Synthesis and Characterization of Silicate Ester Prodrugs and Poly(ethylene glycol)-*b*-poly(lactic-*co*-glycolic acid) Block Copolymers for Formulation into Prodrug-Loaded Nanoparticles

A DISSERTATION SUBMITTED TO THE FACULTY OF THE GRADUATE SCHOOL OF THE UNIVERSITY OF MINNESOTA BY

Adam Richard Wohl

IN PARTIAL FULFILLMENT OF THE REQUIREMENTS FOR THE DEGREE OF

Doctor of Philosophy

Thomas R. Hoye, Advisor

September 2012

September 2012

Acknowledgements

I have been blessed to have the support of my family, friends, and colleagues. Without your help and encouragement, my graduate career would not have been possible.

First of all, I would like to thank my advisor Prof. Tom Hoye. Over the past five years, he has been a consistent and patient mentor that leads first and foremost by setting a world-class example. He has taught me so much about analyzing problems, having fun while working hard, and always paying attention to the details. He has constantly taught me during our experimental discussions, results analysis, and late night (or, as I believe Tom would say, “mid-evening”) grant/manuscript writing sessions. I have learned not only many, many chemical concepts and scientific strategies, but also other valuable skills – how to clearly present ideas and make a compelling presentation to the right audience. Thank you, Tom, for all of the time that you have invested in both my scientific career and life – you have my utmost appreciation and respect.

I would also like to thank Prof. Chris Macosko for all of his time, help, and expertise that he has provided to this collaborative project. With his guidance, my scientific and personal experiences were broadened tremendously. He has also constantly reminded me to keep the “big picture” in view in both science and life, and for that I am truly grateful. I would also like to thank Macosko group students Dr. Zhengxi Zhu, Jing Han, and Kevin Pustulka for their efforts on this project.

In addition, a number of other collaborators have been instrumental to my graduate career. Prof. Jayanth Panyam has provided critical pharmacological expertise to the current project and its future direction during our collaborative biological studies. I owe an especially large debt to his student, Stephen Kalscheuer, for his diligent work on the cell and tumor-bearing animal efficacy studies. Prof. Alon McCormick and Han Seung Lee also provided important theoretical knowledge and experimental skill to the microscopy experiments.

I have been lucky to work with many extraordinarily talented colleagues in the Hoye group as well. Dr. Yutaka Miura conducted the initial experiments to test the viability of the silicate ester prodrug strategy, and Dr. Haitao Qian initiated the block copolymer polyesterification project. I learned much from working with both of these group members, especially as I began my graduate research. I also thank Andrew Michel for carrying on this project into the future, and I wish him the best of luck in all of his upcoming experiments. Many other former and current students in the Hoye group have provided valuable technical advice and an amazing working environment (after all, you have to have some fun!). Thank you to Dr. Matthew Jansma, Dr. Dorian Nelson, Dr. Amanda Schmidt, Dr. Susana Emond, Patrick Willoughby, Brian Woods, Susan Brown, Dawen Niu, and Cagri Izgu.

My parents, Richard and Laura, have always given me their unwavering support and love. From the time that they helped spark my scientific interest by helping me kill a few marigolds in our basement closet, they have always been unbelievably encouraging. I know that they also made many temporal and financial sacrifices to provide me with the resources to pursue my early scientific interests. I will always cherish your support and all that I learned from both of you during those science projects and the life skills that went with those experiences.

Jill, my wife, is my steadfast foundation of support and love throughout the highs and lows that come with graduate school. She celebrated with me in times of success, encouraged me when I was frustrated, and put food in front of me and told me to eat as I studied for my preliminary exams. She has also graciously listened to my incessant “chemistry talk,” patiently allowed me to work late, and always been a much-needed source of balance in my life. Thank you, Jill, for all of the personal sacrifices that you have made in support of my graduate career. Honestly, I couldn’t have done this without your ever-present love and encouragement.

I dedicate this thesis to

my parents and my wife.

Abstract

Fine control of the physical and chemical properties of customized materials is a field that is rapidly advancing. This is especially critical in pursuits to develop and optimize novel nanoparticle drug delivery. Specifically, I aim to apply chemistry concepts to test the hypothesis “Silicate ester prodrugs of paclitaxel, customized to have the proper hydrophobicity and hydrolytic lability, can be formulated with well-defined, biocompatible, amphiphilic block copolymers into nanoparticles that are effective drugs.” Chapter 1 briefly describes the context and motivation of the scientific pursuits described in this thesis. In Chapter 2, a family of model silicate esters is synthesized, the hydrolysis rate of each compound is benchmarked, and trends are established based upon the steric bulk and leaving group ability of the silicate substituents. These trends are then applied to the synthesis of labile silicate ester prodrugs in Chapter 3. The bulk of this chapter focuses on the synthesis, hydrolysis, and cytotoxicity of prodrugs based on paclitaxel, a widely used chemotherapeutic agent. In Chapter 4, a new methodology for the synthesis of narrowly dispersed, “random” poly(lactic-*co*-glycolic acid) polymers by a constant infusion of the glycolide monomer is detailed. Using poly(ethylene glycol) as a macroinitiator, amphiphilic block copolymers were synthesized. Co-formulating a paclitaxel silicate and an amphiphilic block copolymer via flash nanoprecipitation led to highly prodrug-loaded, kinetically trapped nanoparticles. Studies to determine the structure, morphology, behavior, and efficacy of these nanoparticles are described in Chapter 5. Efforts to develop a general strategy for the selective end-functionalization of the polyether block of these amphiphilic block copolymers are discussed in Chapter 6. Examples of this strategy include functionalization of the polyether with an azide or a maleimide. Finally, Chapter 7 provides an outlook for future development of the strategies described in this thesis and summarizes the results and conclusions of the experimental results that led to the development of the therapeutic, paclitaxel silicate-loaded, polymeric nanoparticles.

Table of Contents

List of Tables

List of Figures

List of Schemes

List of Abbreviations

Ac	acetyl
AcOH	acetic acid
AFM	atomic force microscopy
ALT	alanine transaminase
APCI	atmospheric-pressure chemical ionization
app	apparent, in NMR spectroscopy
AST	aspartate transaminase
ATRP	atom transfer radical polymerization
AUC	area under the curve
BCP	block copolymer
BIBS	di-*tertiary*-butylisobutylsilyl
BMS	Bristol-Meyers Squibb
Bn	benzyl
boc	butoxycarbonyl
br	broad, in NMR spectroscopy
brsm	based on recovered starting material
n-Bu (or ^{n}Bu)	*normal*-butyl
t-Bu (or ^{t}Bu)	*tertiary*-butyl
Bz	benzoyl
°C	degree Celsius
Calc'd	calculated

CIJ	confined impingement jet
CIJ-D	confined impingement jet with dilution
clog P	calculated log partition coefficient
CrEL®	Cremophor EL® (i.e., polyoxyethyleneglycerol triricinoleate 35)
d	doublet, in NMR spectroscopy
D	diffusion coefficient
DAD	diode array detector
DBU	1,8-diazabicyclo[5.4.0]-undec-7-ene
DCM	dichloromethane
DEAD	diethyl azodicarboxylate
DHA	docosahexaenoic acid
DIAD	diisopropyl azodicarboxylate
DMAP	4-dimethylaminopyridine
DMF	dimethylformamide
DMSO	dimethyl sulfoxide
d_n/d_c	specific refractive index
DOSY	diffusion oriented spectroscopy
DSC	differential scanning calorimetry
EDCI	1-Ethyl-3-(3-Dimethylaminopropyl)carbodiimide
EPR	enhanced permeation and retention
equiv	equivalent

ESI	electrospray ionization
EtOAc	ethyl acetate
EtOH	ethanol
FDA	Food and Drug Administration
FNP	flash nanoprecipitation
g	gram(s)
GC	gas chromatography
GPC	gel permeation chromatography
h	hour(s)
n-Hex (or ^{n}hex)	*normal*-hexyl
HIV	human immunodeficiency virus
HRMS	high resolution mass spectrometry
Hz	Hertz
IC_{50}	half maximal inhibitory concentration
i,i	isotactic,isotactic
i,s	isotactic,syndiotactic
IR	infrared
IV	intravenous
J	coupling constant, in NMR spectroscopy
k	rate constant
k_{app}	apparent rate constant
k_{obs}	observed rate constant

k_{rel}	relative rate constant
log P	log partition coefficient
m	multiplet, in NMR spectroscopy
M	molar
MAL	maleimide
MALS	multiangle light scattering
Me	methyl
MeOH	methanol
MHz	megahertz
min	minute(s)
MIV	multi-inlet vortex
mmol	millimole(s)
M_n	number average molecular weight
mp	melting point
MPLC	medium pressure liquid chromatography
MS	mass spectrometry
MTBE	methyl *tert*-butyl ether
MTS	3-(4,5-dimethylthiazol-2-yl)-5-(3-carboxymethoxyphyenyl)-2-(4-sulfophenyl)-2H-tetrazolium
MTT	3-(4,5-dimethylthiazol-2-yl)-2,5-diphenyltetrazolium bromide

MW	molecular weight
M_W	weight average molecular weight
n.d.	not determined
ND	none detected
NHS	*N*-hydroxy-succinimide
nm	nanometer(s)
NMR	nuclear magnetic resonance
NSF	National Science Foundation
n-Oct (or ^{n}Oct)	*normal*-octyl
PCL	polycaprolactone
PDI	polydispersity index
PEG	poly(ethylene glycol)
PEO	poly(ethylene oxide)
PGA	poly(glycolic acid)
Ph	phenyl
PLA	poly(lactic acid)
PLGA	poly(lactic-*co*-glycolic acid)
PMMA	poly(methyl methacrylate)
ppm	parts per million
i-Pr (or ^{i}Pr)	*iso*-propyl
PS	polystyrene
PTX	paclitaxel

py	pyridine
q	quartet, in NMR spectroscopy
R	rectus, configuration
RAFT	reversible-addition fragmentation transfer
R_f	ratio to front
rt	room temperature
ROP	ring opening polymerization
S	sinister, configuration
s	singlet, in NMR spectroscopy
sec	second(s)
sept	septet, in NMR spectroscopy
SD	standard deviation
SEC	size-exclusion chromatography
SEM	scanning electron microscopy
SL	sequence length
s,s	syndiotactic,syndiotactic
t	triplet, in NMR spectroscopy
$t_{1/2}$	half life time
TBS	*tertiary*-butyldimethyl
TBD	1,5,7-triazabicyclo[4.4.0]dec-1-ene
TBDPS	*tetrtiary*-butyldiphenylsilyl
TEA (or NEt_3)	triethylamine

TEM	transmission electron microscopy
TEOS	tetraethyl orthosilicate (i.e., tetraethoxysilane)
TFA	trifluoroacetic acid
T_g	glass transition
THF	tetrahydrofuran
THP	terahydropyran
TIPOS	tetraisopropyl orthosilicate (i.e., triisopropoxysilane)
TLC	thin layer chromatography
T_m	melting transition
TMOS	tetramethyl orthosilicate (i.e., tetramethoxysilane)
TMS	trimethyl silyl
vol%	volume percent
wt%	weight percent

Chapter 1

General Overview and Motivation

1. General Overview.

1. A Philosophical Viewpoint. Development of novel and successful drug delivery strategies is arguably one of the most daunting, complex, and important problems faced today. The challenges to developing such techniques are numerous, including (but not limited to): i) control of the physicochemical and biological properties of a small molecule drug, ii) optimization of a biocompatible excipient to facilitate drug delivery, and iii) assurance of both the efficacy and safety of a new formulation. These numerous and widely diverse challenges necessitate a broad-based and highly interdisciplinary approach to achieve progress in the field. In this light, chemists must consider "How can we (as the chemistry community) best apply our knowledge and skills to difficult, inter-disciplinary yet practical problems?" I would argue that our collective expertise in synthesizing precisely customized materials, both discrete small molecules and macromolecules, is one potential key to well-defined and highly generalizable solutions in drug delivery.

2. Flash Nanoprecipitation. One fundamental drawback hindering the development and clinical application of many new drugs is limited aqueous solubility. An emerging technology, termed flash nanoprecipitation (FNP) is one strategy that, in the most general sense, formulates hydrophobic compounds in

an aqueous medium.[1] In this process, water and a miscible organic solvent, in which an amphiphilic block copolymer (BCP) and an organic active are co-dissolved, are rapidly mixed in a confined volume. In the resulting, predominantly aqueous suspension, the organic compound and hydrophobic block of the BCP are co-encapsulated within the newly formed nanoparticle, which is effectively solubilized by the hydrophilic block.

Prud'homme and coworkers further refined the FNP process to optimize it for drug delivery by engineering new impingement jet mixers: the confined impingement jet (CIJ) mixer[2,3] and the multi-inlet vortex (MIV) mixer.[4] In their model work, FNP studies utilized β-carotene as a highly hydrophobic drug model and poly(ethylene glycol)-*b*-poly(styrene) (PEG-*b*-PS) as the amphiphilic block copolymer. These studies demonstrated the potential of FNP methodology; namely, this technique results in nanoparticles that exhibit i) high encapsulation efficiencies, ii) high drug loading, and iii) nanoparticle sizes of approximately 100 nm. Specifically, Dr. Zhengxi Zhu, a student of Prof. Christopher Macosko (Department of Chemical Engineering and Materials Science, University of Minnesota), demonstrated that β-carotene could be loaded in the core of a block copolymer at loading levels > 80 weight percent (wt%)[5] – a loading level that is significantly higher than most commonly employed drug encapsulation methodologies (typically 5-10 wt%).

---

[1] Horn, D.; Rieger, J. Organic Nanoparticles in the Aqueous Phase – Theory, Experiment, and Use. *Angew. Chem. Int. Ed.* **2001**, *40*, 4330–4361.

[2] Johnson, B. K.; Prud'homme, R. K. Chemical Processing and Micromixing in Confined Impinging Jets. *AIChE* **2003**, *49*, 2264–2282.

[3] Johnson, B. K.; Prud'homme, R. K. Flash NanoPrecipitation of Organic Actives and Block Copolymers using a Confined Impinging Jets Mixer. *Aust. J. Chem.* **2003**, *56*, 1021–1024.

[4] Liu, Y.; Cheng, C.; Liu, Y.; Prud'homme, R. K.; Fox, R. O. Mixing in a Multi-Inlet Vortex Mixer (MIVM) for Flash Nano-Precipitation. *Chem. Eng. Sci.* **2008**, *63*, 2829–2842.

[5] Zhu, Z. Polymer Stabilized Nanosuspensions Formed via Flash Nanoprecipitation: Nanoparticle Formation, Formulation, and Stability. Ph.D. Dissertation, University of Minnesota, Minneapolis, MN, **2010**, 1–213.

Members of the Macosko group, with collaborative input from the Hoye group, made advancements in the CIJ mixer design. These efforts led to the development of the modified confined impingement jet (CIJ-D)[6] mixing FNP methodology (Figure 1-1). This simple, hand-operated apparatus allowed for rapid analysis of the particle-forming behavior of new materials and introduced a post-impingement mixing stage. Particles made from this CIJ-D method were shown to produce nanoparticles of similar size and stability as that of the MIV mixer.[6] Thus, the CIJ-D has been used extensively in the production of nanoparticles in this thesis.

Figure 1-1. A modified confined impingement jet mixer for a flash nanoprecipitation: during the rapid impingement mixing, hydrophobic solutes are efficiently trapped in the nanoparticle core and rapidly diluted in bulk water, thereby minimizing aggregation. These well-dispersed particles formed have been shown to remain stable for several days.[6]

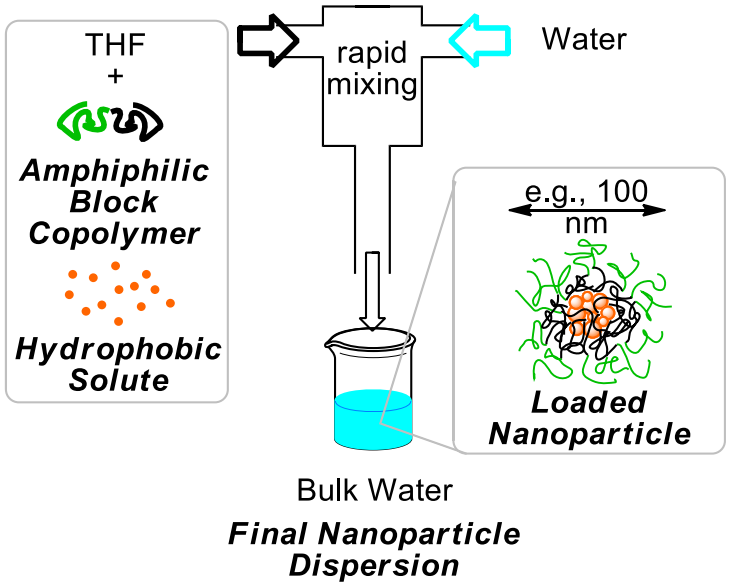

[6] Han, J.; Zhu, Z.; Qian, H.; Wohl, A. R.; Beaman, C. J.; Hoye, T. R.; Macosko, C. W. A Simple Confined Impingement Jets Mixer for Flash NanoPrecipitation. *J. Pharm. Sci.* **2012**, *101*, 4018–4023.

3. Previous Efforts to Encapsulate Paclitaxel via FNP. Previous attempts to expand the β-carotene studies and instead encapsulate a hydrophobic drug, paclitaxel (PTX, **1.01**, the active ingredient in Taxol®), in biocompatible BCPs have been largely unsuccessful.[5,7] These results are attributable to the tendency of PTX to crystallize outside of the nanoparticle core upon aging via Ostwald ripening (i.e., the dissolution of PTX molecules from the nanoparticle core and subsequent crystallization on a bulk PTX crystal). Early work led to improvement of the nanoparticle stability by conjugating PTX to, among others hydrophobic compounds, the nonpolar fatty acid derivative docosanyl diglycolate (**1.02**) to yield the yet more hydrophobic paclitaxel drug derivative **1.03** (Scheme 1-1).[7,8] Altering the physical characteristics of the parent drug molecule successfully created more stable nanoparticles via FNP. However, efficacy of these drug derivatives were found to be significantly (ca. 10-fold) less cytotoxic than the parent drug, presumably due to the unfavorable chemical properties – an exceedingly slow rate of hydrolysis to the active PTX parent – of the new ester drug derivative.[8] The results described above strongly suggest that further optimization of these FNP-based drug delivery systems requires attention to both physical and chemical properties.

[7] Saad, W. S. Drug Nanoparticle Formation via Flash Nanoprecipitation: Conjugation to Encapsulate and Control the Release of Paclitaxel. Ph.D. Dissertation, Princeton University, Princeton, NJ, **2007**. 1–198.

[8] Ansell, S. M.; Johnstone, S. A.; Tardi, P. G.; Lo, L.; Xie, S.; Shu, Y.; Harasym, T. O.; Harasym, N. L.; Williams, L.; Bermudes, D.; Liboiron, B. D.; Saad, W.; Prud'homme, R. K.; Mayer, L. D. Modulating the Therapeutic Activity of Nanoparticle Delivered Paclitaxel by Manipulating the Hydrophobicity of Prodrug Conjugates. *J. Med. Chem.* **2008**, *51*, 3288–3296.

Scheme 1-1. The representative conjugation of **1.01** with **1.02** to synthesize a hydrophobic paclitaxel derivative **1.03**.[8]

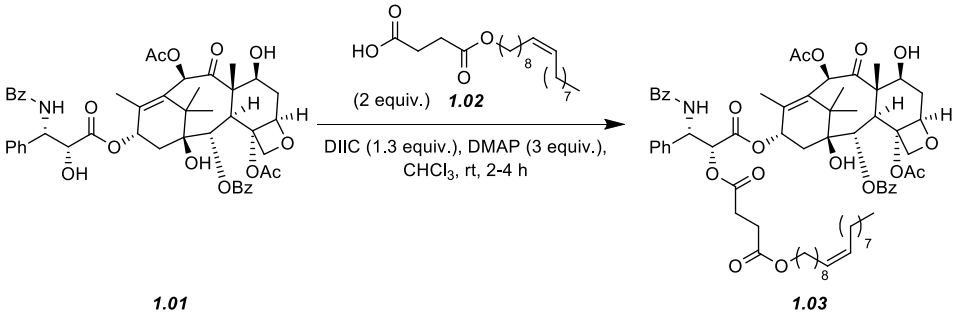

2. General Project Goals.

1. The Over-Arching Hypothesis.

"Silicate ester prodrugs of paclitaxel, customized to have the proper hydrophobicity and hydrolytic lability, can be formulated with well-defined, biocompatible, amphiphilic block copolymers into nanoparticles that are effective drugs."

2. Simultaneous Control of Physical and Chemical Properties of Small Molecules. As alluded earlier, the majority of this thesis is devoted to the development and application of general solutions to far-reaching challenges. Thus, the first aim is to develop novel ideas to independently control the physical *and* chemical properties for application to drug delivery concepts (e.g., FNP). A new, general silicate ester prodrug strategy has been designed to allow for control of *both* the hydrophobic character of a prodrug *and* the rate of hydrolysis to the active parent drug (c.f., Scheme 3-1 and related text in Chapter 3). In pursuing this route, general trends have been established through the analysis of multiple model systems, and this information was most extensively applied to the

synthesis of paclitaxel silicate ester prodrugs. In the course of these studies, the general applicability intentionally incorporated into this methodology was exploited to include other potential drugs, including the synthesis of silicate esters of curcumin (**1.04**, Figure 1-2).

Figure 1-2. The chemical structure of curcumin **1.04**.

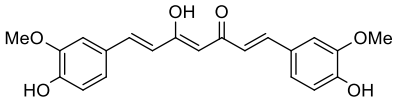

1.04

3. Synthesis of Well-Defined Block Copolymers. Early work on the formulation of loaded nanoparticles suggested that commonly employed, biocompatible BCPs such as poly(ethylene glycol)-*b*-poly(lactic acid) (PEG-*b*-PLA) or poly(ethylene glycol)-*b*-poly(ε-caprolactone) (PEG-*b*-PCL) failed to produce stable nanoparticles, whereas poly(ethylene glycol)-*b*-poly(lactic-*co*-glycolic acid) (PEG-*b*-PLGA) polymers showed promise.[5] However, typical methods for the synthesis of PLGA [i.e., random transesterification of lactide and glycolide with a Sn(II) catalyst] typically give poorly defined, broadly dispersed polymers.[9] Therefore, a new route to synthesize poly(ethylene glycol)-*b*-poly(lactic-*co*-glycolic acid) (PEG-*b*-PLGA) block copolymers of narrow molecular weights was developed in collaboration with Dr. Haitao Qian, a post-doctoral associate in the Hoye group. Additionally, carefully choosing the end groups of these polymers allows selective functionalization of either the hydrophobic or hydrophilic terminus of these block copolymers to induce *in vivo* targeting or imaging. The described unique materials may then be used in a number of applications, including drug delivery projects.

[9] Dechy-Cabaret, O.; Martin-Vaca, B.; Bourissou, D. Controlled Ring-Opening Polymerization of Lactide and Glycolide. *Chem. Rev.* **2004**, *104*, 6147–6176.

Chapter 2

Model Silicate Ester Prodrugs: Synthesis and Determination of Hydrolysis Rate Trends

1. Introduction.

Orthosilicates [$Si(OR)_4$] are a class of organic compounds that have been known for more than 160 years.[10] However, their application to generally control physical and chemical properties is a novel application of an age-old chemical entity. Several attractive features of this new class of prodrugs have the potential to be exploited: i) the ease of synthesis, ii) diversity of amenable compounds, iii) the ability to incorporate alkyl chains of varying lengths to control hydrophobic character, iv) the tunable hydrolysis rate via the steric bulk of the alkoxy substituents, and v) the open "chemical space" in the patent literature.

1. Silicate Nomenclature. Prior to delving into the physical and chemical properties of orthosilicates/alkoxysilanes/silicate esters, it is helpful to unambiguously define the naming system to be used in this thesis for such compounds. Confusion arises from the historical practice of naming such silicon-centric entities as derivatives of different parent compounds. The end result is

[10] Ebelmen, M. *Ann. Chim. Phys.* **1845.** *15,* 319.

that multiple common names are often encountered in the literature for identical compounds.

A series of instructive examples crystallizes many of these issues. Most generally, names for compounds containing silicon are named from the simplest silane, SiH_4. As heavy atom substituents are added, the name of the silane is adjusted appropriately. For instance, $(Et)_3SiH$, $(EtO)_3SiH$, and $Si(OEt)_4$ are named triethylsilane, triethoxysilane, and tetraethoxysilane, respectively. Among these examples, $Si(OEt)_4$ uniquely contains four Si-O bonds, and thus it is commonly named as a derivative of orthosilicic acid [$Si(OH)_4$] rather than as a silane derivative. Therefore, $Si(OEt)_4$ is often referred to as tetraethyl orthosilicate (TEOS).[11]

The naming of $Si(OEt)_4$ and analogous compounds (i.e., those containing four Si-O bonds) is further complicated by repeated references to them as a silicon or silicate esters.[12] Omission of the "ester" and discussion of these compounds merely as "silicates" may induce confusion arising from the prevalence of silicate anions (SiO_4^{4-}) in inorganic chemistry and geology. However, references to "silicates" throughout this thesis will always denote compounds of the general form $Si(OR^1)(OR^2)(OR^3)(OR^4)$ rather than the anion SiO_4^{4-}.

2. Previous Work Utilizing Silicate Esters and Silyl Ethers in Biomaterials and Prodrugs. Prior to work performed in the labs of Prof. Thomas Hoye and

[11] Arkles, B. Silicon Esters. In *Kirk-Othmer Encyclopedia of Chemical Technology, Fourth Edition, Volume 22*; Kroschwitz, J. I.; Howe-Grant, M., ed. John Wiley & Sons, Inc: New York, 1997, 69–81.

[12] Wright, J. R. Bolt, R. O.; Goldschmidt, A.; Abbott, A. D. Silicate Esters and Related Compounds. I. Synthesis of Certain Tetraalkoxysilanes, Polyalkoxysilanes, Bis-(trialkoxysilyl)-alkanes, and Related Intermediates. *J. Am. Chem. Soc.* **1957**, *80*, 1733–1737.

Prof. Christopher Macosko,[13,14] tetraalkoxysilanes attractively lack ample, direct precedent as prodrugs. This feature was viewed as the general innovative strategy described in Chapters 2 and 3 of this thesis. During the preparation of this manuscript, however, multiple reports of related research (i.e., studies using silicon-based derivatives of drugs) appeared in the literature. For instance, Cheng and co-workers published efforts toward trialkoxyalkylsilane drug derivatives to incorporate the drugs into well-defined silica-based nanoparticles.[15] Cheng's general strategy employed derivatization of a drug molecule via a thioether ester linker to form either the trimethoxysilyl camptothecin (Figure 2-1, **2.01**) or trimethoxysilyl paclitaxel (Figure 2-1, **2.02**). Importantly, rather than using the trimethyl silicate ester as a promoiety, the trialkoxyalkylsilane merely "anchored" the drug derivative into nanoparticles comprised of bulk silica. While favorable biocompatibility and biodistribution studies of these compounds were reported, no biological efficacy data of **2.01** or **2.02** has yet been published. In the case of **2.02**, efficacy of this drug may be diminished by the undesirably high *in vivo* stability of the thioether ester linker. Without additional data, this conclusion remains speculative; however, it is consistent with previously reported cytotoxicity data of other paclitaxel drug derivatives functionalized at the C2' position.[16]

---

[13] Hoye, T. R.; Ji, S.; Miura, Y.; Zhu, Z.; Macosko, C. W. PCL-b-PEG Nanoparticles for Drug Delivery: Package and Contents. Presented at IPRIME annual meeting. Minneapolis, MN, May 31, 2007.

[14] Wohl, A. R.; Hoye, T. R.; Zhu, Z.; Macosko, C. W. Orthosilicate Prodrug Models: Synthesis, Hydrolysis, and Encapsulation in Block Copolymer Nanoparticles. National Meeting of the AIChE, Nov. 2010.

[15] Tang, L.; Fan, T. M.; Borst, L. B.; Cheng, J. Synthesis and Biological Response of Size-Specific, Monodisperse Drug-Silica Nanoconjugates. *ACS Nano*, **2012**, *6*, 3954–3966.

[16] Kingston, D. G. I. The Shape of Things to Come: Structural and Synthetic Studies of Taxol and Related Compounds. *Phytochemistry* **2007**, *68*, 1844–1854.

Figure 2-1. The structure of the thioether ester silicate drug derivatives (**2.01** and **2.02**) as reported by Cheng.[15]

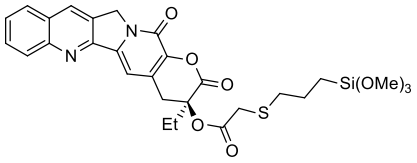

2.01

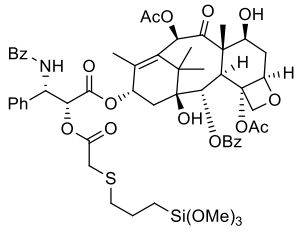

2.02

Alternatively, silyl ethers have been used as hydrolytically degradable biomaterials by DeSimone and co-workers.[17] Their relevant work produced a variety of biomaterials (e.g., drug delivery vehicles, stents, and sutures) based on dialkyldialkoxysilanes that were susceptible to degradation under acid catalysis. Additionally, the rate of degradation was modulated via the steric bulk of the dialkyl substituents (specifically, ethyl, *i*-propyl, and *t*-butyl substituents were examined) composing the silyl ether. Finally, *in vitro* assays established the nontoxic biological properties of the (presumably hydrolyzed) byproducts. This excellent work provides strong encouragement for the general silicate prodrug strategy and motivation to spur the development of tetraalkoxysilanes as prodrugs.

During the preparation of this thesis, DeSimone and co-workers expanded upon their earlier report by publishing the use of dialkoxydialkysilanes as prodrugs of camptothecin (**2.03a-c**), dasatinib (**2.04a-c**), gemcitabine (**2.05a-c**).[18]

[17] Parrott, M. C.; Luft, J. C.; Byrne, J. D.; Fain, J. H.; Napier, M. E.; DeSimone, J. M. Tunable Bifunctional SIlyl Ether Cross-Linkers for the Design of Acid-Sensitive Biomaterials. *J. Am. Chem. Soc.* **2010**, *132*, 17928–17932.

[18] Parrott, M. C.; Finniss, M.; Luft, J. C.; Pandya, A.; Gullapalli, A.; Napier, M. E.; DeSimone, J. M. Incorporation and Controlled Release of Silyl Ether Prodrugs from PRINT Nanoparticles. *J. Am. Chem. Soc.* **2012**, *134*, 7978–7982.

This manuscript expanded upon their previous expertise in biomaterials by incorporating two biologically inert alkyl groups of varying steric bulk [ethyl (**2.03-2.05a**), *i*-propyl (**2.03-2.05b**), *t*-butyl (**2.03-2.05c**)] and hydroxyl ethyl acrylate as the third non-drug substituent. Using the acrylate moiety, they cross-linked the prodrugs with a PEG-diacrylate [**2.06**, molecular weight (MW) = ca. 1000]. These large macromolecules were then formulated into nanoparticles. They further demonstrated that the hydrolysis and release of the free drug was time-dependent and related to the steric bulk of the two alkyl moieties,[18] analogous to their previous biomaterials work.[17]

Figure 2-2. The structure of all reported dialkoxydialkyl silicate drug derivatives **2.03a-c**, **2.04a-c** and **2.05a-c** reported by DeSimone.[18]

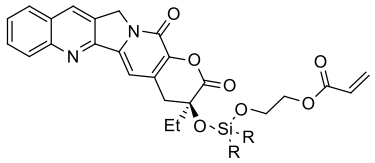

2.03a-c
R = (a) Et (b) ^{i}Pr (c) ^{t}Bu

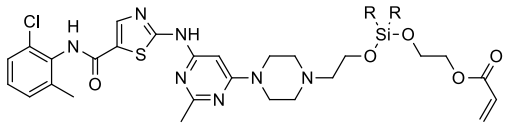

2.04a-c
R = (a) Et (b) ^{i}Pr (c) ^{t}Bu

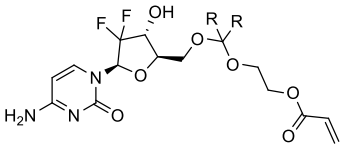

2.05a-c
R = (a) Et (b) ^{i}Pr (c) ^{t}Bu

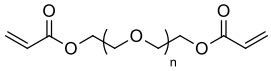

2.06
n = ca. 23

3. Established Orthosilicate Chemistry. Generally, silicate esters (and other organosilicon species[19,20]) have been widely studied for applications other than that of drug delivery.[11] A number of variables (e.g., solvent-dependence,

[19] Bassindale, A. R.; Taylor, P. G. Reaction Mechanisms of Nucleophilic Attack at Silicon. In *The Chemistry of Organic Silicon Comounds*. Patai, S.; Rappoport, Z., eds. John Wiley & Sons, Inc: New York, 1989, 839–892 and references therein.

[20] Holmes, R. R. The Stereochemistry of Nucleophilic Substitution at Tetracoordinated Silicon. *Chem. Rev.* **1990**, *90*, 17–31 and references therein.

catalyst and reagent concentration, etc.) and their effects on both the acid- and base-catalyzed hydrolysis rate of tetramethyl (TMOS) and tetraethyl (TEOS) orthosilicates[21] have been extensively studied. TMOS and TEOS were specifically chosen for these extensive, albeit typically dated, studies due to industrial applications in sol-gel forming processes. The techniques used to monitor the hydrolysis of these silicates include Karl-Fisher titrations,[22] gas chromatography,[23] Raman spectroscopy,[24] and nuclear magnetic resonance (NMR) spectroscopy.[25,26] The most relevant (to this thesis) conclusions resulting from the acid-catalyzed hydrolysis studies are that the hydrolysis occurs via i) an S_N2 mechanism, ii) a solvent-dependent rate, and iii) pseudo-first order kinetics if a large excess of water is present.[27]

Surprisingly, there is relatively little literature data in which the hydrolysis rate of a series of orthosilicates has been systematically and carefully studied under identical reaction conditions. Rather, qualitative inferences have often been drawn from the behavior of these labile compounds. For instance, gelation times (a proxy for hydrolysis) of tetramethyl, tetraethyl, and tetra-*n*-butyl orthosilicates were found to be approximately two days, 10 days, and 25 days,

---

[21] Aelion, R.; Loebel, A.; Eirich, F. Hydrolysis of Ethyl Silicate. *J. Am. Chem. Soc.* **1950**. *69*, 61–75.

[22] Brinker, C. J. Hydrolysis and Condensation of Silicates: Effects on Structure. *J.Non-Cryst. Solids* **1988**, *100*, 31–50.

[23] Ro, J. C.; Chung, I. J. Sol-Gel Kinetics of Tetraethylorthosilicate (TEOS) in Acid Catalyst. *J. Non-Cryst. Solids* **1989**, *110*, 26–32.

[24] Zerda, T. W.; Hoang, G. Effects of Solvents on the Hydrolysis Reaction of Tetramethyl Orthosilicate. *Chem. Mater.* **1990**, *2*, 372–376.

[25] Turner, C. W.; Franklin, K. J. Studies of the Hydrolysis and Condensation of Tetraethylorthosilicate by Multinuclear (^{1}H ^{17}O ^{29}Si) NMR Spectroscopy. *J. Non-Cryst. Solids* **1986**, *91*, 402–415.

[26] Assink, R. A.; Kay, B. D.; Study of Sol-Gel Chemical Reaction Kinetics by NMR. *Annu. Rev. Mater. Sci.* **1991**, *21*, 491–513.

[27] Zerda, T. W.; Hoang, G. Effects of Solvents on the Hydrolysis Reaction of Tetramethyl Orthosilicate. *Chem. Mater.* **1990**, *2*, 372–376.

respectively, when the compounds were stored without "special precautions."[11] While not ultimately satisfying or precisely informative, early observations such as these gave an indication of the subtle steric alterations that influence the rate of hydrolysis of silicate esters.

The most pertinent set of experiments that attempted to quantify the absolute hydrolysis rates of several silicate esters involved four different compounds; all symmetrical tetraalkoxysilanes (see Table 2-1). These experiments demonstrated an approximately six-fold slower hydrolysis rate with increasing aliphatic chain length (from ethyl to *n*-hexyl) and an approximately 17-fold slower hydrolysis rate with a branched side chain.[22] Unfortunately, these studies are compromised by the selected analytical method. The Karl Fisher titration was used determine the change in water concentration during the reaction, but, since the Karl Fisher reagents are now known to consume both water and silanols, the measured rate constants are considered unreliable.[28] These studies provide a degree of precedence regarding the steric dependence of the rate of hydrolysis, but, more precise quantitative measurements of these trends is required to harness orthosilicate esters for novel applications.

[28] Brinker, C. J.; Scherer, G. W. Hydrolysis and Condensation II: Silicates. In *Sol-Gel Science: The Physics and Chemistry of Sol-Gel Processing*. Academic Press, Inc: San Diego, CA, **1990**, 97–233.

Table 2-1. Acid-catalyzed hydrolysis rates, as analyzed by Karl Fisher titrations,[22] of four symmetrical silicate esters.

$Si(OR)_4$ R =	$k\,(10^2)$ [a] $(mol^{-1}\ s^{-1}\ [H^+]^{-1})$
Ethyl	5.1
n-Butyl	1.9
n-Hexyl	0.83
2,3-Dimethylbutyl	0.30

[a] Conducted at 20 °C.

2. Methodology Development.

1. Considerations and Early Attempts. As is the case in many experimental designs, establishing experimental methodology that is capable of differentiating the possible outcomes with confidence is critical. Thus, the first step necessary toward determining the potential of silicate ester prodrugs is to demonstrate that a reliable and accurate measurement of the hydrolysis rate could be achieved. It is important to emphasize at this point that the aim in these studies is to establish *relative* hydrolysis rate trends via observed hydrolysis rates (k_{obs}) rather than the absolute hydrolysis rate constants (k). This goal is guided by both the ease of experimentation (e.g., precise control of temperature within the Varian 500 MHz NMR spectrometer at the University of Minnesota is not trivial) and consideration of the final application (i.e., hydrolysis within a preformed nanoparticle) of the silicate ester hydrolysis. Namely, it is difficult to identify, much less control, the actual microenvironment [e.g., water content,

solvent diffusion rates, effective pH, and physical state (crystalline vs. amorphous) of the silicate ester] within a nanoparticle core. Thus, the model hydrolysis rate trends are needed to guide optimization of the prodrug design based primarily upon empirical observations of the prodrug hydrolysis and/or drug release rates.

Dr. Yutaka Miura, a post-doctoral associate in the Hoye labs, conducted the initial attempts to monitor orthosilicate hydrolysis reactions. He first attempted to employ gas chromatography-mass spectrometry (GC-MS), but this technique yielded irreproducible results.[29] Employing ^{29}Si NMR experiments was found to be impractical due to problems arising from low sensitivity, and the lengthy ^{29}Si NMR experiments that were required to collect the data with sufficient signal-to-noise ratios proved unduly time-consuming and expensive.[29]

2. In situ ^{1}H NMR Spectroscopic Measurements. The more sensitive ^{1}H NMR spectroscopy was considered as a viable alternative. Previous work utilizing ^{1}H NMR spectroscopy to measure kinetic rates has been successful. This tactic is particularly highlighted by the careful and detailed efforts of Raines and co-workers to establish the pD (since the experiments were performed in a deuterated environment, pD is analogous to the more commonly encountered pH values) dependency of hydrazone hydrolysis rates.[30] Proton NMR spectroscopy has also been applied to study hydrolysis intermediates of orthosilicates. However, these experiments employed substoichiometric levels of water, complicating analysis of the hydrolysis rate since pseudo-first order kinetics could not be assumed and the hydrolysis was not exhaustive.[26] Thus, further studies were initiated to develop a technique reliant upon ^{1}H NMR spectroscopy to

[29] Miura, Y. University of Minnesota, Minneapolis, MN. Personal communication, **2008**.

[30] Kalia, J.; Raines, R. T. Hydrolytic Stability of Hydrazones and Oximes. *Angew. Chem. Int. Ed.* **2008**, *47*, 7523–7526.

quickly, *conveniently*, and *accurately* establish the relative hydrolysis rate trends for a series of silicate esters of varying steric and electronic character.

Initially a variety of reactive environments were screened to benchmark standard conditions that would allow: i) solubility of a majority of the silicate ester models and prodrugs, ii) fast yet measurable hydrolysis rates, and iii) a sufficient excess of water to allow pseudo first-order kinetics to be accurately assumed. A series of experiments were conducted by catalyzing the hydrolysis of TEOS with acetic acid [1 volume percent (vol%)] in a mixture of deuterated water and deuterated acetone. In these early experiments, the ratio of the deuterated water/acetone co-solvents was systematically varied. The vol% of water ranged from 90-10% (with deuterated acetone used as the organic solvent in the amount necessary to “balance” the water level). The co-solvent composition corresponded to variations in the observed rate of greater than four orders of magnitude (see Table 2-2). This change in rate represents half-lives ranging from less than two minutes (90 vol% water) to much greater than two weeks (10 vol% water). This correlation of a progressive decrease in the hydrolysis rate that corresponds to increasing acetone content is in agreement with the increased rates previously observed in more polar media. [22,27]

Table 2-2. Acetic acid-catalyzed observed hydrolysis rates of TEOS in co-solvent mixtures containing varying volumes of water.

Entry #	D_2O (vol)%	d_6-acetone (vol)%	acetic acid (vol)%	$t_{1/2}$[a] (observed, min)
1[b]	10	89	1	> 25000
2	50	49	1	55
3	70	29	1	7.4
4	90	9	1	0.86

[a] Error bars are not provided because less than three measurements were taken. The values provided here are thus intended as approximations only.
[b] Measurement taken by Dr. Yutaka Miura.[29]

3. Establishment of "Standard" Hydrolysis Conditions and Reproducibility of the ^{1}H NMR Measurements. Settling upon a set of "standard hydrolysis conditions" took into account multiple factors. First, many of the envisioned silicate ester models and prodrugs are, by design, highly hydrophobic. Therefore, the water content was minimized (to 10 vol%) to allow dissolution of a majority of the silicate models and prodrugs. By default, a large volume of d_6-acetone was then required. A stronger acid catalyst [trifluoroacetic acid (TFA)] was included to illicit observed hydrolysis rates on a reasonable time scale.

Thus, after varying the solvent composition, acid strength, and amount of acid catalyst, we settled upon a solvent mixture composed of 90 vol% d_6-acetone, 9 vol% D_2O, and 1 vol% TFA. Data obtained from this system is used to report the measured k_{obs} and $t_{1/2}$ values analyzed under the assumption of pseudo-first order kinetics. For convenience, the measured k_{rel} values in this section are referenced to the thoroughly studied and readily available TEOS

(**2.07**). The hydrolysis of **2.07** was analyzed to define the reproducibility of this new ^{1}H NMR methodology and "standard" hydrolysis conditions. The results and inferred reproducibility of a series of five sequential hydrolysis experiments (Scheme 2-1) of **2.07** to orthosilicic acid (**2.08**) and four equivalents of ethanol are shown in Table 2-3.

Scheme 2-1. The defined "standard hydrolysis conditions" were used to measure the observed hydrolysis rate of **2.07**, yielding orthosilicic acid **2.08** and ethanol.

2.07 ***2.08***

Table 2-3. The reproducibility of the *in situ* ^{1}H NMR hydrolysis rate measurement of **2.07** was found to be reliable.

Entry [a]	$t_{1/2}$ (min)	k_{obs} (10^{-3} s^{-1})
1	3.3	3.5
2	3.0	3.8
3	3.0	3.9
4	3.2	3.6
5	3.1	3.7

[a] The trials were run sequentially and analyzed immediately thereafter. Experimentation and analysis were completed in less than two total hours for the five trials.

In this study, the variation in the observed hydrolysis rate was confirmed to be approximately ± 5% from the mean value. Further appealing, this technique allows for the rapid accumulation of data – all five trials reported in Table 2-3

were completed in less than two hours. Based upon these results, this methodology was deemed to be fast, convenient, and reproducible; therefore, it was used in the future hydrolysis experiments unless otherwise noted.

3. Hydrolysis Rates of Symmetrical Tetraalkoxy Silicates.

1. Controlling the Hydrophobicity. With the basic ^{1}H NMR methodology established, the opportunity to determine the degree of dependency between the hydrophobic character and the hydrolysis rate of the silicate esters was available. This distinction is one key to the eventual application of silicate esters to a prodrug strategy. The ability to significantly alter physical properties (e.g., hydrophobic character) and chemical properties (e.g., rate of hydrolysis) is a potential, significant advantage of the concept.

Toward this goal, a series of easily obtained, linear, aliphatic, and symmetrical orthosilicate models was examined. The most common of these models [i.e., **2.07** and TMOS (**2.09**)] are readily available from a variety of commercial sources. Other compounds (those with non-obvious commercial applications) such as tetra-*n*-butyl, tetra-*n*-hexyl, tetra-*n*-octyl, and tetraphytyl orthosilicates (**2.11**,[31] **2.12**,[31,32] **2.13**,[32] and **2.14**,[33] respectively) were conveniently prepared via procedures related to those reported in the literature. In a routine experiment, a symmetrical tetraalkoxysilane was prepared by treating silicon tetrachloride ($SiCl_4$, **2.10**) with an excess of the desired alcohol (and often co-dissolved with an amine base) in a hydrocarbon or ethereal solvent (c.f.,

[31] Ridge, D.; Todd, M. Studies in the Formation Mechanisms of Alkyl Orthosilicates. *J. Chem. Soc.* **1949**, 2637–2640.

[32] Gerrard, W.; Woodhead, A. H. Interaction of Alcohols with Silicon Tetrachloride. *J. Chem. Soc.* **1951**, 519–522.

[33] Key resonances observed in crude ^{1}H NMR (500 MHz, $CDCl_3$): δ = 5.37 [br t, *J* = 6 Hz, 4H, $Si(OC\mathit{H}_2CH)_4$] and 4.31 [overlapping d's, 8H, $Si(OCH_2C\mathit{H})_4$, observed as a mixture cis and trans isomers].

Scheme 2-2). As expected, these reactions proceed cleanly to yield the desired, symmetrical orthosilicates of varying hydrophobicities that can be purified via distillation or silica chromatography.

Scheme 2-2. The general synthetic routes utilized to access linear tetraalkoxysilane models.

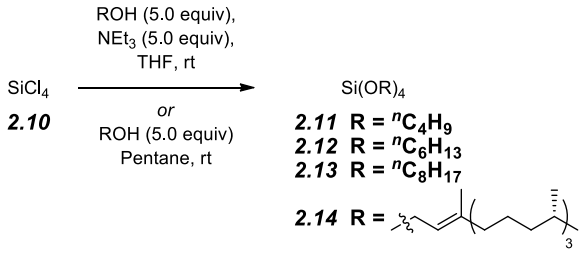

Applying our previously optimized hydrolysis conditions (see Section 2.2.3), the k_{obs} for models **2.07**, **2.09**, and **2.11-2.13** was observed to decrease only slightly with longer (and subtly more sterically encumbered) hydrocarbon chains (Table 2-4, below in section 2.3.2). TMOS (**2.09**) was found to hydrolyze too rapidly ($t_{1/2}$ < 1.5 min) under the described conditions to be measured accurately.[29] However, analysis of the k_{obs} values for the remaining models **2.07** and **2.11-2.13** shows incrementally smaller changes as two additional methylene units were systematically added to the linear hydrocarbon backbone (see Table 2-4). In other words, the data suggests an approaching "plateau effect" of the observed hydrolysis rate as the length of the aliphatic chains progressively increases, consistent with minimal variation of the steric environment at the central silicon atom. The acquisition of data is eventually limited by the solubility of the silicate esters. For instance, attempts to observe the hydrolysis of **2.14** failed due to the compound's insolubility (even in solvent mixtures containing as little as 1 vol% water).

Both chemical intuition and qualitative observations confirm the vast difference in hydrophobicity of the models. For example, **2.07** is a water-soluble

compound while **2.13** is minimally soluble in co-solvent mixtures of acetone:water (10:1 , v/v). On the other hand, quantification[34] of such values [the log partition coefficient (log P) value] is often not rigorously established. Instead, such values are commonly approximated via computation of the calculated log partition coefficient (clog P) by one of a myriad of different software tools. One option that has been used in pharmaceutics[35,36] is the ALOGPS 2.1 program.[37] Using this free online software,[38] clog P values of **2.07** and **2.13** were calculated to be 2.67 and 9.85, respectively – thereby suggesting a difference of greater than seven orders of magnitude in their respective solubilities. It is important to note that these numbers are not meant to be taken as precise measurements; rather, they are reported here simply to confirm that the hydrophobicity of these compounds differ by several orders of magnitude whereas their relative rates of hydrolysis differ by less than a factor of 10. Overall, the described models support the ability to make significant changes in the hydrophobicity of the silicate prodrugs while minimally altering their hydrolysis rate.

2. Slowing the Hydrolysis Rate: Branched Tetraalkoxy Silicates. With preliminary evidence of our ability to control hydrophobicity in hand attention turned to the ability to control the hydrolysis rate. The most obvious solution to

---

[34] Experiment quantification of these differences is historically performed by measuring the equilibrium solubility of a compound in a mixture of water and *n*-octanol and applying the measured concentrations to equation the following equation: log P = [solute$_{octanol}$]/[solute$_{water}$]. A larger log P (or clog P) value is indicative of a more hydrophobic compound. For a comprehensive review of the history and theory, see: Leo, A.; Hansch, C.; Elkins, D. Partition Coefficients and Their Uses. *Chem. Rev.* **1971**, *71*, 525–616 and references cited therein.

[35] Tetko, I. V.; Poda, G. I. Application of ALOGPS 2.1 to Predict log D Distribution Coefficient for Pfizer Proprietary Compounds. *J. Med. Chem*. **2004**, *47*, 5601–5604

[36] Tetko, I. V.; Bruneau, P. Application of ALOGPS to Predict 1-Octanol/Water Distribution Coefficients, logP, and logD, of AstraZeneca In-House Database. *J. Pharm. Sci*. **2004**, *93*, 3103–10.

[37] Tetko, I. V., Tanchuk, V. Y. Application of Associative Neural Networks for Prediction of Lipophilicity in ALOGPS 2.1 Program. *J. Chem. Inf. Comput. Sci.* **2002**, *42*, 1136–1145.

[38] http://www.vcclab.org/lab/alogps/ accessed June 19, 2012.

slow the rate of hydrolysis of the silicate models was to simply increase the steric bulk of the substituents at the central silicon atom.[39,40] Predictably, hydrolysis of the commercially purchased tetra-*i*-propyl orthosilicate (TIPOS, **2.15**) resulted in a significantly slower rate than was observed with the linear silicates (ca. 20-fold slower as compared to **2.07**) – a value consistent with (but not identical to) those previously reported for alpha-branched tetraalkoxysilanes.[22]

Further attempts to analyze the hydrolysis of yet more sterically hindered, symmetrical compounds such as a tetramenthoxy orthosilicate (**2.17**)[41] or a tetra-*t*-butyl orthosilicate (**2.18**) failed. Model **2.17** was successfully synthesized from menthol (2.16) and $SiCl_4$ (Scheme 2-3) and purified, but **2.17** was found to be insoluble in a D_2O:d_6-acetone (1:10, v/v) solution, thus preventing analysis of its k_{obs}. **2.18** is not readily available from commercial sources, and its synthesis is known to result in incomplete substitution of the *tert*-butanol unless silicon fluorides are used, preventing convenient access to the model compound.[42,43]

[39] Clausen, R. P.; Bols, M. The First Tri- and Tetraalkoxysilanes with Four Different Substituents. *J. Org. Chem.* **1997**, *62*, 4457–4464.

[40] Pedlow, G. W., Jr.; Miner, C. S., Jr. Organic Orthosilicates Stable Against Hydrolysis. U.S. Patent 2,566,365, June 15, 1946.

[41] Beckmann, J.; Dakternieks, D.; Tiekink, E. R. T. Chiral Trialkoxysilanols Derived from Terpene Alchols. Molecular Structures of Tris([(1*S*)-*endo*-]-(–)-bornoxy)silanols and tetrakis((–)-menthoxy)silane. *J. Organomet. Chem.* **2002**, *648*, 188–192.

[42] Miner, C. S., Jr.; Bryan, L. A.; Holysz, R. P.; Pedlow, G. W., Jr. *Ind. Eng. Chem.* Tert-Alkoxyaminosilanes. **1947**, *39*, 1368.

[43] Hyde, J. F.; Curry, J. W. The Preparation of Tetra-*i*-butoxysilane and Tri-*t*-butoxyfluorosilane. *J. Am. Chem. Soc.* **1955**, *77*, 3140–3141.

Scheme 2-3. The synthetic efforts toward highly sterically hindered tetraalkoxysilane models **2.17** and **2.18**.

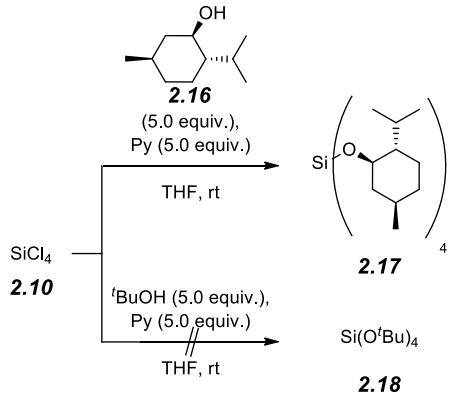

All hydrolysis results for the symmetrical tetraalkoxy silicate ester models are summarized in Table 2-4.

Table 2-4. The observed kinetic data for symmetrical, tetraalkoxysilanes with k_{rel} referenced to TEOS as $k_{rel} = 1$.

Model	R	$t_{1/2}$ (min)	k_{obs} (10^{-3} s^{-1})	k_{rel} [a]
2.09	Methyl	-	> 10	>2
2.07	Ethyl	3.1 ± 0.1	3.7 ± 0.2	1.0 ± 0.05
2.11	*n*-Butyl	12 ± 1	0.94 ± 0.07	0.25 ± 0.02
2.12	*n*-Hexyl	17 ± 1	0.69 ± 0.02	0.19 ± 0.01
2.13	*n*-Octyl	21 ± 1	0.55 ± 0.02	0.15 ± 0.01
2.14 [b]	Phytyl	n.d. [c]	n.d.	n.d.
2.15	*i*-Propyl	81 ± 2	0.15 ± 0.01	0.039 ± 0.002
2.17 [b]	Menthyl	n.d.	n.d.	n.d.
2.18 [d]	*t*-Butyl	n.d.	n.d.	n.d.

[a] $k_{rel} = 1.0$ for **2.07**, hydrolyzed in the 1:10 D_2O:d_6-acetone solution with 1 vol% TFA.
[b] The compound was insoluble in the 1:10 D_2O:d_6-acetone solution.
[c] n.d. = not determined
[d] The synthesis was not readily attainable.

3. Rate Determining Step of the Hydrolytic Cleavage. Throughout these beginning studies, the observed hydrolysis rate was determined by comparative integration of ^{1}H NMR spectra during the *in situ* hydrolysis of the silicate models. This data was also utilized to provide insight to identify the rate determining step of the hydrolysis. Figure 2-3 provides representative ^{1}H NMR spectra taken during the hydrolysis of **2.15** to isopropanol **2.16** (Scheme 2-4) Resonances assigned to the diminishing orthosilicate methine (downfield, ◆) and incoming *i*-propanol (**2.20**) methine (upfield, ■) are obvious in Figure 2-3. it is equally important to note, however, the absence of any spectroscopically observed

intermediates (i.e., **2.19**). While intermediates of the form of **2.19** are undoubtedly formed *in situ*, the spectroscopic evidence verifies that they are rapidly consumed at a rate significantly faster than that of the starting material.

This key observation identifies the initial hydrolysis event as the slow, rate-limiting step. Thus, the four sequential hydrolysis steps may be considered as a "chink in the armor" scenario. In other words, the initial hydrolysis event drastically reduces the steric hindrance at the silicon atom, allowing the subsequent hydrolytic cleavages to proceed at an immeasurably fast rate under the described conditions. Importantly, this leads to a rational hypothesis for the development of more rapidly hydrolyzed prodrugs beyond simple sterics. Specifically, inclusion of a single, rapidly hydrolyzed substituent to a prodrug may potentially yield a clean yet more rapidly hydrolysable moiety while still allowing for control of the hydrophobic character (c.f., section 2.4.4 and 3.3.8).

Scheme 2-4. Hydrolysis of **2.15** and the structure of its presumably formed but unobserved (via spectroscopic analysis) intermediate(s) **2.19**.

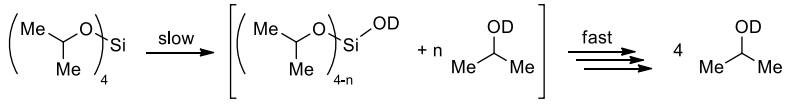

2.15 ***2.19*** ***2.20*** ***2.20***

NOT Observed

Figure 2-3. Selected, representative 1H NMR spectra taken during the hydrolysis of **2.15** (◆) to **2.20** (■). The displayed spectra are at (a) 0.2 half-lives (black, top), (b) 1.0 half-lives (blue, middle), and (c) 2.0 half-lives (red, bottom). For clarity, the black and blue spectra are offset from the scale by ca. 0.2 and 0.1 parts per million (ppm), respectively.

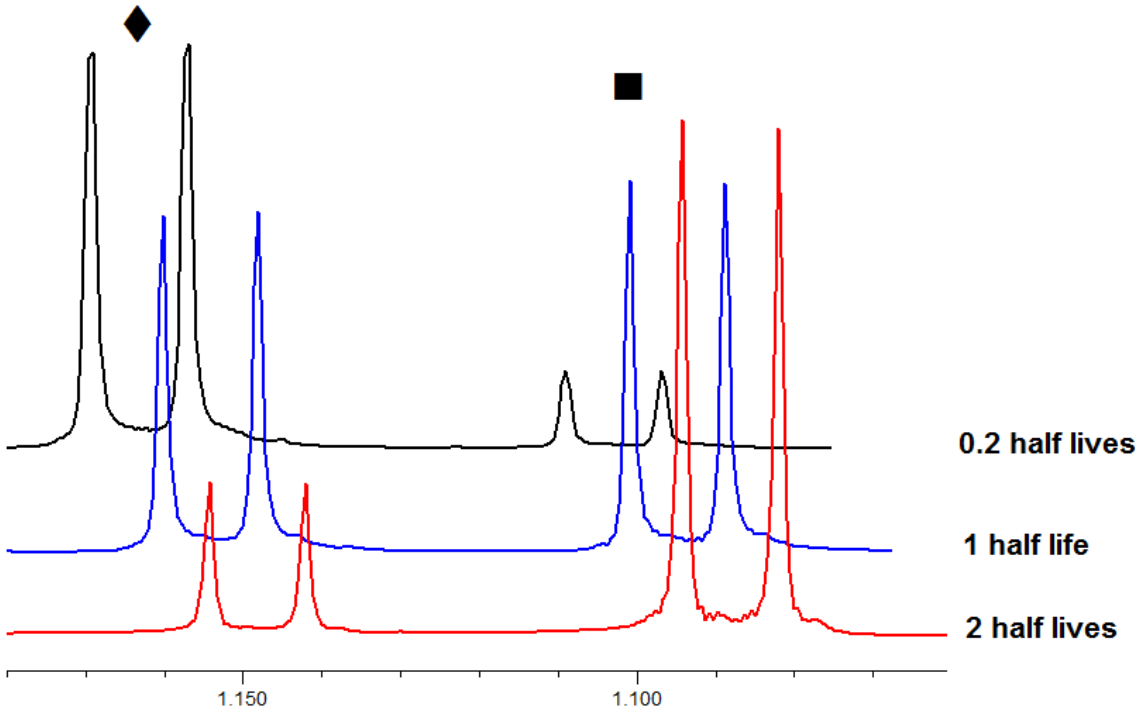

4. Symmetrical Tetraaryl Orthosilicates. In addition to the described tetraalkoxysilane models, tetraarylsilanes were also briefly explored with Dr. Yutaka Miura. His successful synthesis of the tetracresoxy silicate ester **2.23**[44] and tetra-2,4,6-trimethylphenoxy silicate ester **2.24**[45] (from their **2.21** and **2.22**, respectively, see Scheme 2-5)[29] led to hydrolysis studies of these compounds.

[44] Original synthesis performed by Dr. Yutaka Miura. ^{1}H NMR (500 MHz, $CDCl_3$): 7.01 (d, J = 7.0 Hz, 8H, Ar-*H*), 6.89 (d, J = 7.0 Hz, 8H, Ar-*H*), and 2.27 (s, 12H, *p*-C*H*$_3$). ^{13}C NMR (125 MHz, $CDCl_3$): δ = 150.6, 132.3, 130.2, 119.4, and 20.8.

[45] Original synthesis performed by Dr. Yutaka Miura. ^{1}H NMR (500 MHz, $CDCl_3$): δ = 6.76 (s, 8H, Ar-*H*), 2.18 (s, 12H, *p*-C*H*$_3$), and 2.16 (s, 24H, *o*-C*H*$_3$). ^{13}C NMR (125 MHz, $CDCl_3$): δ = 148.4, 131.9, 129.4, 128.4, 20.7, and 17.2.

Again, the increased steric bulk of **2.24** relative to **2.23** slowed the observed hydrolysis rate. Surprisingly, Dr. Miura reported a minimal difference in the measured k_{obs} when comparing the mild acetic acid catalyst with TFA.[29] This is in contrast to model compound **2.24** and, even more starkly, control experiments performed with **2.07** (c.f., section 2.2.3) that noted significantly different k_{obs} values based on acid strength. These experiments advance a strategy for the synthesis of more rapidly hydrolyzing orthosilicates. Namely, the inclusion of substituents that are better leaving groups (in this case, a phenoxy-like compound) may induce a more rapid initial hydrolytic cleavage as the rate-determining first step in the overall hydrolysis.

Scheme 2-5. The synthesis and hydrolysis of tetraaryl orthosilicate models **2.23** and **2.24**.

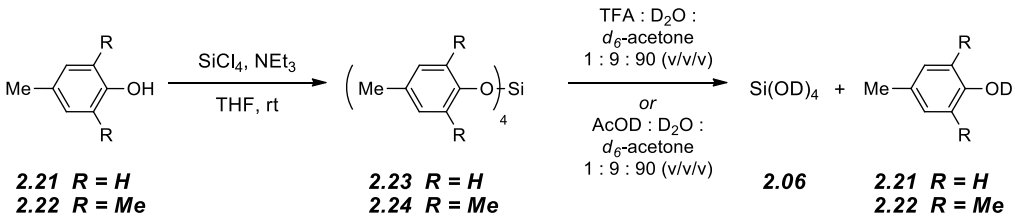

2.21 R = H ***2.22 R = Me*** ***2.23 R = H*** ***2.24 R = Me*** ***2.06*** ***2.21 R = H*** ***2.22 R = Me***

Table 2-5. The observed hydrolysis rate data for tetraaryl orthosilicate models.[a]

Model	Acid	$t_{1/2}$ (min) [b]	k_{obs} (10^{-3} s^{-1}) [b]
2.07	*TFA*	*3.1 ± 0.1*	*3.7 ± 0.2*
2.07	*AcOD*	*>24000*	*--*
2.23 [c]	TFA	6.0	1.9
2.23 [c]	AcOD	10	1.2
2.24	TFA	64	0.18
2.24	AcOD	1300	0.0010

[a] Entries in italics and gray are reproduced from Table 2-2 for convenience.
[b] k_{obs} and $t_{1/2}$ values were not run in triplicate and thus error bars are not included.
[c] Hydrolysis experiments performed by Dr. Yutaka Miura.[29]

4. Observed Hydrolysis Rates of Unsymmetrical, Tetraalkoxy Silicate Esters.

1. Mixed Menthoxy Trialkoxy Silicate Esters. After completing our initial studies, more advanced, mixed model systems were considered to model a silicate ester containing a drug moiety. Considerably fewer examples of such unsymmetrical compounds [e.g., $Si(OR^1)_3(OR^2)$] exist vis-à-vis the number of reports of symmetrical orthosilicates [e.g., $Si(OR^1)_4$]. Yet fewer of these unsymmetrical silicate ester compounds describe product purification via a methodology other than distillation[39] – a requirement for the successful implementation of silicate prodrugs. Therefore, further expansion of the model systems was needed to explore both potential purification strategies and study

the degree to which the relative hydrolysis rates could be controlled by the sacrificial alkoxy substituents. Thus, incorporation of menthol (**2.16**) as an alkoxy, drug-like substituent along with three alkoxy substituents was employed to generate a suite of models (**2.25**-**2.28**) with varying aliphatic character and steric bulk. These compounds are easily synthesized by silylation with a trialkoxychlorosilane and purified by standard silica chromatography via medium pressure liquid chromatography (MPLC). The pure compounds were then subjected to the aforementioned hydrolysis conditions (see Scheme 2-6).

Scheme 2-6. The synthesis of a suite of menthol-containing silicate esters **2.25-2.28** and hydrolysis of these menthoxytrialkoxy silicate ester models.

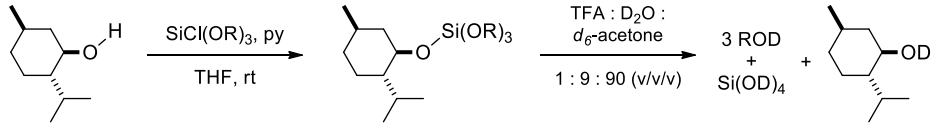

2.16

2.25 R = Et
2.26 R = ^{n}Bu
2.27 R = ^{n}Oct
2.28 R = ^{i}Pr

2.06 ***2.16***

We observed that the previously established trends defined in the symmetrical models **2.07**, **2.11**-**2.13** were generally reproduced. Nonetheless, the absolute rate of hydrolysis was slower, likely owing to the increased steric bulk originating from the inclusion of the menthoxy substituent. Again, these model systems are designed to deduce the *trends* of the hydrolysis rates, and so such differentiation in the absolute rate is not critical.

The trends in these new menthol-containing models are more instructive and detailed in Table 2-6. Specifically, the menthoxytriethoxy silicate ester **2.25** was found to hydrolyze more than five times slower than the tetraethoxysilane **2.07**. Conversely, the menthoxytri-*i*-propoxy silicate **2.25** hydrolyzed only three times more slowly than the TIPOS **2.12**. This likely reflects the similarity in the steric nature of the *i*-propoxy and menthoxy substituents. (i.e., the sterics of an *i*-

propoxy substituent is more similar to menthol than is an ethoxy substituent). Nonetheless, these menthol-based models demonstrate a consistently decreasing hydrolysis rate similar to those observed in the symmetrical orthosilicate models. The similarity of the trends is more pronounced when models **2.25-2.28** are referenced (k_{rel}') to **2.25** rather than **2.07** (Table 2-6). In the case when the menthoxy silicate esters are compared to a more relevant "parent" compound, the trends yet more closely resemble those reported earlier in Table 2-4.

Table 2-6. The observed hydrolysis rates and half-lives for menthoxytrialkoxysilane models **2.25-2.28**.[a]

Prodrug	R	$t_{1/2}$ (min)	k_{obs} (10^{-3} s^{-1})	k_{rel} [b]	k_{rel}' [c]
2.07	*Ethyl*	*3.1 ± 0.1*	*3.7 ± 0.2*	*1.0 ± 0.05*	*N/A*
2.22	Ethyl	17 ± 1	0.67 ± 0.04	0.18 ± 0.01	**1.0 ± 0.06**
2.23	*n*-Butyl	49 ± 2	0.24 ± 0.01	0.065 ± 0.003	**0.36 ± 0.02**
2.24	*n*-Octyl	79 ± 5	0.15 ± 0.01	0.040 ± 0.003	**0.22 ± 0.01**
2.25	*i*-Propyl	210 ± 10	0.056 ± 0.01	0.015 ± 0.001	**0.084 ± 0.004**

[a] Entries in italics and gray are reproduced from Table 2-4 for convenience.
[b] k_{rel} values are referenced to compound **2.07**, k_{rel} = 1.0.
[c] k_{rel}' values are referenced to compound **2.25** , k_{rel}' = 1.0.

2. A Mixed Triethyl Cresol Orthosilicate. In addition to the mixed alkoxy silicate models **2.25-2.28**, a mixed cresol triethyl silicate ester **2.30** was synthesized from cresol **2.29** (see Scheme 2-7). Interest in this compound was motivated by the unusually fast reported rate of hydrolysis during catalysis by a weak acid of **2.23**.[29] Comparing the hydrolysis of **2.30** when catalyzed by acetic acid vis-à-vis TFA again showed a pronounced difference in the observed rates.

Interestingly, the absolute magnitude of these rates were found to be of an intermediate value between the rates observed in TEOS **2.07** and the tetracresoxy silicate ester **2.23** (Table 2-7). This result is suggestive of a silicate ester that exhibits an intermediate number of more labile substituents.

Scheme 2-7. The synthesis of a cresol-containing silicate ester (**2.30**) and its subsequent hydrolysis.

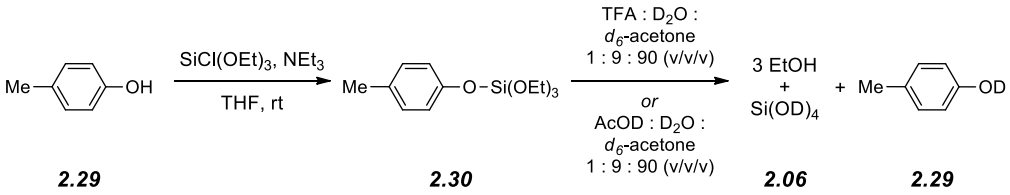

2.29 ***2.30*** ***2.06*** ***2.29***

Table 2-7. Comparison of the observed hydrolysis rate data for **2.30** with TEOS **2.07** and tetraaryloxysilane **2.23.**[a]

Prodrug	Acid	$t_{1/2}$ (min) [b]	k_{obs} (10^{-3} s^{-1}) [b]
2.07	*TFA*	*3.1 ± 0.1*	*3.7 ± 0.2*
2.07	*AcOD*	*>24000*	*--*
2.23 [c]	*TFA*	*6.0*	*1.9*
2.23 [c]	*AcOD*	*10*	*1.2*
2.26	TFA	9.1	1.3
2.26	AcOD	7100	0.0016

[a] Entries in italics and gray are reproduced from Table 2-4 and 2-6 for convenience.

[b] k_{rel} and $t_{1/2}$ values were not run in triplicate and thus error bars are not included.

[c] Hydrolysis experiments performed by Dr. Yutaka Miura.[29]

3. Steroid-Containing Silicate Esters. While estradiol (**2.31**) and hydrocortisone (**2.33**) are not targeted as final prodrug candidates, these two steroidal compounds served as yet more complex and instructive model systems in the development of the silicate ester prodrugs. The trivial silylation of **2.31** with triethoxychlorosilane (Scheme 2-8) yields the bis-triethoxy silicate ester prodrug of estradiol (**2.32**). Similar treatment of **2.33** exclusively gives the *mono*-triethoxy silicate prodrug of hydrocortisone (**2.34**). Notably, even in the presence of up to four equivalents of both the trialkoxychlorosilane and amine base, silylation was not observed at the C11 or C17 hydroxyl. Presumably the increased steric bulk of the hydroxyl groups at these positions severely retards the rate of substitution.

Scheme 2-8. The application of the silicate ester prodrug strategy to synthesize estradiol and hydrocortisone silicate ester prodrugs.

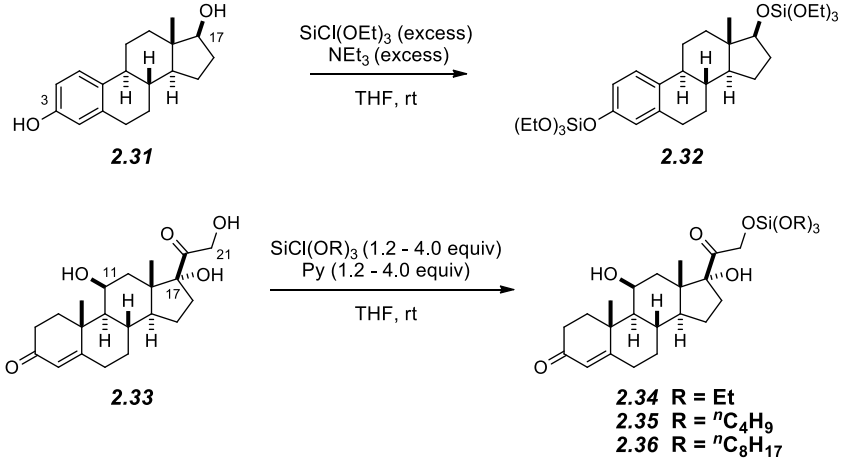

Steroid models **2.32** and **2.34-2.36** present an opportunity to address an outstanding question: will the three sacrificial alkoxy substituents dictate the rate of hydrolysis in different steric and electronic environments? Three different environments are tested in these steroids: an electron-rich aryl hydroxyl (C3 in **2.32**), a sterically hindered, neo-pentyl hydroxyl (C17 in **2.32**), and a sterically accessible hydroxyl (C21 in **2.34-2.36**).

Gratifyingly, the local environment of the silicate ester was found to play only a minor (yet observable) role in the hydrolysis rate [catalyzed by TFA in a co-solvent mixture of 10:1 d_6-acetone:D_2O (v/v) — the "standard hydrolysis" conditions]. Despite the vastly different steric and electronic environments of the prodrug silicates, the observed relative hydrolysis rate varied by less than one order of magnitude from the TEOS model **2.07** (Table 2-8). Specifically, the C17 silicate ester of **2.32** varied by a factor of only four from the TEOS model, despite extreme differences in the steric nature of the fourth substituent – a neo-pentyl hydroxyl in **2.32** vs. an ethoxy in TEOS. Yet more encouraging, the observed hydrolysis rates of **2.32** and the triethoxy cresoxy silicate ester model **2.30** were found to be the same within error. Thus, the dominant influence on the observed hydrolysis rate was the three sacrificial ethoxy groups rather than the single drug-like substrate, and the estradiol silicate prodrug model **2.32** hydrolyzed at rates consistent with previous model systems.

A small series of hydrocortisone silicates of varying aliphatic character were also analyzed. Comparing the hydrolysis rate of the triethoxy hydrocortisone silicate ester (**2.34**) to model compound **2.07** (both silicate esters contained four linear, alkoxy substituents), the observed hydrolysis rates were found to be the same within error (Table 2-8). This further validation of the model system strategy was found to be particularly encouraging – the extensive amount of experimental effort that comprises sections 2.2 and 2.3 was not wasted!

Linear hydrocortisone analogs of the tri-*n*-butoxy (**2.35**) and tri-*n*-octyloxy (**2.36**) silicate esters were also synthesized and hydrolyzed. As observed in the symmetrical silicate ester models, the change in the observed hydrolysis rate was less than one order of magnitude among hydrocortisone prodrugs **2.34-2.36** despite drastically different hydrophobicities. Although the trends do not match precisely to the symmetrical silicate models, this is in fact encouraging – even

less variation was observed in the k_{obs} of between the extremes of the hydrophobic character in the hydrocortisone prodrugs (**2.34** and **2.36**).

Table 2-8. The observed hydrolysis rate data for the estradiol orthosilicate **2.32** and the hydrocortisone orthosilicates **2.34-2.36**. [a]

Prodrug	$t_{1/2}$ (min)	k_{obs} (10^{-3} s^{-1})	k_{rel}
2.07	*3.1 ± 0.1*	*3.7 ± 0.2*	*1.0 ± 0.05*
2.32 (C3)	9.5 ± 0.5	1.3 ± 0.1	0.35 ± 0.02
2.32 (C17)	14 ± 1	0.92 ± 0.04	0.25 ± 0.02
2.34	3.4 ± 0.1	3.4 ± 0.1	0.92 ± 0.03
2.35 [b]	5.0	2.3	0.62
2.36 [b]	7.8	0.15	0.40

[a] Entries in italics and gray are reproduced from Table 2-4 for convenience.
[b] k_{rel} and $t_{1/2}$ values were not run in triplicate and thus error bars are not included.

4. Controlling the Hydrolysis Rate: Acyloxy Silicate Esters. At this point, two of the basic tenets of the novel silicate ester prodrug strategy were on solid experimental ground. Our ability to control the hydrophobic character of the silicate esters largely independent of the hydrolysis rate and the ability to control the rate of hydrolysis through the three sacrificial alkoxy groups had been established. Efforts therefore turned toward the identification of prodrugs with an increasingly fast hydrolysis rate. Previous studies were conducted by Dr. Yutaka Miura. He developed a series of silanes of progressively minimized steric bulk by synthesizing mixed species **2.37-2.41** (Figure 2-4). He confirmed the expected outcome: namely, the inclusion of progressively less bulky alky and/or hydro substituent(s) sped the rate of hydrolysis.[13]

Figure 2-4. The hydrolysis rate trend of menthoxy-based silanes **2.37-2.41** of varying steric bulk as established by Dr. Yutaka Miura. [13,29]

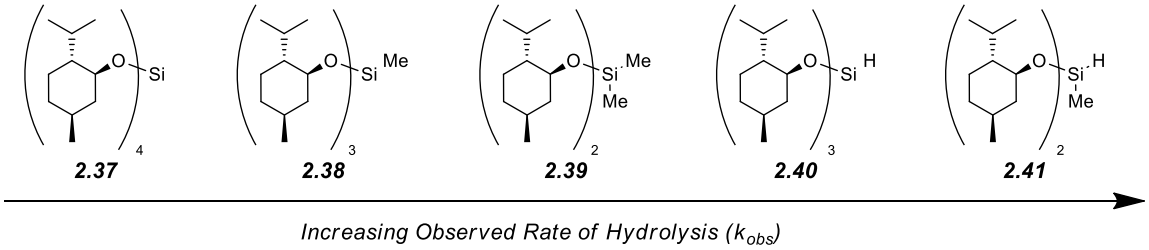

However, the biocompatibility of the byproducts of hydrolysis [e.g., $Si(OH)_{4-n}(R)_n$, where R=alkyl] was doubtful. This, in turn, led to concerns regarding prodrug approval by the FDA in the final drug delivery application. These concerns centered largely on the established toxicity of silanes (especially when inhaled)[46] and the unknown biological consequences arising from the ease of oxidation of such silanes and silanols in the presence of water.[47]

Hesitant to incorporate a potentially insurmountable barrier into the drug delivery strategy, a strategy to speed the hydrolysis of silicate prodrugs would necessitate looking beyond simple steric effects. Building on our previous work (see section 2.3.3) that established the rate-limiting step of the silicate ester hydrolysis as the first Si-O bond cleavage, we hypothesized that incorporation of a single, labile substituent would lead to a more rapid, complete hydrolysis. It is established in the case of mixed organosilicon substrates that better leaving groups would lead to more rapid hydrolysis that is, in our case, desirable.[48] However, incorporation of better leaving groups is a "double-edged sword."

[46] Takebayashi, T. Acute Inhilation Toxicity of High Concentrations of Silane in Male ICR Mice. *Arch. Toxicol.* **1993**, *67*, 55–60.

[47] Anglin, E. J.; Cheng, L.; Freeman, W. R.; Sailor, M. J. Porous Silicon in Drug Delivery Devices and Materials. *Adv. Drug Deliver. Rev.* **2008**, *60*, 1266–1277.

[48] Corriu, R. J. P.; Henner, B. J. L. Mechanism of Nucleophilic Substitution at Silicon: Kinetic Evidence on the Slow Formation of a Penta-Coordinate Silicon Intermediate. *J. Organomet. Chem.* **1975**, *102*, 407–416.

These faster-hydrolyzing prodrugs may be exceptionally sensitive to purification via MPLC silica chromatography and significantly more difficult to isolate.

Reports of tetraacetoxy[49] and mixed acyloxy silicates[50] (and particularly their reported labilities) provided inspiration to assess yet more labile silicate models. These compounds were typically synthesized via an exchange reaction of a tetraalkyl orthosilicate with an anhydride[11,51] followed by distillation to access the pure material. Unfortunately, isolation of high molecular weight prodrugs via distillation is likely unattainable. Therefore, the first step toward applying these concepts to our silicate ester strategy was to determine the practicality of other means of purification.

Previous syntheses of acetoxytriethoxysilane (**2.42**) via a substituent exchange between **2.07** and acetic anhydride under harsh conditions (e.g., prolonged heating up to 180 °C) have led to low yields (e.g., 9%).[52] Thus, we altered the reaction conditions by treating triethoxychlorosilane with an excess of acetic acid and pyridine (despite literature that suggests such reactions fail to proceed cleanly to full conversion).[11] Nonetheless, analysis of the crude ^{1}H NMR and GC/MS data provided ample evidence of at least partial conversion.[53] This allowed attempts to purify **2.42** by eluting the crude mixture through silica gel. However, passing **2.42** through as little as a one inch plug of silica in a Pasteur pipet resulted in extensive (near quantitative) decomposition. Likewise, utilization

[49] Friedel, C.; Ladenburg, A. *Liebigs Annalen der Chemie,* **1868**, *145,* 174–178.

[50] Schuyten, H. A.; Weaver, J. W.; Reid, J. D. Preparation of Substituted Acetoxy Silanes. *J. Am. Chem. Soc.* **1947**, *69*, 2110–2112.

[51] Kopylov, V. M.; Kireev, V. V.; Ivanov, V. V.; Astaf'ev, G. Y.; Kozlov, Y. V. Reaction of Acetoxysilanes with Hydroxy Compounds. *Rus. J. Gen. Chem.* **2001**, *71*, 1924–1928.

[52] Roth, M. J.; Brook, M. A.; Penny, H. B. Hydrosilane Cleavage Reactions Accelerated by Tartaric Acid and Dimethyl Sulphoxide. *J. Organomet. Chem.* **1996**, *521*, 65–74.

[53] Crude ^{1}H NMR data for **2.38** (500 MHz, $CDCl_3$): δ = 3.94 [q, J = 7.1 Hz, 6H, $Si(OCH_2CH_3)_3$], 2.13 [s, 3H, $SiOC(O)CH_3$], and 1.25 [t, J = 7.1 Hz, 6H, $Si(OCH_2CH_3)_3$]. GC/MS: (Method: 50°C, hold for two min; ramp at 20°C/min for 10 min, hold at 250°C for three min) t_R = 5.48 min; *m/z* 222 (5, M^+), 177 (100, M^+ - OEt), and 135 (20).

of salicylic acid **2.43** to synthesize the cyclic organosilane **2.44** succeeded[54] (as previously reported[55]), but decomposition was again observed upon subjecting the crude material to silica chromatography. In contrast to these results, the synthesis of the exceedingly hindered tri-*t*-butoxyacetoxysilane **2.46** [from the commercially available tri-*t*-butoxysilanol (**2.45**), see Scheme 2-9] was synthesized via treatment with acetic anhydride and 4-dimethylaminopyridine (DMAP). These conditions led to greater than 90% conversion to **2.46**. Yet more importantly, **2.46** was isolable by MPLC purification.

Scheme 2-9. Attempts toward the synthesis of labile acyloxy silicate esters.

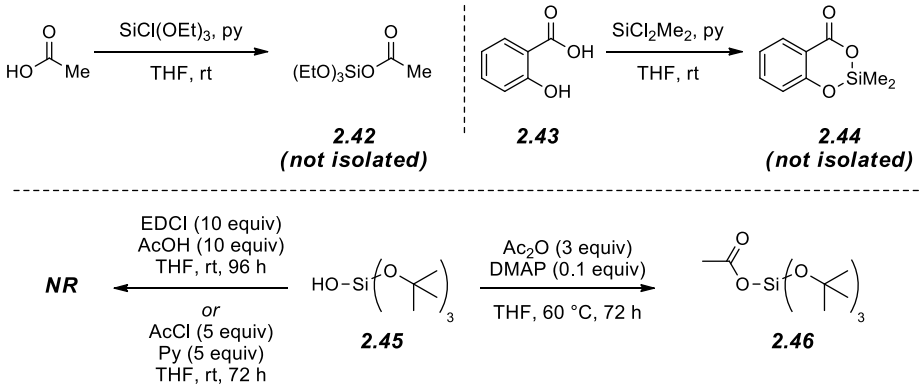

From these preliminary results, it was clear that added steric bulk would be crucial in the development of a new series of chromatographable silicate esters that incorporate a labile acyloxy. Menthol (**2.16**) was utilized as a bulky, secondary alcohol toward this end.[39] A series of trimenthoxysilanes was initially synthesized by a one-pot method in which the trimenthoxychlorosilane **2.47** was not isolated.[41] Yields were seemingly improved by a two pot procedure in which a

[54] Crude ^{1}H NMR data (500 MHz, $CDCl_3$) showed a complex mixture of > 4 different products. Crude GC/MS for **2.40**: (Method: 50°C, hold for two min; ramp at 20°C/min for 11 min, hold at 270°C for three min) t_R = 7.90 min; *m/z* 194 (60, M^+), 179 (50, M^+ - Me), 135 (100), and 91 (10).

[55] Cragg, R. H.; Lane, R. D. Contributios to Group IV Organometallic Chemistry IV. Preparation and Properties of Some Organosilicon Derivatives of Salicylic and Related Acids. *J. Organomet. Chem.* **1981**, *212*, 301–310.

crude sample of **2.47** was subjected to further substitution with the desired carboxylic acid to synthesize either **2.49** or **2.50** (Scheme 2-10). Typical yields for these compounds were ca. 50-60% after purification by MPLC and were likely suppressed due to the instability of the acyloxysilane during exposure to silica gel. Finally, the mixed ethoxytrimenthoxysilane **2.48** was also synthesized, and its observed hydrolysis rate served as an accurate comparison of tetraalkoxysilane vs. trialkoxyacyloxysilane.

Scheme 2-10. The synthesis of trimenthoxyethoxysilane **2.48** and trimenthoxyacyloxysilanes **2.49** and **2.50**.

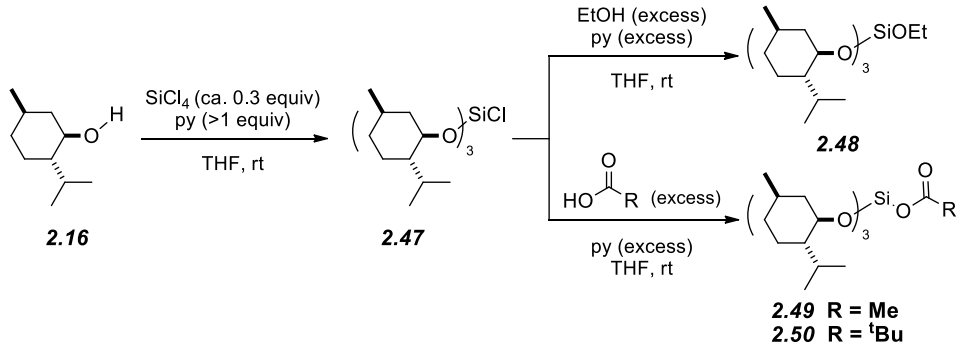

For this family of trimenthoxy models **2.48-2.50**, the "standard" hydrolysis conditions were ineffective; these highly hydrophobic compounds were insoluble in a solution containing 9 vol% water. Thus, a co-solvent system consisting of a 1:1:98 TFA:D_2O:d_6-acetone (v/v/v) solution was used to ensure complete dissolution of these trimenthoxysilane models. Since the S_N2 mechanism of these acid-catalyzed hydrolyses is medium-dependent,[24] the k_{rel} values reported in Table 2-9 have now been referenced to the hydrolysis of **2.07** in this modified co-solvent system. Notably, the absolute rate of hydrolysis was found to be slowed by ca. one order of magnitude in this modified co-solvent ratio.

Consistent with the previous sections (see section 2.3), increasing the steric bulk significantly slowed the observed hydrolysis rates of these menthol-

containing silicate esters. As anticipated, the added steric bulk of **2.48** caused a significant decrease in the observed hydrolysis rate (relative to that of **2.07**). Specifically, ethoxytrimenthoxysilane **2.48** was observed to hydrolyze 400-fold more slowly than **2.07**. Tetramenthoxysilane **2.17** (soluble in this modified co-solvent system) was also found to hydrolyze much more slowly – at least three orders of magnitude more slowly than **2.07.** (The hydrolysis experiment was discontinued after 400 h, by which point less than one half-life was completed.)

Incorporation of an acyloxy substituent to these trimenthoxysilanes resulted in much more readily hydrolyzed analogs than **2.17** and **2.48**. Specific observed rate enhancements include a five-fold faster hydrolysis rate of the pivaloxy-containing **2.50** as compared to **2.48**. This is notable because **2.50** is the more sterically-hindered silicate ester, yet the incorporation of the acyloxy moiety induces a more rapid hydrolysis. The acetoxy-containing silane **2.49**, meanwhile, magnifies this observation. **2.49** exhibited a hydrolysis rate that was > 1500 times faster than the sterically-similar model **2.48**. Furthermore, **2.49** hydrolyzed approximately four times faster than the significantly less encumbered tetraethoxysilane **2.07**. This observation, in particular, effectively highlights the optimism and potential surrounding acyloxysilanes as rapidly hydrolyzing promoieties.

Yet more sterically hindered trialkoxyacyloxysilanes were designed and synthesized to explore the extreme limits of steric hindrance vis-à-vis labile substituents in mixed alkyl/acyl silicate esters. Specifically, di-*t*-butoxydichlorosilane **2.51** was synthesized in the presence of excess *t*-butanol and pyridine. **2.51** could be easily distilled for future use. or utilized crude in a one pot procedure to synthesize species such as the di-*t*-butoxymenthoxychlorosilane **2.52**. Incredibly, **2.52** was (inadvertently) found to

be reasonably stable to purification via MPLC chromatography.[56]. Even when stored neat at room temperature in a vesicle that was not air-tight, **2.52** underwent minimal hydrolysis over the course of several weeks, further highlighting the excessive steric bulk of this compound. Nonetheless, **2.52** was found to remain reactive; dissolving **2.52** in bulk methanol in preparation of characterization via high resolution mass spectrometry (HRMS) resulted in rapid and quantitative conversion to the menthoxymethoxy-di-*t*-butoxysilane.

With a ready supply of pristine **2.52** in hand, a series of derivatization studies were conducted. As in the trimenthoxy series, a mixed tetraalkoxysilane, ethoxymenthoxy-di-*t*-butoxysilane, (**2.53**) was synthesized to serve as a comparable model to the acyloxy-containing silanes (Scheme 2-11).[56] The synthesis of menthoxy-di-*t*-butoxyacetoxysilane **2.54** and menthoxy-di-*t*-butoxypropionoxysilane **2.55** proceeded as expected (Scheme 2-11). However, attempts to synthesize analogous α-branched acyloxy silanes (e.g., **2.56** and **2.57**) failed despite prolonged reaction times and/or treatment with significant reagent excesses.[57]

[56] This work was done jointly with National Science Foundation (NSF)/Lando fellowship undergraduate student Paul Alperin.

[57] No evidence consistent with the synthesis of either **2.56** or **2.57** was observed via TLC, GC/MS, or crude ^{1}H NMR spectroscopy.

Scheme 2-11. The synthesis of menthoxy-di-*t*-butoxyethoxy **2.53** and menthoxy-di-*t*-butoxyacyloxy silicate esters **2.54** and **2.55**.

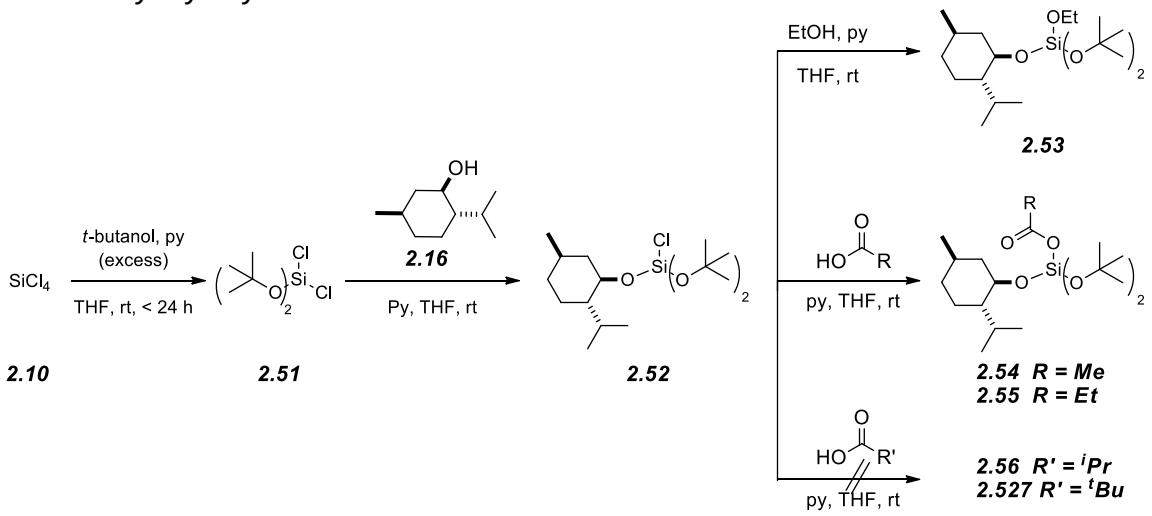

Again, the 1:1:98 TFA:D_2O:d_6-acetone (v/v/v) solution was necessarily employed for the kinetic hydrolysis experiments, thereby ensuring complete dissolution and accurate comparison with models **2.48-2.50**. Similar to **2.48**, the observed hydrolysis rate of **2.53** was exceedingly slow and, in this case, discontinued after > 400 h, prior to complete hydrolysis. Interestingly, the extreme steric bulk from the *t*-butoxy and menthoxy groups exemplified even minor differences in the hydrolysis rates of similar acyloxy silanes. While the acetoxy-containing silane **2.54** hydrolyzed on a reasonable time scale (albeit considerably slower than **2.49**), inclusion of a single methylene unit in the carboxylic acid tail of **2.55** significantly increased the half-life of the hydrolysis, again leading to the discontinuation of the study after greater than 400 h. Full results for all of these models are presented in Table 2-9.

Table 2-9. The observed kinetic data for all acyloxy-containing silicate esters **2.49-2.50** and **2.54-2.55** and comparison to their sterically hindered tetraalkoxysilane analogues **2.48** and **2.53**, respectively. [a]

Silane	R	$t_{1/2}$ (min)	k_{obs} (10^{-3} s^{-1})	k_{rel}', [a]
2.07	Ethyl	33 ± 1	0.35 ± 0.01	1 ± 0.03
2.17	Menthyl	> 24000	n.d. [b]	< 0.001
2.48	Ethyl	13000 ± 1000	0.00092 ± 0.00004	0.0025 ± 0.0002
2.49	$C(O)CH_3$	8.7 ± 0.6	1.3 ± 0.1	3.8 ± 0.3
2.50	$C(O)(CH_3)_3$	2400 ± 300	0.0048 ± 0.0001	0.014 ± 0.002
2.53	Ethyl	> 24000	n.d.	< 0.001
2.54	$C(O)CH_3$	5100 ± 200	0.0022 ± 0.0001	0.0065 ± 0.0003
2.55	$C(O)CH_2CH_3$	> 24000	n.d.	< 0.001

[a] k_{rel}' are referenced to TEOS **2.07** in a 1:98 D_2O:d_6-acetone solution.
[b] n.d. = not determined.

In addition to providing important, new information regarding the relative rates of hydrolysis of these highly hindered, acyloxy-containing models (**2.54** and **2.55**), these experiments also provided the first spectral evidence of a sufficiently long-lived hydrolysis intermediate. This unique intermediate (see Scheme 2-12) is hypothesized to be the menthoxy-di-*t*-butoxysilanol **2.58** based on the results of analogous work done on a related, paclitaxel-based system (see section 3.3.8) and a publication that describes the synthesis of a trimenthoxysilanol[41] and another that claims to identify of a silanol (although the lack of spectroscopic data presented makes it difficult to validate this claim).[58] However, no incontrovertible

[58] Theis, B.; Weib, J.; Lippert, W. P.; Bertermann, R.; Burschka, C.; Tacke, R. Zwitterionic and Anionic Multinuclear Pentacoordinate Silicon(IV) Complexes with Bridging (R,R)-Tartrato(4) Ligands and SiO_5 Skeletons: Synthesis and Reactivity in Aqueous Solution. *Chem. Eur. J.* **2012**, *18*, 2202–2206.

data was collected that indisputably corroborates this claim the structure of **2.58**. Regardless, the significant rate enhancement observed as a result of the inclusion of acyloxy substituents provides strong evidence to support our ability to accelerate silicate prodrug hydrolysis if it is deemed necessary in the prodrug work.

Scheme 2-12. The hydrolysis of labile di-t-butoxymenthoxysilanes.

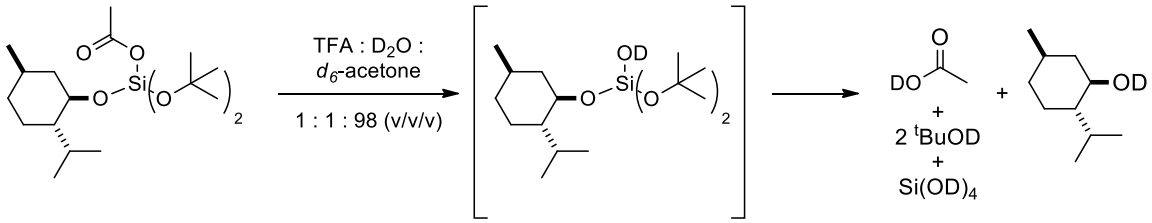

2.54 ***2.58*** ***2.06*** ***2.16***

5. Aminotrialkoxysilanes.

1. Introduction. Interest in developing mixed, cyclic aminoalkoxysilane prodrugs was prompted by compounds such as doxorubicin (Figure 2-5, **2.59**). Doxorubicin, a small molecule with chemotherapeutic properties, is currently administered after formulation in a pegylated liposome[59] – making it an attractive target for further prodrug loading optimization via synthesis of a silicate prodrug and subsequent FNP techniques. To undertake this task, pursuit of a novel class of cyclic aminoalkoxy silicate esters was necessary. General encouragement for such endeavors was found in the large number of 1,3,2-dioxasilolanes (81 examples found during a Reaxys® search) and 1,3,2-dioxasilinanes (96 examples found during a Reaxys® search). Interest in models for compounds

[59] Gabizon, A.; Shmeeda, H.; Barenholz, Y. Pharmacokinetics of Pegylated Liposomal Doxorubicin. *Clin. Pharmacokinet.* **2003**, *42*, 419–436.

such as **2.60** was further piqued by the lack of analogous nitrogen-containing examples, with only one characterized, tetravalent silicon compound reported.[60]

Figure 2-5. The structure of doxorubicin and a proposed aminotrialkoxysilanes prodrug.

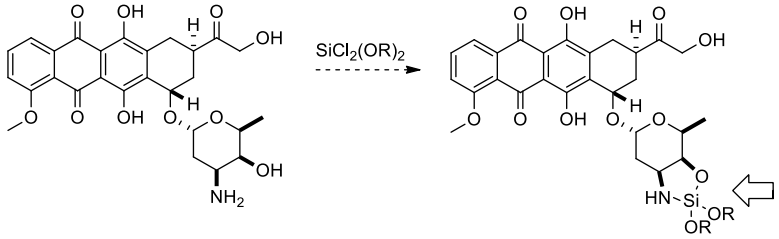

2.59 ***2.60 proposed prodrug***

2. Attempts to Synthesize Mixed Cyclic Aminoalkoxy Silicate Esters.

Again, design of a model system to determine the feasibility of prodrugs such as structure **2.60** was deemed especially crucial due to the limited literature precedent, as was the case for the phosphonic acid silicate esters. An obvious first reaction was the cyclization of racemic 1-aminopropan-2-ol (**2.61**). Anticipating lability in the uncommon Si-N bond,[61] di-*t*-butoxydichlorosilane was chosen as the first silylating agent in these initial experiments. Unfortunately, all attempts to synthesize the 1,3,2-azaoxsilolane (e.g., **2.64** in Scheme 2-13) failed despite repeated attempts to optimize reagent stoichiometry, molarity, and reaction time. In the presence of substoichiometric amounts of the dichlorosilane, the reaction proceeded to give a complex mixture of products,

[60] Diedrich, F.; Ebker, C.; Klingbiel, U.; Reiche, C.; Labahn, T.; Magull, J.; Noltemeyer, M. N,N-Bis(silyl)ethylenediamine und 1,3-Diaza-2-silacyclopentane – Synthese, Reaktionen, Strukturen. *Z. Naturforsch., B: Chem. Sci.* **2002**, *57*, 99–106.

[61] Wutz, P. G. M.; Greene, T. W. Protection for the Amino Group. In *Greene's Protective Groups in Organic Synthesis, Fourth Edition*. John Wiley & Sons, Inc: Hoboken, NJ, 2007.

including the tentatively assigned **2.63** (Scheme 2-13).[62] While crude GC/MS data from early time points were suggestive of the formation of intermediate **2.62**, none of the compounds observed via GC/MS analysis could be correlated with the five-membered, cyclized (and desired) product **2.64**.

Likewise, attempts to synthesize a 1,3,2-diazasilinanes (e.g., **2.67** in Scheme 2-14) from propane 1,3-diamine **2.65** resulted predominantly in the mono-substitution of the dichlorosilane to give **2.66**[63] (Scheme 2-13). In this case, evidence for the transient cyclized product **2.67**[64] was obtained, albeit in low quantities [< 10% of the area under the curve (AUC) in the GC/MS trace]. In an effort to illicit more complete conversion, the reaction times was prolonged, but **2.67** was not observed to any extent. Instead, a larger molecular weight peak (hypothesized to be an oligomeric compound) was observed, growing in intensity with the reaction progress.[65]

[62] Crude GC/MS data for **2.63** (Method: 30°C, hold for 1.5 min; ramp at 27°C/min for 13 min, hold at 300°C for 1.5 min) t_R = 11.75 min; *m/z* 249 (20 M^+ - O^{t}Bu), 192 {40, Si(O)[O(CH_3)$CHCH_2NH_2$]$_2$}, 175 (300), 136 {100, Si(OH)$_2$[O(CH_3)$CHCH_2NH_2$]$_2$}, 97 (20), and 57 (20).

[63] Crude GC/MS data for **2.66** (Method: 30°C, hold for two min; ramp at 20°C/min for 14 min, hold at 310°C for five min) t_R = 9.34 min; *m/z* 282 (<5, M^+), 267/269 (100, M^+ - Me), 211/213 (80), 169/171 (40), 155/157 (40), 97 (30), and 57 (20).

[64] Crude GC/MS data for **2.67** (Method: 50°C, hold for two min; ramp at 20°C/min for 10 min, hold at 250°C for three min) t_R = 9.34 min; *m/z* 246 (5), M^+), 231 (20, M^+ - Me), 173 (20, M^+ - O^{t}Bu), 133 (40), and 117 (100).

[65] Alternatively, attempts to synthesize 1,3,2-azaoxasilinanes by treating 3-amino-1-propanol with di-*t*-butoxydichlorosilane again led to a disappointing mixture of products in the GC/MS trace. None of the products could be reliably assigned as a cyclized, non-chlorinated substrate.

Scheme 2-13. Failed attempts to synthesize of cyclic aminotrialkoxysilanes.

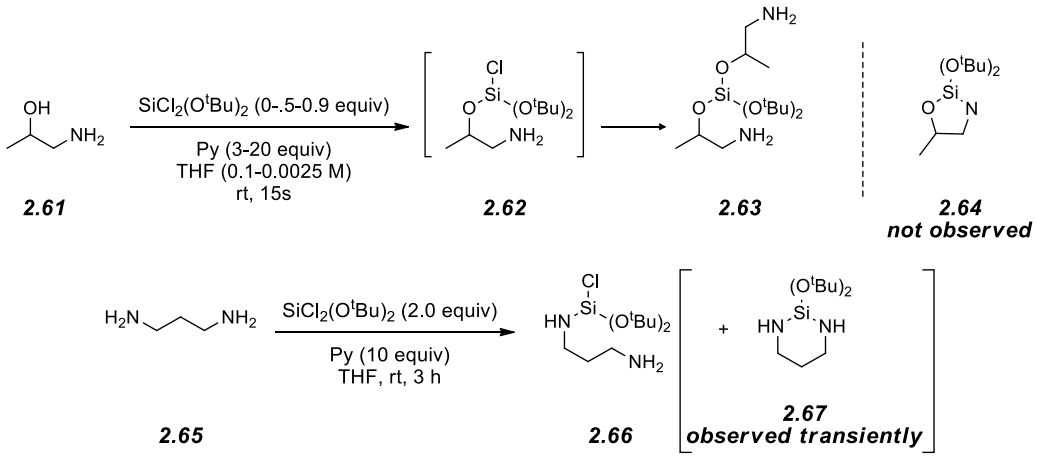

3. Control Experiments. Discouraged by these unsatisfying results, a series of controls were designed to elucidate the cause of the failed reactions in Scheme 2-14. First, to determine if the long silicon-heteroatom bonds in the potential product(s) was somehow untenable, di-*t*-butoxydichlorosilane was treated with ethylene glycol (**2.68**) and, in a separate reaction, 1,3-propanediol (**2.70**). The data obtained via GC/MS analysis of these reactions confirmed the synthesis of the five- and six-membered rings (**2.69**[66] and **2.71**,[67] respectively), as has been previously reported (Scheme 2-15).[40] Confident that established cyclic silicate ester chemistry was not only feasible but also achievable in my hands, the extreme steric bulk of the dichlorosilane was next hypothesized as the limiting factor.

[66] Crude GC/MS data for **2.68** (Method: Method: 30°C, hold for 1.5 min; ramp at 27°C/min for 13 min, hold at 300°C for 1.5 min) t_R = 9.07 min; *m/z* 219 (40, M^+ - Me) and 163 (100, M^+ - O^{t}Bu).

[67] Crude GC/MS data for **2.70** (Method: 50°C, hold for two min; ramp at 20°C/min for 10 min, hold at 250°C for three min) t_R = 5.05 min; *m/z* 233 (40, M^+ - Me), 177 (100), and 119 (20).

Scheme 2-14. The first generation of control experiments: synthesis of cyclic tetraalkoxysilanes.

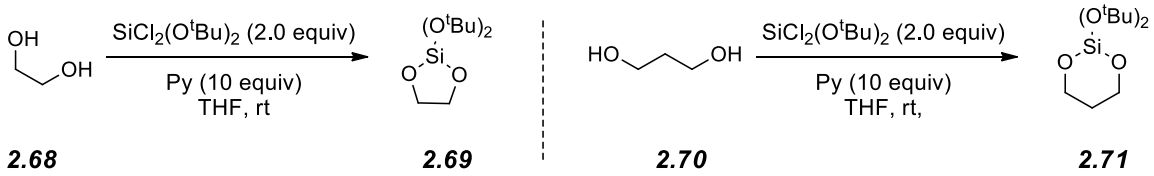

2.68 ***2.69*** ***2.70*** ***2.71***

To fully eliminate the steric congestion induced by the *t*-butoxy substituents as the reason for the lack of observed cyclization, sterically constrained aminotrialkoxysilane model systems were designed as further control experiments. These systems were analogous to the previous (single) report of dimethylaminotri-*t*-butoxysilane that was obtained pure upon distillation.[68] Specifically, in the control experiments reported here, benzylamino-*i*-propoxy-di-*t*-butoxysilane (**2.73**) and benzylamino-tri-*t*-butoxysilane (**2.72**) were envisioned. Analysis of GC/MS data during both experiments confirmed the synthesis of **2.73**[69] and **2.72**, respectively (Scheme 2-15). This result, coupled with the synthesis of **2.69** and **2.71**, firmly established that steric congestion is not the cause of the failed reactions described in Scheme 2-13.

[68] Ismail, V. R. M. Herstellung von Tertiarbutoxy-(halogenphenoxy)-silanen. XIV. *Z. anorg. allg. Chem.* **1969**, *371,* 23–31.

[69] Crude GC/MS data for **2.73** (Method: Method: 30°C, hold for 1.5 min; ramp at 27°C/min for 13 min, hold at 300°C for 1.5 min) t_R = 12.46 min; *m/z* 339 (40, M^+), 324 (50, M^+ - Me), 282 (100, M^+ - ^{t}Bu), 268 (20), 226 (60), 184 (30), 139 (30), and 91 (20, Bn^+).

Scheme 2-15. Second generation of control experiments: synthesis of sterically encumbered (di)aminoalkoxysilanes.

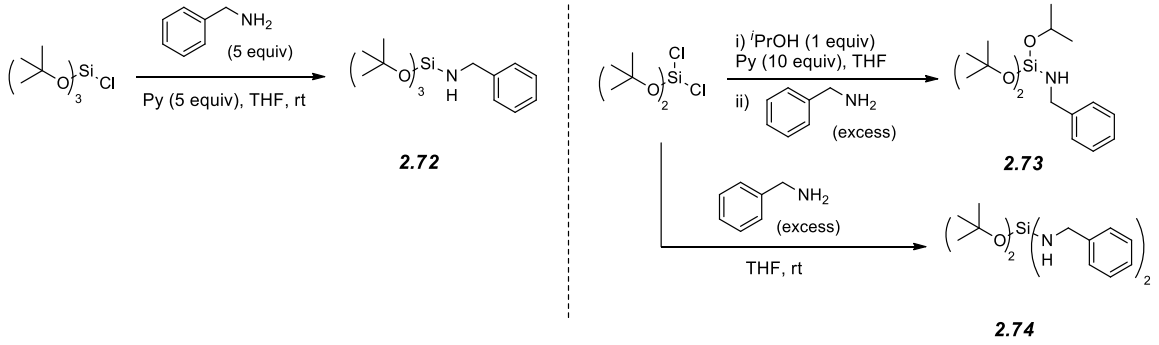

Two final tests were designed to lend guidance to the stability of the potential aminosilane products. First, the stability of **2.72** was tested by subjecting it to purification via MPLC. Compound **2.72** was isolated in low yields from the chromatographic experiment, and resubjecting the pure compound to a short silica plug returned ca. 97% of the submitted material. Second, the presumably more labile bis(benzylamino)di-*t*-butoxysilane (**2.74**) was designed, synthesized, and successfully filtered through a silica plug (Scheme 2-16).[70] Stability of both of these compounds to silica gel is unusual compared to other amino-silicate esters that are typically used crude or purified by distillation. These results, (namely, the observation of a presumably more labile aminosilane species such as **2.74**) suggest that, if cyclic compounds such as **2.64** and **2.67** were the primary product of their respective reactions, they would be observed.

Taken as a whole, the above results further suggest that neither extreme lability nor steric hindrance is the likely source of the undesired outcomes in Scheme 2-14. Further experimentation with, for example, a di-*i*-

[70] Crude GC/MS data for **2.73** (Method: 50°C, hold for two min; ramp at 20°C/min for 10 min, hold at 250°C for three min) t_R = 5.05 min; *m/z* 386 (20, M^+), 371 (10, M^+ - Me), 329 (20, M^+ - ^{t}Bu), 313 (5, M^+ - O^{t}Bu), 295 (80, M^+ - Bn), 273 (30), 257 (10), 239 (40), 183 (100), 168 (30), 139 (40), 106 (30), and 91 (30, Bn^+).

propyldichlorosilane could yield a less sterically hindered cyclic 1,3,2-azaoxsilolane, but the increased lability of the compound would probably render it non-isolable. Nonetheless, the ability to synthesize and (as discussed next) readily hydrolyze these silicate esters opens possibilities to the use of silicate esters as labile amine protecting groups.

4. Trialkoxy Silicate Esters as Labile Amine Protecting Groups. Silyl-based protecting groups (trialkylsilylamines) have not received extensive use in synthesis due to their high reactivity to moisture.[61] However, a few such examples of have shown that the use of sterically hindered silyl protecting groups hold promise. Notably, reacting *t*-butyldiphenylchlorosilane (TBDPS-Cl) with a wide scope of primary amines gave high yields of the desired silylamines. Further encouraging, these protecting groups were stable to chromatography and hydrolytic conditions, and the Si-N bond could be cleaved by treatment with 80% acetic acid or pyridine-HF.[71] Recently, a yet more hindered silyl protecting group, the di-*tert*-butylisobutylsilyl (BIBS) group, has been reported.[72] This strategy allows the protection of primary amines and subsequent purification via flash chromatography in high (typically, > 90%) yields. Also noteworthy, in both of these literature reports, secondary amines were found to be unreactive under these conditions[72] (although addition of carbon dioxide allows for formation of the protected carbamate[73]).

Only one reported use of a protecting group strategy involving a trialkoxysilane was found in the literature. In this case, the published graphical scheme depicts the use of a triisopropoxysilane [$NSi(O^iPr)_3$] as a nitrogen

[71] Overman, L. E.; Okazako, M. E.; Mishra, P. *tert*-Butyldipenylsilylamines: A Useful Protecting Group for Primary Amines. *Tet. Lett.* **1986**, *27*, 4391–4394.

[72] Liang, H.; Hu, L.; Corey, E. J. Di-*tert*-butylisobutylsilyl, Another Useful Protecting Group. *Org. Lett.* **2011**, *13*, 4120–4123.

[73] Lipshutz, B. H.; Papa, P.; Keith, J. M. Triisopropylsiloxycarbonyl (“Tsoc”): A New Protecting Group for 1° and 2° Amines. *J. Org. Chem.* **1999**, *64*, 3792–3793.

protecting group, but ambiguity remains regarding the true chemical compound. The text refers to the protecting group as a traditional "triisopropylsilyl" (as opposed to a "triisopropoxysilyl" as depicted in the scheme) group. Further complicating matters, the article contains minimal characterization or proof of constitution related to the compound.[74]

Given the relatively limited development of silicon-based nitrogen protecting groups, tri-*t*-butoxysilyls were envisioned as novel, labile protecting groups for amines. Thus, the purified **2.72** was dissolved in a co-solvent mixture of deionized water:acetonitrile (5:95) and monitored via GC/MS methodology in an effort to test for stability. Consistent with the previously noted lability of the attempted prodrug models, a rapid hydrolysis was observed ($t_{1/2}$ < 2 h) in these neutral conditions. Furthermore, dissolving **2.72** in ethyl acetate saturated with water yielded complete cleavage of the Si-N bond in less than 24 hours.

The potential utility of silicate ester protecting groups was further expanded by the discovery that, for the first time, unbranched secondary amines (diethylamine, **2.75**) could be successfully silylated with sterically encumbered silyl reagents to yield **2.76**[75] (Scheme 2-16). Notably, similar reaction conditions failed to provide the silylated analog when TBDPS-Cl was used as the silylating agent. Competition studies that subjected **2.75** to equal molar quantities of $SiCl(O^tBu)_3$ and TBDPS-Cl yielded exclusively **2.76**. Presumably, the ability of the $SiCl(O^tBu)_3$ reagent to successfully functionalize these more hindered systems in cases were TBDPS-Cl and BIBS-OTf failed is the result of the longer

[74] Tao, M.; Park, C. H.; Bihovsky, R.; Wells, G. J.; Husten, J.; Ator, M. A.; Hudkins, R. L. Synthesis and Structure-Activity Relationships of Novel Poly(ADP-ribose) Polymerase-1 Inhibitors. *Bioorg. Med. Chem. Lett.* **2006**, *16*, 938–942.

[75] Crude GC/MS data for **2.76** (Method: 50°C, hold for two min; ramp at 20°C/min for six min, hold at 170°C for six min) t_R = 9.44 min; *m/z* 319 (5, M^+), 304 (100, M^+ - Me), 248 (20), 192 (20), and 136 (20).

Si-O bond, thus providing a less crowded and more readily functionalized silicon center.

Scheme 2-16. Synthesis of a secondary aminotri-*t*-butoxysilane **2.76**.

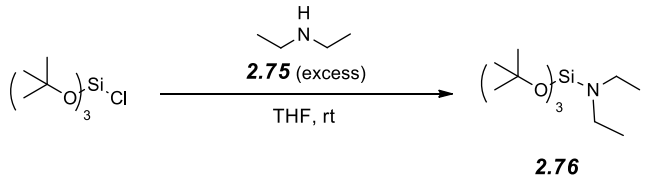

2.76

Attempts to expand silicate ester chemistry to branched secondary amines (e.g., diisopropylamine) were, however, unsuccessful. Nonetheless, the synthesis of both primary and unbranched secondary amino silicate esters and the purification of a subset of these compounds via column chromatography is highly advantageous to their development as protecting groups. These preliminary studies have established the labile nature that accounts for rapid hydrolysis under neutral conditions and warrant further development of the general concepts described here.[76] These attractive features open the possibility to their use as a new class of protecting groups that may be removed under exceedingly mild co-solvent conditions.

6. Conclusions.

The work described in Chapter 2 has established silicate esters as a viable promoiety. Both physical (i.e., hydrophobic character) and chemical (i.e., rate of hydrolysis) characteristics can be controlled, largely independently, through the choice of the sacrificial substituents. Under acid-catalyzed conditions, all but the most sterically hinder of these silicate ester prodrug models

[76] Development of hindered amonotrialkoxysilanes is continuing in collaboration with the laboratory of Prof. Michael Wentzel, Augsburg College, Minneapolis, MN.

cleanly return the parent compound(s). The principals developed within this chapter have been applied, with varying degrees of success, to specific model systems that are designed to mimic a variety of drug molecules containing aliphatic hydroxyls, aryl hydroxyls, phosphonic acids, and amines. With the guiding data regarding the rate of silicate ester hydrolysis trends now established, it is logical to advance these concepts to therapeutically relevant prodrugs.

7. Experimental Section.

Tetramethyl orthosilicate, tetraethyl orthosilicate, and menthol were purchased and used as received. Silicon tetrachloride was purchased and transferred to a Schlenk flask for storage. Tetraisopropyl orthosilicate and triethoxychlorosilane were purchased and used as received. Estradiol was purchased and used as received. Hydrocortisone was purchased and used as received. *n*-Butanol, *n*-hexanol, *n*-octanol, *i*-propanol, and *t*-butanol were dried over activated 3 or 4 Å molecular sieves overnight. Tetra-*n*-butoxysilane,[31] tetra-*n*-hexoxysilane,[31,32] and tetra-*n*-octoxysilane,[32] tri-n-butoxychlorosilane,[77] tri-*n*-octyloxychlorosilane,[78] tri-*i*-propoxychlorosilane,[79] and di-*t*-butoxydichlorosilane[32] were synthesized according to literature precedent. Tri-*t*-butoxychlorosilane was either purchased or prepared according to literature precedent.[80]

[77] Gerrard, W.; Jones, J. V. Stability of Isomeric Butoxysilanes with Respect to Silicon Tetrachloride and Hydrogen Chloride. *J. Chem. Soc.* **1952**, 1690–1693.

[78] Gerrard, W.; Howe, B. K. The Behaviour of 1:1:1:3:3:3-hexachloropropan-2-ol with Inorganic Non-Metal Halides. *J. Chem. Soc.* **1955**, 505–510.

[79] Chappelow, C. C.; Elliot, R. L.; Goodwin, J. T. The Phenylation and Methylation of Alkoxychlorosilanes. *J. Org. Chem.* **1960**, *25*, 435–439.

[80] Pedlow, G. W.; Miner, C. S. Tertiary-Alkoxy Chlorosilanes. U.S. Patent 2,566,957, September 4, 1951.

Triethylamine and pyridine were purchased and purified by distillation over CaH_2. Tetrahydrofuran was purchased and dried by being passed through an activated alumina column. Ethanol (anhydrous) was further dried by storing overnight over activated 3Å molecular sieves. Ethyl acetate (ACS grade) was and hexanes (ACS grade) were used as received. The d_6-acetone and *d*-chloroform were dried over activated 3Å molecular sieves overnight. D_2O was purchased and used as received.

Medium pressure liquid chromatography (MPLC) purifications were performed using columns dry-packed with ca. 25-35 μm silica gel. The MPLC apparatus was pressurized with a chromatography pump. Compound detection was performed by using a UV absorbance detector at 254 nm and a differential refractometer in series. All thin layer chromatography (TLC) data were collected on glass-backed plates coated with F-254 indicator. Visualization was completed via UV-light and/or staining with phosphomolybdic acid (PMA). ^{1}H NMR spectra were taken on a 500 MHz (^{1}H) instrument. All ^{1}H characterization spectra were taken in $CDCl_3$ and chemical shifts (δ) are referenced to tetramethylsilane at δ = 0.00. All ^{13}C NMR characterization spectra were taken in $CDCl_3$ on either a 125 MHz (^{13}C) or a 75 MHz (^{13}C) instrument and referenced to $CHCl_3$ at δ = 77.23. The following abbreviations are used to describe the NMR signals: s (singlet), d (doublet), t (triplet), q (quartet), sept (septet), m (multiplet), br (broad), and app (apparent). Coupling constants (J) are reported in Hz. Infrared spectra were recorded using an FT-IR instrument. All samples were collected in attenuated total reflectance (ATR) mode as thin films on a germanium window. Melting point data were collected on a hot stage and are uncorrected. High resolution mass spectra were collected on a BioTOF II (ESI-TOF) instrument using poly(ethylene glycol) (PEG) or poly(propylene glycol) (PPG) as an internal standard.

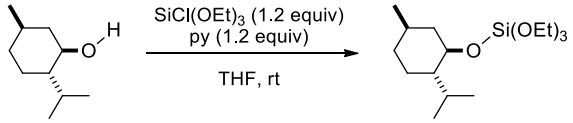

2.16 ***2.25***

Triethoxy (1*R*,2*S*,5*R*)-2-isopropyl-5-methylcyclohexoxysilane (2.25). To an oven-dried 5 mL culture tube containing a stir bar, menthol (98.0 mg, 0.628 mmol, 1.0 equiv) was added. This was dissolved in 3 mL of dry THF. Distilled pyridine (60 µL, 0.742 mmol, 1.2 equiv) and triethoxychlorosilane (150 µL, 0.764 mmol 1.2 equiv) were added. Immediately, a white precipitate formed. The vessel was closed with a Teflon®-lined culture tube and allowed to stir for 0.5 h while being monitored by GC/MS. The reaction mixture was diluted with a 1:1 mixture of hexanes:ethyl acetate (EtOAc), filtered through Celite®, concentrated under reduced pressure, and redissolved in a minimal amount of 49:1 hexanes:EtOAc. If a slurry resulted, this was filtered prior to being loaded onto a silica gel column. Purification by MPLC was performed using 49:1 hexanes:EtOAc as the eluent to yield the title silicate (165 mg, 82.3%) as a colorless oil.

^{1}H NMR (500 MHz, $CDCl_3$): δ 3.84 [q, *J* = 7.0 Hz, 6H, OSi(OC*H*$_2$CH$_3$)$_3$], 3.67 (ddd, *J* = 4.3, 10.5, 10.5 Hz, 1H, SiOC*H*), 2.23 [dsept, *J* = 2.6, 7.0 Hz, 1H, (CH$_3$)$_2$C*H*], 2.02 (m, 1H, SiOCHCH$_A$C*H*$_E$), 1.64-1.56 [m, 2H, (CH$_3$)$_2$CHCHCH$_A$C*H*$_E$CH$_A$C*H*$_E$], 1.40 (ddddq, *J* = 3.5, 3.5, 11.6, 11.6, 6.7, 1H, CH$_3$C*H*), 1.23 [t, *J* = 7.0 Hz, 9H, OSi(OCH$_2$C*H*$_3$)$_3$], 1.19 (dddd, *J* = 3, 3, 10, 12 Hz, 1H, (CH$_3$)$_2$CHC*H*), 1.05 (ddd, *J* = 10.5, 12.0, 12.0 Hz, 1H, SiOCHC*H*$_A$H$_E$), 0.95 [dddd, *J* = 3.0, 12.3, 12.3, 12.3 Hz, 1H, (CH$_3$)$_2$CHCHC*H*$_A$H$_E$], 0.90 (d, *J* = 6.5 Hz, 3H, C*H*$_3$CH), 0.89 (d, *J* = 7.1 Hz, 3H, C*H*$_3$CHCH), 0.83 (dddd, *J* = 3.2, 12.4, 12.4, 12.4 Hz, 1H, (CH$_3$)$_2$CHCHCH$_2$C*H*$_A$CH$_E$), and 0.77 (d, *J* = 6.9 Hz, 3H, C*H*$_3$CHCH).

^{13}C NMR (75 MHz, $CDCl_3$): δ 73.3, 59.3, 49.9, 44.8, 34.7, 31.8, 25.5, 22.9, 22.4, 21.4, 18.3, and 15.8.

HRMS (ESI) Calc'd for $C_{16}H_{34}NaO_4Si^+$ ($M + Na^+$): 341.2119, found 341.2114.

GC/MS (Method: 50 °C, hold for two min; ramp at 20 °C/min for 10 min, hold at 250 °C for three min) t_R = 7.75 min; *m/z* 318 (5, M^+), 303 (10. M^+-Me), 233 (100), 181 (10), and 138 (20).

IR (thin film) 2956, 2923, 1456, 1392, 1294, 1168, 1102, 1082, 1002, 963, 883, 829, and 791.

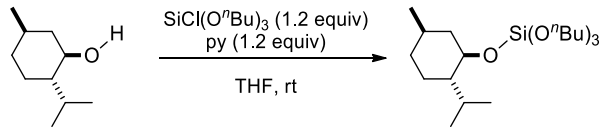

2.16 ***2.26***

Tri-*n*-butoxy (1*R*,2*S*,5*R*)-2-isopropyl-5-methylcyclohexoxysilane (2.26). To an oven dried 5 mL culture tube containing a stir bar, menthol (177.5 mg, 1.14 mmol, 1 equiv) was added. This was dissolved in 3 mL of dry THF. Distilled pyridine (0.11 mL, 1.37 mmol, 1.2 equiv) and a 2.5:1 mixture of SiCl(O^{n}Bu)$_3$:Si(O^{n}Bu)$_4$ [533 mg 1.37 mmol of SiCl(O^{n}Bu)$_3$, 1.2 equiv] were added. Immediately, a white precipitate formed. The vessel was closed with a Teflon®-lined cap and the mixture was allowed to stir for 16 h. The slurry was filtered through Celite®, concentrated under reduced pressure, and redissolved in a minimal amount of 49:1 hexanes:EtOAc. If a slurry resulted, this was filtered prior to being loaded onto a silica gel column. Purification by MPLC led to two overlapping peaks, and the pure title product was obtained by taking the front of the faster eluting substance, yielding the title silicate (180.3 mg, 68.6%) as a

colorless oil. The remainder of the peak corresponded to the $Si(O^nBu)_4$ (^{1}H NMR) present in the starting silylating reagent.

^{1}H NMR (500 MHz, $CDCl_3$): δ 3.76 [t, *J* = 6.7 Hz, 6H, $OSi(OCH_2CH_2)_3$], 3.66 (ddd, *J* = 4.4, 10.5, 10.5 Hz, 1H, SiOC*H*), 2.24 [dsept, *J* = 2.7, 7.0 Hz, 1H $(CH_3)_2CH$], 2.05-2.00 (m, 1H, $SiOCHCH_ACH_E$), 1.66-1.56 [m, 2H, $(CH_3)_2CHCHCH_ACH_ECH_ACH_E$], 1.56 [tt, *J* = 6.6, 7.0 Hz, 6H, $Si(OCH_2CH_2)_3$], 1.37-1.28 [tq, *J* = 7, 7 Hz, 6H, $Si(OCH_2CH_2CH_2CH_3)_3$ and m, 1H, CH_3CH), 1.19 [dddd, *J* = 3.0, 4.6, 9.9, 12.2 Hz, 1H, $(CH_3)_2CHCH$], 1.04 [ddd, *J* = 10.5, 12.0, 12.0 Hz, 1H, $SiOCHCH_AH_E$), 1.00-0.90 (m, 1H, $(CH_3)_2CHCHCH_AH_E$], 0.92 [t, *J* = 7.4 Hz, 9H, $Si(OCH_2CH_2CH_2CH_3)_3$], 0.90 (d, *J* = 6.5 Hz, 3H, CH_3), 0.89 [d, *J* = 7.1 Hz, 3H, CH_3], 0.85 [dddd, *J* = 3.5, 12.0, 12.0, 12.0 Hz, 1H, $(CH_3)_2CHCHCH_2CH_ACH_E$], and 0.77 (d, *J* = 6.9 Hz, 3H, CH_3).

^{13}C NMR (75 MHz, $CDCl_3$): δ 73.4, 63.3, 49.9, 44.9, 34.7, 34.6, 31.9, 25.5, 23.0, 22.5, 21.4, 19.1, 15.9, and 14.1.

HRMS (ESI) Calc'd for $C_{22}H_{46}NaO_4Si^+$ ($M + Na^+$): 425.3058, found 425.3082.

GC/MS (Method: 50 °C, hold for two min; ramp at 20 °C/min for 10 min, hold at 250 °C for three min) t_R = 10.12 min; *m/z* 402 (10, M^+), 359 (20. M^+-$CH_2CH_2CH_3$), 317 (100), 265 (30), and 138 (40).

IR (thin film) 2957, 2931, 2873, 1456, 1383, 1235, 1151, 1089, 1051, 989, 938, 895, 832, 802, and 734.

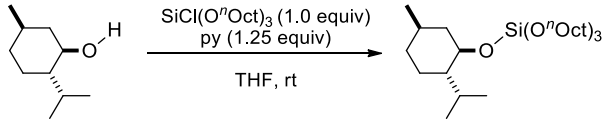

2.16 ***2.27***

Tri-*n*-octyloxy (1*R*,2*S*,5*R*)-2-isopropyl-5-methylcyclohexoxysilane (2.27). Menthol (342 mg, 2.19 mmol, 1 equiv) was added to an oven-dried 12 mL culture tube containing a stir bar. This was dissolved in 10 mL of dry THF. Distilled pyridine (0.22 mL, 2.74 mmol, 1.25 equiv) and a 1:0.55 mixture of SiCl(O^{n}Oct)$_3$:Si(O^{n}Oct)$_4$ [1.79 g, 2.19 mmol, 1.0 equiv of SiCl(O^{n}Oct)$_3$] were added. Immediately, a white precipitate formed. The vessel was closed with a Teflon®-lined cap and allowed to stir for 2 h. The reaction mixture was filtered through a paper filter to remove the pyridinium chloride salt, concentrated under reduced pressure, and redissolved in a minimal amount of 99:1 hexanes:EtOAc. If a slurry resulted, this was filtered prior to being loaded onto a silica gel column. Purification by MPLC provided two overlapping peaks, and the pure title product was obtained by taking the front of the faster eluting substance, yielding the title silicate (858 mg, 68.6%) as a colorless oil. The remainder of the peak corresponded to the Si(O^{n}Oct)$_4$ (^{1}H NMR) present in the starting silylating reagent.

^{1}H NMR (500 MHz, $CDCl_3$): δ 3.74 [t, *J* = 6.6 Hz, 6H, OSi(OC*H*$_2$CH$_2$)$_3$], 3.66 (ddd, *J* = 4.3, 10.5, 10.5 Hz, 1H, SiOC*H*), 2.22 [dsept, *J* = 2.6, 7.0 Hz, 1H (CH$_3$)$_2$C*H*], 2.02 (m, 1H, SiOCHCH$_A$C*H*$_E$), 1.68-1.50 [m, 8H, (CH$_3$)$_2$CHCHCH$_A$C*H*$_E$CH$_A$C*H*$_E$ and Si(OCH$_2$C*H*$_2$CH$_2$)$_3$], 1.40-1.10 {m, 32H, CH$_3$C*H*, (CH$_3$)$_2$CHC*H*, and Si[OCH$_2$CH$_2$(C*H*$_2$)$_5$CH$_3$]$_3$}, 1.03 (ddd, *J* = 10.5, 12.0, 12.0 Hz, 1H, SiOCHC*H*$_A$H$_E$), 0.99-0.83 {m,17H, Si[O(CH$_2$)$_7$C*H*$_3$]$_3$, (CH$_3$)$_2$CHCHCH$_2$C*H*$_A$CH$_E$, (CH$_3$)$_2$CHCHCH$_2$C*H*$_A$H$_E$, C*H*$_3$, and C*H*$_3$}, and 0.76 (d, *J* = 6.9 Hz, 3H, C*H*$_3$).

^{13}C NMR (75 MHz, $CDCl_3$): δ 73.4, 63.7, 49.9, 44.9, 34.7, 32.6, 32.1, 31.9, 29.62, 29.59, 26.0, 25.5, 23.0, 22.9, 22.5, 21.4, 15.9, and 14.3.

HRMS (ESI) Calc'd for $C_{34}H_{74}NO_4Si^+$ ($M + NH_4^+$): 588.5382, found 588.5376.

GC/MS (Method: 50 °C, hold for two min; ramp at 20 °C/min for 12 min, hold at 250 °C for seven min) t_R = 14.23 min; *m/z* 570/571 (10, M^+), 527 (10), 486 (100), 433 (30), and 138 (40).

IR (thin film) 2953, 2924, 2855, 1458, 1380, 1095, 1054, 1002, 936, 888, 836, 807, and 725.

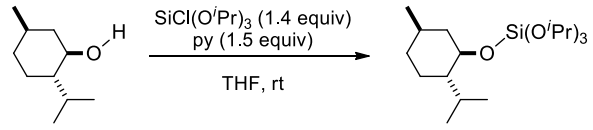

2.16 ***2.28***

Tri-*i*-propoxy (1*R*,2*S*,5*R*)-2-isopropyl-5-methylcyclohexoxysilane (2.28). Menthol (71.6 mg, 0.458 mmol, 1 equiv) was added to an oven-dried 12 mL culture tube containing a stir bar. This was dissolved in 2 mL of dry THF. Distilled pyridine (55 µL, 0.687 mmol, 1.5 equiv) and a 2.9:1 mixture of $SiCl(OiPr)_3$:$Si(OiPr)_4$ [206 mg, 0.620mmol, 1.4 equiv of $SiCl(OiPr)_3$] were added. Immediately, a white precipitate formed. The reaction vessel was closed with a Teflon®-lined cap and monitored by GC/MS. After 2 h, no starting material remained, and the reaction mixture was filtered through Celite® to remove the pyridinium chloride salt, concentrated under reduced pressure, and redissolved in a minimal amount of 99:1 hexanes:EtOAc. If a slurry resulted, this was filtered prior to being loaded onto a silica gel column. Purification by MPLC was

performed using 99:1 hexanes:EtOAc as the eluent to yield the title silicate (133 mg, 0.369 mmol, 80.7%) as a colorless oil.

^{1}H NMR (500 MHz, $CDCl_3$): δ 4.22 [sept, *J* = 6.1 Hz, 3H, OSiOC*H*$(CH_3)_2$], 3.66 (ddd, *J* = 4.3, 10.5, 10.5 Hz, 1H, SiOC*H*), 2.25 [dsept, *J* = 2.6, 7.0 Hz, 1H $(CH_3)_2$C*H*], 2.08-2.02 (m, 1H, SiOCHCH_AC*H*$_E$), 1.65-1.55 [m, 2H, $(CH_3)_2$CHCHCH_AC*H*$_E$CH_AC*H*$_E$], 1.38 (ddddq, *J* = 3, 3, 10, 12, 7 Hz, 1H, CH_3C*H*), 1.19 [d, *J* = 6.0 Hz, 18H, SiOCH(C*H*$_3)_2$], 1.02 (ddd *J* = 10, 12, 12 Hz, 1H, SiOCHC*H*$_A$H$_E$), 0.94 [dddd, *J* = 3.2, 12.8, 12.8, 12.8 Hz, 1H, $(CH_3)_2$CHCHC*H*$_A$H$_E$], 0.90 (d, *J* = 6.5 Hz, 3H, C*H*$_3$), 0.89 (d, *J* = 7.1 Hz, 3H, C*H*$_3$), 0.81 [dddd, *J* = 3.2, 12.7, 12.7, 12.7 Hz, 1H, $(CH_3)_2$CHCHCH_2C*H*$_A$CH$_E$], and 0.76 (d, *J* = 6.9 Hz, 3H, C*H*$_3$).

^{13}C NMR (75 MHz, $CDCl_3$): δ 73.3, 65.9, 50.0, 44.9, 34.8, 31.9, 25.6, 25.4, 23.0, 22.5, 21.4, and 15.9.

HRMS (ESI) Calcd for $C_{19}H_{40}NaO_4Si^+$ ($M + Na^+$): 383.2588, found 383.2585.

GC/MS (Method: 50 °C, hold for two min; ramp at 20 °C/min for 10 min, hold at 250 °C for three min) t_R = 7.32 min; m/z 360 (10, M^+), 345 (40, M^+-CH_3), 275 (100), and 138 (30).

IR (thin film) 2971, 2924, 2872, 1455, 1380, 1371, 1172, 1120, 1085, 1042, 935, 890, 825, 807, 769, 687, 649, 635, and 611.

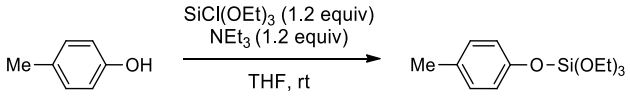

2.29 ***2.30***

Triethoxy *p*-tolyloxysilane (2.30). *P*-cresol (1.50 g, 13.9 mmol, 1 equiv) was dissolved in dry THF (60 mL) in a round bottom flask with a magnetic stir bar. Triethylamine (2.32 mL, 16.6 mmol, 1.2 equiv) and triethoxychlorosilane (3.27 mL, 16.6 mmol, 1.2 equiv) were added to this solution. A white precipitate was immediately observed upon addition of the triethoxychlorosilane. The mixture was allowed to stir for 2 hours, after which the crude reaction mixture was centrifuged, the solution decanted, and the remaining solid was washed with dry THF (3x). The collected solution was concentrated under reduced pressure, and the crude product (2.36 g) was purified by flash column chromatography (SiO_2, 20:1 hexanes:EtOAc) to afford the title compound as a colorless oil (2.25 g, 8.3 mmol, 60%).

^{1}H NMR (500 MHz, $CDCl_3$): δ 7.04 (d, *J* = 8.5 Hz, 2H, CH_3CCH), 6.91 (d, *J* = 8.5 Hz, 2H, SiOCC*H*), 3.91 [q, *J* = 7.0 Hz, 6H, $Si(OCH_2CH_3)_3$], 2.28 (s, 3H, $CH_3C_6H_4$), and 1.24 [t, *J* = 8.0 Hz, 9H, $Si(OCH_2CH_3)_3$].

^{13}C NMR (125 MHz, $CDCl_3$): δ 151.4, 131.2, 129.9, 119.0, 59.6, 20.6, and 18.0.

HRMS (ESI) Calc'd for $C_{13}H_{22}NaO_4Si^+$ ($M + Na^+$): 293.1180, found 293.1187.

TLC (20:1 hexanes:EtOAc) R_f = 0.40

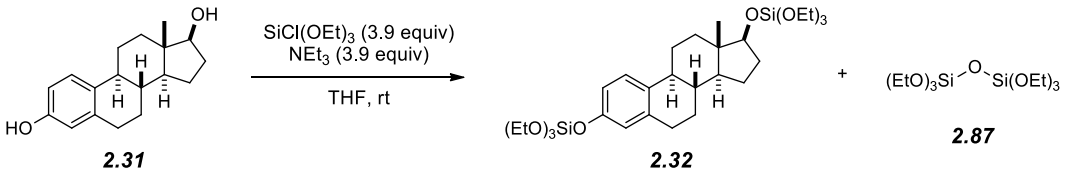

2.31 ***2.32*** ***2.87***

3,17-Di-*O*-(Triethoxysilyl) estradiol (2.32). Estradiol (50.0 mg, 0.184 mmol, 1 equiv) was dissolved in 0.75 mL of dry THF in a 4 mL glass vial containing a stir bar. Triethylamine (100 µL, 0.72 mmol, 3.9 equiv) and triethoxychlorosilane (145 µL, 0.74 mmol, 3.9 equiv) were added. The vessel was capped and allowed to stir overnight at ambient temperature. Incomplete conversion was noted by TLC; an additional aliquot of triethylamine (60 µL, 0.43 mmol, 2.3 equiv) and triethoxychlorosilane (80 µL, 0.41 mmol, 2.3 equiv) were added. The vial was again capped and stirred overnight. The reaction mixture was diluted with dry THF, the slurry centrifuged, the organic layer decanted, and the solution dried under reduced pressure. The product was redissolved in a minimal volume of 9:1 hexanes:EtOAc and purified via flash column chromatography using 9:1 hexanes:EtOAc as the eluent. A volatile contaminant was removed by high vacuum for 72 h, yielding the title compound (64.5 mg, 0.168 mmol, 91.3%) as a colorless oil.

^{1}H NMR (500 MHz, $CDCl_3$)[81]: δ 7.15 (d, *J* = 8.5 Hz, 1H, H1), 6.79 (dd, *J* = 8.4, 2.6 Hz, 1H, H2), 6.73 (d, *J* = 2.5 Hz, 1H, H4), 3.91 [overlapping q, *J* = 7.0 Hz, 6H, $OSi(OC\mathit{H_2}CH_3)_3$ and d, 1H, H17], 3.86 [q, *J* = 7.0 Hz, 6H, $OSi(OC\mathit{H_2}CH_3)_3$], 2.81, (m, 2H, H6α and H6β), 2.28 (ddd, *J* = 13.3, 7.0, 3.9 Hz, 1H, H11α), 2.17 (ddd, *J* = 11.3, 11.3, 4.2 Hz, 1H, H9), 2.06 (m, 1H, H16β), 1.97 (ddd, *J* = 12.6, 3.2, 3.2 Hz, 1H, H7β), 1.86 (dddd, *J* = 11.0, 8.0, 2.6, 2.6 Hz, 1H, H15α), 1.70-1.10 [m, 26H,

[81] ^{1}H NMR assignments were made with the assistance of: Ciuffreda, P.; Casati, S.; Manzocchi, A. Complete ^{1}H and ^{13}C NMR Spectral Assignment of 17-Hydroxy Epimeric Sterols with Planar A or A and B Rings. *Magn. Reson. Chem.* **2004**, *42*, 360–363.

H7α, H8, H11β, H12α, H12β, H14, H15β, H16α, $OSi(OCH_2CH_3)_3$, $OSi(OCH_2CH_3)_3$], and 0.79 (s, 3H, C18H_3).

^{13}C NMR (75 MHz, $CDCl_3$): δ 151.5, 138.1, 134.1, 126.4, 119.3, 116.5, 82.3, 59.8, 59.4, 49.8, 44.3, 43.7, 39.0, 37.0, 30.5, 29.8, 27.4, 26.5, 23.3, 18.4, 18.3, and 11.5.

HRMS (ESI) Calc'd for $C_{30}H_{52}NaO_8Si_2$ $[M + Na]^+$ 619.3093, found 619.3098

TLC R_f (1:1 hexanes:EtOAc) = 0.5.

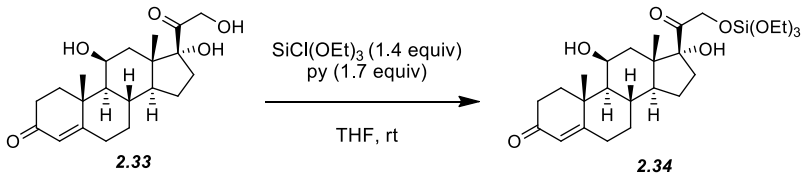

2.33 *2.34*

19-*O*-(Triethoxysilyl) hydrocortisone (2.34). Hydrocortisone (53.3 mg, 0.147 mmol, 1.0 equiv) was transferred to an oven-dried culture tube containing a stir bar. The hydrocortisone was dissolved with gentle heating in dry THF (1.0 mL). Pyridine (20 µL, 0.247 mmol, 1.7 equiv) and triethoxychlorosilane (40 µL, 0.204 mmol, 1.4 equiv) were added by Wiretrol®. Immediately, a white precipitate was observed. The vessel was sealed with a Teflon®-lined cap, and the solution was stirred at room temperature while being monitored by TLC. After stirring for 3 h, the reaction mixture was diluted with hexanes:ethyl acetate (1:1), filtered through a short plug of Celite® to remove the pyridinium salt, concentrated under reduced pressure, and redissolved in a minimal amount of hexanes:ethyl acetate (1:1). If a slurry resulted, this was filtered prior to being loaded onto a silica gel column. Subsequent chromatography (SiO_2, 1:1 hexanes: ethyl acetate) via medium

pressure liquid chromatography and concentration under reduced pressure yielded the title compound (65.2 mg, 0.124 mmol, 84.5%) as a colorless oil.

^{1}H NMR (500 MHz, CD_3OD)[82]: δ δ 5.67 (s, 1H, H4), 4.91 (d, *J* = 18.7 Hz, 1H, H21a), 4.55 (d, *J* = 18.7 Hz, 1H, H21b), 4.40 (app q, *J* = 3.3 Hz, 1H, H11α), 3.88 (q, *J* = 7.0 Hz, 6H, $OSiOC\mathit{H_2}CH_3$), 2.72 (ddd, *J* = 14.3, 11.1, 2.5 Hz, 1H, 16β), 2.56 (dddd, *J* = 14.3, 14.3, 5.5, 1.9, 1H, H6β), 2.49 (ddd, *J* = 16.7, 13.6, 5.0 1H, H2β), 2.35-2.18 (m, 3H, H2α, H6α, and H1β), 2.10-1.99 (m, 3H, H8, H7β, and H12α), 1.88 (ddd, *J* = 13.5, 13.5, 4.4 Hz, 1H, H1α), 1.82-1.71 (m, 2H, H14 and H15α), 1.63 (dd, *J* = 13.6, 2.7 Hz, 1H, H12β), 1.50-1.34 (m, 5H, H16α, C19$\mathit{H_3}$, and H15β), 1.23 [t, *J* = 7.0 Hz, 9H, $OSi(OCH_2C\mathit{H_3})_3$], 1.11 (dddd, *J* = 4, 11.5, 11.5, 11.5 Hz, 1H, H7α), 1.00 (dd, *J* = 11.1, 3.3 Hz, 1H, H9), and 0.90 (s, 3H, C18$\mathit{H_3}$).

^{13}C NMR (125 MHz, $CDCl_3$): 206.0, 199.8, 172.5, 122.5,89.5, 68.6, 68.4, 59.7, 56.2, 51.8, 47.7, 40.1, 39.4, 35.2, 34.0, 34.0, 32.9, 32.3, 31.6, 23.9, 21.2, 18.3, and 17.7.

HRMS (ESI) Calc'd for $C_{27}H_{44}NaO_8Si$ $[M + Na]^+$ 547.2698, found 547.2705.

IR (thin film) 3450 (br), 2974, 2930, 1744, 1723, 1657, 1614, 1442, 1390, 1364, 1271, 1232, 1165, 1104, 1079, 1007, 965, 947, 908, 865, 846, 793 and 736.

TLC R_f (1:1 hexanes:EtOAc) = 0.55.

[82] ^{1}H NMR assignments were made with the assistance of: Kirk, D. N.; Toms, H. C.; Douglas, C.; White, K. A.; Smith, K. E.; Latif, S.; Hubbard, R. W. P. A Survey of the High-Field ^{1}H NMR Spectra of the Steroid Hormones, their Hydroxylated Derivatives, and Related Compounds. *J. Chem. Soc. Perkin Trans. 2* **1990**, 1567–1594.

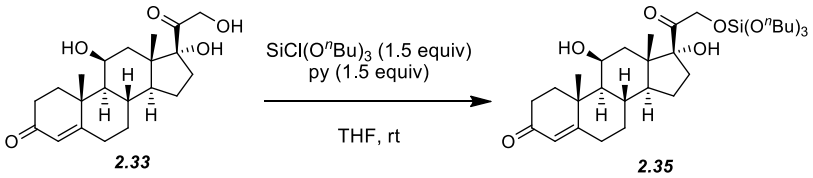

2.33 *2.35*

19-*O*-(Tri-*n*-butoxysilyl) hydrocortisone (2.35). Hydrocortisone (44.0 mg, 0.121 mmol, 1.0 equiv) was transferred to an oven-dried culture tube with a Teflon-lined cap and stir bar and dissolved in dry THF (2.0 mL). Pyridine (15 µL, 0.185 mmol, 1.5 equiv) was added by Wiretrol.® A 1:1.05 mixture of tri-*n*-butoxychlorosilane:tetra-*n*-butoxysilane (0.108 mg, 0.179 mmol, 1.5 equiv of tri-*n*-butoxychlorosilane) was then added and a white precipitate was immediately observed. The culture tube was sealed and the solution was stirred at room temperature while being monitored by TLC. After stirring for 3 h, the reaction was diluted with a mixture of hexane:ethyl acetate (1:1), filtered through a short plug of Celite® to remove the pyridinium salt, concentrated under reduced pressure, and redissolved in a mixture of hexane:ethyl acetate (2:1). Subsequent chromatography (SiO_2, 3:1 hexanes: ethyl acetate) via medium pressure liquid chromatography and drying under reduced pressure yielded the title compound as a colorless oil (60.4 mg, 0.096 mmol, 79.3%).

^{1}H NMR (500 MHz, CD_3OD) [82]: δ 5.66 (s, 1H, H4), 4.90 (d, *J* = 18.7 Hz, 1H, H21), 4.54 (d, *J* = 18.7 Hz, 1H, H21), 4.40 (app. q, *J* = 3.3 Hz, 1H, H11α), 3.82 [t, *J* = 6.5 Hz, 6H, $OSi(OC\mathit{H}_2CH_2CH_2CH_3)_3$], 2.72 (ddd, *J* = 14.3, 11.1, 2.5 Hz, 1H, 16β), 2.56 (dddd, *J* = 14.3, 14.3, 5.5, 1.8 Hz, 1H, H6β), 2.49 (ddd, *J* = 16.7, 13.7, 5.0 Hz, 1H, H2β), 2.35-2.19 (m, 3H, H2α, H6α, and H1β), 2.11-2.01 (m, 3H, H8, H7β, and H12α), 1.88 (ddd, *J* = 13.5, 13.5, 4.5 Hz, 1H, H1α), 1.82-1.72 (m, 2H, H14 and H15α), 1.62 (dd, *J* = 13.6, 2.7 Hz, 1H, H12β), 1.56 [tt, *J* = 6.6, 6.6 Hz, 6H, $OSi(OCH_2C\mathit{H}_2CH_2CH_3)_3$], 1.47 (s, 3H, C19$\mathit{H}_3$), 1.46-1.33 [m, 8H, H16α, H15β,

and $OSi(OCH_2CH_2C\mathit{H}_2CH_3)_3$], 1.12 (m, 1H, H7α), 1.00 (dd, *J* = 11.1, 3.4 Hz, 1H, H9), 0.94 [t, *J* = 7.4 Hz, 9H, $OSi(OCH_2CH_2CH_2C\mathit{H}_3)_3$], and 0.90 (s, 3H, C18$\mathit{H}_3$).

^{13}C NMR (125 MHz, $CDCl_3$): 208.5, 199.7, 172.5, 122.5, 89.5, 68.6, 68.5, 63.7, 56.2, 51.8, 47.6, 40.2, 39.4, 35.2, 34.6, 34.0, 33.9, 32.9, 32.3, 31.6, 23.9, 21.2, 19.0, 17.7, and 14.0.

HRMS (ESI) Calc'd for $C_{33}H_{56}NaO_8Si$ $[M + Na]^+$ 631.3637, found 631.3650.

IR (thin film) 3475 (br), 2956, 2934, 2875, 1724, 1658, 1615, 1455, 1388, 1269, 1233, 1091, 1042, 1008, 989, 945, 906, 864, 803, 763, 701, 637, and 623.

TLC R_f (2:1 hexanes:EtOAc) = 0.35.

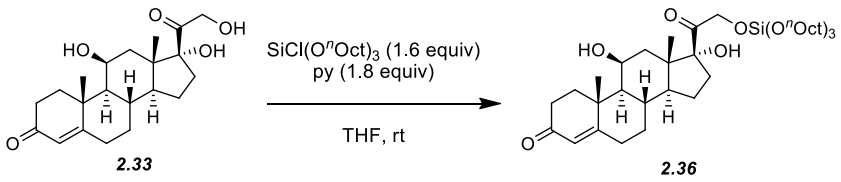

19-*O*-(Tri-*n*-octyloxysilyl) hydrocortisone (2.36). Hydrocortisone (48.5 mg, 0.134 mmol, 1.0 equiv) was transferred to an oven-dried culture tube with a Teflon-lined cap and stir bar and dissolved with gentle heating in dry THF (2.0 mL). Pyridine (20 µL, 0.247 mmol, 1.8 equiv) was added by Wiretrol®. A 1.67:1 mixture of tri-*n*-octyloxychlorosilane:tetra-*n*-octyloxysilane (0.165 mg, 0.212 mmol, 1.6 equiv of tri-*n*-octyloxychlorosilane) was then added and a white precipitate was immediately observed. The culture tube was sealed and the solution was stirred at room temperature while being monitored by TLC. After stirring for 4 h, the reaction was diluted with a mixture of hexane:ethyl acetate (1:1), filtered through a short plug of Celite® to remove the pyridinium salt, concentrated under reduced pressure, and redissolved in a mixture of

hexane:ethyl acetate (3:1). Subsequent chromatography (SiO_2, 3:1 hexanes: ethyl acetate) via medium pressure liquid chromatography and drying under reduced pressure yielded the title compound as a colorless oil (82.1 mg, 0.106 mmol, 78.8%).

^{1}H NMR (500 MHz, CD_3OD)[82]: δ 5.66 (s, 1H, H4), 4.89 (d, *J* = 18.7 Hz, 1H, H21), 4.55 (d, *J* = 18.7 Hz, 1H, H21), 4.40 (app. q, *J* = 3.3 Hz, 1H, H11α), 3.81 {t, *J* = 6.5 Hz, 6H, OSi[OC*H*$_2$CH$_2$(CH$_2$)$_5$CH$_3$]$_3$}, 2.72 (ddd, *J* = 14.3, 11.1, 2.5 Hz, 1H, 16β), 2.56 (dddd, *J* = 14.3, 14.3, 5.5, 1.8 Hz, 1H, H6β), 2.50 (ddd, *J* = 16.7, 13.7, 5.0 Hz, 1H, H2β), 2.35-2.19 (m, 3H, H2α, H6α, and H1β), 2.12-2.00 (m, 3H, H8, H7β, and H12α), 1.87 (ddd, *J* = 13.5, 13.5, 4.4 Hz, 1H, H1α), 1.82-1.72 (m, 2H, H14, and H15α), 1.63 (dd, *J* = 13.6, 2.7 Hz, 1H, H12β), 1.58 {tt, *J* = 6.6, 6.6 Hz, 6H, OSi[OCH$_2$C*H*$_2$(CH$_2$)$_5$CH$_3$]$_3$}, 1.50-1.25 {m,35H, H16α, C19*H*$_3$, H15β, and OSi[OCH$_2$CH$_2$(C*H*$_2$)$_5$CH$_3$]$_3$}, 1.12 (br dddd, *J* = 13.7, 13.7, 13.7, 4.4 Hz, 1H, H7α), 1.00 (dd, *J* = 11.1, 3.4 Hz, 1H, H9), and 0.94-0.88 {overlapping s, 3H, C18*H*$_3$ and t, *J* = 6.9 Hz, 9H, OSi[OCH$_2$CH$_2$(CH$_2$)$_5$C*H*$_3$]$_3$}.

^{13}C NMR (125 MHz, $CDCl_3$): 208.5, 199.6, 172.4, 122.5, 89.5, 68.6, 68.5, 64.1, 56.2, 51.8, 47.7, 40.3, 39.4, 35.2, 34.0, 33.9, 32.9, 32.5, 32.3, 32.0, 31.6, 29.6, 29.5, 25.9, 24.0, 22.8, 21.2, 17.8, and 14.3.

HRMS (ESI) Calc'd for $C_{45}H_{80}NaO_8Si$ $[M + Na]^+$ 799.5515, found 799.5564.

IR (thin film) 3400 (br), 2926, 2855, 1724, 1659, 1615, 1459, 1389, 1347, 1271, 1232, 1183, 1096, 1059, 1006, 986, 907, 865, 813, 762, 742 and 725.

TLC R_f (3:1 hexanes:EtOAc) = 0.35.

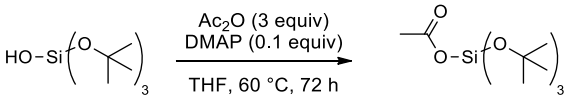

2.45 ***2.46***

Tri-*t*-butoxyacetoxysilane (2.46). To an oven-dried culture tube with stir bar, 0.2980 g (1.127 mmol, 1 equiv) of tri-*tert*-butoxysilanol was added. This was then dissolved in 5 mL of dry THF. Next, 0.30 mL of acetic anhydride (3.18 mmol, 2.8 equiv) followed by 0.010 g of DMAP (0.082 mmol, 0.073 equiv). The reaction was sealed with a Teflon-lined, heated to 60 °C in an oil bath, and monitored by GC-MS. After 72 h, the volatile organic compounds were removed under concentrated under reduced pressure, and the residue redissolved in a mixture of 99:1 hexanes:EtOAc. The dissolved residue was split into two portions and purified sequentially by MPLC in 99:1 hexanes:EtOAc. The product was concentrated under reduced pressure to yield 0.1605 g (0.525 mmol, 46.5%) of the pure title product as a colorless oil.

^{1}H NMR (500 MHz, $CDCl_3$): δ 2.09 [s, 3H, SiOC(O)CH_3] and 1.33 {s, 27H, Si[OC(CH_3)$_3$]$_3$}.

LRMS (ESI) Calc'd for $C_{14}H_{30}NaO_5Si^+$ (M + Na^+): 329.2, found 329.2.

GC/MS (Method: 50 °C, hold for two min; ramp at 20 °C/min for 10 min, hold at 250 °C for three min) t_R = 5.21 min; *m/z* 291 (20, M^+-CH_3), 233 [60, M^+-$OC(CH_3)$], 177 (30), and 121 (100).

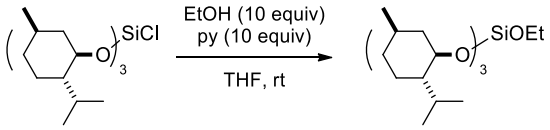

2.47 ***2.48***

Ethoxy-tri-(1*R*,2*S*,5*R*)-2-isopropyl-5-methylcyclohexoxysilane (2.48). Trimenthyloxychlorosilane[39] (166.2 mg, 0.306 mmol, 1 equiv) was added to an oven-dried 5 mL culture tube containing a stir bar and then dissolved in 3 mL of dry THF. Distilled pyridine (0.25 mL, 3.06 mmol, 10 equiv) and anhydrous ethanol, which had been dried over activated 3Å molecular sieves (0.18 mL, 3.06 mmol, 10 equiv), were added. A white precipitate quickly formed. The reaction vessel was sealed with a Teflon®-lined cap, the reaction mixture was stirred at room temperature, and the reaction progress was monitored by GC/MS. After 0.5 h no starting material remained, and the reaction slurry was filtered through a plug of glass wool to remove the pyridinium salt, concentrated under reduced pressure, and redissolved in a minimal amount of hexanes. If a slurry resulted, this was filtered prior to being loaded onto a silica gel column. Purification by MPLC using pure hexanes as the eluent yielded 0.0125 g of tetramenthyloxy orthosilicate and, in a later eluting fraction, the pure title product (113.6 mg, 0.211 mmol, 69.0%) as a colorless oil.

^{1}H NMR (500 MHz, $CDCl_3$): δ 3.816 (dq, *J* = 10.1, 7.0 Hz, 1H, $SiOC\mathit{H}_aH_bCH_3$), 3.809 (dq, *J* = 10.2, 7.0 Hz, 1H, $SiOCH_a\mathit{H}_bCH_3$), 3.67 [ddd, *J* = 4.3, 10.4, 10.4 Hz, 3H, $Si(OC\mathit{H})_3$], 2.26 {dsept, *J* = 2.6, 7.1 Hz, 3H $[(CH_3)_2C\mathit{H}]_3$}, 2.10-2.01 [m, 3H, $Si(OCHCH_AC\mathit{H}_E)_3$], 1.67-1.54 {m, 6H, $[(CH_3)_2CHCHCH_AC\mathit{H}_ECH_AC\mathit{H}_E]_3$}, 1.36 [ddddq, *J* = 3.5, 3.5, 12, 12, 7 Hz, 3H, $(CH_3C\mathit{H})_3$], 1.23 (t, *J* = 7.0 Hz, 3H, $SiOCH_2C\mathit{H}_3$), 1.23-1.12 {m, 3H $[(CH_3)_2CHC\mathit{H}]_3$}, 1.02 {ddd, *J* = 10.7, 12.1, 12.1 Hz, 3H, $Si[OCHC\mathit{H}_AH_E]_3$}, 0.94 {dddd, *J* = 3, 12, 12, 12 Hz, 3H, $[(CH_3)_2CHCHC\mathit{H}_AH_E]_3$}, 0.90 [d, *J* = 6.5 Hz, 9H, $(C\mathit{H}_3)_3$], 0.89 [d, *J* = 7.1 Hz, 9H,

($C\mathit{H}_3$)$_3$], 0.88-0.76 {m, 3H, [$(CH_3)_2CHCHCH_2C\mathit{H}_A\mathit{H}_E$]$_3$}, and 0.75 [d, J = 6.9 Hz, 9H, ($C\mathit{H}_3$)$_3$].

^{13}C NMR (75 MHz, $CDCl_3$): δ 73.4, 59.0, 50.0, 45.0, 34.8, 31.9, 25.4, 22.9, 22.5, 21.5, 18.3, and 15.8.

HRMS (ESI) Calc'd for $C_{32}H_{62}NaO_4Si^+$ (M + Na^+): 561.4310 found 561.4292.

GC/MS (Method: 50 °C, hold for two min; ramp at 20 °C/min for 10 min, hold at 250 °C for three min) t_R = 12.16 min; *m/z* 538 (40, M^+), 523 (10. M^+-Me), 453 (100), 399 (90), 315 (20), 261 (20), and 138 (60).

IR (thin film) 2953, 2921, 2870, 1455, 1387, 1371, 1280, 1155, 1101, 1083, 1070, 1052, 1002, 980, 963,939, 889, 831, 804, and 757.

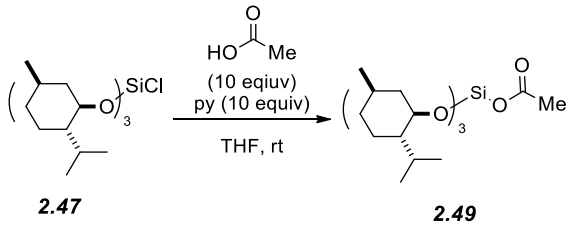

2.47 ***2.49***

Tri-(1*R*,2*S*,5*R*)-2-isopropyl-5-methylcyclohexoxyacetoxysilane (2.49). Trimenthyloxychlorosilane[39] (226.3 mg, 0.428 mmol, 1 equiv) was added to an oven-dried 5 mL culture tube containing a stir bar and dissolved in 5 mL of dry THF. Distilled pyridine (0.34 mL, 4.20 mmol, 10 equiv) and glacial acetic acid (0.24 mL, 4.19 mmol, 10 equiv) were added. Within minutes, a white precipitate formed. The vessel was sealed with a Teflon®-lined cap and monitored by GC/MS. After 4 h, no starting material remained, and the reaction was filtered through a plug of glass wool to remove the pyridinium salt, concentrated under reduced pressure, and redissolved in a minimal amount of 49:1 hexanes:EtOAc.

If a slurry resulted, this was filtered prior to being loaded onto a silica gel column. Purification by MPLC was completed using 49:1 hexanes:EtOAc as the eluent. The product was concentrated under reduced pressure to yield 0.0133 g of tetramenthyloxy orthosilicate and, in a later eluting fraction, the pure title product (139.2 mg, 0.252 mmol, 58.9%) as a colorless oil.

^{1}H NMR (500 MHz, $CDCl_3$): δ 3.68 [ddd, *J* = 4.3, 10.5, 10.5 Hz, 3H, $Si(OCH)_3$], 2.23 {dsept, *J* = 2.3, 6.8 Hz, 3H $[(CH_3)_2CH]_3$}, 2.10-2.01 [m, 3H, $Si(OCHCH_ACH_E)_3$], 2.07 [s, 3H, $C(O)CH_3$], 1.67-1.56 {m, 6H, $[(CH_3)_2CHCHCH_ACH_ECH_ACH_E]_3$}, 1.37 [ddddq, *J* = 3, 3, 12, 12, 7 Hz, 3H, $(CH_3CH)_3$], 1.18 {dddd, *J* = 3.1, 4.6, 9.9, 12.2 Hz, 3H $[(CH_3)_2CHCH]_3$}, 1.05 [ddd, *J* = 10.5, 12.1, 12.1 Hz, 3H, $Si(OCHCH_AH_E)_3$], 0.95 {dddd, *J* = 2.8, 12.5, 12.5, 12.5 Hz, 3H, $[(CH_3)_2CHCHCH_AH_E]_3$}, 0.90 [d, *J* = 6.5 Hz, 9H, $(CH_3)_3$], 0.89 [d, *J* = 7.1 Hz, 9H, $(CH_3)_3$], 0.83 {dddd, *J* = 3.1, 12.7, 12.7, 12.7 Hz, 3H, $[(CH_3)_2CHCHCH_2CH_AH_E]_3$}, and 0.76 [d, *J* = 6.9 Hz, 9H, $(CH_3)_3$].

^{13}C NMR (75 MHz, $CDCl_3$): δ 169.4, 74.2, 49.8, 44.7, 34.6, 31.8, 25.4, 23.0, 22.9, 22.4, 21.4, and 15.9.

HRMS (ESI) Calc'd for $C_{32}H_{62}NaO_5Si^+$ ($M + Na^+$): 575.4102 found 575.4144.

GC/MS (Method: 50 °C, hold for two min; ramp at 20 °C/min for 12 min, hold at 290 °C for seven min) t_R = 14.59 min; *m/z* 509 (100), 425 (10), 371 (20), and 139 (40).

IR (thin film) 2955, 2925, 2871, 1740, 1455, 1370, 1248, 1181, 1086, 1054, 1020, 1004, 946, 893, 833, 794, 768, 749, and 715.

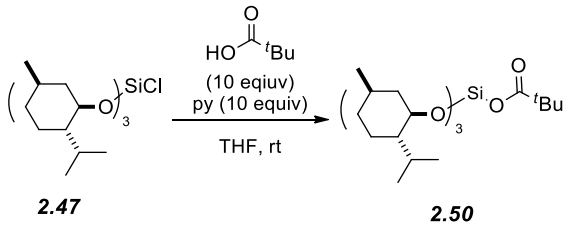

2.47 ***2.50***

Tri-(1*R*,2*S*,5*R*)-2-isopropyl-5-methylcyclohexoxypivaloxysilane (2.50). Trimenthyloxychlorosilane[39] (227.2 mg, 0.429 mmol, 1 equiv) was added to an oven-dried 5 mL culture tube containing a stir bar and dissolved in 5 mL of dry THF. Distilled pyridine (0.34 mL, 4.20 mmol, 10 equiv) and pivalic acid (437 mg, 4.29 mmol, 10 equiv) were added. Within minutes, a white precipitate formed. The reaction was sealed with a Teflon®-lined cap, stirred at room temperature, and monitored by GC/MS. After 5 h, no starting material remained, and the reaction was filtered through a plug of glass wool to remove the pyridinium salt, concentrated under reduced pressure, and redissolved in a minimal amount of 99:1 hexanes:EtOAc. If a slurry resulted, this was filtered prior to being loaded onto a silica gel column. Purification by MPLC was completed using 99:1 hexanes:EtOAc as the eluent to yield the title product (137.9 mg, 0.232 mmol, 54.1%) as a colorless oil.

^{1}H NMR (300 MHz, $CDCl_3$): δ 3.77 [ddd, *J* = 4.3, 10.5, 10.5 Hz, 3H, $Si(OCH)_3$], 2.22 {dsept, *J* = 2.4, 7.0 Hz, 3H, $[(CH_3)_2CH]_3$}, 2.10-2.00 [br m, 3H, $Si(OCHCH_AC\mathit{H}_E)_3$], 1.68-1.52 {m, 6H, $[(CH_3)_2CHCHCH_AC\mathit{H}_ECH_AC\mathit{H}_E]_3$}, 1.44-1.27 [br m, 3H, $(CH_3C\mathit{H})_3$], 1.23-1.12 {m, 3H $[(CH_3)_2CHC\mathit{H}]_3$}, 1.21 [s, 9H, $SiOC(O)C(C\mathit{H}_3)_3$], 1.04 [ddd, *J* = 10.6, 12.0, 12.0 Hz, 6H, $Si(OCHC\mathit{H}_AH_E)_3$], 0.95 {dddd, *J* = 3.2, 12.2, 12.2, 12.2 Hz, 3H, $[(CH_3)_2CHCHC\mathit{H}_AH_E]_3$}, 0.89 [d, *J* = 6.5 Hz, 9H, $(C\mathit{H}_3)_3$], 0.88 [d, *J* = 7.0 Hz, 9H, $(C\mathit{H}_3)_3$], 0.89-0.74 {m, 3H, $[(CH_3)_2CHCHCH_2C\mathit{H}_ACH_E]_3$}, and 0.74 [d, *J* = 6.9 Hz, 9H, $(C\mathit{H}_3)_3$].

^{13}C NMR (75 MHz, $CDCl_3$): δ 177.1, 74.2, 49.8, 44.7, 39.7, 34.7, 31.8, 27.3, 25.5, 23.0, 22.4, 21.4, and 16.0.

HRMS (ESI) Calc'd for $C_{32}H_{62}NaO_4Si^+$ (M + Na^+): 617.4572 found 617.4572.

GC/MS (Method: 50 °C, hold for two min; ramp at 20 °C/min for 12 min, hold at 290 °C for seven min) t_R = 13.35 min; *m/z* 493 (10), 455 (30), 317 (30), 301 (20), 179 (30), 163 (100), and 137 (20).

IR (thin film) 2954, 2923, 2871, 1727, 1456, 1370, 1291, 1236, 1175, 1101, 1086, 1054, 1003, 941, 905, 893, 831, 827, 813, and 730.

An alternative, one-pot procedure for the synthesis of 2.49 and 2.50. An oven-dried two-neck round bottom flask fitted with an oven-dried addition funnel and stir bar was purged with dry N_2. To this vessel, dry THF was added followed by the transfer of $SiCl_4$ via a dried, glass syringe. Menthol (3.1-3.4 equiv) and pyridine (3.1-3.4 equiv) were co-dissolved in dry THF and transferred to the closed addition funnel. The solution of menthol/pyridine was added dropwise to the solution of $SiCl_4$. The mixture was allowed to stir overnight. A final THF solution consisting of an excess of the carboxylic acid and pyridine (equimolar amounts) was prepared and transferred to the addition funnel, again allowing the solution to add to the bulk reaction dropwise. The reaction was again stirred at room temperature overnight. The reaction was filtered through a paper filter to remove the pyridinium salt, concentrated under reduced pressure, and redissolved in a mixture of hexanes and EtOAc. The product was then purified by MPLC with a mixture of hexanes and EtOAc as the mobile phase.

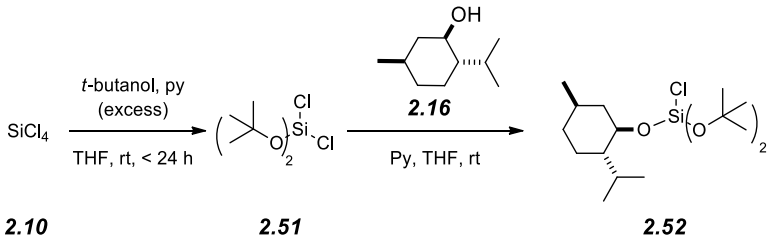

2.10 ***2.51*** ***2.52***

Di-*t*-butoxy-(1*R*,2*S*,5*R*)-2-isopropyl-5-methylcyclohexoxychlorosilane (2.52). An oven-dried 100 mL, 3-neck round bottom flask with an attached addition funnel and containing a magnetic stir bar was purged with N_2 (g). To this apparatus, 15 mL of dry THF was added followed by the addition of $SiCl_4$ (0.50 mL, 4.36 mmol, 1.0 equiv) in an dry, air-tight glass syringe. Pyridine (1.1 mL, 13.6 mmol, 3.1 equiv) was co-dissolved with *t*-butanol (1.3 mL, 13.6 mmol, 3.1 equiv) in 10 mL of dry THF and transferred to the addition funnel. The solution of pyridine and *t*-butanol was added dropwise over the course of ca. 15 minutes to the solution of $SiCl_4$ at room temperature. The reaction was monitored by GC/MS. After stirring at room temperature for 20 h under N_2, a solution of pyridine (50 µL, 0.654 mmol, 1.5 equiv) and menthol (0.101 g, 0.654 mmol, 1.5 equiv) co-dissolved in 10 mL of dry THF was added dropwise over the course of ca. five minutes. The reaction mixture was stirred for an additional 22 h overnight at room temperature. The reaction mixture was filtered through a paper filter, concentrated under reduced pressure, and redissolved in a minimal amount of 99:1 hexanes:ethyl acetate. If a slurry resulted, this was filtered prior to being loaded onto a silica gel column. Purification by MPLC using 99:1 hexanes:ethyl acetate as the eluent yielded the title compound (0.510 g, 1.40 mmol, 32%) as a colorless oil.

^{1}H NMR (500 MHz, $CDCl_3$): δ 3.74 (ddd, *J* = 4.3, 10.4, 10.4 Hz, 1H, SiOC*H*), 2.24 [dsept, *J* = 2.6, 7.1 Hz, 1H $(CH_3)_2CH$], 2.15-2.10 (m, 1H, $SiOCHCH_ACH_E$), 1.66-1.57 [m, 2H, $(CH_3)_2CHCHCH_ACH_ECH_ACH_E$], 1.44-1.28 (m, 1H, CH_3CH), 1.354 [s,

9H, SiOC(C*H*$_3$)], 1.350 [s, 9H, OSiOC(C*H*$_3$)], 1.20 [dddd, *J* = 2.5, 2.5, 10.1, 12.6 Hz, 1H $(CH_3)_2CHCH$], 1.04 [ddd, *J* = 10.6, 12.2, 12.2 Hz, 1H, SiOCHCH_AH_E], 0.95 [dddd, *J* = 3.1, 12.7, 12.7, 12.7 Hz, 1H, $(CH_3)_2CHCHCH_AH_E$], 0.90 (d, *J* = 6.5 Hz, 3H, C*H*$_3$), 0.89 (d, *J* = 7.1 Hz, 3H, C*H*$_3$), 0.82 [dddd, *J* = 3.3, 12.4, 12.4, 12.4 Hz, 1H, $(CH_3)_2CHCHCH_2CH_ACH_E$], and 0.77 (d, *J* = 6.9 Hz, 3H, C*H*$_3$).

^{13}C NMR (75 MHz, $CDCl_3$): δ 75.4, 75.3, 74.6, 49.8, 44.4, 34.7, 31.8, 31.4, 31.4, 25.4, 22.9, 22.5, 21.4, and 16.0.

GC/MS (Method: 50 °C, hold for two min; ramp at 20 °C/min for 10 min, hold at 250 °C for five min) t_R = 8.42 min; *m/z* 364/366 (5, M^+), 349/351 (60, M^+ - Me), 279/281 (100), 223 (20), 155 (100), and 81 (90).

IR (thin film) 2976, 2956, 2930, 2871, 1456, 1390, 1367, 1244, 1184, 1078, 1031, 1003, 935, 883, 832, 800, and 760.

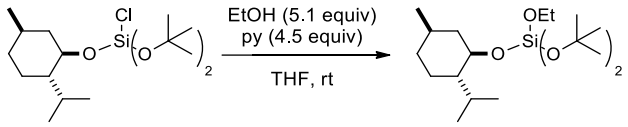

2.52 ***2.53***

Di-*t*-butoxyethoxy-(1*R*,2*S*,5*R*)-2-isopropyl-5-methylcyclohexoxysilane (2.53). Di-*t*-butoxychloro((2-isopropyl-5-methylcyclohexyl)oxy)silane (200. mg, 0.549 mmol, 1 equiv) was added to an oven-dried 5 mL culture tube containing a stir bar, and dissolved in a premixed solution of pyridine (0.20 mL, 2.5 mmol, 4.5 equiv) and anhdrous ethanol (0.16 mL, 2.8 mmol, 5.1 equiv) in 5.5 mL of dry THF. The reaction vessel was sealed with a Teflon®-lined cap and stirred at room temperature. A white precipitate was observed after stirring under the sealed tube for 60 h, at which time the reaction mixture was decanted to remove the

pyridinium salt, concentrated under reduced pressure, and redissolved in a minimal amount of 49:1 hexanes:EtOAc. If a slurry resulted, this was filtered prior to being loaded onto a silica gel column. The solution was filtered through glass wool, and purfied by MPLC using 49:1 hexanes:EtOAc as the eluent. The product was concentrated under reduced pressure to yield the title product (133 mg, 0.355 mmol, 64.7%) as a colorless oil.

^{1}H NMR (300 MHz, $CDCl_3$): δ 3.78 (q, *J* = 7.0 Hz, 2H, SiOC$H_2$$CH_3$) 3.64 (ddd, *J* = 4.3, 10.5, 10.5 Hz, 1H, SiOC*H*), 2.30 [dsept, *J* = 2.7, 7.0 Hz, 1H $(CH_3)_2$C*H*], 2.13-2.06 (m, 1H, SiOCHCH_ACH_E), 1.65-1.55 [m, 2H,$(CH_3)_2$CHCHCH_ACH_ECH_ACH_E], 1.38 (ddddq, *J* = 3.1, 3.1, 11.9, 11.9, 6.7 Hz, 1H, CH_3C*H*), 1.31 [s, 18H, SiOC(CH_3)$_3$ and SiOC(CH_3)$_3$], 1.20 (t, *J* = 7.0 Hz, 3H, SiOCH_2CH_3), 1.16 [dddd, *J* = 3.0, 3.0, 10.2, 12.9 Hz, 1H $(CH_3)_2$CHC*H*], 1.01 [ddd, *J* = 10.7, 12.2, 12.2 Hz, 1H, SiOCHC$H_A$$H_E$), 0.96, [dddd, *J* = 3.2, 12.8, 12.8, 12.8 Hz, 1H, $(CH_3)_2$CHCHC$H_A$$H_E$], 0.89 (d, *J* = 6.6 Hz, 3H, CH_3), 0.88 (d, *J* = 7.1 Hz, 3H, CH_3), 0.81 [dddd, *J* = 3.2, 12.5, 12.5, 12.5 Hz, 1H, $(CH_3)_2$CHCHCH_2CH_ACH_E], and 0.77 (d, *J* = 7.0 Hz, 3H, CH_3).

^{13}C NMR (125 MHz, $CDCl_3$): δ 73.0, 72.6, 72.5, 56.6, 49.8, 44.6, 34.6, 31.7, 31.4, 31.3, 25.1, 22.7, 22.4, 21.3, 18.1, and 15.6.

HRMS (ESI) Calc'd for $C_{20}H_{40}NaO_4Si^+$ (M + Na^+): 397.2745 found 397.2746.

IR (thin film) 2972, 2922, 2871, 1455, 1388, 1365, 1242, 1191, 1062, 1029, 1001, 959, 882, 832, 815, 757, and 703.

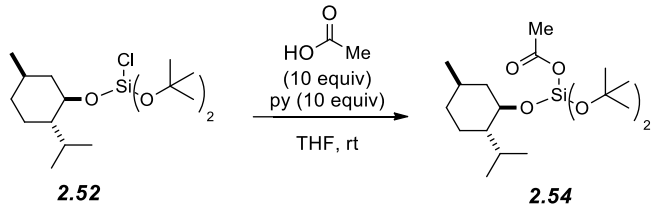

2.52 ***2.54***

Di-*t*-butoxy-(1*R*,2*S*,5*R*)-2-isopropyl-5-methylcyclohexoxyacetoxysilane (2.54). Di-*t*-butoxychloro((2-isopropyl-5-methylcyclohexyl)oxy)silane (96.4 mg, 0.264 mmol, 1 equiv) was added to an oven-dried 5 mL culture tube containing a stir bar and dissolved in 1.0 mL of dry THF. Pyridine (0.21 mL, 2.6 mmol, 10 equiv) and glacial acetic acid (0.15 mL, 2.6 mmol, 10 equiv) were added. The reaction vessel was sealed with a Teflon®-lined cap and stirred at room temperature. A white precipitate was formed after stirring for 16 h. The reaction was decanted to remove the pyridinium salt, concentrated under reduced pressure, and redissolved in a minimal amount of 99:1 hexanes:EtOAc, upon which a white precipitate formed immediately. The solution was filtered through glass wool, and purification by MPLC was completed using 99:1 hexanes:EtOAc followed 19:1 hexanes:EtOAc as the eleuents. The product was concentrated under reduced pressure to yield the title product (73.9 mg, 72.0%) as a colorless oil.

^{1}H NMR (300 MHz, $CDCl_3$): δ 3.76 (ddd, *J* = 4.4, 10.5, 10.5 Hz, 1H, SiOC*H*), 2.26 [dsept, *J* = 2.4, 7.0 Hz, 1H $(CH_3)_2CH$], 2.12-2.04 (m, 1H, $SiOCHCH_ACH_E$), 2.09 (s, 3H, $COCH_3$), 1.67-1.52 [m, 2H, $(CH_3)_2CHCHCH_ACH_ECH_ACH_E$], 1.46-1.35 (m, 1H, CH_3CH), 1.33 [s, 9H, $SiOC(CH_3)$], 1.32 [s, 9H, $SiOC(CH_3)$], 1.18 [dddd, *J* = 2.7, 2.7, 10.3, 12.7 Hz, 1H $(CH_3)_2CHCH$], 1.02 (ddd, *J* = 10.5, 12.0, 12.0 Hz, 1H, $SiOCHCH_ACH_E$), 0.91 [dddd, *J* = 2.9, 12.0, 12.0, 12.0 Hz, 1H, $(CH_3)_2CHCHCH_AH_E$], 0.90 (d, *J* = 6.4 Hz, 9H, CH_3), 0.89 (d, *J* = 7.1 Hz, 9H, CH_3),

0.85 [dddd, J = 3.0, 11.9, 11.9, 11.9 Hz, 1H, $(CH_3)_2CHCHCH_2CH_AH_E$], and 0.76 [d, J = 6.9 Hz, 9H, CH_3).

^{13}C NMR (125 MHz, $CDCl_3$): δ 168.6, 74.4, 74.3, 74.1, 49.9, 44.6, 34.7, 31.8, 31.4, 31.4, 25.4, 23.4, 22.9, 22.5, 21.4, and 15.9.

HRMS (ESI) Calc'd for $C_{20}H_{40}NaO_5Si^+$ (M + Na^+): 411.2537 found 411.2529.

GC/MS (Method: 50 °C, hold for two min; ramp at 20 °C/min for 13 min, hold at 310 °C for seven min) t_R = 8.18 min; *m/z* 373 (10, M^+ - Me), 315 (50, M^+ - O^{t}Bu), 275 (20), 233 (20), 177 (20), and 121 (100).

IR (thin film) 2975, 2955, 2928, 2871, 1740, 1456, 1389, 1367, 1245, 1194, 1079, 1020, 944, 884, 834, 804, and 737.

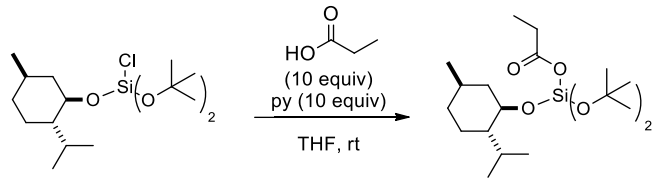

2.52 ***2.55***

Di-*t*-butoxy-(1*R*,2*S*,5*R*)-2-isopropyl-5-methylcyclohexoxypropionoxysilane (2.55). Di-*t*-butoxychloro((2-isopropyl-5-methylcyclohexyl)oxy)silane (85.0 mg, 0.233 mmol, 1 equiv) was added to an oven-dried 5 mL culture tube containing a stir bar and dissolved in 1.0 mL of dry THF. Pyridine (0.19 mL, 2.3 mmol, 10 equiv) and propanoic acid (0.17 mL, 2.3 mmol, 10 equiv) were added. The reaction vessel was capped with a Teflon®-lined cap and stirred at room temperature. After stirring for 22 h, a white precipitate was observed. The reaction was decanted to remove the pyridinium salt, concentrated under reduced pressure, and redissolved in a minimal amount of 19:1 hexanes:EtOAc.

The slurry was filtered through glass wool, and purification by MPLC was completed by using 19:1 hexanes:EtOAc as the eluent. The product was concentrated under reduced pressure to yield the title product (81.6 mg, 90.2%) as a colorless oil.

^{1}H NMR (500 MHz, $CDCl_3$): δ 3.76 (ddd, *J* = 4.3, 10.5, 10.5 Hz, 1H, SiOC*H*), 2.35 [q, *J* = 7.5 Hz, 2H, SiOC(O)CH_2CH$_3$], 2.26 [dsept, *J* = 2.6, 7.0 Hz, 1H $(CH_3)_2$C*H*], 2.11-2.05 (m, 1H, SiOCHCH$_A$CH_E), 1.66-1.56 [m, 2H,$(CH_3)_2$CHCHCH$_A$CH_ECH$_A$CH_E], 1.38 (ddddq, *J* = 3.1, 3.1, 8.5, 8.5, 6.8 Hz, 1H, CH$_3$C*H*), 1.33 [s, 9H, SiOC(CH_3)$_3$], 1.32 [s, 9H, SiOC(CH_3)$_3$], 1.18 [dddd, *J* = 3.1, 3.1, 10.4, 12.9 Hz, 1H $(CH_3)_2$CHC*H*], 1.13 [t, J = 7.5 Hz, 3H, SiOC(O)CH$_2$CH_3], 1.02 (ddd, *J* = 10.6, 12.2, 12.2 Hz, 1H, SiOCHCH_ACH$_E$), 0.94 (dddd, *J* = 3.1, 12.7, 12.7, 12.7 Hz, 1H, $(CH_3)_2$CHCHCH_AH$_E$], 0.90 (d, *J* = 6.6 Hz, 3H, CH_3), 0.89 (d, *J* = 7.1 Hz, 3H, CH_3), 0.81 (dddd, *J* = 3.2, 12.3, 12.3, 12.3 Hz, 1H, $(CH_3)_2$CHCHCH$_2$CH_AH$_E$], and 0.76 (d, *J* = 6.9 Hz, 3H, CH_3).

^{13}C NMR (75 MHz, $CDCl_3$): δ 172.4, 74.25, 74.22, 74.1, 49.9, 44.6, 34.7, 31.8, 31.4 (x2), 29.7, 25.3, 22.8, 22.5, 21.4, and 15.9.

HRMS (ESI) Calc'd for $C_{21}H_{42}NaO_5Si^+$ (M + Na^+): 425.2694 found 425.2702.

GC/MS (Method: 50 °C, hold for two min; ramp at 20 °C/min for 13 min, hold at 310 °C for seven min) t_R = 8.54 min; *m/z* 387 (5, M^+ - Me), 329 (60, M^+ - O^{t}Bu), 289 (20), 247 (20), 191 (10), and 135 (100).

IR (thin film) 2975, 2956, 2926, 2871, 1738, 1459, 1389, 1366, 1243, 1182, 1079, 1031, 1001, 935, 895, 835, 804, 756, and 703.

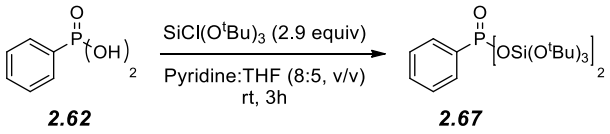

2.62 ***2.67***

Di (tri-*t*-butoxysilyl) phenyl phosphonic acid (2.67). Phenylphosphonic acid (81.7 mg, 0.517 mmol, 1 equiv) was suspended in a 1:1 mixture of dry THF and dry pyridine (1 mL total volume) in a 5 mL, oven-dried culture tube with a stir bar. The suspension was stirred for 10 mins, in which time the solution became homogenous. The purified tri-*t*-butoxychlorosilane (0.4262 g, 1.51 mmol, 2.9 equiv) was added and immediately a white precipitate was observed. The culture tube was capped and allowed to stir for 4 h. The crude material was passed through a short Celite® plug and passed through a silica plug. Concentration under reduced pressure and redissolution in a mixture of 9:1 hexanes:EtOAc and subsequent purification by two MPLC columns in 9:1 hexanes:EtOAc. An unsymmetrical MPLC peak was noted. The title compound was obtained pure as a white solid. (116.5 mg, 34.7%)

^{1}H NMR (500 MHz, $CDCl_3$): δ 7.93 (ddd, *J* = 1.3, 8.3, 14.4 Hz, 2H, *o*-Ar), 7.46 (ttd, *J* = 1.3, 1.3, 7.5 Hz, 1H, *p*-Ar), 7.40 (ddd, *J* = 4.2, 7.6, 7.6 Hz, 2H, *m*-Ar), and 1.27 [s, 54H, SiOC(C*H*$_3$)$_3$].

^{13}C NMR (125 MHz, $CDCl_3$): δ 132.7 (*J* = 196.8 Hz), 132.3 (*J* = 10.7 Hz), 131.2 (*J* = 3.2 Hz), 127.5 (*J* = 15.7 Hz), 73.9, and 31.4.

HRMS (ESI) Calc'd for $C_{30}H_{60}O_9PSi_2^+$ ($M + H^+$):651.3508, found 651.3512.

GC/MS (Method: 50 °C, hold for two min; ramp at 20 °C/min for 10 min, hold at 250 °C for three min) t_R = 11.23 min; *m/z* 577 (100, M^+ -O^{t}Bu), 521 (10), and 279 (30).

LC/MS (Method: C_8 column, gradient 50-98% methanol content over two min, then isocratic at 98% methanol content for 13 min, DAD 215 nm, 254 nm, 300 nm, and 350 nm, MW 121-1000, MM-ES+APCI Positive and MM-ES+APCI Negative) t_R = 13.9 min ($M\text{-}H^+$ 651.1).

IR (thin film) 2976, 1473, 1391, 1367, 1264, 1245, 1187, 1135, 1074, 1030, 998, 910, 837, 812, and 734.

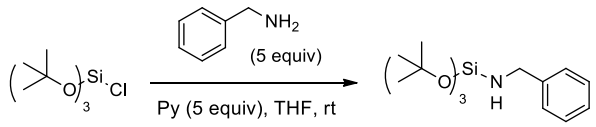

2.78

Benzylamino-tri-*t*-butoxysilane (2.78): Tri-*t*-butoxychlorosilane (200 µL, 0.71 mmol, 1.0 equiv) was transferred to an oven-dried culture tube with a Teflon-lined cap and stir bar and dissolved in dry THF (2.0 mL). Pyridine (100 µL, 1.24 mmol, 1.75 equiv) was added by Wiretrol®. Dry benzylamine (120 µL, 1.10 mmol, 1.55 equiv) was then added, and a white precipitate was observed in seconds. The culture tube was sealed and the solution was stirred at room temperature while being monitored by GC/MS. After stirring for 40 m, the tri-*t*-butoxychlorosilane was > 90% consumed. After a total of 75 m, the reaction was diluted with hexanes (3 mL), filtered through a short plug of Celite®, concentrated under reduced pressure, and redissolved in a mixture of hexane:ethyl acetate (99:1). Silica chromatography (SiO_2, 99:1 hexanes: ethyl acetate) via medium pressure liquid chromatography and drying under reduced pressure yielded the title compound as a colorless oil (39.6 mg, 0.11 mmol, 15.8%).

^{1}H NMR (300 MHz, $CDCl_3$): δ 7.40 (dd, *J* = 7.4, 2.1 Hz, 2H, CH_2-*o*-Ph), 7.30 (dd, *J* = 7.6, 7.1 Hz, 2H, CH_2-*m*-Ph), 7.20 (tt, *J* = 7.2, 2.3 Hz, 2H, CH_2-*p*-Ph), 3.97 (s, 2H, C*H*$_2$Ph), and 1.31 {s, 27H, SiO[C(C*H*$_3$)$_3$]$_3$}.

^{13}C NMR (75 MHz, $CDCl_3$): 128.3, 127.5, 126.4, 72.4, 45.9, and 31.7.

HRMS (ESI) Calc'd for $C_{19}H_{36}NO_3Si$ $[M + H]^+$ 354.2459, found 354.2467.

IR (thin film) 2974, 2930, 2870, 1495, 1471, 1454, 1388, 1364, 1240, 1191, 1054, 1027, 909, 828, 786, and 739.

GC/MS (Method: 30 °C, hold for two min; ramp at 20 °C/min for 14 min, hold at 310 °C for five min) t_R = 12.70 min; *m/z* 353 (25, M^+), 338 (40, M^+ - Me), 296 (100, M^+ - ^{t}Bu), 282 (10), 240 (30), 184 (70), 168 (40), 139 (30), 91 (20), and 77 (10).

General procedure for the hydrolysis studies of 2.25-2.28. The silicate ester (0.016 mmol) was dissolved in 900 µL of d_6-acetone. To this homogenous solution, 100 µL of a 9:1 v/v solution of D_2O : TFA was added, and the solution was vigorously mixed. The ^{1}H NMR spectra were recorded (16 transients) on a 500 MHz instrument at multiple time points over the course of multiple half-lives. The study was conducted at ambient temperature (ca. 22.5 °C ± 1.0 °C). To judge the extent of conversion, the H1 resonances in the menthyl moiety of the starting material menthyl silicate and product menthol were integrated in a baseline-corrected NMR spectrum using MestRe-C® software. The relative integration values were used to determine the extent of hydrolysis. Data from three replications were plotted on a semi-log scale to determine the k_{obs} values that were then converted to the k_{rel} data as presented. Errors are defined as the standard deviation of the three trials.

Chapter 3

Synthesis and Development of Silicate Ester Prodrugs of Paclitaxel.

1. Introduction.

Use of a prodrug that has altered the physical, chemical, and/or biological characteristics (e.g., metabolic stability, solubility, or pharmacokinetics) of a drug is a widely known tactic.[83,84] Most commonly, a prodrug is formed by a strategic chemical modification of the drug structure to impart advantageous physical, chemical, and/or biological properties. The prodrug is often therapeutically inert prior to activation by an *in vivo* chemical event (e.g., either chemical or metabolic hydrolysis, oxidation, or reduction) to regenerate the active agent. This concept of temporarily masking a property that is restored following a subsequent chemical cleavage event – not dissimilar to that of protecting group use in synthetic chemistry – has been widely applied to therapeutically relevant drugs,[85,86] including the antitumor agent paclitaxel (PTX, **1.01**).[87]

---

[83] Stella, V. J. A Case for Prodrugs. In *Prodrugs.* Stella, V. J.; Borchardt, R. T.; Hageman, M. J.; Oliyai, R.; Maag, H.; Tilley, J. W., eds. Springer Science: New York, 2007, 3–33.

[84] Stella, V. J. Prodrugs as Therapeutics. *Expert Opin. Ther. Patents*, **2004**, *14*, 277–280.

[85] Ettmayer, P.; Amidon, G. L.; Clement, B.; Testa, B. Lessons Learned from Marketed and Investigational Prodrugs. *J. Med. Chem.* **2004**, *47*, 2393–2404.

[86] Testa, B. Prodrug Research: Futile or Fertile? *Biochem. Pharmacol.* **2004**, *68*, 2097–2106.

2. The Silicate Ester Prodrug Strategy.[88]

1. Silicate Esters as Prodrugs. This fundamentally new prodrug strategy (Figure 3-1) is novel. As this concept was initially conceived and undertaken, the application of silicate esters as prodrugs was unprecedented,[5,13,18] leading to an inherently "high risk, high reward" scenario that necessitated extensive work on multiple model systems (described in Chapter 2). The results from these proof-of-principle studies led to the conclusion that silicate esters hold significant promise as a promoiety with strong potential to finely control physical *and* chemical properties.

Figure 3-1. The silicate prodrug strategy: modification of a hydroxyl group in the drug with a trialkoxychlorosilane generates the (labile) silicate prodrug, which, following administration, undergoes hydrolysis to return the free drug along with alcohol and orthosilicic acid byproducts.

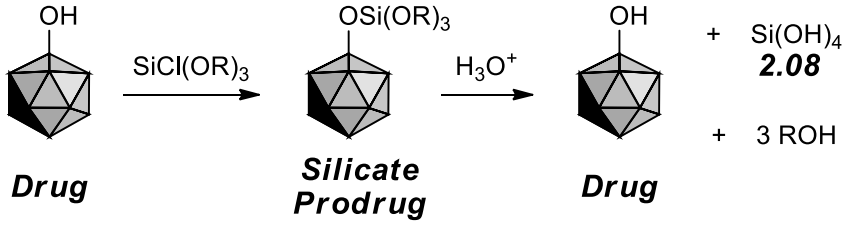

The innovative silicate ester prodrug design is predicated upon the hypothesis that a hydrolytically-labile orthosilicate ester (i.e., a tetraalkoxysilane) is an enabling platform. In principle, any drug with a derivitizable hydroxyl group (c.f., "**Drug**" in Figure 3-1) can be modified with an electrophilic silylating agent,

[87] Skwarczynski, M.; Hayashi, Y.; Kiso, Y. Paclitaxel Prodrugs: Toward Smarter Delivery of Anticancer Agents. *J. Med. Chem.* **2006**, *49*, 7253–7269.

[88] Wohl, A. R.; Kalscheuer, S.; Lee, H. S.; Han, J.; McCormick, A.; Macosko, C. W.; Panyam, J.; Hoye, T. R. A Silicate Ester Prodrug Strategy and in vivo Efficacy of Paclitaxel Prodrug-loaded Nanoparticles. *J. Am. Chem. Soc., submitted.*

such as a trialkoxychlorosilane,[89] resulting in a silicate ester prodrug (c.f., "**Prodrug**" in Figure 3-1). Hydrolytic cleavage catalyzed by a weak acid returns the parent drug while simultaneously liberating three equivalents of the sacrificial alcohol and orthosilicic acid (**2.08**). This basic strategy is attractive for both its simplicity as well as its general applicability to a variety of drug molecules

2. Toxicological Profile of Orthosilicic Acid. Orthosilicic acid [a.k.a., silicic acid, $Si(OH)_4$, compound **2.08**] is an unavoidable byproduct of the prodrug cleavage depicted in Figure 3-1. Given the intended application of these prodrugs, it is prudent to preemptively consider the biological profile of $Si(OH)_4$ and its oligomers. Notably, orthosilicic acid (and oligomers thereof) are, in fact, present in humans; we excrete such species at a rate of approximately 75 mg/day.[90,91]

Significant toxicological issues from the use of silicate prodrugs are not anticipated, and numerous studies on biological silicon support this assertion. For example, the degradation of cross-linked microparticles of dialkoxydialkysilanes demonstrated no toxicity at concentrations up to 100 µg/mL in HeLa or SKOV3 cells.[17] Additionally, implanted medical devices constructed from elemental silicon metal (Si°) are approved by the Food and Drug Administration (FDA). These materials are known to oxidatively degrade to silicic acids, and no significant detrimental effects have been reported.[47,92] Another study showed that a multi-gram charge of glass shards implanted subdermally in the back of a

[89] Corriu R. J. P.; Granier M.; Lanneau G. F. Synthesis and Reactivity of Bis(triethoxysilyl)methane, Tris(triethoxysilyl)methane and Some Derivatives. **1998** *J. Organomet. Chem. 562*, 79–88.

[90] Gitelman, H. J.; Alderman, F.; Perry, S. J. Renal Hnadling of Silicon in Normals and Patients with Renal Insufficiency. *Kidney Int.* **1992**, *42*, 957–959.

[91] Marco-Franco, J. E.; Torres, V. E.; Nixon, D. E.; Wilson, D. M; James, E. M.; Bergstrahl, E J.; McCarthy, J. T. Oxalate, Silicon, and Vanadium in Acquired Cystic Kidney Disease. *Clin. Nephrol.* **1991**, *35*, 52–58.

[92] Lai, W.; Garino, J.; Flaitz, C.; Ducheyne, P. Excretion of Resorption Products from Bioactive Glass Impanted in Rabbit Muscle. *J. Biomed. Mater. Res. Part A* **2005**, *75A*, 398–407.

rabbit was cleared over a period of several months by hydrolytic breakdown to (and excretion of) $Si(OH)_4$.[92] Furthermore, "no toxicity was observed" upon treatment of rat neuronal cells with silicic acid at concentrations up to 100μM,[93] and studies where human subjects orally ingested aqueous silicic acid noted excretion within 24 h.[90,91]

Despite this ample (albeit somewhat indirect) evidence for the *in vitro* and *in vivo* safety of orthosilicic acid and its oligomers, a control experiment was designed in collaboration with Stephen Kalscheuer, a graduate student in the laboratory of Prof. Jayanth Panyam (Department of Pharmaceutics, University of Minnesota) to further establish the safety of the byproducts of these degraded silicate prodrugs.[94] In this study, tetraethoxysilane (**2.07**) and triethoxymenthoxysilane (**2.25**) were subjected to an *in vitro* cytotoxicity assay. MDA-MB-231 cells were treated with a solution of either **2.07** or **2.25** dissolved in dimethyl sulfoxide (DMSO) and compared to control cells that were exposed only to pure DMSO. After 48 hours, the cells were treated with 3-(4,5-dimethylthiazol-2-yl)-5-(3-carboxymethoxyphyenyl)-2-(4-sulfophenyl)-2H-tetrazolium (MTS) to assess the viability of the cell culture.[95] In all cases (up to 10 μM concentrations of the silanes), cell viability was greater than 90% of the untreated control (Figure 3-2). Generally, the results of the model silicate ester treatments and the control were the same within error, further demonstrating the *in vitro* safety of the prodrug degradation byproducts.

---

[93] Mayne, A. H.; Bayliss, S. C.; Barr, P. Tobin, M.; Buckberry, L. D. Biologically Interfaced Porous Silicon Devices. *Phys. Status Solidi A – Appl. Res*. **2000**, *182*, 505–513.

[94] Kalscheuer, S.; Panyam, J. University of Minnesota, Minneapolis, MN. Personal communication, **2012**.

[95] Cory, A. H.; Owen, T. C.; Barltrop, J. A.; Cory, J. G. Use of an Aqueous Soluble Tetrazolium/Formazan Assay for Cell Growth Assays in Culture. *Cancer Comm.* **1991**, *3*, 207–212.

Figure 3-2. The cell viability of two representative silicate ester prodrug models [tetraethoxysilane (**2.07**), blue and triethoxymenthoxysilane (**2.25**), red] was found to be similar to the control groups at all concentrations examined.[94]

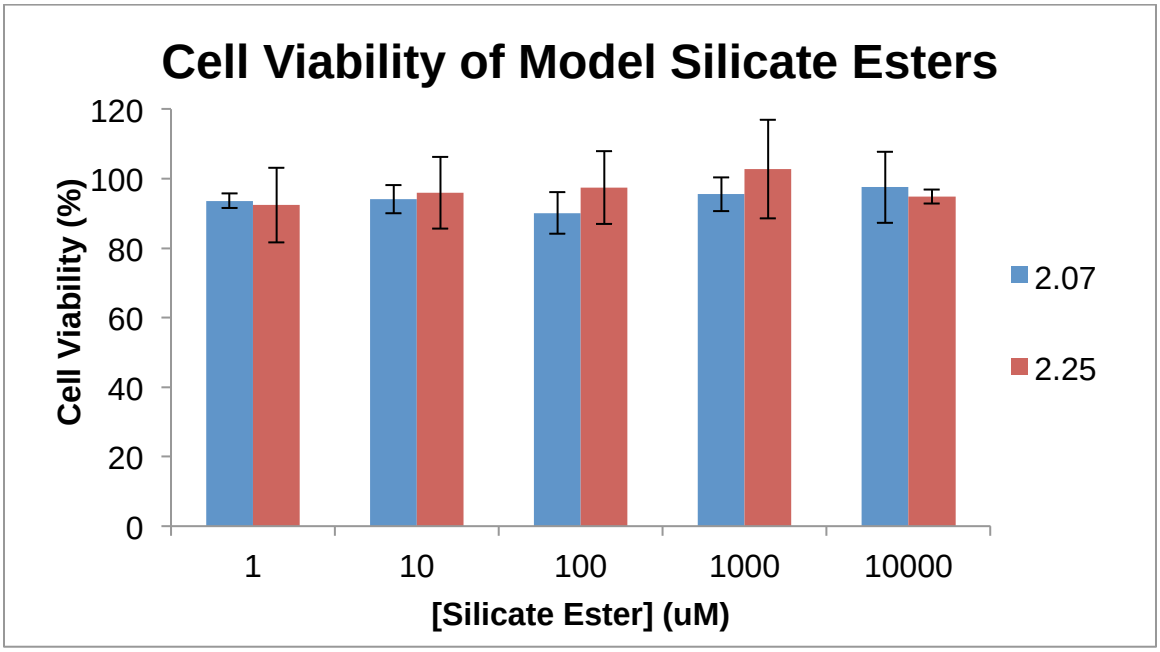

Error bars represent ± the standard deviation (SD) of the data.

3. Paclitaxel (PTX).

1. A Brief Overview of Clinical Formulations of Paclitaxel. Paclitaxel[96] (PTX, c.f. Scheme 1-1, **1.01**), the most famous natural product of the taxane

[96] Originally, compound **1.01** was named "taxol," leading to the still persistent confusion over the name of the drug molecule (i.e., taxol with a lower case "t") vs. the drug formulation (i.e., Taxol® with an upper case "T"). Historically, it was found after the name taxol was in widespread use, Taxol® was a previously trademarked name of a minor drug. By the time this came to be common knowledge, "taxol" was already widely recognized by the general public as a "miracle drug." To maintain the positive publicity that had already been garnered by this molecule, Bristol-Meyers Squibb (BMS), the eventual commercial producer and marketer of this chemotherapeutic, purchased the legal rights to the name Taxol® during commercialization. Thus, the chemical entity was renamed "paclitaxel" to attempt to alleviate further confusion and to reserve the name Taxol® for the clinical formulation of paclitaxel in Cremophor EL® (CrEL®). For a more detailed history and commentary on this subject, see Kingston, D. G. I. The Shape of Things to Come: Structural

family, was originally isolated from the bark of the Pacific Yew tree. After its structure was elucidated,[97] Horwitz and co-workers discovered that PTX induced cell death by the inhibition of tubulin depolymerization during cellular division – a mode of action unique at its time of discovery.[98] PTX continues to draw considerable interest due to its highly desirable anticancer efficacy.[99] However, despite promising cytotoxicity, it is too hydrophobic to be merely dissolved in, for instance, a saline solution and administered by traditional clinical routes [e.g., intravenous (IV) delivery]. Therefore, significant effort has been expended over the course of decades toward devising methods to formulate PTX for clinical use. Most often, this is done by employing the use of an excipient.

In Taxol®, the most widely used commercial drug formulation of PTX, Cremophor EL® (CrEL®, a 1:1 (v/v) mixture of polyethoxylated castor oil and absolute ethanol)[100] is used as an emulsification agent to effectively solubilize PTX. Previously, CrEL® has been safely used to formulate a wide variety of other drugs, including other antineoplastics, sedatives, and immunosuppressant. In these cases, the small volume (typically, only a few milliliters) of CrEL® that was necessarily administered had minimal side effects.[101] In the Taxol® formulation, however, especially high loads of CrEL® are required for successful administration (specifically, Taxol® contains only 1.14 wt% of PTX and a typical

---

and Synthetic Studies of Taxol and Related Compounds. *Phytochemistry* **2007**, *68*, 1844–1854 and references therein.

[97] Wani, M.C.; Taylor, H.L.; Wall, M.E.; Coggon, P.; McPhail, A.T. Plant Antitumor Agents. VI. The Isolation and Structure of Taxol, a Novel Antileukemic and Antitumor Agent from *Taxus brevifolia*. *J. Am. Chem. Soc.* **1971**, 2325–2327.

[98] Schiff, P. B.; Fant, J.; Horwitz, S. B. Promotion of Microtubule Assembly in vitro By Taxol. *Nature* **1979,** *277*, 665–667.

[99] Wang, Y.-F.; Shi, Q.-W.; Dong, M.; Kiyota, H.; Gu, Y.-C.; Cong, B. Natural Taxanes: Developments Since 1828. *Chem. Rev.* **2011**, *111*, 7652–7709.

[100] U.S. Food and Drug Administration. *TAXOL® (paclitaxel) INJECTION*. **2007**.

[101] ten Tije, A. J.; Verweij, J.; Loos, W. L.; Sparreboom, A. Pharmacological Effects of Formulation Vehicles: Implications for Cancer Therapy. *Clin. Pharmacokinet.* **2003**, *42*, 665–685.

dose is composed of ca. 25 mL of CrEL®). Unfortunately, at these high levels, pharmacologically and biologically of CrEL® is particularly dangerous. This onerous biological activity hindered the early development of Taxol®, with a dramatic example of two deaths that were attributed to the dosed CrEL.® Thankfully, this issue has been mitigated by a 24 hour infusion protocol.[102] Even today, however, a subpopulation of patients receiving Taxol® chemotherapy still experience significant, undesirable side effects, including, among others, serious acute hypersensitivity and peripheral neurotoxicity.[101,103,104]

Accordingly, significant efforts have been devoted to eliminating the use of CrEL® by replacement with a more benign adjuvant. These have included studies of formulations based on nanoparticles, liposomes, emulsions, and micelles.[103] It is beyond the scope of this (or any) thesis to comprehensively review all of these cases. Most notably, Abraxane® is a drug formulation of PTX that has been developed, earned FDA-approval, and brought to the market. It eliminates CrEL® and its associated hypersensitivity[105,106] by formulating PTX in human serum albumin at a much higher loading level than in Taxol® (Abraxane® is administered as approximately 10 wt% PTX).[107] In addition to eliminating the CrEL®-induced side effects, the efficacy of Abraxane® may be improved by its proposed ability to

[102] Wiernik, P. H.; Schwartz, E. L.; Einzig, A.; Strauman, J. J.; Lipton, R. B.; Dutcher, J. P. Phase I Trial of Taxol Given as a 24-Hour Infusion Every 21 Days: Responses Observed in Metastatic Melanoma. *J. Clin. Oncol.* **1987**, *5*, 1232–1239.

[103] Hennenfent, K. L.; Govindan, R. New Formulations of Taxol: A Review. Old Wine in a New Bottle? *Ann. Oncol.* **2006**, *17*, 735–749 and references therein.

[104] Gelderblom, H.; Verweij, J.; Nooter, K.; Sparreboom, A. Cremophor EL: The Drawbacks and Advantages of Vehicle Selection for Drug Formulation. *Eur. J. Cancer* **2001**, *37*, 1590–1598.

[105] Scripture, C. D.; Figg, W. D.; Sparreboom, A. Paclitaxel Chemotherapy: From Empiricism to a Mechanism-Based Formulation Strategy. *Ther. Clin. Risk Manag.* **2005**, *1*, 107–114.

[106] Sparreboom, A.; Baker, S. D.; Verweij, J. Paclitaxel Repackaged in an Albumin-Stabilized Nanoparticle: Handy or Just Dandy? *J. Clin. Oncol.* **2005**, *23*, 7765–7767.

[107] U.S. Food and Drug Administration. ABRAXANE™ for Injectable Suspension (paclitaxel protein-bound particles for injectable suspension) (albumin-bound). **2005**.

uniquely target the albumin-specific gp60 receptors that are prolific on tumors.[108] However, the use of Abraxane® remains limited due to its high financial costs and its failure to increase the survival time of "first-line" cancer patients (i.e., those that have not yet received chemotherapy).[109] Thus, it is currently approved only for "second-line" metastatic breast cancer patients (i.e., those patients that have been ineffectively treated with well-established chemotherapeutics).[110]

2. Selected, Relevant Pre-Clinical Formulations of Paclitaxel. Another noteworthy effort that aims to eliminate CrEL® from PTX-containing chemotherapeutics is the relatively recent development of Genexol-PM®. This formulation utilizes poly(ethylene glycol)-*b*-poly(lactic acid) (PEG-*b*-PLA) to create micelles containing PTX trapped in the hydrophobic micellular core. The inventors of this work claim loading levels of 16.7[111] to 25 wt% PTX.[112] These drug-loaded micelles are then lyophilized and redispersed in a 5% dextrose solution prior to administration. Genexol-PM® has shown considerable promise for the treatment of breast cancer, and it has completed Phase II clinical trials,[113] although it has not yet achieved full FDA-approval.

---

[108] Ibrahim, N. K.; Desai, N.; Legha, S.; Soon-Shiong, P.; Theriault, R. L.; Rivera, E.; Esmaeli, B.; Ring, S. E.; Bedikian, A.; Hortobagyi, G. N.; Ellerhorst, J. A. Phase I and Pharmacokinetics Study of ABI-007, a Cremophor-Free, Protein-Stabilized, Nanoparticle Formulation of Paclitaxel. *Clin. Cancer Res.* **2002**, *8*, 1038–1044.

[109] Gradishar, W. J.; Tjulandin, S.; Davidson, N.; Shaw, H.; Desai, N.; Bhar, P.; Hawkins, M.; O'Shaughnessy, J. Phase III Trial of Nanoparticle-Albumin Bound Paclitaxel Compared with Polyethylated Castor Oil-Based Paclitaxel in Women with Breast Cancer. *J. Clin. Oncol.* **2005**, *23*, 7794–7803.

[110] Harries, M.; Ellis, P.; Harper, P. Nanoparticle Albumin-bound Paclitaxel for Metastatic Breast Cancer. *J. Clin. Oncol.* **2005**, *23*, 7768–7771.

[111] Kim, S. C.; Kim, D. W.; Shim, Y. H.; Bang, J. S.; Oh, H. S.; Kim, S. W.; Seo, M. H. In vivo Evaluation of Polymeric Micellar Paclitaxel Formulation: Toxicity and Efficacy. *J. Control. Release* **2001**, *72*, 191–202.

[112] Hangal-Joshi, R.; Gore, A. Y.; Rubinfeld, J.; Shrotriya, R. Paclitaxel Formulation. U.S. Patent 6,538,020, August 1, 2002.

[113] Lee, K. S.; Chung, H. C.; Im, S. A.; Park, Y. H.; Kim, C. S.; Kim, S.-B.; Rha, S. Y.; Lee, M. Y.; Ro, J. Multicenter Phase II Trial of Genexol-PM, a Cremophor-Free Polymeric Micelle

A second, recently reported formulation tactic for PTX was used to create Nanotax®.[114] This innovation is notable in that it consists solely of PTX – no excipient is needed. This achievement is realized by spraying small droplets of an organic solvent containing dissolved PTX into supercritical carbon dioxide. Upon evaporation of the solvent, the resulting precipitated PTX microcrystal is approximately 600-700 nm.[114] Administration of the Nanotax® suspension has shown preliminary promise in mouse *in vivo* tumor models[115] and Phase I studies.[116]

3. Docetaxel and its Formulation as Taxotere®. An additional on-the-market taxane drug is significant. Docetaxel (**3.01** in Figure 3-3) has been incorporated with polysorbate 80 (i.e., Tween 80®, **3.02** in Figure 3-3) to create Taxotere®.[117,118] The structure of docetaxel varies subtly from PTX (the C3' benzoyl amide is replaced by a C3' boc carbamate and the C10 acetate in PTX is a hydroxyl in docetaxel), and it is slightly more water-soluble than PTX. The administration of docetaxel as Taxotere® eliminates the need for CrEL®, leading

---

Formulation of Paclitasel, in Patients with Metastatic Breast Cancer. *Breast Cancer Res. Treat.* **2008**, *108*, 241–250.

[114] Niu, F.; Roby, K. F.; Rajewski, R. A.; Decedue, C.; Subramaniam, B. Paclitaxel Nanoparticles: Production Using Compressed CO_2 as Antisolvent: Characterization and Animal Studies. In *Polymeric Drug Delivery II;* Svenson, S., ed. American Chemical Society: Washington, D. C., 2006, 262–277.

[115] Roby, K. F.; Niu, F.; Rajewski, R. A.; Decedue, C.; Subramaniam, B.; Terranova, P. F. Syngenic Mouse Model of Epithelial Ovarian Cancer: Effects of Nanoparticle Paclitaxel, Nanotax®. *Adv. Exp. Med. Biol.* **2008**, *622*, 169–181.

[116] Axiak, S. M.; Selting, K. A.; Decedue, C. J.; Henry, C. J.; Tate, D.; Howell, J.; Bilof, K. J.; Kim, D. Y. Phase I Does Escalation Study of Nanoparticulate Paclitaxel (CTI 52010) in Normal Dogs. *Int. J. Nanomedicine* **2011**, *6*, 2205–2212.

[117] Crown, J. Docetaxel and Paclitaxel in the Treatment of Breast Cancer: A Review of Clinical Experience. *Oncologist* **2004**, *9*, 24–32.

[118] Bernstein, B. Docetaxel as an Alternative to Paclitaxel after Acute Hypersensitivity Reactions. *Ann. Pharmacother.* **2000**, *34*, 1332–1335.

to minimal hypersensitivity in patients; however, neurotoxicity and poor drug distribution/clearance are still reported.[119,120]

Figure 3-3. The chemical structures of the components of Taxotere® – docetaxel **3.01** and Tween 80® **3.02**.

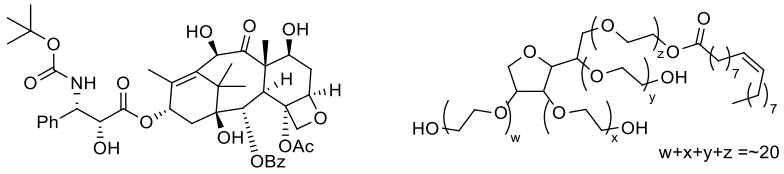

3.01 ***3.02***

4. Hydrophilic Derivatives of PTX. Beyond improving PTX-containing chemotherapeutic formulations solely by improving the excipient load and properties, structural modifications of PTX have also been considered. Various PTX [and other taxane-based (e.g., docetaxel)] prodrugs and drug conjugates have been explored, in part with an eye toward identification of a bioactive agent that might no longer require the use of any formulation agent. Typically, these efforts have centered on increasing the hydro*philicity* of the parent taxane, thereby improving its classical solubility parameters.[87] For example, a non-inclusive list of PTX prodrugs includes phosphate ester prodrugs,[121,122] amino

[119] Norris, L. B.; Qureshi, Z. P.; Bookstaver, P. B.; Raisch, D. W.; Sartor, O.; Chen, H.; Bennet, C. L. Polysorbate 80 Hypersensitivity Reactions: A Renewed Call to Action. *Commun. Oncol.* **2010**, *7*, 425–428.

[120] Echhoff, L.; Nielsen, M.; Moeller, S.; Knoop, A. TAXTOX – A Retrospective Study Regarding the Side Effects of Docetaxel Given as Part of the Adjuvant Treatment to Patients with Primary Breast Cancer in Denmark from 2007 to 2009. *Acta. Oncologica.* **2011**, *50*, 1075–1082.

[121] Vyas, D. M.; Wong, H.; Crosswell, A. R.; Casazza, A. M.; Knipe, J.O.; Mamber, S. W.; Doyle, T. W. Tumor targeting by covalent conjugation of a natural fatty acid to paclita. *Bioorg. Med. Chem. Lett*. **1993**, *3*, 1357–1360.

[122] Moosavi-Movahedi, A. A.; Hakimelahi, S.; Chamani, J.; Khodarahmi, G. A.; Hassanzadeh, F.; Luo, F. T.; Ly, T. W.; Shia, K.-S.; Yen, C. F.; Jain, M. L.; Kulatheeswaran, R.; Xue, C.; Pasdar, M.; Hakimelahi, G. H. Design, Synthesis, and Anticancer Activity of Phosphonic Acid Diphosphate Derivative of Adenine-Containing Butenolide and its Water Soluble Derivatives of Paclitaxel with High Antitumor Activity. *Bioorg. Med. Chem.* **2003**, *11*, 4303–4313.

acid conjugates,[123] succinates,[124] and sugar conjugates.[125] Further efforts have been directed toward covalent conjugation of PTX to macromolecules such as poly(ethylene glycol),[126,127,128] polysaccharides,[129] and poly(amino acids).[130] All of these compounds have been synthesized in attempts to increase the aqueous solubility of PTX.

5. Hydrophobic Derivatives of PTX. Conversely (and, perhaps, ironically), the use of PTX prodrugs that are *more hydrophobic* than PTX itself has also been explored. The motivating hypothesis is that such prodrugs can be more efficiently loaded into the hydrophobic regions of the various encapsulating vehicles, thereby reducing the overall amount of excipient. Examples of such hydrophobic derivatives include modification of PTX as a steroidal (cholesterol) carbonate,[131] phospholipid,[132] fullerene,[133] α-bromo fatty ester,[134] or as a fatty

---

[123] Paradis, R.; Page, M. New Active Paclitaxel Amino Acid Derivatives with Improved Water Solubility. *Anticancer Res.* **1998**, *18*, 2711–2716.

[124] Deutsch, H. M.; Glinski, J. A.; Hernandez, M.; Haugwitz, R. D.; Narayanan, V. L.; Suffness, M.; Zalkow, L. H. Synthesis of Congeners and Prodrugs. 3. Water-Soluble Prodrugs of Taxol with Potent Antitumor Activity. *J. Med. Chem.* **1989**, *32*, 788–792.

[125] Khmelnitsky, Y. L.; Budde, C.; Arnold, M. J.; Usyatinsky, A.; Clark, D. S.; Dordick, J. S. Synthesis of Water-Soluble Paclitaxel Derivatives by Enzymatic Acylation*. J. Am. Chem. Soc.* **1997**, *119*, 11554–11555.

[126] Greenwald, R. B.; Pendri, A.; Bolikal, D.; Gilbert, C. W. Highly Water Soluble Taxol Derivatives: 2-Polyethylene Glycol Esters as Potential Prodrugs. *Bioorg. Med. Chem. Lett*. **1994**, *4*, 2465–2470.

[127] Greenwald, R. B.; Gilbert, C. W.; Pendri, A.; Conover, C. D.; Xia, J.; Martinez, A. Drug Delivery Systems: Water Soluble Taxol 2'-Poly-(Ethylene Glycol) Ester Prodrugs. Design and in vivo Effectiveness. *J. Med. Chem*. **1996**, *39*, 424–431.

[128] Rodrigues, P. C. A.; Scheuermann, K.; Stockmar, C.; Maier, G.; Fiebig, H. H.; Unger, C.; Muelhaupt, R.; Kratz, F. Synthesis and in vitro Efficacy of Acid-Sensitive Poly(ethylene glycol) Paclitaxel Conjugates. *Bioorg. Med. Chem. Lett*. **2003**, *13*, 355–360.

[129] Luo, Y.; Prestwich, G. D. Synthesis and Selective Cytotoxicity of a Hyaluronic Acid-Antitumor Bioconjugate. *Bioconjugate Chem.* **1999**, *10*, 755–763.

[130] Li, C.; Yu, D. F.; Newman, R. A.; Cabral, F.; Stephens, L. C.; Hunter, N.; Milas, L.; Wallace, S. Complete Regression of Well-Established Tumors using a Novel Water-Soluble Poly(L-glutamic acid)-Paclitaxel Conjugate. *Cancer Res.* **1998**, *58*, 2404–2409.

[131] Stevens, P. J.; Sekido, M.; Lee, R. J. A Folate Receptor-Targeted Lipid Nanoparticle Formulation for a Lipophilic Paclitaxel Prodrug. *Pharm. Res.* **2004**, *21*, 2153–2157.

ester derivatives.[8,135,136] Most notably, however, is the conjugation of docosahexaenoate (DHA) via ester bond formation at the C2' hydroxyl to give a new DHA-PTX drug conjugate (**3.03**, Figure 3-4).[137] **3.03** has been studied in Phase III clinical trials.[138]

Figure 3-4. The chemical structure of the DHA ester of PTX (**3.03**).

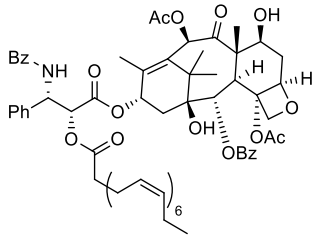

3.03

All of these hydrophobic derivatives have demonstrated notably higher load levels within drug delivery vehicles. However, the PTX derivatives demonstrated lower (or no) *in vitro* activity at equimolar concentration vis-à-vis

[132] Ansell, S. Lipophilic Drug Derivatives for Use in Liposomes. U.S. Patent 5,534,499, July 9, 1996.

[133] Zakharian, T. Y.; Seryshev, A.; Sitharaman, B.; Gilbert, B. E.; Knight, V.; Wilson, L. J. A Fullerene-Paclitaxel Chemotherapeutic: Synthesis, Characterization and Study of Biological Activity in Tissue Culture. *J. Am. Chem. Soc.* **2005**, *127*, 12508–12509.

[134] Ali, S.; Ahmad, I.; Peters, A.; Masters, G.; Minchey, S.; Janoff, A. S.; Mayhew, E. Hydrolyzable Hydrophobic Taxanes: Synthesis and Anticancer Activities. *Anti-Cancer Drugs* **2001**, *12*, 117–128.

[135] Lundberg, B. B.; Risovic, V.; Ramaswamy, M.; Wasan, K. M. A Lipophilic Pacltaxel Derivative Incorporated in a Lipid Emulsion for Parenteral Administration. *J. Control. Release* **2003**, *86*, 93–100.

[136] Rodrigues, D. C.; Maria, D. A.; Fernandes, D. C.; Valduga, C. J.; Couto, R. D.; Ibanez, O. C. M.; Maranhao, R. C. Improvement of Paclitaxel Therapeutic Index by Derivatization and Association to a Cholesterol-Rich Microemulsion: in vitro and in vivo Studies. *Cancer Chemother. Pharmacol.* **2005**, *55*, 565–576.

[137] Bradley, M. O.; Webb, N. L.; Anthony, F. H.; Devanesan, P.; Witman, P. A.; Hemamalini, S.; Chander, M. C.; Baker, S. D.; He, L.; Horwitz, S. B.; Swindell, C. S. Tumor Targeting by Covalent Conjugation of a Natural Fatty Acid to Paclitaxel. *Clin. Cancer Res*. **2001**, *7*, 3229–3238.

[138] Bedikian, A. Y.; DeConti, R. C.; Conry, R.; Agarwala, S.; Papadopoulos, N.; Kim, K. B.; Ernstoff, M. Phase 3 Study of Docosahexaenoic Acid-Paclitaxel Versus Dacarbazine in Patients with Metastatic Malignant Melanoma. *Ann. Oncol.* **2011**, *22*, 787–793.

PTX against cancer cell lines,[8,131,137] despite their higher loading capacity into encapsulating vehicles. Formulation of the PTX-DHA conjugate **3.03**, for instance, is able to be formulated using ca. 20% less CrEL® than is required for PTX. Promising behavior in *in vivo* studies has been further observed, allowing the advancement of the DHA ester to a Phase III human clinical trial under the trade name of Taxoprexin®, but has not yet been FDA-approved or marketed.[138,139]

These encouraging indications have further motivated our interest in the development of the novel silicate prodrug strategy introduced above, specifically in the context of (and as a forerunner to) PTX prodrug therapy. We aim to demonstrate the ability to control *both* the extent of hydrophobicity and the hydrolysis rate of a series of PTX-silicate prodrug candidates analogous to the alkoxy silicate ester models described in Chapter 2. We further note that this strategy has considerable potential for general applicability to many other prodrugs beyond PTX – as is detailed in sections 3.4 and 3.5.

6. PTX Silicate Prodrug Design and Synthesis of Tetraalkoxy PTX Silicate Prodrugs.[140] A suite of PTX silicate ester prodrugs **3.04**-**3.12** (Figure 3-5) was selected for study and synthesized in moderate to high yields. The members of this family differed in their i) hydrophobicity (e.g., **3.04** vs. **3.05**), ii) anticipated hydrolytic lability based on steric differences (e.g., **3.04** vs. **3.06** vs. **3.07**), iii) and sites of the silylated hydroxyl group (e.g., **3.04** vs. **3.08** vs. **3.11**). The rationale for each of these systematic changes is described hereafter.

[139] Harries, M.; O'Donnell, A.; Scurr, M.; Reade, S.; Cole, C.; Judson, I.; Greystoke, A.; Twelves, C.; Kaye, S. Phase I/II study of DHA-Paclitaxel in Combination with Carboplatin in Patients with Advanced Malignant Solid Tumours. *Br. J. Cancer* **2004**, *91*, 1651–1655.

[140] Hoye, T. R.; Wohl, A. W.; Macosko, C. W.; Panyam, J. Silicate Prodrugs and Nanoparticles. U.S. Patent Application PCT/US2012/040247, May 31, 2012. This application claims priority to a provisional application filed on May 31, 2011.

Figure 3-5. The chemical structure of selected *mono*- and *bis*- trialkoxy silicate ester prodrugs of PTX.

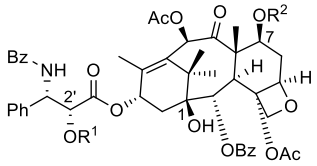

Prodrug #	R^1	R^2
1.01 (PTX)	H	H
3.04	$Si(OEt)_3$	H
3.05	$Si(O^nOct)_3$	H
3.06	$Si(O^iPr)_3$	H
3.07	$Si(O^tBu)_2OEt$	H
3.08	$Si(OEt)_3$	$Si(OEt)_3$
3.09	$Si(O^nOct)_3$	$Si(O^nOct)_3$
3.10	$Si(O^iPr)_3$	$Si(O^iPr)_3$
3.11	H	$Si(OEt)_3$
3.12	H	$Si(O^nOct)_3$

The differences in aliphatic chain length (e.g., **3.04** vs. **3.05**) of the PTX silicate esters could yield three significant advantages. First, and most obviously, the differing hydrophobicities imparted from the sacrificial alkoxy substituents will lead to varied solubility in water. This, in turn, will likely affect the loading levels, encapsulation efficiencies, and/or stability of prodrug-loaded nanoparticles produced from the FNP process.[8] Secondly, delivery of a highly nonpolar has the potential to result in improved cellular uptake[8,131] and prolonged retention in the lipophilic portion of the cell wall prior to hydrolysis. This may, in turn, provide an improved cell kill. Additionally, inclusion of oily hydrocarbon side chains (e.g., *n*-octyl as in **3.08**) could minimize or eliminate the crystallinity of the silicate prodrug in the nanoparticle core – thereby favorably altering the drug release profile by depressing the initial "burst" release of the drug.[141,142]

Variations in the steric bulk of the alkoxy substituents (e.g., **3.04** vs. **3.06** vs. **3.07**) build upon the well-established trends detailed in Chapter 2. While the

[141] Kim, I.-S.; Kim, S.-H. Development of a Polymeric Nanoparticulate Drug Delivery System: In vitro Characterization of Nanoparticles based on Sugar-Containing Particles. *Int. J. Pharm.* **2002**, *245*, 67–73.

[142] Görner, T.; Gref, R.; Michenot, D.; Sommer, F.; Tran, M. N.; Dellacherie, E. Lidocaine-loaded Biodegradable Nanospheres. I. Optimization of the Drug Incorporation into the Polymer Matrix. *J. Control. Release* **1999**, *57*, 259–268.

hydrolysis rate trends have been well-established in fully solvated model systems, the absolute hydrolysis rate of a prodrug encapsulated within a nanoparticle is difficult, if not impossible, to predict. Thus, prodrugs that will hydrolyze at substantially different rates (due to varying steric bulk and varying leaving group ability) were prepared and tested in IC_{50} studies. Feedback from these concurrent biological assays performed by our collaborators Stephen Kalscheuer and Prof. Jayanth Panyam will be crucial to the selection of prodrug with an acceptable rate of hydrolysis.

Finally, the prodrugs were designed considering the literature precedent that the C2'-hydroxyl of PTX is both the most reactive of the three hydroxyls as well as critical to the bioactivity of the drug.[143] The vast majority of true prodrugs (i.e., those for which there is evidence for formation of PTX after administration) functionalize PTX at this C2' site.[87] Alternatively, the C7-hydroxyl is also reasonably reactive, and the biological activity of PTX is less sensitive to minor alterations at this site. Such C7 derivatives often exhibit efficacy similar to the parent PTX, but many of the PTX conjugates at this position fail to provide convincing evidence of the true structure of the bioactive agent.[87] The C1 hydroxyl is generally inert to typical reaction conditions. Therefore, this family of PTX silicates (e.g., **3.04** vs. **3.08** vs. **3.11**) conscientiously includes mono-substituted prodrugs at either the C2' and C7 positions as well as bis-silylated silicate prodrugs to further examine these issues.

[143] Zhu, Q.; Guo, Z.; Huang, N.; Wang, M.; Chu, F. Comparative Molecular Field Analysis of a Series of Paclitaxel Analogs. *J. Med. Chem*. **1997**, *40*, 4319–4328.

Scheme 3-1. Synthesis of the silicate prodrugs of PTX. Conditions: (a) $SiCl(OR^1)_3$, NEt_3, THF. (b) i) $SiCl_2(O^tBu)_2$, py, THF; ii) EtOH, py. (c) $SiCl(OR)_3$, py, THF. (d) d_6-acetone, D_2O, TFA (90:9:1 v/v/v). Yields of chromatographed product: **3.04** (91%); **3.05** (81%); **3.06** (65%); **3.07** (84%); **3.08** (85%); **3.09** (77%); **3.10** (67%) **3.11** (91%, brsm); and **3.12** (66%, brsm). brsm = based on recovered starting material.

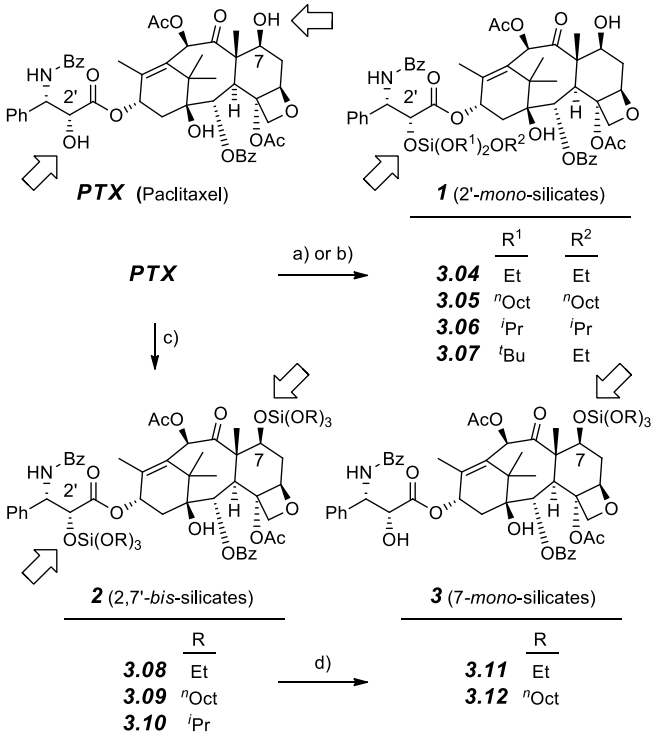

Each compound was synthesized from PTX as outlined in Scheme 3-1. The 2'-triethoxy (**3.04**), 2'-trioctyloxy (**3.05**), and 2'-tri-*i*-propoxy (**3.06**) PTX silicates were synthesized via treatment with triethylamine (TEA) and the appropriate trialkoxychlorosilane. Subjecting PTX to tri-*t*-butoxychlorosilane in the presence of either TEA or pyridine led to no evidence of conversion to the desired 2'-tri-*t*-butoxy PTX silicate. (A similar observation has been made by my colleague in the Hoye labs, Andrew Michel, when using docetaxel as the taxane

substituent.[144]) Thus, the di-*t*-butoxyethoxy PTX silicate (**3.07**) was synthesized by treatment with the di-*t*-butoxydichlorosilane and pyridine. The reaction progress was followed by ^{1}H NMR spectroscopy, and, upon observing complete consumption of PTX, a 100-fold excess of ethanol was added, yielding compound **3.07**.

Treating PTX with a stoichiometric excess (i.e., > two equivalents) of a trialkoxychlorosilane in the presence of TEA failed to provide any notable [via thin layer chromatography, (TLC)] conversion to the 2',7-bis PTX silicate esters. Fortunately, optimization of the amine base led to the desired bis-silylation. Replacing TEA with the less basic but more nucleophilic pyridine as the amine base leads to high conversion of PTX to the bis-silicate esters. In this way, the 2',7-bis(triethoxy) (**3.08**), 2',7-bis(tri-*n*-octyloxy) (**3.09**), and 2',7-bis(tri-*i*-propoxy) (**3.10**) were successfully accessed.

Finally, **3.08** and **3.09** were treated with TFA in a mixed d_6-acetone/D_2O co-solvent (precisely the same as the hydrolysis conditions utilized in the kinetic experiments; refer to sections 2.2.3 or 3.3.7). The selective degradation of the C2' silicate ester was monitored by *in situ* ^{1}H NMR spectroscopy. After ca. 2 half-lives were observed, the reactions were quenched with a saturated $NaHCO_3$ solution, extracted, and purified from the starting material and PTX, resulting in reasonable yields of the 7-triethoxy (**3.11**) and 7-tri-*n*-octyloxy (**3.12**) PTX silicates.

7. PTX Tetraalkoxy Silicate Prodrug Hydrolysis Studies. As in the models studies described in Chapter 2, ^{1}H NMR spectroscopy was again used to establish relative hydrolysis rates and trends thereof for compounds **3.04-3.12**. Using the previously established "standard hydrolysis conditions" (c.f., section 2.2.3), each prodrug was dissolved in a solution of d_6-acetone, D_2O, and TFA in

[144] Michel, A. University of Minnesota, Minneapolis, MN. Personal communication, **2012**.

a 90:9:1 ratio (v/v/v). Resonances of, e.g., H2' in the reactant silicate vs. product carbinol were monitored. None of the partially hydrolyzed silanol intermediates arising from the tetraalkoxy silicates were observed in these compounds, reinforcing that the initial hydrolysis event (i.e., cleavage of the first Si–OR bond) is the rate-limiting step in the hydrolysis.

Table 3-1. The hydrolysis rates of the PTX silicate prodrugs relative to that of the slowest (**3.07**).

Prodrug	at C2'			at C7		
	$t_{1/2}$ (min)	k_{obs} (10^{-3} s^{-1})	k_{rel} [a]	$t_{1/2}$ (min)	k_{obs} (10^{-3} s^{-1})	k_{rel} [a]
3.04	4.0 ± 1.3	3.1 ± 0.9	**2200 ± 600**	n/a [b]	n/a	n/a
3.05	12 ± 1	0.10 ± .04	**710 ± 30**	n/a	n/a	n/a
3.06	120 ± 10	0.097 ± 0.006	**69 ± 4**	n/a	n/a	n/a
3.07	1200 ± 100	0.0014 ± 0.0001	**1.0 ± 0.1**	n/a	n/a	n/a
3.08	4.6 ± 0.1	2.5 ± 0.1	**1800 ± 100**	33 ± 2	0.35 ± 0.02	**250 ± 10** [c]
3.09	18 ± 1	0.64 ± 0.01	**460 ±10**	200 ± 10	0.058 ± 0.004	**41 ± 3** [d]
3.10	n.d. [e]	n.d.	n.d.	n.d.	n.d.	ca. **50** [f]
3.11	n/a	n/a	n/a	31 ± 1	0.38 ± 0.01	**270 ± 10**
3.12	n/a	n/a	n/a	150 ± 10	.077 ± .005	**55 ± 3**

[a] The k_{rel} values displayed in Table3-1 are referenced such that the most slowly-hydrolyzing prodrug, **3.07**, k_{rel} = 1.

[b] n/a = not applicable

[c] The rate of hydrolysis of in situ generated **3.07** to PTX.

[d] The rate of hydrolysis of in situ generated **3.08** to PTX.

[e] n.d. = not determined

[f] The rate of hydrolysis of in situ generated of 7-*O*-(tri-*i*-propoxysilyl)paclitaxel to PTX was not rigorously established because it was not a candidate for biological studies described in section 3.3.8.

As anticipated, the results (Table 3-1) show that increasing the steric bulk of the silicate prodrug slows its hydrolysis rate. The k_{rel} values (here, referenced to the most slowly hydrolyzed prodrug, **3.07**) differ by > 2000-fold between the extremes of the 2'-triethyl PTX-silicate **3.04** to the hindered 2'-di-*t*-butylethyl PTX-silicate **3.07**. The hydrolysis rates for **3.04** and **3.05** were similar (k_{rel} of a factor of ca. 3), demonstrating that the hydrophobicity of the PTX silicate can be significantly increased with only a small change in the relative hydrolysis rate. (This result is in line with expectations derived from the menthol-based silane model systems in section 2.3.1.) As a group, prodrugs bearing the silicate at C7 hydrolyzed ca. 10x slower than those at C2'.

It is interesting to note that the absolute rate of hydrolysis in the PTX-based silicate ester prodrugs was faster than predicted from the menthol models. Specifically, TEOS **2.07** and triethoxymenthoxysilane **2.25** were found to exhibit k_{obs} values of 3.7 ± 0.2 s^{-1} and 0.67 ± 0.04 s^{-1}, respectively. In contrast, the k_{obs} value measured for the related secondary, PTX-based triethoxy silicate **3.04** was 3.1 ± 0.9 s^{-1}. An analysis based purely upon steric bulk would suggest that **2.25**, consisting of a branched secondary hydroxyl, would be a more reasonable model for **3.04**.

Previous, related work has shown that a nucleophilic primary amine at the C3' position in isotaxel (**3.13**) is able to rapidly ($t_{1/2}$ = 15 min at pH = 7.4) induce an O-N acyl migration.[145,146] The hydrolysis rate variance from the menthol model in our PTX silicate prodrugs may be attributed to similar nucleophilic capabilities of the C3' amide, generating a transient, highly activated tetravalent silicon

[145] Hayashi, Y.; Skwarczynski, M.; Hamada, Y.; Sohma, Y.; Kumura, T.; Kiso, Y. A Novel Approach of Water-Soluble Paclitaxel Prodrug with No Auxiliary and no Byproduct: Design and Synthesis of Isotaxel. *J. Med. Chem.* **2003**, *46*, 3782–3784.

[146] Sohma, Y.; Hayashi, Y.; Skwarczynski, M.; Hamada, Y.; Sasaki, M.; Kimura, T.; Kiso, Y. O-N Intramolecular Acyl Migration Reaction in the Development of Prodrugs and the Synthesis of Difficult Sequence-Containing Bioactive Peptides. *Biopolymers* **2004**, *76*, 344–356.

moiety (i.e., **3.14** in Scheme 3-2) to substitute the first alkoxy substituent. This potential, short-lived intermediate may then be consumed by water more rapidly than originally anticipated.

Scheme 3-2. O-N Acyl transfer of isotaxel (**3.13**) and the postulated, related participation of the benzoyl amide functioning as an activator (**3.14**) of the rapid silicate hydrolysis.

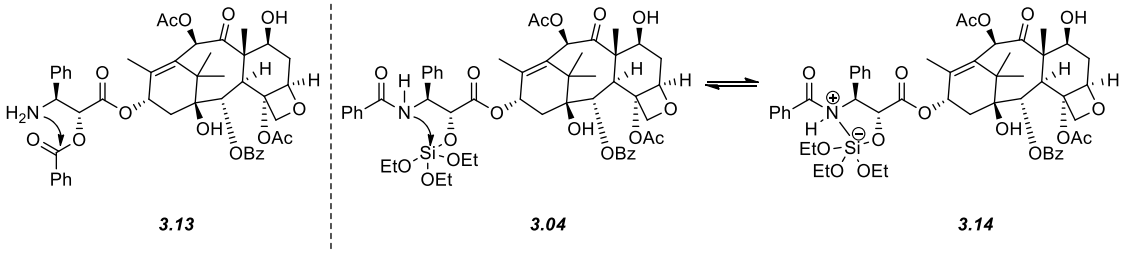

However, despite differences from the expected (but ultimately inconsequential) absolute rate, the observed trends were quite comparable to those measured for the menthol-containing silicate ester models (Table 3-2). For example, the bis-trialkoxy PTX silicates **3.08**, **3.09**, and **3.10** were compared with the analogous menthol models **2.25**, **2.27**, and **2.28** (ethyl, *n*-octyl, and *i*-propyl, respectively). When the k_{rel} values of all compounds were referenced to the respective parent triethoxy silicate ester, the PTX trends aligned well with the patterns found in the menthoxy silicate ester models. In addition to further validating the model work performed in Chapter 2, the desired generality of these trends was supported by the closely related patterns observed for both C2' and C7 silicates.

Table 3-2. A comparison of observed hydrolysis rates of the PTX silicate prodrugs and the menthoxytrialkoxysilanes.

Menthoxy Silicate	k_{rel} [a]	**PTX Silicate**	at C2' k_{rel} [b]	at C7 k_{rel} [c]
2.25	1.0 ± 0.06	**3.08**	1.0 ± 0.06	1.0 ± 0.06
2.27	0.22 ± 0.01	**3.09**	0.22 ± 0.01	0.17 ± 0.01
2.28	0.084 ± 0.004	**3.06 / 3.10** [d]	0.033 ± 0.002	ca. 0.028

[a] The rate of hydrolysis referenced to k_{rel} = 1 for **2.25**.
[b] The rate of hydrolysis referenced to k_{rel} = 1 for the C2' silicate of **3.08**.
[c] The rate of hydrolysis referenced to k_{rel} = 1 for the C7 silicate of **3.08**.
[d] The k_{rel} for the C2' silicate is taken from the mono-silicate **3.06** and the k_{rel} for the C7 silicate is taken from the bis-silicate **3.10**.

8. Acyloxy-Containing PTX Silicate Prodrug Design and Synthesis.

Encouraged by the reliable translation of the menthoxy silicate ester models, I aimed to apply the principles delineated in section 2.3.4 and synthesize PTX silicate esters that were yet more labile than **3.04**. Thus, the expansion of the acyloxy-containing silicate esters was applied to the design of a rapidly hydrolyzing PTX analog. Anticipating a highly labile compound, *t*-butoxy groups were chosen as the sacrificial alkoxies during this prodrug development. An initial attempt to pre-form the acetoxy-di-*t*-butoxychlorosilane *in situ* followed by addition of PTX was unsuccessful. However, following a strategy similar to the synthesis of **3.07**, PTX was treated with di-*t*-butoxydichlorosilane, leading to the successful formation of intermediate **3.15** (Scheme 3-3).[147] It was often necessary to add an excess of acetic acid and pyridine prior to quantitative

[147] Analysis of crude ^{1}H NMR data demonstrated a characteristic shift of the C2' methine from a doublet (δ = 4.78) to a pair of diastereotopic doublets (δ = 5.03 and 5.01 in an ca. 3:2 ratio) assigned to **3.14**.

conversion of PTX to **3.15** (due to the observation of a byproduct[148] in the crude ^{1}H NMR spectrum), the major product was isolated in a moderate yield after MPLC chromatography. Spectroscopic and mass analysis confirmed this compound as the desired PTX silicate ester prodrugs **3.16**.

Interestingly, compound **3.18** was isolated (in low yield) when the crude reagent di-*t*-butoxydichlorosilane (i.e., a sample still containing unreacted *t*-butanol) was used during attempts to synthesize **3.15** (Scheme 3-3). As previously discussed, attempts to synthesize **3.18** by treatment of PTX with tri-*t*-butoxychlorosilane, even at elevated temperatures and large reagent excesses, led to no evidence of conversion to **3.18**. (Similar observations have been made with docetaxel.[144]) The origin of this apparent discrepancy is not clear — both PTX and *t*-butanol are bulky substituents leading to highly hindered chlorosilanes. It is difficult to imagine a scenario in which there is a notable difference in substitution at the silicon center. Further efforts toward the synthesis of **3.18** were not pursued, as **3.07** could be synthesized reliably to serve as a "slowly hydrolyzing" PTX prodrug in biological studies.[149]

An analogous strategy was exploited to synthesize a presumably more stable acyloxy silicate, **3.19** (Scheme 3-3). Pivalic acid was used in place of acetic acid, but *in situ* analysis by ^{1}H NMR of the preformed chlorosilane **3.15** showed a significantly slower rate of incorporation. The reaction was sufficiently slow (Table 3-3) such that hydrolysis of **3.15** by adventitious water was competitive with acyl substitution. Thus, the reaction was stopped prior to full conversion, and the desired PTX silicate **3.17** was isolated only in a low yield.

[148] This byproduct was later found to be the PTX-containing di-*t*-butoxysilanol **3.18**, confirmed by the HR-MS and the independent synthesis of **3.18**.

[149] Subjecting **3.17** to the "standard hydrolysis conditions" led to a $t_{1/2}$ > 400 h, at which point the experiment was discontinued.

Scheme 3-3. The synthetic route used to access the acyloxy-di-*t*-butoxy PTX silicate ester prodrugs **3.16** and **3.17** and the unexpected byproduct **3.18**.

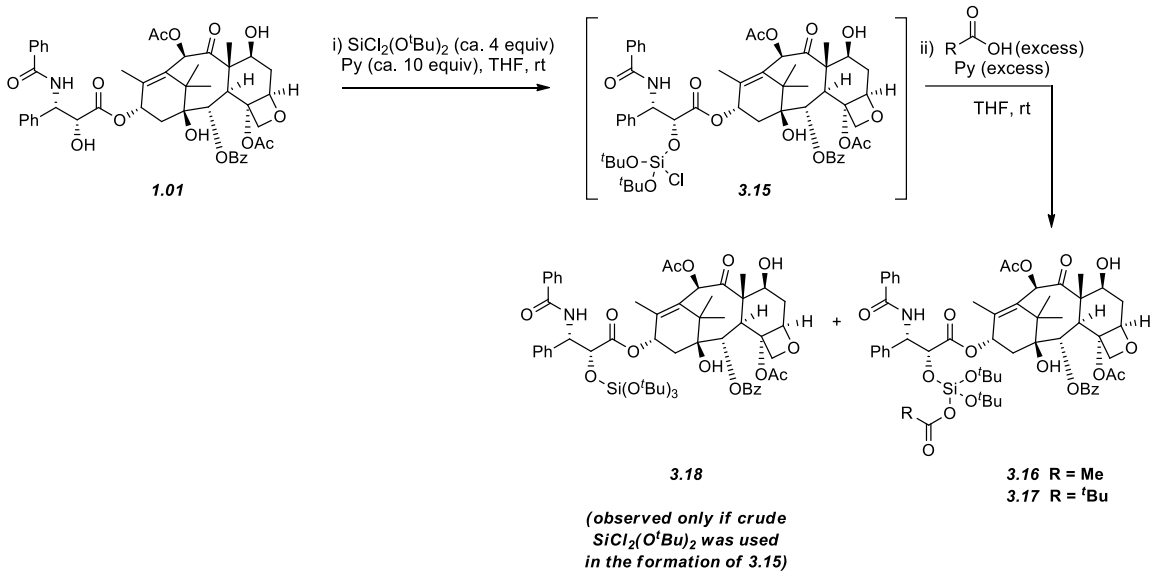

Table 3-3. A correlation of time and conversion of PTX acyloxy silicate prodrugs.

Prodrug	Substituent	Time (h)	Conversion (%)
3.07	Ethoxy	72	> 99
3.16	Acetoxy	24	85
3.17	Pivaloxy	120	20

9. PTX Acyloxy Silicate Prodrug Hydrolysis Studies. ^{1}H NMR spectroscopy and the extensively used hydrolytic conditions [90:9:1 d_6-acetone:D_2O:TFA

(v/v/v)] were again employed to study the degradation of **3.16**. The k_{rel}, as defined by the degradation of the parent compound **3.16** and referenced to **3.07**, was found to be 240 ± 10 ($t_{1/2}$ = 35 ± 2 mins). This is a significantly faster hydrolysis than that observed for **3.07** (a prodrug of similar steric bulk), but, unfortunately, still slower than the triethoxy PTX silicate **3.04**.

Perhaps the most interesting experimental result during the hydrolysis of **3.16** was the detection of a long-lived intermediate (Figure 3-6). This intermediate was found to be sufficiently stable, allowing isolation via MPLC and, subsequently, full characterization. This work led to the identification of the intermediate it as the PTX-silanol **3.19** (Scheme 3-4). (The observation of a silanol is not unprecedented – recall that an intermediate silanol was detected in the hydrolysis of the highly hindered silicate ester model **2.58**.) The pure silanol **3.19** was subjected to identical hydrolysis conditions, and the k_{rel} value (relative to **3.07** as k_{rel} = 1) was measured to be 4.8 ± 0.2 ($t_{1/2}$ = 250 ± 10 mins).

Scheme 3-4. The hydrolysis of **3.16** to a stable, isolable silanol intermediate **3.19** that reverts to free PTX upon further exposure to the hydrolytic conditions.

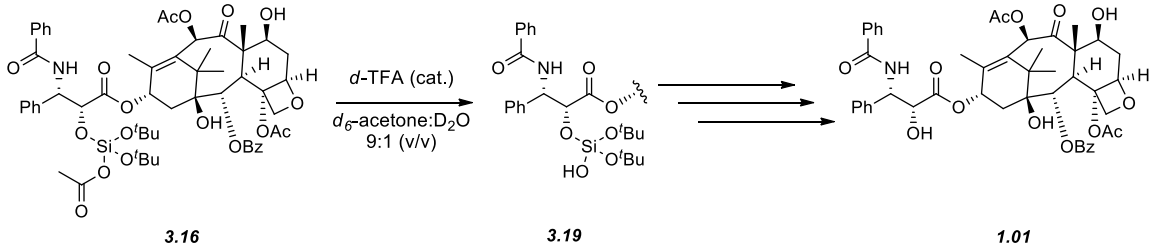

Figure 3-6. Representative ^{1}H NMR spectra showing the hydrolysis of starting material **3.16** (H2' resonance most downfield, ◆) to stable intermediate **3.19** (H2' resonance center, ■) and subsequent hydrolysis of **3.19** to free PTX **1.01** (H2' resonance most upfield, ●).

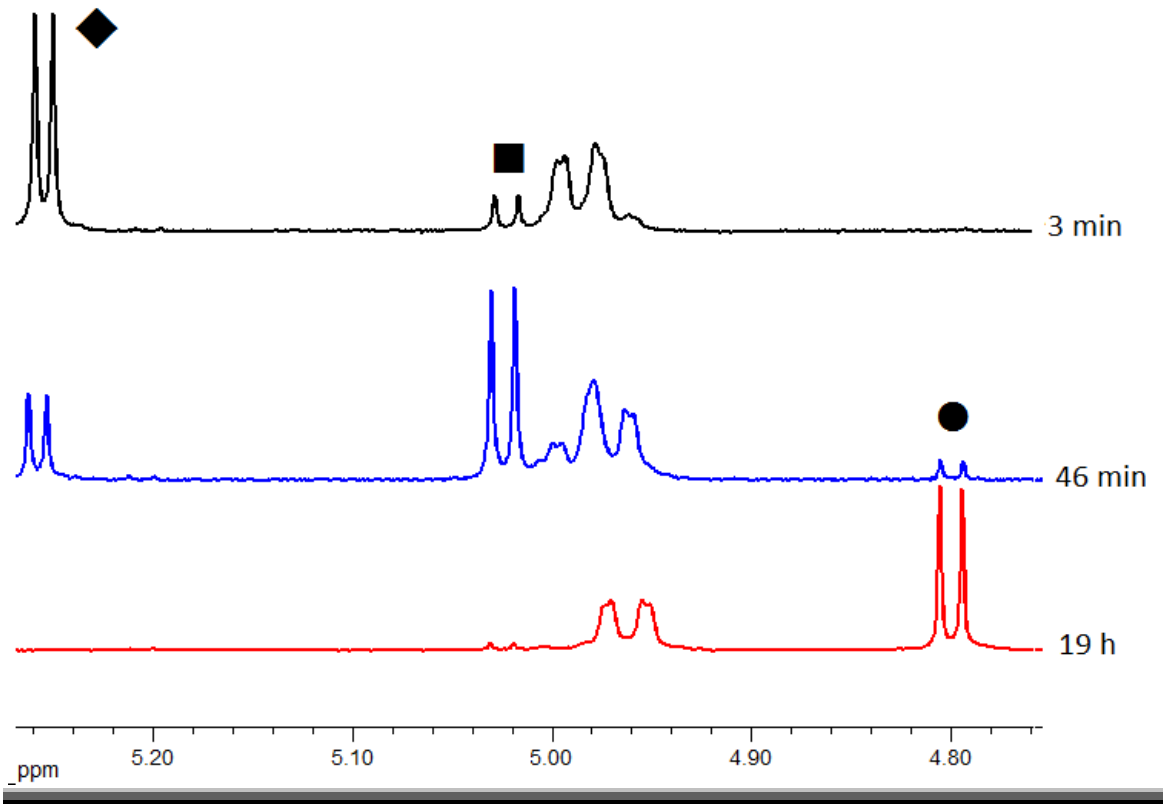

These observations led to limited analysis of the more stable (and thus more slowly hydrolyzing) pivalate derivative **3.17**. In the case of **3.17**, the rate limiting step of the hydrolysis could be either cleavage of the initial Si-O-*acyl* or the hydrolysis of silanol **3.19**. Regardless, compound **3.17** would ultimately prove to be ineffective as a "more rapidly hydrolyzing prodrug," as both **3.17** and **3.19** would hydrolyze significantly more slowly than **3.04**. If more rapidly hydrolyzing silicate prodrugs were deemed necessary, future work could incorporate *i*-propoxy rather than *t*-butoxy substituents, opening the possibility of faster hydrolysis and reasonable stability to chromatography. This work has not yet

been pursued, however, due to feedback from concurrent biological studies detailed in the upcoming section 3.3.11. Briefly, these studies indicate that numerous trialkoxy PTX silicates hydrolyze at sufficiently fast rates, thereby diminishing motivation for the optimization of acyloxy-containing PTX silicate prodrugs.

*10. Mechanistic Studies of the Hydrolysis of **3.16**.* During the hydrolysis of **3.16**, the initial bond cleavage of the Si-O-*acyl* was not the rate limiting step. This led to the unique (among the other PTX-prodrugs) formation of a PTX-based silanol, **3.19**. While the formation of an intermediate is decidedly negative from an application viewpoint, [the FDA would require safety data to be obtained separately for all intermediate(s)] the stability of **3.19** allows us to address an important scientific question. Namely, are the acyloxysilanes more rapidly hydrolyzed because the acyl group is a better leaving group or because there is a less sterically congested, electrophilic carbonyl carbon available to the nucleophilic water?

While the S_N2 nature of tetraalkoxy silicate ester substitution is well accepted,[27] the stereochemical result of acyloxysilanes is considerably less studied. Minimally, precedent exists to suggest nucleophilic attack selectively at the electrophilic carbonyl is favored over direct substitution at silicon in specific, sterically constrained examples. Notably, Eaborn and co-workers have reported exclusive acyl-oxygen fission in the methanolysis of extremely hindered trisyl derivatives of trialkylacetoxysilanes.[150] If this result held true in the case of **3.16**, the mechanism of hydrolysis could proceed through a mechanism other than an S_N2 mechanism.

[150] Damja, R. I.; Eaborn, C.; Saxena, A. K. Acyl-Oxygen Fission in Reactions of Oragnosilicon Carboxylates with Sodium Methoxide in Methanol. *J. Chem. Soc. Perkin Trans. II* **1985**, *2*, 597–598.

Defining the mechanism of hydrolysis in our PTX system (i.e., **3.16**) was deemed critical to the rational design of future silicate ester prodrugs – not just in the specific case of PTX silicate esters but also for the development of this strategy more generally. Thus, isolation of the silanol intermediate **3.19** was undertaken to aid in the identification of the atomic location of the nucleophilic substitution. Namely, if substitution occurs directly at silicon (blue dashed arrow, Figure 3-7), the lability of the silicate ester is controlled at least primarily by the steric bulk and leaving group ability of the substituents. However, it is plausible that the accelerated rate of hydrolysis is the result of water attacking the electrophilic carbonyl in the acyloxy substituent (red solid arrow, Figure 3-7), resulting in cleavage of the O-acyl bond as the first step in the hydrolysis.

Figure 3-7. The potential modes of nucleophilic attack in the acyloxy-containing PTX silicate ester prodrug **3.16** include direct displacement at the silicon (solid blue arrow) or the electrophilic carbonyl (dashed red arrow).

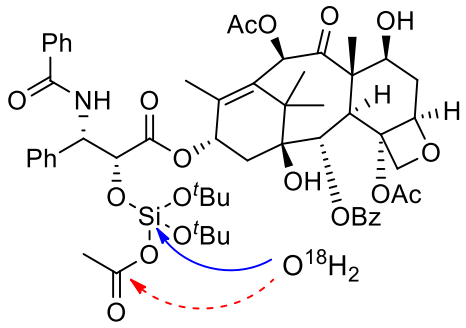

3.16

The possible results described above in Figure 3-7 may be distinguished by a properly controlled isotopic labeling study. In this vein, the mechanistic study was conducting by partially hydrolyzing **3.16** in the presence of O^{18}-labeled water (Scheme 3-5). Such conditions resulted in isolation (via MPLC) of solely the ^{18}O-labeled silanol **3.20** (as determined by ESI-HRMS). While such results are

strongly indicative of direct substitution of water at silicon, this single result fails to rule out post-hydrolysis exchange of ^{16}O and ^{18}O. Therefore, as an additional control, pure **3.20** was resubjected to the reaction conditions containing ^{16}O water to test for hydroxyl exchange. Gratifyingly, even after submitting **3.20** to an identical acid catalyst load for an identical amount of time, only **3.20** and PTX (**1.01**) were obtained upon purification.

Scheme 3-5. The hydrolysis of **3.16** in the presence of ^{18}O-labeled water resulted in the exclusive formation of the ^{18}O-labeled PTX silanols **3.20**.

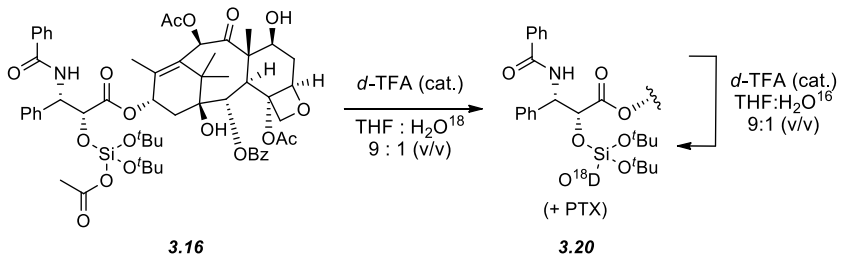

In the specific context of PTX prodrugs, **3.16** hydrolyzed at a faster rate than the analogous di-*t*-butoxyethoxy PTX silicate **3.07**, but its measured k_{obs} value was still considerably slower than several of the other prodrug consisting of less hindered alkoxies (i.e., **3.04**). However, potential exists for yet faster hydrolyzing prodrugs to be synthesized by, for instance, incorporating *i*-propoxy rather than *t*-butoxy alkoxy substituents. These compounds were not further pursued because ongoing biological studies (see section 3.3.10) indicated that linear, aliphatic prodrugs such as **3.04**, **3.05**, and **3.08** were hydrolyzing at sufficiently fast rates in *in vitro* studies to maintain drug efficacy. In a broader sense, these results offer convincing evidence of direct nucleophilic substitution of water at silicon. The leaving group ability, rather than inclusion of an electrophilic carbonyl, is the key to the generation of rapidly hydrolyzed prodrugs.

This information will instruct the design of potential, future, labile silicate prodrugs of other active agents.

11. PTX Silicate Prodrug in Vitro Cytotoxicity Studies.[88,151] A subset of PTX silicate prodrugs (**3.04**, **3.05**, **3.06**, **3.07**, **3.08**, **3.11**, and **3.12**) were selected for *in vitro* cell cytotoxicity assays during a productive collaboration with the group of Prof. Jayanth Panyam. Stephen Kalscheuer, a student in the Panyam group, grew and plated MDA-MB-231 cells prior to treatment with DMSO solutions of varying concentrations of a PTX silicate prodrug. Following an incubation period of 48 hours, the cells were treated with a solution of 3-(4,5-dimethylthiazol-2-yl)-2,5-diphenyltetrazolium bromide (MTT) reagent. Viable cells are known to reduce MTT, and absorbance measurements taken at 490 nm are reliably correlated to the number of viable cells.[152]

The IC_{50} results are summarized in Table 3-4. Generally, the faster hydrolyzing prodrugs **3.04**, **3.05**, **3.06**, **3.08**, and **3.11** all exhibited IC_{50} values statistically equivalent to the parent PTX compound. Prodrug **3.07** which hydrolyzes exceedingly slowly was found to have significantly decreased efficacy. Comparatively, prodrugs **3.04-3.06** and **3.08**, all of which hydrolyze at much faster relative rates than **3.07**, demonstrated IC_{50} values statistically equivalent to that of the free PTX.

Interestingly, silylation at the less sensitive C7 position, as in prodrugs **3.11** and **3.12** gave differing results. The faster hydrolyzing prodrug **3.11** resulted in a statistically equal cytotoxicity value as PTX. However, the more slowly hydrolyzing and marginally bulkier silicate, **3.12**, demonstrated a significantly diminished cytotoxic effect. Given this result, we found that we were unable to

[151] These IC_{50} cytotoxicity studies were performed by Stephen Kalscheuer. Kalscheuer, S. University of Minnesota, Minneapolis, MN. Personal communication, **2012**.

[152] Mosmann, T. Rapid Colorimetric Assay for Cellular Growth and Survival: Application to Proliferation and Cytotoxicity Assays. *J. Immunol. Methods* **1983**, *65*, 55–63.

infinitely increase the lipophilicity of the prodrug at the at the C7 position while retaining sufficient efficacy. Presumably, the reported biological tolerance at this site is, as are all parameters, relative. Clearly, the rate of hydrolysis back to the parent drug needs to be considered at both the C2' and C7 hydroxyls.

Table 3-4.[151] The measured cytotoxicity of PTX and PTX silicate prodrugs in MDA-MB-231 cells.[a]

Compound	IC_{50} (nM) [b]
PTX (1.01)	23.6(± 9.8)
3.04	23.0 (± 10.7)
3.05	35.6 (± 19.4)
3.06	24.5 (± 12.7)
3.07	8140. (± 1320)
3.08	74.4 (± 35.0)
3.11	21.4 (± 12.5)
3.12	540. (± 113)

[a] The cell viability was measured after 48 h.
[b] The data are reported as the mean (± SD).

12. Summary and Future Work. The development of PTX-based silicate prodrugs has validated the tetraalkoxysilane models used in Chapter 2 and yielded significant advances toward a novel prodrug family. A series of prodrugs of varying hydrophobicity and hydrolytic lability has been synthesized, purified, and hydrolyzed. IC_{50} values for a subset of seven were measured in the labs of our collaborator, Prof. Paynyam,[151] and the outcomes were correlated with the prodrug rate of hydrolysis. These experiments resulted in the identification of five prodrugs that displayed cytotoxicity equivalent to the parent PTX. Consideration

of many relevant factors – ease of synthesis and handling, hydrophobic character, rate of hydrolysis, cytotoxicity, and nature of the byproducts – led to the selection of PTX prodrug **3.08** to be formulated into nanoparticles via flash nanoprecipitation. These prodrug-loaded nanoparticles were utilized in collaborative *in vivo* mouse model studies, described in Chapter 5.

4. Curcumin.

1. Introduction. Curcumin (**1.04**), the yellow/orange natural product derived from turmeric, has long been viewed as a potential therapeutic.[153] Prominently featured among a host of potential health benefits is its use as a preventative chemotherapeutic. These aspirations center on the antioxidant prospects of this highly conjugated molecule. However, practical application of **1.04** has been limited by, among other issues, low bioavailability. The low bioavailability frequently observed in treatments of **1.04** results largely from the known glucuronidation of an aryl hydroxyl (occurring via UDP-glucuronosyltransferase activity[154]) upon oral administration to yield species such as **3.21** (Scheme 3-6). Additionally, action by reductases (occurring upon intravenous or intraperitoneal administration) gives undesired degradation to a variety of products of the form of **3.22** (Scheme 3-6).[153,155]

[153] Anand, P.; Kunnumakkara, A. B.; Newman, R. A.; Aggarwal, B. B. Bioavailability of Curcumin: Problems and Promises. *Mol. Pharm.* **2007**, *4*, 807–818.

[154] Hoehle, S. I.; Pfeiffer, E.; Metzler, M. Glucuronidation of Curcuminoids by Human Microsomal and Recombinant UDP-Glucuronosyltransferases. *Mol. Nutr. Food Res.* **2007**, *51*, 932–938.

[155] Pan, M.-H.; Huang, T.-M.; Lin, J.-K. Biotransformation of Curcumin through Reduction and Glucoronidation in Mice. *Drug Metab. Dispos.* .**1998**, *27,* 486–494.

Scheme 3-6. Two of the known degradation pathways to which curcumin is susceptible: Glucuronidation to yield **3.21** and reduction to yield **3.22**.

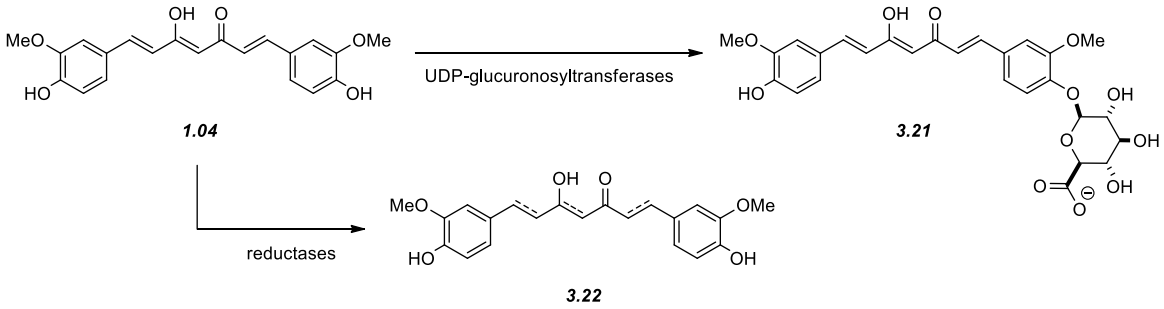

2. Efforts toward a Curcumin Silicate Ester. The silicate prodrug strategy was applied to curcumin to modify its biochemical properties. We hypothesized that silylation of the phenols may render these functional groups unreactive toward *in vivo* biological glucuronidation following oral administration. Additionally, recent results have suggested that, while curcumin has been efficiently encapsulated within chitosan/Tween 20 microparticles, there is an extremely rapid release of the drug (ca. 40% released within five mins and full release in less than 2 h).[156] Thus, as an added benefit, formation of silicate ester prodrugs would allow control of the release kinetics from future formulations.

Strongly motivated by these factors, initial attempts to synthesize the bis-triethoxy curcumin prodrug **3.23** were undertaken, resulted in low yields. This is likely the result of *in situ* oxidation that was qualitatively observed by the considerable darkening of the reaction solution. This minor complication could be easily avoided by carefully minimizing the reaction time. Controlling this variable, the bis-triethoxy and bis-tri-*i*-propoxy curcumin silicate prodrugs (**3.24** and **3.26**,

[156] O'Toole, M. G.; Henderson, R. M.; Soucy, P. A.; Fasciotto, B. H.; Hoblitzell, P. J.; Keynton, R. S.; Ehringer, W. D.; Gobin, A. S. Curcumin Encapsulation in Sub-Micron Chitosan/Tween 20 Particles. *Biomacromolecules*, **2012**, *13*, 2309–2314.

respectively) were readily synthesized by treating curcumin with the appropriate trialkoxychlorosilane and pyridine (Scheme 3-7). The purification of these compounds was mildly problematic, in that the starting curcumin was only ca. 94% pure. The contaminant, the monomethoxy derivative **3.23**, was silylated, giving **3.25** or **3.27**. These undesired byproducts were found to elute during silica chromatography with retention times similar to that of the desired, bis-silylated prodrugs. The only solution found to this complication was to take only specific fractions from the purifications, allowing isolation of the pure products, albeit in depressed yields.

Scheme 3-7. The synthesis of the bis-triethoxy and bis-*i*-isopropoxy curcumin silicate prodrugs **3.24** and **3.26**. The monomethoxy byproducts **3.25** and **3.27** co-eluted with the desired products.

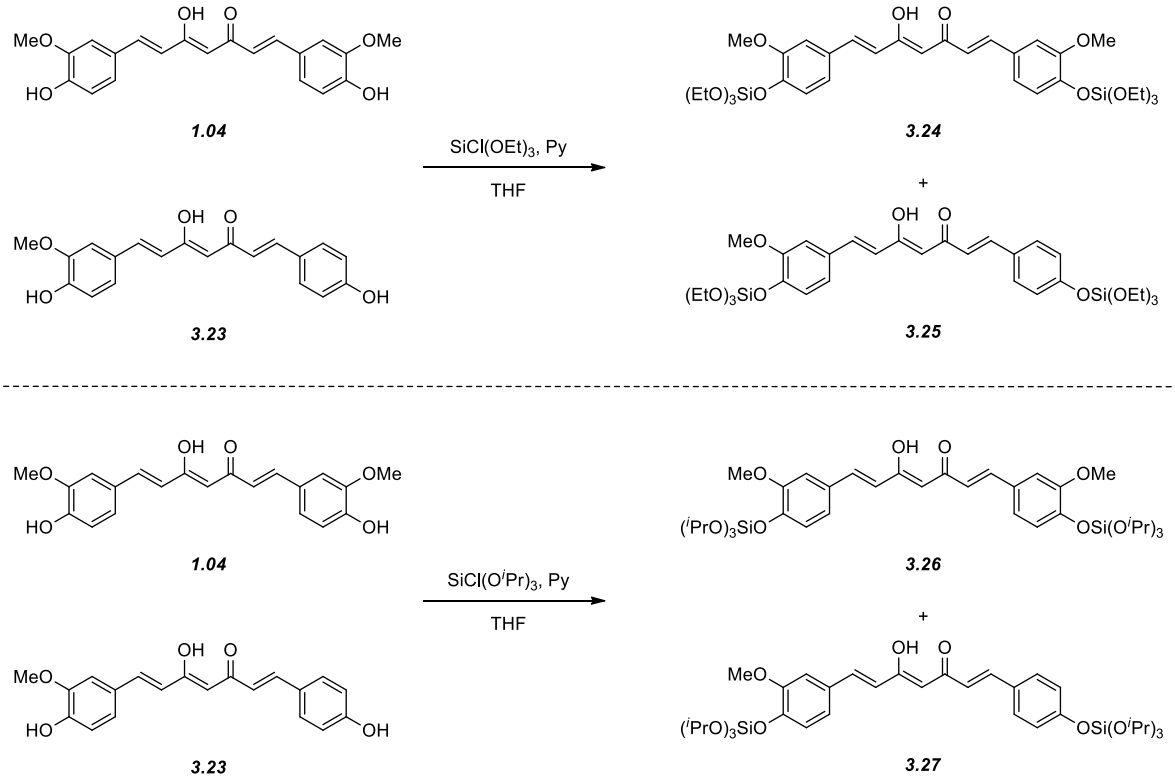

3. General Results of Collaborative Biological Assays.[157] The biological assays involving prodrugs **3.24** and **3.26** were again performed in collaboration with Prof. Jayanth Panyam. Curcumin silicates **3.24** and **3.26** were given to Alex Grill, another graduate student studying in the Panyam labs, for further testing. Briefly, **3.24** was found to be far too labile, hydrolyzing in DMSO during preparation for biological assays.[157] To our delight, prodrug **3.26** remained stable during experimentation and prevented glucuronidation during the *in vitro* assays. Thus, Alex Grill formulated **3.26** and injected the mixture into a live animal model. While glucuronidation was not observed *in vivo*, neither **3.26** nor free curcumin was detected after circulation.[157] This observation suggests that, while conjugation to a silicate ester prevented glucuronidation, the curcumin was likely shunted to a secondary metabolic pathway via reductase and/or dehydrogenase activity.[155,158] Given these disappointing results and no obvious strategy to minimize a secondary metabolic pathway, efforts toward curcumin silicate prodrugs were suspended.

5. Conclusions.

The silicate ester prodrug strategy has been applied to three fundamentally diverse hydroxyl environments in two different drugs: paclitaxel (two secondary alkyl hydroxyls) and curcumin (a phenol). The paclitaxel silicate ester prodrugs have been extensively developed, with efforts yielding a suite of prodrugs that vary in both their hydrophobic character and rate of hydrolysis. All but the most slowly hydrolyzing of this family demonstrated cytotoxicity

[157] These biological experiments were performed by Alex Grill. Grill, A. University of Minnesota, Minneapolis, MN. Personal communication, **2011**.

[158] Ireson, C. R.; Jones, D. J. L.; Orr, S.; Coughtrie, M. W. H.; Boocock, D. J.; Williams, M. L.; Farmer, P. B.; Steward, W. P.; Gescher, A. J. Metabolism of the Cancer Chemopreventive Agent Curcumin in Human and Rat Intestine. *Cancer Epidemiol. Biomarkers Prevent.* **2002**, *11*, 105–111.

equivalent to that of underivitized paclitaxel. This work has led to the selection of a 2',7-Di-*O*-(triethoxysilyl)paclitaxel silicate prodrug (**3.08**) for work in formulation studies and subsequent *in vivo* work in animal models, as detailed in Chapter 5. Furthermore, the synthesis of the di-*t*-butoxyacetoxy paclitaxel silicate ester uniquely led to the observation of a stable di-*t*-butoxy paclitaxel silanol during hydrolysis. The mechanism of hydrolysis for these species was determined via ^{18}O-labeling studies to be direct S_N2 substitution at the silicon atom (rather than nucleophilic attack at the electrophilic carbonyl).

Additional efforts to expand the silicate ester prodrug strategy beyond paclitaxel resulted in the synthesis of curcumin-based silicate prodrugs. The curcumin silicates were successfully designed to prevent glucuronidation, but the bioavailability of the drug remained low in preliminary *in vivo* experiments. This observation is likely due to degradation via a secondary metabolic pathway. Taken together, these applications of the general silicate ester prodrug strategy further confirm that this novel idea is both general and effective. Further exploitation of this concept to alter the physical, chemical, and/or biological properties of additional drugs could advance its utility to yet more active agents.

6. Experimental Section.

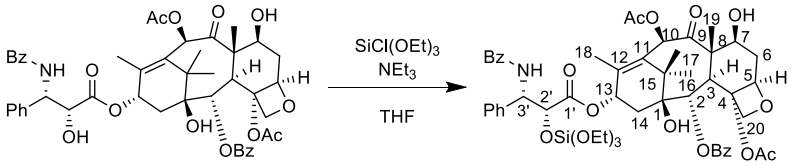

PTX (1.01) *3.04*

2'-*O*-(Triethoxysilyl)paclitaxel (3.04)[159]. Paclitaxel (55.3 mg, 0.0648 mmol, 1.0 equiv) was dissolved in dry THF (1.0 mL) in an oven-dried culture tube fitted with a Teflon-lined cap and magnetic stir bar. Triethylamine (20 µL, 0.130 mmol, 2.0 equiv) was added by Wiretrol®. Chlorotriethoxysilane (25 µL, 0.0127 mmol, 2.0 equiv) was then added, and a white precipitate was immediately observed. The culture tube was sealed and the suspension was allowed to stir for 1 hour at room temperature. The reaction slurry was diluted with a mixture of hexanes :EtOAc (1:1) and filtered through a short plug of Celite® to remove the triethylammonium salt. The filtrate was concentrated under reduced pressure, and the residue redissolved in a mixture of hexanes:EtOAc (1:1). Chromatography (SiO_2, 1:1 hexanes:EtOAc) via MPLC yielded the title compound as a white, crystalline solid (59.6 mg, 0.0587 mmol, 90.6%). If necessary, residual EtOAc was removed by storage under high vacuum for ≥ 24h.

^{1}H NMR (500 MHz, $CDCl_3$): δ 8.12 (dd, *J* = 8.5, 1.4 Hz, 2H, C2O_2C-*o*-Ph), 7.78 (dd, *J* = 8.5, 1.3 Hz, 2H, C3'NHCO-*o*-Ph), 7.62 (tt, *J* = 7.5, 1.2 Hz, 1H, C2O_2C-*p*-Ph, 1H), 7.56-7.46 (m, 3H, C2O_2C-*m*-Ph and C3'NHCO-*p*-Ph), 7.43-7.36 (m, 6H, C3'-*o*-Ph, C3'-*m*-Ph and C3'NHCO-*m*-Ph), 7.29 (tt, *J* = 6.5, 2.2 Hz, 1H, C3'-*p*-Ph), 7.19 (d, *J* = 8.6 Hz, 1H, C3'NH), 6.28 (s, 1H, H10), 6.24 (br dd, *J* = 9, 9 Hz,

[159] ^{1}H NMR assignments were made with the consideration of Oyama, M.; Itokawa, H. Physical Methods for Identification of the Structures of Taxoids. In *Taxus: The Genus Taxus*. Itokawa, H.; Lee, K.-H., Eds. Taylor & Francis, Inc: New York, **2003**, *32*; 79-133.

1H, H13), 5.72 (dd, *J* = 8.5, 3.2 Hz, 1H, H3'), 5.68 (d, *J* = 7.1 Hz, 1H, H2), 4.97 (dd, *J* = 9.4, 2.0 Hz, 1H, H5), 4.96 (d, *J* = 3.3 Hz, 1H, H2'), 4.43 (ddd, *J* = 10.9, 6.4, 4.5 Hz, 1H, H7), 4.32 (d, *J* = 8.5 Hz, 1H, H20α), 4.20 (d, *J* = 8.5 Hz, 1H, H20β), 3.80 (d, *J* = 7.2 Hz, 1H, H3), 3.71 [q, *J* = 7.0 Hz, 6H, C2'OSi(OC*H*$_2$CH$_3$)$_3$], 2.56 (ddd, *J* = 14.7, 9.6, 6.5 Hz, 1H, H6α), 2.45 (s, 3H, C4OAc), 2.44 (br s, 1H, C7OH), 2.32 (dd, *J* = 15.4, 9.4, Hz, 1H, H14α), 2.24 (s, 3H, C10OAc), 2.08 (dd, *J* = 15.2, 8.8 Hz, 1H, H14β), 1.90 (d, *J* = 1.2 Hz, 3H, C18H$_3$), 1.89 (ddd, *J* = 14.5, 11.0, 2.4 Hz, 1H, H6β), 1.68 (s, 3H, C19H$_3$), 1.64 (br s, 1H, C1OH), 1.24 (s, 3H, C17H$_3$), 1.15 [t, *J* = 7.0 Hz, 9H, C2'OSi(OCH$_2$C*H*$_3$)$_3$], and 1.13 (s, 3H, C16H$_3$).

^{13}C NMR (75 MHz, $CDCl_3$): δ 204.0, 171.6, 171.0, 170.1, 167.3, 167.2, 143.0, 138.2, 134.2, 133.9, 132.9, 132.0, 130.4, 129.3, 128.9 (x2), 128.8, 128.2, 127.3, 126.8, 84.6, 81.2, 79.3, 76.7, 75.8, 75.3, 75.1, 72.3, 71.5, 59.7, 58.7, 55.6, 45.7, 43.4, 35.7, 35.6, 27.0, 23.0, 22.4, 21.1, 18.2, 14.9, and 9.8.

HRMS (ESI) Calc'd for $C_{53}H_{65}NNaO_{17}Si$ $[M + Na]^+$ 1038.3914, found 1038.3942.

IR (thin film) 3500 (br), 2977, 2898, 1744, 1730, 1636, 1580, 1540, 1487, 1452, 1371, 1314, 1268, 1240, 1170, 1145, 1078, 1025, 978, 908, 854, 797, and 710 cm^{-1}.

mp = 131-134 °C.

TLC R_f (1:1 Hexanes:EtOAc) = 0.45.

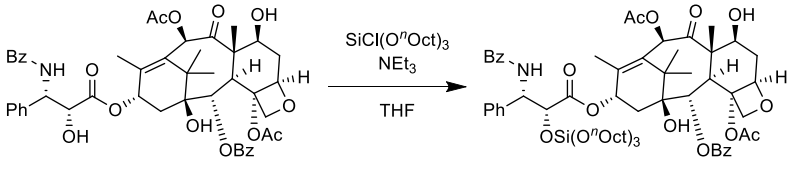

PTX (1.01) **3.05**

2-*O*-(Tri-*n*-octyloxysilyl)paclitaxel (3.05). Paclitaxel (76.0 mg, 0.0890 mmol, 1.0 equiv) was dissolved in dry THF (1.5 mL) in an oven-dried culture tube fitted

with a Teflon-lined cap and magnetic stir bar. Triethylamine (60 µL, 0.430 mmol, 4.8 equiv) was added by Wiretrol®. A 1.67:1 mixture of tri-*n*-octyloxychlorosilane:tetra-*n*-octyloxysilane (0.200 mg, 0.257 mmol, 2.9 equiv of tri-*n*-octyloxychlorosilane) was added and a white precipitate was immediately observed. The culture tube was sealed and the suspension was allowed to stir for 22 h at room temperature. The reaction slurry was diluted with a mixture of hexanes:EtOAc (1:1), the slurry filtered through a short plug of Celite® to remove the triethylammonium salt, the filtrate concentrated under reduced pressure, and the residue redissolved in a mixture of hexanes:EtOAc (2:1). Chromatography (SiO_2, 2:1 hexanes:EtOAc) via MPLC yielded the title compound as a white, crystalline solid (91.5 mg, 0.0721 mmol, 81.0%). If necessary, residual EtOAc was removed by storage under high vacuum for ≥ 24 h.

^{1}H NMR (500 MHz, $CDCl_3$): δ 8.13 (dd, *J* = 8.5, 1.5 Hz, 2H, C2O_2C-*o*-Ph), 7.77 (dd, *J* = 8.5, 1.4 Hz, 2H, C3'NHCO-*o*-Ph), 7.62 (tt, *J* = 7.4, 1.3 Hz, 1H, C2O_2C-*p*-Ph), 7.55-7.46 (m, 3H, C2O_2C-*m*-Ph and C3'NHCO-*p*-Ph), 7.43-7.35 (m, 6H, C3'-*o*-Ph, C3'-*m*-Ph and C3'NHCO-*m*-Ph), 7.28 (tt, *J* = 6.9, 1.7 Hz, 1H, C3'-*p*-Ph), 7.19 (d, *J* = 8.6 Hz, 1H, C3'NH), 6.28 (s, 1H, H10), 6.25 (br dd, *J* = 9, 9 Hz, 1H, H13), 5.72 (dd, *J* = 8.6, 3.2 Hz, 1H, H3'), 5.68 (d, *J* = 7.1 Hz, 1H, H2), 4.97 (dd, *J* = 9.8, 2.1 Hz, 1H, H5), 4.96 (d, *J* = 3.2 Hz, 1H, H2'), 4.44 (ddd, *J* = 10.9, 6.7, 4.2 Hz, 1H, H7), 4.31 (d, *J* = 8.4 Hz, 1H, H20α), 4.20 (d, *J* = 8.3 Hz, 1H, H20β), 3.80 (d, *J* = 7.1 Hz, 1H, H3), 3.61 {t, *J* = 6.8 Hz, 6H, C2'OSi[OC*H*$_2$(CH_2)$_6$$CH_3$]$_3$}, 2.56 (ddd, *J* = 14.8, 9.6, 6.6 Hz, 1H, H6α), 2.47 (d, *J* = 4.1 Hz, 1H, C7OH), 2.44 (s, 3H, C4OAc), 2.32 (dd, *J* = 15.4, 9.4 Hz, 1H, H14α), 2.24 (s, 3H, C10OAc), 2.07 (dd, *J* = 15.4, 8.8 Hz, 1H, H14β), 1.89 (d, *J* = 1.4 Hz, 3H, C18H_3), 1.89 (m, 1H, H6β), 1.68 (s, 3H, C19H_3), 1.65 (br s, 1H, C1OH), 1.48 [tt, *J* = 6.9, 6.9 Hz, 6H, C2'OSi(OCH_2C*H*$_2$(CH_2)$_5$$CH_3$)$_3$], 1.32-1.22 {m, 33H, C2'OSi[OCH_2CH_2(C*H*$_2$)$_5$$CH_3$]$_3$ and C17H_3}, 1.13 (s, 3H, C16H_3), and 0.88 {t, *J* = 6.9 Hz, 9H, C2'OSi[OCH_2CH_2(CH_2)$_5$C*H*$_3$]$_3$}.

^{13}C NMR (75 MHz, $CDCl_3$): δ 204.0, 171.5, 170.9, 170.1, 167.2, 167.2, 143.0, 138.3, 134.3, 133.9, 132.9, 132.0, 130.4, 129.3, 128.9 (x2), 128.8, 128.1, 127.3, 126.8, 84.7, 81.2, 79.3, 76.6, 75.8, 75.3, 74.9, 72.4, 71.4, 64.1, 58.7, 55.5, 45.7, 43.4, 35.8, 35.7, 32.4, 32.0, 29.54, 29.52, 27.0, 25.8, 23.0, 22.9, 22.4, 21.1, 14.9, 14.3, and 9.8.

HRMS (ESI) Calc'd for $C_{71}H_{101}NNaO_{17}Si$ $[M + Na]^+$ 1290.6731; found 1290.6749.

IR (thin film) 2926, 2855, 1730, 1665, 1643, 1602, 1581, 1518, 1484, 1453, 1371, 1312, 1271, 1240, 1174, 1094, 1025, 985, 926, 907, 851, 801, 777, and 711 cm^{-1}.

mp = 60-63 °C.

TLC R_f (3:1 Hexanes:EtOAc) = 0.15.

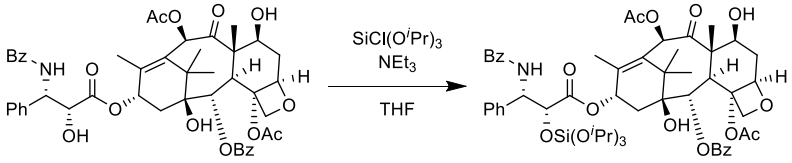

PTX (1.01) ***3.06***

2'-*O*-(Tri-*i*-propoxysilyl)paclitaxel (3.06). Paclitaxel (38.8 mg, 0.0454 mmol, 1.0 equiv) was dissolved in dry THF (1.0 mL) in an oven-dried culture tube fitted with a Teflon-lined cap and magnetic stir bar. Triethylamine (25 µL, 0.179 mmol, 3.9 equiv) was added by Wiretrol®. A 2.9:1 mixture of tri-*i*-propoxychlorosilane:tetra-*i*-propoxysilane (0.155 mg, 0.132 mmol, 2.9 equiv of tri-*i*-propoxychlorosilane) was added. The culture tube was sealed and a white precipitate was observed within minutes. The suspension was stirred at room temperature for 48 hours and the cloudy, heterogeneous reaction mixture was noted to be slightly yellowed. The suspension was diluted with a mixture of hexanes:EtOAc (1:1), the slurry filtered through a short plug of Celite® to remove the triethylammonium salt, the filtrate

concentrated under reduced pressure, and the residue redissolved in a mixture of hexanes:EtOAc (1:1). Chromatography (SiO_2, 1:1 hexanes:ethyl acetate) via MPLC yielded the title compound as a white, crystalline solid (31.1 mg, 0.0294 mmol, 64.7%). If necessary, residual EtOAc was removed by storage under high vacuum for ≥ 24h.

^{1}H NMR (500 MHz, $CDCl_3$): δ 8.11 (dd, *J* = 8.5, 1.4 Hz, 2H, C2O_2C-*o*-Ph), 7.79 (dd, *J* = 8.4, 1.3 Hz, 2H, C3'NHCO-*o*-Ph), 7.62 (tt, *J* = 7.6, 1.3 Hz, 1H, C2O_2C-*p*-Ph, 1H), 7.55-7.47 (m, 3H, C2O_2C-*m*-Ph and C3'NHCO-*p*-Ph), 7.44-7.35 (m, 6H, C3'-*o*-Ph, C3'-*m*-Ph and C3'NHCO-*m*-Ph), 7.27 (tt, *J* = 7.0, 1.7 Hz, 1H, C3'-*p*-Ph), 7.17 (d, *J* = 8.5 Hz, 1H, C3'NH), 6.28 (s, 1H, H10), 6.19 (br dd, *J* = 9, 9 Hz, 1H, H13), 5.69 (dd, *J* = 8.5, 3.6 Hz, 1H, H3'), 5.68 (d, *J* = 6.7 Hz, 1H, H2), 4.98 (d, *J* = 3.6 Hz, 1H, H2'), 4.96 (dd, *J* = 9.7, 2.4 Hz, 1H, H5), 4.44 (ddd, *J* = 10.9, 6.6, 4.1 Hz, 1H, H7), 4.31 (d, *J* = 8.4 Hz, 1H, H20α), 4.20 (d, *J* = 8.4 Hz, 1H, H20β), 4.13 {sept, *J* = 6.1 Hz, 3H, C2'OSi[OC*H*$(CH_3)_2]_3$}, 3.80 (d, *J* = 7.1 Hz, 1H, H3), 2.56 (ddd, *J* = 14.8, 9.8, 6.6 Hz, 1H, H6α), 2.47 (d, *J* = 4.1 Hz, 1H, C7OH), 2.42 (s, 3H, C4OAc), 2.29 (dd, *J* = 15.4, 9.4 Hz, 1H, H14α), 2.24 (s, 3H, C10OAc), 2.06 (dd, *J* = 15.4, 8.9 Hz, 1H, H14β), 1.91 (d, *J* = 1.4 Hz, 3H, C18H_3), 1.88 (ddd, *J* = 14.3, 11.0, 2.4 Hz, 1H, H6β), 1.76 (br s, 1H, C1OH), 1.68 (s, 3H, C19H_3), 1.23 (s, 3H, C17H_3), 1.15 {d, *J* = 6.1 Hz, 9H, C2'OSi[OCH$(CH_3)_a$(C*H*$_3)_b]_3$}, 1.12 {d, *J* = 6.1 Hz, 9H, C2'OSi[OCH$(CH_3)_a$(C*H*$_3)_b]_3$}, and 1.12 (s, 3H, C16H_3).

^{13}C NMR (125 MHz, $CDCl_3$): δ 204.1, 171.5, 171.1, 170.1, 167.3, 167.2, 143.1, 138.3, 134.4, 133.9, 132.9, 131.9, 130.4, 129.4, 128.9 (x2), 128.8, 128.1, 127.3, 127.0, 84.7, 81.2, 79.3, 76.7, 75.9, 75.3, 74.9, 72.3, 71.5, 66.7, 58.7, 55.8, 45.7, 43.4, 35.8, 35.7, 27.0, 25.44, 25.42, 23.0, 22.4, 21.1, 15.2, and 9.8.

HRMS (ESI) Calc'd for $C_{56}H_{71}NNaO_{17}Si$ $[M + Na]^+$ 1080.4383; found 1080.4380.

IR (thin film) 3500 (br), 2974, 2934, 1729, 1666, 1603, 1583, 1515, 1485, 1452, 1371, 1313, 1269, 1241, 1174, 1114, 1052, 985, 897, 850, 800, 773, and 712 cm^{-1}.

mp = 126-129 °C.

TLC R_f (1:1 Hexanes:EtOAc) = 0.45.

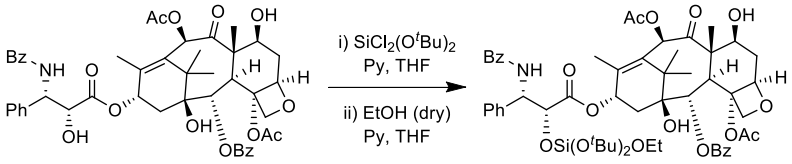

PTX (1.01) **3.07**

2'-*O*-(Ethoxydi-*t*-butoxysilyl)paclitaxel (3.07). Paclitaxel (49.3 mg, 0.0577 mmol, 1.0 equiv) was dissolved in dry THF (1.0 mL) in an oven-dried culture tube with a Teflon-lined cap and magnetic stir bar. Pyridine (0.12 mL, 1.48 mmol, 26 equiv) was added by syringe. A distilled sample of di-*t*-butoxydichlorosilane (0.349 mg, 1.42 mmol, 25 equiv) was added by Wiretrol®. The culture tube was sealed and the solution was allowed to stir at room temperature. A small amount of a white precipitate was observed after ca. 30 minutes, and the reaction mixture was noted to be cloudy and heterogeneous after stirring for 6 hours. To the suspension, pyridine was again added (0.47 mL, 5.81 mmol, 100 equiv). Immediately afterward, anhydrous ethanol (dried overnight over 3Å molecular sieves, 0.68 mL, 11.7 mmol, 200 equiv) was added. The mixture was allowed to stir for one additional hour at room temperature. Analysis of the crude mixture was completed by removing a 0.1 mL aliquot of the reaction solution, removing the volatile components under reduced pressure, and analyzing the crude ^1H NMR spectrum. The results indicated that the reaction was complete. The remainder of the reaction suspension was diluted with a mixture of hexanes:EtOAc (1:1), the slurry filtered through a short plug of Celite® to remove

the pyridinium salt, the filtrate concentrated under reduced pressure, and the residue redissolved in a mixture of hexanes:EtOAc (2:1). Chromatography (SiO_2, 2:1 hexanes:EtOAc) via MPLC yielded the title compound as a white, crystalline solid (52.0 mg, 0.0485 mmol, 84.1%). If necessary, residual EtOAc was removed by storage under high vacuum for ≥ 24h.

^{1}H NMR (500 MHz, $CDCl_3$): δ 8.11 (dd, *J* = 8.5, 1.4 Hz, 2H, C2O_2C-*o*-Ph), 7.79 (dd, *J* = 8.4, 1.4 Hz, 2H, C3'NHCO-*o*-Ph), 7.62 (tt, *J* = 7.4, 1.3 Hz, 1H, C2O_2C-*p*-Ph, 1H), 7.56-7.46 (m, 3H, C2O_2C-*m*-Ph and C3'NHCO-*p*-Ph), 7.45-7.33 (m, 6H, C3'-*o*-Ph, C3'-*m*-Ph and C3'NHCO-*m*-Ph), 7.30-7.22 (m, 1H, C3'-*p*-Ph), 7.15 (d, *J* = 8.4 Hz, 1H, C3'NH), 6.28 (s, 1H, H10), 6.18 (br dd, *J* = 9, 9 Hz, 1H, H13), 5.68 (d, *J* = 7.2 Hz, 1H, H2), 5.66 (dd, *J* = 8.3, 3.6 Hz, 1H, H3'), 5.01 (d, *J* = 3.6 Hz, 1H, H2'), 4.97 (dd, *J* = 9.7, 2.3 Hz, 1H, H5), 4.44 (ddd, *J* = 10.8, 6.6, 4.1 Hz, 1H, H7), 4.31 (d, *J* = 8.4 Hz, 1H, H20α), 4.19 (d, *J* = 8.4 Hz, 1H, H20β), 3.79 (d, *J* = 7.0 Hz, 1H, H3), 3.64 (q, *J* = 7.0 Hz, 2H, C2'OSiOC*H_2*CH_3), 2.56 (ddd, *J* = 14.8, 9.7, 6.6 Hz, 1H, H6α), 2.45 (d, *J* = 4.1 Hz, 1H, C7OH), 2.41 (s, 3H, C4OAc), 2.28 (dd, *J* = 15.4, 9.4, Hz, 1H, H14α), 2.24 (s, 3H, C10OAc), 2.05 (dd, *J* = 15.3, 9.0 Hz, 1H, H14β), 1.90 (d, *J* = 1.4 Hz, 3H, C18H_3), 1.88 (ddd, *J* = 14.4, 11.1, 2.5 Hz, 1H, H6β), 1.68 (s, 4H, C1OH and C19H_3), 1.26 (s, 9H, C2'OSiOC(C*H_3*)$_2$], 1.25 (s, 9H, C2'OSiOC(C*H_3*)$_2$], 1.23 (s, 3H, C17H_3), and 1.13 (overlapping t, *J* = 7.0 Hz, 3H, C2'OSiCH_2C*H_3* and s, 3H, C16H_3).

^{13}C NMR (125 MHz, $CDCl_3$): δ 204.1, 171.5, 171.0, 170.0, 167.3, 167.2, 143.1, 138.4, 134.4, 133.9, 132.8, 131.9, 130.4, 129.4, 128.90, 128.89, 128.8, 128.1, 127.3, 127.0, 84.7, 81.2, 79.3, 76.6, 75.9, 75.3, 74.9, 73.99, 73.98, 72.3, 71.4, 59.3, 58.7, 55.8, 45.7, 43.4, 35.8, 35.7, 31.41, 31.38, 27.0, 22.9, 22.3, 21.1, 18.2, 15.1, and 9.8.

IR (thin film) 3500 (br), 2976, 2936, 1726, 1665, 1603, 1582, 1514, 1485, 1452, 1389, 1368, 1312, 1270, 1242, 1179, 1128, 1069, 1025, 981, 909, 853, 821, 800, 775, 733, and 711 cm^{-1}.

HRMS (ESI) Calc'd for $C_{57}H_{73}NNaO_{17}Si$ $[M + Na]^+$ 1094.4540; found 1094.4579.

mp = 130-134 °C.

TLC R_f (2:1 Hexanes:EtOAc) = 0.2.

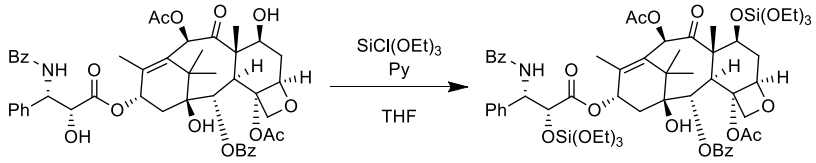

PTX (1.01) **3.08**

2',7-Di-*O*-(Triethoxysilyl)paclitaxel (3.08). Paclitaxel (58.0 mg, 0.0679 mmol, 1.0 equiv) was dissolved in dry THF (1.0 mL) in an oven-dried culture tube fitted with a Teflon-lined cap and a stir bar. Pyridine (25 µL, 0.309 mmol, 4.5 equiv) was added by Wiretrol®. Chlorotriethoxysilane (50 µL, 0.255 mmol, 3.8 equiv) was added, and a white precipitate was immediately observed. The suspension was allowed to stir for 2 hours at room temperature and then diluted with hexanes:EtOAc (1:1). The slurry was filtered through a short plug of Celite® to remove the pyridinium salt, and the filtrate concentrated under reduced pressure. The residue was purified by MPLC (SiO_2, 2:1 hexanes:EtOAc) to yield **2a** as a white crystalline solid (68.0 mg, 0.058 mmol, 85%). If necessary, residual EtOAc was removed by storage under high vacuum for ≥ 24 h.

^{1}H NMR (500 MHz, $CDCl_3$): δ 8.12 (dd, *J* = 8.5, 1.5 Hz, 2H, C2O_2C-*o*-Ph), 7.78 (dd, *J* = 8.5, 1.5 Hz, 2H, C3'NHCO-*o*-Ph), 7.62 (tt, *J* = 7.5, 1.0 Hz, 1H, C2O_2C-*p*-Ph, 1H), 7.54-7.46 (m, 3H, C2O_2C-*m*-Ph and C3'NHCO-*p*-Ph), 7.44-7.36 (m, 6H, C3'-*o*-Ph, C3'-*m*-Ph and C3'NHCO-*m*-Ph), 7.29 (tt, *J* = 7.0, 1.5 Hz, 1H, C3'-*p*-Ph), 7.20 (d, *J* = 8.5 Hz, 1H, C3'NH), 6.58 (s, 1H, H10), 6.18 (br dd, *J* = 9, 9 Hz, 1H, H13), 5.72 (dd, *J* = 8.5, 3.0 Hz, 1H, H3'), 5.71 (d, *J* = 6.5 Hz, 1H, H2), 4.98 (d, *J* = 3.0 Hz, 1H, 2'H), 4.96 (dd, *J* = 10.0, 2.0 Hz, 1H, H5), 4.62 (dd, *J* = 10.5,

6.7 Hz, 1H, H7), 4.31 (d, *J* = 8.5 Hz, 1H, H20α), 4.20 (d, *J* = 8.5 Hz, 1H, H20β), 3.85 (d, *J* = 7.0 Hz, 1H, H3), 3.76 [q, *J* = 7.0 Hz, 6H, C7OSi(OC$H_2$$CH_3$)$_3$], 3.71 [q, *J* = 7.0 Hz, 6H, C2'OSi(OC$H_2$$CH_3$)$_3$], 2.66 (ddd, *J* = 14.5, 9.5, 6.5 Hz, 1H, H6α), 2.45 (s, 3H, C4OAc), 2.33 (dd, *J* = 15.4, 9.4Hz, 1H, H14α), 2.15 (s, 3H, C10OAc),2.08 (d, *J* = 1.5 Hz, 3H, C18H_3), 2.07 (dd, *J* = 15.1, 9.0 Hz, 1H, H14β), 1.96 (ddd, *J* = 14.5, 10.8, 2.2 Hz, 1H, H6β), 1.73 (s, 3H, C19H_3), 1.65 (br s, 1H, C1OH), 1.23 (s, 3H, C17H_3), 1.19 [t, *J* = 7.0 Hz, 9H, C7OSi(OCH$_2$CH_3)$_3$], 1.17 (s, 3H, C16H_3), and 1.15 [t, *J* = 7.0 Hz, 9H, C2'OSi(OCH$_2$CH_3)$_3$].

^{13}C NMR (75 MHz, $CDCl_3$): δ 202.6, 171.0, 169.8, 169.0, 167.3, 167.2, 141.0, 138.2, 134.3, 133.9, 133.3, 132.0, 130.4, 129.4, 128.9, 128.8, 128.7, 128.1, 127.3, 126.8, 84.5, 81.2, 78.9, 76.7, 75.9, 75.02, 74.99, 72.1, 71.6, 59.7, 59.5, 58.3, 55.5, 46.9, 43.4, 36.5, 35.5, 26.7, 23.0, 21.4, 21.0, 18.0 (x2), 14.2, and 10.4.

HRMS (ESI) Calc'd for $C_{59}H_{79}NNaO_{20}Si_2$ $[M + Na]^+$ 1200.4626, found 1200.4631.

IR (thin film) 3500 (br), 2976, 2928, 2896, 1744, 1725, 1644, 1603, 1580, 1541, 1486, 1451, 1370, 1314, 1268, 1238, 1169, 1098, 1080, 1027, 969, 891, 842, 795, and 708 cm^{-1}.

mp = 121-123 °C.

TLC R_f (2:1 Hexanes:EtOAc) = 0.4.

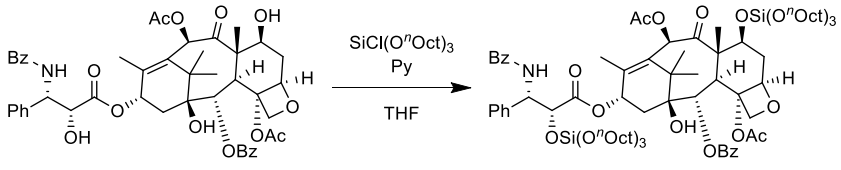

PTX (1.01) ***3.09***

2',7-Di-*O*-(Tri-*n*-octyloxysilyl)paclitaxel (3.09). Paclitaxel (57.8 mg, 0.0677 mmol, 1.0 equiv) was dissolved in dry THF (1.5 mL) in an oven-dried culture tube

fitted with a Teflon-lined cap and magnetic stir bar. Pyridine (25 µL, 0.309 mmol, 4.6 equiv) was added by Wiretrol®. A 1.67:1 mixture of tri-*n*-octyloxychlorosilane:tetra-*n*-octyloxysilane (0.155 mg, 0.199 mmol, 2.9 equiv of tri-*n*-octyloxychlorosilane) was added, and formation of a white precipitate was immediately observed. The culture tube was sealed and the suspension was allowed to stir for 5 h at room temperature. The reaction mixture was diluted with a mixture of hexanes:EtOAc (1:1), and the slurry filtered through a short plug of Celite® to remove the pyridinium salt. The filtrate was concentrated under reduced pressure, and the residue purified by MPLC (SiO_2, 9:1 hexanes:EtOAc) to yield **2b** as a viscous oil (88.1 mg, 0.0523 mmol, 77.3%). Additional elution in hexanes:EtOAc (2:1) yielded **1b** (1.7 mg, 0.0013mmol, 2.0 %). If necessary, residual EtOAc was removed from **2b** by storage under high vacuum for ≥ 24 h.

^{1}H NMR (500 MHz, $CDCl_3$): δ 8.13 (dd, *J* = 8.6, 1.4 Hz, 2H, C2O_2C-*o*-Ph), 7.78 (dd, *J* = 8.6, 1.5 Hz, 2H, C3'NHCO-*o*-Ph), 7.60 (tt, *J* = 7.4, 1.2 Hz, 1H, C2O_2C-*p*-Ph, 1H), 7.54-7.46 (m, 3H, C2O_2C-*m*-Ph and C3'NHCO-*p*-Ph), 7.44-7.35 (m, 6H, C3'-*o*-Ph, C3'-*m*-Ph and C3'NHCO-*m*-Ph), 7.28 (tt, *J* = 7.2, 1.3 Hz, 1H, C3'-*p*-Ph), 7.22 (d, *J* = 8.7 Hz, 1H, C3'NH), 6.55 (s, 1H, H10), 6.23 (br dd, *J* = 10, 9 Hz, 1H, H13), 5.74 (dd, *J* = 8.6, 3.0 Hz, 1H, H3'), 5.70 (d, *J* = 7.1 Hz, 1H, H2), 4.99 (d, *J* = 3.0 Hz, 1H, 2'H), 4.94 (dd, *J* = 9.7, 1.9 Hz, 1H, H5), 4.61 (dd, *J* = 10.6, 6.8 Hz, 1H, H7), 4.31 (d, *J* = 8.4 Hz, 1H, H20α), 4.20 (d, *J* = 8.4 Hz, 1H, H20β), 3.86 (d, *J* = 7.0 Hz, 1H, H3), 3.67 {t, *J* = 6.7 Hz, 6H, C7OSi[OCH_2(CH_2)$_6$$CH_3$]$_3$}, 3.61 {t, *J* = 6.7 Hz, 6H, C2'OSi[OCH_2(CH_2)$_6$$CH_3$]$_3$}, 2.65 (ddd, *J* = 14.7, 9.7, 6.8 Hz, 1H, H6α), 2.45 (s, 3H, C4OAc), 2.33 (dd, *J* = 15.3, 9.4 Hz, 1H, H14α) 2.13 (s, 3H, C10OAc),), 2.06 (d, *J* = 1.2 Hz, 3H, C18H_3), 2.09-2.02 (m, 1H, H14β), 1.96 (ddd, *J* = 14.5, 10.8, 2.2 Hz, 1H, H6β), 1.73 (s, 3H, C19H_3), 1.66 (br s, 1H, C1OH), 1.56-1.44 {m, 12H, C2'OSi[OCH_2CH_2(CH_2)$_5$$CH_3$]$_3$ and C7OSi[OCH_2CH_2(CH_2)$_5$$CH_3$]$_3$}, 1.34-1.21 {m, 63H, C17H_3, C2'OSi[OCH_2CH_2(CH_2)$_5$$CH_3$]$_3$, and C7OSi[OC$H_2CH_2$(C$H_2$)$_5$$CH_3$]$_3$}, 1.17 (s, 3H,

$C16H_3$), and 0.88 {overlapping t's, *J* = 6.8 Hz, 18H, C2'OSi[$OCH_2CH_2(CH_2)_5CH_3$]$_3$ and C7OSi[$OCH_2CH_2(CH_2)_5CH_3$]$_3$}.

^{13}C NMR (75 MHz, $CDCl_3$): δ 202.4, 170.9, 169.8, 168.7, 167.3, 167.2, 140.9, 138.3, 134.3, 133.8, 133.3, 131.9, 130.4, 129.4, 128.91, 128.89, 128.8, 128.1, 127.3, 126.8, 84.6, 81.2, 79.0, 76.8, 75.8, 75.1, 74.9, 72.0, 71.5, 64.1, 63.9, 58.3, 55.5, 46.8, 43.5, 36.6, 35.6, 32.5, 32.4, 32.1, 32.0, 29.6, 29.63, 29.60, 29.57, 26.7, 25.92, 25.89, 23.0, 22.91, 22.90, 21.6, 21.1, 14.3 (x2), 14.1, and 10.4.

HRMS (ESI) Calc'd for $C_{95}H_{151}NNaO_{20}Si_2$ $[M + Na]^+$ 1705.0260; found 1705.0228.

IR (thin film) 3500 (br), 2927, 2856, 1728, 1741, 1721, 1634, 1580, 1545, 1456, 1371, 1315, 1270, 1239, 1174, 1095, 1028, 989, 968, 924, 893, 843, 779, and 709 cm^{-1}.

TLC R_f (3:1 Hexanes:EtOAc) = 0.55.

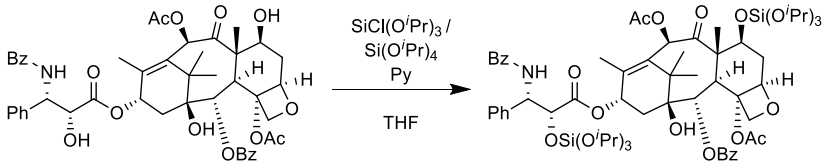

PTX (1.01) **3.10**

2',7-Di-*O*-(Tri-*i*-propoxysilyl)paclitaxel (3.10). Paclitaxel (30.1 mg, 0.0352 mmol, 1.0 equiv) was dissolved in dry THF (1.0 mL) in an oven-dried culture tube fitted with a Teflon-lined cap and magnetic stir bar. Pyridine (15 µL, 0.185 mmol, 5.3 equiv) was added by Wiretrol®. A 3.5:1 mixture of tri-*i*-propoxychlorosilane:tetra-*i*-propoxysilane (0.0424 mg, 0.134 mmol, 2.9 equiv of tri-*i*-propoxychlorosilane) was added. The culture tube was sealed and a white precipitate was observed within minutes. The suspension was stirred at room

temperature for 18 hours. The suspension was directly filtered through a short plug of Celite® to remove the triethylammonium salt, the filtrate concentrated under reduced pressure, and the residue redissolved in a mixture of hexanes:EtOAc (2:1). Chromatography (SiO_2, 2:1 hexanes:ethyl acetate) via MPLC yielded the title compound as a white, crystalline solid (29.8 mg, 0.0236 mmol, 67.0%). If necessary, residual EtOAc was removed by storage under high vacuum for ≥ 24h.

^{1}H NMR (500 MHz, $CDCl_3$): δ 8.12 (dd, *J* = 8.5, 1.5 Hz, 2H, C2O_2C-*o*-Ph), 7.80 (dd, *J* = 8.4, 1.5 Hz, 2H, C3'NHCO-*o*-Ph), 7.62 (tt, *J* = 7.4, 1.7 Hz, 1H, C2O_2C-*p*-Ph, 1H), 7.55-7.46 (m, 3H, C2O_2C-*m*-Ph and C3'NHCO-*p*-Ph), 7.43-7.34 (m, 6H, C3'-*o*-Ph, C3'-*m*-Ph and C3'NHCO-*m*-Ph), 7.29-7.24 (m, 1H, C3'-*p*-Ph), 7.17 (d, *J* = 8.4 Hz, 1H, C3'NH), 6.53 (s, 1H, H10), 6.14 (br dd, *J* = 9, 9 Hz, 1H, H13), 5.70 (d, *J* = 7.3 Hz, 1H, H2), 5.67 (dd, *J* = 8.4, 3.6 Hz, 1H, H3'), 5.00 (d, *J* = 3.6 Hz, 1H, H2'), 4.96 (dd, *J* = 9.4, 2.0 Hz, 1H, H5), 4.61 (dd, *J* = 10.7, 6.7, Hz, 1H, H7), 4.31 (d, *J* = 8.8 Hz, 1H, H20α), 4.19 (d, *J* = 8.6 Hz, 1H, H20β), 4.13 and 4.12 {overlapping septs, *J* = 6.2 Hz, 6H, C2'OSi[OC*H*$(CH_3)_2]_3$ and C7OSi[OC*H*$(CH_3)_2]_3$}, 3.85 (d, *J* = 7.4 Hz, 1H, H3), 2.68 (ddd, *J* = 14.7, 9.7, 6.8 Hz, 1H, H6α), 2.41 (s, 3H, C4OAc), 2.30 (dd, *J* = 15.1, 9.3 Hz, 1H, H14α), 2.14 (s, 3H, C10OAc), 2.10 (d, *J* = 1.2 Hz, 3H, C18H_3), 2.03 (dd, *J* = 15.7, 9.5 Hz, 1H, H14β), 1.95 (ddd, *J* = 14.6, 10.9, 2.2 Hz, 1H, H6β), 1.72 (s, 3H, C19H_3), 1.61 (br s, 1H, C1OH), 1.23 (m, 3H, C17H_3), 1.18-1.10 {m, 39H, C2'OSi[OCH$(CH_3)_a$(C*H*$_3)_b]_3$}, C2'OSi[OCH$(CH_3)_a$(C*H*$_3)_b]_3$, C7OSi[OCH$(CH_3)_a$(C*H*$_3)_b]_3$}, C7OSi[OCH$(CH_3)_a$(C*H*$_3)_b]_3$, and C16H_3}.

^{13}C NMR (125 MHz, $CDCl_3$): δ 202.6, 171.1, 169.6, 168.9, 167.3, 167.2, 141.2, 138.4, 134.4, 133.8, 133.3, 131.9, 130.4, 129.5, 128.9 (x2), 128.8, 128.1, 127.3, 127.0, 84.6, 81.2, 80.0, 76.8, 75.9, 75.2, 74.9, 72.3, 71.7, 66.6, 66.2, 58.3, 55.9, 46.8, 43.5, 36.7, 35.5, 26.8,25.5, 25.4, 25.4, 25.4, 23.0, 21.5, 21.1, 14.7, 10.5

HRMS (ESI) Calc'd for $C_{65}H_{91}NNaO_{20}Si_2$ $[M + Na]^+$ 1284.5565, found 1284.5563

IR (thin film) 3500 (br), 2973, 2933, 1725, 1671, 1603, 1582, 1512, 1484, 1452, 1371, 1313, 1267, 1238, 1173, 1116, 1047, 989, 893, 839, 767, and 711.

MP = 108-113°C

TLC R_f (2:1 Hexanes:EtOAc) = 0.55

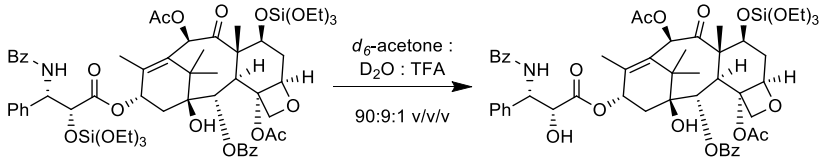

3.08 ***3.11***

7-*O*-(Triethoxysilyl)paclitaxel (3.11). Bis-silicate ester **3.08** (99.5 mg, 0.0845 mmol, 1.0 equiv) was dissolved in *d*$_6$-acetone (1.8 mL, dried over 3Å molecular sieves) in an NMR tube. A 9:1 mixture of D_2O:TFA was added (200 µL) and the reaction progress was monitored by ^{1}H NMR spectroscopy. After eight minutes at 21.4 °C, the mixture was transferred into saturated aqueous $NaHCO_3$ (2 mL). This mixture was extracted with CH_2Cl_2 (3 x 5 mL). The combined organic extracts were dried over $MgSO_4$. and concentrated under reduced pressure. The residue was purified by MPLC (SiO_2, 2:1 hexanes:EtOAc) to provide recovered starting material **2a** (27.3 mg, 0.0232 mmol, 27.4%). Additional elution in 1:1 hexanes:EtOAc gave the title compound as a white, crystalline solid [56.9 mg, 0.0560 mmol, 66.3% (91.4% brsm)]. If necessary, residual EtOAc was removed by storage under high vacuum for ≥ 24 h.

^{1}H NMR (500 MHz, $CDCl_3$): δ 8.12 (dd, *J* = 8.5, 1.3 Hz, 2H, C2O_2C-*o*-Ph), 7.75 (dd, *J* = 8.5, 1.4 Hz, 2H, C3'NHCO-*o*-Ph), 7.61 (tt, *J* = 7.5, 1.2 Hz, 1H, C2O_2C-*p*-Ph, 1H), 7.53-7.46 (m, 5H, C2O_2C-*m*-Ph, C3'NHCO-*p*-Ph, and C3'-*o*-Ph,), 7.43-

7.37 (m, 4H, C3'-*m*-Ph and C3'NHCO-*m*-Ph), 7.34 (tt, *J* = 7.3, 1.2 Hz, 1H, C3'-*p*-Ph), 7.09 (d, *J* = 9.0 Hz, 1H, C3'NH), 6.56 (s, 1H, H10), 6.18 (br dd, *J* = 9, 9 Hz, 1H, H13), 5.80 (dd, *J* = 6.9, 2.5 Hz, 1H, H3'), 5.69 (d, *J* = 6.9 Hz, 1H, H2), 4.93 (dd, *J* = 9.6, 1.7 Hz, 1H, H5), 4.78 (dd, *J* = 4.9, 2.7 Hz, 1H, 2'H), 4.57 (dd, *J* = 10.5, 6.9 Hz, 1H, H7), 4.30 (d, *J* = 8.4 Hz, 1H, H20α), 4.19 (dd, *J* = 8.3, 0.9 Hz, 1H, H20β), 3.83 (d, *J* = 6.9 Hz, 1H, H3), 3.76 [q, *J* = 7.0 Hz, 6H, C7OSi(OC*H*$_2$CH$_3$)$_3$], 3.69 (br s, 1H, C2'OH), 2.65 (ddd, *J* = 14.7, 9.7, 6.9 Hz, 1H, H6α), 2.37 (s, 3H, C4OAc), 2.35-2.25 (m, 2H, H14α and H14β), 2.15 (s, 3H, C10OAc), 1.95 (ddd, *J* =14.6, 10.7, 2.1 Hz, 1H, H6β), 1.93 (d, *J* = 1.3 Hz, 3H, C18H$_3$), 1.76 (br s, 1H, C1OH), 1.73 (s, 3H, C19H$_3$), 1.23 (s, 3H, C17H$_3$), 1.19 [t, *J* = 7.0 Hz, 9H, C7OSi(OCH$_2$C*H*$_3$)$_3$], and 1.16 (s, 3H, C16H$_3$).

^{13}C NMR (125 MHz, CDCl$_3$): δ 202.4, 172.6, 170.4, 169.0, 167.2, 167.1, 140.1, 138.2, 133.9, 133.8, 132.1, 130.3, 129.4, 129.1, 128.89, 128.87, 128.5, 127.3, 127.24, 127.23, 84.4, 81.5, 78.8, 76.8, 76.1, 74.8, 73.4, 72.5, 72.1, 59.5, 58.6, 55.0, 47.0, 43.4, 36.7, 35.6, 26.8, 22.9, 21.1, 21.0, 18.2, 14.5, and 10.3.

HRMS (ESI) Calc'd for C$_{53}$H$_{65}$NNaO$_{17}$Si [M + Na]$^+$ 1038.3914, found 1038.3914.

IR (thin film) 3500 (br), 2975, 2898, 1724, 1653, 1602, 1580, 1515, 1485, 1451, 1394, 1370, 1314, 1266, 1240, 1172, 1079, 1025, 969, 913, 888, 839, 797, and 712 cm^{-1}.

mp = 141-146 °C.

TLC R_f (1:1 Hexanes:EtOAc) = 0.5.

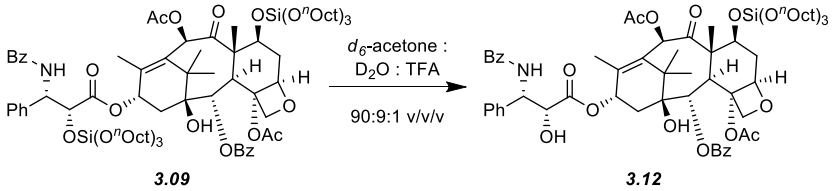

3.09 ***3.12***

7-*O*-(Tri-*n*-octyloxysilyl)paclitaxel (3.12). Bis-silicate ester **3.09** (88.1 mg, 0.0523 mmol, 1.0 equiv) was dissolved in d_6-acetone (1.8 mL, dried over 3Å molecular sieves) in an NMR tube. A 9:1 mixture of D_2O:TFA was added (200 µL) and the solution became white and cloudy. Upon vigorous mixing for 30 seconds, the mixture became homogeneous and transparent. The hydrolysis progress was monitored by ^{1}H NMR spectroscopy. After 30 minutes at room temperature, the solution was transferred into saturated aqueous $NaHCO_3$ (2 mL). This mixture was extracted with CH_2Cl_2 (3 x 5 mL). The combined organic layers were dried over $MgSO_4$ and concentrated under reduced pressure. The residue was purified by MPLC (SiO_2, 3:1 hexanes:EtOAc) to provide recovered **2b** (12.9 mg, 0.0076 mmol, 27.4%). Additional elution in 2:1 hexanes:EtOAc gave the title compound as a crystalline solid [37.3 mg, 0.0294 mmol, 56.2% (65.7% brsm)]. If necessary, residual EtOAc was removed by storage under high vacuum for ≥ 24 h.

^{1}H NMR (500 MHz, $CDCl_3$): δ 8.12 (dd, *J* = 8.5, 1.3 Hz, 2H, C2O_2C-*o*-Ph), 7.75 (dd, *J* = 8.5, 1.4 Hz, 2H, C3'NHCO-*o*-Ph), 7.61 (tt, *J* = 7.4, 1.3 Hz, 1H, C2O_2C-*p*-Ph, 1H), 7.53-7.47 (m, 5H, C2O_2C-*m*-Ph, C3'NHCO-*p*-Ph, and C3'-*o*-Ph,), 7.43-7.38 (m, 4H, C3'-*m*-Ph and C3'NHCO-*m*-Ph), 7.34 (tt, *J* = 7.2, 1.3 Hz, 1H, C3'-*p*-Ph), 7.06 (d, *J* = 9.0 Hz, 1H, C3'NH), 6.53 (s, 1H, H10), 6.17 (br dd, *J* = 9, 9 Hz, 1H, H13), 5.81 (dd, *J* = 6.8, 2.4 Hz, 1H, H3'), 5.68 (d, *J* = 6.9 Hz, 1H, H2), 4.92 (dd, *J* = 9.6, 1.8 Hz, 1H, H5), 4.78 (dd, *J* = 4.8, 2.6 Hz, 1H, 2'H), 4.56 (dd, *J* = 6.7, 10.5 Hz, 1H, H7), 4.29 (d, *J* = 8.3 Hz, 1H, H20α), 4.19 (d, *J* = 8.5 Hz, 1H, H20β), 3.83 (d, *J* = 7.0 Hz, 1H, H3), 3.66 {t, *J* = 6.7 Hz, 6H,

C7OSi[OCH_2(CH_2)$_6$$CH_3$]$_3$}, 3.60 (d, *J* = 4.9 Hz, 1H, C2'OH), 2.64 (ddd, *J* = 14.7, 9.7, 6.9 Hz, 1H, H6α), 2.37 (s, 3H, C4OAc), 2.34-2.27 (m, 2H, H14α and H14β), 2.14 (s, 3H, C10OAc), 1.97-1.90 (m, 4H, H6β and C18H_3), 1.74-1.70 (m, 4H, C1OH and C19H_3), 1.52 {tt, *J* = 6.8, 6.8 Hz, 6H, C7OSi[OCH_2CH_2(CH_2)$_5$$CH_3$]$_3$}, 1.34-1.22 {m, 33H, C17H_3 and C7OSi[OCH_2CH_2(CH_2)$_5$$CH_3$]$_3$}, 1.16 (s, 3H, C16$H_3$), and 0.88 {t, *J* = 6.8 Hz, 9H, C7OSi[OCH_2CH_2(CH_2)$_5$CH_3]$_3$}.

^{13}C NMR (125 MHz, $CDCl_3$): δ 202.2, 172.7, 170.3, 168.8, 167.2, 167.0, 140.0, 138.3, 133.93, 133.89, 132.1, 130.4, 129.4, 129.1, 128.9 (x3), 128.5, 127.3, 127.2, 84.5, 81.5, 78.8, 76.8, 76.0, 74.9, 73.3, 72.1, 63.9, 58.6, 54.9, 47.0, 43.4, 36.6, 35.6, 32.5, 32.1, 29.62, 29.57, 26.8, 25.9, 22.91, 22.88, 21.1, 21.0, 14.5, 14.3, and 10.3.

HRMS (ESI) Calc'd for $C_{71}H_{101}NNaO_{17}Si$ $[M + Na]^+$ 1290.6731; found 1290.6738.

IR (thin film) 3500 (br), 2926, 2855, 1732, 1710, 1673, 1602, 1582, 1452, 1396, 1370, 1317, 1281, 1269, 1241, 1179, 1093, 1025, 988, 968, 890, 844, 809, and 712 cm^{-1}.

mp = 69-73 °C.

TLC R_f (2:1 Hexanes:EtOAc) =0.4.

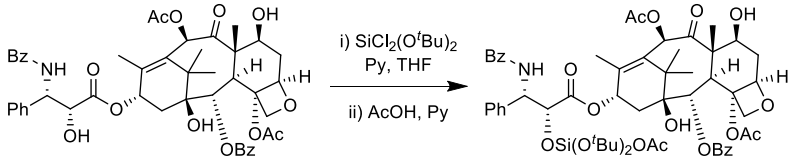

PTX (1.01) ***3.16***

2'-*O*-(Di-*t*-butoxyacetoxysilyl)paclitaxel (3.16). Paclitaxel (33.5 mg, 0.0392 mmol, 1.0 equiv) was dissolved in THF (1.0 mL, dried by distillation from sodium/benzophenone) in an oven-dried culture tube with a Teflon-lined cap and magnetic stir bar. Pyridine (50 µL, 0.618 mmol, 16 equiv) was added by

Wiretrol®. A distilled sample of di-*t*-butoxydichlorosilane (0.0524 mg, 0.214 mmol, 5.5 equiv) was added by Wiretrol®. The culture tube was sealed and the solution was allowed to stir at room temperature for 24 hours. The reaction mixture was noted to be cloudy and heterogeneous after stirring overnight. To the suspension, pyridine was again added (50 µL, 0.618 mmol, 16 equiv). Immediately afterward, glacial acetic acid (50 µL, 0.873 mmol, 22 equiv) was added. The mixture was allowed to stir for an additional 24 hours at room temperature. The reaction suspension was diluted with EtOAc, the slurry filtered through a short plug of Celite® to remove the pyridinium salt, the filtrate concentrated under reduced pressure, and the residue redissolved in a mixture of hexanes:EtOAc (2:1). Chromatography (SiO_2, 2:1 hexanes:EtOAc) via MPLC yielded the title compound (28.0 mg, 0.0258 mmol, 65.8%). If necessary, residual EtOAc was removed by storage under high vacuum for ≥ 24h.

^{1}H NMR (500 MHz, $CDCl_3$): δ 8.13 (dd, *J* = 8.5, 1.4 Hz, 2H, C2O_2C-*o*-Ph), 7.81 (dd, *J* = 8.5, 1.4 Hz, 2H, C3'NHCO-*o*-Ph), 7.63 (tt, *J* = 7.4, 1.3 Hz, 1H, C2O_2C-*p*-Ph), 7.54 (t, *J* = 7.9 Hz, 2H, C2O_2C-*m*-Ph), 7.48 (tt, *J* = 7.4, 1.9 Hz, 1H, C3'NHCO-*p*-Ph), 7.43-7.34 (m, 6H, C3'-*o*-Ph, C3'-*m*-Ph, and C3'NHCO-*m*-Ph), 7.30-7.21 (m, 2H, C3'-*p*-Ph and C3'NH), 6.28 (s, 1H, H10), 6.13 (br dd, *J* = 9, 9 Hz, 1H, H13), 5.69 (dd, *J* = 8.5, 3.9 Hz, 1H, H3'), 5.66 (d, *J* = 7.2 Hz, 1H, H2), 5.19 (d, *J* = 4.0 Hz, 1H, H2'), 4.96 (dd, *J* = 9.6, 2.1 Hz, 1H, H5), 4.44 (ddd, *J* = 10.8, 6.4, 4.3 Hz, 1H, H7), 4.31 (d, *J* = 8.4 Hz, 1H, H20α), 4.20 (d, *J* = 8.3 Hz, 1H, H20β), 3.79 (d, *J* = 7.0 Hz, 1H, H3), 2.56 (ddd, *J* = 14.9, 9.9, 6.6 Hz, 1H, H6α), 2.45 (overlapping m, 1H, C7OH and s, 3H, C4OAc), 2.30-2.18 (overlapping m, 1H, H14α and s, 3H, C10OAc), 1.97-1.84 (m, 8H, H14β, C18H_3, SiOAc, and H6β), 1.67 (s, 3H, C19H_3), 1.61 (s, 1H, C1OH), 1.30 (s, 9H, C2'OSiOC(CH_3)$_2$], 1.26 (overlapping s, 9H, C2'OSiOC(CH_3)$_2$], 1.22 (s, 3H, C17H_3), and 1.12 (s, 3H, C16H_3).

^{13}C NMR (75 MHz, $CDCl_3$): δ 204.1, 171.6, 170.9, 170.2, 167.2, 167.1, 143.2, 138.2, 134.4, 133.9, 132.7, 131.8, 130.4, 129.4, 128.92, 128.85, 128.7, 128.1, 127.4, 127.1, 84.7, 81.1, 79.3, 76.6, 75.9, 75.4, 75.31, 75.27 (x2), 72.3, 71.6, 58.7, 56.1, 45.7, 43.3, 35.7 (x2), 31.34, 31.32, 26.9, 23.1, 22.9, 22.4, 21.1, 15.2, and 9.8.

HRMS (ESI) Calc'd for $C_{57}H_{71}NNaO_{18}Si$ $[M + Na]^+$ 1108.4333; found 1108.4360.

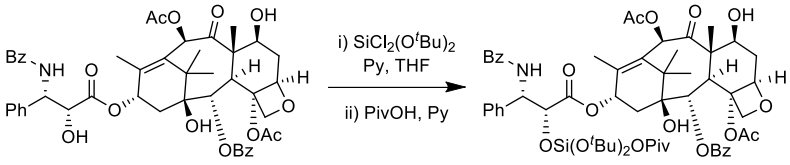

PTX (1.01) ***3.17***

2'-*O*-(Di-*t*-butoxypivaloxysilyl)paclitaxel (3.17). Paclitaxel (30.0 mg, 0.0351 mmol, 1.0 equiv) was dissolved in THF (1.0 mL) in an oven-dried culture tube with a Teflon-lined cap and magnetic stir bar. Pyridine (25 µL, 0.31 mmol, 8.8 equiv) was added by Wiretrol®. A distilled sample of di-*t*-butoxydichlorosilane (0.050 mg, 0.20 mmol, 6 equiv) was added by Wiretrol®. The culture tube was sealed and the solution was allowed to stir at room temperature for 96 hours. Pyridine ((40 µL, 0.49 mmol, 14 equiv) and pivalic acid (48.0 mg, 0.470 mmol, 13.4 equiv) were co-dissolved in dry THF (1 mL), and the solution was added in a single portion to the reaction vesicle., The mixture was allowed to stir for an additional 24 hours at room temperature. An aliquot of the reaction mixture was removed, concentrated to dryness under reduced pressure, and analyzed by crude ^{1}H NMR spectroscopy. Analysis showed that ca. 10% conversion to **3.16**. The remainder of the reaction slurry was heated to 60 °C and stirred for 18 hours. A second aliquot of the reaction mixture was removed, concentrated to dryness under reduced pressure, and analyzed by crude ^{1}H NMR spectroscopy. Analysis showed an ca. 1:1:2 mixture of **3.17:**PTX:PTX-2'OSi(OtBu)$_2$Cl. The

reaction was capped and allowed to stir at 60 °C for an additional 24 hours. A third aliquot of the reaction mixture was removed, concentrated to dryness under reduced pressure, and analyzed by crude ^{1}H NMR spectroscopy. The results showed no further conversion of the chlorosilane to **3.16** and a larger resonance corresponding to PTX. The remainder of the reaction suspension was diluted with EtOAc, the slurry filtered through a short plug of Celite® to remove the pyridinium salt, the filtrate concentrated under reduced pressure, and the residue redissolved in a mixture of hexanes:EtOAc (2:1). Chromatography (SiO_2, 2:1 hexanes:EtOAc) via MPLC yielded the title compound (4.8 mg, 0.0043 mmol, 12%). If necessary, residual EtOAc was removed by storage under high vacuum for ≥ 24h.

^{1}H NMR (500 MHz, $CDCl_3$)[160]: δ 8.12 (dd, *J* = 8.6, 1.4 Hz, 2H, C2O_2C-*o*-Ph), 7.80 (dd, *J* = 8.2, 1.1 Hz, 2H, C3'NHCO-*o*-Ph), 7.60 (br tt, *J* = 7, 1 Hz, 1H, C2O_2C-*p*-Ph), 7.54-7.35 (m, 9H, C2O_2C-*m*-Ph, C3'NHCO-*p*-Ph, C3'-*o*-Ph, C3'-*m*-Ph, and C3'NHCO-*m*-Ph), 7.31 (t, *J* = 7.0 Hz, 1H, C3'-*p*-Ph), 7.07 (d, *J* = 9.3 Hz, 1H, C3'NH), 6.28 (s, 1H, H10), 6.22 (br dd, *J* = 9, 8 Hz, 1H, H13), 5.82 (dd, *J* = 9.0, 2.5 Hz, 1H, H3'), 5.68 (d, *J* = 7.5 Hz, 1H, H2), 5.20 (d, *J* = 2.4 Hz, 1H, H2'), 4.96 (dd, *J* = 9.3, 2.2 Hz, 1H, H5), 4.44 (br m, 1H, H7), 4.30 (d, *J* = 8.8 Hz, 1H, H20α), 4.20 (d, *J* = 8.6 Hz, 1H, H20β), 3.80 (d, *J* = 6.9 Hz, 1H, H3), 2.56 (ddd, *J* = 14.4, 9.7, 6.3 Hz, 1H, H6α), 2.45 (overlapping m, 1H, C7OH and s, 3H, C4OAc), 2.37 (dd, *J* = 14.8, 8.5 Hz, 1H, H14α), 2.25 (s, 3H, C10OAc), 1.97-1.84 (overlapping m, 1H, H14β and s, 3H, C18H_3), 1.68 (overlapping m, 1H, H6β and s, 3H, C19H_3), 1.59 (br s, 1H, C1OH), 1.33 [s, 9H, C2'OSiOC(CH_3)$_2$], 1.32 [s, 9H, C2'OSiOC(O)C(CH_3)$_3$], 1.31 [s, 9H, C2'OSiOC(CH_3)$_2$],, 1.22 (s, 3H, C17H_3), and 1.13 (s, 3H, C16H_3).

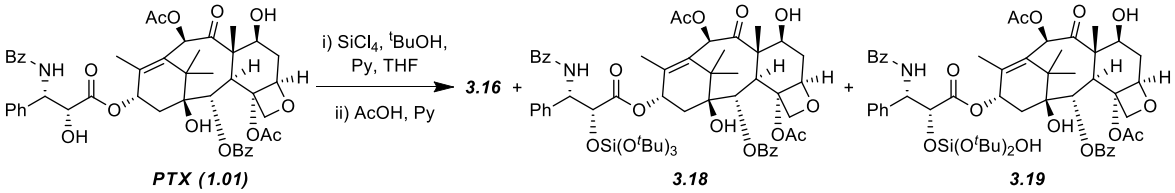

PTX-2'OSi(OtBu)$_3$2'-*O*-(Tri-*t*-butoxyacetoxysilyl)paclitaxel (3.18). Paclitaxel (49.8 mg, 0.0583 mmol, 1.0 equiv) was dissolved in dry THF (1.0 mL) in an oven-dried culture tube with a Teflon-lined cap and magnetic stir bar. A 1.0 mL aliquot containing ca. 0.40 mL of $SiCl_4$ (2.6 mmol), 0.84 mL of pyridine (10. mmol), and 0.73 mL of *t*-butanol (7.6 mmol) in THF (pre-mixed for 24 h) was added crude to the reaction vessel. The culture tube was sealed and the solution was allowed to stir at room temperature overnight. To the suspension, pyridine was again added (50 µL, 0.62 mmol, 13 equiv). Immediately afterward, glacial acetic acid (50 µL, 0.87 mmol, 24 equiv) was added. The mixture was allowed to stir for an additional 48 hours at room temperature. The reaction suspension was diluted with EtOAc, the slurry filtered through a short plug of Celite® to remove the pyridinium salt, the filtrate concentrated under reduced pressure, and the residue redissolved in a mixture of hexanes:EtOAc (2:1). Chromatography (SiO_2, 2:1 hexanes:EtOAc) via MPLC yielded **3.18** (11.2 mg, 0.0107 mmol, 18.4%) and, in the second fraction to elute **3.15** (23.0 mg, 0.0212 mmol, 36.3%), and finally, in the third fraction to elute, **3.17** (8.6 mg, 0.0078 mmol, 13.4%). If necessary, residual EtOAc was removed by storage under high vacuum for ≥ 24h.

For **3.18**:

^{1}H NMR (500 MHz, $CDCl_3$)[160]: δ 8.11 (dd, *J* = 8.8, 1.7 Hz, 2H, C2O_2C-*o*-Ph), 7.78 (dd, *J* = 8.8, 1.8 Hz, 2H, C3'NHCO-*o*-Ph), 7.61 (tt, *J* = 7.3, 1.2 Hz, 1H, C2O_2C-*p*-Ph, 1H), 7.56-7.34 (m, 9H, C2O_2C-*m*-Ph, C3'NHCO-*p*-Ph, C3'-*o*-Ph, C3'-*m*-Ph,

[160] Minor impurities were noted in the alkyl region of this product.

and C3'NHCO-*m*-Ph), 7.30-7.24 (m, 1H, C3'-*p*-Ph), 7.05 (d, *J* = 8.5 Hz, 1H, C3'NH), 6.29 (s, 1H, H10), 6.17 (br dd, *J* = 9, 9 Hz, 1H, H13), 5.74-5.66 (m, 2H, H2 and H3'), 5.16 (d, *J* = 2.9 Hz, 1H, H2'), 4.97 (dd, *J* = 9.2, 2.3 Hz, 1H, H5), 4.45 (app br dd, *J* = 11, 6 Hz, 1H, H7), 4.31 (d, *J* = 8.4 Hz, 1H, H20α), 4.20 (d, *J* = 8.6 Hz, 1H, H20β), 3.80 (d, *J* = 7.0 Hz, 1H, H3), 2.57 (ddd, *J* = 15.2, 9.9, 6.7 Hz, 1H, H6α), 2.47 (br d, *J* = 4 Hz, 1H, C7OH), 2.42 (s, 3H, C4OAc), 2.32 (dd, *J* = 15.9, 9.6, Hz, 1H, H14α), 2.25 (s, 3H, C10OAc), 2.17 (br dd, *J* = 14, 5 Hz, 1H, H14β), 1.93 (br d, *J* = 1 Hz, 3H, $C18H_3$), 1.89 (br m, 1H, H6β), 1.78 (br s, 1H C1OH), 1.68 (s, 3H, $C19H_3$), 1.24 {overlapping s, 27H, C2'OSi[OC(CH_3)]$_3$ and s, 3H, $C17H_3$}, and 1.13 (s, 3H, $C16H_3$).

^{13}C NMR (125 MHz, $CDCl_3$): δ 204.1, 171.6, 171.1, 170.1, 167.4, 167.2, 143.2, 138.3, 134.5, 133.9, 132.8, 131.9, 130.4, 129.4, 128.97, 128.95, 128.8, 128.0, 127.3, 126.9, 84.7, 81.2, 79.3, 76.7, 75.9, 75.3, 74.2, 73.9, 72.4, 71.4, 58.7, 55.5, 45.7, 43.4, 36.0, 35.7, 31.4, 27.0, 23.0, 22.4, 21.1, 15.3, and 9.8.

IR (thin film) 3500 (br), 2973, 2929, 1729, 1670, 1511, 1483, 1452, 1389, 1367, 1268, 1242, 1183, 1124, 1069, 1025, 985, 835, 800, 758, and 711 cm^{-1}.
HRMS (ESI) Calc'd for $C_{59}H_{77}NNaO_{17}Si$ $[M + Na]^+$ 1122.4853; found 1122.4901

mp = 134-138°C.

For **3.19**:

^{1}H NMR (500 MHz, d_6-acetone): δ 8.13 (dd, *J* = 8.5, 1.4 Hz, 2H, $C2O_2C$-*o*-Ph), 7.89 (dd, *J* = 8.5, 1.4 Hz, 2H, C3'NHCO-*o*-Ph), 7.69 (tt, *J* = 7.3, 1.3 Hz, 1H, $C2O_2C$-*p*-Ph), 7.63-7.26 (m, 10H, $C2O_2C$-*m*-Ph, C3'NHCO-*p*-Ph, C3'-*o*-Ph, C3'-*m*-Ph, C3'NHCO-*m*-Ph, and C3'-*p*-Ph), 6.41 (s, 1H, H10), 6.16 (br dd, *J* = 9, 9 Hz, 1H, H13), 5.72-5.68 (m, 2H, H3' and H2), 5.08 (d, *J* = 5.5 Hz, 1H, H2'), 4.97 (dd, *J* = 9.8, 2.0 Hz, 1H, H5), 4.41 (dd, *J* = 10.7, 6.5 Hz, 1H, H7), 4.17 (d, *J* = 8.2 Hz, 1H, H20α), 4.15 (d, *J* = 8.1 Hz, 1H, H20β), 3.85 (d, *J* = 6.9 Hz, 1H, H3), 2.57-2.31 (m, 5H, H6α, C4OAc, and H14α), 2.16 (s, 3H, C10OAc), 2.0-1.9 (m, 4H,

H14β, and C18H_3), 1.78 (ddd, *J* = 14.0, 10.8, 2.3 Hz, 1H, H6β), 1.66 (s, 3H, C19H_3), 1.30 (s, 9H, C2'OSiOC(C*H*$_3$)$_2$], 1.28 (s, 9H, C2'OSiOC(C*H*$_3$)$_2$], 1.21 (s, 3H, C17H_3), and 1.18 (s, 3H, C16H_3).

HRMS (ESI) Calc'd for $C_{57}H_{71}NNaO_{18}Si$ $[M + Na]^+$ 1066.4227; found 1066.4251

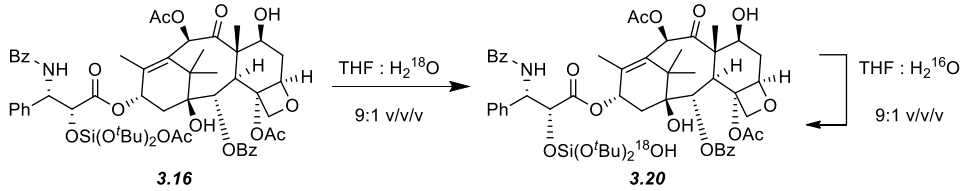

3.16 ***3.20***

2'-*O*-(Di-*t*-butoxysilanol)paclitaxel (3.20). Compound **3.16** (10.4 mg, 0.0096 mmol, 1 equiv) was dissolved in THF (0.45 mL, dried by distillation from sodium/benzophenone) and to this solution ^{18}O-labeled water (50 µL) was added. The solution was sealed with a Teflon-lined cap and allowed to stir at room temperature for two hours. The solution was diluted with 5 mL of $CDCl_3$ (dried over 3Å molecular sieves) and dried over magnesium sulfate. The solution was filtered, concentrated under reduced pressure, and analyzed by ESI HR-MS.

HRMS (ESI) Calc'd for $C_{57}H_{71}NNaO_{17}{}^{18}OSi$ $[M + Na]^+$ 1068.4269; found 1068.4267

Approximately half of the recovered silanol **3.20** was dissolved in THF (0.45 mL, dried by distillation from sodium/benzophenone) and water (50 µL) was added. The solution was sealed with a Teflon-lined cap and allowed to stir at room temperature for two hours. The solution was diluted with 5 mL of $CDCl_3$ (dried over 3Å molecular sieves) and dried over magnesium sulfate. The solution was filtered, concentrated under reduced pressure, and analyzed by ESI HR-MS.

HRMS (ESI) Calc'd for $C_{57}H_{71}NNaO_{17}{}^{18}OSi$ $[M + Na]^+$ 1068.4269; found 1068.4281

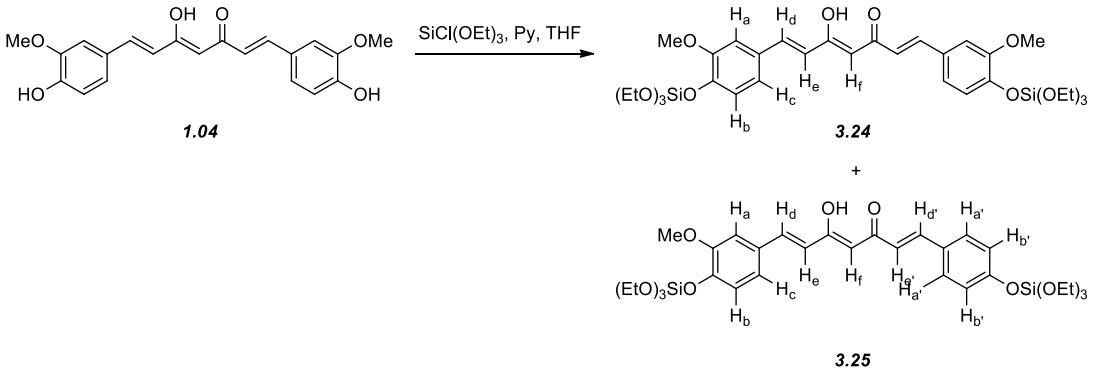

Di-*O*-(Triethoxysilyl)curcumin (3.24). Curcumin (≥94% purity as received, 19.7 mg, 0.0535 mmol, 1.0 equiv) was dissolved in dry THF (1.0 mL) in an oven-dried culture tube fitted with a Teflon-lined cap and a stir bar. Pyridine (20 µL, 0.25 mmol, 4.6 equiv) was added by Wiretrol®. Chlorotriethoxysilane (50 µL, 0.26 mmol, 4.8 equiv) was added, and a white precipitate was immediately observed. The suspension was observed to be cloudy and orange, and it was allowed to stir for 15 minutes at room temperature, at which time it was diluted with ca. 5 mL of dry THF. The slurry was filtered through a short plug of Celite® to remove the pyridinium salt, and the filtrate concentrated under reduced pressure. The residue was redissolved in hexanes:EtOAc (9:1), filtered through a plug of glass wool, and purified by MPLC (SiO_2, 9:1 hexanes:EtOAc) to yield the monomethoxy byproduct as an orange solid (ca. 2 mg). In a second, slightly overlapping fraction, the desired product **3.23** was eluted. Yield of the pure **3.23** (22.0 mg, 0.0318, 59.4%) was achieved by discarding fractions containing the co-eluted byproduct and **3.23**. If necessary, residual EtOAc was removed by storage under high vacuum for ≥ 24 h.

^{1}H NMR of **3.24** (500 MHz, $CDCl_3$): δ 7.60 (d, *J* = 15.8, Hz, 2H, H_d), 7.10-7.03 (m, 6H, H_a, H_b, and H_c), 6.51 (d, *J* = 15.8, Hz, 2H, H_e), 5.82 (s, 1H, H_f), 3.93 [q, *J* = 7.0 Hz, 12H, $OSi(OCH_2CH_3)_3$ and $OSi(OCH_2CH_3)_3$], 3.89 (s, 6H, OCH_3), and 1.24 [t, *J* = 7.0 Hz, 18H, $OSi(OCH_2CH_3)_3$ and $OSi(OCH_2CH_3)_3$].

^{1}H NMR of **3.25** (500 MHz, $CDCl_3$): δ 7.62 (d, *J* = 15.8, Hz, 1H, $H_{d'}$), 7.60 (d, *J* = 15.7, Hz, 1H, H_d), 7.47 (d, *J* = 8.6 Hz, 2H, $H_{a'}$) 7.10-7.02 (m, 5H, H_a, H_b, H_c, and $H_{b'}$), 6.511 (d, *J* = 15.8, Hz, 1H, $H_{e'}$), 6.507 (d, *J* = 15.8, Hz, 1H, H_e), 5.80 (s, 1H, H_f), 3.93 [q, *J* = 7.0 Hz, 12H, $OSi(OCH_2CH_3)_3$ and $OSi(OCH_2CH_3)_3$], 3.89 (s, 3H, OCH_3), 1.26 and 1.24 [overlapping t's, *J* = 7.0 Hz, 18H, $OSi(OCH_2CH_3)_3$ and $OSi(OCH_2CH_3)_3$].

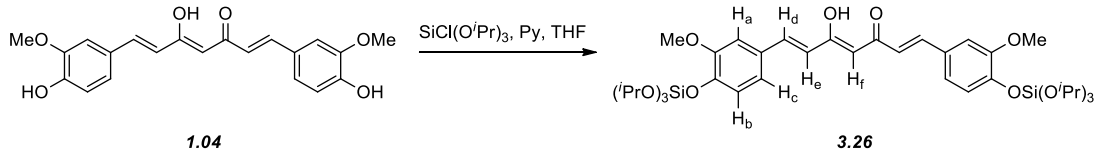

1.04 *3.26*

Di-*O*-(Tri-*i*-propoxysilyl)curcumin (3.26). Curcumin (≥94% purity as received, 17.2 mg, 0.0467 mmol, 1.0 equiv) was dissolved in dry THF (1.0 mL) in an oven-dried culture tube fitted with a Teflon-lined cap and a stir bar. Pyridine (15 µL, 0.25 mmol, 4.0 equiv) was added by Wiretrol®. An approximately 3:1 mixture of tri-*i*-propoxychlorosilane:tetra-*i*-propoxysilane (0.0472 mg, 0.14 mmol, 3 equiv of tri-*i*-propoxychlorosilane) was added. The orange solution gradually became cloudy while it stirred for 3.5 hours at room temperature. The suspension was diluted with dry THF, the slurry filtered through a short plug of Celite® to remove the pyridinium salt, and the filtrate concentrated under reduced pressure. The residue was redissolved in hexanes:EtOAc (99:1), filtered through a plug of glass wool, and subjected to MPLC (SiO_2, 99:1 hexanes:EtOAc) to remove the tetra-*i*-propoxysilane byproduct. The solvent mixture was changed (3:1 hexanes:EtOAc) to yield 3.24 contaminated with a column impurity. In a second MPLC

experiment, the impure 3.24 was subjected to MPLC (19:1 hexanes:EtOAc), to yield of the pure **3.24** (7.8 mg, 0.0129, 27.6%). If necessary, residual EtOAc was removed by storage under high vacuum for ≥ 24 h.

^{1}H NMR (500 MHz, $CDCl_3$): δ 7.60 (d, *J* = 15.8, Hz, 2H, H_d), 7.10-7.05 (m, 6H, H_a, H_b, and H_c), 6.50 (d, *J* = 15.8, Hz, 2H, H_e), 5.81 (s, 1H, H_f), 4.34 {sept, *J* = 6.1 Hz, 6H, $[OSi(OC\mathit{H}(CH_3)_2]_3$ and $[OSi(OC\mathit{H}(CH_3)_2]_3$}, 3.87 (s, 6H, $OC\mathit{H_3}$), and 1.22 {d, *J* = 6.1 Hz, 18H, $OSi[OCH(C\mathit{H_3})_2]_3$ and $OSi[OCH(C\mathit{H_3})_2]_3$}.

A representative, general experimental procedure for the PTX silicate prodrug hydrolysis studies The PTX silicate prodrug was dissolved in 900 µL of d_6-acetone. To this homogenous solution, 100 µL of a 9:1 v/v solution of D_2O:TFA was added, and the solution was vigorously mixed. The ^{1}H NMR spectra were taken (16 transients) on a 500 MHz Varian instrument at multiple time points over the course of more than three half-lives. The study was conducted at room temperature (rt = 22.5 °C ± 1.0 °C). Upon completion of the study, the H2' and/or H7 methine resonances were integrated in a baseline-corrected NMR spectrum using MestRe-C® software. The relative integration values were used to determine the extent of hydrolysis. Data from three replications were plotted on a semi-log scale to determine the k_{obs} values that were then converted to the k_{rel} data as presented (Table 3-1), where the rate of the most slowly hydrolyzed prodrug (**3.07**) is taken to be k_{rel} = 1.0. Errors are defined as the standard deviation of the three trials.

Chapter 4

A Strategy for Control of "Random" Copolymerization of Lactide and Glycolide: Application to the Synthesis of PEG-*b*-PLGA Block Copolymers Having Narrow Polydispersity.

Efforts toward the development of a random copolymerization of glycolide and lactide were motivated by the need for acceptably hydrophobic, non-crystalline, and biocompatible block copolymers for use in the FNP experiments. Toward that end, Dr. Haitao Qian initiated research designed to synthesis PEG-*b*-PLGA block copolymers having varying molecular weights and lactide to glycolide ratios. In the course of his studies, he adapted work originally published by the Waymouth, Hedrick, and co-workers detailing the use of 1,8-diazabicyclo[5.4.0]-undec-7-ene (DBU) as a catalyst for the polymerization of, among other lactones, lactide.[161] Dr. Qian's work applying this literature precedent to the copolymerization of lactide and glycolide included: i) the determination of the DBU-catalyzed polymerization kinetics of lactide and

[161] Lohmeijer, B. G. G.; Pratt, R. C.; Leibfarth, F.; Logan, J. W.; Long, D. A.; Dove, A. P.; Nederberg, F.; Choi, J.; Wade, C.; Waymouth, R. M.; Hedrick, J. L. Guanidine and Amidine Organo-Catalysts for Ring-Opening Polymerization of Cyclic Esters. *Macromolecules* **2006**, *39*, 8574–8583.

glycolide, ii) the synthesis of PEG-*b*-PLA and PEG-*b*-PLGA block copolymers via Method A (see section 4.4.3), and iii) the measurement of the extent of randomization in the PLGA backbone via ^{13}C NMR spectroscopy.

As Dr. Qian prepared to leave the Hoye lab to accept a new position, the research progress of the polyesterification project was gradually transferred to my responsibility. Working with Dr. Qian, I repeated a number of his experiments and subsequently began to advance the project goals. In doing so, I made experimental contributions, including: i) the optimization of the Method B (see section 4.4.4) to render the synthesis of PEG-*b*-PLA and PEG-*b*-PLGA block copolymers more efficient and convenient, ii) the synthesis of the high molecular weight PEG-*b*-PLGAs (with the help of an undergraduate student, Jordan Crow, under my direction), iii) the demonstration of the proof of principle of PEG-*b*-PLGA polymerizations with high lactide consumption, and iv) the SEC/MALS characterization of a subset of polymers. In addition to these experimental efforts, I took a primary role in analyzing the data, compiling the experimental results and analysis for publication, and writing/editing the *Macromolecules* manuscript. These joint, collaborative efforts were crucial to the project's success and eventual publication of this research.[162]

[162] Qian, H.; Wohl, A. R.; Crow, J. T.; Macosko, C. W.; Hoye, T. R. A Strategy for Control of "Random" Copolymerization of Lactide and Glycolide: Application to Synthesis of PEG-*b*-PLGA Block Polymers Having Narrow Dispersity. *Macromolecules*, **2011**, *44*, 7132–7140.

1. Introduction.

Poly(lactic-*co*-glycolic acid) (PLGA) is a biodegradable copolymer that is also acceptable for use in a variety of biomedical applications. Typically, a random PLGA polymer is synthesized in a bulk batch polymerization using a tin-based catalyst at high temperatures. This methodology results in relatively broad polydispersity indexes (PDIs) due to transesterification, and the polymer product is often discolored. We report here the use of 1,8-diazabicyclo[5.4.0]-undec-7-ene (DBU), a known, effective, and convenient organocatalyst for the ring-opening polymerization of cyclic esters, to synthesize random copolymers of lactide and glycolide. The polymerization kinetics of the homo- and copolymerizations of lactide and glycolide were explored via NMR spectroscopy. A novel strategy that employs a controlled addition of the more reactive glycolide monomer to a solution containing the lactide monomer, the poly(ethylene glycol) (PEG) macroinitiator, and DBU catalyst was developed. Using this tactic (semi-batch polymerization), we synthesized a series of block copolymers that exhibited excellent correlation of the expected and observed molecular weights and possessed narrow PDIs. We also measured the thermal properties of these block copolymers and observed trends based on the composition of the block copolymer. We also explored the need for experimental rigor in several aspects of the preparations and have identified a set of convenient reaction conditions that provide polymer products that retain the aforementioned desirable characteristics. These polymerizations proceed rapidly at room temperature and without the need for tin-based catalysts to provide PEG-*b*-PLGAs suitable for use in biomedical investigations.

2. Lactide and Glycolide Polyester Synthesis Background.

Polyesters synthesized from ring-opening polymerization (ROP) of cyclic ester[163] monomers [lactones and dilactones (diolides)] have found wide application in the fields of drug delivery (microparticles, nanoparticles, or micelles),[164] tissue engineering (sutures and other biodegradable implants),[165,166] medical devices,[167] and single-use plastics[168] because of their biocompatibility and biodegradability. The most extensively studied of these polyesters are poly(lactic acid) (PLA) and poly(lactic-*co*-glycolic acid) (PLGA), the homopolymer of lactide (**4.01**) or random copolymer of **4.01** and glycolide (**4.02**), respectively.[169,170] Tin(II) octoate is widely used as a catalyst for the synthesis of PLA or PLGA.[171] However, tin-based catalysts are less than ideal from both chemical [e.g., broad polydispersities (PDIs)] and biological (e.g., toxicity) perspectives, especially in the synthesis of the more readily transesterified PLGAs.

---

[163] Jerome, C.; Lecomte, P. Recent Advances in the Synthesis of Aliphatic Polyesters by Ring-Opening Polymerization. *Adv. Drug Deliver. Rev*. **2008**, *60*, 1056–1076.

[164] Astente, C. E.; Sabliov, C. M. Synthesis and Characterization of PLGA Nanoparticles, *J. Biomater. Sci. Polymer Edn.* **2006**, *17*, 247–289.

[165] Albertsson, A. C.; Varma, I. K. Recent Developments in Ring Opening Polymerization of Lactones for Biomedical Applications. *Biomacromolecules* **2003**, *4*, 1466–1486.

[166] Mohamed, F.; Van der Walle, C. F. Engineering Biodegradable Polyester Particles with Specific Drug Targeting and Drug Release Properties. *J. Pharm. Sci.* **2008**, *97*, 71–87.

[167] Middleton, J. C.; Tipton, A. J. Synthetic Biodegradable Polymers as Orthopedic Devices. *Biomaterials* **2000**, *21*, 2335–2346.

[168] Drumright, R. E.; Gruber, P. R.; Henton, D. E. Polylactic Acid Technology. *Adv. Mater.* **2000**, *12*, 1841–1846.

[169] Chu, C. C. Biodegradable Polymeric Biomaterials: an Updated Overview. In *Biomaterials*; Wong, J. Y., Bronzino, J. D. CRC Press: Boca Raton, FL, 2007; 6/1–6/22.

[170] Vert, M. Polyglycolide and Copolyesters with Lactide. *Biopolymers* **2002**, *4*, 179–202.

[171] Stjerndahl, A.; Wistrand, A. F.; Albertsson, A. C. Industrial Utilization of Tin-Initiated Resorbable Polymers: Synthesis on a Large Scale with a Low Amount of Initiator. *Biomacromolecules* **2007**, *8*, 937–940.

The importance of PLGA microstructure has been demonstrated in a study of polyester hydrolytic degradation by Meyer and coworkers.[172] They demonstrated that microspheres made from PLGA copolymers having alternating lactic and glycolic acid units [from condensation polymerization of (*S*)-2-(2-hydroxyacetoxy)propanoic acid monomer] undergo chain scission ca. two times more slowly than those prepared from PLGA copolymers containing longer blocks of lactic and glycolic units. The observed difference in degradation rates was attributed to the difference in the rate of nucleophilic attach at the less sterically hindered glycolic carbonyls present in the blocks of glycolic repeat units.

Controlled homopolymerization of glycolide (**4.02**) is challenging because of the low solubility of both the monomer and resulting poly(glycolic acid) (PGA) homopolymer (or block copolymers) in common organic solvents. Copolymerization of glycolide (**4.02**) and lactide (**4.01**) provides an effective way to modify the chemical and physical properties of these polyesters for various applications, and PLGAs that comprise up to a 1:1 ratio of lactic to glycolic units are of practical interest.[9] Dong et al. developed a strategy for obtaining PLGA with exactly a 1:1 molar ratio of lactic to glycolic acid by polymerizing 3-methylglycolide (tin(II) octoate).[173] These polymerizations were shown to proceed with high monomer conversion and typical PDIs of 1.6-1.7. However, we are unaware of any protocols for random copolymerization of glycolide (**4.02**) and lactide (**4.01**) that produce PLGAs having well-controlled molecular weights and narrow PDIs while minimizing the sequence length of the lactic and glycolic repeat units. This largely reflects differences in reactivity and solubility of these

[172] Li, J.; Stayshich, R. M.; Meyer, T. Y. Exploiting Sequence to Control the Hydrolysis Behavior of Biodegradable PLGA Copolymers. *J. Am. Chem. Soc.* **2011**, *133*, 6910–6913.

[173] Dong, C.-M.; Qiu, K.-Y.; Gu, Z.-W.; Feng, X.-D. Synthesis of Poly(D,L-lactic acid-*alt*-glycolic acid) from D,L-3-methylglycolide. *J. Polym. Sci., Part A: Polym. Chem.* **2000**, *38*, 4179–4184.

two monomers.[174] Thus, simple use of equimolar charges of glycolide (**4.02**) and lactide (**4.01**) results in polymers containing long glycolic blocks (at least in the absence of chain transfer). This adversely affects the solubility and PDI of the copolymer. Melt copolymerization of glycolide (**4.02**) and lactide (**4.01**) has often been used to prepare PLGA with high glycolic content. Under these conditions *in situ* transesterification of the polymer both randomizes the sequence and broadens the distribution of the PLGA.[9] During our attempts to synthesize PEG-*b*-PLGAs using Sn(II)-catalysis, we observed PDI values greater than 1.7 and significant discoloration of the resulting PLGA copolymer. Thus, we felt there was room for improvement in the methods for preparation of well-defined PLGAs.

In addition to tin(II) octoate, other metal-containing catalysts have been studied for the ROP of lactide (**4.01**), glycolide (**4.02**), ring strained lactones, and cyclic carbonates. These include zinc or aluminum alkoxides[9,175,176,177,178] and rare earth metal compounds.[175,178,179,180,181] Some of these catalysts also raise

---

[174] Kreiser-Saunders, I.; Kricheldorf, H. R. Polylactones. Part 39. Zn Lactate-Catalyzed Copolymerization of L-lactide with Glycolide or ε-caprolactone. *Macromol. Chem. Phys.* **1998**, *199*, 1081–1087.

[175] O'Keefe, B. J.; Hillmyer, M. A.; Tolman, W. B Polymerization of Lactide and Related Cyclic Esters by Discrete Metal Complexes. *J. Chem. Soc., Dalton Trans.* **2001**, 2215–2224.

[176] Barakat, I.; Dubois, P.; Jérôme, R.; Teyssié, P. Living Polymerization and Selective End Functionalization of ε-caprolactone using Zinc Alkoxides as Initiators. *Macromolecules* **1991,** *24***,** 6542–6545.

[177] Baran, J.; Duda, A.; Kowalski, A.; Szymanski, R.; Penczek, S. Quantitative Comparison of Selectivities in the Polymerization of Cyclic Esters. *Macromol. Symp.* **1997**, *123*, 93–101.

[178] Ovitt, T. M.; Coates, G. W. Stereochemistry of Lactide Polymerization with Chiral Catalysts: New Opportunities for Stereocontrol using Polymer Exchange Mechanisms. *J. Am. Chem. Soc.* **2002**, *124*, 1316–1326.

[179] Shen, Y.; Shen, Z.; Shen, J.; Zhang, Y.; Yao, K. Characteristics and Mechanism of ε-caprolactone Polymerization with Rare Earth Halide Systems. *Macromolecules* **1996***, 29*, 3441–3446.

[180] Ravi, P.; Gröb, T.; Dehnicke, K.; Greiner, A. Novel $[Sm_2I(NPPh_3)_5(DME)]$ Initiator for the Living Ring-Opening Polymerization of ε-caprolactone and δ-valerolactone, *Macromolecules* **2001**, *34*, 8649–8653.

health safety concerns. Enzymatic ROP of lactones, lactide (**4.01**), and glycolide (**4.02**) has also been studied to address concerns about possible toxicity of heavy metal catalysts and initiators.[182]

A decade ago the first organocatalytic ROP of lactide (**4.01**) was reported, using 4-dimethylaminopyridine (DMAP) and pyrrolidinopyridine as catalysts.[183] This was followed by the investigation of several other classes of organic small molecules as more potent catalysts for ROP of lactide (**4.01**) and lactones. Among these, *N*-heterocyclic carbenes,[184] phosphines,[185] phosphazenes,[186] and amidines and guanidines[161] have been demonstrated to have unique properties that influence the synthesis of polyesters from different monomers. Many of these allow for better control of molecular weight and molecular weight distribution; some show enhanced functional group compatibility.

Here we report a strategy for the successful controlled "random" copolymerization (Scheme 4-1) of glycolide (**4.02**) and a racemic mixture of D- and L-lactide [50:50 **R,R-4.01** and **S,S-4.01**, which we will refer to as **(±)-4.01**] using poly(ethylene glycol) monomethyl ether (**4.03**, mPEG-OH) as a

---

[181] Chamberlin, B. M.; Jazdzewski, B. A.; Pink, M.; Hillmyer, M. A.; Tolman, W. B. Controlled Polymerization of DL-lactide and ε-caprolactone by Structurally Well-Defined Alkoxo-Bridged Di- and Triyttrium(III) Complexes. *Macromolecules* **2000**, *33*, 3970–3977.

[182] Albertsson, A. C.; Srivastava, R. K. Recent Developments in Enzyme-Catalyzed Ring-Opening Polymerization. *Adv. Drug Deliver. Rev.* **2008**, *60*, 1077–1093.

[183] Nederberg, F.; Connor, E. F.; Möller, M.; Glauser, T.; Hedrick, J. L. New Paradigms for Organic Catalysts: the First Organocatalytic Living Polymerization. *Angew. Chem. Int. Ed.* **2001**, *40*, 2712–2715.

[184] Dove, A. P.; Pratt, R. C.; Lohmeijer, B. G. G.; Culkin, D. A.; Hagberg, E. C.; Nyce, G. W.; Waymouth, R. M.; Hedrick, J. L. *N*-Heterocyclic Carbenes: Effective Organic Catalysts for Living Polymerization. *Polymer* **2006**, *47*, 4018–4025.

[185] Myers, M.; Connor, E. F.; Glauser, T.; Mock, A.; Nyce, G.; Hedrick, J. L. Phosphines: Nucleophilic Organic Catalysts for the Controlled Ring-Opening Polymerization of Lactides. *J. Polym. Sci., Part A: Polym. Chem.* **2002**, *40*, 844–851.

[186] Zhang, L.; Nederberg, F.; Messman, J. M.; Pratt, R. C.; Hedrick, J. L.; Wade, C. G. Organocatalytic Stereoselective Ring-Opening Polymerization of Lactide with Dimeric Phosphazene Bases. *J. Am. Chem. Soc.* **2007,** *129*, 12610–12611.

macroinitiator. The resulting amphiphilic mPEG-*b*-PLGA block copolymers (**4.04**) have well-controlled molecular weights (MWs) and MW distributions. The resulting poly(ethylene glycol) (PEG)-containing amphiphilic block copolymers (BCPs) of PLA and PLGA have practical applications in drug delivery systems.[187,188,189] Specifically, they can be used to formulate aqueous dispersions of hydrogels or nanoparticles. The use of well-defined PEG-*b*-PLAs and/or PEG-*b*-PLGAs to fabricate drug-containing nanoparticles may lead to more precise control of size, degradability, thermal properties (T_m and T_g), and release profiles in these applications.

Scheme 4-1. The co-polymerization of *rac*-lactide [**(±)-4.01**] and glycolide (**4.02**) yields the PEG-*b*-PLGA block copolymer **4.04**.

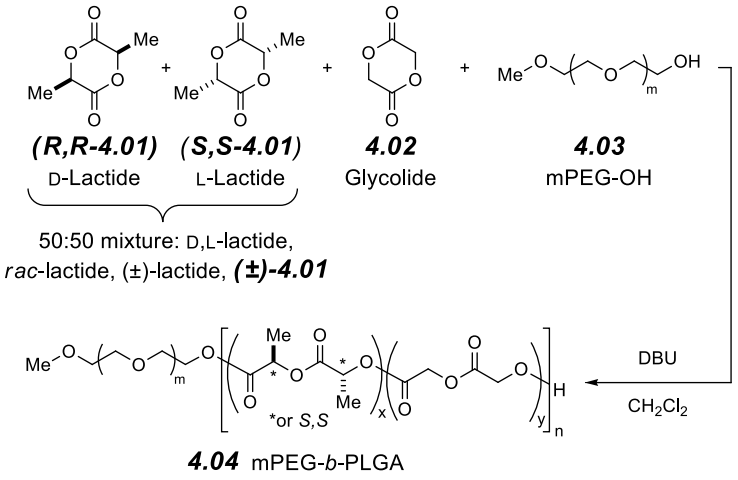

[187] Dong, J.; Jiang, S.; Ping, Q. Development of Injectable Biodegradable in-situ forming Gel Implants. *Yaoxue Jinzhan* **2007**, *31*, 110–113.

[188] Avgoustakis, K. Pegylated Poly(lactide) and Poly(lactide-*co*-glycolide) Nanoparticles: Preparation, Properties and Possible Applications in Drug Delivery. *Curr. Drug Deliver*. **2004**, *1*, 321–333.

[189] Huh, K. M.; Cho, Y. W.; Park, K. PLGA-PEG Block Copolymers for Drug Formulations. *Drug Deliver. Tech*. **2003**, *42*, 44–49.

3. Shorthand Designation of the Polymer Nomenclature.

PEG_x-PL_yA is used to designate our PEG-*b*-PLA diblock copolymers and PEG_x-PL_yG_zA is used for PEG-*b*-PLGA. PEG is used interchangeably with poly(ethyele oxide) (PEO) due to the prevalent use of the PEG nomenclature in the biological sciences. PEG_x-PL_yA has a PEG block with the number average molecular weight (Mn) of x kilodaltons and a lactic acid (LA) block with the average MW of y kilodaltons. Similarly, PEG_x-PL_yG_zA has a PEG block with the average MW of x kilodaltons and a lactic-*co*-glycolic acid (LGA) block comprising LA and GA of y and z kilodaltons, respectively. PEG_x-PLL_yA refers to a PEG-*b*-PLA polymer in which pure L-lactide (i.e., **S,S-4.01**) was used rather than **(±)-4.01**. Essential data for each of the polymer samples prepared in this study are presented in Table 4-1.

4. Methods for PEG-*b*-PLA and PEG-*b*-PLGA Synthesis.

1. Method A for PEG-b-PLA Synthesis. The following reaction mixture was prepared in a controlled atmosphere (N_2) glove box. To a solution of *rac*-lactide [**(±)-4.01**, 100 mg, 0.694 mmol] and mPEG-OH (**4.03**, 5K) (100 mg, 0.02 mmol) in 1 mL of chloroform was added DBU [1 mg, 1 mol% relative to **(±)-4.01**] in a screw-capped glass reaction vessel (e.g., culture tube). The solution was removed from the glove box and stirred for 1 h. The vessel was opened, hydrochloric acid (1N) was added immediately, and the mixture was washed with water and brine. The polymer was precipitated by dropwise addition of the chloroform solution with stirring into excess isopropanol. Solvent was removed from the resulting suspension of white polymer by either filtration or decantation, and the polymer was dried under vacuum at 50 °C overnight.

2. Method B for PEG-b-PLA Synthesis. The following reaction mixture was prepared under ambient atmosphere in a fume hood. A solution of mPEG-OH

(**4.03)** in dry CH_2Cl_2 (0.5 g mL^{-1}) was dried over 3 Å molecular sieves overnight. A portion of this solution (2.0 mL) was added to a solution of *rac*-lactide [**(±)-4.01**] in 8 mL of dry CH_2Cl_2 in an oven-dried, screw-capped glass reaction vessel. DBU was added (10 µL) and the reaction vessel was tightly capped. The resulting solution was stirred for 1 h, and benzoic acid (150 mg) was added. This solution was concentrated to approximately 30% of the original volume and then added dropwise with stirring into excess isopropanol. Solvent was removed from the resulting suspension of white polymer by either filtration or decantation, and the polymer was dried under vacuum at 50 °C overnight.

3. Method A for PEG-b-PLGA Synthesis. The following operations were performed in a controlled atmosphere (N_2) glove box. i) mPEG-OH (**4.03**, 5K, 150 mg) in CH_2Cl_2 (7 mL) together with a predetermined amount of *rac*-lactide [**(±)-4.01**] were combined in a round-bottomed flask containing a magnetic stir bar and closed with a septum. ii) DBU was dissolved in CH_2Cl_2 at a concentration of 11 µL mL^{-1} in a round-bottomed flask closed with a septum. iii) Glycolide (**4.02**) was dissolved in THF (2 mL) and taken up in a syringe. All three solutions i-iii) were removed from the glove box. Solution i) was vigorously stirred. *Immediately* after the addition of solution ii) (1 mL), solution iii) was infused into the reaction vessel via a syringe pump at the rate of 0.2 mL min^{-1}. At the end of the infusion (10 min), solid benzoic acid (50 mg) was added to arrest the polymerization. The PEG-*b*-PLGA (**4.04**) was purified by precipitation twice into isopropanol from CH_2Cl_2 and dried at 50 °C under vacuum overnight.

4. Method B for PEG-b-PLGA Synthesis. The following three solutions were prepared in ambient atmosphere in a fume hood. i) mPEG-OH (**4.03**, 5K, 450 mg) was dissolved in CH_2Cl_2 (22 mL) together with a predetermined amount of *rac*-lactide [**(±)-4.01**] in an oven-dried round-bottomed flask containing a magnetic stir bar and closed with a septum. ii) DBU was dissolved in CH_2Cl_2 at a concentration of 16.7 µL mL^{-1} in a screw-capped vial. iii) Glycolide (**4.02**) was

dissolved in THF (6 mL) and taken up in a syringe. Solution i) was vigorously stirred. *Immediately* after the addition of solution ii) (2 mL), solution iii) was infused into the reaction vessel via a syringe pump at the rate of 0.6 mL min^{-1}. At the end of the infusion (10 min), solid benzoic acid (150 mg) was added to arrest the polymerization. As above, the PEG-*b*-PLGA (**4.04**) was purified by precipitation twice into isopropanol from CH_2Cl_2 and dried at 50 °C under vacuum overnight.

5. Synthesis of PEG-*b*-PLA.

1. Introduction and Replication of Waymouth and Hedrick's PLA Polymerization. DBU is an organic base of low nucleophilicity that has found wide application as a catalyst for transesterification-like reactions. Waymouth, Hedrick, et al. [161] have demonstrated that DBU and other superbases, such as 1,5,7-triazabicyclo[4.4.0]dec-1-ene (TBD), catalyze ring-opening polymerization of lactide and other lactones. Moreover, these polymerizations occur in solution, at ambient temperature, and with impressive effectiveness to afford polyesters that have defined structure, controlled molecular weight, and controlled molecular weight distribution. Their findings that DBU is a less active catalyst than TBD [and thus more manageable for controlling undesired transesterification (chain transfer) during polymerization] prompted us to investigate its use for the preparation of PLGA moieties. Our interest in use of poly(ethylene oxide)-containing, amphiphilic block copolymers for various drug delivery applications led us to target PEG-*b*-PLGAs. Hence, we selected mPEG-OH as the (macro)initiator in the work reported here.

We used the Waymouth/Hedrick methodology[161] first to prepare a series of PEG-*b*-PLA block copolymers using only lactide as the monomer. Thus, *rac*-lactide [**(±)-4.01**] was polymerized using mPEG-OH (MW= 2K or 5K) as the

macroinitiator to afford PEG-*b*-PLA. When 1 mol% of DBU and monomer concentrations of ca. 0.5-2M were used for polymerization at room temperature, >95% monomer conversions were observed in less than 1 h. We prepared a series of mPEG-*b*-PLA diblock copolymers of different molecular weight ratios. Each had a small PDI (cf. entries 1-6, Table 4-1) and was monomodal. This is in accordance with the fact that DBU does not cause extensive transesterification of PLA on the time scale of lactide ROP.[161] We observed (^{1}H NMR spectroscopy) a preference for production of isotactic arrays in these DBU-catalyzed ROPs of *rac*-lactide [**(±)-4.01**]. Interestingly, this contrasts with the known syndiotactic preference when tin(II) octoate is used as the polymerization catalyst[190] but is in agreement with the slight isotactic preference noted in TBD-catalyzed ROPs.[161]

2. Tacticity Analysis of PEG-b-PLAs. A representative ^{1}H NMR spectrum of one of the PEG-*b*-PLAs (PEG_5-$PL_{10}A$) is shown in Figure 4-1. The tacticity of the PLA block can be judged from analysis of the methine proton resonances between δ = 5.10-5.25 ppm.[190,191] The array of overlapped quartets centered at ca. 5.16 ppm arises from backbone methine protons flanked on both sides by a lactic acid moiety of the same configuration (*isotactic,isotactic* or *i,i*) while the array at ca. 5.21 ppm reflects flanking by one lactic acid moiety of the same and a second of opposite configuration (*isotactic,syndiotactic,* or *i,s*) . Racemic lactide [**(±)-4.01**] was used as the monomer for these ROPs. Since each monomer lactide in **(±)-4.01** (**R,R-4.01** or **S,S-4.01)** bears two lactic acid moieties of the *same* configuration, there are no individual lactic acid moieties in the PLA that are flanked on both sides by ones of opposite configuration (and thus there are no *syndiotactic,syndiotactic,* or *s,s* relationships). Arrays of similar quartets rather

[190] Thakur, K. A. M.; Kean, R. T.; Hall, E. S.; Kolstad, J. J.; Munson, E. J. Stereochemical Aspects of Lactide Stereo-Polymerization Investigated by ^{1}H NMR: A Case of Changing Stereospecificity. *Macromolecules* **1998**, *21*, 1487–1497.

[191] Thillaye du Boullay, O.; Marchal, E.; Martin-Vaca, B.; Cossio, F. P.; Bourissou, D. An Activated Equivalent of Lactide toward Organocatalytic Ring-Opening Polymerization. *J. Am. Chem. Soc*. **2006**, *128*, 16442–16443.

than a single discrete quartet are observed because of small influences on the precise chemical shifts from longer-range, relative configurational relationships. If the rates for homochiral (PLA-*R* with **R,R-1** or PLA-*S* with **S,S-1**) vs. heterochiral (PLA-*R* with **S,S-1** or PLA-*S* with **R,R-1**) propagation were identical, the intensity of each of the two multiplets at δ = 5.16 and 5.21 (proportional to the #*i,i* and #*i,s*, respectively) would be equal. The average sequence length (SL, the number of adjacent lactic acid moieties of the same configuration) is [(#*i,i* + #*i,s*)/(#*i,s*/2)],[192] and in this scenario SL would be 4. Since, instead, the ratio of these resonances is 3, the average SL is 8. Finally, from the SL, one can deduce the reactivity ratio[193] (*r*) for homo- vs. heterochiral propagation events; namely, *r* = (SL-2)/2[194] or 3.

[192] Each run of *i,i* moieties is terminated at each of its ends by a *i,s* moiety; there are two *i,s* moieties per run; and the number of runs is one half the number of *i,s* moieties. The average sequence length in any sample is the total number of lactic acid units (#*i,i* + #*i,s*) divided by the total number of runs (#*i,s*/2).

[193] Hiemenz, P. C.; Lodge, T. P. Copolymers, Microstructure, and Stereoregularity. In *Polymer Chemistry*, 2nd Ed.; Taylor & Francis Group, LLC: Boca Raton, **2007**, *1*; 165–216.

[194] The reactivity ratio for a growing chain whose reactive terminal carbinol center has the *R* configuration is $r_{PLA\text{-}R}$ = (SL-2)/(2*[**R,R-1**]/[**S,S-1**]). Likewise, $r_{PLA\text{-}S}$ = (SL-2)/(2*[**S,S-1**]/[**R,R-1**]). Since **(±)-1** was used here, [**S,S-1**]/[**R,R-1**] = 1 and $r_{PLA\text{-}R}$ = $r_{PLA\text{-}S}$ = *r* = (SL-2)/2.

Figure 4-1. ^{1}H NMR spectrum of the PEG-*b*-PLA copolymer PEG_5-$PL_{10}A$ ($CDCl_3$) The ratio of the methine multiplets at ca. δ 5.16 and 5.21 ppm indicates that the DBU catalyst favors the formation of isotactic sequences with a homochiral/heterochiral reactivity ratio of 3 (see text).

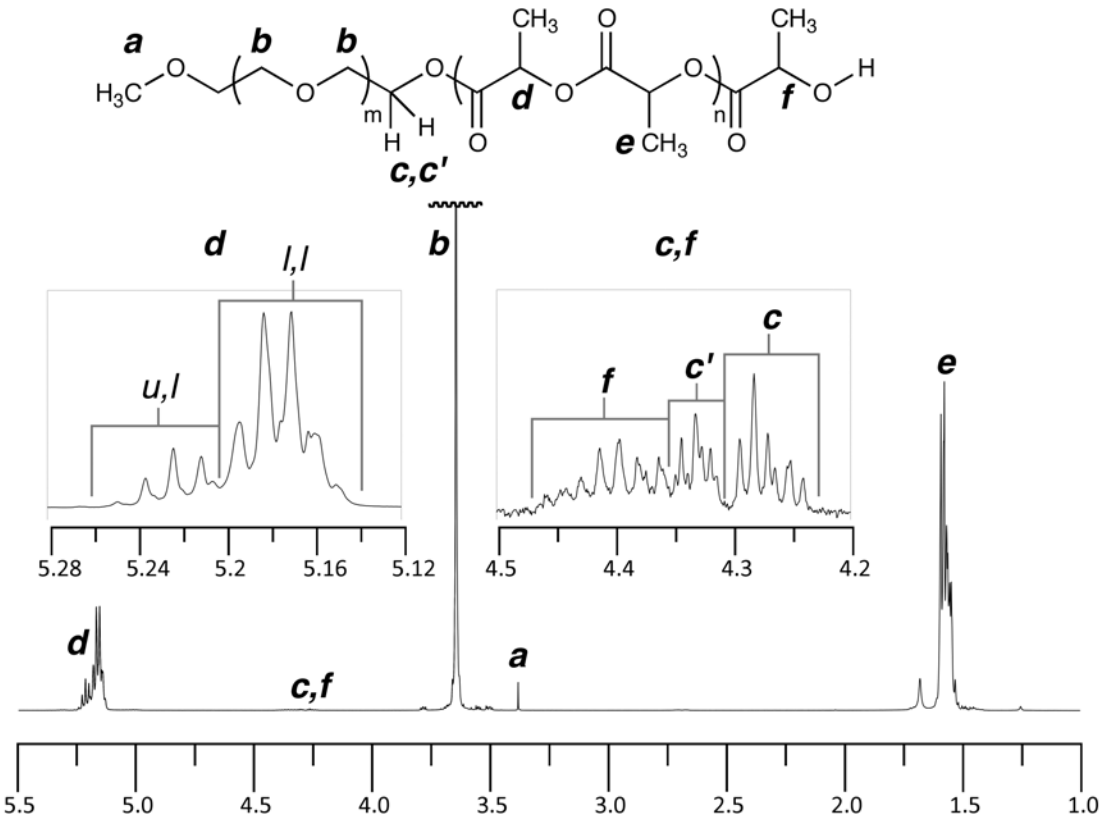

6. Synthesis of PEG-*b*-PLGA.

1. Determining Glycolide to Lactide Reactivity Ratio during DBU-Catalyzed Polymerization. The organocatalyzed copolymerization of glycolide (**4.02**) with lactide (**4.01**) is challenging. The low solubility in common organic solvents of both the monomeric glycolide and, especially, growing polymers that have a high glycolyl content can make the experiment problematic. Additionally, glycolide is, of course, much more reactive than lactide.[9,174] Thus, batch copolymerizations

that have equimolar ratios of the glycolide and lactide monomers result in the synthesis of long blocks of polyglycolide, further reducing polymer solubility during copolymerization (as previously observed for cationic polymerizations[195]). Consequently, we are unaware of reports that describe either homopolymerization or copolymerization of glycolide by organocatalysis. We were interested in determining the relative reactivity of glycolide and lactide in order to design an essentially "random" copolymerization protocol.

Initial attempts to quantify the reactivity ratios of glycolide (**4.01**) and lactide (**4.02**) by subjecting a 1:1 mixture of the two monomers to mPEG-initiated, DBU-catalyzed polymerization followed by NMR analysis were only marginally successful. Instead of observing copolymerization of both monomers, we noted the rapid consumption of the glycolide monomer via ROP, while nearly all of the lactide remained intact. Thus, we were unable to directly measure the copolymerization reactivity ratio, but it was clear that the glycolide had polymerized significantly faster than the lactide.

We then explored the relative reactivity of glycolide and lactide via parallel, independent homopolymerization experiments. Thus, analogous kinetic experiments utilizing lactide [**(±)-4.01**] vs. glycolide (**4.02**) were conducted, leading eventually to the following sets of conditions from which comparative reactivities could be assessed. For lactide, [$mPEG_{2k}$] = 5.0mM and a ratio of [**(±)-4.01**]:[$mPEG_{2k}$]:[DBU] = 264:1:1.32 was used. For the more reactive glycolide, much lower catalyst and initial monomer concentrations were used—namely, [$mPEG_{2k}$] = 5.1mM and the ratio of [**4.02**]:[$mPEG_{2k}$]:[DBU] was 2.94:1:0.0022. In the case of glycolide (**4.02**), only polymers having short PGA blocks could be prepared because of solubility limitations of the oligomeric product. Waymouth and Hedrick have demonstrated that similar amidine-catalyzed ROPs (of

[195] Kricheldorf, H. R.; Kreiser, I. Polylactones, 11. Cationic Copolymerization of Glycolide with L,L-Dilactide. *Makromol. Chem*. **1987**, *188*, 1861–1873.

valerolactone) show a first-order dependency on the monomer, alcohol initiator, and amine catalyst conentrations.[161] We assumed that this would also be the case for lactide or glycolide polymerizations, which is reflected in the rate expression shown in equation 4-1. The concentration of propagating hydroxyl groups equals the concentration of alcohol initiator used and remains constant throughout the polymerization as does, of course, the concentration of DBU catalyst. Thus, we hypothesized the reaction to be pseudo first-order in monomer, since the apparent rate constant (k_{app}, eq 4-2) remains unchanged under a given set of conditions. This was then supported by observing linearity in the plots of ln[1/(1-x)] vs. time (x = monomer conversion) for both glycolide and lactide as shown in Figure 4-2A.

$$\frac{d\,[\text{monomer}]}{dt} = -k\,[\text{DBU}][\text{propagating-OH}][\text{monomer}] \qquad \text{(eq 4-1)}$$

$$k_{app} = k\,[\text{DBU}][\text{propagating-OH}] \qquad \text{(eq 4-2)}$$

Figure 4-2. Lactide and glycolide homopolymerizations in $CDCl_3$ solvent at ambient temperature (reaction progress measured by ^1H NMR spectroscopic analysis) under the following conditions (cf. Table 4-1). For lactide [**(±)-4.01**]: {[$mPEG_{2k}$] = 5.0mM; [**(±)-4.01**]$_0$:[$mPEG_{2k}$]:[DBU] = 264:1:1.32}; for glycolide (**4.02**): {[$mPEG_{2k}$] = 5.1mM, [**4.02**]$_0$:[$mPEG_{2k}$]:[DBU] = 2.94:1:0.0066. **Panel A**: Plot of ln[1/(1-x)] vs. time (x = monomer conversion). **Panel B**: Experimentally observed (red) exponential decay of monomer concentration for lactide polymerization. The blue line denotes the approximate linear conversion during the first half-life of lactide consumption, which we then used to guide the choice of the (constant) rate of glycolide addition during subsequent syntheses of the PEG-*b*-PLGA copolymers.

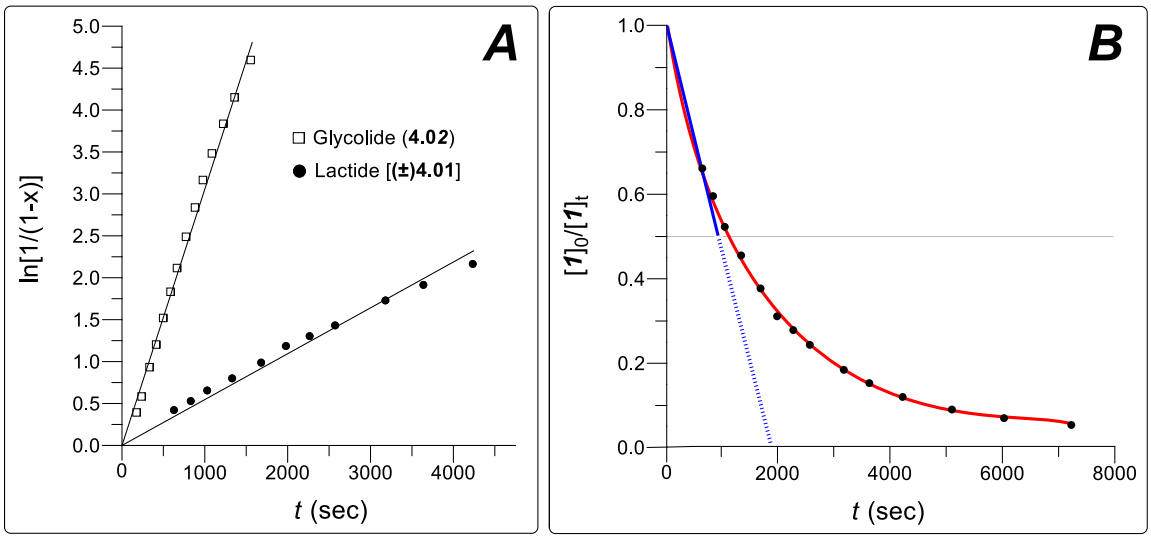

The apparent first-order rate constant (k_{app}, cf. eq 4-2) for each of these two pseudo-first order polymerizations is given in Table 4-1 (column 4). The third order rate constant (k) for each, calculated according to eq 4-1, is given in column 5. The ratio of this latter pair of rate constants is ca. 10^3, favoring the more reactive glycolide monomer. This is larger than the reported relative

reactivity of glycolide to lactide using tin(II) octoate at 200 °C, where the k_{rel} for these two monomers is 14:1.[196]

Table 4-1. Rate constants for glycolide and lactide polymerization.

Monomer	[mPEG$_{2K}$] (mM)	[DBU] (mM)	k_{app}[a] (s^{-1})	k[b] (10^5 $(L/mol)^2$ s^{-1})
Lactide [**(±)-1**, 1.3M]	5.0	6.6	550	1.7
Glycolide (**2**, 15mM)	5.1	0.033	3100	1800

[a] Apparent rate constant of pseudo-first order ROP (cf. eq 4-2)
[b] Third order rate constant (cf. eq 4-1).

The large difference in ROP reactivity of the two monomers reflects collective differences in steric hindrance of both the electrophilic monomer and the nucleophilic hydroxyl group of the propagating polymer chain in this pair of homopolymerizations.[196] Knowledge of this reactivity difference guided our design of the following copolymerization experiments in which, of course, both monomers were simultaneously exposed to identical concentrations of catalyst and propagating hydroxyl groups. Thus, alteration of the relative amounts of each monomer was the obvious exploitable experimental variable.

2. Initial PEG-b-PLGA Synthesis by Method A. One strategy for copolymerization of monomers with different propagation rate constants is to add the fast-reacting monomer continuously during the polymerization. In this

[196] Gilding, D. K.; Reed, A. M. Biodegradable Polymers for Use in Surgery – Polyglycolic/Poly(lactic acid) Homo- and Copolymers: 1. *Polymer* **1979**, *20,* 1459–1464.

manner, the inherent reactivity imbalance is compensated by the fact that at any instant the slow-reacting monomer is in excess. We adopted this "semi-batch polymerization"[197] strategy to target copolymers of lactide (**4.01**) and glycolide (**4.02**) having approximately equal composition by mass. We initiated polymerization of lactide with mPEG-OH, immediately (<1 sec) began addition of glycolide at a constant rate, set the glycolide addition to finish at the time required to reach ca. 50% conversion of the lactide, and quenched the reaction (by addition of excess benzoic acid[161]) immediately upon completion of glycolide addition. A control experiment demonstrated that pretreatment of mPEG-OH/lactide with excess benzoic acid followed by addition of DBU did not result in polymerization. Because it was convenient to add glycolide at a constant rate, we approximated lactide consumption as if it were linear during its first half-life (see blue line in Figure 4-2B). In a typical run a solution containing [mPEG-OH] = 4mM and [**(±)-4.01**]$_0$ = 0.3M in anhydrous CH_2Cl_2 was charged to the reaction vessel. The DBU catalyst (1 mol% based on the amount of mPEG-OH) was injected to this rapidly stirred solution. Addition via syringe pump of a solution of glycolide (**4.02**, 0.5 equiv vs. the initial charge of lactide) was immediately (<1 sec) begun. We judged the $t_{1/2}$ for lactide consumption to ca. ten minutes under these conditions, which we therefore set as the glycolide addition time. The polymerization progress was immediately then arrested, and the excess unreacted lactide was removed by precipitation.

The purified PEG-*b*-PLGA polymers were characterized by gel permeation chromatography (GPC) and NMR analyses. The ^{1}H NMR spectrum of a typical product is shown in Figure 4-3. The small resonances for the carbinol protons ***f*** and for the methylene protons ***c*** at the linkage point between the PEG and PLGA blocks indicate that, again, the polymerization occurred with good functional

[197] Dotson, N. A.; Galván, R.; Laurence, R. L.; Tirrell, M. Reactor Configuration. In *Polymerization Process Modeling*; VCH Publishers, Inc.: New York, NY, **1996**; 259–303.

fidelity. It can be inferred from this spectrum (i.e., from the integration ratio or resonances ***g*** to ***d***) that we were able to achieve the targeted 50:50 mass ratio of glycolate to lactate reasonably well (cf., Tables 4-2 and 4-4). Finally, we judged from analysis of ^{13}C NMR data that the glycolide and lactide monomers were incorporated into the PLGA blocks with nearly random monomer distributions (see sequence length discussion, below).

Figure 4-3. ^{1}H NMR spectrum of PEG-PLA block copolymer PEG_5-PL_5G_5A obtained in $CDCl_3$.

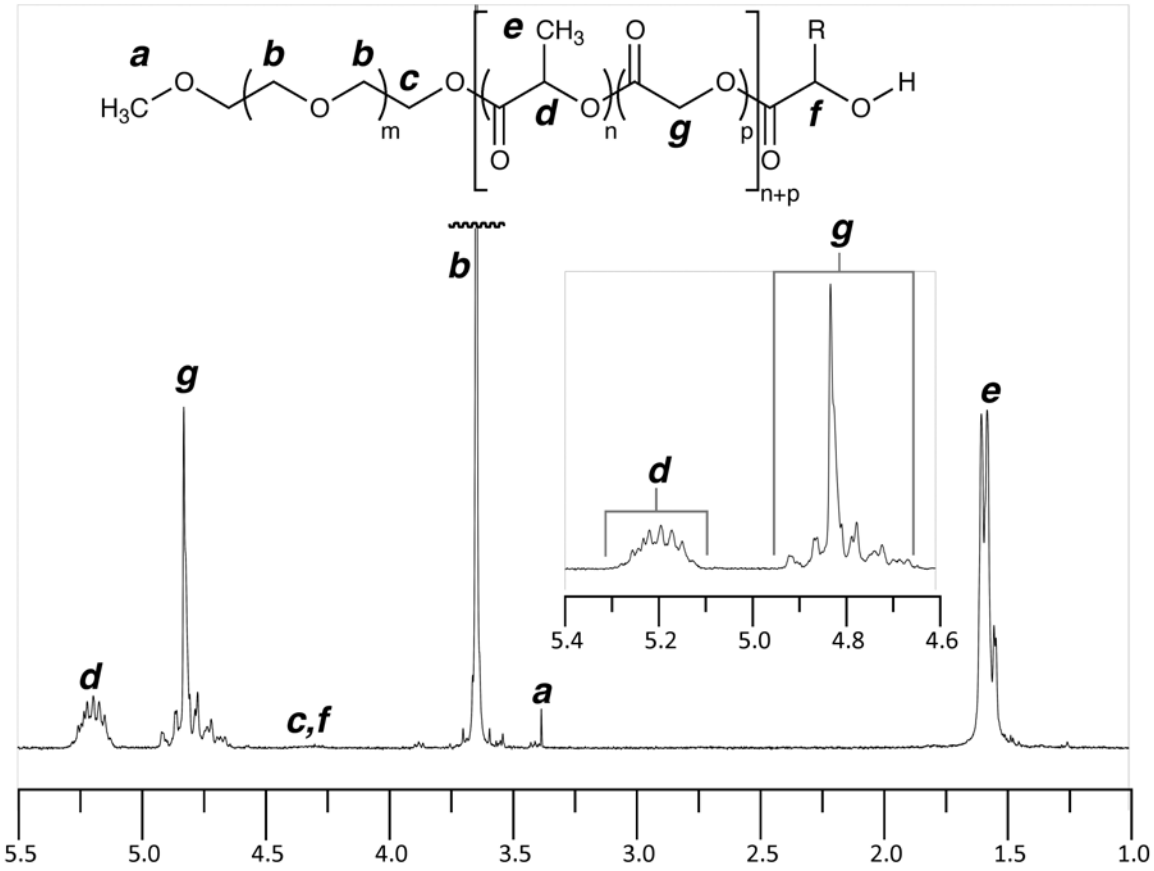

3. Alternative PEG-b-PLGA Synthesis by Method B. We then explored whether less rigorous polymerization conditions, those described as Method B in the Experimental Section, would allow us to obtain polymers of comparable

quality and with similar levels of control, thereby reducing the time and effort necessary to complete a polymerization experiment vis-à-vis the more careful protocols of Method A. We compared the preparation of five polymers using both Methods A and B. The results are given in Table 4-2 and demonstrate that in all cases, both methods yielded polymers having molecular weights and monomer ratios similarly close to the targets. Note that in several instances we judged that the copolymers made by Method B had slightly higher PDI values. Two of the polymerizations were carried out in triplicate, and the results were quite consistent among runs. Therefore, use of the less stringent Method B conditions did not adversely affect the process or product.

Table 4-2. A comparison of polymers made by DBU-catalyzed ROP using Methods A vs. B.

Polymer (targeted)	**Method**	**$M_{n(PEG)}$**	**$M_{n(PLGA)}$ [a]**	**Ratio [a,b] LA : GA**	**PDI [c]**
PEG_2-PL_2A	A	2K	2.16K	100 : 0	1.08
PEG_2-PL_2A	B	2K	2.03K	100 : 0	1.15
PEG_5-PL_5A	A	5K	5.62K	100 : 0	1.06
PEG_5-PL_5A	B	5K	5.09K	100 : 0	1.06
PEG_5-$PL_{10}A$	A	5K	10.8K	100 : 0	1.05
PEG_5-$PL_{10}A$ [d]	B	5K	10.1–10.2K	100 : 0	1.08–1.09
PEG_5-$PL_{2.5}G_{2.5}A$	A	5K	4.90K	46 : 54	1.06
PEG_5-$PL_{2.5}G_{2.5}A$	B	5K	4.79K	50 : 50	1.05
PEG_5-PL_5G_5A	A	5K	10.4K	54 : 46	1.08
PEG_5-PL_5G_5A [d]	B	5K	10.2–10.3K	52-54 : 46-48	1.09–1.17

[a] Results based on NMR spectroscopy[198]
[b] Mass ratio of the repeat units
[c] Results based on GPC measurements against a polystyrene standard
[d] Run in triplicate, giving the indicated ranges of values

4. Molecular Weight Determination via SEC/MALS. To assess the accuracy of our determinations of M_n via ^1H NMR spectroscopy, we further analyzed three polymers by SEC/MALS to determine the absolute molecular

[198] To assess the accuracy of determining M_n via ^1H NMR spectroscopy, we analyzed three polymer samples by SEC/MALS to measure the absolute molecular weight each. The M_n values by these two approaches showed reasonably good agreement.

weight of the samples. The results are summarized in Table 4-3. The specific refractive index (dn/dc) of a polymer is a concentration-dependent value of the difference in the refractive index of a dilute solution of the polymer and the corresponding pure solvent. If we assume a 100% recovery of the polymeric sample through the SEC column, then the value we measured for the specific refractive index (dn/dc) for the PEG sample was lower than its known value. This results in an M_n value that is higher than expected (i.e., 5K for the mPEG–OH sample, entry 1) or measured (for the block copolymers in entries 2 and 3) via ^{1}H NMR spectroscopy. Specifically, if we assume 100% recovery in the analysis of the 5K PEG-OH (run as a control), the experimentally determined dn/dc value was only 0.055 mL/g and the calculated M_n was 6.0 K. However, when the reported dn/dc value for poly(ethylene oxide) in THF of 0.068 mL/g was used,[199] the M_n was determined to be 4.9K–in good agreement with the value reported by the supplier of this commercial sample. Presumably, sample loss during filtration prior to injection and/or during elution from the SEC column is responsible for the need to correct the data in this manner.

Similarly, the observed dn/dc values for both the PEG-*b*-PLA and PEG-*b*-PLGA samples were also lower than expected, resulting, again, in correspondingly high M_n values. In this case, the known dn/dc value in THF for PLA of 0.042 was used,[199] for either the PLA block or as an approximation for the PLGA block. The weighted average of the dn/dc values for the PEG and polyester blocks were then used to calculate a dn/dc value for the block copolymer.[200] Using this approach, satisfactory correlation was found between the corrected M_n values found via SEC/MALS and ^{1}H NMR spectroscopy.

---

[199] Bandrup, J.; Immergut, E. H.; Grulke, E. A.; Abe, A.; Bloch, D. R. Polymer Handbook, 4th Edition, John Wiley & Sons, Inc. New York, 1999.

[200] Medrano, R.; Laguna, M. T. R.; Saiz, E.; Tarazona, M. P. Analysis of Copolymers of Styrene and Methyl Methacrylate using Size Exclusion Chromatography with Multiple Detection. *Phys. Chem. Chem. Phys.* **2003**, *5*, 151–157.

Table 4-3. A comparison of M_n values obtained via ^{1}H NMR spectroscopy and SEC/MALS.

Polymer	dn/dc (mL/g) (measured)	M_n [a] (MALS)	dn/dc (mL/g) (literature)	M_n (MALS/corrected)	M_n (^{1}H NMR)
PEG_5-OH	0.055	6.0 K	0.068	4.9 K [b]	5.0 K
PEG_5-$PL_{10}A$	0.042	19.0 K	0.051	15.5 K [c]	14.5 K
PEG_5-PL_5G_5A	0.031	24.2 K	0.051	14.7 K [c]	14.2 K

[a] M_n value assuming 100% recovery of the polymer sample during the SEC analysis.

[b] M_n value using the reported dn/dc value for PEG (0.068).[199]

[c] M_n value using a weighted average (0.33/0.67) for the reported dn/dc values for PEG (0.068) and PLA (0.042).

5. Improvements to the Extent of Lactide Consumption during PEG-b-PLGA Synthesis. Quenching the copolymerization at ca. 50% lactide conversion effectively establishes the proof of principle of the described semi-batch methodology. From a practical perspective, it likely would be advantageous to convert the lactide to a higher degree of polymerization. We demonstrated proof of principle by polymerizing the lactide through three half-lives. To maintain a the near "random" lactyl to glycolyl distribution in the product, a total of 87.5 mol% of glycolide relative to lactide was added and the rate of its infusion was halved after each of the first and second half-times (i.e., after and 10 and 20 minutes with a total addition time of 30 minutes). In the experiment we targeted a PEG_5-$PL_{4.38}G_{4,38}A$ polymer. A small aliquot was removed from the polymerization mixture after 10 and 20 minutes. They contained polymers with compositions that were measured to be PEG_5-$PL_{3.1}G_{2.5}A$ and PEG_5-$PL_{3.8}G_{3.4}A$ vs. the theoretical

PEG_5-$PL_{2,5}G_{2.5}A$ and PEG_5-$PL_{3.75}G_{3.75}A$, respectively (^{1}H NMR). The final sample of bulk polymer had a composition of PEG_5-$PL_{4.4}G_{4.3}A$ and a PDI of 1.19. While unoptimized, this experiment establishes the ability to achieve higher levels of lactide conversion while maintaining narrow polydispersities.

6. High MW PEG-b-PLGA Synthesis. Because polyesters with high glycolate content are notorious for their limited solubility,[201] we viewed it important to establish some of the limits of both the PEG and PLGA block sizes as well as the PLGA compositions that could be prepared using this new methodology. The results of these experiments are reported in entries 14-21 of Table 4-4. It can be seen from entries 7-10 that we were able to consistently and reproducibly generate PEG-*b*-PLGAs having PLGA blocks of MW up to 10K. However, attempts to synthesize a 5K-15K PEG-*b*-PLGA (PEG_5-$PL_{7.5}G_{7.5}A$ Entry 9) revealed a limitation. In this case, the reaction mixture became heterogeneous prior to conclusion of the polymerization and resulted in abnormally high lactic acid content. Presumably the inhomogeneity is the result of the growing glycolic acid content (total mass% of the block copolymer), which ultimately caused the polymer to become insoluble. Characterization of this sample showed that it possessed a PLGA block having a molecular weight lower than that targeted and an atypically broad PDI.

[201] Huffman, K. R.; Casey, D. J. Effect of Carboxyl End Groups on Polyglycolic Acid. *J. Polym. Sci: Polym. Chem. Ed.* **1985**, *23*, 1939–1954.

Table 4-4. Data for all block copolymers synthesized in this chapter.[a]

entry	Polymer (targeted)	Method	$M_{n(PEG)}$	$M_{n(PLGA)}$ [b] LA : GA	Ratio [c]	PDI [d]	T_g [e] (°C)	T_m [e] (°C)
1	PEG_2-PL_2A	A	2K	2.16K	100 : 0	1.08	ND	39.3
2	PEG_2-PL_5A	A	2K	5.11K	100 : 0	1.07	1.6	ND
3	PEG_5-PL_2A	A	5K	2.10K	100 : 0	1.04	ND	54.1
4	PEG_5-PL_5A	A	5K	5.62K	100 : 0	1.06	ND	51.0
5	PEG_5-$PL_{10}A$	A	5K	10.8K	100 : 0	1.05	1.8	ND
6	PEG_5-$PL_{15}A$	A	5K	16.3K	100 : 0	1.07	16.1	ND
7	PEG_5-$PL_{2.5}G_{2.5}A$	A	5K	4.90K	46 : 54	1.06	-24.2	50.1
8	PEG_5-PL_5G_5A	A	5K	10.4K	54 : 46	1.08	-4.8	ND
9	PEG_5-$PL_{7.5}G_{7.5}A$	A	5K	16.1K	58 : 42	1.13	7.5	ND
10	PEG_5-$PL_{7.5}G_{7.5}A$	B [f]	5K	13.5K	47 : 53	1.15 [g]	-2.8	ND
11	PEG_5-PLL_5G_5A	A	5K	9.43K	56 : 44	1.10	-6.1	ND
12	PEG_5-$PL_{7.5}G_{2.5}A$	A	5K	8.44K	76 : 24	1.08	-12.9	ND
13	PEG_5-$PL_{15}G_5A$	B	5K	18.5K	77 : 23	1.65 [h]	-0.8	ND
14	PEG_{10}-$PL_{2.5}G_{2.5}A$	B	10K	4.64K	53 : 47	1.04	ND	57.0
15	PEG_{10}-PL_5G_5A	B	10K	10.9K	54 : 46	1.04	-19.2	55.1
16	PEG_{10}-$PL_{7.5}G_{7.5}A$	B [i]	10K	15.7K	51 : 49	1.22 [g]	-18.6	55.3
17	PEG_{10}-$PL_{10}G_{10}A$	B [f]	10K	16K	50 : 50	2.29 [h]	--	--
18	PEG_{10}-$PL_{3.75}G_{1.25}A$	B [f,j]	10K	4.30K	72 : 28	1.05	ND	56.5
19	PEG_{10}-$PL_{7.5}G_{2.5}A$	B [f,j]	10K	10.3K	78 : 22	1.05	ND	51.5
20	PEG_{10}-$PL_{11.75}G_{3.75}A$	B [f,j]	10K	12.0K	71 : 29	1.07	-23.3	50.1
21	PEG_{10}-$PL_{15}G_5A$ [g]	B [f,j]	10K	20.3K	77 : 23	1.39	-3.5	ND

[a] Grayed information is reproduced from Table 4-2 and included here for comparison within sets having the same PEG block size and same polyester composition

[b] Results based on NMR spectroscopy

[c] Results based on NMR spectroscopy and presented as the mass ratio of the repeat units

[d] Results based on GPC measurements against a polystyrene standard

[e] Results obtained by DSC measurements (ND = none detected)

[f] Reaction performed at 8-fold lower concentration than Method B

[g] Minor asymmetric broadening noted in the GPC trace

[h] Asymmetric broadening noted in the GPC trace

[i] Reaction performed at 2-fold lower concentration than Method B

[j] The amounts of glycolide and lactide used were 0.5 and 1.5 times those used in Method B, in order to target a final 1:3 mass ratio within the PLGA block

We then turned to a different strategy—the use of lower reaction concentration to improve product solubility as the PLGA blocks grew larger. Thus, performing the reaction 8-fold more dilute than in Method B allowed the synthesis of the 5K-15K PEG-*b*-PLGA (PEG_5-$PL_{7.5}G_{7.5}A$, entry 10). However, that modification alone still fell short when we attempted to prepare the yet larger 5K-20K analog (i.e., PEG_5-$PL_{10}G_{10}A$); again heterogeneity prior to the end of the polymerization time was observed. Increasing solubility by use of a longer 10K PEG macroinitiator led to no substantial improvement (entry 17). However, we were finally able to prepare the 5K-20K PEG-*b*-PLGA PEG_{10}-$PL_{15}G_5A$ (entry 21, albeit with an atypically large PDI) by increasing the lactic acid content of the PLGA block to 75 wt%. From these experiments, we conclude that if one desires polymers having PLGA blocks with narrow PDIs, the scope of the reported methodology is limited to the synthesis of PEG-*b*-PLGAs having PLGA block sizes of less than ca. 20K.

7. Thermal Properties of the Block Copolymers. The melting and glass transition properties (T_g and T_m) of the PEG-*b*-PLA and PEG-*b*-PLGA block copolymers were measured by DSC and the results for each block copolymer are presented in Table 4-4. High molecular weight PEG homopolymer is highly crystalline (T_m ~ 63 °C). Consistent with this fact and as the data in Table 4-4

clearly show, every block copolymer sample containing a PEG block of greater than 40 wt% showed a melting exotherm at ca. 50 °C. This observation indicates that the polyether and polyester blocks in these samples are phase-separated (likely into lamellar phases) so that the PEG is able to crystallize.[202] One example (entry 7 in Table 4-4) is shown in Figure 4-4A.

The diblock copolymers with PEG blocks of less than 40 wt% show a single T_g but no evidence of a melting exotherm (e.g., Figure 4-4B, entry 8 in Table 4-4), suggesting that the polyether and polyester blocks are phase mixed. The T_g of PEG, PGA, and PLA homopolymers are approximately -40 °C, 35 °C, and 55 °C, respectively.[196,203] The T_g values of the diblock copolymers with PEG fraction <0.4 follow a general trend that can be rationalized by the Fox equation; that is, the T_gs of these copolymers are correlated with the weighted average of the T_gs for each of the PEG, lactyl, and glycolyl components. This is also consistent with the interpretation that a PEG-*b*-PLGA copolymer with <40 wt% PEG is a single phase at room temperature.

[202] Khandpur, A. K.; Förster, S.; Bates, F. S.; Hamley, I W.; Ryan, A. J.; Bras, W.; Almdal, K.; Mortensen, K. Polyisoprene-Polystyrene Diblock Copolymer Phase Diagram near the Order-Disorder Transition. *Macromolecules* **1995**, *28*, 8796–8806.

[203] Bandrup, J.; Immergut, E. H.; Grulke, E. A.; Abe, A.; Bloch, D. R. Polymer Handbook, 4th Edition, John Wiley & Sons, Inc. New York, 1999.

Figure 4-4. Representative DSC plots showing typical melting (A) and glass transition (B) behavior.

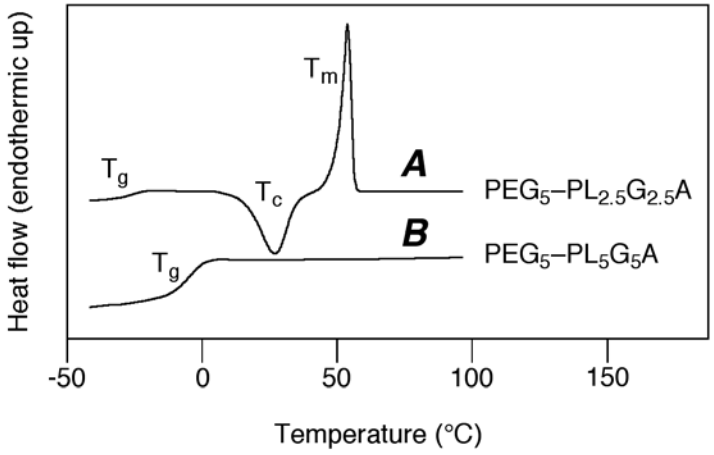

A few additional general trends can be seen in the T_m and T_g data in Table 4-4: *i*) increased MW of the polyether block tends to result in lower T_g values; *ii*) increased MW of the polyester block tends to result in higher T_g values; and *iii*) increased lactic (relative to glycolic) acid content in the polyester block tends to result in higher T_g values. These observations offer guidance for the design of PEG-*b*-PLGAs having compositions leading to specific thermal properties.

8. Sequence Length of Monomer Units in the PLGAs. Because the chemical shifts of the ester carbonyl carbons are sensitive to subtle electronic differences, ^{13}C NMR spectroscopy can be used to ascertain the average number of adjacent lactide (or glycolide) dyads in a PLGA backbone.[195,204] The NMR spectral data for several PLGA samples (Table 4-5) were used to calculate sequence lengths of both LA and GA repeating units using equations 3 and

[204] Kricheldorf, H. R.; Mang, T.; Jonte, J. M. Polylactones. 1. Copolymerization of Glycolide and ε-caprolactone. *Macromolecules* **1984**, *17*, 2173–2181.

4.[174,205] Representative data for two of these, having a 50:50 vs. a 75:25 LA:GA composition, are shown in Figure 4-5. $\overline{L_L}$ and $\overline{L_G}$ are the average sequence lengths of both the lactyl and glycolyl repeat units, respectively; I_{LL}, I_{LG}, I_{GG}, and I_{GL} are the signal intensities of the lactyl-lactyl, lactyl-glycolyl, glycolyl-glycolyl and glycolyl-lactyl structures (I_{LG} should be equivalent to I_{GL} if the carbonyl resonances are equally sensitive). Good agreement was observed by comparing the ratio of lactide to glycolide sequence lengths deduced from this ^{13}C NMR analysis ($\overline{L_L}/\overline{L_G}$) to that observed by integration of the methine vs. methylene resonances of the backbone protons for lactic to glycolic units, which lends confidence to the reliability of the ^{13}C NMR method.

[205] Grujpma, D. W.; Nijenhuis, A. J.; Pennings, A. J. Synthesis and Hydrolytic Degradation Behaviour of High-Molecular-Weight L-Lactide and Glycolide Copolymers. *Polymer* **1990**, *31*, 2201–2206.

Figure 4-5. ^{13}C NMR spectra (in hexafluoroisopropanol[195,204]) of two PEG-*b*-PLGA block copolymers of different compositions.

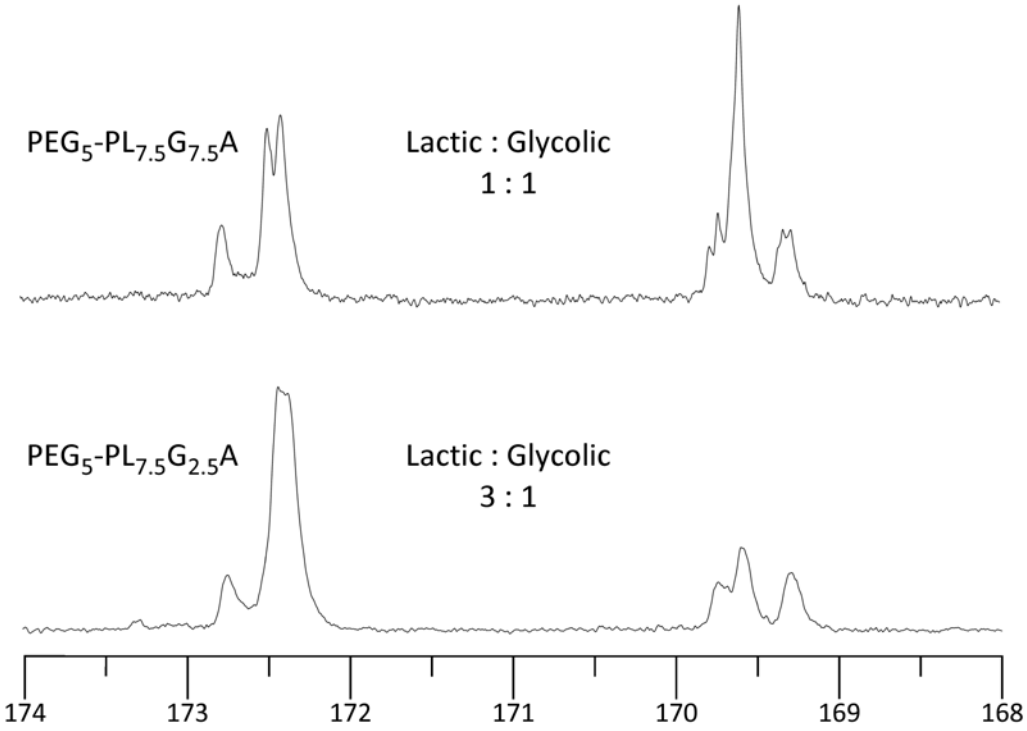

Table 4-5. Average sequence length of lactide ($\overline{L_L}$) and glycolide ($\overline{L_G}$) as measured by ^{13}C vs. ^{1}H NMR spectroscopies.

Entry	Polymer (Targeted)	$\overline{L_L}$ [a]	$\overline{L_G}$ [a]	$\overline{L_L}/\overline{L_G}$ [a]	LA/GA [b]
1	PEG_5-$PL_{2.5}G_{2.5}A$	3.68	5.31	40.9/59.1	40.3/59.7
2	PEG_5-PL_5G_5A	4.57	4.31	51.5/48.5	48.8/51.2
3	PEG_5-$PL_{7.5}G_{2.5}A$	7.73	3.00	72.0/28.0	71.7/28.3
4	PEG_5-PLL_5G_5A	4.90	4.57	51.7/48.3	50.7/49.3
5	PEG_5-$PL_{7.5}G_{7.5}A$	4.90	4.54	51.9/48.1	52.2/47.8

[a] Sequence lengths and their ratio calculated from ^{13}C NMR results according to eq 4-3 and 4-4.

[b] Molar ratio of lactic to glycol units calculated from integration of ^{1}H NMR data.

$$\overline{L_L} = 2 \times \frac{I_{LL}}{I_{LG}} + 2 \qquad \text{(eq 4-3)}$$

$$\overline{L_G} = 2 \times \frac{I_{GG}}{I_{GL}} + 2 \qquad \text{(eq 4-4)}$$

The expectation value for each of the sequence lengths of both lactic and glycolic dyads for a truly random copolymerization of lactide and glycolide is 4.00 (recall that each propagation event delivers two of the same acid backbone units since each monomer is dimeric).[206] In the case of PEG_5-PL_5G_5A (Table 4-5, entry

[206] Odian, G., Principles of Polymerization, 4th Edition, Wiley-Interscience, New York, 2004, p 470.

2) the average sequence of the lactyl unit, $\overline{L}_L$, is 4.57 and of $\overline{L}_G$ is 4.31. These differences from the theoretical likely arise from some combination of the use of constant rather than a diminishing rate of addition of glycolide, error in the measured rate constant ratio, imperfect mixing, and inherent difference in cross reactivity ratios that attend each of four possible propagation partners. When the glycolide feed rate was decreased to obtain the PEG_5-$PL_{7.5}G_{2.5}A$ polymer, $\overline{L}_G$ was observed to decrease to 3 while $\overline{L}_L$ increased to 7.73 (Table 4-5, entry 3).

7. Collaborative Circulation Studies with Nanoparticles Comprised of Narrowly Dispersed PEG-*b*-PLGA and PEG-*b*-PLA BCPs.[207]

Using the methodology described above, a series of PEG-*b*-PLGA and PEG-*b*-PLA BCPs were prepared and, in collaboration with Suzanne D'Addio and Prof. Robert Prud'homme (Department of Chemical Engineering, Princeton University) used to synthesize nanoparticles via FNP. Fine analysis and control of the PL(G)A MW, PLGA monomer ratio, and PLGA microstructure was necessary to systematically examine the effects of these parameters on nanoparticle stability and accurately compare them to nanoparticles made from either PEG-*b*-PS or PEG-*b*-PCL of varying MWs.

Briefly, the result of this study suggested general guidelines for the design of stable, PEG-protected, drug-loaded nanoparticles. Characteristics to be considered are: i) the area ratio of PEG block vis-à-vis the hydrophobic block, ii) the hydrophobicity of the hydrophobic block relative to the PEG solvation energy, iii) the absolute MW of the PEG block, and iv) the physical state (i.e., crystalline

[207] D'Addio, S. M.; Saad, W.; Ansell, S. M.; Squiers, J. J.; Adamson, D.; Herrera-Alonso, M.; Wohl, A. R.; Hoye, T. R.; Macosko, C. W.; Mayer, L. D.; Vauthier, C.; Prud'homme, R. K. Effects of Block Copolymer Properties on Nanocarrier Protection from *in vivo* Clearance. *J. Control. Release* **2012**, *162*, 208–217.

vs. amorphous) of the hydrophobic block.[207] In these studies, the PEG-*b*-PLA and PEG-*b*-PLGA synthesis methodology was used to control three of these critical parameters in the PLA/PLGA polyester blocks: i) absolute polyester MW and, correspondingly, its area ratio, ii) the hydrophobicity of the polyester block via control of both the absolute PLA/PLGA MW as well as the ratio of lactide:glycolide, and iii) the crystallinity of the polyester via incorporation of a "random" PLGA. These studies indicate the utility of the PLGA synthesis methodology described within Chapter 4.

8. Conclusions.

The high activity of DBU makes it a convenient catalyst for the synthesis of PEG-*b*-PLA block copolymers having well-controlled sizes and narrow distribution. To expand this chemistry to the synthesis of PEG-*b*-PLGAs, with a "random" PLGA copolymer block, we determined the reactivity ratio of **4.02:4.01** to be approximately 1000:1 for glycolide (**4.02**) to lactide (**4.01**) in homopolymerizations. We developed a new, semi-batch PEG-*b*-PLGA synthesis strategy in which the continuous addition of glycolide approximated the conversion curve of lactide throughout its first half-life. This resulted in a convenient method for the preparation of PEG-*b*-PLGAs of various block sizes and monomer ratios. As a consequence of the controlled copolymerization of lactide and glycolide, MW, composition, sequence length and distribution (and therefore physical properties) of PEG-*b*-PLGA block copolymers could be easily manipulated for different applications. We determined that the limitation of this method was the synthesis of PLGA blocks with MW greater than 20K, likely due precipitation before completion of the polymerization. This strategy was found to give reproducible results, allowing the convenient preparation of PEG-*b*-PLGA block copolymers that could be useful in a variety of applications, including the

synthesis of well-defined BCPs for systematic studies of nanoparticle circulation behavior. The general principles explored here should be applicable to the copolymerization of glycolide and lactide with other less reactive lactones for the preparation of various copolymers.

9. Experimental Section.

General Materials. *Rac*-Lactide [**(±)-4.01**] was purchased from Altasorb was purified by recrystallization from toluene. L-Lactide (**S,S-4.01**) was purchased from Purac, recrystallized twice from toluene, and stored in a dry box. Glycolide (**4.02**) was purchased from Altasorb and was purified by recrystallization from dry THF. 1,8-Diazabicyclo[5.4.0]-undec-7-ene (DBU) was purchased from Sigma Aldrich, dried over calcium hydride, and distilled. mPEG-OH of molecular weight 2 and 5 kg mol^{-1} (K) was purchased from Aldrich and 10 K from JenKem Technology. All polymerizations were conducted at ambient temperature.

Method A for reagent and catalyst purification, storage, and handling (more rigorous). Chloroform was washed with water and distilled from phosphorus pentoxide. Dichloromethane (CH_2Cl_2) was first dried by being passed through an activated alumina column and then distilled from calcium hydride (CaH_2). Tetrahydrofuran (THF) was first dried by being passed through an activated alumina column and then distilled from sodium and benzophenone. DBU was purified by distillation twice from CaH_2. Lactides and glycolide were stored and handled in a controlled atmosphere dry box. mPEG-OHs were dried by azeotropic distillation with toluene at atmospheric pressure.

Method B for reagent and catalyst purification, storage, and handling (less rigorous). CH_2Cl_2 and THF were dried by passing through an activated alumina column. DBU was purified by one distillation from CaH_2. Lactide and glycolide were stored in screw-capped containers under ambient lab atmosphere. mPEG-OHs were dried as a solution in dry dichloromethane and overnight over activated molecular sieves (4 Å) in an airtight culture tube.

Polymer Characterization. ^{1}H NMR spectra were obtained on a Varian VI-300, Varian VXR-300, or Varian VXR-500 spectrometer in $CDCl_3$. Number-average molecular weight was calculated by comparison of the ratio of the integrations of the methine and methylene signals of PLA and PGA residues vs. the methylene signal of PEG residues assuming the manufacturer-provided molecular weight of the mPEG–OH macroinitiator. For sequence analysis, ^{13}C NMR spectra were obtained on a Varian 400 instrument at 100 MHz in hexafluoroisopropanol; a 45 degree pulse and a relaxation delay of 5 s were used. Size-exclusion chromatography (SEC) was performed on an Agilent Technologies 1100 series liquid chromatograph equipped with a Hewlett-Packard 1047A refractive index detector. Chloroform was used as the mobile phase at an elution rate of 1 mL min^{-1}. The instrument was operated at 35 °C using a series of three PLgel 5 µm Mixed-C columns (Polymer Laboratories) with molecular weight range of 0.4-400 K. PDIs are reported with respect to polystyrene standards having molecular weights ranging from 5 to 1000 K (Polymer Laboratories). Size-exclusion chromatography/multiangle light scattering (SEC/MALS) was performed using an Alltech 426 HPLC pump equipped with a Wyatt Technology Corporation Dawn DSP Laser photometer and an Optilab refractive index detector. Laser light scattering data were collected using a 633

nm wavelength at a 90° scattering angle. Tetrahydrofuran containing 1% tetramethylethylenediamine was used as the mobile phase at an elution rate of 1 mL min^{-1}. The instrument was operated at 25 °C using a series of three Phenomenex columns containing Phenogel 5 µm cross-linked styrene divinyl benzene with a molecular weight range of 5-500 K. The results were analyzed with ASTRA software. Differential scanning calorimetry (DSC) was performed using a TA Instruments model Q1000 Differential Scanning Calorimeter that was calibrated using high purity indium at a heating rate of 10 °C min^{-1}. Transitions were recorded during the second scan.

Chapter 5

Studies on Silicate-Loaded Nanoparticles: Characterization, Structure, and Efficacy.

1. Introduction.

1. A Brief Discussion of Common Encapsulation Methodologies. General strategies to encapsulate drugs into polymeric and/or liposomal carriers have been rigorously explored over the last several decades. While a number of highly customized polymers have been synthesized exclusively for drug delivery applications, more often, common, easily prepared polymeric species are preferred for these applications. One chief example of a frequently used polymer is PLGA, which has been used to encapsulate drugs and/or prodrugs via a variety of formulation techniques, including single emulsions, double emulsions, coacervation, and spray drying.[208]

Unfortunately, when these strategies are applied to encapsulate PTX, they frequently result in rather low drug loading levels. For example, PTX-loaded liposomes often contain exceptionally low PTX content (e.g., 3.4 wt%[209] or 6.5

[208] Jain, R. A. The Manufacturing Techniques of Various Drug-Loaded Biodegradable Poly(lactide-*co*-glycolide) (PLGA) Devices. *Biomaterials*, **2000**, *21*, 2475–2490.

[209] Fetterly, G. J.; Straubinger, R. M. Pharmacokinetics of Paclitaxel-Containing Liposomes in Rats. *AAPS PharmSci.* **2003**, *5*, 90-100.

wt%[210]), with the remainder of the mass consisting of non-therapeutic excipient(s). Another example of PTX-loaded BCPs can be found in the construction of PTX-containing thin films of PEG and/or PLGA. Such efforts have resulted in encapsulation of up to 10 wt% PTX in PLGA films containing systematically varied PEG content.[211]

Perhaps the most common tactic to load PTX into a polymeric excipient, however, is through the creation of micelles. The most clinically relevant example of this strategy is Genexol-PM®. Depending upon the publication referenced, 16.7-25 wt% PTX loading in ca. 2k-2k PEG-*b*-PLA micelles has been claimed.[111,112] Unfortunately, it is difficult to independently analyze either the micellar structure of these preparations or the loading levels since only formulation procedures are reported –detailed data to corroborate full encapsulation or particle size are not readily available.[111,112]

In addition to Genexol-PM®, numerous other reports demonstrate that emulsion techniques are an exceedingly common strategy to encapsulate PTX into micelles consisting of PEG and PLA/PLGA.[212,213] These reports describe achievement of a wide variety of loading levels of PTX, but these levels are generally below 15 wt%.[214,215,216,217] These typical, relatively low loading levels

---

[210] Koudelka, S.; Turaneck-Knotigova, P.; Masek, J.; Korvasova, Z.; Skrbalova, M.; Plockova, J.; Bartheldyova, E.; Turanek, J. Liposomes with High Encapsulation Capacity for Paclitaxel: Preparation, Characterization, and *in vivo* Anticancer Effect. *J. Pharm. Sci.* **2010**, *99*, 2309–2319.

[211] Steele, T. W. J.; Huang, C. L.; Widjaja, E.; Boey, F. Y. C.; Loo, J. S. C.; Venkatraman, S. S.; The Effect of Polyethylene Glycol Strutcture on Paclitaxel Drug Release and Mechanical Properties of PLGA Thin Films. *Acta Biomater.* **2011**, *7*, 1973–1983.

[212] Quintanar-Guerrero, D.; Allèmann, E.; Fessi, H.; Doelker, E. Preparation Techniques and Mechanisms of Fromation of Biodegradable Nanoparticles from Preformed Polymers. *Drug Dev. Ind. Pharm.* **1998**, *24*, 1113–1128.

[213] Torchilin, V. P. Micellar Nanocarriers: Pharmaceutical Perspectives. *Pharm. Res.* **2007**, *24*, 1–16.

[214] Chavanpatil, M. D.; Patil, Y.; Panyam, J. Susceptibility of Nanoparticle-Encapsulated Paclitaxel to P-glycoprotein-mediated Drug Efflux. *Int. J. Pharm.* **2006**, *320*, 150–156.

are likely a result of the encapsulation level reaching a maximum dictated by the thermodynamic (rather than kinetic) physical properties of the polymeric excipient and/or PTX small molecule.

2. Flash Nanoprecipitation (FNP). As opposed to the emulsion and micellization processes, flash nanoprecipitation is a technique that is capable of kinetically entrapping hydrophobic solutes. This fundamentally different concept has demonstrated the ability to increase the maximum loading level of hydrophobic small molecules during development of the methodology.[1] Prud'homme and coworkers were the first to realize the potential of the FNP process as applied to drug delivery. Both the Prud'homme group and the Macosko/Hoye groups expanded the fundamental understanding of FNP by establishing several trends: i) relationships of jet diameters, chamber diameters, and outlet configurations to micromixing performance;[2] ii) impact of matching the aggregation time of the polymer with the nucleation time of the hydrophobic solute;[3] and iii) plateau effect of the nanoparticle size at sufficiently large Reynolds number.[5] These (and other) principles were successfully used to encapsulate β-carotene as a model hydrophobic solute.[5,218] Additionally, these

---

[215] Patil, Y. B.; Toti, U. S.; Khdair, A.; Ma, L.; Panyam, J. Single-Step Surface Functionalization of Polymeric Nanoparticles for Targeted Drug Delivery. *Biomaterials*, **2009**, *30*, 859–866.

[216] Danhier, F.; Lecouturier, N.; Vroman, B.; Jèröme, C.; Marchand-Brynaert, J.; Feron, O.; Prèat, V. Paclitaxel-loaded PEGylated PLGA-based Nanoparticles: In vitro and in vivo Evaluation. *J. Control. Release* **2009**, *133*, 11–17.

[217] He, G.; Lwin, L.; Pan, J.; Venkatraman, S. ABA and BAB Type Triblock Copolymer of PEG and PLA: A Comparative Study of Drug Release Properties and "Stealth" Particle Characteristics. *Int. J. Pharm.* **2007**, *334*, 48–55.

[218] Johnson, B. K. Flash NanoPrecipitation of Organic Actives via Confined Micromixing and Block Copolymer Stabilization. Ph.D. Dissertation, Princeton University, Princeton, NJ, **2003**, 1–291.

trends were used more broadly to, for example, establish the ability to precipitate an *in situ* formed BCP via reactive flash nanoprecipitation.[219]

Despite the high encapsulation efficiencies and solute loading levels (> 80 wt% β-carotene) in model studies, weaknesses remained in the overall design. Namely, impingement mixing via the CIJ mixer required the use of equal volumes of the solvent and anti-solvent – a potentially limiting feature when attempting to reach supersaturation. Thus, the Prud'homme group advanced the FNP mixing science with the invention and development of the multi-inlet vortex (MIV) mixer.[4] This device consisted of four separate solvent streams that mix tangentially, allowing alterations in the mixing physics and the production of dispersions of varied solvent composition. While an effective device, especially for larger scale experiments, the capital costs of the apparatus, inconvenient set-up, and larger material requirements reduced the applicability to experiments that are material-limited, such as those with high-value prodrug or end-functionalized BCPs.

Thus, a collaborative effort between the Macosko group and Hoye group continued to advance the CIJ mixer design. This work led to the development of a confined impingement jet with dilution (CIJ-D)[6] mixing FNP methodology (Figure 5-1; also, c.f. Figure 1-1). This simple, hand-operated apparatus allowed for: i) rapid creation and analysis of nanoparticles derived from new materials, ii) small material requirements, and iii) a post-impingement dilution stage to increase the range of co-solvent mixtures that could be accessed. Particles made from this CIJ-D method were shown to produce nanoparticles of similar size and stability as that of the MIVM, and thus the CIJ-D mixer served as a useful device for the screening of new materials (both silicate ester prodrugs and BCPs).[6]

[219] Zhu, Z.; Anacker, J. L.; Ji, S.; Hoye, T. R.; Macosko, C. W.; Prud'homme, R. K. Formation of Block Copolymer-Protected Nanoparticles via Reactive Impingement Mixing. *Langmuir*, **2007**, *23*, 10499–10504.

Figure 5-1. The design and dimensions of the modified confined impingement jet mixer for flash nanoprecipitation.[6]

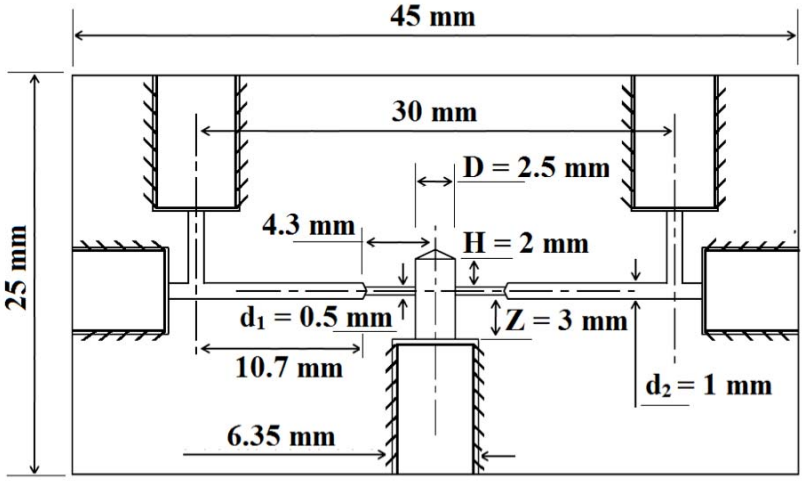

With ample tools (i.e., silicate ester prodrugs and PEG-*b*-PLGA BCPs) and methodologies (i.e., FNP) customized for highly efficient encapsulation in hand, a notable scientific inquiry remained. Namely, will these modifications overcome the propensity of PTX to rapidly crystallize outside of a nanoparticle core? Furthermore, other tangential questions related to the creation of defined nanoparticles exist. For instance, since these are *kinetically* trapped particles, it is likely that they are less uniform than traditional micelles or liposomes – an assumption that is validated by the relatively large size distribution observed in both DLS and microscopy experiments.[5] One can thus ask a number of pertinent questions regarding these nanostructures. Is the water soluble PEG block and hydrophobic PLGA block phase segregated or interspersed in the final nanoparticle? Is the silicate ester prodrug distributed uniformly throughout the polymer, highly localized in the nanoparticle core, or some blend of the two extremes? Is the PTX silicate ester amorphous or crystalline? What analytical techniques can we employ to attain data to answer such questions?

2. Studies of Model Silicate Ester-Loaded Nanoparticles.

1. Behavior of PEG-b-PLA in Co-Solvents of Varying Aqueous Content.

The power of NMR spectroscopic techniques is one of many options that provide insight into block copolymer self-assembly and micellization.[220] Such studies have been conducted on a variety of BCPs, but the most pertinent and informative to the materials addressed in this thesis is the work by Davis and co-workers on PEG-*b*-PLA. They have extensively detailed the behavior of micellized PEG-*b*-PLA (of a variety of MWs) BCPs via ^{1}H NMR spectroscopy and correlated it with the particle sizes obtained from DLS.[221] Briefly, they deduced that the traditional micellization technique that they employed (dissolution of the BCP in a water miscible organic solvent, slow addition of the two co-solvents, and finally, removal of the organic solvent) resulted in a miclle with a traditional core-shell structure. Notably, they observed significantly large PLA resonances (as judged relative to an internal standard) for low MW polyester blocks (< 3K). They interpreted this result as significant polymer mobility at these low MWs. In contrast to these findings, analogous resonances were not observed for BCPs with a PEG MW >6K.[221] Additionally, quantitative integration of the PEG block suggested minimal penetration of the PEG chains into the micelle core, indicative of a solid-like PLA core.[221,222]

---

[220] Riess, G. Micellization of Block Copolymers. *Prog. Polym. Sci.* **2003**, *28*, 1107–1170 and references therein.

[221] Riley, T.; Stolnik, S.; Heald, C. R.; Xiong, C. D.; Garnett, M. C.; Illum, L; Davis, S. S.; Purkiss, S. C.; Barlow, R. J.; Gellert, P. R. Physicochemical Evaluation of Nanoparticles Assembled from Poly(lactic acid)-Poly(ethylene glycol) (PLA-PEG) Block Copolymers as Drug Delivery Vehicles. *Langmuir* **2001**, *17*, 3168–3174.

[222] Heald, C. R.; Stolnik, S.; Kujawinski, K. S.; De Matteis, C.; Garnett, M. C.; Illum, L.; Davis, S. S.; Purkiss, S. C.; Barlow, R. J.; Gellert, P. R. Poly(lactic acid)-Poly(ethylene oxide) (PLA-PEG) Nanoparticles: NMR Studies of the Central Solidlike PLA Core and the Liquid PEG Corona. *Langmuir*, **2002**, *18*, 3669–3675.

While these excellent studies provide a wealth of information potentially applicable to our PEG-*b*-PLGA copolymers, a key difference (other than the use of a PLGA polyester block) remained. Unlike the thermodynamically-stable micelles formed in the Davis work, FNP-produced nanoparticles are kinetically trapped. Thus, the possibility for PEG entrapment within the core, extraneous PLGA corona material, or mobile PLGA chains within the core (potentially due to entrapped solvent) remained reasonable propositions. Understanding the structure of these nanoparticles is of fundamental scientific interest. Additionally, the physical state of the polyester block could provide key insights and guidance into the results of, for example, future drug release studies.[223]

The initial experiment was a simple derivation of the Davis study[221] – a 5K-5K PEG-*b*-PLGA BCP was dissolved in d_6-acetone (a precisely known concentration of methanol was included as an internal standard). D_2O was progressively titrated into the solution and the proton NMR resonances attributable to the ethylene oxide, lactic, and glycolic repeat units were integrated. With the progressive addition of D_2O, the PLGA resonances broadened significantly during the experiment, becoming unrecognizable at >50 vol% D_2O content (see Table 5-1). In contrast, the PEG-related proton resonance remained sharp, and its integration value remained essentially constant throughout the experiment (up to 90 vol% D_2O).

After successfully emulating the Davis work in the related PEG-*b*-PLGA system, the precipitation method was altered such that unloaded particles were prepared via FNP. Yet, even in the case of a kinetic arrest of particle growth, the results were essentially the same. After precipitation via FNP, the PLGA resonances were broadened such that they were indistinguishable from the

[223] Papadimitriou, S.; Bikiaris, D. Novel Self-Assembled Core–Shell Nanoparticles Based on Crystalline Amorphous Moieties of Aliphatic Copolyesters for Efficient Controlled Drug Release. *J. Control. Release* **2009**, *138*, 177–184.

baseline, whereas the PEG resonances remained well-defined and integrated to the "full" value relative to the internal standard. Both of these sets of results are consistent with the Davis conclusion of a solubilized PEG corona and a solid-like PLGA core.[221,222]

Table 5-1. The observed resonance integration for a PEG-*b*-PLGA BCP relative to an internal standard.

Method	D_2O content (%)[a]	ethylene glycol integration (%)[b]	glycolyl integration (%)[b]	lactyl integration (%)[b]
A[c]	0	100	100	100
A	20	99.5	82.1	96.1
A	33	98.9	65.9[d]	92.8[d]
A	50	95.7	17.9[d]	48.8[d]
A	75	99.6	n.o.[e]	n.o.
A	90	94.2	n.o.	n.o.
B[f]	0	100	100	100
B	90	88.5	n.o.	n.o.

[a] The percent D_2O content is relative to the d_6-acetone content (v/v).
[b] The percent integration is presented as the percentage of the full solubilized (100% acetone) NMR sample relative to an internal standard
[c] Method A consists of slow addition of the anti-solvent (water).
[d] The resonances were noted to be very broad.
[e] n.o. = not observed. The resonances were too broad to reliably integrate.
[f] Method B consists of mixing by FNP (CIJ-D).

2. Tetra-n-butoxysilane-Loaded Nanoparticles: Analysis by DOSY NMR Methodologies. While analysis of nanocarrier contents via spectroscopic techniques is invariably difficult (the use of ^{1}H NMR spectroscopy in conjunction

with a pH dependent chemical shift is a notable exception[224]), defining the size of macrostructures via spectroscopy and/or microscopy has realized substantially more success. The most common means encountered in the literature of measuring particle sizes on the nanometer scale is DLS. While this is typically effective for (near) monodisperse samples, rigorous analysis of DLS methodology as it is most commonly practiced, (i.e., with a single angle detector) fails to identify bimodal distributions. Typically, in these cases microscopic techniques [e.g., atomic force microscopy (AFM) scanning electron microscopy (SEM), or transmission electron microscopy (TEM)] are better able to provide a more accurate "snapshot" of mixtures containing a significant size distribution.[5,225]

Even in these cases, however, there is no way to know the constitution of the particles containing only low atomic weight atoms – only the size is measured. In the case of our FNP-produced nanoparticles, one of the critical parameters is not just the size of the particles, but also their composition. Namely, is there a way to determine that the hydrophobic silicate was indeed encapsulated in a polymer-protected nanoparticle (rather than merely self-aggregated)?

We turned to advanced NMR techniques to gain further definition of both the nanoparticle size and composition.[226] Specifically, we employed diffusion oriented spectroscopy (DOSY) to determine if the silicate esters were being

---

[224] Zhang, X.-M.; Patel, A. B.; de Graaf, R. A.; Behar, K. L. Determindation of Liposomal Encapsulation Efficiency Using Proton NMR Spectroscopy. *Chem. Phys. Lipids* **2004**, *127*, 113–120.

[225] Hoo, C. M.; Starostin, N.; West, P.; Mecartney, M. L. A Comparison of Atomic Force Microscopy (AFM) and Dynamic Light Scattering (DLS) Methods to Characterize Nanoparticle Size Distributions. *J. Nanopart. Res.* **2008**, *10*, 89–96.

[226] Valentini, M.; Vaccaro, A.; Rehor, A.; Napoli, A.; Hubbell, J. A.; Tirelli, N. Diffusion NMR Spectroscopy for the Characterization of the Size and Interactions of Colloidal Matter: The Case of Vesicles and Nanoparticles. *J. Am. Chem. Soc.* **2004**, *126*, 2142–2147.

efficiently encapsulated within the BCP nanoparticle.[227] A series of silicate esters were initially screened for these studies: tetra-*n*-butylsilane (**2.11**) tetraphytylsilane (**2.14**), tetramenthoxysilane (**2.17**) and the bis-triethoxy PTX silicate (**3.08**) were considered. Compounds **2.17** and **3.08** were quickly eliminated from consideration because these compounds were likely entrapped in the solid state within the solid PLGA core. Thus, the proton resonances from **2.17** and **3.08** species were not observed. Fortunately, the oily silicate esters **2.11** and **2.14** exhibited distinctive resonances that were easily discernible after FNP formulation. Silicate **2.11** was chosen over **2.14** for further study, however, because a small degree of water solubility in the model was desirable for control experiments involving non-polymer protected, self-aggregation of the tetraalkoxysilane in D_2O. Successful completion of this control necessitates the ability to observe resonances associated with the model compound in pure D_2O.

Thus, **2.11** was subjected to FNP with a PEG-*b*-PLGA BCP using D_2O/d_6-acetone as the co-solvents (9:1 v/v). The dispersion was analyzed by ^1H and DOSY NMR spectroscopy after the addition of a water-soluble, small molecule internal standard (monomethoxy diethylene glycol). The internal standard served as a check for the diffusion coefficient (D) of a solubilized small molecule.

The Stokes-Einstein equation is sometimes employed to determine absolute sizes of the particulate species. However, this equation is only valid if the substrate is a perfectly spherical particle that behaves identically to the standard in the given medium, and neither of these assumptions is rigorously true in the case of FNP-derived nanoparticles. Instead, we chose to focus on the differences of the diffusion coefficients (ΔD) that are observed in the silane resonances relative to the monomethoxy diethylene glycol standard.

[227] Garcia-Fuentes, M.; Torres, D.; Martin-Pastor, M.; Alonso, M. J. Application of NMR Spectroscopy to the Characterization of PEG-Stabilized Lipid Nanoparticles. *Langmuir*, **2004**, *20*, 8839–8845.

Interestingly, comparison of the diffusion coefficients of the (presumably encapsulated) silane **2.11** and soluble monomethoxy diethylene glycol produced a ΔD = ca. 10^6 m^2 s^{-1} (compare resonances ■ and ● in Figure 5-2)! This large difference is consistent with incorporation of the tetraalkoxysilane into the much larger (and more slowly diffusing) nanoparticle. [The "smeared" resonances (◆) are a frequent artifact from overlapping resonances of different diffusion coefficients and are disregarded in the analysis.[228]] To rule out simple aggregation of the silane **2.11** as the cause of the large ΔD, **2.11** was dissolved in a d_6-acetone solution and added to D_2O in the same concentration and solvent ratio. In this case, comparison to the internal standard yielded a ΔD = ca. 10^2 m^2 s^{-1} (data not shown).

[228] Dr. Letitia Yao provided critical expertise and assistance during these DOSY NMR experiments. Yao, L. University of Minnesota, Minneapolis, MN. Personal communication, **2011**.

Figure 5-2. DOSY spectrum showing the $\Delta D = 10^6$ of the (presumably) encapsulated tetra-*n*-butylsilane (●, ❖, and ⌘) as compared to the monomethoxy diethylene glycol (■) in D_2O (❍).

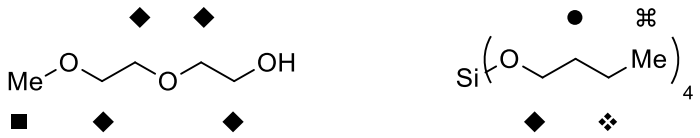

2.11

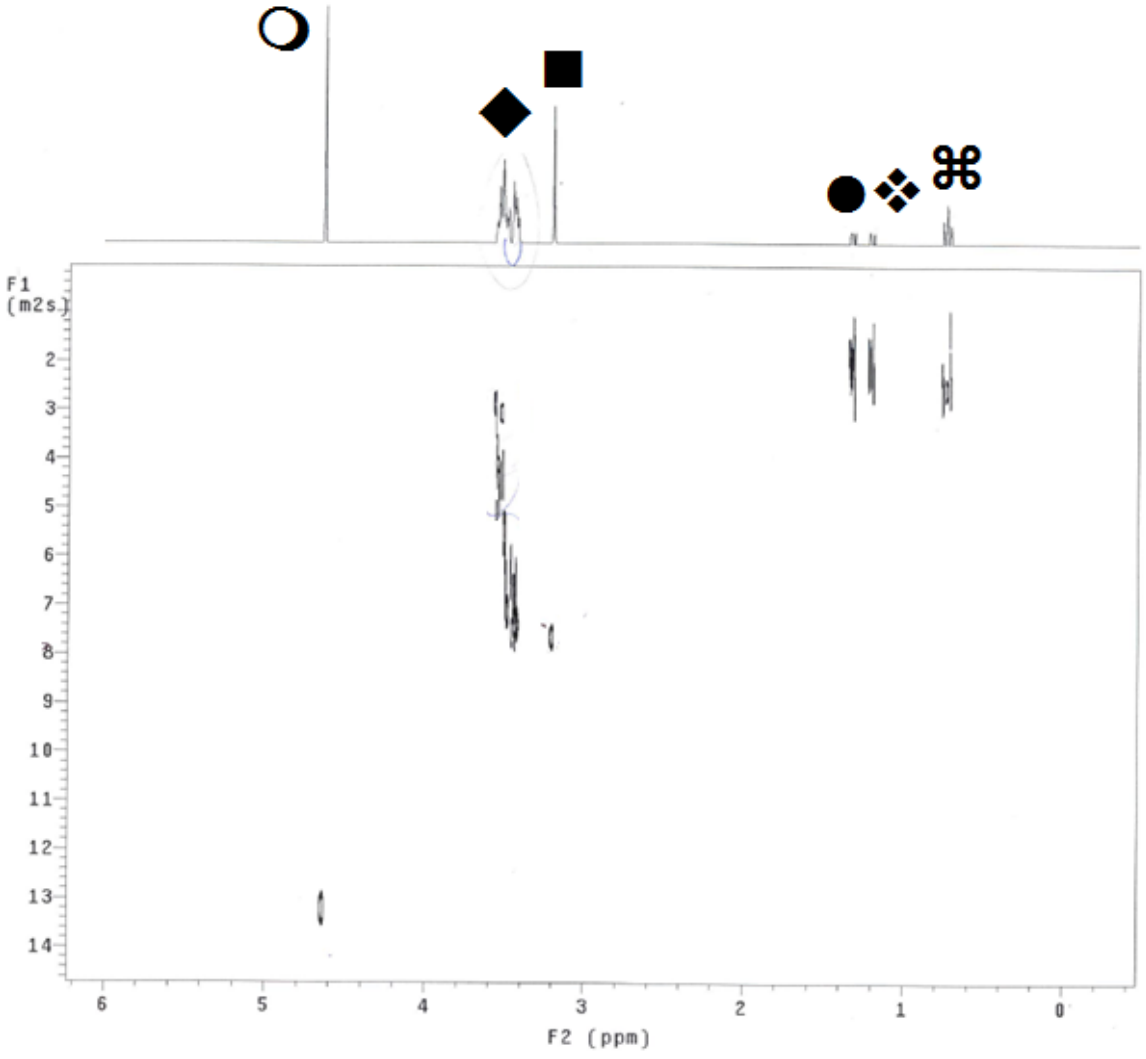

As evidenced by the ΔD of the non-polymer protected silane, it is likely that some aggregation of the silane exists in the absence of the BCP. However, aggregation only fails to account for the magnitude of the change in the diffusion coefficient. Coupling these diffusion coefficient results from DOSY measurements with qualitative observations (e.g., the apparent homogeneity of the FNP dispersion), it is highly probable that the silane is encapsulated within the nanoparticle. These qualitative observations are further expanded in the context of PTX silicates in section 5.3.2. While far from an "open and shut case," the evidence remains consistent with the tentative conclusion expressed here.

3. Selected Studies of PTX Silicate Prodrug-Loaded Nanoparticles.

1. FNP Encapsulation of PTX and a PTX-Silicate in a PEG-b-PLGA Nanoparticle. Recall that FNP is an attractive technique for producing nanoparticles loaded with high levels of hydrophobic compounds, including pharmaceutically relevant agents. Co-precipitation of varying hydrophobes with an amphiphilic block copolymer (BCP) provides dispersions of kinetically protected NPs in the size range of 50-200 nm.[2,3,6] However, attempts to incorporate PTX within a PEG-*b*-PCL BCP via FNP led to unstable NPs.[7] The PTX is sufficiently hydrophilic that it quickly partitions out of the NP cores. The PTX crystallizes from the aqueous medium via Ostwald ripening. In the end result, the crystalline form of the drug acts as an infinite sink in a partitioning experiment, resulting in rapid loss of encapsulated drug from the nanoparticle core. This is ironic given that PTX is too hydrophobic to be formulated as an aqueous solution for conventional intravenous delivery.

Working together with Dr. Zhengxi Zhu of the Macosko group, efforts toward the successful incorporation of the PTX silicates were initiated by altering the Saad experimental procedure[7] by substituting a PEG-*b*-PLGA (2K-10K) as

the BCP. This reasonable control experiment was predicated on both repeating the previously described results in our hands, but also because the more amorphous PLGA polyester will potentially precipitate at a different rate and/or in an alternate morphology. Either of these outcomes could lead more efficient PTX encapsulation. Specifically, the FNP of 25 mg of both PTX and PEG-*b*-PLGA were impinged in the MIVM mixer [final ratio of THF:water was 5:95 (v/v)]. Immediately (i.e., one minute) after FNP-mixing, the suspension was homogeneous. Dr. Zhu prepared an SEM sample (Figure 5-3a) which visualized a broad dispersion of spherical particles. However, approximately 90 mins later, a significant change in the dispersion was noted. A white, crystalline precipitate was readily observed. Dr. Zhu's subsequently prepared SEM (Figure 5-3b), confirmed the presence of micron-sized crystals.[5]

With the instability of FNP-produced,l PTX-loaded nanoparticles reaffirmed, the focus of the study quickly shifted to incorporation of a PTX silicate in its place. Guided by its mosaic of prodrug characteristics (ease of synthesis and handling, hydrophobic character, rate of hydrolysis, cytotoxicity, and nature of the byproducts), we selected the bis-triethoxysilicate prodrug **3.08** for formulation into nanoparticles. Again in collaboration with Dr. Zhengxi Zhu, the first FNP experiment utilizing a PTX silicate was conducted. In this experiment, 35 mg of **3.08** (an equimolar amount of PTX as used in the above experiment) and 25 mg of a 2K-10K PEG-*b*-PLGA were impinged in a MIV mixing device [final ratio of THF:water was again 5:95 (v/v)]. In this case, the dispersion was again initially homogeneous, but in this trial, only negligible changes in the measured particle size (ca. 100 nm by DLS) were observed over the course of several days. SEM images prepared by Dr. Zhu 90 minutes (Figure 5-3c and d) and eight days (Figure 5-3e) were virtually indistinguishable. Both images confirmed the qualitative observations and DLS measurements that indicated a moderately broad size range of spherical particles with no crystallization.[5]

Figure 5-3. The SEM images taken by Dr. Zhu from collaboratively formulated nanoparticles show (a) the kinetically trapped nanoparticles consisting of PEG-*b*-PLGA and PTX one minute after formulation, (b) the crystal growth of PTX 90 minutes after formulation, (c) the kinetically trapped nanoparticles consisting of PEG-*b*-PLGA and **3.08** 90 minutes after formulation, (d) a magnified image of panel c, and (e) the maintained size and shape of the silicate-containing particles after eight days.[5]

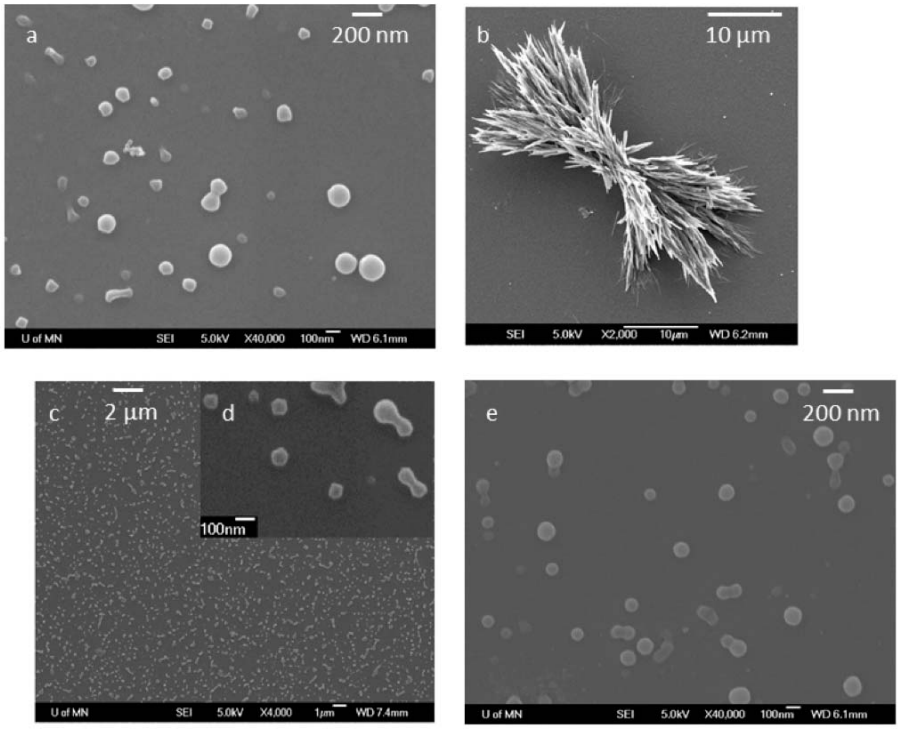

For convenience, future nanoprecipitation experiments were conducted on the CIJ-D mixer unless otherwise indicated. A cartoon depicting a representative FNP experiment is given (with typical amounts) in Figure 5-4 to yield PEG-*b*-PLGA based nanoparticles loaded with PTX silicate **3.08** (hereafter, **3.08-NPs**). While these results led to highly prodrug-loaded nanoparticles (up to 58 wt%),

the maximum loading level of these PTX silicate prodrugs within FNP-derived PEG-*b*-PLGA nanoparticles has yet to be defined.[229]

Figure 5-4. A typical experiment that utilizes the CIJ-D mixer to impinge water against a THF solution containing 35 mg of the PTX silicate **3.08** in 25 mg of a 5K-10K PEG-*b*-PLGA BCP co-dissolved. The final ratio of THF:H_2O is 95:5.

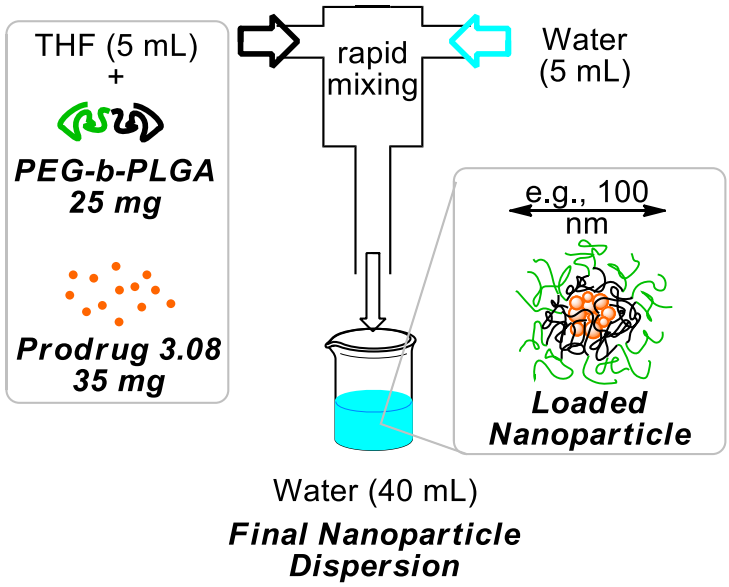

2. Qualitative Observations of PTX Silicate Aggregates and Nanoparticles. With one of the basic concepts (specifically, that the hydrophobicity of the silicate prodrug can be tailored to improve the nanoparticle stability) of the silicate prodrug strategy now practically applied, efforts turned toward understanding the nature of these kinetically trapped particles. Due largely to the absence of visible aggregation after FNP, full encapsulation of the PTX silicate in the nanoparticle was assumed. However, running a simple control experiment cast doubt on such an assumption. An FNP experiment in which only **3.08** (without a protective BCP present) was dissolved in the organic solvent did *not* lead to rapid formation of large aggregates. Instead, a cloudy but seemingly homogeneous suspension

[229] These studies are ongoing in collaboration with Ms. Jing Han and Prof. Christopher Macosko.

was attained (Figure 5-5a). Analyzing this mixture by DLS led to the measurement of larger, (ca. 200-300 nm) but still nano-sized, particles. Fortunately, rapid aggregation (in less than one min) was observed upon addition of 0.9 wt% NaCl (Figure 5-5d) – an observation consistent with "unprotected" drug aggregates in a solution of the same ionic strength as blood. In contrast, varying the ionic strength of the polymer-protected PTX silicate nanoparticles resulted in no visible changes in the nanoparticle size, even at extended times (Figure 5-5c and d).

Figure 5-5. The photographs show a visual analysis of FNP mixing experiments of 3.08 in various conditions: (a) the impinged PTX silicate in H_2O/THF, (b) the impinged PTX silicate in H_2O/THF with 0.9 wt% NaCl added, (c) the impinged PEG-*b*-PLGA BCP and PTX silicate in H_2O/THF, and (d) the impinged PEG-*b*-PLGA BCP and PTX silicate in H_2O/THF with 0.9 wt% NaCl added.

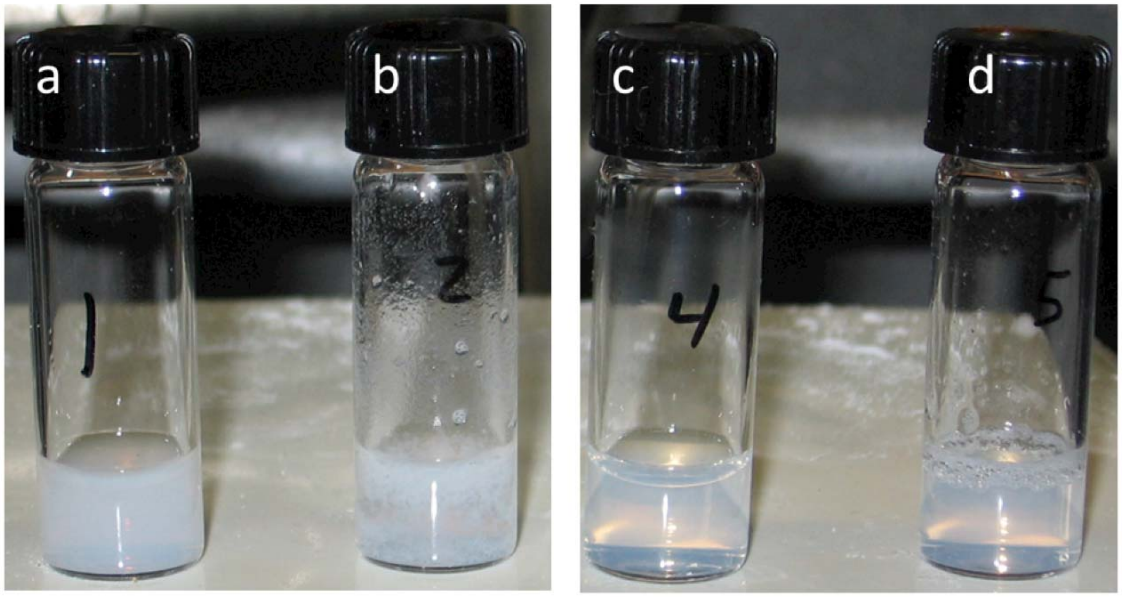

3. NMR Studies of FNP-produced, PTX Silicate Loaded Nanoparticles.

While the qualitative results discussed above provided data consistent with silicate prodrug encapsulation within the PEG-*b*-PLGA nanoparticles, more

quantitative and definitive experiments were desired. In other words, many questions still remained. For instance, a necessary step for future *in vivo* work requires complete removal of the solvents. However, this necessary freeze drying (i.e., lyophilization) step consisted of several experimental unknowns. Most important to these discussions, however, was determining if the PTX silicate survives the FNP and subsequent freeze drying procedure.

This question was addressed by dissolving lyophilized, **3.08**-loaded, PEG-*b*-PLGA nanoparticles in a $CDCl_3$ solution (Figure 5-6). This NMR spectrum provides convincing evidence that the PTX silicate survived intact, as judged by the readily observed, diagnostic resonances associated with the ethoxy groups at ppm = 3.76 and 3.71 (■ in Figure 5-6). Integration of these resonances against the, e.g., aromatic and alkyl PTX-derived resonances demonstrated that minimal, if any, hydrolysis occurred during FNP and subsequent handling. Furthermore, integration of the ethoxy resonances vis-à-vis the polymer resonances (● in Figure 5-6) confirmed that the ratio of the silicate:polymer was within experimental error of the material used. Finally, THF-related resonances were not observed in the spectrum, confirming that the organic solvent is fully removed during the freeze-drying process.

Figure 5-6. The ^{1}H NMR spectrum in $CDCl_3$ of a lyophilized nanoparticle suspension shows resonances from the PTX silicate prodrug **3.08** (silicate ester ethoxy resonances labeled as ■) and PEG-*b*-PLGA BCP (all polymer resonances labeled as ●).

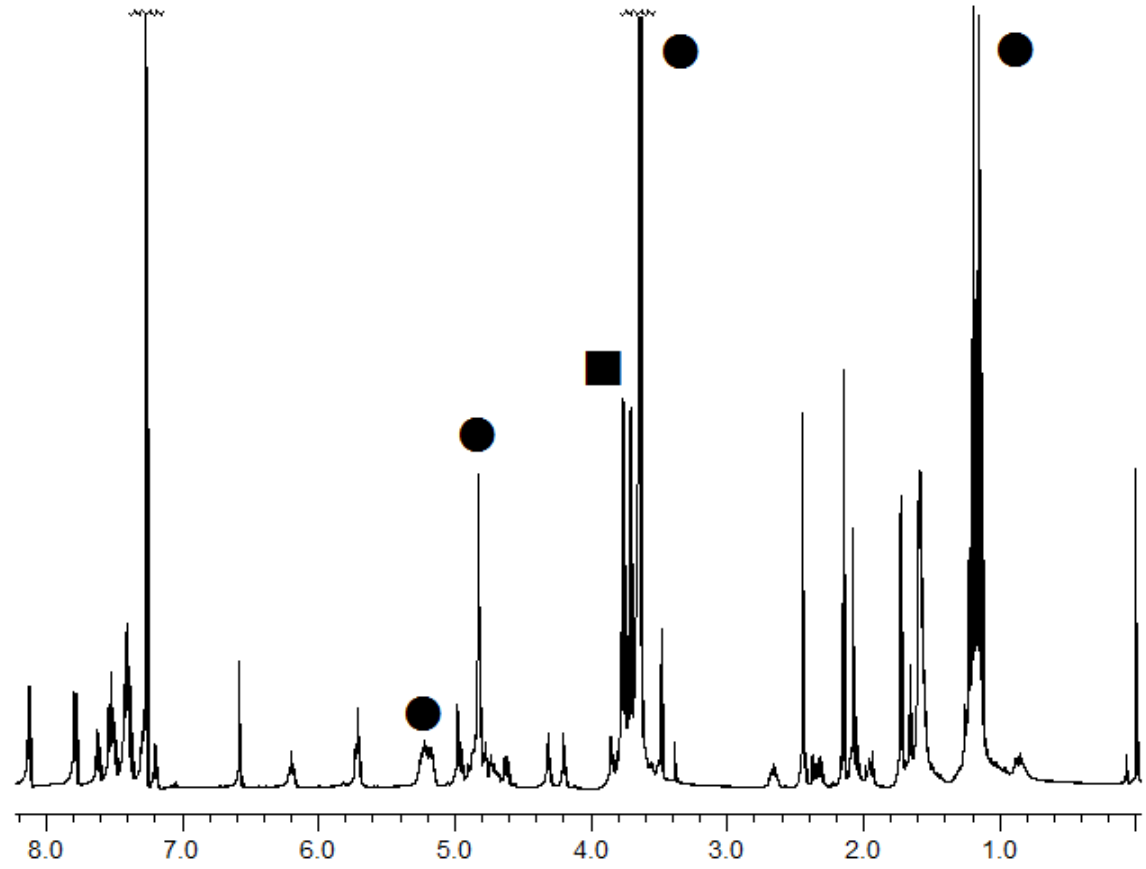

4. Quantification of Encapsulated PTX Silicate by Differential Solubilities. While the ^{1}H NMR results (c.f., Figure 5-6) confirm the overall constitution of the freeze dried powder, they fail to provide any information about the macrostructure of the nanoparticles. Essentially, the NMR spectrum tells us *what* is in the freeze dried powder but not *where* the silicate is located relative to the BCP. This is an especially critical point, given that previous work has suggested

that PTX itself partitions into the PEG component of PEG/PLGA thin films.[230] Therefore, further studies were designed to supplement the conclusions drawn from the qualitative observations in section 5.3.2. Understanding the distribution of the PTX silicate within the nanoparticle has implications for both the stability of the FNP particles and the hydrolysis/release rate of the prodrug/drug more generally.[230,231]

Techniques to quantify encapsulated PTX that are reported in the literature rely almost exclusively on HPLC analysis of the nanoparticle contents and quantification against a standard curve. Unfortunately, "extracting" the PTX from PEG-*b*-PLGA particles in, for example, acetonitrile is ineffective because the BCP is readily soluble in this solvent. Thus, this strategy is capable of quantifying the total amount of PTX (or the PTX silicate prodrug) in the freeze dried powder, but it is insufficient to differentiate the total amount of encapsulated taxane from the total amount present. Furthermore, because the PTX silicate aggregates if the protecting polymer is not included, techniques (e.g., centrifugation) intended to separate the bigger particles from molecularily dissolved species were not anticipated to be effective. Instead, to better understand the amount of *encapsulated* PTX silicate, we employed a simple strategy exploiting the differential solubilities of PEG and the PTX silicate.

Specifically, PEG homopolymers are minimally soluble in diethyl ether, whereas the PTX silicate prodrugs (including **3.08**) are freely soluble. Thus, extracting an aqueous FNP suspension with multiple diethyl ether washes would, in principle, readily solubilize and remove any unprotected (i.e., non-

[230] Kang, E.; Robinson, J.; Park, K.; Cheng, J.-X. Paclitaxel Distribution in Poly(ethylene glycol) / Poly(lactide-*co*-glycolide) Blends and its Release by Coherent Anti-Stokes Raman Scattering Microscopy. *J. Control. Release* **2007**, *122*, 261–268.

[231] Mu, L.; Teo, M. M.; Ning, H. Z.; Tan, C. S.; Feng, S. S. Novel Powder Formulations for Controlled Delivery of Poorly Soluble Anticancer Drug: Application and Investigation of TPGS and PEG in Spray-Dried Particulate System. *J. Control. Release* **2005**, *103*, 565–575.

encapsulated) PTX silicate while the prodrug that is encapsulated within the BCP (with a solubilized PEG block) would reasonably be expected to remain entrapped in the nanoparticle core within the dispersion. Interestingly, investigation of this theory with a **3.08**-**NP** resulted in less than 7% of **3.08** recovered, even after multiple washes (Table 5-2). Conversely, washing FNP-produced aggregates (i.e., non-encapsulated) of **3.08** yielded > 85% recovery of the PTX silicate (see Table 5-2). While again not overwhelming proof of encapsulation, these results provide strong corroboration for the high encapsulation efficiency of the PTX silicate prodrug in PEG-*b*-PLGA based nanoparticles.

Table 5-2. The recovered PTX silicate from either polymer protected nanoparticles or prodrug aggregates derived from two different FNP experiments.

FNP Materials [a]	Encapsulated Amount [b] (mg)	Recovered ^{1}H NMR [c] (mg)	Recovered HPLC [d] (mg)
3.08 + BCP	3.5	n.o. [e]	0.23
3.08 only	3.5	3.01	3.05

[a] The materials dissolved in THF during the FNP process.
[b] The mass of PTX silicate **3.08** that was dissolved in THF and subjected to FNP.
[c] The amount of **3.08** that was quantified by 1H NMR relative to an internal standard of known quantity.
[d] The amount of **3.08** that was quantified by HPLC relative to a calibration curve of **3.08**.
[e] n.o. = not observed. The amount of the PTX prodrug was below the level of detection.

5. Differential Scanning Calorimetry Studies of FNP-produced Nanoparticles. DSC techniques have been extensively employed for the general characterization of polymeric thermal behavior and phase transitions,[193] including in Chapter 4 of this thesis.[162] However, the use of DSC analysis in drug delivery vehicles is not viewed as standard, and it is decidedly less often utilized to answer important questions related to the macrostructure of drug delivery vehicles. Nonetheless, DSC studies on lipids[232] and oil-in-water emulsions[233] have been conducted.

While informative, these studies were on thermodynamically stable, rather than kinetically trapped, nanostructures. We, therefore, set out to determine if DSC could provide complementary data related to the structure and morphology of these nanoparticles. The first structure examined was the simplest – the FNP-precipitated and subsequently freeze-dried 5K-10K PEG-*b*-PLGA BCP. Typically, DSC studies utilize the "second run" (i.e., the behavior of a polymer after a single heating/cooling cycle) of a DSC trace so that the polymer properties that are measured are independent of the polymer's the thermal history. In the special case of a flash nanoprecipitated polymer, however, the "first run" is the most interesting – the handling history of the material and the induced morphological changes are the factors that we aim to probe. Interestingly, the "first run" DSC trace (Figure 5-7, black line) of the FNP-produced polymer exhibited a strong T_m of the crystalline PEG block at ca. 50 °C. This is a depressed melting transition temperature relative to the pure PEG homopolymer (which exhibited a T_m of ca. 60 °C in a control experiment). This observation is consistent with incomplete

[232] Ali, H.; El-Sayed, K.; Sylvester, P. W.; Nazzal, S. Molecular Interaction and Localization of Tocotrienol-Rich Fraction (TRF) within the Matrices of Lipid Nanoparticles: Evidence Studied by Differential Scanning Calorimetry (DSC and Proton Nuclear Magnetic Resonance Spectroscopy (^{1}H NMR). *Colloids Surf., B.* **2010**, *77*, 286–297.

[233] Essa, S.; Rabanel, J. M.; Hildgen, P. Effects of Polyethylene Glycol (PEG) Chain Organization on the Physicochemical Properties of Poly(D, L -lactide) (PLA) Based Nanoparticles. *Eur. J. Pharm. Biopharm.* **2010**, *75*, 96–106.

phase segregation. The T_g from the PLGA block was not as obvious in the trace, but it is conceivable that there is a weak, broad T_g transition at ca. 20 °C. While this value is less than what is predicted from the Fox equation (essentially, a mass weighting of the T_g values derived from the pure PLA and PGA homopolymers), this may be accounted for via a combination of the relatively low MW of the polyester block and the previously observed polyether/polyester mixing in other systems leading to polyester plasticization.[234]

Interestingly, no recrystallization of the PEG was noted upon cooling (cooling trace omitted for clarity in Figure 5-7), and the "second run" DSC trace (Figure 5-7, gray line) exhibited a single T_g. This result was reproduced even when the polymer was cooled at an exceedingly slow rate (1 °C s^{-1}), consistent with a thermodynamically stable, phase mixed system (and in contrast to PEG-PLLA BCPs[235]) observed in the polymer characterization studies reported in Chapter 4. Based upon these results, a reasonable conclusion is that the polymer blocks are largely, but not exclusively, phase segregated following FNP and lyophilization. This working knowledge further confirms the core-shell nature of these nanoparticles and may lead to further understanding of issues related to redispersion and drug release of these nanoparticles.

[234] Kulinski, Z.; Piorkowska, E.; Gadzinowska, K.; Stasiak, M. Plasticization of Poly(L-lactide with Poly(propylene glycol). *Biomacromolecules*, **2006**, *7*, 2128–2135.

[235] Lee, J. H.; Jho, J. Y. A Morphological Study of Semicrystalline Poly(L-lactic acid-*b*-ethylene oxide-*b*-L-lacitic acid) Triblock Copolymer. *Macromolecules* **2005**, *38*, 104–109.

Figure 5-7. The DSC trace of the FNP-precipitated and freeze-dried 5K-10K PEG-*b*-PLGA BCP shows a strong PEG T_m on the "first run" (black trace) indicative of significant phase segregation of the kinetically trapped nanoparticle and a single T_g on the "second run" (gray trace) that suggests a phase mixed state at equilibrium.

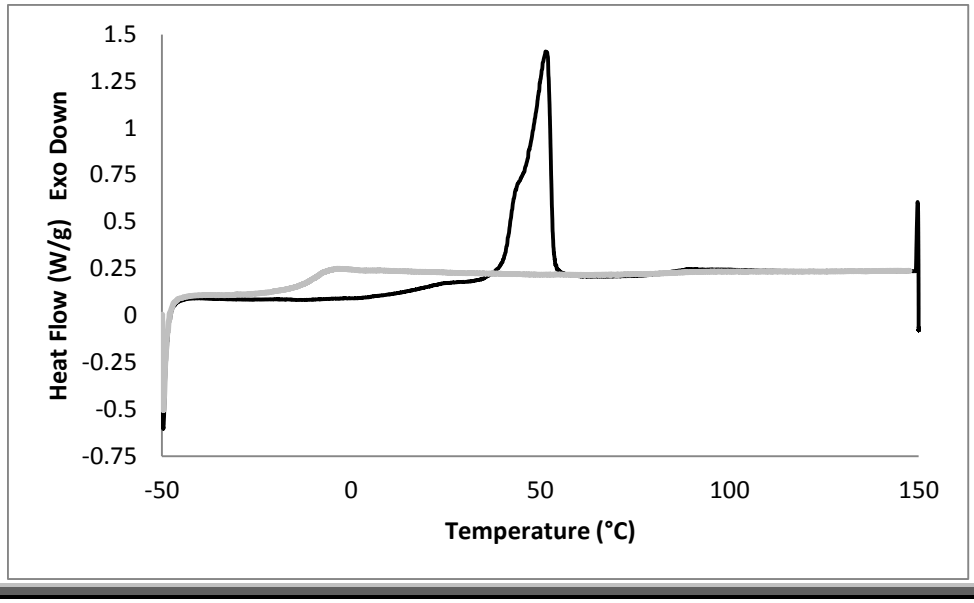

With a basic understanding of the DSC behavior of the precipitated polymer, focus shifted to the analysis of **3.08-NP**. An FNP experiment was conducted using typical mixing parameters (c.f., Figure 5-6) and lyophilized immediately after the nanoprecipitation. Due to the nature of the freeze dried powder [i.e., the high static charge as evidenced (albeit not explained) by the measured zeta potential[5]] only 0.8 mg of the fluffy white powder could be loaded into the experimental pan for analysis by DSC. Again, the "first run" was analyzed as the most informative (black line, Figure 5-8). In this case, there is again a strong, depressed PEG T_m at ca. 50 °C. Due to the small amount of material that was used, it is particularly difficult to postulate on the presence (or absence) of a PLGA T_g in this experiment. However, a more easily identifiable feature of this trace that was clearly unique to the PTX silicate-loaded nanoparticles was the

broad melting point centered at ca. 105 °C. I postulate that this endothermic peak is a result of an impure, crystalline melting transition of PTX silicate **3.08**. (It is interesting to note that, upon heating **3.08-NPs** to 250 °C, decomposition of, presumably, **3.08**, was observed.) After cooling (trace not shown), a single T_g is again noted during the second heating cycle, a feature consistent with a well-mixed, prodrug-loaded thin film (rather than a nanoparticle).

Figure 5-8. The DSC trace of the FNP-precipitated and freeze-dried nanoparticles composed of PTX silicate **3.08** and 5K-10K PEG-*b*-PLGA BCP shows a strong PEG T_m and a broad melting point attributed to a depressed melting of **3.08** on the "first run" (black trace) and a single T_g associated with a phase-mixed film in the "second run" (gray line).

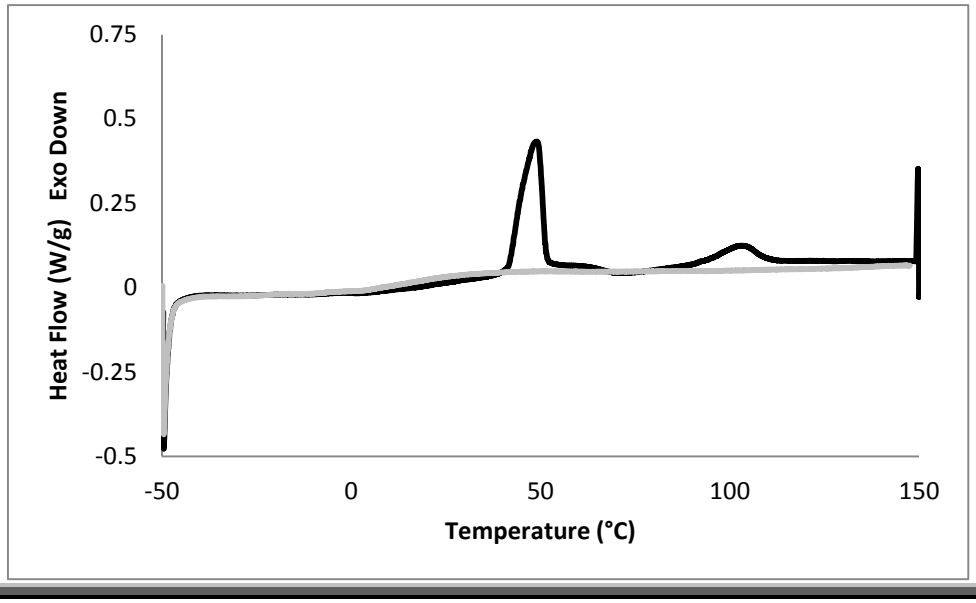

*6. Collaborative Cryo Transmission Electron Microscopy Studies of **3.08-NPs**.*[88,236] We collaborated with Han Seung Kim and Prof. Alon McCormick (Department of Chemical Engineering and Materials Science) to employ cryo-TEM and obtain further definition of the nanoscopic structures of these particles.

[236] The cryo-TEM images were obtained by Mr. Han Seung Lee, a member of Prof. Alon McCormick's research group in Chemical Engineering and Materials Science.

Images like that shown in Figure 5-9a show the size-distribution and predominantly spherical nature of the loaded PEG-*b*-PLGA nanoparticles presumably loaded with PTX silicate **3.08**. A subset of substantially smaller NPs, perhaps indicative of unloaded block-polymer, can also be seen; similar structures have been observed in a pluronics-based PTX NP system.[237] The higher resolution micrographs in Figure 5-9b and Figure 5-9c suggest a core-shell microstructure.[237]

Figure 5-9. Cryo-TEM micrographs of nanoparticles loaded with PTX silicate **3.08** (defocus parameter: -4 to -8 µm). (a) A low magnification image showing spherical NPs and their size distribution. (b) A higher magnification image of a portion of that field in which one can discern core-shell features. (c) An under focused image that emphasizes the core-shell nature of one particle. This particle is a prolate spheroid (long diameter is ca. 10% greater than the short). Only minor beam damage was observed during the under focused microscopy experiment.

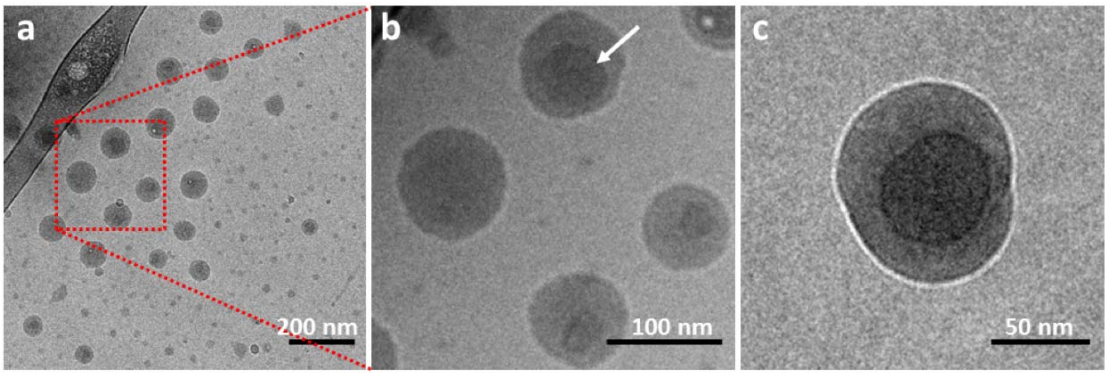

*7. NMR Release Studies of **3.08-NPs**.* Given that the known bioactivity of PTX is critically dependent upon an unmodified C2' hydroxyl,[143] efforts were pursued to analyze the hydrolysis of prodrug **3.08** after FNP-loading into a PEG-*b*-PLGA nanoparticle. Accordingly, a freeze-dried sample of these polymers was

[237] Oh, K. S.; Song, J. Y.; Cho, S. H.; Lee, B. S.; Kim, S. Y.; Kim, K.; Jeon, H.; Kwon, I. C.; Yuk, S. H. Paclitaxel-loaded Pluronic Nanoparticles Formed by a Temperature-Induced Phase Transition for Cancer Therapy. *J. Control. Release* **2010**, *148*, 344–350.

redispersed in buffered D_2O (pD = 6.4) at ambient temperature and an internal standard [methyl *tert*-butyl ether (MTBE)] was added. Since the low solubility of both the PTX silicate and PTX itself in water will render both species unobservable, the production of the water-soluble byproduct ethanol was observed during the experiment and quantified against the internal standard.

In contrast to Ms. Jing Han's collaborative dialysis studies that suggested nearly quantitative hydrolysis and release in several hours,[238] the evolution of ethanol was markedly slower in these NMR experiments. After 162 h (ca. one week), only 25% of the maximum molar equivalents of ethanol (dashed line in Figure 5-10) was observed. Even if this quantity of ethanol was the result of exclusive hydrolysis at the C2' position of **3.08**, this result still accounts for only half of the molar quantity of ethanol that is expected (Figure 5-10). This observation is consistent with a nanostructure in which there is a large amount of the PTX silicate prodrug protected deep within the nanoparticle core. A delayed, prolonged release could prove beneficial during *in vivo* experiments by potentially subjecting a cancerous tumor to a more prolonged chemotherapeutic dose and/or minimizing undesirable side effects.

[238] Han, J. University of Minnesota,Minneapolis, M. Personal communication, **2012**.

Figure 5-10. The graph depicts the evolution of ethanol in the hydrolysis of encapsulated **3.08**. The dashed line represents the expected amount of ethanol upon complete hydrolysis of the PTX *bis*-silicate.

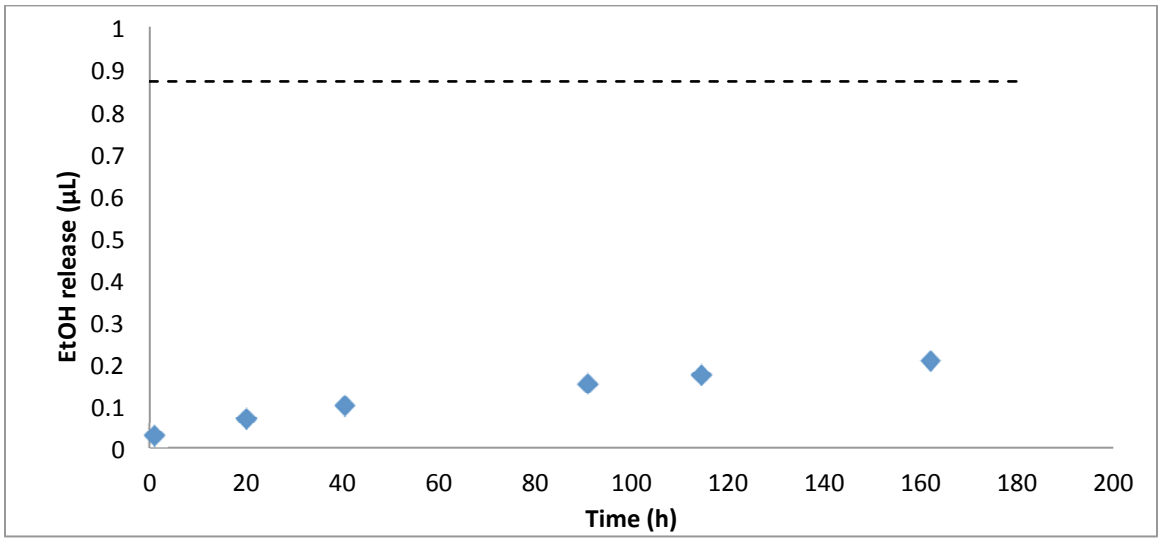

4. Efficacy of the PTX Silicate Ester-Loaded Nanoparticles.[88]

*1. In vivo Efficacy Study of **3.08-NPs**.* The *in vitro* efficacy of the PTX silicate-loaded nanoparticles **3.08-NPs** was next tested by Mr. Stephen Kalscheuer and Dr. Barath Guru in the lab of Prof. Jayanth Panyam (Department of Pharmaceutics). Briefly, his studies demonstrated that the efficacy of **3.08-NPs** are statistically equivalent to clinical PTX formulations (Taxol® and Abraxane®).[144,239] The *in vivo* efficacy of the **3.08-NPs** was evaluated in mice carrying orthotopic MDA-MB-231 tumor xenografts. This cell line was stably transfected with luciferase to enable subsequent quantitative bioluminescence imaging of tumor growth. The prodrug-loaded particles were prepared by FNP and immediately lyophilized to remove THF and water. The resulting white

[239] Guru, B. University of Minnesota, Minneapolis, MN. Personal communication, **2010**.

powder was then resuspended into a phosphate buffered saline (PBS) solution (1 wt%, probe tip sonication) directly prior to injection into tumor-bearing animals.

Three active PTX-based drug formulations were administered (n≥5 for each group): **3.08-NPs**, PTX-CrEL® (formulated as in Taxol®), and Abraxane®. Equimolar quantities of PTX were used in each dosing regimen to enable comparison of the therapeutic response of **3.08-NP** vis-à-vis the current clinical formulations of PTX. Non-drug loaded CrEL® and PEG-*b*-PLGA NP (hereafter, blank NPs) control groups were also included.

Quantitative luminescence was used to determine therapeutic response. Luciferase-catalyzed oxidation of luciferin is an ATP-dependent reaction, and the intensity of the resulting photon emission is taken to be indicative of the number of viable grafted luc+ MDA-MB-231 cells at the primary tumor site.[240] The relative antitumor efficacy of **3.08-NP**, PTX-CrEL®, and Abraxane® was determined by photon flux from the primary tumor site via bioluminescence imaging. Luciferin was administered at 150 mg•kg^{-1} by i.p. injection on an every 8 day schedule. Each time point reflects the number of days following initiation of either PTX-containing or control formulation dosing schedule. The images of the three animals in Figure 5-11a (one from each test PTX treatment group at the end of the experiment) are representative of the data provided by this quantitative luminescence assay. A full panel of images from one mouse from each treatment group at each of 5 time points (22 to 54 days post-treatment) is provided in Figure 5-11b.

[240] Jenkins, D. E.; Oei, Y.; Hornig, Y. S.; Yu, S.-F.; Dusich, J.; Purchio, T.; Contag, P. R. Bioluminescent Imaging (BLI) to Improve and Redefine Traditional Murine Models of Tumor Growth and Metastasis. *Clin. Exp. Metastasis* **2003**, *20*, 733–744.

Figure 5-11. A summary of the quantitative luminescence data (a) Luminescence images from one representative mouse from each of the three PTX-based treatments at the completion of the study and (b) luminescence images from one representative mouse from each time point. Images were autoscaled to insure uniformity. The pseudocolor scale represents photon flux [photons sec^{-1} $(cm^2)^{-1}$ sr^{-1}] from a defined region of interest at the primary tumor site. Red boxes indicate death of the animal.[88]

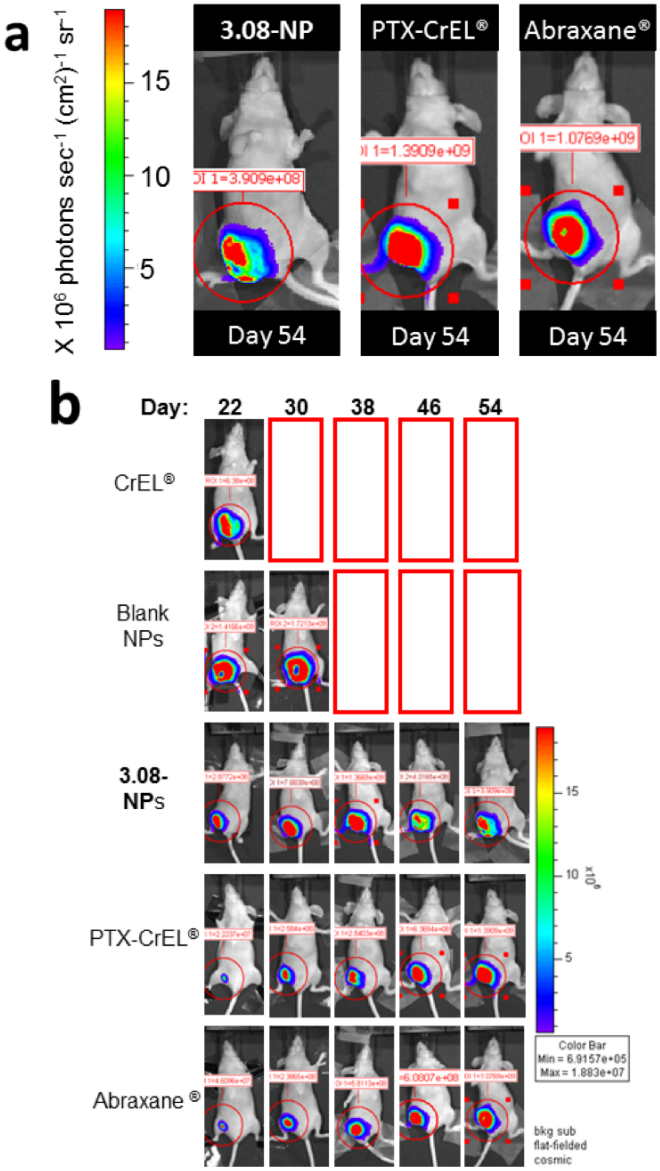

The data in Figure 5-12 summarize the luminescence response from all animals in a given test group at the indicated time points. Highlights are that treatment with each of **3.08-NPs**, PTX-CrEL®, and Abraxane® showed significant inhibition of tumor growth relative to the controls and that all three of **3.08-NPs**, PTX-CrEL®, and Abraxane® were statistically comparable in their protective capacity. Recall that the dosage of PTX or PTX prodrug was identical (50 μmol kg^{-1}) for all treatment groups.

Figure 5-12. The mean luminescence quantitation is correlated with photon intensity from the primary tumor site was determined for ≥4 mice at each time point. CrEL® and blank NP groups are shown up to the time point preceding euthanasia or death of a majority of the group. "x" indicates too few surviving animals for meaningful data interpretation. Data are presented as mean ± S.D.[88]

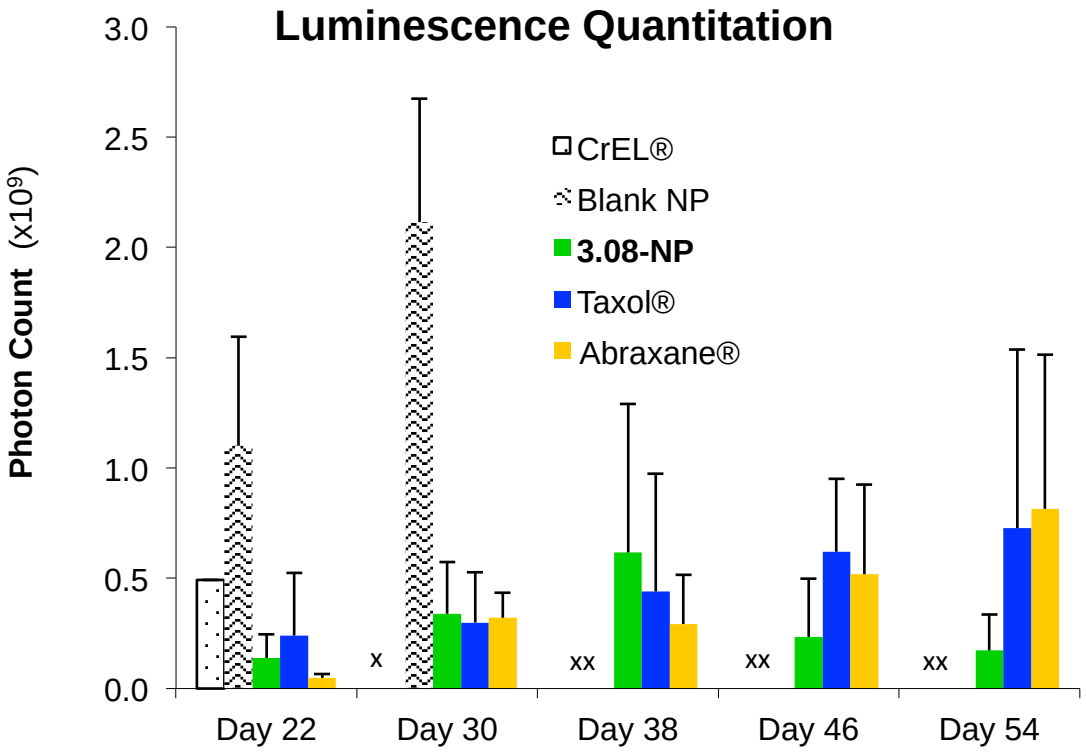

2. Toxicological Analysis of the in vivo Study. Because the wt% of prodrug in **3.08-NPs** (47 ± 5 wt%) was considerably higher than that of PTX in PTX-CrEL® (1.1%) or Abraxane® (10%), much lower amounts of excipient were administered to the animals receiving **3.08-NPs**. Qualitatively, tail tissue near the injection site in the mice treated with CrEL® alone (control) or PTX-CrEL® were found to exhibit necrotic characteristics, suggesting significant toxic side effects from the CrEL® excipient.[104] Upon conclusion of the luminescence study, a liver

and blood toxicology profile [aspartate transaminase (AST) and alanine transaminase (ALT) levels and %neutrophils vs. %lymphocytes] showed less pronounced toxicity in the mice receiving **3.08-NPs** vis-à-vis PTX-CrEL® and Abraxane® Figure 5-13. This is at least consistent with the hypothesis that **3.08-NPs** is the source of lower levels of toxic agent over a longer duration by virtue of slow release of PTX from NPs.

Figure 5-13. Hepatological and hematological data from animals treated with **3.08-NP**, PTX-CrEL®, and Abraxane®. (a) Measured AST levels. (b) Measured ALT levels. (c) Ratio of %Neutrophils to %Lymphocytes (Table 5-3). In all graphs, each diamond represents the value for an individual animal, the solid bar represents the mean value with error bars denoting ± S.D., and the dashed horizontal line represents the "expected" values for this strain of female mice, as provided by the supplier.[241] For a and b n=4 (**3.08-NP**), n=6 (PTX-CrEL®), and n=5 (Abraxane®). For c n=3 for each group due to hemolysis of the blood samples during analysis.

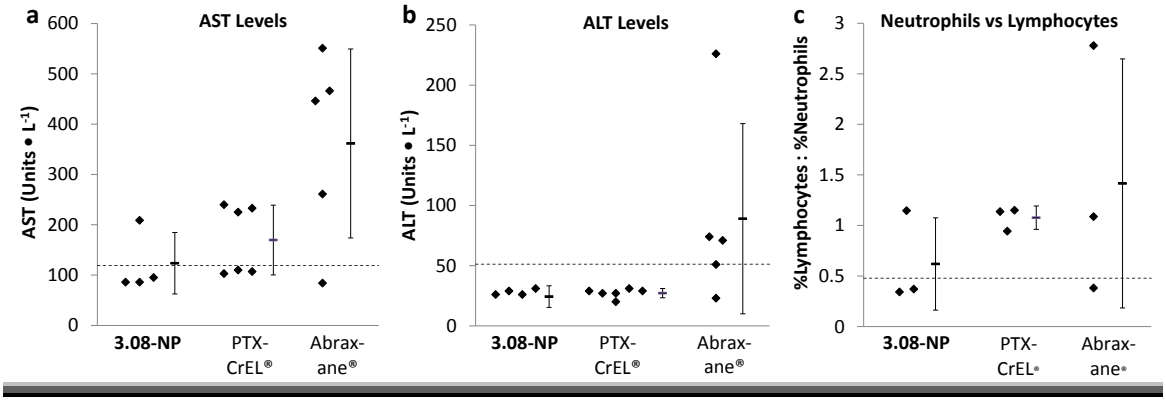

[241] http://www.criver.com/sitecollectiondocuments/rm_rm_r_NUNU_mouse_hematology_2008.pdf and http://www.criver.com/sitecollectiondocuments/rm_rm_r_NUNU_mouse_biochemistry_2008.pdf at http://www.criver.com/en-US/ProdServ/ByType/ResModOver/ResMod/Pages/NuNuNudeMouse.aspx (accessed May 31, 2012).

Table 5-3. Toxicological data for the mice treated with **3.08-NP**, PTX-CrEL®, and Abraxane®.

Treatment	ALT (U/L)	AST (U/L)	Mean Cell Hemoglobin ($g \bullet dL^{-1}$)
Expected [a]	51.3 (± 18.8)	119.4 (± 95.5)	30.4 (± 2.7)
3.08-NP	24.3 (± 9.0)	123.6 (± 61.1)	27.6 (± 0.6)
PTX-CrEL®	27.2 (± 3.8)	170.0 (± 69.2)	27.9 (± 3.3)
Abraxane®	89.0 (± 79.2)	361.6 (± 187.8)	30.5 (± 1.7)

	Lymphocytes (%)	Neutrophils (%)
Expected	62.5 (± 10.3)	29.9 (± 8.4)
3.08-NP	59.7 (± 16.2)	32.0 (± 13.0)
PTX-CrEL®	43.7 (± 5.0)	46.7 (± 2.1)
Abraxane®	46.0 (± 21.1)	49.0 (± 23.5)

[a] Expected values for this strain of mouse, as provided by the vendor.[241]

The bioluminescence imaging data (Figure 5-11a and b) also suggest that tumors in mice treated with **3.08-NPs** were decellularized (i.e., less dense at the tumor core) relative to Abraxane®-and PTX-CrEL®-treated mice. Histologic assessment of tumors at the study endpoint [hematoxylin and eosin (H&E) as well as caspase-3 staining assays] showed a trend towards a larger central non-viable core in the **3.08-NPs** relative to the PTX-CrEL® and Abraxane® treatment groups (Figure 5-13). Again, this is suggestive of a prolonged release profile of PTX from **2a-NPs** at the tumor site. Collectively, these *in vivo* results suggest

that prodrug- and dose-optimization studies should be performed with an eye toward further improving the therapeutic window of PTX silicate prodrug formulations.

Figure 5-14. The representative histology images are from animals treated with (a-c) **3.08-NP;** (a'-c'')PTX-CrEL®; and (a''-c'')Abraxane®. (a,a',a'') Hematoxylin and eosin (H&E) tumor periphery (10X) staining. (b,b',b'') Full tumor H&E staining (1X). (c,c',c'') Cleaved caspase-3 (1x) assays. The larger decellularized core and thinner cellular margin of mitotically active cells among these tumors suggests a greater (apoptotic) cytotoxic effect of **3.08-NP**s compared to PTX-CrEL® or Abraxane®.

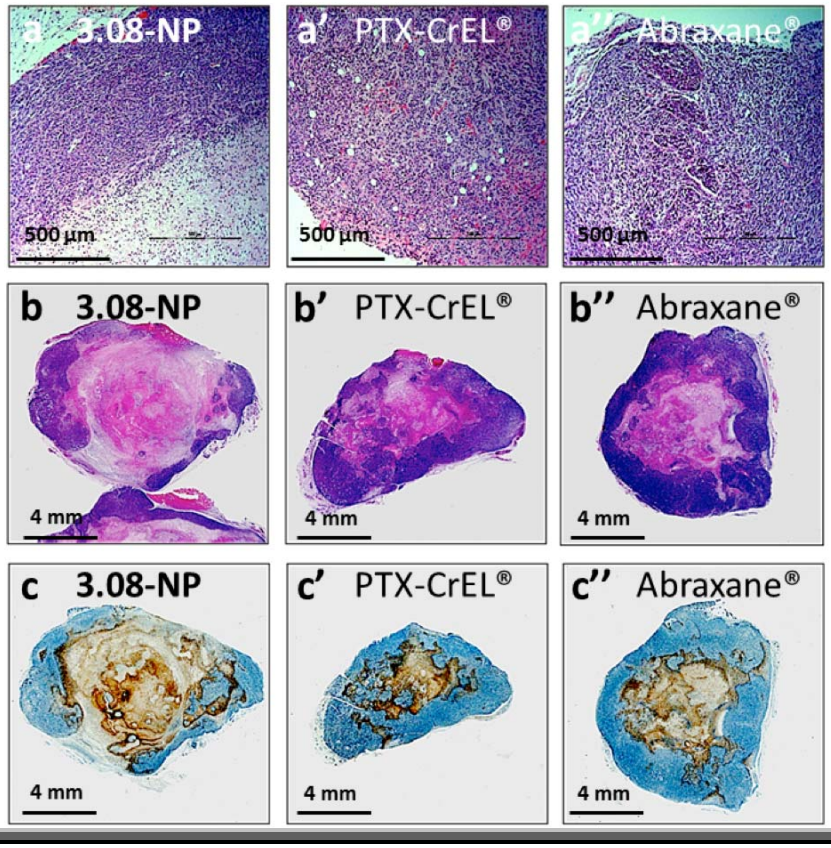

5. Conclusion.

Nanoparticles derived from flash nanoprecipitation are unique from those that are made via more traditional (e.g., emulsion) techniques. A key difference is that FNP-derived particles are kinetically-trapped species, and thus traits commonly associated with thermodynamically stable nano carriers (e.g., micelles or liposomes) did not necessarily apply. A series of experiments were designed and conducted to further define the structure of these FNP-formulated nanoparticles. Analysis by ^{1}H NMR spectroscopy, DOSY NMR spectroscopy, and DSC, studies, in addition to collaborative SEM and cryo-TEM provided valuable information on the organization (or disorganization) of both encapsulated silicates and the PEG-*b*-PLGA BCP. While it is difficult to know with certainty, the evidence obtained from these broadly diverse studies is consistent with a nanoparticle whose solid core is composed largely of the crystalline PTX silicate co-mixed with the PLGA block. The water-soluble PEG forms a corona that effectively prevents aggregation.

The bis-ethoxy PTX silicate prodrug **3.08** was formulated via FNP to provide nanoparticles **3.08-NP**, which contained very high levels (47 ± 5 wt%) of prodrug load. Tumor-bearing mouse models were dosed with three taxane-containing agents, and quantitative luminescence was used to assess comparative *in vivo* antitumor efficacy. The **3.08-NPs** were found to display similar effectiveness as the clinically used formulations PTX-CrEL® and Abraxane®. Importantly, liver and blood toxicology and histology studies showed that the **3.08-NP** treatment group demonstrated minimal toxicity. Notably, the amount of excipient used in the **3.08-NP** formulations is significantly lower than that in the PTX-CrEL® and Abraxane® drugs. Together, these results suggest that prodrug- and dose-optimization studies should be performed with an eye toward further improving the therapeutic window of PTX silicate prodrug formulations.

6. Experimental Section.

A Typical FNP Experiment to Synthesizes 3.08-NPs. Prodrug **3.08**-loaded nanoparticles were produced with a confined-impingement jet (CIJ) mixer.[6] A 5K-10K PEG-*b*-PLGA polymer (25 mg) and prodrug **3.08** (35 mg) were dissolved in THF (2.5 mL) and impinged against 2.5 mL of DI water in the CIJ mixer over the course of 5 s. The resulting nanoparticle suspension was immediately diluted in 45 mL of DI water, resulting in a nanosuspension of 1.2 mg/mL in a mixture of THF and DI water (5:95). This suspension was lyophilized and kept frozen at -80 ˚C until used. In preparation for injection into mice, the NP powder was redispersed in 0.9%NaCl (ca. 10 mg/mL, 1 wt%) while cooling in an ice bath using probe sonication at 20 kHz for five minutes.

DOSY Parameters. DOSY NMR measurements were performed on a 300 MHz Varian NMR spectrometry with the temperature unregulated at ambient temperature. The 1D ^{1}H NMR experiment was run first (number of transients = 16), calibrated at 90°, and the 1D ^{1}H NMR experiment repeated. Parameters were obtained from the 1D experiment (pulse width = 17 ms, spectral width =2007.3 Hz, transmitter offset -628.4 Hz, and gain = 50) and applied to the DOSY experiment. A series of spectra were then obtained (with the diffusion time set to be 0.03 s) such that the final signals decayed to approximately 10% of their original intensity. The spectra were baseline-corrected and processed using the Varian-supplied software.

SEM Sample Preparation. SEM samples were prepared by Zhengxi Zhu as previously described.[242]

Quantification of PTX Silicate from Nanoparticles. 3.08-NPs were prepared as described in section 5.6.1 and 3.08 aggregates were prepared by omitting the polymeric component but otherwise identically to the procedure in section 5.6.1. The THF/H_2O sample was extracted with diethyl ether (x3), the organic washes were combined, the solution dried over $MgSO_4$, and then concentrated under reduced pressure. The 1H NMR quantification was performed in CDCl3 with ethanol as the internal standard. The HPLC quantification was performed on a C-18 column (4.6 mm x 25 cm) with 5 μm packing and eluted with a 75:25 mixture of acetonitrile:water at a rate of one mL•min^{-1}. The amount of **3.08** was quantified by measuring the UV absorbance at 228 nm and comparing to a standard curve.

DSC Analysis of the Nanoparticles. Differential scanning calorimetry (DSC) was performed using a Discovery DSC that was calibrated using high purity indium. The samples were analyzed over a temperature range of -50 °C – 150 °C due to decomposition of the PTX silicate prodrug at higher temperatures. Runs were conducted at a heating rate of 10 °C min^{-1} unless otherwise noted. Transitions of the nanoparticles were recorded during the first scan and compared to the transitions recorded during the second scan.

[242] Zhu, Z.; Margulis-Goshen, K.; Magdassi, S.; Talmon, Y.; Macosko, C. W. Polyelectrolyte Stabilized Drug Nanoparticles via Flash Nanoprecipitation: A Model Study With β-Carotene. *J. Pharm. Sci.* **2010**, *99*, 4295–4306.

Cryo-TEM Sample Preparation. A lacey carbon Cu grid (200-mesh) was glow-discharged in a vacuum evaporator at 70 mTorr (DV-502A) for 30 s. A 7.0 µL portion of a fresh sample (i.e., one hour after FNP) of **3.08-NP** was pipetted onto the carbon coated side of the grid at 22 °C in a Mark III Vitrobot chamber with a relative humidity of 100%. The sample was blotted with filter paper for five seconds and relaxed for three seconds before being submerged in liquid ethane. The vitrified sample was transferred to a Gatan 626 cryo-transfer unit (Gatan,) at -193 °C and characterized at -179 °C in a low-dose mode. A 120 kV FEI Tecnai Spirit BioTWIN was used and images were taken with Eagle™ 2k CCD camera . The images were processed with TEM Imaging and Analysis and Image J software.

MDA-MB-231 Luciferase-positive Orthotopic Xenograft. Balb/c nu/nu immunocompromised female mice were purchased from Charles River Labs (strain code 088, Charles River Labs, Wilmington MA, USA). For xenograft studies, $7.5*10^5$ MDA-MB-231 Luc+ cells were resuspended in 100 µL of Dulbecco's phosphate buffered saline (DPBS) and mixed with an equal volume of matrigel. Subcutaneous injection to mammary pad 9 located near the left flank was performed with a 26-gauge needle attached to 0.5 cc syringe. Subcutaneous tumors reached >100 mm^3 within three-four weeks.

PTX-CrEL®, Abraxane®, and 3.08-NP injections. Once tumors had grown to 100 mm^3, animals were randomly assigned to treatment groups. A dosing schedule of three sequential doses of either PTX-CrEL®, Abraxane®, or **3.08-NP**, each containing 40 $mg•kg^{-1}$ of PTX equivalent, was given on days 0, 4,

and 8. For PTX-CrEL® a 7.5 mg•mL^{-1} stock solution of PTX in CrEL®-ethanol (1:1 v/v) was prepared and diluted to the appropriate working concentration in 0.9% NaCl. Abraxane® was diluted to the appropriate concentration in 0.9% NaCl. Calculation of the PTX-equivalent dosing for the prodrug-loaded PEG-*b*-PLGA NPs (**3.08-NP**) took into consideration both the prodrug loading level (i.e., 47 wt%) and the molecular weight of the prodrug. In all cases the final volume of agent administered (by tail vein injection using a 26 gauge needle) was 200 µL. Two control groups were also included. Mice in the first received a working dilution in 0.9%NaCl with an identical CrEL® concentration to that in the PTX-CrEL® treatment. Mice in the second received blank (i.e., empty) PEG-*b*-PLGA nanoparticles, administered at an identical level to the amount of PEG-*b*-PLGA polymer administered as **3.08-NP**. Animal body weights were monitored. Mice displaying ≥20% reduction in body weight, greater than 2000 mm^3 tumor volume, or ulcerations of the tumor were euthanized.

***In Vivo* Bioluminescence Measurements.** Quantitation of luminescence was determined following i.p. administration, beginning at day 22 following initial dosing, of D-luciferin on an every 8-day schedule. Mice were anesthetized with 2% inhalational isoflurane prior to whole animal luminescence imaging. Luminescence was monitored longitudinally for all mice. Luminescence quantitation was performed using the Xenogen IVIS® whole animal imaging system located in the Biomedical Image Processing Lab at the University of Minnesota. D-Luciferin stock solutions of 15 mg•mL^{-1} were prepared in PBS and stored at -70 °C until used. D-Luciferin was administered at 150 mg•kg^{-1} by i.p.

injection. A 15-minute delay between injection and imaging was used.[243] Photographic overlay images were obtained simultaneous to luminescence detection (30 s exposure). The region of interest was defined to contain all photon emission. Photon flux was calculated using Living Image Pro 4.2 software).

Histopathological, Hematological, and Hepatological Analyses. At the endpoint of the study, blood was collected by cardiac puncture from mice that had received an active PTX agent, and complete blood count analysis and hepatic profiling was performed by Marshfield Labs. Tumors were then excised and fixed in 10% buffered formalin phosphate for 48 hours. Tumors were washed and subsequently stored in 70% ethanol. Histology and immunohistochemistry in formalin-fixed tumors was performed with assistance from the Comparative Pathology shared resource, University of Minnesota Masonic Cancer Research Center.

[243] Paroo, Z.; Bollinger, R. A.; Braasch, D. A.; Richer, E.; Corey, D. R.; Antich, P. P.; Mason, R. P. Validating Bioluminescence Imaging as a High-Throughput, Quantitative Modality for Assessing Tumor Burden. *Mol. Imaging* **2004**, *3*, 117–124.

Chapter 6

Selective End-Functionalization of PEG-*b*-PLGA Block Copolymers.

1. Introduction.

"High value" (e.g., customized, functionalized, and well-defined) polymers represent tremendous potential in a wide variety of fields in both academic as well as industrial environments. This belief was aptly summarized Hawker and Wooley in a recent review, as they stated *"Applications for advanced functional soft materials that possess precisely engineered properties and functional groups have been expanding significantly with the development of nanotechnology and the growing need to address resource, health, and energy issues."*[244] As is the theme throughout this thesis, the aim of Chapter 6 is to develop a general strategy that can solve immediate, practical problems and be amenable to a wide variety of future uses. Specifically, the covalent conjugation of a targeting agent on the water-soluble polyether block could serve to selectively localize

[244] Iha, R. K.; Wooley, K. L.; Nyström, A. M.; Burke, D. J.; Kade, M. J.; Hawker, C. J. Applications of Orthogonal "Click" Chemistries in the Synthesis of Functional Soft Materials. *Chem. Rev.* **2009**, *109*, 5620–5686.

nanoparticles *in vivo.* In doing so, material of potentially tremendous value to both the fundamental scientific inquiries involving the nanoparticles as well as the overall efficacy of the drug delivery project would be created. Furthermore, these efforts will be directed toward the development of a general route toward selectively end-functionalized block polymers that could be expanded to include numerous other functional ligands and fluorescent imaging agents.

2. A General Strategy toward a Common Polymeric Precursor.

1. Generalized Route Design. The use of PEG-*b*-PLGA BCPs (i.e., those described in Chapter 4) to synthesize **3.08-NPs** via FNP experiments generally produced particles that were ca. 100 nm in diameter.[5] This size is generally advantageous for passive particle localization via the Enhanced Permeation and Retention (EPR) effect.[245,246,247] This localization is an artifact of the "leaky" vasculature that results from the rapid angiogenesis of cancer tumors. Since these loose junctions occur primarily in a cancer tumor, a variable degree of passive but somewhat selective localization of nano-sized particles at a cancerous tumor is a generally accepted phenomenon. However, the range of particle sizes reported to be conducive to the EPR effect varies widely in the literature.[248] Additionally, the EPR effect alone is unlikely to optimize localization

[245] Acharya, S.; Sahoo, S. K. PLGA Nanoparticles Containing Various Agents and Tumour Delivery by EPR Effect. *Adv. Drug Deliver. Rev.* **2011**, *63*, 170–183.

[246] Brannon-Peppas, L.; Blanchette, J. O. Nanoparticle and Target Systems for Cancer Therapy. *Adv.Drug Delivery Rev*. **2004**, *56*, 1649–1659.

[247] Maeda, H.; Sawa, T.; Konno, T. Mechanism of Tumor-Targeted Delivery of Macromolecular Drugs,Including the EPR Effect in Solid Tumor and Clinical Overview of the Prototype Polymeric DrumSMANCS. *J. Control. Release* **2001**, *74*, 47–61.

[248] Peer, D.; Karp, J. M.; Hong, S.; Farokhzad, O. C.; Margalit, R.; Langer, R. Nanocarriers as an Emerging Platform for Cancer Therapy. *Nature Nanotech.* **2007**, *2*, 751–760.

of particles,especially so for tumors of small volume (i.e., < 100 mm^3).[249] Potential improvements in both efficacy and safety of prodrug-loaded nanoparticles could be realized by including an active (e.g., ligand-based) targeting strategy,.

As described in Chapter 5, PTX silicate-loaded PEG-*b*-PLGA BCPs demonstrated a statistically equivalent chemotherapeutic effect as compared to the clinical formulations of PTX, Taxol® and Abraxane®.[88] While the efficacy of this **3.08-NP** treatment may have been aided by the EPR effect, the pursuit of BCPs that display a targeting ligand (and thus function as more than a simple, biocompatible excipient) was viewed as especially promising for further improved efficacy. Therefore, BCPs functionalized with a biologically relevant small molecule or ligand to improve taxane delivery in future drug-loaded nanoparticle applications were desired. The advances made in highly efficient polymer functionalization (of both end groups and repeat units)[244] and advances in the generation of a wide variety of nanomedicines that are conjugated to effective targeting ligands is particularly are examples of earlier work proving this field to be a growing area of fertile research.[250,251]

To achieve a targeted BCP, multiple options toward the synthesis of end-differentiated BCPs have been previously reported. For example, end group differentiation of the commercially available and inexpensive dihydroxyl PEG homopolymers has been explored, but this strategy is greatly hindered by the generation of statistical mixtures of products and/or challenging separations and

[249] Adiseshaiah, P. P,. Hall, J. B., McNeil, S. E. Nanomaterial Standards for Efficacy and Toxicity Assessment. *Wiley Interdiscip. Rev. Nanomed. Nanobiotechnol.* **2010**, *2*, 99–112.

[250] Petros, R. A. & DeSimone, J. M. Strategies in the Design of Nanoparticles for Therapeutic Applications. *Nat. Rev. Drug Discov.* **2010**, *9*, 615–627.

[251] Betancourt, T.; Doiron, A.; Brannon-Peppas, L. Polymeric Nanoparticles for Tumor-Targeted Drug Delivery. In *Nanotechnology for Cancer Therapy.* Amiji, M. M., ed. CRC Press: Boca Raton, FL, 2007, pp 2115–229.

purifications.[252] Conversely, numerous reports that detail the use of specific, functional initiators for the synthesis of PEO homopolymers have also been published.[253] For instance, initiation of an ethylene oxide polymerization by allyl-containing (for metathesis reactions)[254,255] and cyano-containing (for reduction to a primary amine)[256] have been synthesized. This strategy effectively produces PEO homopolymers with defined, differentiated end groups, but it suffers from a rather limited scope. Often, a new initiator and, correspondingly, a new PEO polymer is necessary for each unique conjugation reaction scheme.

As has been thematic throughout this thesis, an approach that is practical and widely applicable to a variety of functionalization reactions and substrates was desired. A "PEG-protecting group" approach fit these criteria and was adapted to meet the challenging synthesis of these BCPs. To access these materials, a general strategy was designed that included the following features: i) independent functionalization of either the polyether or polyester terminus, ii) chemical reactions that are compatible with the hydrolytically-susceptible polyester block, iii) highly efficient end-functionalization reactions to maximize the incorporation of precious targeting ligands, and iv) strategic route design to allow access to multiple, functionalized block copolymers from a common, late-stage intermediate.

---

[252] Jäschke, A.; Fürste, J. P.; Cech, D.; Erdmann, V. A. Automated Incorporation of Polyethylene Glycol into Synthetic Oligonucleotides. *Tet. Lett.* **1993**, *34*, 301–304.

[253] Thompson, M. S.; Vadala, T. P.; Vadala, M. L.; Lin, Y.; Riffle, J. S. Synthesis and Applications of Heterobifunctional Poly(ethylene oxide) Oligomers. *Polymer* **2008**, *49*, 345–373 and references therein.

[254] Yagci, Y.; Ito, K. Macromolecular Architecture Based on Anionically Prepared Poly(ethylene oxide) Macromonomers. *Macromol. Symp.* **2005**, *226*, 87–96.

[255] Hiki, S.; Kataoka, K. A Facile Synthesis of Azido-Terminated Heterobifunctional Poly(ethylene glycol)s for "Click" Conjugation. *Bioconjugate. Chem.* **2007**, *18*, 2191–2196.

[256] Nagasaki, Y.; Iijima, M.; Kato, M.; Kataoka, K. Primary Amino-Terminal Heterobifunctional Poly(ethylene oxide). Facile Synthesis of Poly(ethylene oxide) with a Primary Amino Group on One End and a Hydroxyl Group at the Other End. *Bioconjugate Chem.* **1995**, *6*, 702–704.

Given the extensive research already devoted to hydroxyl protecting group chemistry, multiple protecting groups have been considered to mask a PEO hydroxyl group. For instance, initiating an ethylene oxide polymerization with a potassium salt of an ethylene glycol *tert*-butyldimethyl (TBS) ether has been reported to successfully provide TBS-protected PEG homopolymers of narrow polydispersity and controlled molecular weights.[257] However, subsequent work has identified difficulties arising from the *in situ* deprotection of the TBS group during the quench with an acidic resin. This, of course, leads to undesireable contamination by a significant amount of the PEO diol. [258] Additional reports of mono-tetrahydropyran (THP)-protected ethylene glycol initiators have also been utilized to synthesize monoTHP-protected PEOs.[259] However, removal of the THP group is conducted with acidic methanol – conditions that are less optimal in a BCP with an incorporated PLGA block.

In view of the above, a general route to a common polymeric intermediate (Scheme 6-1) was envisioned. This scheme began with initiation of the anionic polymerization of ethylene oxide **6.02** with mono-protected diol **6.01**, in turn yielding mono-protected PEG homopolymer **6.03**. Using **6.03** as a macroinitiator, the co-polymerization of lactide **4.01** and glycolide **4.02** via the previously established continuous addition methodology[162] could be employed to yield the hydroxyl-terminated polyester block of **6.04**. At this stage, the polyester could be functionalized selectively, by, for example, an esterification reaction. Alternatively, the polyester could be simply rendered inactive by acetylation, with

[257] Ito, K.; Hashimura, K.; Itsuno, S. Poly(ethylene oxide) Macromolecules. 8. Preparation and Polymerization of ω-Hydroxypoly(ethylene oxide) Macromonomers. *Macromolecules* **1991**, *24*, 3977–3981.

[258] Reed, N. N,; Janda, K. D. A One-Step Synthesis of Monoprotected Polyethylene Glycol Ethers. *J. Org. Chem.* **2000**, *65*, 5843–5845.

[259] Hiki, S.; Kataoka, K. Versatile and Selective Synthesis of “Click Chemistry” Compatible Heterobifunctional Poly(ethylene glycol)s Possessing Azide and Alkyne Functionalities. *Bioconjugate Chem.* **2010**, *21*, 248–254.

either route giving a BCP of the general form **6.05**. From this intermediate, the deprotection at the PEG terminus would yield BCP **6.06** that displays a primary hydroxyl. This readily-diversified functional group could be manipulated by a variety of amenable to chemical reactions, including, among others, substitutions, esterifications, and oxidations.

Scheme 6-1. Schematic of the general strategy for selective end-functionalization of the PEG-*b*-PLGA block copolymers.

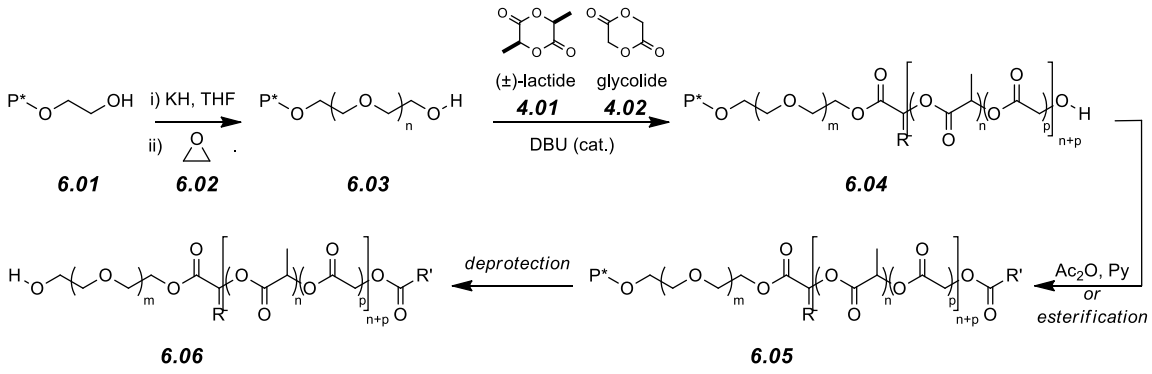

2. A Brief Description of Nomenclature. Within Chapter 6, it is critical that the end groups of all polymers be unambiguously defined. As in Chapter 4, PEG is used interchangeably with PEO for consistency with previous chapters and due to the prevalence of the PEG nomenclature in the biological sciences. The description of the BCP's in text will use the general format of XXX-PEG-YYY, XXX-PEG-*b*-PLA-YYY, and XXX-PEG-*b*-PLGA-YYY. "XXX" will denote the terminus of the PEG block (always appearing on the left-hand side) while "YYY" will describe the terminus of the PLGA block (always appearing on the right-hand side). In the case of the symmetrical PEG homopolymers, the XXX and YYY end groups are used without regard for the left- or right-hand designation. As the absolute MW of the BCPs is not critical in this chapter, the block sizes are not specified in text, but, for completeness, are included parenthetically after the compound number in all schemes, with the PEG block size written first and

followed by the total MW of the polyester written second. For consistency, the described general format will read from left to write as the PEG then PLGA blocks, and this system will be used throughout the text.

3. Synthesis of a Common, Derivitizable Intermediate: HO-PEG-*b*-PLGA-OAc.

1. Synthesis of BnO-PEG-OH. In line with one of the project goals (i.e., developing a methodology that is readily adaptable to a variety of compatible chemistries), a common, readily diversified intermediate analogous to **6.06** was sought. Efforts toward a polymeric intermediate were initiated by synthesizing the mono-benzyl-protected PEG **6.08** following the precedent of Janda and co-workers (Scheme 6-2).[258] 2-(benzyloxy)ethanol **6.07** was utilized as to initiate the ethylene oxide polymerization. During this methodology, extreme care was taken in the drying of the reagents, monomer, and solvent to minimize the production of the PEG diol. Gratifyingly, SEC analysis of the precipitated product showed a narrow (PDI = 1.06), symmetrical, and monomodal peak during elution of **6.08**, indicating nearly exclusive initiation by **6.07**. Further analysis via ^{1}H NMR spectroscopy resulted in confirmation of the product purity and determination of a M_n of 3,300 g mol^{-1}.

Scheme 6-2. Synthesis of a poly(ethylene glycol) mono benzyl ether.

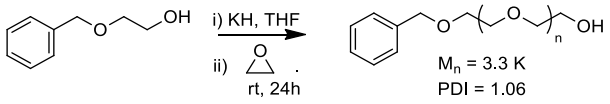

6.07 ***6.02*** ***6.08***

2. Synthesis and Derivatization of the Polyester Block. With **6.08** (and other BnO-PEG-OH's[260] of differing MW) in hand, polymerizations of both a pure PLA block (**6.09**) and a "random" PLGA polyester (**6.10**) were completed (Scheme 6-3).[162] Both polymerizations proceeded as expected – the targeted PLA and PLGA MWs were readily achieved using the techniques described in Chapter 4. With these mono-benzylated block polymers **6.09** and **6.10** synthesized, the focus turned toward selectively functionalized of the hydrophobic polyester block via, for example, esterification reactions.

Scheme 6-3. Synthesis of a PEG-*b*-PLA mono benzyl ether and PEG-*b*-PLGA mono benzyl ether.

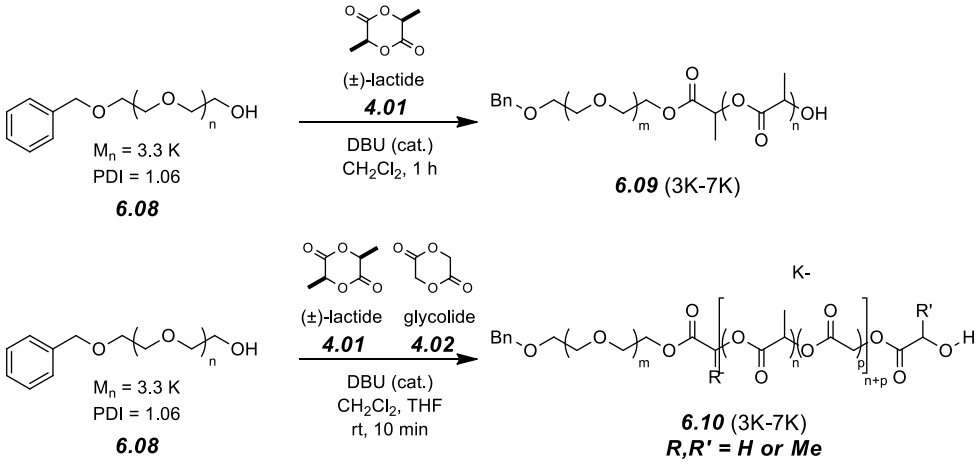

While functionalization of the polyester is ineffective for the incorporation of targeting ligands (the targeting agent would most likely be buried in the nanoparticle core and thus unable to interact with a cellular receptor), conjugation of a fluorescent imaging agent at the polyester end may be advantageous. Specifically, functionalization of PEG-*b*-PLA (as a model proxy for **6.09)** with the carboxylic acid-derivitized pyrene **6.11** has been quantitatively

[260] Additional samples (ca. 2K and 6K) were purchased at a later date from Adavanced Polymer Materials, Inc.

conjugated to the polyester block of a MeO-PEG-*b*-PLA-OH BCP (see Scheme 6-4 for a representative example). The synthesis of **6.12** demonstrated the proof of principle and our ability to derivative the polyester block of these BCPs.

Scheme 6-4. Representative esterifications of BnO-PEG-*b*-PLA-OH to a pyrene fluorophore.

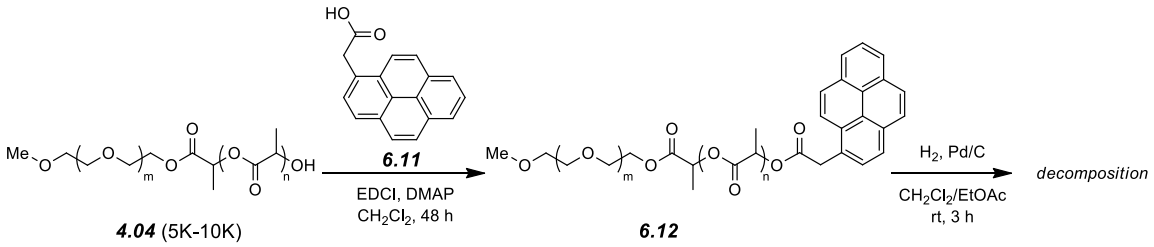

The practicality of pyrene-derivatized polymer **6.12** (and related analogs), is somewhat limited to applications other than those involving animal models. The maximum emission wavelength of pyrene is < 400 nm, significantly shorter than the ca. 600-800 nm wavelengths that are desired for quantitative *in vivo* work. Nonetheless, converting polymers such as **6.12** into bis-functionalized BCPs consisting of both a targeting and imaging agent could prove more innovative and useful in fundamental studies of nanoparticle formation and/or micellization.[261]

Utilization toward a bis-functionalized BCP was explored by subjecting **6.12** to debenzylation conditions to examine its stability under the deprotection conditions. These experiments led to extensive decomposition of the pyrene moiety. While benzylated analogs of **6.12** would likely prove ineffective for the synthesis of bis-derivatitized BCPs, the incorporation of a longer wavelength fluorophores (e.g., rhodamine dyes[262]) remains a possibility. These studies would

[261] Zhao, C.-L.; Winnik, M. A.; Riess, G.; Croucher, M. D. Fluorescence Probe Techniques Used to Study Micelle Formation in Water-Soluble Block Copolymers. *Langmuir*, **1990**, *6*, 514–516.

[262] Savic, R.; Luo, L.; Eisenberg, A.; Maysinger, D. Micellar Nanocontainers Distribute to Defined Cytoplasmic Organelles. *Science* **2009**, *300*, 615–618.

further benefit from the ability to accommodate *in vivo* and/or intracellular imaging in future studies. Regardless, these preliminary studies demonstrate unambiguously that terminal polyester hydroxyls are readily and quantitatively derivitizable.

3. Acetylation of the Polyester block. In the pursuit of derivatized BCPs that display a targeting ligand at the water soluble polyether block, there was typically no need to functionalize the polyester terminus. To avoid competing reactions, simple acetylation of the polyester block was completed prior to debenzylation. Initial attempts to employ a one-pot procedure by quenching the polyesterification reaction with an excess of acetyl chloride were encouraging; the PDI measurements of these polymers remained narrow. However, future studies demonstrated that the end groups were not quantitatively acetylated.

This problem became apparent after debenzylation of **6.10**to give **6.06**. Esterification of this polymer with, for example, 5-hexynoic acid gave an inseparable byproduct. ^{1}H NMR analysis confirmed that the byproduct contained a second alkyne, with the structure later being identified as **6.13** (Figure 6-1). This was confirmed through the synthesis of multiple small molecule analogs and comparison of their ^{1}H NMR resonances. The esterification of a second hexyne ester on the PLGA end was finally confirmed by an independent synthesis of **6.14** and further correlation of the key ^{1}H NMR resonances with the previously observed impurity.

Figure 6-1. Structures of the bis-esterified byproduct **6.13** via independent synthesis and 1H NMR analysis of **6.14**.

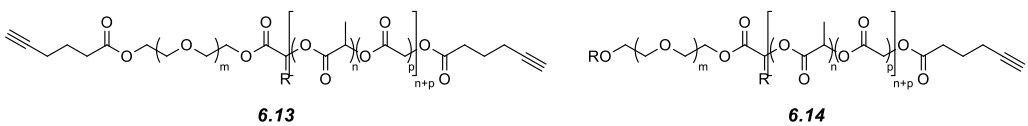

6.13 ***6.14***

A two-step "polymerization-then-acetylation" procedure was instead employed. The polyesterification was halted by addition of benzoic acid as previously described,[162] the polymer purified, and the acetylated to yield the ca. 100% acetylated BnO-PEG-*b*-PLGA-OAc (**6.15**). It is worth noting that spectroscopic analysis via ^{1}H NMR of these polymer end-groups is complicated by the varying ratios of lactic vs. glycolic terminated polymers, thereby leading to different integration nvalues of the resonances of the acetate CH_3's. This ratio changes with each polymer "batch," and the characteristic ratios can be used as a tool to "track" aliquots that originate from the same polymerization.

Polymer **6.15** (and other analogous polymers of varying MWs) was now primed for a selective deprotection of the PEG terminus. Indeed, placing the solution of **6.15** in a H_2 gas atmosphere in the presence of catalytic palladium on carbon cleanly and quantitatively debenzylated the block copolymer to yield **6.16**.[258] With gram-quantities of the versatile intermediate **6.16** in hand, attention was turned to the selective functionalization of the water soluble PEG block.

Scheme 6-5. Sequential acetylation and debenzylation of a BnO-PEG-*b*-PLGA-OH **6.10** to yield a HO-PEG-*b*-PLGA-OAc that may act as a common intermediate for further derivatization of the water-soluble polyether.

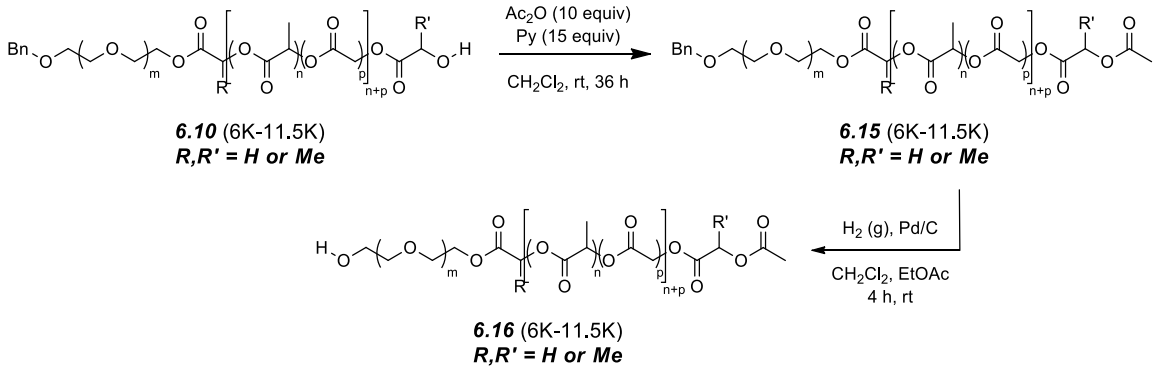

6.10 (6K-11.5K)
R,R' = H or Me

6.15 (6K-11.5K)
R,R' = H or Me

6.16 (6K-11.5K)
R,R' = H or Me

4. Attempts to Conjugate Biotin to HO-PEG-*b*-PLGA-OAc BCPs.

1. Conjugation of Biotin via Esterification. Early efforts to add a discrete targeting molecule to the water-soluble, polyether terminus of PEG-*b*-PLGA BCPs first centered on an extensively studied ligand, biotin (**3.17**). Due to its exceptionally strong binding with avidin and streptavidin linkers [dissociation constant = ca. 10^{-15}],[263] biotin has been widely studied for many different uses. For example, it has been used as an affinity tag for protein identification in which exceedingly specific interactions are necessary.[264] Relevant to nanoparticle-based chemotherapy, biotin tagged therapies been exploited by conjugation of biotin to the surface of nanoparticles, thus inducing active targeting of breast cancer cells[265] because breast cancer cells overexpress biotin receptors.[266]

An (overly) simplistic approach was taken toward the first generation of biotin labeled PEG-*b*-PLGA BCPs. Treating **6.16** with an excess of **6.17** in the presence of EDCI and DMAP efficiently led to the near quantitative functionalization of the biotin-tagged BCP **6.18**. However, despite the ease of synthesis, biological studies were not performed on (pro)drug-loaded nanoparticles consisting of polymer **6.18** due to concerns regarding the stability of the exposed ester bond in eventual *in vivo* work. Nonetheless, this work provided material that was easily characterized for use as a standard during the NMR characterization of future biotin-tagged particles.

---

[263] Laitinen, O. H.; Hytönen, V. P.; Nordlund, H. R.; Kulomaa, M. S. Genetically Engineered Avidins and Streptavidins. *Cell Mol. Life Sci.* **2006**, *63*, 2992–3017.

[264] Tashiro, E.; Imoto, M. Target Identification of Bioactive Compounds. *Bioorg. Med. Chem.* **2012**, *20*, 1910–1921.

[265] Patil, Y.; Sadhukha, T.; Ma, L.; Panyam, J. Nanoparticle-Mediated Simultaneous and Targeted Delivery of Paclitaxel and Tariquidar Overcomes Tumor Drug Resistance. *J. Control. Rel.* **2009**, *136*, 21–29.

[266] Lee, E. S.; Na, K.; Bee, Y. H. Super pH-Sensitive Multifunctional Polymeric Micelle. *Nano Lett.* **2005**, *5*, 325–329.

Scheme 6-6. Biotinylation of HO-PEG-*b*-PLGA-OAc **6.16** via esterification to yield **6.18**.

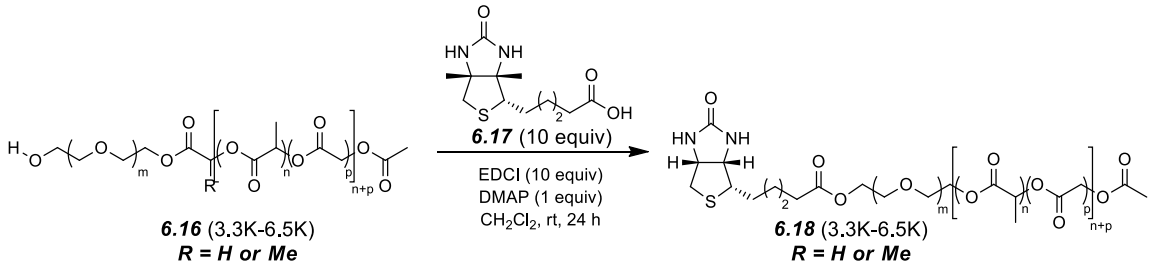

2. Attempts to Conjugate Biotin via an Amide Bond. In light of the potential, detrimental degradation of the biotin/PEG ester linkage during *in vivo* applications, a secondary, less direct route was explored. For example, biotinylated PEG-*b*-PLA BCPs were prepared by conjugation of an *N*-hydroxy-succinimide (NHS)-activated biotin with a heterobifunctional α-hydroxy-ω-amine PEG block to form the amide-linked biotin. This species was then utilized as a macroinitiator for the polymerization of lactide to form the final product.[267]

With this precedent, focus turned briefly from the synthesis of a biotin-tagged BCP from common polymeric precursor **6.16** to the synthesis of a BnO-PEG-NH_2 polymer. To avoid unnecessarily consuming large amounts of the precious (and expensive) benzylated PEG **6.08**, model work was performed utilizing MeO-PEG-OH **4.03** as a model system. Accordingly, **4.03** was treated with mesyl chloride to give **6.19**. The purified product could then be redissolved in a saturated aqueous solution of ammonium hydroxide to produce **6.20** in high yield (Scheme 6-7).

[267] Salem, A. K.; Cannizzaro, S. M.; Davies, M. C.; Tendler, S. J. B.; Roberts, C. J.; Williams, P. M.; Shakesheff, K. M. Synthesis and Characterization of a Degradable Poly(lactic acid)-Poly(ethylene glycol) Copolymer with Biotinylated End Groups. *Biomacromolecules* **2001**, *2*, 575–580.

A similar route was employed to access the activated MsO-PEG-*b*-PLA-OAc **6.21**. While possibly counterintuitive, **6.21** was considered as a candidate for direct displacement of the mesylate by ammonia. I hypothesized that pre-organization of the BCP in its nanoparticulate form may result in the rate of displacement of the mesylate being significantly faster than the diffusion of the water-soluble ammonia into the hydrophobic nanoparticle core. If this proved true, the end-group may be effectively functionalized with minimal degradation of the polyester core. Alas, this hypothesis proved to be incorrect, as treatment of a nanoparticle suspension of **6.21** resulted in rapid consumption of the PLA block (Scheme 6-7).

Scheme 6-7. Synthesis of model polymer NH_2-PEG-OMe **6.20** and attempted direct synthesis of NH_2-PEG-*b*-PLA-OAc by displacement of **6.21**.

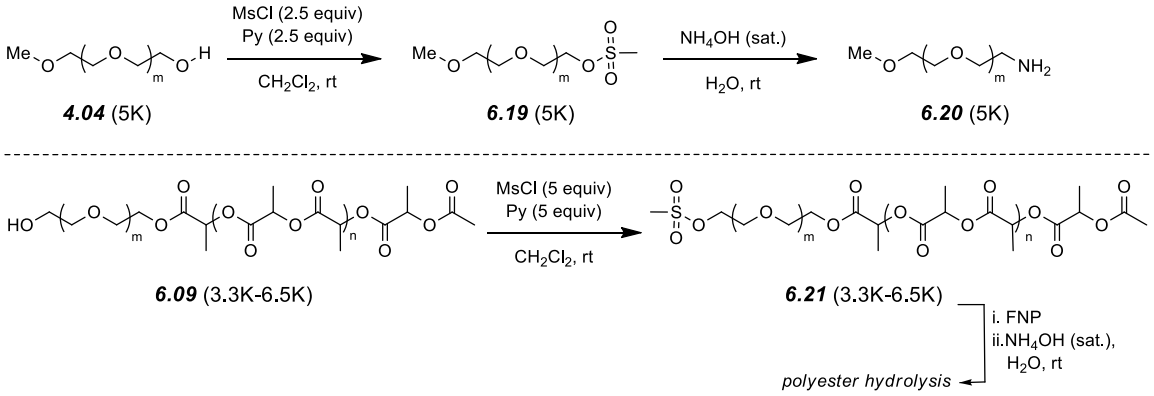

With the failure of the direct displacement of the mesylate-funtionalized, pre-organized PEG-*b*-PLA BCP, other means to biotinylate **6.08** were pursued. Treatment of **6.08** with mesyl chloride afforded the end-differentiated polymer **6.22**, and dissolution of this polymer in a saturated ammonium hydroxide solution cleanly yielded the α-benzoxy-ω-amine PEG (BnO-PEG-NH_2) **6.23**. Encouragingly, formation of the biotin amide also proceeded smoothly in the presence of the carbodiimide EDCI and DMAP, giving **6.24**. However, the final

deprotection step proved problematic. Following literature precedent,[268] **6.24** was exposed to 10 wt% Pd/C (10 %) in a hydrogen atmosphere. Unfortunately, this led to only ca. 25% debenzylation of the polymer in three hours. Conversely, debenzylation of, for example, **6.09** and **6.10** were found to be fully deprotected under these conditions, likely a result of catalyst poisoning by the sulfide. Further disappointment was realized when subjecting **6.24** to the reduction conditions for prolonged time periods resulted in significant degradation of the biotin end group.

Scheme 6-8. Synthesis of model polymer NH_2-PEG-OMe **6.20**, biotinylation, and attempted debenzylation of **6.23**.

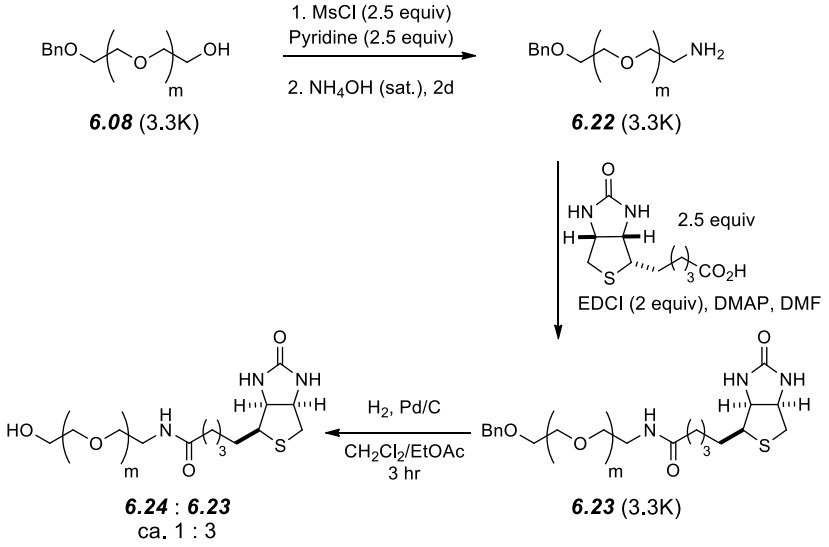

Thus, an N_3-PEG-*b*-PLGA-OAc **6.27** was next envisioned as an ideal monofunctional BCP. The azide functionality could be reduced under palladium-catalyzed hydrogenation[269] or Staudinger reduction conditions,[270,271] revealing a

[268] Despras, G.; Robert, R.; Sendid, B.; Machez, E.; Poulain, D.; Mallet, J.-M. Biotin Sulfone Tagged Oligomannosides as Immunogens for Eliciting Antibodies against Specific Mannan Epitopes. *Bioorg. Med. Chem.* **2012**, *20*, 1817–1831.

[269] Newkome, G. R.; Kotta, K. K.; Mishra, A.; Moorefield, C. N. Synthesis of Water-Soluble Ester-Terminated Dendrons and Dendrimers Containing Internal PEG Linkages. *Macromolecules* **2004**, *37*, 8262–8268.

primary amine under conditions compatible with both the polyether and polyester blocks of the BCP. Furthermore, with the exploding popularity of Huisgen (i.e., "click") cycloadditions in polymer chemistry and materials science,[272] an azide-tagged BCP was viewed as an attractive functional polymer target with extensive potential for functionalization. Again, initial studies employed the readily available monomethoxy PEG homopolymer as a model system. Accordingly, **6.19** was treated with an excess of sodium azide to give **6.25** in high conversion, as anticipated.[273]

Scheme 6-9. Synthesis of model polymer N_3-PEG-OMe **6.25**.

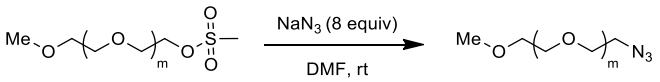

6.19 (5K) ***6.25*** (5K)

Accordingly**,** the treatment of HO-PEG-b-PLGA-OAc **6.21** with mesyl chloride readily produced **6.26** was unexpectedly problematic. Conversion to the mesylate functionalized BCP was irreproducible, and the rate was sluggish as compared to the PEG model system. Attempts to further explore the cause of these observations by measuring conversion with respect to time suggested a sudden (and currently inexplicable) halt to the reaction progress. For instance, temporal monitoring of the treatment of **6.26** with an excess of mesyl chloride and an amine base allowed, e.g., 40% conversion, at which point, additional

[270] Menger, F. M.; Zhang, H. Self-Adhesion among Phospholipid Vesicles. *J. Am. Chem. Soc.* **2006**, *128*, 1414–1415.

[271] Ryu, J.-H.; Jang, C.-J.; Yoo, Y.-S.; Lim, S.-G.; Lee, M. Supramolecular Reactor in an Aqueous Environment: Aromatic Cross Suzuki Coupling Reaction at Room Temperature. *J. Org. Chem.* **2005**, *70*, 8956–8962.

[272] Binder, W. H.; Sachsenhofer, R. "Click" Chemistry in Polymer and Materials Science. *Macromol. Rapid Commun.* **2007**, *28*, 15–54 and references therein.

[273] Opsteen, J. A.; van Hest, J. C. M. Modular Synthesis of Block Copolymers via Cycloaddition of Terminal Azide and Alkyne Functionalized Polymers. *Chem. Commun.* **2005**, 57–59.

substitution was no longer observed. Surprisingly, additional reagents did not lead to further conversion over time.

Unfortunately, a solution to this problematic and currently unexplained low conversion has remained elusive. It was deemed prudent to continue the line of experimentation with a BCP that is, typically, ca. 40-60% mesylated. This decision was made in part because it is not necessary to formulate a nanoparticle with a 100% end-capped BCP. Fortunately, conversion of **6.26** to the azide-tagged PEG-*b*-PLGA proceeded cleanly – the mesylate was quantitatively substituted with the azide nucleophile to yield **6.27**.

Scheme 6-10. Synthesis of N_3-PEG-*b*-PLGA-OAc **6.27**.

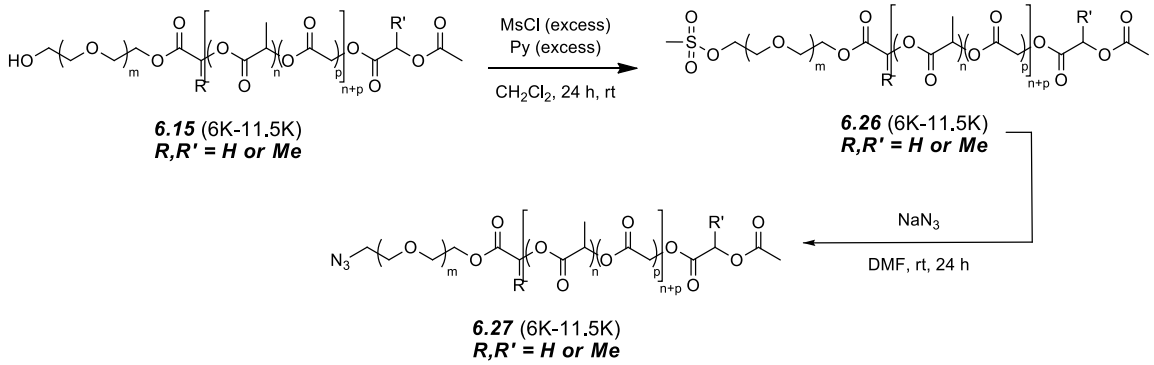

With both the azido PEG model **6.25** and N_3-PEG-*b*-PLGA-OAc BCP **6.27** in hand, efforts were turned toward finding suitable reduction conditions to reveal the desired amino-terminated polymers. Preliminary reduction conditions were explored using model **6.25** in dry DCM and allowing it to stir at room temperature in the presence of Pd/C under a hydrogen atmosphere (Scheme 6-11). These conditions resulted in incomplete conversion after two hours, but conversion reached greater than 90% (as judged by the diminishing intensity of the methylene resonances assigned to those adjacent to the azide as in Figure 6-2) after 24 hours, yielding **6.28.**

The identity of **6.28** necessitated added study because the methylene resonance observed at δ = 2.89 ppm in **6.20** formed via ammonia displacement of the mesylate was conspicuously absent in the spectra obtained from the purified polymer depicted in Scheme 6-11 (Figure 6-2). The identity of the polymer was confirmed by multiple control experiments. Treatment of the reduced and purified MeO-PEG-NH_2 with an excess of acetyl chloride yielded the methyl amide **6.29**. Correlation of the new amide resonance intensity to that of the menthoxy end-group allowed for quantitation of the amine functionality as > 70%. To remove all doubt regarding the constitution of **6.28** (i.e., that the new singlet in the ^{1}H NMR spectrum of **6.29** was not, in fact, simply an impurity), a carbodiimide amidification with octanoic acid experiment was run to obtain a product containing several new resonances in the ^{1}H NMR spectrum of **6.30**. Subjecting **6.31** (a PLA rather than PLGA polyester block) as a proxy for **6.27** to a 24 hour-long hydrogenation led to new, unassigned resonances in the polymer even after purification via standard precipitation techniques.

Scheme 6-11. The synthesis of NH_2-PEG-OMe **6.28** from **6.25** was successful and confirmed by ^1H NMR spectroscopic analysis of the analog amide, but subjecting BCP **6.31** to identical conditions lead to multiple byproducts.

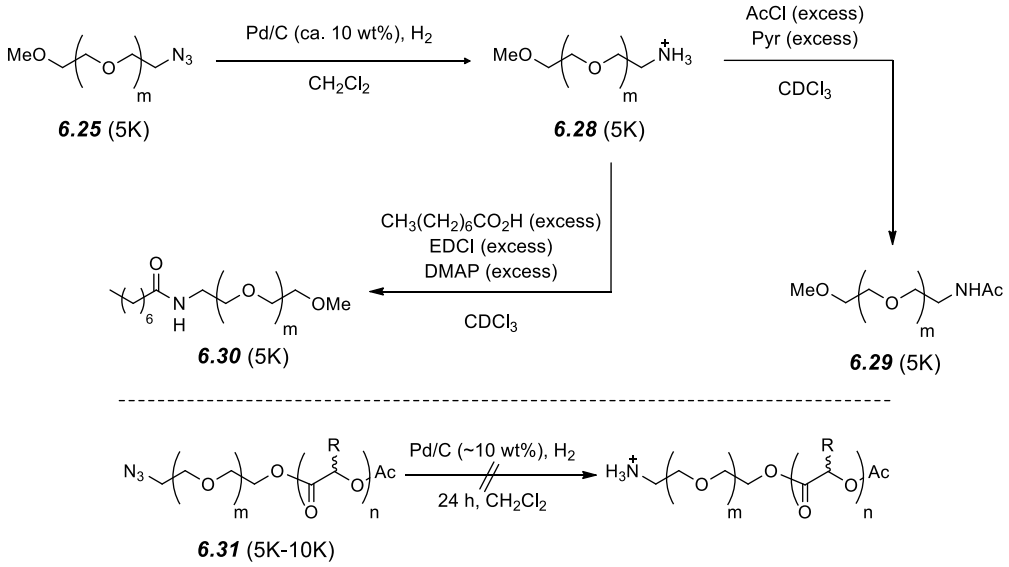

Figure 6-2. The reduction of N3-PEG-OMe **6.25** (top black trace) to NH_2-PEG-OMe **6.28** (bottome blue trace) was successful. The identity of **6.28** was confirmed by derivatization to the methyl amide and subsequent ^{1}H NMR spectroscopic analysis.

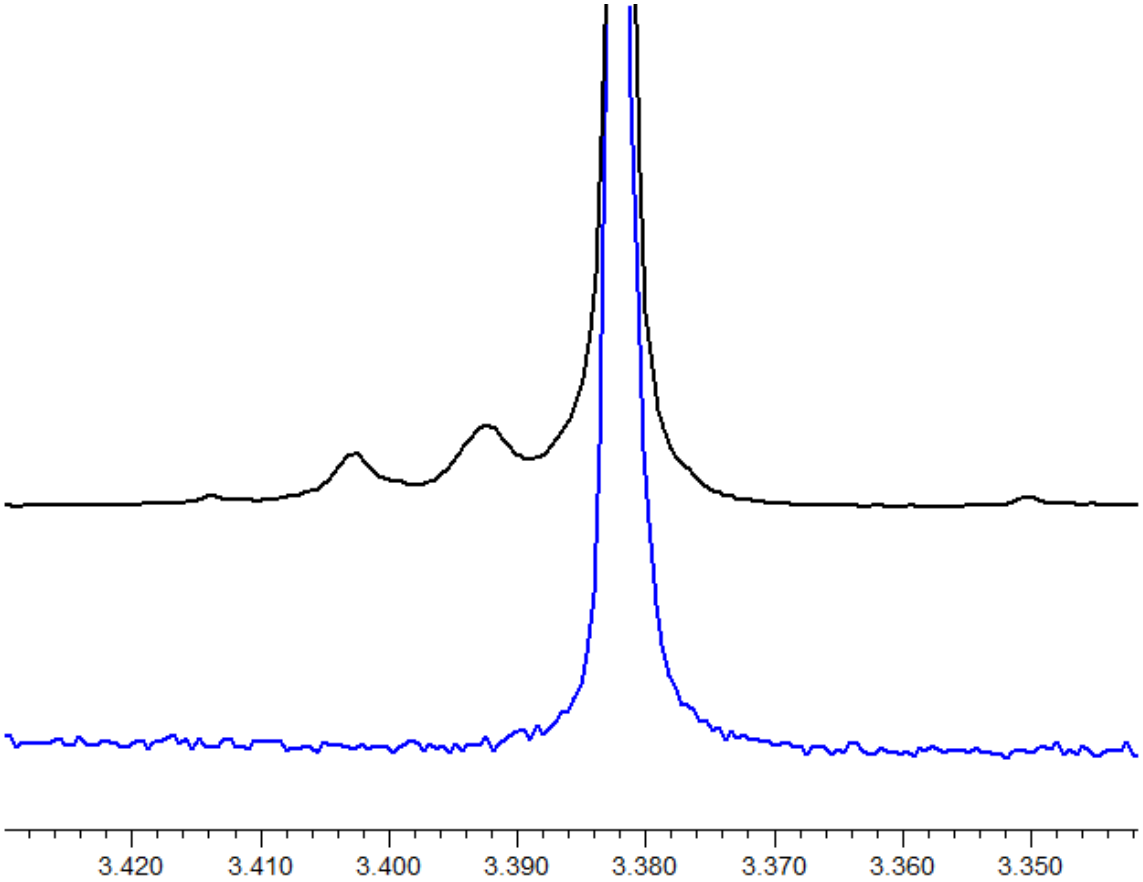

Attention was next turned toward the Staudinger reduction as a means to reduce the BCP azide. Again, **6.25** functioned as a model system and a successful Staudinger reduction was completed (Scheme 6-12). Complications arose only in the purification of the product – removal of the triphenylphosphine oxide was problematic because it was not readily soluble in cold diethyl ether during the normal PEG precipitation procedure.

Fortunately, this hinderance was alleviated upon experimentation with the BCP. Subjecting **6.27** to standard Staudinger conditions provided encouraging initial results, and the purification proceeded to easily remove the triphenylphosphine oxide via precipitation in *i*-propanol. The analysis by ^{1}H NMR spectroscopy showed a conspicuous disappearance of the azido methylene resonance (Figure 6-3). However, attempts to conclusively establish the amine functionality were disappointing. Treatment of **6.32** with either acetyl chloride to form the methyl amide or 3,5-bis(trifluoromethyl)benzaldehyde (BTBFA)[274] to form an imine failed to producing convincing evidence of amine functionality.

Scheme 6-12. The Staudinger reduction of NH_2-PEG-OMe **6.28** was successful. Subjecting the block copolymer **6.31** to identical conditions led to multiple byproducts.

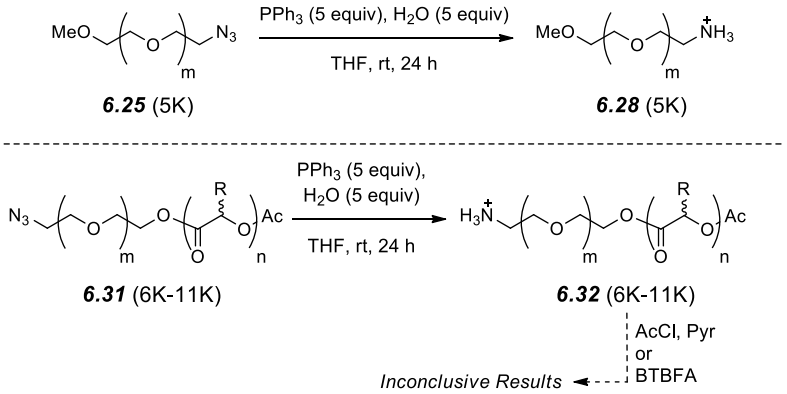

[274] Ji, S.; Hoye, T. R.; Macosko, C. W. Primary Amine (-NH_2) Quantification in Polymers: Functionality by ^{19}F NMR Spectroscopy. *Macromolecules* **2005**, *38*, 4679–4686.

Figure 6-3. Analysis of the product of the reduction of N_3-PEG-*b*-PLGA **6.31** by ^{1}H NMR spectroscopy showed a disappearance of the azide resonance.

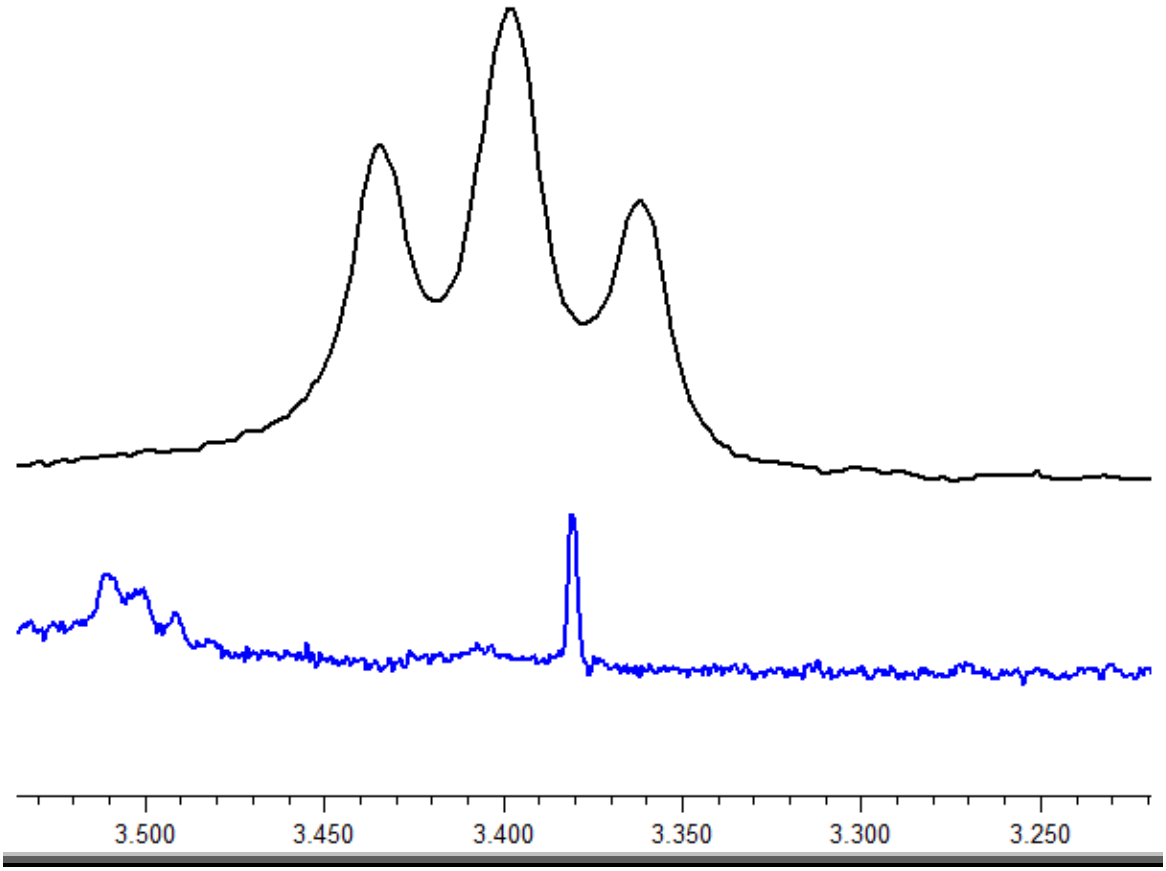

3. Conjugation of Biotin via a [3 + 2] Cycloaddition. Despite the anticipated ease, incontrovertible proof of the production and isolation of **6.32** remained elusive. Thus, efforts were shifted to the application of click chemistry in order to i) successfully conjugate biotin to a PEG-*b*-PLGA and ii) to develop expertise in polymer-based "click" chemistry to be used in future derivatizations. Previously, alkyne-tagged biotin molecules have been successfully prepared and conjugated

to magnetic nanoparticles[275] and cellulosic films.[276] At this time, experiments to successfully complete the [3 + 2] cycloaddition of a propargylated biotin[276] and a N3-PEG-PLGA-OAc **6.27** are ongoing in collaboration with Mr. Andrew Michel.

5. Conjugation of Mannose to HO-PEG-*b*-PLGA-OAc BCPs.

1. Motivation. In concert with the stated objective of this chapter – namely, to synthesize a dearth of varied but useful end-functionalized BCPs from a common polymeric precursor – a mannose targeting agent was sought on the advice of Prof. Robert Prud'homme, a collaborator at Princeton University. Different from the majority of research in this thesis, which focuses on chemotherapeutic applications, mannose is thought to be particularly useful as a targeting agent in immunological (particularly tuberculosis) diseases. Mannose [and other (oligo)saccharides] have drawn increasing interest over the last two decades as landmark studies have shown key, selective sugar-protein complexes.[277] Further motivation is found in recent studies that detail several key attractions for use of mannose in PEG-*b*-PLGA BCP-based formulations: i) a number of potential targets within the immune system are known,[278] particularly in the mononuclear phagocyte system,[279] making this a widely applicable concept, ii) binding to mannose receptors is known to induce endocytosis without

[275] Lin, P.-C.; Ueng, S.-H.; Yu, S.-C.; Jan, M.-D.; Adak, A. K.; Yu, C.-C.; Lin, L.-C. Surface Modification of Magnetic Nanoparticle via Cu(I)-Catalyzed Alkyne-azide [2 + 3] Cycloaddition. *Org. Lett.* **2007**, *9*, 2131–2134.

[276] Xu, W. Z.; Zhang, X.; Kadla, J. F. Design of Functionalized Cellulosic Honeycomb Films: Site-Specific Biomolecule Modification via "Click Chemistry." *Biomacromolecules* **2012**, *13*, 350–357.

[277] Weis, W. I.; Drickamer, K.; Hendrickson, W. A. Structure of a C-type Mannose-Binding Protein Complexed with an Oligosaccharide. *Nature* **1992**, *360*, 127–134.

[278] Irache, J. M.; Salman, H. H.; Gamazo, C.; Espuelas, S. Mannose-Targeted Systems for the Delivery of Therapeutics. *Expert Opin. Drug Dis.* **2008**, *5*, 703–724.

[279] Foged, C. Arigita, C.; Sundblad, A.; Jiskoot, W.; Storm, G.; Frokjaer, S. Interaction of Dendritic Cells with Antigen-Containing Liposomes: Effect of Bilayer Composition. *Vaccine* **2004**, *22*, 1903–1913.

receptor oligomerization,[280] iii) conjugation to a PEG linker has been shown to increase receptor binding and correspondingly decrease nonspecific uptake,[281] and iv) sufficient ligand density is critical to effective binding and uptake.[282] Furthermore, motivation is found in recent reports of the effective targeting of nanoparticles that are mannosylated.[283] Thus, such-mannose (MAN) capped MAN-PEG-*b*-PLGA polymers could readily find use in FNP-derived nanoparticles with interesting and varied drug delivery applications.

2. Synthesis of an Alkyne-Functionalized BCP and Conjugation to Mannose via "Click" Chemistry. A combination of multiple reports of PEG-linked mannose derivatives synthesized via "click chemistry"[284,285,286] and youthful ignorance of the prevalent esterase activity[287] *in vivo* inspired the first foray into the field of mannose conjugation. In doing so, HO-PEG-*b*-PLGA-OAc **6.16** was readily converted in a single synthetic step to an alkyne-containing polymer **6.34** via esterification with 5-hexynoic acid [treatment of mPEG-OH (**4.03**) with 5-

[280] Taylor, M. E.; Drickamer, K. Structural Requirements for High-Affinity Binding of Complex Ligands by the Macrophage Mannose Receptor. *J. Bio. Chem.* **1993**, *268*, 399–404.

[281] Engel, A.; Chatterjee, S. K.; Al-arifi, A.; Riemann, D.; Langner, J.; Nuhn, P. Influence of Spacer Length on Interaction of Mannosylated Liposomes with Human Phagocytic Cells. *Pharm. Res.* **2003**, *20*, 51–57.

[282] Yeeprae, W.; Kawakami, S.; Yamashita, F.; Hashida, M. Effect of Mannose Density on Mannose Receptor-Mediated Cellular Uptake of Mannosylated O/W Emulstions by Macrophages. *J. Control. Release* **2006**, *114*, 193–201.

[283] Mahajan, S.; Prashant, C. K.; Koul, V.; Choudhary, V.; Dinda, A. K. Receptor Specific Macrophage Targeting by Mannose-Conjugated Gelatin Nanoparticles: An *in vitro* and *in vivo* Study. *Curr. Nanosci.* **2010**, *6*, 413–421.

[284] Nagahori, N.; Nishimura, S.-I. Tailoring Glycopolymers: Controlling the Carbohydrate-Protein Interaction Based on Template Effects. *Biomacromolecules* **2001**, *2*, 22–24.

[285] Hotha, S.; Kashyap, S.; "Click Chemistry" Inspired Synthesis of *pseudo*-Oligosaccharides and Amino Acid Glycoconjugates. *J. Org. Chem.* **2006**, *71*, 364–367.

[286] Fernandez-Megia, E.; Novoa-Carballal, R.; Quio, E.; Riguera, R. Conjugation of Bioactive Ligands to PEG-Grated Chitosan at the Distal End of PEG. *Biomacromolecules*, **2007**, *8*, 833–842.

[287] Berry, L. M.; Wollenberg, L.; Zhao, Z. Esterase Activities in the Blood, Liver and Intestine of Several Preclinical Species and Humans. *Drug Metab. Lett.* **2009**, *3*, 70–77.

hexynoic chloride was equally effective to produce the PEG homopolymer analog **6.33**[288]].

Scheme 6-13. Esterification of a monomethoxy polyether block to the alkyne-tagged **6.33** and **6.34**.

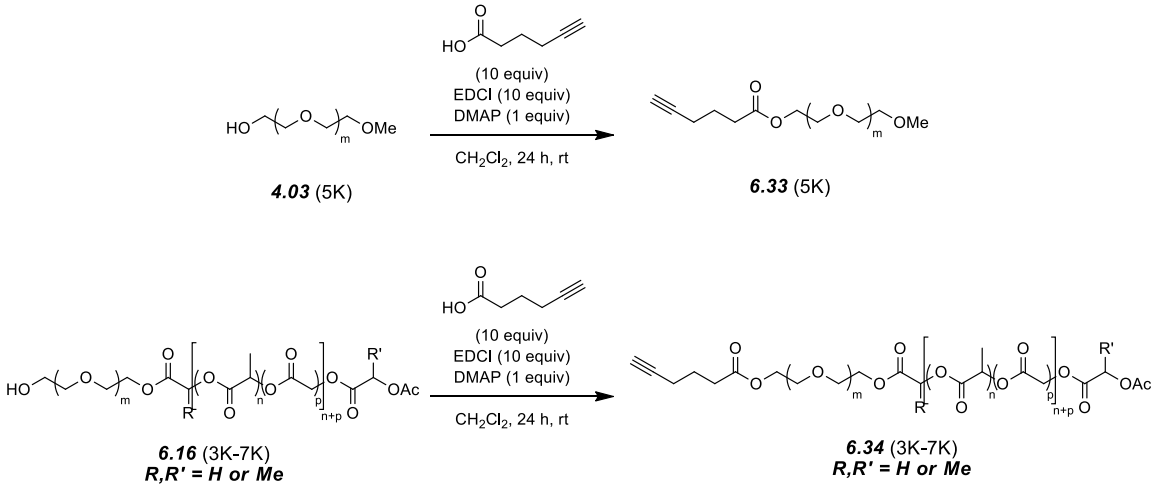

The azido mannose moiety **6.39** was synthesized as previously described (Scheme 6-14).[284] Consistent with this previous report, mannose **6.35** was penta-acetylated, after which the C2 acetate was selectively removed by treatment with benzyl amine, and the trichloroimidate of mannose (**6.36**) was formed of the trichloroimidate. An acid-catalyzed reaction with an azide-containing ethylene

[288] Synthesis of the mPEG-C(O)O(CH_2)$_3$CCH proceeded as expected and to high conversion. The key ^{1}H NMR resonances (500 MHz, $CDCl_3$): δ 4.24 [non-uniform t, *J* = 4.8 Hz, 2H, $CH_3O(CH_2CH_2O)_mCH_2CH_2OC(O)CH_2CH_2CH_2CCH$], 3.65 [s, 455 H, $CH_3O(CH_2CH_2O)_mCH_2CH_2OC(O)CH_2CH_2CH_2CCH$], 3.38 [s, 3H, $CH_3O(CH_2CH_2O)_mCH_2CH_2OC(O)CH_2CH_2CH_2CCH$], 2.49 [t, *J* = 7.5 Hz, 3H $CH_3O(CH_2CH_2O)_mCH_2CH_2OC(O)CH_2CH_2CH_2CCH$], 2.27 [dt, *J* = 7.0, 2.7 Hz, 2H, $CH_3O(CH_2CH_2O)_mCH_2CH_2OC(O)CH_2CH_2CH_2CCH$], 1.98 [t, *J* = 2.6 Hz, 1H, $CH_3O(CH_2CH_2O)_mCH_2CH_2OC(O)CH_2CH_2CH_2CCH$], and 1.85 [app pent, *J* = 7.1 Hz, 2H $CH_3O(CH_2CH_2O)_mCH_2CH_2OC(O)CH_2CH_2CH_2CCH$].

glycol oligomer {**6.38**, prepared from (2-[2-(2-chloroethoxy)ethoxy]ethanol) **6.37** according to known precedent[289]} provided the acetylated mannose azide **6.39**.

Scheme 6-14. The precedented, synthetic route of azido mannose **6.39**.[284]

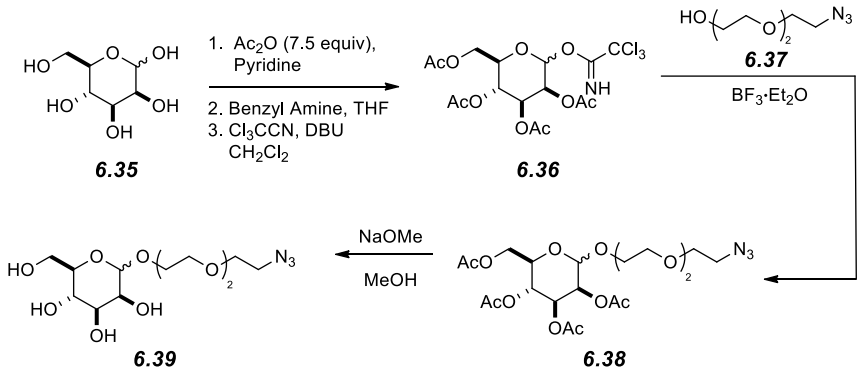

With both "click" chemistry partners (**6.34** and **6.39**) now in hand, attention turned to the strategic cyclization of the mannose azide and polymeric alkyne. As has been standard, the first such reactions were run not with the desired materials, but rather model systems were used. Specifically, **6.33** and **6.38** were selected for their i) ready synthetic accessibility, ii) conspicuous ^{1}H NMR resonances in analysis, and iii) potential to provide insight into the chemical and spectroscopic properties of the desired system. In accordance with this plan, partners **6.33** and **6.38** were subjected to copper(I)-catalyzed Huisgen reaction conditions and, gratifyingly, strong evidence of the mannose-tagged azide **6.40** was realized. In this case, the presence of the four remaining acetates (and their three proton singlet resonances) was useful in providing further evidence of the extent of conjugation. With this data in hand, the procedure was expanded to the cyclization of partners **6.33** and **6.39**. Again, the reaction proceeded as expected. NMR analysis of product **6.41** demonstrated a significant shift of many of the

[289] Iyer, S. S.; Anderson, A. S.; Reed, S.; Swanson, B.; Schmidt, J. G. Synthesis of Orthogonal End Functinoaled Oligotheylene Glycols of Defined Lengths. *Tetrahedron Lett.* **2004**, *45*, 4285–4288.

mannose-related resonances, presumably to ppm's that coincide with the PEG backbone and a significant broadening of several other key resonances. This data proved useful in the analysis of the PEG-*b*-PLGA end functionalization reactions.

Scheme 6-15. The synthesis of the mannose-labeled PEG model systems.

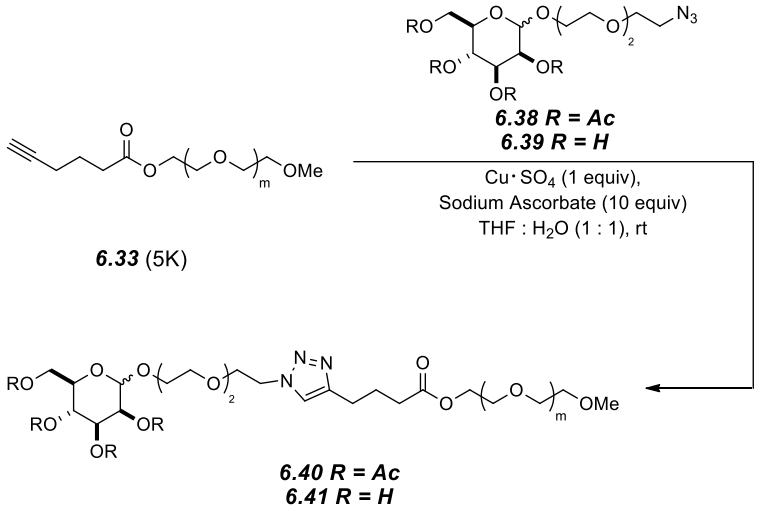

Now armed with confidence and data regarding the NMR shifts of key spectroscopic resonances, the click chemistry was applied toward the synthesis of **6.43**. In acknowledgement of the previous inconsistencies regarding the application of PEG model systems to the block copolymers, however, a final model system was designed prior to pursuit of **6.43**. Accordingly, **6.34** and **6.38** were cyclized to yield **6.42** (Scheme 6-16). Confidence in the success of this reaction (i.e., ca. 100% conversion) is attributable to the observance of several key resonances that were predicted by model **6.40** to be non-overlapping with the broad lactic and glycolic signals.

Finally, the hexyne-terminated PEG-*b*-PLGA block copolymer **6.34** was subjected yo copper(I) conditions to conjugate it to the deacetylated mannose **6.39** (Scheme 6-16). After the reaction and purification, analysis of the final

product was not trivial due to the number of small mannose resonances that overlapped with the much broader polymer peaks. However, relying particularly on model **6.41** as a guide, sufficient correlation to confidently conclude the cycloaddition occurred and ca. 25-50% conversion was obtained.

Scheme 6-16. The synthesis of the mannose-labeled PEG-b-PLGA BCPs via a [3 + 2] cycloaddition of an azido mannose and hexyne-functionalized BCP.

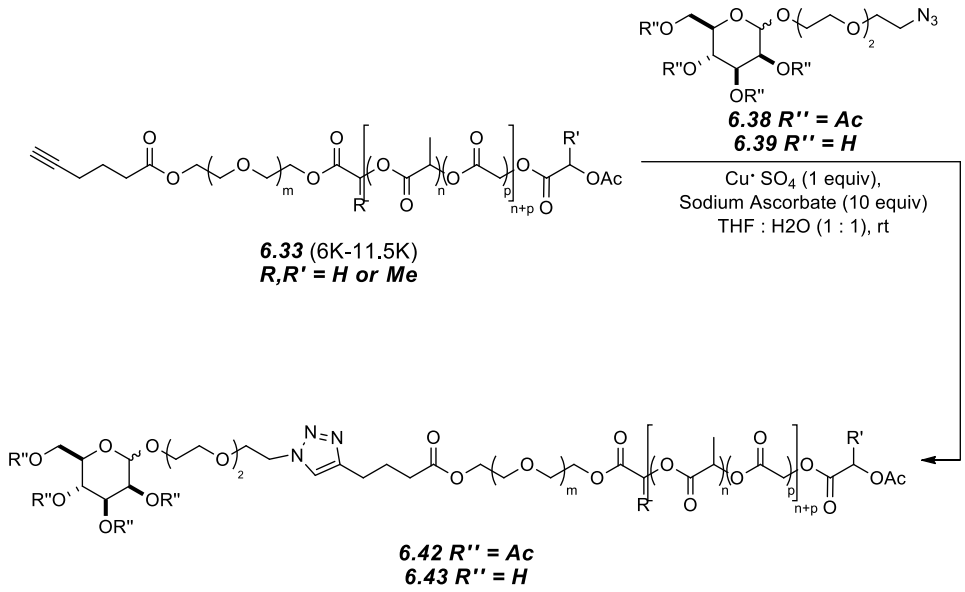

With the intent of synthesizing a biologically-relevant mannose tagged polymer for FNP, multiple routes to access a hexyne-functionalized polymer through the HO-PEG-*b*-PLGA-OAc **6.15** were explored. Unfortunately, treatment of **6.15** with either NaH/propargyl bromide nor a trichloroacetimidate/TMSOTf or TfOH resulted in efficient propargylation of **6.15**. Instead, apparent decomposition of the block copolymer was observed. Both of these reactions were especially disappointing because reactions of the mPEG-OH model system were successful under both sets of conditions. Likely, the inability to fully dry the BCP and/or the presence of small amounts of adventitious water may have

resulted in minor hydrolysis in the polyester block, leading to a significant loss of material and concurrent broadening of the PDI.

3. Synthesis of a Hexyne-Containing Mannose and Conjugation via "Click" Chemistry. While polymer **6.43** was not ultimately applicable from a biological perspective due to esterase activity,[287] experiments with mannose-tagged models **6.40**-**6.43** provided hands-on experience during early efforts to utilize "click" chemistry in polymer end-functionalization. Furthermore, this work provided important clues regarding our ability to analyze block copolymer conjugation via standard ^{1}H NMR spectroscopy.

Attention was next turned to utilizing the previously described N_3-PEG-*b*-PLGA-OAc **6.25** and a hexyne-labeled mannose. Compounds such as the alkyne-tagged mannose **6.45** have been previously synthesized[290] and utilized in click reactions to both PEG macromolecules[291] and small molecules.[285,292] Access to the propargylated mannose moiety **6.45** was accomplished via penta-acetylation of mannose **6.35** and treatment of this compound with propargyl alcohol in the presence of a strong acid, yielding **6.44**. **6.44** could be subjected to strongly basic conditions, thereby giving **6.45** in a three step sequence (Scheme 6-17).[290]

[290] Mereyala, H. B.; Gurrala, S. R. A Highly Diastereoselctive, Practical Synthesis of Allyl, Propargyl, 2,3,4,6-tetra-*O*-acetyl-β-D-gluco, β-D-galactopyranosides and Allyl, Propargyl, Heptaacetyl-β-D-lactosides. *Carbohydr. Res.* **1998**, *307*, 351–354.

[291] Wang, R.; Chen, G.-T.; Du, F.-S.; Li, Z.-C. Preparation and Aggregation Behavior of Mannose-Terminated Poly(ethylene glycol)-*b*-poly(L-leucine) in Water. *Colloids Surf., B* **2011**, *85*, 56–62.

[292] Kumar, K. K.; Kumar, R. M.; Subramanian, V.; Das, T. M. Expedient Synthesis of Coumarin-Coupled Triazoles via 'Click Chemistry' Leading to the Formation of Coumarin-Triazole-Sugar Hybrids. *Carbohydr. Res.* **2010**, *345*, 2297–2304.

Scheme 6-17. The precedented synthesis of the hexyne mannose **6.45**.[290]

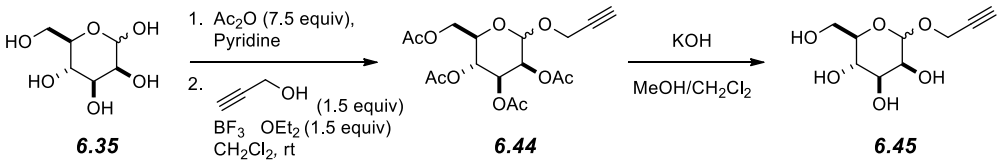

With **6.45** in hand, initial efforts once again centered on establishing the feasibility of click chemistry on an mPEG-OH model system. As in section 6.5.2, copper(I) catalysis was employed to couple **4.03** and **6.44** to confirm both the chemical methodology on these substrates and further confirm the shifts of the key resonances in the NMR spectrum. **6.46** was readily synthesized (Scheme 6-18). Again, analysis of this ^{1}H NMR spectrum suggested that analysis of a polyester-containing block copolymer would be far more challenging. Several diagnostic resonances of the mannose sugar were located at ppm values that are predicted to fall within the same range as the polyether resonances.

Scheme 6-18. The cycloaddition of **6.25** and **6.45** gave the mannosylated PEG homopolymer **6.46**.

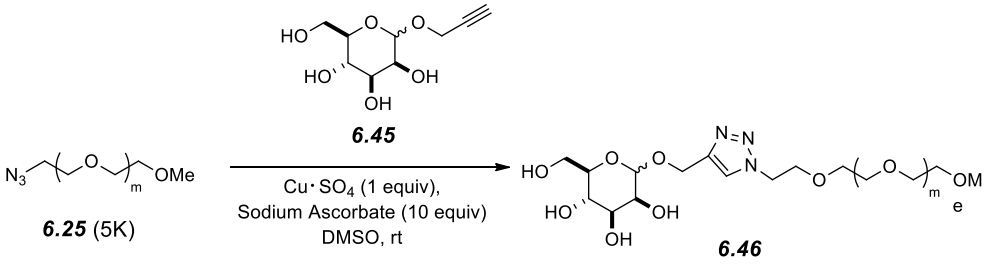

The azido functionalized PEG-PLGA BCP **6.31** was treated with a copper (I) source and the alkynylated mannose **6.45**. The first experiments were run under reaction conditions utilizing equal volumes of water and THF as the reaction solvent, akin to those utilized in Scheme 6-16.). Unfortunately, the small, one proton aromatic singlet of the triazole could not be convincingly

observed. This negative result may be attributable to a number of factors: the minimal amount of material, low signal-to-noise ratio, and previously observed broadness of this peak in $CDCl_3$. However, there were encouraging changes in the ^1H NMR spectrum of the product as well. Most notably, two resonances consistent with the (in this case, somewhat broadened) triplets assigned as the PEG methylenes that are α and β to the triazole (at δ = 4.56 and 3.87 ppm) are entirely consistent with model **6.46**. The integrations of these resonances suggested that 20-25% of the BCP was mannose-functionalized – a 100% conversion after considering that the starting material, **6.31**, was only 20% azide functionalized (owing to the difficulties in mesylation discussed previously in section 6.4.2

Scheme 6-19. The [3 + 2] cycloaddition of **6.31** and **6.45** gave the mannosylated BCP **6.47**.

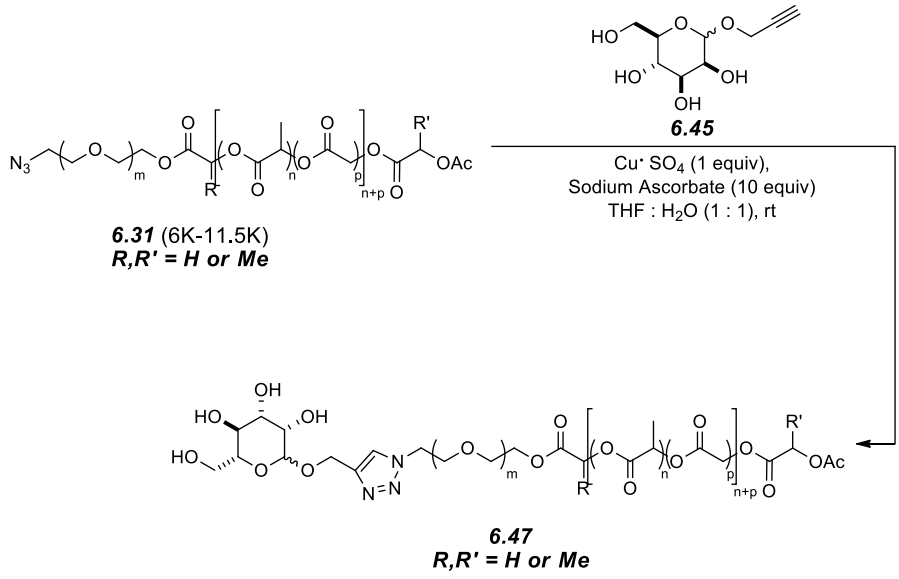

Attempts to obtain further proof of structure by treating **6.47** with large (> 30 equiv) excess of acetic anhydride and pyridine did not yield an unambiguous result. Namely, while additional singlets were noted at ppm shifts consistent with

acetates, conversion was incomplete, likely owing to the significant dilution of polymeric solution. Regardless, evidence remains for successful [3 + 2] cycloaddition of **6.31** and **6.45**. Further work involving a mannose derivative alkynylated with 3-butyn-1-ol has been initiated (to allow for additional resonance in the alkyl region to be monitored) and passed on to Mr. Andrew Michel for further work. While this conjugate would provide further evidence for the cyclization on the polymer end-group, it is likely that mannose-functionalized PEG-PLGA BCPs have been successfully accessed from the common precursor **6.15**. This result opens the possibility for the biological study of targeted nanoparticles of this BCP.

6. Maleimide Conjugation to HO-PEG-*b*-PLGA-OAc BCPs via the Mitsunobu Reaction.

1. Motivation and Literature Precedent. In addition to the azide/alkyne "click" chemistry that is discussed in sections 6.4 and 6.5, further diversity was sought in the materials applications of these end-functionalized polymers. After considering a number of functionalities associated with clean, high-yielding reactions, we settled upon the use of a maleimide (**6.48**, MAL) end group. This versatile chemical functionality is primarily employed in materials applications via the Diels-Alder [4 + 2] reaction as well as thiol conjugation to the α,β-unsaturation.[244] We sought to access a family of MAL-PEG-*b*-PLGA BCPs in order to eventually take advantage of its Michael-accepting properties, especially in applications that exploit the rapid conjugation of the thiol within cysteine residues of peptides and/or proteins for bioconjugation of targeting peptides.[293]

Previously, maleimide has been incorporated into the polymer end groups in a variety of ways. For example, multiple highly cited reports have described

[293] Singh, R. A Sensitive Assay for Maleimide Groups. *Bioconjugate Chem.* **1994**, *5*, 348–351.

the use of a furan-protected, maleimide-terminated initiator (e.g., **6.49** or **6.50**) to successfully synthesize poly(methyl methacrylate) (PMMA) macromolecules via atom transfer radical polymerization (ATRP)[294,295] or poly(ethylene glycol) methyl ether acrylate via reversible-addition fragmentation transfer (RAFT) polymerization (Figure 6-4). Alternatively, polyacrylates that co-polymerize protected maleimide-containing monomers (e.g., **6.51**) have been accessed via radical polymerization.[296]

Figure 6-4. The structures of maleimide (**6.48**) and representative examples of a maleimide-functionalized ATRP initiator (**6.49**), RAFT initiator (**6.50**) and acrylate monomer (**6.51**).

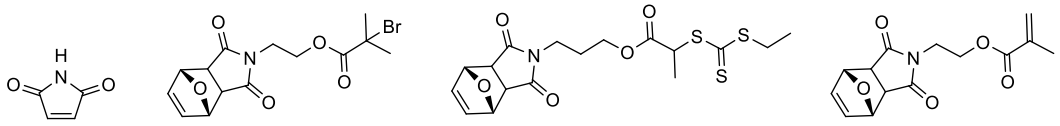

6.48 ***6.49*** ***6.50*** ***6.51***

Specific to this thesis, the ability to display a maleimido group on the water-soluble PEG block of a BCP is critical to its successful implementation in the nanoparticle-based drug delivery systems described here. PEG homopolymers such as **4.03** have been derivatized with succinic acid and then esterified with a maleimide derivative to yield a PEG homopolymer that is end-functionalized with an unprotected maleimide.[297,298] [However, the use of a MAL-

[294] Durmaz, H.; Colakoglu, B.; Tunca, U.; Hizal, G. J. Preparation of Block Copolymers Via Diels Alder Reaction of Maleimide- and Anthracene-End Functionalized Polymers. *J. Polym. Sci., Part A: Polym. Chem.* **2006**, *44*, 1667–1675.

[295] Dag, A.; Durmaz, H.; Demir, E.; Hizai, G.; Tunca, U. Heterograft Copolymers via Double Click Reactions Using One-Pot Technique. *J. Polym. Sci., Part A: Polym. Chem.***2008**, *46*, 6969–6977.

[296] Kosif, I.; Park, E.-J.; Sanyal, R.; Sanyal, A. Fabrication of Maleimide Containing Thiol Reactive Hydrogels via Diels-Alder/Retro Diels-Alder Strategy. *Macromolecules* **2010**, *43*, 4140–4148.

[297] Durmaz, H.; Dag, A.; Altintas, O.; Erdogan, T.; Hizal, G.; Tunca, U. One Pot Synthesis of ABC Type Triblock Copolymers via in situ Click [3 + 2] and [4 + 2] Reactions. *Macromolecules* **2007**, *40*, 191–198.

PEG-OH in the literature is frequently referenced as a commercially purchased commodity (rather than synthesized) from now-defunct companies as well.[299,300]] The work of Gao and co-workers, particularly, is noteworthy in that they used the heterobifunctional MAL-PEG-OH as a macroinitiator of caprolactone, generating a MAL-PEG-*b*-PCL that was utilized in the delivery of doxorubicin.

Much more limited precedent is available for the selective end functionalization with maleimide. A notable example is an alternative synthesis of a MAL-PEG-*b*-PCL that was performed previously in the Hoye labs.[301] This work synthesized the PEG-*b*-PCL block polymer via an esterification of a PCL acid chloride with a large (ca. 10-fold) excess of a PEG diol. The PCL-*b*-PEG-OH moiety could then be further functionalized with an acid chloride-containing maleimide derivative to yield the final MAL-PEG-*b*-PCL. This strategy served as a viable route to MAL-PEG-*b*-PCL's of varying MWs, but it is still limited by the PEG-maleimide ester linkage – a chemical bond susceptible to esterase activity.

2. Maleimide Substitution under Mitsunobu Conditions. While the acid-catalyzed reaction of an amine with maleic anhydride has been known for decades,[302] interest in applying the Mitsunobu reaction[303] to incorporate

---

[298] Gacal, B.; Durmaz, H.; Tasdelen, M. A.; Hizal, G.; Tunca, U.; Yagel, Y.; Demirel, A. L. Anthracene-Maleimide-Based Diels-Alder "Click Chemistry" as a Novel Route to Graft Copolymers. *Macromolecules* **2006**, *39*, 5330–5336.

[299] Olivier, J.-C.; Huertas, R.; Lee, H. J.; Calon, F.; Pardridge, W. M. Synthesis of Pegylated Immunonanoparticles. *Pharm. Res.* **2002**, *19*, 1137–1143.

[300] Nasongkla, N.; Shuai, X.; Ai, H.; Weinberg, B. D.; Pink, J.; Boothman, D. A.; Gao, J. cRGD-Functionalized Polymer Micelles for Targeted Doxorubicin Delivery. *Angew. Chem., Int. Ed*. **2004**, *116*, 6483–6487.

[301] Ji, S.; Hoye, T. R.; Zhu, Z.; Macosko, C. W. Maleimide Functionalized Poly(ε-caprolactone)-*b*-poly(ethylene glycol) (PCL-PEG-MAL) Nanoparticles: Formation and Thiol Conjugation. *Macromol. Chem. Phys.* **2009**, *210*, 823–831.

[302] Mehta, N. B.; Phillips, A. P.; Lui, F. F.; Brooks, R. E. Maleamic and Citraconamic Acids, Methyl Esters, and Imides. *J. Org. Chem.* **1960**, *25*, 1012–1015.

[303] Mitsunobu, O. The Use of Diethyl Azodicarboxylate and Triphenylphosphine in Synthesis and Transformation of Natural Products. *Synthesis* **1981** 1–28.

maleimide has only been explored for the last ca. 20 years.[304] These initial efforts by Walker yielded the Mitsunobu-derived maleimide compounds from activated primary alcohols in moderate yield.[304] Especially relevant to the proposed PEG functionalization, when an ethylene glycol oligomer (n = 4, **6.53**) was used as the alcohol, a reasonable (66%) yield was reported.[304] Similar Mitsunobu reactions have been reported by others, with mixed results. For instance, utilization of 2-methoxyethanol **6.52** has been reported to yield an approximately 70% yield of the maleimide-substituted Mitsunobu product.[301] Conversely, others have reported the use of oligomeric ethylene glycols (n = 6, **6.54**) providing low (ca. 25%) yields under nearly identical conditions.[305] The lone report of an attempt to activate a true PEG homopolymer **4.03** for displacement by maleimide resulted in minimal (ca. 10%) conversion.[301] In this case, isolation of the pure maleimido functionalized polymer is not reported, likely owing to the difficulty associated with separation of starting material from product.

Scheme 6-20. Previous efforts toward the Mitsunobu reaction of maleimide (**6.48**) and ethylene glycol oligomers (**6.52-6.54**) and polymers (**4.03**).[301,304,305]

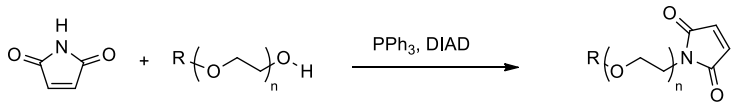

6.48 ***see Table 6-1*** ***see Table 6-1***

[304] Walker, M. A. The Mitsunobu Reaction: A Novel Method for the Synthesis of Bifunctional Maleimide Linkers. *Tetrahedron Lett.* **1994**, *35*, 665–668.

[305] Gill, H. S.; Tinianow, J. N.; Ogasawara, A.; Flores, J. E.; Vanderbilt, A. N.; Raab, H.; Scheer, J. M.; Vandlen, R.; Williams, S.-P.; Marik, J. A Modular Platform for the Rapid Site-Specific Radiolabelling of Proteins with ^{18}F Exemplified by Quantitative Positron Emission Tomography of Human Epidermal Growth Factor Receptor 2. *J. Med. Chem.* **2009**, *52*, 5826–5825.

Table 6-1. Previously reported results of maleimide substitution under Mitsunobu reaction condtions with ethylene glycol oligomers and PEG.[301,304,305]

Starting Material	n	R	Product	Yield
6.52	1	CH_3	**6.55**	ca. 70%
6.53	4	CH_3	**6.56**	66%
6.54	6	CCH	**6.57**	25%
4.03	110	CH_3	**6.58**	ca. 10%

Future optimization of Walker's study utilized an excess of the primary alcohol substrate or inclusion of a "dummy" neo-pentyl alcohol (to render the unreacted betaine inactive, thereby minimizing the reaction between the betaine and the maleimide) to significantly improve the yields, now up to 92% in the case of primary alkyl alcohols.[306] However, application of even these conditions to bifunctional oligomeric ethylene glycols (n = 3-6) resulted in disappointingly variable yields (25-68%).[307] Given these results, Mitsunobu chemistry for the incorporation maleimide into a BCP is promising, but there remains room for improvement and optimization in these synthetic procedures.

3. Mitsunobu Model Studies and Optimization of the Synthetic Procedure. In response to the apparent difficulties in reproducing the maleimide substitution with ethylene glycols under Mitsunobu conditions, the first goal of this project was

[306] Walker, M. A. A High Yielding Synthesis of *N*-alkyl Maleimides Using a Novel Modification of the Mitsunobu Reaction. *J. Org. Chem.* **1995**, *60*, 5352–5355.

[307] Warnecke, A.; Kratz, F. Maleimide-oligo(ethylene glycol) Derivative of Camptothecin as Albumin-Binding Prodrugs: Synthesis and Antitumor Efficacy. *Bioconjugate Chem.* **2003**, *14*, 377–387.

to replicate the published results. The diethylene glycol monomethyl ether (**6.59**) was first tested under the Mitsunobu conditions containing neo-pentyl alcohol and diisopropyl azodicarboxylate (DIAD) rather than diethyl azodicarboxylate (DEAD), as per literature precedent.[306] Accordingly, **6.59** was subjected to the neo-pentyl alcohol-containing Mitsunobu conditions, and GC/MS analysis of the crude reaction mixture provided convincing evidence of significant conversion to the substituted product **6.60**. Encouraged by this first result, the extent of conversion was not rigorously analyzed by ^{1}H NMR spectroscopy. Instead, a dried, 2K mPEG-OH polymer was subjected to identical reaction conditions. In the case of this (relatively small) macromolecule, however, the conversion was depressed to only 44% of the desired product **6.61**. Further attempts to substitute a larger, 5K PEG homopolymer yielded an even further depressed conversion – approximately 15% of **6.62**.

Dismayed by these progressively less desirable results, focus shifted away from incorporation of a dummy alcohol due to the less than ideal results of ethylene glycol oligomeric substrates reported.[307] Reasoning that 100% maleimide incorporation was not critical in the final BCP application efforts were turned toward an excess of the desired alcohol.[306] Taking (1.5 equivalents of) **6.59** as a model system, the substitution of **6.59** was judged to be 72% (recall that the limiting reagent was not the alcohol – conversion of the alcohol was measured to be 48% crude). This result is well in line with the previously reported findings (66%[304] and ca. 70%[301]).

Once again encouraged by the prospect of the Mitsunobu chemistry, 1.1 equivalents of the 5K PEG model system **4.03** was treated with triphenylphosphine, DIAD, and maleimide. Unfortunately, conversion of this reaction reverted back to the low levels (in this case, 26%) of conversion previously observed for the synthesis of **6.62**. Interestingly, in this experiment, the reaction was noted to be slightly heterogeneous after addition of the

maleimide and stirring at -78 °C for ca. 10 min. This heterogeneity upon prolonged stirring after step i (Scheme 6-21) proved to be reproducible.

Originally, I postulated that this observation was attributable to the PEG insolubility in an ethereal co-solvent (THF/DCM) mixture at a low temperature. In an attempt to overcome this, an additional volume of room temperature DCM was added to the reaction mixture upon observation of a white solid. Initially, this solvent addition appeared to correct the issue – the reaction again became homogeneous. However, upon further stirring at -78 °C, the white precipitate reappeared. A second addition of room temperature DCM once again resolvated the reactant, but again this proved to be only temporary. [As a control, a THF/DCM solution of **4.03** was prepared (at the same concentration as the reactions in Scheme 6-21) and cooled to -78 °C. In this case, however, the solution remained homogeneous indefinitely.] Upon the third addition of room temperature DCM, the dissolved maleimide was immediately added. Despite the decreased concentration of this reaction, a notable increase in the extent of conversion (55%) was noted upon analysis of the crude reaction.

The hypothesis for the cause of the unanticipated insolubility was revised in light of the above results. Instead, the cause of the heterogeneity was thought to be a result of the cold temperature resulting in the insolubility of the PEG dioxaphosphorane intermediate rather than attributable to the co-solvent composition. The dissolution of the white precipitate in the experiment described above was instead the result of the solution warming from the room temperature solvent rather than increasing the DCM:THF solvent ratio. In accordance with this theory, the concentration of **4.03** was reduced and the temperature of the reaction was adjusted at step ii. After addition of the maleimide, the reaction was allowed to warm to -40 °C and stirred for 1 h. Satisfyingly, the reaction remained fully solvated throughout this incubation. Afterwards, the reaction was warmed to room temperature. ^{1}H NMR spectroscopic analysis of the crude reaction mixture

provided evidence of a 60% conversion. While the Mitsunobu reaction of a dithiophenolmaleimide with PEG **4.03** has been reported in high (73%) yield,[308] this especially high conversion rate reported here is, to the best of my knowledge, unprecedented in a PEG/maleimide Mitsunobu reaction.

Scheme 6-21. The optimization of Mitsunobu conditions for the reaction of maleimide (**6.48**) and diethylene glycol monomethyl ether (**6.59**) and PEG (**4.03**).

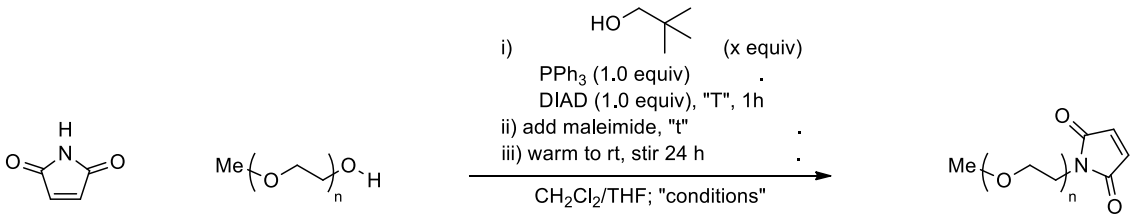

6.53 1.0-1.1 equiv

see Table 6-2

see Table 6-2

[308] Given the limited discussion and spectroscopic data, it is difficult to judge the conversion (rather than the mass-based percent yield) of this reaction. See Schumacher, F. F.; Nobles, M.; Ryan, C. P.; Smith, M. E. B.; Tinker, A.; Caddick, S.; Baker, J. R. In Situ Maleimide Bridging of Disulfides and a New Approach to Protein PEGylation. *Bioconjugate Chem.* **2011**, *22*, 132–136.

Table 6-2. The optimization of the Mitsunobu reaction condtions for the substitution of ethylene glycol or PEG with maleimide.

Starting Material	n	**6.48** (equiv)	*n*-pentanol (equiv)	T (°C)	t (min)	Product	Conversion [a] (%)
6.59	2	1.0	0.5	-78	10	**6.60**	n.d.[b]
4.03	45	1.0	0.5	-78	10	**6.61**	44
4.03	110	0.5	1.0	-78	10	**6.62**	15
6.59	2	1.5	0	-78	10	**6.60**	48 [c]
4.03	110	1.1	0	-78	10	**6.62**	26
4.03	110	0.5	0	-78 to -40	60	**6.62**	60

[a] Conversion based on ^{1}H NMR analysis.
[b] n.d. = not determined; product observed via GC/MS
[a] 72% conversion based on limiting reagent.

The final hurdle to declaring these model systems a rousing success was the need to purify the final product **6.62**. It proved particularly difficult to remove the triphenylphosphine oxide from the PEG mixture – attempts to selectively precipitate the substituted PEG from the most frequently encountered solvents yielded little improvement in the purity. After extensive optimization, a multistep sequence of precipitations was established to effectively purify the maleimido-functionalized polymer. In this procedure, the crude polymer was dissolved in EtOAc and added dropwise to an equal volume of hexanes pre-cooled to 0 °C, filtered, the solid redissolved in DCM, precipitated into isopropanol pre-cooled to 0 °C, filtered, the solid redissolved in EtOAc and again added dropwise to an equal volume of hexanes pre-cooled to 0 °C and finally filtered for a third time. This resulted in the recovery of a pure, maleimide-substituted polymer.

4. Maleimide-Thiol Conjugation Model Studies. With the maleimido-functionalized **6.60** and **6.62** now in hand, control experiments were run to establish viability of thiol conjugation.[309] In anticipation of future applications of amino-acid derived ligands, we aimed to establish our ability to conjugate the thiol of a cysteine ethyl ester (**6.63**) to **6.60**, thereby forming the thioether **6.64**. To our delight, addition of 1.1 equivalents of the cysteine ethyl ester to a D_2O solution buffered at pD = 7.4 (note that it is pD rather than pH due to the deuterated buffer) resulted in > 85% conversion (as judged by ^{1}H NMR analysis) to **6.64**. The identity of this compound was further confirmed by the identification of the di/tri-deuterated species (the deuteration of the amine exchanged rapidly in methanol during analysis, and thus only two-three deuterium isotopes were detected) as the major peak in the LC-MS trace.[310]

Scheme 6-22. The Michael addition of cysteine ethyl ester **6.63** to the maleimide model systems **6.60** and **6.62** in a buffered aqueous solvent resulted in significant conversion to the thiolated products **6.64** and **6.65**.

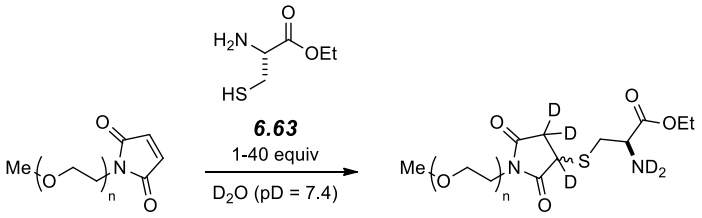

##	n
6.60	2
6.62	110

##	n
6.64	2
6.65	110

[309] Veronese, F. M. Peptide and Protein PEGylation: A Review of Problems and Solutions. *Biomaterials* **2001**, *22*, 405–417 and references therein.

[310] Model **6.60** (17.5 mg, 0.088 mmol, 1 equiv) was co-dissolved with cysteine ethyl ester hydrochloride salt **6.68** (17.4 mg, 0.094 mmol, 1.1 equiv) in a buffered D_2O solution (pD = 7.4) in a 3 mL vial with stir bar. The vessel was capped with a Teflon-lined cap and allowed to stir for overnight at rt. The product was analyzed crude and the major product was found to be **6.69**.LC/MS (Method: C18 column, gradient 50-100% methanol content MM-ES+APCI Positive and MM-ES+APCI Negative) t_R = 1.8 min (M-H$^+$ 349.0 and 350.0 for the di- and tri-deuterated species).

Expanding these results to the PEG system, conversion to **6.65** was noted when **6.62** (30 % functionalized) was incubated with 12 equivalents of the cysteine ethyl ester for 18 hours. This encouraging result was judged by the observation of several new resonances in the ^{1}H NMR spectrum: most notably a quartet at ppm = 4.27, two doublet of doublets at 3.01 and 2.99. Equally uplifting, the resonances associated with the α,β-unsaturation of the maleimide were no longer present. Encouraged by our ability to induce the thioether formation under mild, biologically compatible conditions, we proceeded forward with efforts toward the maleimido BCP.

5. Initial Results of HO-PEG-b-PLGA-OAc Mitsunobu Reactions and Future Work. With extensive and encouraging data in hand from the successful model systems, attention turned toward functionalization of the targeted system: the HO-PEG-*b*-PLGA-OAc BCP **6.16**. Specifically, a 0.435 g sample of **6.16** was treated under the optimized conditions (Scheme 6-21, entry 6) in an attempt to access the maleimido BCP. Unfortunately, this first experiment resulted in no detectable maleimide substitution at the PEG terminus.

Scheme 6-23. The attempted application of the optimized Mitsunobu conditions to **6.16** resulted in none of the desired product.

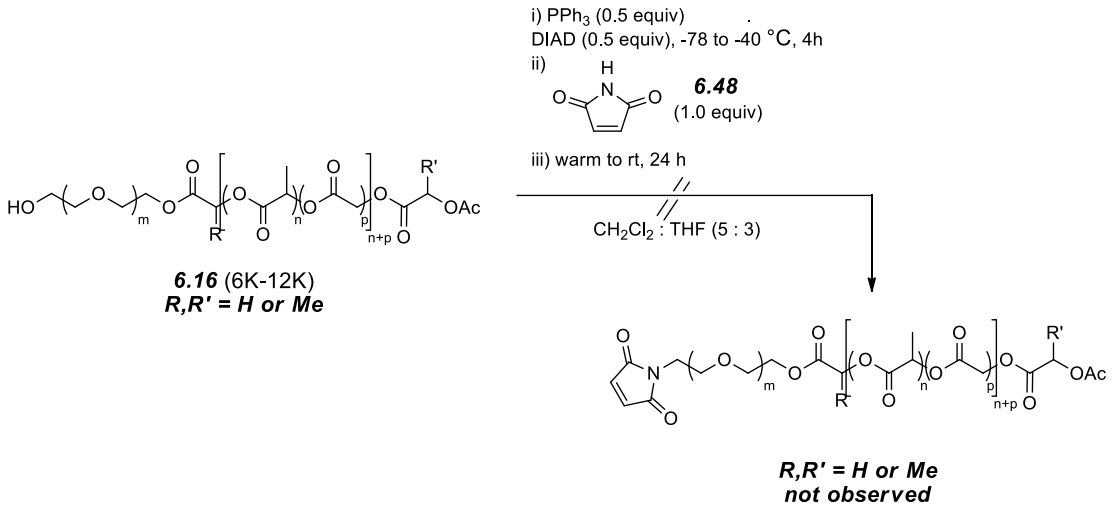

This disappointing failure could be most easily attributed to the small amount of material subjected to the reaction – 0.435 g of a 6K-12K BCP is only 0.024 mmol. To put the reaction conditions in proper context, use of almost a half gram of the polymer starting material would initially seem sufficient, that is, until one realizes that a molar equivalent of water is only ca. 440 nL (yes, *nano*liters!). Combining the unavoidable introduction of adventitious water with the previously described difficulties in completely drying PEG-*b*-PLGA BCPs, it is easy to understand how a small quantity of water could out-compete the poorly nucleophilic maleimide. Further complicating the practical difficulties of this transformation is the reduced molarity of this reaction. Specifically, the BCP was soluble to only 0.003 M – only one half the concentration of the successful PEG model systems.

If maleimide substitution results with HO-PEG-*b*-PLGA-OAc from Mitsunobu conditions continue to be disappointing, alternatives exist. For instance, subjecting a BnO-PEG-OH species via a sequence of Mitsunobu

substitution with s furan-protected maleimide, debenzylation, and finally a retro Diels-Alder reaction to yield HO-PEG-MAL [commercial purchase of HO-PEG-MAL is also an (expensive) option[311]]. The HO-PEG-MAL, with the maleimide in either its protected or unprotected form, may be used as a macroinitiator. This route is attractive as a second option because preliminary tests in which **6.60** was incubated with DBU showed no decomposition over the time period of a normal PLGA polymerization (degradation of the small molecule to baseline material was noted after extended incubation). Thus, polyesterification of lactide and glycolide with MAL-PEG-OH could yield the MAL-PEG-PLGA-OH BCP. This polymer could then, in turn, be used as for thiol conjugation reactions.

7. Conclusions.

Efforts to utilize the PEG-*b*-PLGA copolymer as a targeting or imaging agent (rather than merely as an excipient/carrier) in drug delivery applications are reported. Notably, an efficient and readily reproducible route to a common polymeric precursor of the BCP (HO-PEG-*b*-PLGA-OAc) has been established. Multiple chemical transformations on this entity have been examined by using mPEG-OH as a model substrate, but these results, surprisingly, did not translate well to the PEG-*b*-PLGA BCPs in all cases. This may be due to the add difficulty of drying and limited solubility (and correspondingly dilute reaction conditions) of the PEG-*b*-PLGA copolymer. Nonetheless, significant advances have been made through the synthesis of the N_3-PEG-*b*-PLGA-OAc BCP, leading to the successful incorporation of a mannose targeting moiety. Additionally, significant effort has led to the optimization of Mitsunobu conditions for the synthesis of maleimido-functionalized PEG polymers. Further efforts toward applying this

[311] http://www.creativepegworks.com/heterobifunctional%20PEG.html accessed July 18th, 2012.

chemistry to the synthesis of a MAL-PEG-*b*-PLGA-OAc remains a strong possibility.

8. Experimental Section.

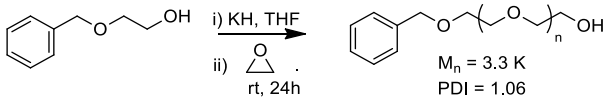

6.07 ***6.02*** ***6.08***

Mono benzyl ether poly(ethylene glycol) (6.08).[258,312] To prepare for the polymerization of ethylene oxide, the following purifications were performed. 2-(Benzyloxy)ethanol was distilled under N_2 gas after stirring over CaH_2, immediately transferred to an oven-dried Schlenk flask under N_2 gas with a Teflon seal, and stored for future use. Potassium hydride (30 wt% dispersion in mineral oil) was washed with distilled hexanes (4x), dried under high vacuum, and transferred to a glove box for future use. Ethylene oxide (*CAUTION: poisonous gas*) was transferred to a flame-dried 2-neck flask that had been previously evacuated and back-filled with argon (3x) and cooled in an *i*-propanol/dry ice bath. The liquid ethylene oxide was subjected to three freeze-pump-thaw cycles and transferred to a flame dried flask containing neat butyl magnesium chloride and stirred for four hours at 0 °C. The drying procedure for ethylene oxide involving neat butyl magnesium chloride was repeated by transferring the ethylene oxide to another flask containing a fresh aliquot of the butyl magnesium chloride. The ethylene oxide was again stirred at 0 °C for four hours. Upon completion of the drying procedure, the ethylene oxide was transferred to a flame-dried Schlenk flask, and the flask was packed in solid dry ice to store the ethylene oxide for future use. THF was first passed through an

[312] This procedure was completed with the help of Mr. Ligeng Yin in the lab of Prof. Marc Hillmyer. Their expertise, assistance, and provision of materials are greatly appreciated.

alumina column directly into an oven-dried 2-neck flask containing neat butyl magnesium chloride and allowed to stir at room temperature for six hours. The THF was then transferred to a clean, flame-dried 1L flask under argon, subjected to three freeze-pump-thaw cycles, and stored under argon for future use.

To complete the polymerization, a 1L, 5-neck round bottom flask fitted with a burette attachment, syringe attachment, and stir bar was heat under dynamic vacuum overnight. Following three fill-evacuate cycles, the argon-filled five-neck round bottom flask was transferred to a glove box. Inside the glove box, the pre-dried THF (ca. 500 mL), 2-(benzyloxy)ethanol (0.61 mL, 4.3 mmol, 1.0 equiv), and KH (0.19 g, 4.8 mmol, 1.1 equiv) were added. The five-neck flask was removed from the glove box, returned to a fume food, and stirred for four hours. The burette containing the ethylene oxide monomer was attached while maintaining the ethylene oxide at 0 °C, and the tubing was flame dried. The monomer burette was removed from the ice bath and, with the stopcock to the five-neck flask open, inverted to added the ethylene oxide (21.5 g, 0.489 mol, 114 equiv). After stirring for 24 hours at room temperature, the flask was opened and 8 g of Amberlyst-15 acidic resin was added and stirred for an additional two hours. Because the pH of the solution remained basic, dry *i*-propanol was acidified with concentrated HCl and added until a neutral pH was reached. The solution was then concentrated under reduced pressure, yielding a viscous, yellow oil that was precipitated in diethyl ether at 0 °C. After filtration, the title product was recovered as a white powder (10.44 g, 48.6%) with M_n = 3,300 g mol^{-1}.

^{1}H NMR (500 MHz, DMSO): δ 7.37-7.26 (m, 5H, OCH_2-*o*-Ph, OCH_2-*m*-Ph, and OCH_2-*p*-Ph), 4.58 [t, *J* = 5.6 Hz, 1H, $BnO(CH_2CH_2O)_nCH_2CH_2O\mathit{H}$], 4.49 (s, 2H, $OC\mathit{H}_2Ph$), and 3.51 [s, 332 H, $BnO(C\mathit{H}_2C\mathit{H}_2O)_nC\mathit{H}_2C\mathit{H}_2OH$].

SEC (Polystyrene standards) PDI = 1.06.

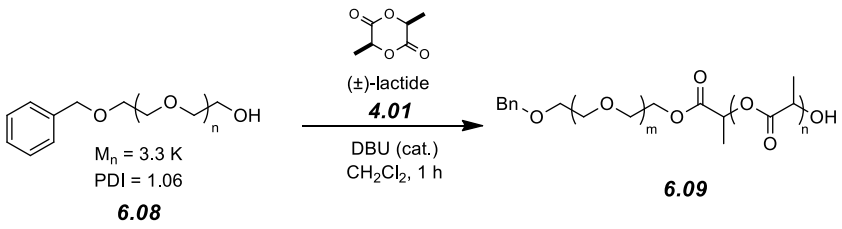

Mono benzyl ether poly(ethylene glycol)-b-poly(lactic acid) (6.09). Representative procedure utilizing Method A from (see section 4.D.1); other PEG-*b*-PLA polymers have been prepared via Method B (see 4.D.2).

The following reaction mixture was prepared in a controlled atmosphere (N_2) glove box. To a solution of *rac*-lactide [**(±)-4.01**, 0.500 g, 3.47 mmol] and BnO-PEG-OH (3.3K) (0.250 g, 0.076 mmol) in 5.5 mL of dichloromethane was added DBU [10 µL] in a screw-capped glass reaction vessel (e.g., culture tube). The solution was removed from the glove box and stirred for 1 h. The vessel was opened, hydrochloric acid (1N) was added immediately, and the mixture was washed with water and brine. The polymer was precipitated by dropwise addition of the chloroform solution with stirring into excess isopropanol. Solvent was removed from the resulting suspension of white polymer by decantation, and the polymer was dried under vacuum at 50 °C overnight, yielding the desired product as a white solid with M_n (PLA) = 6,700 g mol^{-1}.

^{1}H NMR (500 MHz, $CDCl_3$): δ 7.37-7.27 (m, 5H, OCH_2-*o*-Ph, OCH_2-*m*-Ph, and OCH_2-*p*-Ph), 5.28-5.10 {m, 93H, BnO-PEG-[OC(O)C*H*(CH_3)]$_n$OC(O)CH(CH_3)OH}, 4.57 (s, 2H, OC*H*$_2$Ph), 4.40-4.23 [m, 4H, BnO-PEG-OCH_2C*H*$_2$OC(O)C*H*(CH_3)-PLA-C(O)C*H*(CH_3)OH], 3.65 [s, 323 H, BnO-(C*H*$_2$C*H*$_2$O)$_n$C*H*$_2$$CH_2$O-PLA], and 1.63-1.51 {m, 302 H, BnO-PEG-[OC(O)CH(C*H*$_3$)]$_n$OC(O)CH(C*H*$_3$)OH}.

SEC (Polystyrene standards) PDI = 1.12.

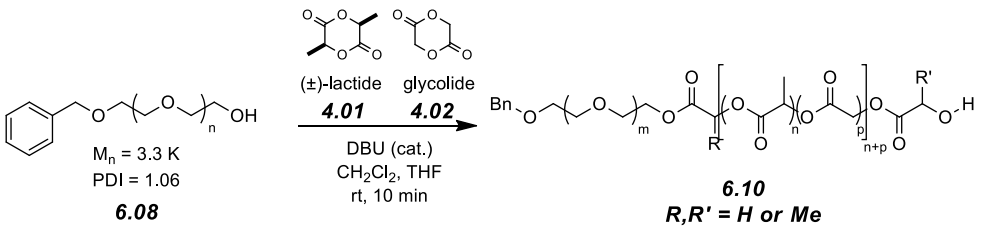

Mono benzyl ether poly(ethylene glycol)-*b*-poly(lactic-*co*-glycolic acid) (6.10). Representative procedure utilizing Method B from (see section 4.D.4); PEG-*b*-PLGA polymers of different MWs and lactic:glycolic ratios have also been prepared via Method B.

The following three solutions were prepared in ambient atmosphere in a fume hood. i) BnO-PEG-OH (3.3K, 450 mg) was dissolved in CH_2Cl_2 (21 mL) together with a predetermined amount of *rac*-lactide [**(±)-4.01**] in an oven-dried round-bottomed flask containing a magnetic stir bar and closed with a septum. ii) DBU was dissolved in CH_2Cl_2 at a concentration of 16.7 µL mL^{-1} in a screw-capped vial. iii) Glycolide (**4.02**) was dissolved in THF (6 mL) and taken up in a syringe. Solution i) was vigorously stirred. *Immediately* after the addition of solution ii) (2 mL), solution iii) was infused into the reaction vessel via a syringe pump at the rate of 0.6 mL min^{-1}. At the end of the infusion (10 min), solid benzoic acid (150 mg) was added to arrest the polymerization. The BnO-PEG-*b*-PLGA-OH (**6.10**) was purified by precipitation twice into isopropanol from CH_2Cl_2 and dried at 50 °C under vacuum overnight yielding the desired product as a white solid with M_n (PLGA) = 9,000 g mol^{-1}, ca. 60:40 lactic:glycolic ratio by mass.

^{1}H NMR (500 MHz, $CDCl_3$): δ 7.37-7.27 (m, 5H, OCH_2-*o*-Ph, OCH_2-*m*-Ph, and OCH_2-*p*-Ph), 5.29-5.12 {m, 78H, BnO-PEG-{[OC(O)C*H*$(CH_3)]_n$[OC(O)$CH_2]_n$}OH}, 4.90-4.65 {m, 123H, BnO-PEG-{[OC(O)CH$(CH_3)]_n$[OC(O)C*H*$_2]_n$}OH}, 4.57 (s, 2H, OC*H*$_2$Ph), 4.41-4.22 {m, 4H, BnO-PEG-OCH_2C*H*$_2$O-C(O)C*H*(R)-{[OC(O)CH$(CH_3)]_n$[OC(O)C*H*$_2]_n$}-C(O)C*H*(R)OH}, 3.65 [s, 313 H,

BnO(CH_2CH_2O)$_n$CH_2CH$_2$O-PLGA], and 1.61-1.44 {m, 239 H, BnO-PEG-[OC(O)CH(CH_3)]$_n$OC(O)CH(CH_3)OH}.

SEC (Polystyrene standards) PDI = 1.12.

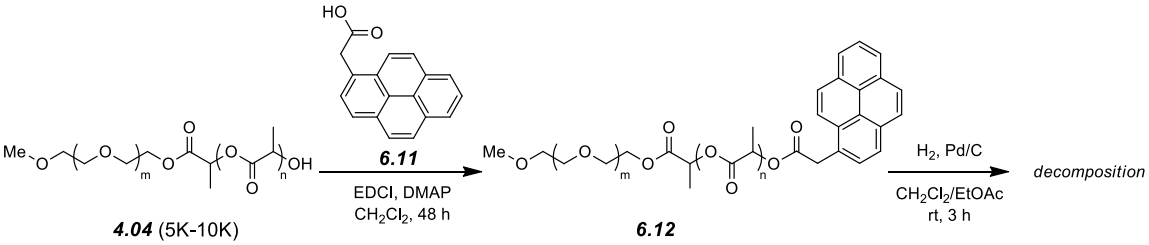

Mono benzyl ether poly(ethylene glycol)-*b*-poly(lactic-*co*-glycolic acid) mono 1-pyreneacetate (6.13). Polymer **6.09** (0.91 g, 0.061 mmol, 1 equiv) was transferred to an oven-dried culture tube with stir bar and dissolved in 5 mL of dry CH_2Cl_2. 1-Pyreneacetic acid (0.063 g, 0.242 mmol, 4 equiv), *N*-(3-dimethylaminopropyl)-*N*'-ethylcarbodiimide hydrochloride (0.136 mg, 0.709 mmol, 12 equiv), and 4-(dimethylamino)pyridine (0.018 g, 0.147 mmol, 2.4 equiv) were added sequentially. The reaction was sealed with a Teflon-lined cap and stirred for 48 hours. The reaction mixture was precipitated directly into *i*-propanol, decanted, and the solid dried under high vacuum at 50 °C overnight. A brown solid (0.710 g, 0.047 mmol, 78%) was obtained.

^{1}H NMR (500 MHz, $CDCl_3$): δ 8.30-7.90 (m, 9H, CH_2-*Pyr*), 5.25-5.11 {m, 133H, MeO-PEG-[OC(O)C*H*(CH$_3$)]$_n$OC(O)CH(CH$_3$)OH}, 4.48-4.23 {m, 4H, MeO-PEG-OCH$_2$CH_2OC(O)C*H*(CH$_3$)[OC(O)CH(CH$_3$)]$_n$C(O)C*H*(CH$_3$)OH}, 3.65 [s, 455 H, MeO(CH_2CH_2O)$_n$CH_2CH$_2$O], 3.38 [s, 3H, CH_3O(CH$_2$CH$_2$O)$_n$-PLA], and 2.80 [s, 2H, Pyr-CH_2C(O)O].

6.13 (105 mg) was redissolved in 4 mL of a 3:1 mixture of CH_2Cl_2:EtOAc and transferred to a round bottom flask containing Pd/C (30 mg, 10% Pd) and a stir bar. The reaction mixture was flushed with N_2 and subsequently purged with

H_2. The reaction was allowed to stir under a hydrogen atmosphere for three hours. The reaction slurry was then filtered through celite, concentrated under reduced pressure, and precipitated into diethyl ether at 0 °C. ^{1}H NMR spectroscopic analysis suggested decomposition of the pyrene moiety.

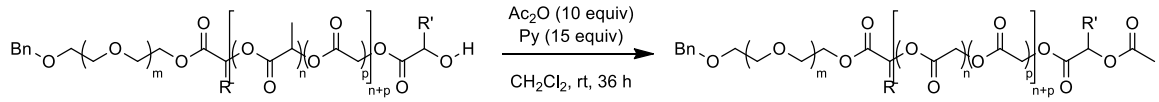

6.10 (6K-11.5K)
R,R' = H or Me

6.15 (6K-11.5K)
R,R' = H or Me

Mono benzyl ether poly(ethylene glycol)-*b*-poly(lactic-*co*-glycolic acid) mono acetate (6.15). Representative procedure; BnO-PEG-*b*-PLGA-OH polymers of different MWs and lactic:glycolic ratios have also been prepared via similar methodology.

BnO-PEG-*b*-PLGA-OH **6.10** (4.61 g, 0.263 mmol, 1 equiv) was transferred to an oven-dried culture tube with a stir bar and dissolved in 20 mL of dry CH_2Cl_2. Pyridine (0.3 mL, 3.88 mmol, 15 equiv) and acetic anhydride (0.25 mL, 2.64 mmol, 10 equiv) were added by syringe. The reaction was capped with a Teflon-lined cap and allowed to stir at room temperature for 36 hours. After the reaction solution was then precipitated directly into ca. 250 mL of *i*-propanol at room temperature. Upon complete precipitation, the *i*-propanol was decanted, and the polymer was dried under high vacuum at 50 °C overnight, yielding the desired product as a white solid (4.16 g, 0.238 mmol, 90.2%) with ca. 100 % acetylation at the polyester terminus.

^{1}H NMR (500 MHz, $CDCl_3$): δ 7.37-7.30 (m, 5H, OCH_2-*o*-Ph, OCH_2-*m*-Ph, and OCH_2-*p*-Ph), 5.29-5.13 {m, 94H, BnO-PEG-{[OC(O)C*H*(CH_3)]$_n$[OC(O)CH_2]$_p$}OAc}, 4.91-4.62 {m, 164H, BnO-PEG-{[OC(O)CH(CH_3)]$_n$[OC(O)C*H*$_2$]$_p$}OAc}, 4.57 (s, 2H, OC*H*$_2$Ph), 4.40-4.22 (m, 3-4H,

BnO-PEG-OCH$_2$C*H$_2$*-OC(O)C*H*(R)-PLGA-C(O)C*H*(R)OAc}, 3.65 [s, 545 H, BnO(C*H$_2$*C*H$_2$*O)$_m$C*H$_2$*CH$_2$O-PLGA], 2.17 {overlapping s's, 1.5H,[313] BnO-PEG-PLGA-C(O)CH$_2$OC(O)C*H$_3$*}, 2.13 {s, 1.5H,[313] BnO-PEG-PLGA-C(O)CH(CH$_3$)OC(O)C*H$_3$*}, and 1.62-1.50 {m, 304 H BnO-PEG-{[OC(O)CH(C*H$_3$*)]$_n$[OC(O)CH$_2$]$_p$}OAc }.

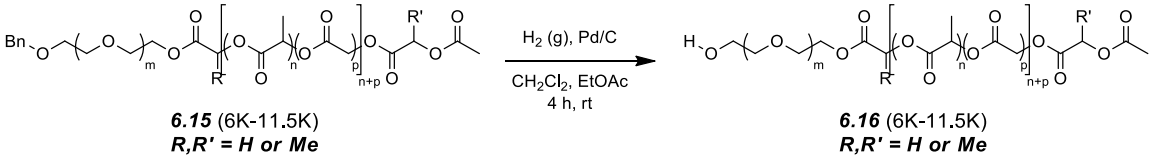

6.15 (6K-11.5K)
R,R' = H or Me

6.16 (6K-11.5K)
R,R' = H or Me

Poly(ethylene glycol)-*b*-poly(lactic-*co*-glycolic acid) mono acetate (6.16). Representative procedure; BnO-PEG-*b*-PLGA-OH polymers of different MWs and lactic:glycolic ratios have also been prepared via similar methodology.

BnO-PEG-*b*-PLGA-OAc **6.15** (4.16 g, 0.238 mmol, 1 equiv) was dissolved in 60 mL of a 1:2 mixture of CH$_2$Cl$_2$:EtOAc. This homogeneous solution was transferred to an oven-dried round bottom flask containing a stir bar and 10 wt% palladium on carbon (0.452 g). The resulting slurry was mixture was flushed sequentially with N$_2$ and then H$_2$. The reaction was maintained under a H$_2$ atmosphere and allowed to stir for four hours. The reaction slurry was then filtered through celite and centrifuged for 20 hours. The supernatant was decanted from the black pellet that resulted from prolonged centrifugation, the supernatant was concentrated under reduced pressure, redissolved in CH$_2$Cl$_2$, and precipitated into ca. 225 mL of *i*-propanol at room temperature. Upon complete precipitation, the *i*-propanol was decanted, and the polymer was dried

[313] Two primary singlets (and associated minor peaks due to differing repeat unit and/or stereoisomer patterns at the end of the polyester) are observed in the ^{1}H NMR spectrum. The total integration of these resonances in the fully acetylated BCP is 3H, although the ratio of the integrations varies by BCP batch.

under high vacuum at 50 °C overnight, yielding the desired product as an off-white solid (4.15 g, 0.237 mmol, 99.5%) with ca. 100 % debenzylation at the polyether terminus.

^{1}H NMR (500 MHz, $CDCl_3$): δ 5.28-5.12 {m, 89H, HO-PEG-{[OC(O)C*H*(CH_3)]$_n$[OC(O)CH_2]$_p$}OAc}, 4.92-4.64 {m, 158H, HO-PEG-{[OC(O)CH(CH_3)]$_n$[OC(O)C*H*$_2$]$_p$}OAc}, 4.38-4.22 (m, 3-4H, HO-PEG-$OCH_2CH_2OC(O)CH$(R){[OC(O)CH(CH_3)]$_n$[OC(O)C*H*$_2$]$_p$}C(O)C*H*(R)OAc}, 3.65 [s, 545 H, HO(CH_2CH_2O)$_m$C*H*$_2$$CH_2$O-PLGA], 2.17 {overlapping s's, 1.5H,[313] HO-PEG-{[OC(O)CH(CH_3)]$_n$[OC(O)CH_2]$_p$}C(O)CH_2OC(O)C*H*$_3$}, 2.13 {s, 1.5H,[313] HO-PEG-{[OC(O)CH(CH_3)]$_n$[OC(O)CH_2]$_p$}C(O)CH(CH_3)OC(O)C*H*$_3$}, and 1.62-1.50 {m, 296 H HO-PEG-{[OC(O)CH(C*H*$_3$)]$_n$[OC(O)CH_2]$_p$}OAc }.

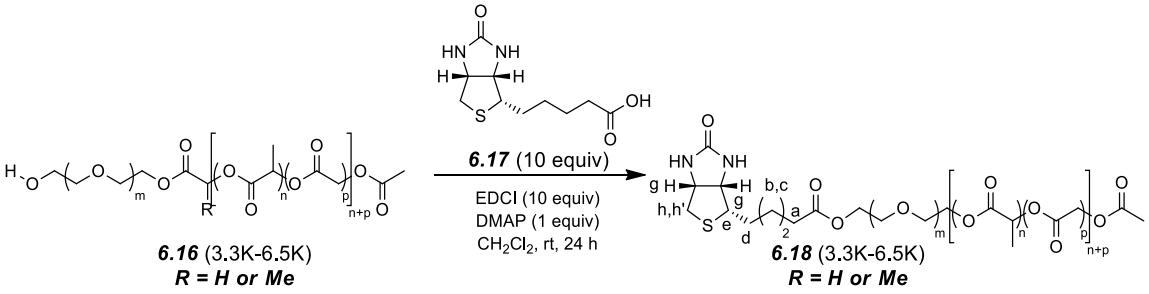

Mono biotin poly(ethylene glycol)-*b*-poly(lactic-*co*-glycolic acid) acetate (6.18). HO-PEG-*b*-PLGA-OAc **6.16** (0.146 g, 0.0146 mmol, 1 equiv) was dissolved in 1.5 mL of dry CH_2Cl_2, and this homogeneous solution was transferred to an oven-dried culture tube with stir bar. Biotin was added (35.6 mg, 0.146 mmol, 10 equiv), EDCI (28.0 mg, 0.146 mmol, 10 equiv), and DMAP (1.8 mg, 0.0146 mmol, 1 equiv) were added sequentially. The reaction vessel was capped with a Teflon-lined cap and allowed to stir for 24 hours. The reaction was then precipitated directly into *i*-propanol at room temperature, filtered over a glass frit, and dried under high vacuum at 50 °C overnight. ^{1}H NMR

spectroscopic analysis determined that unreacted biotin likely was contaminating the sample. The polymer was redissolved in dichloromethane, filtered through a cotton plug, re-precipitated into *i*-propanol at room temperature, and again dried under high vacuum at 50 °C overnight, yielding the desired product as a white solid (0.088 g, 0.0088 mmol, 69.3%).

^{1}H NMR (500 MHz, $CDCl_3$): δ 5.29-5.10 {m, 44H, Biotin-PEG-{[OC(O)C*H*(CH_3)]$_n$[OC(O)CH_2]$_p$}OAc}, 4.93-4.63 {m, 112H, Biotin-PEG-{[OC(O)CH(CH_3)]$_n$[OC(O)C*H*$_2$]$_p$}OAc}, 4.54-4.51 (m, 1H, H_g), 4.34-4.20 {m, 4-5H, Biotin-PEG-OCH_2C*H*$_2$-OC(O)C*H*(R)-PLGA-C(O)C*H*(R)OAc and H_f}, 3.65 [s, 300 H, Biotin-(C*H*$_2$C*H*$_2$O)$_m$C*H*$_2$$CH_2$O-PLGA], 3.19-3.15 (m, 1H, H_e), 2.93 (dd, *J* = 12.9, 5.1 Hz, 1H, H_h), 2.74 (d, *J* = 12.9 Hz, 1H, $H_{h'}$), 2.37 (t, *J* = 7.3 Hz, 2H, H_a), 2.22-2.17 [overlapping s's, 1.5H,[313] Biotin-PEG-PLGA-C(O)CH_2OC(O)C*H*$_3$ and H_a], 2.13 [s, 1.5H,[313] Biotin-PEG-PLGA-C(O)CH(CH_3)OC(O)C*H*$_3$], and 1.62-1.50 {m, 147 H Biotin-PEG-{[OC(O)CH(C*H*$_3$)]$_n$[OC(O)CH_2]$_p$}OAc, H_b, H_c, and H_d}.

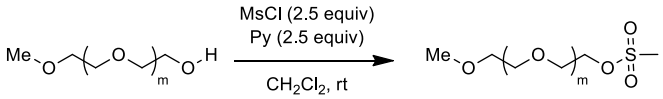

4.03 (5K) ***6.19*** (5K)

Mono methyl ether poly(ethylene glycol) mesylate (6.19). MeO-PEG-OH **4.03** (1.00 g, 0.200 mmol, 1 equiv) was dissolved in 5 mL of dry CH_2Cl_2, and allowed to sit over activated 3Å molecular sieves overnight. This homogeneous solution was then transferred to an oven-dried culture tube with stir bar, and pyridine (80 µL, 0.989 mmol, 5 equiv) and methanesulphonyl chloride (75 µL, 0.969 mmol, 4.8 equiv) were added sequentially. The reaction vessel was capped with a Teflon-lined cap and allowed to stir overnight. The reaction was then precipitated directly into diethyl ether at 0 °C, filtered through a paper filter on a Buchner

funnel, and dried under house vacuum. The product was isolated as a white solid (0.697 g, 0.139 mmol, 69.7%).

^{1}H NMR (500 MHz, $CDCl_3$): δ 4.39 [non-first order t, *J* = 4.4 Hz, 2H, MeO-PEG-CH_2CH_2O-S(O)$_2CH_3$], 3.65 [s, 455 H, OMe-(C*H*$_2$C*H*$_2$O)$_m$C*H*$_2$CH$_2$O-S(O)$_2CH_3$], 3.38 [s, 3H, C*H*$_3$O-PEG-CH_2CH_2O-S(O)$_2CH_3$], and 3.09 [s, 3H, CH_3O-PEG-CH_2CH_2O-S(O)$_2$C*H*$_3$].

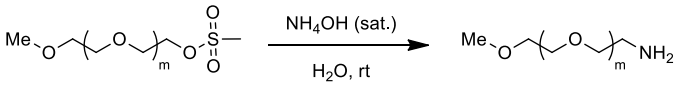

6.19 (5K) ***6.20*** (5K)

Mono methyl ether poly(ethylene glycol) amine (6.20). MeO-PEG-OMs **6.19** (0.780 g, 0.0156 mmol, 1 equiv) was dissolved in 4.0 mL of dry DMF, in an oven-dried culture tube with stir bar. Sodium azide (0.101 g, 1.55 mmol, 10 equiv) was added and the originally water-white solution was noted to quickly turn to a yellow/brown tint. The reaction vessel was capped with a Teflon-lined cap and allowed to stir overnight. The reaction was then precipitated directly into diethyl ether at 0 °C, filtered through a paper filter on a Buchner funnel, and dried under high vacuum for three hours at 80 °C and then under high vacuum at room temperature for 48 hours. The product was isolated as a slightly brown solid (0.680 g, 0.136 mmol, 87.2%).

^{1}H NMR (500 MHz, $CDCl_3$): δ 3.65 [s, 455 H, OMe-(C*H*$_2$C*H*$_2$O)$_m$C*H*$_2$CH$_2$O-NH_2], 3.38 [s, 3H, C*H*$_3$O-PEG-NH_2], 2.89 [t, *J* = 5.2 Hz, 2H, CH_3O-PEG-CH_2C*H*$_2$O-NH_2], and 1.9 [br s, 2H, CH_3O-PEG-N*H*$_2$].

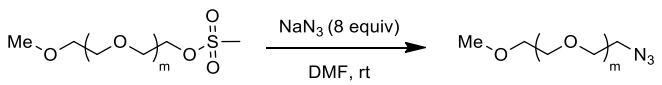

6.19 (5K) ***6.25*** (5K)

Mono methyl ether poly(ethylene glycol) azide (6.20). MeO-PEG-OMs **6.19** (3.0 g, 0.60 mmol, 1 equiv) was dissolved in 20 mL of distilled water in an oven-dried round bottom flask containing a stir bar and fitted with a condenser. The solution was buffered with $NaHCO_3$ (ca. 150 mg), and the pH of the solution was measured to be eight. Sodium azide (0.078 g, 1.2 mmol, 2 equiv) was added and the solution was refluxed overnight. The reaction was extracted with 250 mL of DCM (x2), dried over $MgSO_4$, the solid removed by filtration through a paper filter, and dried under reduced pressure. The residue was redissolved in DCM and precipitated into diethyl ether at 0 °C. The resulting white powder was dried high vacuum overnight The product was isolated as a white solid (2.21 g, 0.442 mmol, 74%).

^{1}H NMR (500 MHz, $CDCl_3$): δ 3.65 [s, 455 H, OMe-(CH_2CH_2O)$_m$CH_2CH_2O-N_3], 3.40 [t, *J* = 5.1 Hz, 2H, CH_3O-PEG-CH_2CH_2O-N_3] and 3.38 [s, 3H, CH_3O-PEG-N_3].

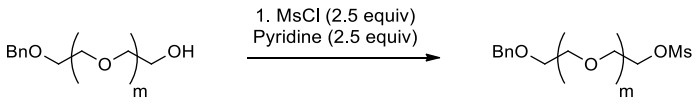

6.08 (3.3K) ***6.22*** (3.3K)

Mono benzyl ether poly(ethylene glycol) mesylate (6.22). BnO-PEG-OH **6.08** (0.452 g, 0.137 mmol, 1 equiv) was dissolved in 2.0 mL of dry CH_2Cl_2, in an oven-dried 3 mL vial with stir bar. Pyridine was added (60 µL, 0.742 mmol, 5.4 equiv) and methanesulphonyl chloride (50 µL, 0.646 mmol, 4.7 equiv) were added sequentially. The reaction vessel was capped with a Teflon-lined cap and

allowed to stir for 18 hours. The reaction was then precipitated directly into 50 mL of diethyl ether at 0 °C, filtered through a paper filter, and dried under house vacuum for three hours. The product was isolated as a white solid (0.407 g, 0.123 mmol, 89.8%).

^{1}H NMR (500 MHz, $CDCl_3$): δ 7.36-7.26 (m, 5H, *o*-Ph, *m*-Ph, *p*-Ph), 4.57 [s, 2H, PhC*H*$_2$O-PEG-OTs], 4.39 [non-first order t, 2H, *J* = 4.5 Hz, PhCH_2O-PEG-CH_2C*H*$_2$O-S(O)$_2$CH_3], 3.65 [s, 455 H, BnO-(C*H*$_2$C*H*$_2$O)$_m$C*H*$_2$CH_2O-OTs], and 3.07 [s, *J* = 5.2 Hz, 3H, BnO-PEG-CH_2CH_2O-S(O)$_2$C*H*$_3$].

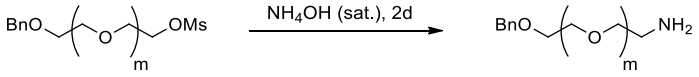

6.08 (3.3K) ***6.22*** (3.3K)

Mono benzyl ether poly(ethylene glycol) amine (6.22).

BnO-PEG-OMs (0.892 g, 0.270 mmol, 1 equiv) was dissolved in 5 mL of distilled water, and this homogeneous solution was transferred to an oven-dried culture tube with stir bar. The solution was further diluted with 20 mL of an NH_4OH (sat) aqueous solution. The reaction vessel was capped with a Teflon-lined cap and allowed to stir at room temperature for two days. The aqueous solution was extracted with 100 mL of CH_2Cl_2 (x3), the extract dried over $MgSO_4$, the solid removed via filtration, and the DCM solution concentrated under reduced pressure. The residue was redissolved in CH_2Cl_2 and precipitated into diethyl ether at 0 °C. The white solid was filtered through a paper filter and dried under house vacuum at room temperature for four days, yielding the desired product as a white solid (0.701 g, 0.212 mmol, 78.5%).

^{1}H NMR (500 MHz, $CDCl_3$): δ 7.36-7.26 (m, 5H, *o*-Ph, *m*-Ph, *p*-Ph), 4.57 [s, 2H, PhC*H*$_2$O-PEG-NH_2], 3.65 [s, 300 H, BnO-(C*H*$_2$C*H*$_2$O)$_m$C*H*$_2$CH_2-NH_2], 2.89 [t, *J* =

5.2 Hz, 2H, BnO-PEG-OCH_2CH_2-NH_2], and 1.9 [br s, 2H, BnO-$(CH_2CH_2O)_mCH_2CH_2$-NH_2].

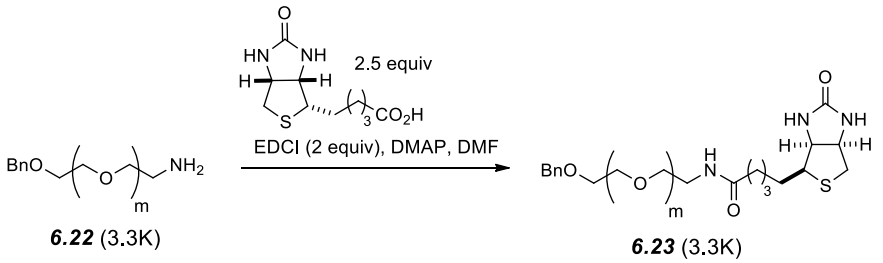

Mono benzyl ether poly(ethylene glycol) biotin (6.23). BnO-PEG-NH_2 **6.22** (0.088 g, 0.029 mmol, 1 equiv) was dissolved in 0.5 mL of dry DMF (dried over 3Å MS overnight), and this homogeneous solution was transferred to an oven-dried vial with stir bar. In a separate, oven-dried culture tube with stir bar, biotin (17.9 mg, 0.072 mmol, 2.5 equiv), EDCI (11.2 mg, 0.058 mmol, 2 equiv), and DMAP (3.2 mg, 0.026 mmol, 0.9 equiv) were co-dissolved. The solution of **6.22** was added, the reaction vessel was capped with a Teflon-lined cap and allowed to stir overnight. The reaction was then diluted with 5 mL of distilled water, extracted three times with 20 mL of CH_2Cl_2, dried over $MgSO_4$, concentrated under reduced pressure, redissolved in CH_2Cl_2, and finally precipitated into *i*-propanol at 0 °C. The heterogeneous suspension was cooled further in a freezer for several hours, filtered, and dried under high vacuum at 50 °C overnight. ^{1}H NMR spectroscopic analysis determined approximately 90% conversion in the isolated product, a white solid (0.013 g, 0.0043 mmol, 15%).

^{1}H NMR (500 MHz, $CDCl_3$): δ 4.57 [s, 2H, PhCH_2O-$(CH_2CH_2O)_mCH_2CH_2$O-NH-Biotin], 4.51 (br dd, J = 7, 6 Hz, 1H, H_g), 4.33 (br dd, J = 5, 4 Hz, 1H, H_f), 3.65 [s, 300 H, BnO-($CH_2CH_2O)_mCH_2CH_2$O-NH-Biotin], 3.17 [m, 2H, BnO-$(CH_2CH_2O)_mCH_2CH_2$-NH-Biotin], 2.93 (dd, J = 12.9, 5.1 Hz, 1H, H_h), 2.74 (d, J =

12.9 Hz, 1H, $H_{h'}$), 2.22 (m, 2H, H_a), 1.72-1.62 (m, 4H, H_d and H_b), and 1.46 (ddt, xx Hz 2H, H_c).

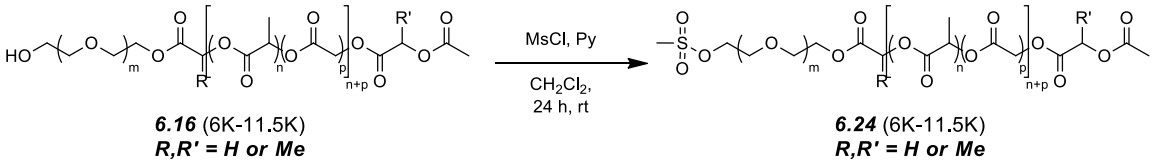

6.16 (6K-11.5K)
R,R' = H or Me

6.24 (6K-11.5K)
R,R' = H or Me

Tosyl poly(ethylene glycol)-*b*-poly(lactic-*co*-glycolic acid) acetate (6.24). Representative procedure; HO-PEG-*b*-PLGA-OH and HO-PEG-*b*-PLA-OH polymers of different MWs and lactic:glycolic ratios have also been prepared via similar methodology.

HO-PEG-*b*-PLGA-OAc **6.16** (3.6 g, 0.181 mmol, 1 equiv) was dissolved in 10 mL of dry CH_2Cl_2. This homogeneous solution was transferred to an oven-dried culture tube containing a stir bar. To the solution, pyridine (0.50 mL, 6.18 mmol, 34 equiv) and mesyl chloride (0.47 mL, 6.07 mmol, 34 equiv) were added sequentially. The reaction was capped with a Teflon-lined cap and allowed to stir at room temperature for 24 hours. The slightly yellowed solution was then precipitated directly into *i*-propanol, the solvent decanted, and the solid polymer dried under high vacuum at 50 °C overnight, yielding the desired product as a white solid (2.25 g, 0.129 mmol, 71.3% recovery, ca. 35% yield) with ca. 40-50 % mesylation at the polyether terminus.

^{1}H NMR (500 MHz, $CDCl_3$): δ 5.28-5.12 {m, 86H, MsO-PEG-{[OC(O)C*H*(CH_3)]$_n$[OC(O)CH_2]$_p$}OAc}, 4.92-4.64 {m, 162H, MsO-PEG-{[OC(O)CH(CH_3)]$_n$[OC(O)C*H*$_2$]$_p$}OAc}, 4.39 [non-uniform t, *J* = 4.4 Hz, 2H (integration of 1H due to 50% conversion), $CH_3S(O)_2OCH_2CH_2O$-PEG-PLGA-OAc], 4.34-4.23 (m, 3-4H, MsO-PEG-OCH_2C*H*$_2$OC(O)C*H*(R)-PLGA-C(O)C*H*(R)OAc}, 3.65 [s, 545 H, MsO-(C*H*$_2$C*H*$_2$O)$_m$C*H*$_2$CH_2O-PLGA], 3.07 [s, 3H

(integration of 1H due to 50% conversion), C*H*$_3$S(O)$_2$O-PEG-PLGA-OAc], 2.17 {overlapping s's, 1.5H,[313] MsO-PEG-PLGA-C(O)CH$_2$OC(O)C*H*$_3$}, 2.13 {s, 1.5H,[313] MsO-PEG-PLGA-C(O)CH(CH$_3$)OC(O)C*H*$_3$}, and 1.62-1.50 {m, 288 H MsO-PEG-{[OC(O)CH(C*H*$_3$)]$_n$[OC(O)CH$_2$]$_p$}OAc }.

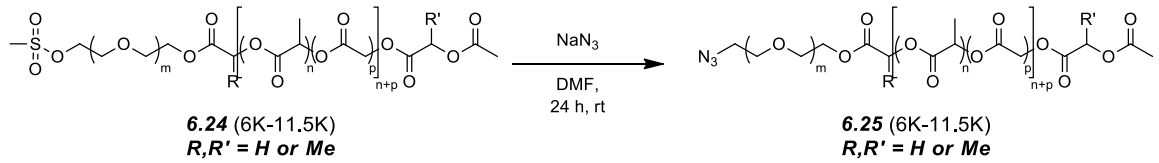

6.24 (6K-11.5K)
R,R' = H or Me

6.25 (6K-11.5K)
R,R' = H or Me

Azido poly(ethylene glycol)-*b*-poly(lactic-*co*-glycolic acid) acetate (6.25). Representative procedure; MsO-PEG-*b*-PLGA-OH and MsO-PEG-*b*-PLA-OH polymers of different MWs and lactic:glycolic ratios have also been prepared via similar methodology.

MsO-PEG-*b*-PLGA-OAc **6.24** (1.65 g, 0.094 mmol, 1 equiv) was dissolved in 7 mL of DMSO dried over activated 4Å sieves and transferred to an oven-dried culture tube containing a stir bar. Sodium azide (71 mg, 1.09 mmol, 12 equiv) was added. This homogeneous solution was capped with a Teflon-lined cap and slowly became tinted light orange as it stirred was at room temperature for 24 hours. The slightly orange solution was then precipitated directly into *i*-propanol, the solvent decanted, and the solid polymer dried under high vacuum at 50 °C overnight, yielding the desired product (0.91 g, 0.052 mmol, 57.1%) with ca. 40-50 % azide incorporation at the polyether terminus.

^{1}H NMR (500 MHz, $CDCl_3$): δ 5.28-5.12 {m, 86H, N_3-PEG-{[OC(O)C*H*(CH$_3$)]$_n$[OC(O)CH$_2$]$_p$}OAc}, 4.92-4.64 {m, 162H, N_3-PEG-{[OC(O)CH(CH$_3$)]$_n$[OC(O)C*H*$_2$]$_p$}OAc}, 4.39 [non-uniform t, *J* = 4.4 Hz, 2H (integration of 1H due to 50% conversion), N_3-C*H*$_2$CH$_2$O-PEG-PLGA-OAc], 4.34-4.23 (m, 3-4H, N_3-PEG-OCH$_2$C*H*$_2$OC(O)C*H*(R)-PLGA-C(O)C*H*(R)OAc}, 3.65 [s,

545 H, N_3-(C*H*$_2$C*H*$_2$O)$_m$C*H*$_2$CH$_2$O-PLGA-OAc], 2.17 {overlapping s's, 1.5H,[313] N_3-PEG-PLGA-C(O)CH$_2$OC(O)C*H*$_3$}, 2.13 {s, 1.5H,[313] N_3-PEG-PLGA-C(O)CH(CH$_3$)OC(O)C*H*$_3$}, and 1.62-1.50 {m, 288 N_3-PEG-{[OC(O)CH(C*H*$_3$)]$_n$[OC(O)CH$_2$]$_p$}OAc }.

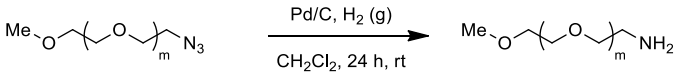

6.25 (5K) ***6.20*** (5K)

Mono methyl ether poly(ethylene glycol) amine (6.20). MeO-PEG-N_3 **6.25** (0.180 g, 0.0360 mmol, 1 equiv) was dissolved with gentle heating in 10 mL of absolute ethanol, in a round bottom flask containing a stir bar and palladium on carbon (0.055 g). The flask was purged with N_2 and subsequently purged with H_2. After stirring under a hydrogen atmosphere for 24 hours, five mL of the solution was removed, filtered through Celite,® and precipitated directly into diethyl ether at 0 °C. The solvent was decanted from the white solid and dried under vacuum. Analysis by ^{1}H NMR spectroscopy showed a quantitative disappearance of the methylene resonance adjacent to the azide.

^{1}H NMR (500 MHz, $CDCl_3$) matched the previously reported data.

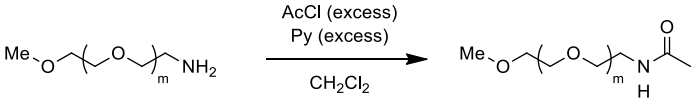

6.20 (5K) ***6.29*** (5K)

Mono methyl ether poly(ethylene glycol) methyl amide (6.29). MeO-PEG-NH_2 **6.20** (0.045 g, 0.009 mmol, 1 equiv) was dissolved in 0.5 mL of $CDCl_3$ in a 3mL vial containing a stir bar. Pyridine (12 µL, 0.148 mmol, 16.4 equiv) and acetyl chloride (10 µL, 0.141 mmol, 15.7 equiv) were added sequentially to the solution.

The reaction was capped and stirred overnight. Analysis of the crude ^{1}H NMR spectrum was inconclusive. The $CDCl_3$ solution was then precipitated into diethyl ether at 0 °C, the solvent decanted from the solute, and the isolated solid dried. The purified ^{1}H NMR spectrum confirmed the absence of a methylene adjacent to an azide and the presence of an amide in the isolated, slightly yellow solid (0.012 g, 0.0024 mmol, 26.7%).

^{1}H NMR (500 MHz, $CDCl_3$)[314]: δ 4.32 and 4.22 [non-first order t's, *J* = 5 Hz, 2H total, OMe-$(CH_2CH_2O)_mCH_2CH_2$-NHAc], 3.65 [s, 455 H, OMe-$(CH_2CH_2O)_mCH_2CH_2$-NHAc], 3.38 [s, 3H, CH_3O-PEG-NHAc], and 2.08 [t, *J* = 5.2 Hz, 3H, CH_3O-PEG-NHC(O)CH_3].

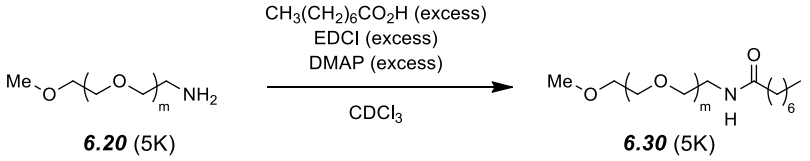

6.20 (5K) ***6.30*** (5K)

Mono methyl ether poly(ethylene glycol) octyl amide (6.30). MeO-PEG-NH_2 **6.20** (0.045 g, 0.009 mmol, 1 equiv) was dissolved in 0.5 mL of $CDCl_3$ in a 3mL vial containing a stir bar. In a separate vial, octanoic acid (20 µL, 0.126 mmol, 14 equiv), EDCI (15 mg 0.078 mmol, 10 equiv), and DMAP (3 mg 0.025 mmol, 3 equiv) were added co-dissolved in 0.5 mL of dry $CDCl_3$. The two solutions were mixed and stirred overnight. Analysis of the crude ^{1}H NMR spectrum was inconclusive. The $CDCl_3$ solution was then precipitated into *i*-propanol at 0 °C, the solvent decanted from the solute, and the isolated solid dried. The purified ^{1}H NMR spectrum confirmed the absence of a methylene adjacent to an azide and the presence of an amide in the isolated white solid.

[314] The ^{1}H NMR spectrum also exhibited resonances consistent with pyridine contamination.

^{1}H NMR (500 MHz, $CDCl_3$): δ 4.33 and 4.22 [non-first order t's, *J* = 5 Hz, 2H total, OMe-PEG-CH_2CH_2-NHC(O)$(CH_2)_6CH_3$], 3.65 [s, 455 H, OMe-$(CH_2CH_2O)_mCH_2CH_2$-NHC(O)$(CH_2)_6CH_3$], 3.38 [s, 3H, CH_3O-PEG-NHC(O)$(CH_2)_6CH_3$], 2.33 [t, *J* = 7.5 Hz, 2H, CH_3O-PEG-NHC(O)$CH_2(CH_2)_5CH_3$], 1.62 [app pent, *J* = 7.1 Hz, 2H, CH_3O-PEG-NHC(O)$CH_2CH_2(CH_2)_4CH_3$], 1.62 [m, 8H, CH_3O-PEG-NHC(O)$CH_2CH_2(CH_2)_4CH_3$], and 0.88 [t, *J* = 6.6 Hz, 3H, CH_3O-PEG-NHC(O)$(CH_2)_6CH_3$].

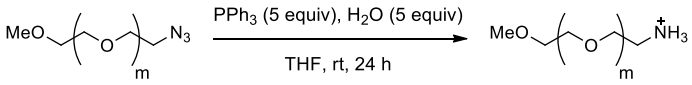

6.25 (5K) ***6.28*** (5K)

Mono methyl ether poly(ethylene glycol) amine (6.28). MeO-PEG-N_3 **6.25** (1.0 g, 0.20 mmol, 1 equiv) was dissolved in seven mL of THF, in a culture tube containing a stir bar. Triphenylphosphine (0.262 g, 1.0 mmol, 5 equiv) and water (20 µL, 1.1 mmol, 11 equiv) were added sequentially to the polymer solution. The reaction was capped with a Teflon-lined cap and stirred overnight. The reaction was concentrated under reduced pressure, the residue redissolved in CH_2Cl_2, the solution precipitated into diethyl ether at 0 °C, and the solid filtered. Triphenylphosphine oxide was a noted contaminant, and so the polymer was redissolved in water, extracted with CH_2Cl_2 (x3), the organic phase washed with brine and then dried over $MgSO_4$. The CH_2Cl_2 layer was then filtered through a paper filter, concentrated to a small volume under reduced pressure, and precipitated in diethyl ether at 0 °C. The isolated solid still retained triphenylphosphine oxide, and so the polymer was redissolved in CH_2Cl_2, precipitated into *i*-propanol, and cooled in a freezer. The liquid was decanted, and the solid dried under vacuum.

^{1}H NMR (500 MHz, $CDCl_3$) matched the previously reported data with a small amount of contaminating triphenylphosphine oxide.

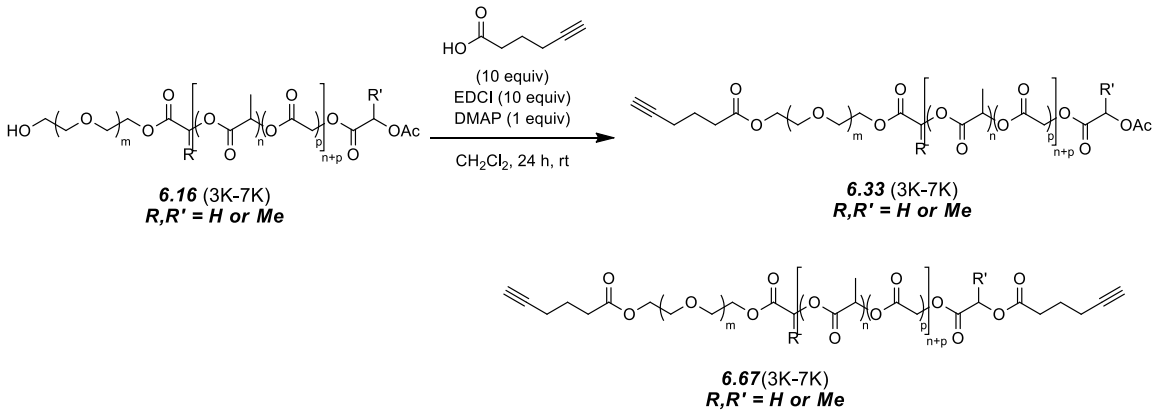

Mono 5-hexyne ester poly(ethylene glycol)-*b*-poly(lactic-*co*-glycolic acid) acetate (6.33). HO-PEG-*b*-PLGA-OAc **6.16** (.114 g, 0.011 mmol, 1 equiv) was dissolved in one mL of dry CH_2Cl_2 in an oven-dried culture tube with stir bar. To this homogeneous solution, hexynoic acid (15 µL, 0.136 mmol, 12 equiv), EDCI (22 mg 0.114 mmol, 10 equiv), and DMAP were added. The reaction was sealed with a Teflon-lined cap and allowed to stir at room temperature overnight. The solution was then precipitated directly into *i*-propanol at room temperature, the solvent decanted, and the solid polymer dried under high vacuum at 50 °C overnight, yielding the desired product as a white solid (0.085 g, 0.0095 mmol, 75% yield). Due to incomplete acetylation at the polyester terminus, the product was an ca. 2:1 mixture of **6.33**:di-esterified compound **6.67**.

^{1}H NMR (500 MHz, $CDCl_3$): δ 5.29-5.10 {m, 53H, $HCCCH_2CH_2CH_2C(O)O$-PEG-{[$OC(O)CH(CH_3)]_n[OC(O)CH_2]_p$}OAc}, 4.92-4.65 {m, 118H, $HCCCH_2CH_2CH_2C(O)O$-PEG-{[$OC(O)CH(CH_3)]_n[OC(O)CH_2]_p$}OAc}, 4.34-4.23 (m, 5H, $HCCCH_2CH_2CH_2C(O)O$-CH_2CH_2O-PEG-$OCH_2CH_2OC(O)CH$(R)-PLGA-

C(O)C*H*(R)OAc}, 3.65 [s, 330 H, HCCCH$_2$CH$_2$CH$_2$C(O)O(C*H$_2$*C*H$_2$*O)$_m$C*H$_2$*CH$_2$O-PLGA-OAc], 2.49 [t, *J* = 7.4 Hz, 3H HCCCH$_2$CH$_2$C*H$_2$*C(O)O-PEG-PLGA-OAc], 2.27 [dt, *J* = 6.9, 2.6 Hz, 2H, HCCC*H$_2$*CH$_2$CH$_2$C(O)O-PEG-PLGA-OAc], 2.17 {overlapping s's, 1.3H,[313] HCCCH$_2$CH$_2$CH$_2$C(O)O-PEG-PLGA-OC(O)C*H$_3$*}, 2.13 [s, 1.7H,[313] HCCCH$_2$CH$_2$CH$_2$C(O)O-PEG-PLGA-OC(O)C*H$_3$*], 1.98 [t, *J* = 2.6 Hz, 1H, *H*CCCH$_2$CH$_2$CH$_2$C(O)O-PEG-PLGA-OAc], and 1.85 [app pent, *J* = 7.2 Hz, 2H HCCCH$_2$C*H$_2$*CH$_2$C(O)O-PEG-PLGA-OAc], and 1.61-1.51 {m, 176 H, HCCCH$_2$CH$_2$CH$_2$C(O)O-PEG-{[OC(O)CH(C*H$_3$*)]$_n$[OC(O)CH$_2$]$_p$}OAc}.

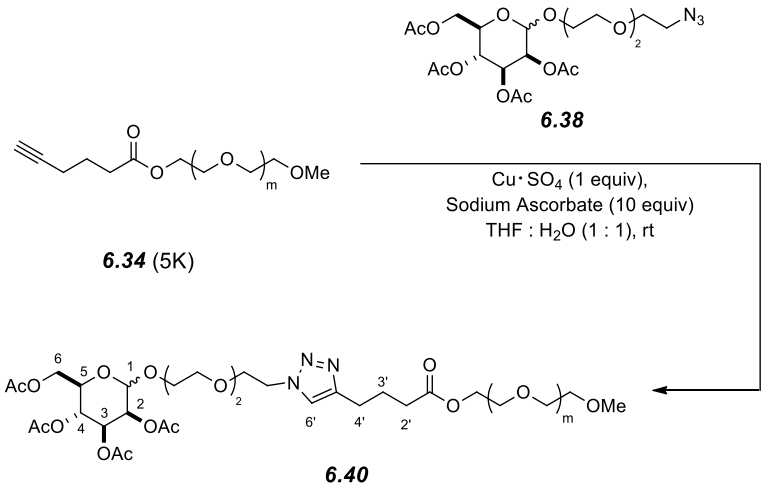

Mono methyl ether poly(ethylene glycol) penta-acetate mannose (6.40). OMe-PEG-OC(O)CH$_2$CH$_2$CH$_2$CCH **6.34** (0.080 g, 0.016 mmol, 1 equiv) was dissolved in 0.5 mL of dry THF in an oven-dried culture tube with stir bar. In a separate vial, **6.38** (7.5 mg, 0.015 mmol, 1 equiv) was dissolved in 0.5 mL of dry THF. The two solutions were combined. In a third vial, copper (II) sulfate pentahydrate (5 mg, 0.020 mmol, 1.3 equiv) and sodium ascorbate (25 mg 0.126 mmol, 7.9 equiv) were dissolved in distilled water. The solutions were combined and sealed with a Teflon-lined cap and allowed to stir at room temperature for 14 h. The reaction was diluted with 10 mL of a 0.01 M EDTA aqueous solution,

extracted with 75 mL of DCM (3x), dried over $MgSO_4$, and concentrated under reduced pressure, returning 58.6 mg of crude material. The residue was then precipitated into diethyl ether at 0 °C, the solid filtered through a paper filter, and the solid polymer dried under high vacuum at 50 °C overnight, yielding the desired product as a white solid (0.0125 g, 0.003 mmol, 75% conversion, 16% yield).

^{1}H NMR (500 MHz, $CDCl_3$): δ 7.49 (s, 1H, H6'), 5.38-5.25 (m, 3H, H2, H3, and H4), 4.88 (d, *J* = 1.3 Hz, 1H, H1), 4.52 [t, *J* = 5.3 Hz, MeO-PEG-triazole-C*H*$_2$CH$_2$O(CH$_2$CH$_2$O)$_2$-mannose], 4.29 (dd, *J* = 12.2, 4.9 Hz, H6a), 4.23 (m, 2H, , MeO-PEG-triazole-(CH$_2$CH$_2$O)$_2$CH$_2$C*H*$_2$O-mannose), 4.11 (dd, *J* = 12.2, 2.2 Hz, 1H, H6b), 4.05 (m, 1H, H5), 3.65 [s, 461 H, mannose-triazole-(C*H*$_2$C*H*$_2$O)$_m$-OMe], 3.38 (s, 3H, C*H*$_3$O-(CH$_2$CH$_2$O)$_m$-triazole-mannose], 2.77 [t, *J* = 7.5 Hz, 2H, H4'], 2.42 (t, *J* = 7.4 Hz, 2H, H2'), 2.16 (s, 3H, OC(O)C*H*$_3$], 2.11 (s, 3H, OC(O)C*H*$_3$], 2.07-1.96 (m, 2H, H3'), 2.04 (s, 3H, OC(O)C*H*$_3$], and 2.00 (s, 3H, OC(O)C*H*$_3$].

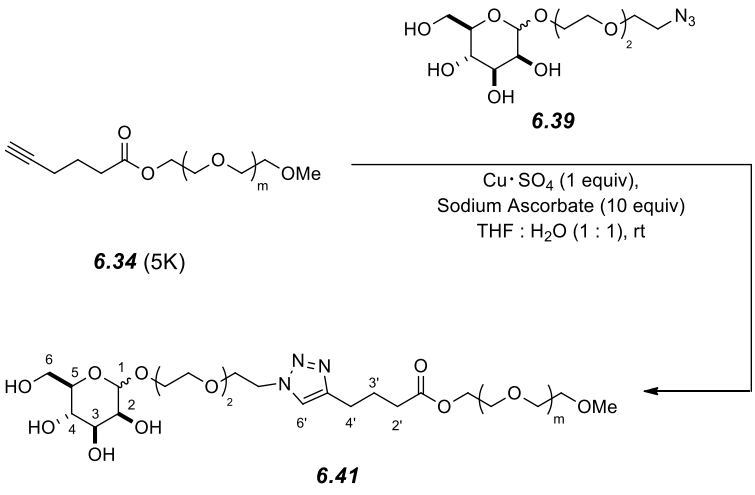

Mono methyl ether poly(ethylene glycol) mannose (6.41). OMe-PEG-OC(O)CH$_2$CH$_2$CH$_2$CCH **6.34** (0.075 g, 0.015 mmol, 1 equiv) was dissolved in 1.0 mL of dry THF in an oven-dried culture tube with stir bar. In a separate vial, **6.39**

(5.1 mg, 0.015 mmol, 1 equiv) was dissolved in 0.5 mL of distilled water. The two solutions were combined. In a third vial, copper (II) sulfate pentahydrate (5 mg, 0.020 mmol, 1.3 equiv) and sodium ascorbate (25 mg 0.126 mmol, 7.9 equiv) were dissolved in 0.5 mL of distilled water. The solutions were combined and sealed with a Teflon-lined cap and allowed to stir at room temperature for overnight. The reaction was extracted with 150 mL of DCM, dried over $MgSO_4$, and concentrated under reduced pressure. The residue was then precipitated into diethyl ether at 0 °C, the solid filtered through a paper filter, and the solid polymer dried under vacuum. The residue was redissolved in DCM, washed with 10 mL of a 0.01 M EDTA aqueous solution, and re-precipitated.

^{1}H NMR (500 MHz, $CDCl_3$): δ 7.6 (br s, 1H, H6'), 4.54 [app br s, MeO-PEG-triazole-C*H*$_2$CH$_2$O(CH$_2$CH$_2$O)$_2$-mannose], 4.23 (br t, *J* = 5 Hz, 2H, MeO-PEG-triazole-(CH$_2$CH$_2$O)$_2$CH$_2$C*H*$_2$O-mannose), 3.65 [s, 468 H, MeO-(C*H*$_2$C*H*$_2$O)$_m$-triazole-mannose, H1, H2, H3, H4, H5, H6a, H6b], 3.38 (s, 3H, C*H*$_3$O(CH$_2$CH$_2$O)$_m$-triazole-mannose], 2.78 [app br s, 2H, H4'], 2.43 (br t, *J* = 6 Hz, 2H, H2'), and 2.09-1.97 (br m, 2H, H3').

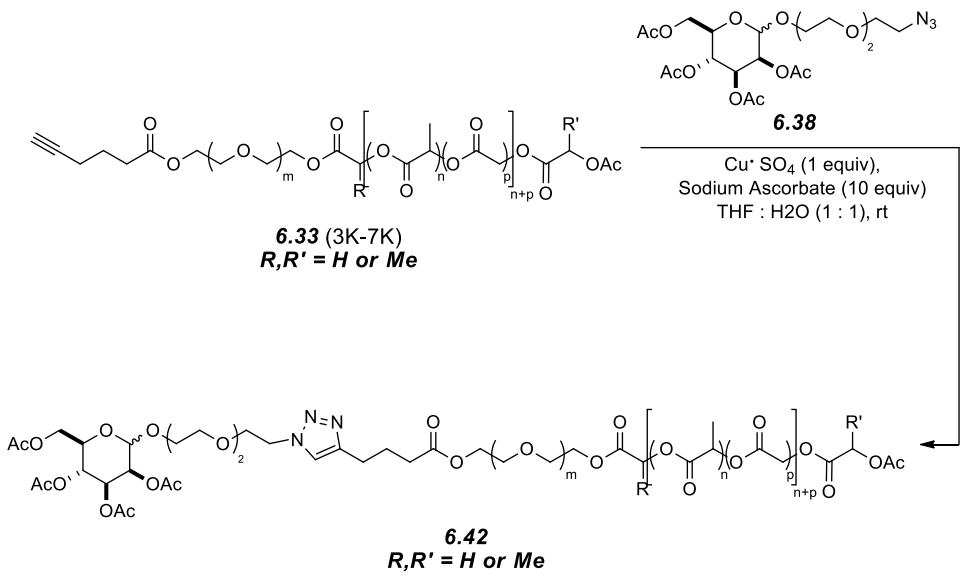

Pentaacetate mannose poly(ethylene glycol)-*b*-poly(lactic-*co*-glycolic acid) acetate (6.42). $HCCCH_2CH_2CH_2O(O)C$-PEG-PLGA-OAc **6.33** (0.100 g, 0.010 mmol, 1 equiv) was dissolved in 0.5 mL of dry THF in an oven-dried culture tube with stir bar. In a separate vial, **6.38** (7.5 mg, 0.015 mmol, 1.5 equiv) was dissolved in 0.5 mL of dry THF. The two solutions were combined. In a third vial, copper (II) sulfate pentahydrate (2.5 mg, 0.010 mmol, 1 equiv) and sodium ascorbate (20 mg 0.1 mmol, 10 equiv) were dissolved in distilled water. The solutions were combined and sealed with a Teflon-lined cap and allowed to stir at room temperature for overnight. The reaction was diluted with 10 mL of a 0.01 M EDTA aqueous solution, extracted with 75 mL of DCM (3x), dried over $MgSO_4$, and concentrated under reduced pressure. The residue was then precipitated into diethyl ether at 0 °C, the solid filtered through a paper filter, and the solid polymer dried under high vacuum at 50 °C overnight, yielding the desired product as a white solid (0.022 g, 0.002 mmol, > 90% conversion, 22% yield).

^{1}H NMR (500 MHz, $CDCl_3$):[315] δ 7.49 (s, 1H, H6'), 5.35 (dd, *J* = 10, 4 Hz, 1H, H3), 5.32-5.08 {m, 43H, mannose-triazole-$CH_2CH_2CH_2C(O)O$-PEG-{[$OC(O)CH(CH_3)]_n[OC(O)CH_2]_p$}OAc, H2, and H4}, 4.91-4.65 {m, 95H, mannose-triazole-$CH_2CH_2CH_2C(O)O$-PEG-{[$OC(O)CH(CH_3)]_n[OC(O)CH_2]_p$}OAc and H1}, 4.52 [t, *J* = 5.0 Hz, mannose-$(OCH_2CH_2)_2OCH_2CH_2$-triazole-$CH_2CH_2CH_2C(O)O$-PEG-PLGA-OAc], 4.34-4.23 (m, ca. 7H, mannose-$OCH_2CH_2(OCH_2CH_2)_2$-triazole-$CH_2CH_2CH_2C(O)O$-PEG-$OCH_2CH_2OC(O)CH$(R)-PLGA-C(O)CH(R)OAc and H6a}, 4.11 (app br d, *J* = 12 Hz, 1H, H6b), 4.06 (m, 1H, H5), 3.65 [s, 336 H, -mannose-triazole-$CH_2CH_2CH_2C(O)O$-$(CH_2CH_2O)_m$-PLGA-OAc], 2.77 [t, *J* = 7.9 Hz, 2H, H4'], 2.42 (t, *J* = 7.4 Hz, 2H, H2'), 2.17 {overlapping s's, 1.3H,[313] mannose-triazole-$CH_2CH_2CH_2C(O)O$-PEG-PLGA-$OC(O)CH_3$}, 2.16 (s, 3H, $OC(O)CH_3$], 2.13 [s, 1.7H,[313] mannose-triazole-$CH_2CH_2CH_2C(O)O$-PEG-PLGA-$OC(O)CH_3$], 2.11 (s, 3H, $OC(O)CH_3$], 2.07-1.96 (m, 2H, H3'), 2.04 (s, 3H, $OC(O)CH_3$], and 1.99 (s, 3H, $OC(O)CH_3$].

[315] Some contaimination was noted from a PEG-*b*-PLGA polymer bearing the alkyne at both the polyether and polyester termini.

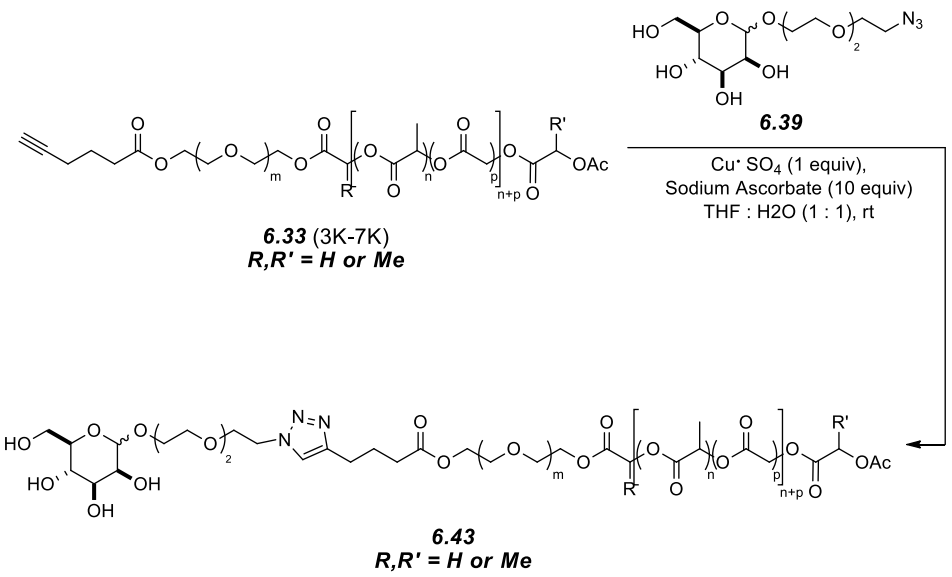

Mannose poly(ethylene glycol)-*b*-poly(lactic-*co*-glycolic acid) acetate (6.43). $HCCCH_2CH_2CH_2O(O)C$-PEG-PLGA-OAc **6.33** (0.096 g, 0.0096 mmol, 1 equiv) was dissolved in 1.0 mL of dry THF in an oven-dried culture tube with stir bar. In a separate vial, **6.39** (8.0 mg, 0.021 mmol, 2.1 equiv) was dissolved in 1.0 mL of distilled water. The two solutions were combined. In a third vial, copper (II) sulfate pentahydrate (6.0 mg, 0.024 mmol, 2.5 equiv) and sodium ascorbate (47 mg 0.24 mmol, 25 equiv) were added, and the culture tube was sealed with a Teflon-lined cap, wrapped in tinfoil, and allowed to stir at room temperature overnight. The reaction was diluted with 2 mL of a 0.01 M EDTA aqueous solution, extracted with 100 mL of DCM (5x), dried over $MgSO_4$, filtered and concentrated under reduced pressure. The residue was then precipitated into ca. 25 mL of diethyl ether, but no obvious precipitate was noted. The cloudy suspension was centrifuged for one hour (4x), and the solid polymer recovered after each hour. The isolated solid material was observed to become whiter with each subsequent centrifuge procedure. The polymer was isolated (0.117 g, 0.0117 mmol, ca. 25-50% conversion).

^{1}H NMR (500 MHz, $CDCl_3$): δ 7.55 (br s, 1H, H6'), 5.32-5.08 {m, 48H, mannose-triazole-$CH_2CH_2CH_2C(O)O$-PEG-{[$OC(O)CH(CH_3)]_n[OC(O)CH_2]_p$}OAc}, 4.91-4.65 {m, 110H, mannose-triazole-$CH_2CH_2CH_2C(O)O$-PEG-{[$OC(O)CH(CH_3)]_n[OC(O)CH_2]_p$}OAc}, 4.52 [br t, *J* = 5 Hz, mannose-$(OCH_2CH_2)_2OCH_2CH_2$-triazole-$CH_2CH_2CH_2C(O)O$-PEG-PLGA-OAc], 4.34-4.23 (m, ca. 6H, mannose-$OCH_2CH_2(OCH_2CH_2)_2$-triazole-$CH_2CH_2CH_2C(O)O$-$(CH_2CH_2O)_m$-$OCH_2CH_2OC(O)CH(R)$\{[$OC(O)CH(CH_3)]_n[OC(O)CH_2]_p$\}$C(O)CH(R)OAc$}, 3.65 [s, 343 H, -$(CH_2CH_2O)_m$-, H1, H2, H3, H4, H5, H6a, and H6b], 2.77 [br t, *J* = 8 Hz, 2H, H4'], 2.57-2.38 (m, 2H, H2'), 2.17 {overlapping s's, 0.8H,[313] PEG-PLGA-$OC(O)CH_3$}, 2.16 (s, 3H, $OC(O)CH_3$], 2.13 [s, 2.2H,[313] PEG-PLGA-$OC(O)CH_3$], and 2.06-1.96 (m, 2H, H3').

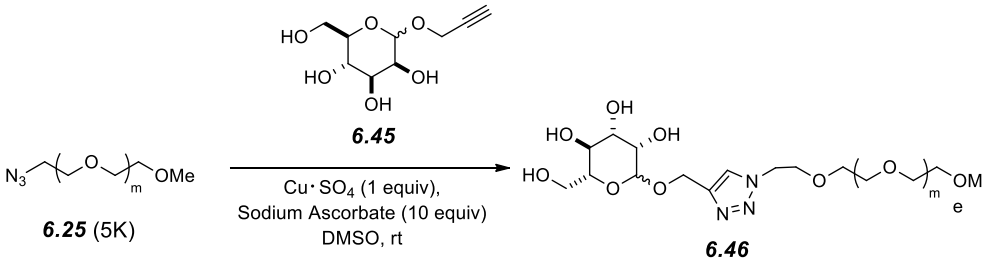

Mono methyl ether poly(ethylene glycol) mannose (6.46). MeO-PEG-N_3 **6.25** (0.175 g, 0.035 mmol, 1 equiv) was dissolved in 1.0 mL of dry DMSO in an oven-dried culture tube with stir bar. Copper (II) sulfate pentahydrate (8.8 mg, 0.035 mmol, 1 equiv) and ascorbic acid (32.9 mg, 0.187 mmol, 5 equiv) were added and observed to dissolve, resulting in a yellow solution. Crude **6.50** (62 mg crude) was dissolved in 0.5 mL of DMSO and added to the reaction solution. The culture tube was purged with nitrogen gas and sealed with a Teflon-lined cap and allowed to stir at room temperature for 48 h. The reaction was filtered through glass wool precipitated into ca. 40 mL of iPrOH at 0 °C, the solid filtered

through a Buchner funnel, and the solid polymer dried under vacuum. The filtrate was centrifuged to yield an additional aliquot of the product, a white solid (0.1366g, 0.027 mmol, 78% yield, ca. 85% conversion).

^{1}H NMR (500 MHz, $CDCl_3$): δ 7.84 (s, 1H, H6'), 4.97 (br s, 1H, H3), 4.82 (d, *J* = 12.4 Hz, 1H, H2), 4.82 (d, *J* = 12.4 Hz, 1H, H4), 4.55 [br t, J = 4.7 Hz, 2H, $CH_3O(CH_2CH_2O)_m$-CH_2CH_2-triazole-CH_2-mannose], 3.89 [t, *J* = 4.8 Hz, 2H, $CH_3O(CH_2CH_2O)_m$-CH_2CH_2-triazole-CH_2-mannose], and 3.65 [s, 460 H, $CH_3O(CH_2CH_2O)_m$-CH_2CH_2-triazole-CH_2-mannose, H6b, H1, H5], and 3.38 [s, 3H, $CH_3O(CH_2CH_2O)_m$-CH_2CH_2-triazole-CH_2-mannose].

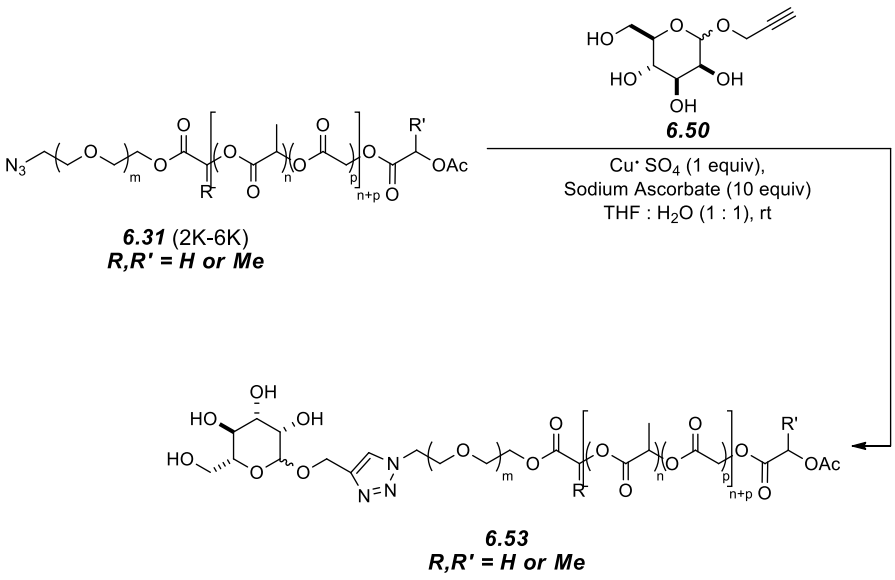

Mannose poly(ethylene glycol)-*b*-poly(lactic-*co*-glycolic acid) acetate (6.48). N_3-PEG-PLGA-OAc **6.31** (0.152 g, 0.019 mmol, 1 equiv) was dissolved in 1.5 mL of dry THF in an oven-dried culture tube with stir bar. In a separate vial, **6.50** (ca. 90 mg crude) was dissolved in 1.5 mL of distilled water. The two solutions were combined. copper (II) sulfate pentahydrate (2.4 mg, 0.001 mmol, 0.5 equiv) and ascorbic acid (9.4 mg 0.0475 mmol, 2.5 equiv) were added, and the culture tube

was sealed with a Teflon-lined cap, wrapped in tinfoil, and allowed to stir at room temperature overnight. The reaction was concentrated under reduced pressure, extracted with dry DCM, and precipitated into ca. 30 mL of isopropanol. The cloudy suspension was centrifuged and the solid polymer recovered. The polymer was isolated (0.015 g, 0.002 mmol, 10%).

^{1}H NMR (500 MHz, $CDCl_3$):[316] δ 5.32-5.08 {m, 38H, mannose-CH_2-triazole-PEG-{[OC(O)C*H*$(CH_3)]_n$[OC(O)$CH_2]_p$}OAc}, 4.91-4.65 {m, 62H, mannose-CH_2-triazole-PEG-{[OC(O)CH$(CH_3)]_n$[OC(O)C*H*$_2]_p$}OAc}, 4.56 [br t, *J* = 4 Hz, 2H (ca. 20% conversion), mannose-CH_2-triazole-C*H*$_2$$CH_2$O-PEG-PLGA-OAc], 4.34-4.23 (m, ca. 3H, mannose-CH_2-triazole-PEG-OC(O)C*H*(R)-PLGA-C(O)C*H*(R)OAc}, 3.87 [br t, *J* = 5 Hz, 2H (ca. 20% conversion), mannose-CH_2-triazole-CH_2C*H*$_2$O-PEG-PLGA-OAc], 3.65 [s, 115 H, mannose-C*H*$_2$-triazole-(C*H*$_2$C*H*$_2$O)$_m$-OC(O)C*H*(R)-PLGA-C(O)CH(R)OAc, H1, H2, H3, H4, H5, H6a, and H6b], 2.17 {overlapping s's, 1.2 H, mannose-C*H*$_2$-triazole-PEG-PLGA-OC(O)C*H*$_3$}, 2.16 (s, 3H, OC(O)C*H*$_3$], and 2.13 [s, 1.8 H, mannose-C*H*$_2$-triazole-PEG-PLGA-OC(O)C*H*$_3$].

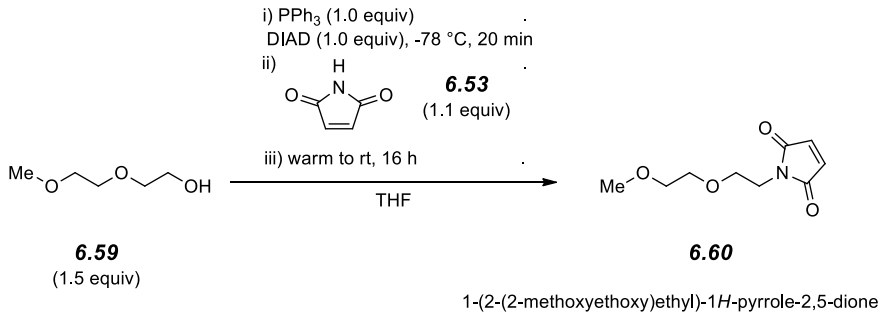

1(2-(2-methoxyethoxy)ethyl)-1*H*-pyrrolye-2,5-dione (6.60).

Triphenylphosphine (0.167 g, 0.637 mmol, 1.05 equiv) was added to an oven-

[316] The aromatic traizole resonance could not be observed, likely due to the minimal amount of material, low signal-to-noise ratio, and/or previously observed broadness of this resonance in $CDCl_3$.

dried round bottom flask with stir bar and the vessel was evacuated and filled with nitrogen (3x). The triphenylphosphine was dissolved by the addition of 5.0 mL of dry THF. DIAD (0.12 mL, 0. 609, 1 equiv) was added via a plastic syringe. The reaction was cooled to -78 °C and stirred for five minutes. Diethylene glycol monomethyl ether **6.64** (0.112 g, 0.932 mmol, 1.5 equiv) was added, and the homogeneous mixture was stirred for an additional 20 mins at -78 °C. In a separate vial, maleimide (0.0625 g, 0.644 mmol, 1.06 equiv) was dissolved in 3.0 mL of dry THF, and this solution was added to the bulk reaction via a plastic syringe. The solution was allowed to stir at -78 °C for 10 mins after which the solution was warmed to rt and stirred for an additional 16 h. After stirring overnight, the reaction was noted to be a light yellow color. The reaction was then concentrated under reduced pressure, the residue dissolved in hexanes:EtOAc (1:1), and purified via MPLC, yielding 6.65 (44.4 mg, 0.223 mmol, 36.6% based on limiting reagent) as a colorless, viscous oil.

^{1}H NMR (500 MHz, $CDCl_3$): δ 6.71 [s, 2H, NC(O)C*H*C*H*C(O)], 3.74 (t, *J* = 6.1 Hz, 2H, NCH_2CH_2O), 3.66 (t, *J* = 5.7 Hz, 2H, NCH_2CH_2O), 3.61 (m, 2H, and $CH_3OCH_2CH_2O$), 3.50 (m, 2H, and $CH_3OCH_2CH_2O$), and 3.35 (s, 3H, $CH_3OCH_2CH_2O$).

GC/MS (Method: 50 °C, hold for two min; ramp at 20 °C/min for 10 min, hold at 250 °C for three min) t_R = 6.79 min; *m/z* 199 (10, M^+), 154 (20, M^+-$MeOCH_2$), 124 (100, M^+-$MeOCH_2CH_2O$), 110 (20, M^+-$MeOCH_2CH_2OCH_2$), and 59 (30).

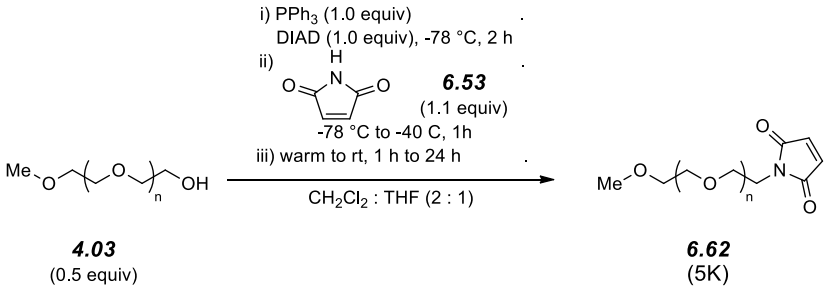

Mono methyl ether Poly(ethylene glycol) maleimide (6.62).

Triphenylphosphine (0.167 g, 0.637 mmol, 1.05 equiv) was added to an oven-dried round bottom flask with stir bar and the vessel was purged with nitrogen. The triphenylphosphine was dissolved by the addition of 5.0 mL of dry THF. DIAD (0.12 mL, 0. 609, 1 equiv) was added via a plastic syringe. The reaction was cooled to -78 °C and stirred for 15 mins. A 4 mL solution of mPEG-OH **4.03** (1.56 g, 0.312 mmol, 0.5 equiv) was added, and the mixture was stirred for an additional 15 mins at -78 °C. A white precipitate was noted, and the reaction was allowed to warm to -40 °C. After stirring at -40 °C, the reaction was again homogeneous. In a separate vial, maleimide (0.0625 g, 0.644 mmol, 1.06 equiv) was dissolved in 2.0 mL of dry THF, and this solution was added to the bulk reaction via a plastic syringe. The solution was allowed to stir at -40 °C for 1 h, after which the solution was warmed to rt and stirred for an additional 1 h. After 1 h, a 5 mL aliquot was removed from the reaction flask, concentrated under reduced pressure, dissolved in EtOAc, precipitated into an equal volume of hexanes cooled to 0 °C, filtered, the solid redissolved in CH_2Cl_2, and precipitated into isopropanol at 0 °C. The solid was collected by filtration, dried under high vacuum, and analyzed by ^{1}H NMR, suggesting a 60% conversion. The remainder of the reaction was stirred overnight, and purified as described. No significant further conversion was noted.

^{1}H NMR (500 MHz, $CDCl_3$): δ 6.71 [s, 2H, NC(O)C*H*C*H*C(O)], 3.65 (s, 455H, MeO-(CH_2CH_2O)$_n$-CH_2CH_2maleimide), and 3.38 (s, 3H, CH_3O-(CH_2CH_2O)$_n$-CH_2CH_2maleimide).

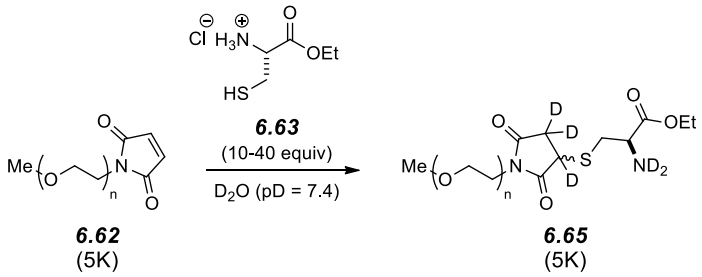

Mono methyl ether Poly(ethylene glycol) maleimide cysteine ethyl ester (6.65). Model **6.67** (93 mg, 0.019 mmol, 1 equiv) was co-dissolved with cysteine ethyl ester hydrochloride salt **6.68** (40.9 mg, 0.22 mmol, 12 equiv) in 0.8 mL of a buffered D_2O solution (pD = 7.4) in an oven-dried culture tube with stir bar. The vessel was capped with a Teflon-lined cap and allowed to stir for overnight at rt. The solution was then precipitated directly into isopropanol at 0 °C. Attempts to filter the fine precipitate failed, and so the heterogeneous suspension was concentrated to dryness under reduced pressure, redissolved, and precipitated into isopropanol at 0 °C. The suspension was centrifuged for two hours, the solvent decanted, and the solid dried under high vacuum at 50 °C. The solid white precipitate was identified as **6.70**.

^{1}H NMR (500 MHz, D_2O):[317] δ 4.27 [q, *J* = 7.2 Hz, 2H, C(O)CC$H_2$$CH_3$], 3.65 (s, 455 H, MeO-(CH_2CH_2O)$_n$), 3.38 (s, 3H, CH_3O-(CH_2CH_2O)$_n$), 3.01 (dd, *J* = 13.6, 8.6 Hz, 1H, SC$H_a$$H_b$CH), 2.91 (dd, *J* = 13.5, 7.8 Hz, 1H, SCH_aH_bCH), and 1.31 [t, overlapping with impurities, 3H, $C(O)CCH_2CH_3$].

[317] Relavent ^{1}H NMR data are reported from an impure sample. Impurities are omitted.

Chapter 7

Overall Conclusions and Future Outlook

Through the experiments described in this thesis, there have been a number of discoveries that are of interest from both a fundamental as well as practical viewpoint. The general strategic concept of silicate esters as promoieties has been validated, a novel synthesis for the production of "random" PLGA block copolymers has been established, and the utility of these materials in biological studies has been confirmed. These studies provide optimism for the outlook of these silicate-loaded, FNP-produced nanoparticles.

1. The Silicate Ester Prodrug Strategy.

The synthesis, purification, and characterization of a wide variety of tetraalkoxysilanes and acyloxytrialkoxysilanes are detailed, and the relative hydrolysis rates of these compounds have been benchmarked. The structural diversity within this family of compounds was designed to allow for the control of two primary physicochemical properties: hydrophobic character and rate of hydrolysis of the silicate esters. Based on the study of these models, multiple, important trends were established. First, increasing the length of aliphatic, linear alkoxy substituents has the power to dramatically alter the solubility of a silicate while the rate of hydrolysis differs minimally. The hydrolysis rate, on the other

hand, can be slowed by inclusion of sterically bulky substituents or quickened by the inclusion of a labile acetoxy group.

In order to obtain data relevant to future silicate ester prodrugs, the necessity of a well-chosen model study was apparent in these studies. Even in the tetraalkoxysilane model system, subtle variations in one of the four sacrificial alkoxy groups elicited measurable changes in the observed hydrolysis rate. The trends developed from the tetraalkoxysilane models were effectively translated to the design of PTX silicate ester prodrugs. Efforts from these studies resulted in a class of novel silicate ester prodrugs that varied in their hydrophobicity, hydrolysis rate, and site of silylation. An interesting study of a hindered, acetoxy-containing silicate ester of PTX uniquely allowed for the isolation of a PTX silanol intermediate. This study further established the S_N2 nature of the hydrolysis mechanism. Collaborative efforts measured the IC_{50} values of a subset of these PTX silicate esters, and, encouragingly, found all but two of the most slowly hydrolyzing species to be equally as cytotoxic as PTX itself.

2. Block Copolymer Synthesis Methodology and End-Functionalization.

The biocompatible copolymer PLGA has been widely used in biomedical applications. However, the traditional synthetic route to PLGAs has typically utilized tin catalysis to access random copolymers via a polymerization that incurs significant transesterification, resulting in products that are polydisperse. The methodology described in this thesis has demonstrated that the synthesis of essentially random, narrowly dispersed PLGA copolymer blocks is achievable. This task was accomplished through the use of the organocatalyst DBU and the controlled infusion of the glycolide monomer to match the consumption of the lactide monomer. Using a monomethoxy PEG as a macroinitiator, PEG-*b*-PLGA

BCPs of varying MWs, and correspondingly different physical properties, were synthesized.

Expanding the utility of this methodology, use of a monobenzyl ether PEG (rather than a monomethyl ether PEG) as a macroinitiator allowed access to a family of BnO-PEG-*b*-PLGA BCPs whose termini were end-differentiated and amenable to a variety of chemical transformations. Following acetylation of the polyester block, the polyether could be efficiently debenzylated to yield a polymer (HO-PEG-*b*-PLGA-OAc) that could be further functionalized selectively at the polyether terminus. Studies reported here focus on efforts to render these polymers amenable to various “click” chemistries such as [3 + 2] cycloadditions and thiol-maleimide conjugations.

3. PTX Silicate-Loaded Nanoparticles.

The bis-triethoxy PTX silicate prodrug was co-formulated via FNP with a 5K-10K PEG-*b*-PLGA BCP into highly prodrug-loaded, stable nanoparticles. In collaboration with a number of colleagues of varying expertise, the morphology and behavior of these nanoparticles was examined by a variety of spectroscopy, calorimetry, and microscopy techniques. While it is difficult to definitively characterize these inherently broadly dispersed, kinetically trapped nanoparticles, the preponderance of the evidence suggests that the nanoparticles are composed of a solid core that consists of the crystalline PTX silicate and amorphous PLGA polymer block. The nanoparticles are effectively dispersed in water by a PEG corona that crystallizes upon freeze drying, leading to difficulties during redispersion at high concentration in aqueous buffers.

PTX silicate loaded nanoparticles were extensively tested in collaborative biological studies. These prodrug loaded formulations were dosed to cancer tumor-bearing mice to test for *in vivo* efficacy. In a highly encouraging result,

groups of mice receiving equimolar doses of the PTX silicate nanoparticles, Taxol®, and Abraxane® all demonstrated statistically equivalent levels of tumor growth suppression. Due to the high loading levels in the PTX silicate nanoparticles, notably less excipient was dosed to this group. In addition, the PTX silicate may have hydrolyzed and released over a more prolonged period, thereby allowing a more sustained drug delivery. These two traits are consistent with the critical observation that mice receiving these PTX silicate nanoparticles exhibited minimal side effects such as liver and blood toxicity vis-à-vis the clinical treatment groups.

4. Future Outlook.

Several aspects of this thesis deserve yet greater study. The silicate ester prodrug strategy has been well established in the case of tetraalkoxysilanes and PTX silicate ester prodrugs, but application of the silicate ester prodrug strategy to other hydrophobic, hydroxyl-containing drugs could lead to additional new drug formulations. Additionally, silicate esters consisting of other functional groups could also prove to be productive. For example, further development of aminosilanes and phosphonic acid silicates could expand the utility of this concept. In the case of the end-functionalized BCPs, a reliable route to a readily derivatized polymeric intermediate (HO-PEG-*b*-PLGA-OAc) has been established. While initial studies have demonstrated that end-functionalization of these PEG-*b*-PLGAs is achievable, optimization of reaction conditions and incorporation of high-value imaging, targeting, and cytotoxic agents could advance this strategy. Eventually, with the appropriate materials in hand, loading these customized BCPs with silicate prodrugs could yield selective and highly efficacious therapeutic agents.

The efficacy and minimal toxicity of PTX silicates in PEG-*b*-PLGA nanoparticles is an outcome that inspires future study. However, a number of opportunities still exist to further understand the fundamental science as well as improve the end application. For instance, specific to these PTX silicate-loaded nanoparticles, carefully matching the precipitation rate of the silicate and polyester block during the FNP formulation may result in alterations of the morphology of the nanoparticle, thereby potentially affecting the hydrolysis/release rate. Alternatively, optimization of the loading level of the PTX silicate (via either inclusion of higher wt% in the FNP experiment or increasing the hydrophobic character of the silicate prodrug) may further minimize any undesirable toxicity. Upon conclusion of these optimization studies, determination of the maximum tolerated dose is essential. Any one of these studies could individually or collectively improve the overall efficacy of this PTX silicate nanoparticle formulation.

References and Notes

[1] Horn, D.; Rieger, J. Organic Nanoparticles in the Aqueous Phase – Theory, Experiment, and Use. *Angew. Chem. Int. Ed.* **2001**, *40*, 4330–4361.

[2] Johnson, B. K.; Prud'homme, R. K. Chemical Processing and Micromixing in Confined Impinging Jets. *AIChE* **2003**, *49*, 2264–2282.

[3] Johnson, B. K.; Prud'homme, R. K. Flash NanoPrecipitation of Organic Actives and Block Copolymers using a Confined Impinging Jets Mixer. *Aust. J. Chem.* **2003**, *56*, 1021–1024.

[4] Liu, Y.; Cheng, C.; Liu, Y.; Prud'homme, R. K.; Fox, R. O. Mixing in a Multi-Inlet Vortex Mixer (MIVM) for Flash Nano-Precipitation. *Chem. Eng. Sci.* **2008**, *63*, 2829–2842.

[5] Zhu, Z. Polymer Stabilized Nanosuspensions Formed via Flash Nanoprecipitation: Nanoparticle Formation, Formulation, and Stability. Ph.D. Dissertation, University of Minnesota, Minneapolis, MN, **2010**, 1–213.

[6] Han, J.; Zhu, Z.; Qian, H.; Wohl, A. R.; Beaman, C. J.; Hoye, T. R.; Macosko, C. W. A Simple Confined Impingement Jets Mixer for Flash NanoPrecipitation. *J. Pharm. Sci.* **2012**, *101*, 4018–4023.

[7] Saad, W. S. Drug Nanoparticle Formation via Flash Nanoprecipitation: Conjugation to Encapsulate and Control the Release of Paclitaxel. Ph.D. Dissertation, Princeton University, Princeton, NJ, **2007**. 1–198.

[8] Ansell, S. M.; Johnstone, S. A.; Tardi, P. G.; Lo, L.; Xie, S.; Shu, Y.; Harasym, T. O.; Harasym, N. L.; Williams, L.; Bermudes, D.; Liboiron, B. D.; Saad, W.; Prud'homme, R. K.; Mayer, L. D. Modulating the Therapeutic Activity of Nanoparticle Delivered Paclitaxel by Manipulating the Hydrophobicity of Prodrug Conjugates. *J. Med. Chem.* **2008**, *51*, 3288–3296.

[9] Dechy-Cabaret, O.; Martin-Vaca, B.; Bourissou, D. Controlled Ring-Opening Polymerization of Lactide and Glycolide. *Chem. Rev.* **2004**, *104*, 6147–6176.

[10] Ebelmen, M. *Ann. Chim. Phys.* **1845.** *15,* 319.

[11] Arkles, B. Silicon Esters. In *Kirk-Othmer Encyclopedia of Chemical Technology, Fourth Edition, Volume 22*; Kroschwitz, J. I.; Howe-Grant, M., ed. John Wiley & Sons, Inc: New York, 1997, 69–81.

[12] Wright, J. R. Bolt, R. O.; Goldschmidt, A.; Abbott, A. D. Silicate Esters and Related Compounds. I. Synthesis of Certain Tetraalkoxysilanes, Polyalkoxysilanes, Bis-(trialkoxysilyl)-alkanes, and Related Intermediates. *J. Am. Chem. Soc.* **1957**, *80*, 1733–1737.

[13] Hoye, T. R.; Ji, S.; Miura, Y.; Zhu, Z.; Macosko, C. W. PCL-b-PEG Nanoparticles for Drug Delivery: Package and Contents. Presented at IPRIME annual meeting. Minneapolis, MN, May 31, 2007.

[14] Wohl, A. R.; Hoye, T. R.; Zhu, Z.; Macosko, C. W. Orthosilicate Prodrug Models: Synthesis, Hydrolysis, and Encapsulation in Block Copolymer Nanoparticles. National Meeting of the AIChE, Nov. 2010.

[15] Tang, L.; Fan, T. M.; Borst, L. B.; Cheng, J. Synthesis and Biological Response of Size-Specific, Monodisperse Drug-Silica Nanoconjugates. *ACS Nano*, **2012**, *6*, 3954–3966.

[16] Kingston, D. G. I. The Shape of Things to Come: Structural and Synthetic Studies of Taxol and Related Compounds. *Phytochemistry* **2007**, *68*, 1844–1854.

[17] Parrott, M. C.; Luft, J. C.; Byrne, J. D.; Fain, J. H.; Napier, M. E.; DeSimone, J. M. Tunable Bifunctional SIlyl Ether Cross-Linkers for the Design of Acid-Sensitive Biomaterials. *J. Am. Chem. Soc.* **2010**, *132*, 17928–17932.

[18] Parrott, M. C.; Finniss, M.; Luft, J. C.; Pandya, A.; Gullapalli, A.; Napier, M. E.; DeSimone, J. M. Incorporation and Controlled Release of Silyl Ether Prodrugs from PRINT Nanoparticles. *J. Am. Chem. Soc.* **2012**, *134*, 7978–7982.

[19] Bassindale, A. R.; Taylor, P. G. Reaction Mechanisms of Nucleophilic Attack at Silicon. In *The Chemistry of Organic Silicon Comounds*. Patai, S.; Rappoport, Z., eds. John Wiley & Sons, Inc: New York, 1989, 839–892 and references therein.

[20] Holmes, R. R. The Stereochemistry of Nucleophilic Substitution at Tetracoordinated Silicon. *Chem. Rev.* **1990**, *90*, 17–31 and references therein.

[21] Aelion, R.; Loebel, A.; Eirich, F. Hydrolysis of Ethyl Silicate. *J. Am. Chem. Soc.* **1950**. *69*, 61–75.

[22] Brinker, C. J. Hydrolysis and Condensation of Silicates: Effects on Structure. *J.Non-Cryst. Solids* **1988**, *100*, 31–50.

[23] Ro, J. C.; Chung, I. J. Sol-Gel Kinetics of Tetraethylorthosilicate (TEOS) in Acid Catalyst. *J. Non-Cryst. Solids* **1989**, *110*, 26–32.

[24] Zerda, T. W.; Hoang, G. Effects of Solvents on the Hydrolysis Reaction of Tetramethyl Orthosilicate. *Chem. Mater.* **1990**, *2*, 372–376.

[25] Turner, C. W.; Franklin, K. J. Studies of the Hydrolysis and Condensation of Tetraethylorthosilicate by Multinuclear (^{1}H ^{17}O ^{29}Si) NMR Spectroscopy. *J. Non-Cryst. Solids* **1986**, *91*, 402–415.

[26] Assink, R. A.; Kay, B. D.; Study of Sol-Gel Chemical Reaction Kinetics by NMR. *Annu. Rev. Mater. Sci.* **1991**, *21*, 491–513.

[27] Zerda, T. W.; Hoang, G. Effects of Solvents on the Hydrolysis Reaction of Tetramethyl Orthosilicate. *Chem. Mater.* **1990**, *2*, 372–376.

[28] Brinker, C. J.; Scherer, G. W. Hydrolysis and Condensation II: Silicates. In *Sol-Gel Science: The Physics and Chemistry of Sol-Gel Processing*. Academic Press, Inc: San Diego, CA, **1990**, 97–233.

[29] Miura, Y. University of Minnesota, Minneapolis, MN. Personal communication, **2008**.

[30] Kalia, J.; Raines, R. T. Hydrolytic Stability of Hydrazones and Oximes. *Angew. Chem. Int. Ed.* **2008**, *47*, 7523–7526.

[31] Ridge, D.; Todd, M. Studies in the Formation Mechanisms of Alkyl Orthosilicates. *J. Chem. Soc.* **1949**, 2637–2640.

[32] Gerrard, W.; Woodhead, A. H. Interaction of Alcohols with Silicon Tetrachloride. *J. Chem. Soc.* **1951**, 519–522.

[33] Key resonances observed in crude ^{1}H NMR (500 MHz, $CDCl_3$): δ = 5.37 [br t, *J* = 6 Hz, 4H, $Si(OCH_2CH)_4$] and 4.31 [overlapping d's, 8H, $Si(OCH_2CH)_4$, observed as a mixture cis and trans isomers].

[34] Experiment quantification of these differences is historically performed by measuring the equilibrium solubility of a compound in a mixture of water and *n*-octanol and applying the measured concentrations to equation the following equation: log P = $[solute_{octanol}]/[solute_{water}]$. A larger log P (or clog

P) value is indicative of a more hydrophobic compound. For a comprehensive review of the history and theory, see: Leo, A.; Hansch, C.; Elkins, D. Partition Coefficients and Their Uses. *Chem. Rev.* **1971**, *71*, 525–616 and references cited therein.

[35] Tetko, I. V.; Poda, G. I. Application of ALOGPS 2.1 to Predict log D Distribution Coefficient for Pfizer Proprietary Compounds. *J. Med. Chem*. **2004**, *47*, 5601–5604

[36] Tetko, I. V.; Bruneau, P. Application of ALOGPS to Predict 1-Octanol/Water Distribution Coefficients, logP, and logD, of AstraZeneca In-House Database. *J. Pharm. Sci*. **2004**, *93*, 3103–10.

[37] Tetko, I. V., Tanchuk, V. Y. Application of Associative Neural Networks for Prediction of Lipophilicity in ALOGPS 2.1 Program. *J. Chem. Inf. Comput. Sci.* **2002**, *42*, 1136–1145.

[38] http://www.vcclab.org/lab/alogps/ accessed June 19, 2012.

[39] Clausen, R. P.; Bols, M. The First Tri- and Tetraalkoxysilanes with Four Different Substituents. *J. Org. Chem.* **1997**, *62*, 4457–4464.

[40] Pedlow, G. W., Jr.; Miner, C. S., Jr. Organic Orthosilicates Stable Against Hydrolysis. U.S. Patent 2,566,365, June 15, 1946.

[41] Beckmann, J.; Dakternieks, D.; Tiekink, E. R. T. Chiral Trialkoxysilanols Derived from Terpene Alchols. Molecular Structures of Tris([(1*S*)-*endo*-]-(–)-bornoxy)silanols and tetrakis((–)-menthoxy)silane. *J. Organomet. Chem.* **2002**, *648*, 188–192.

[42] Miner, C. S., Jr.; Bryan, L. A.; Holysz, R. P.; Pedlow, G. W., Jr. *Ind. Eng. Chem.* Tert-Alkoxyaminosilanes. **1947**, *39*, 1368.

[43] Hyde, J. F.; Curry, J. W. The Preparation of Tetra-*i*-butoxysilane and Tri-*t*-butoxyfluorosilane. *J. Am. Chem. Soc.* **1955**, *77*, 3140–3141.

[44] Original synthesis performed by Dr. Yutaka Miura. ^{1}H NMR (500 MHz, $CDCl_3$): 7.01 (d, *J* = 7.0 Hz, 8H, Ar-*H*), 6.89 (d, *J* = 7.0 Hz, 8H, Ar-*H*), and 2.27 (s, 12H, *p*-C*H*$_3$). ^{13}C NMR (125 MHz, $CDCl_3$): δ = 150.6, 132.3, 130.2, 119.4, and 20.8.

[45] Original synthesis performed by Dr. Yutaka Miura. ^{1}H NMR (500 MHz, $CDCl_3$): δ = 6.76 (s, 8H, Ar-*H*), 2.18 (s, 12H, *p*-C*H*$_3$), and 2.16 (s, 24H, *o*-C*H*$_3$). ^{13}C NMR (125 MHz, $CDCl_3$): δ = 148.4, 131.9, 129.4, 128.4, 20.7, and 17.2.

[46] Takebayashi, T. Acute Inhilation Toxicity of High Concentrations of Silane in Male ICR Mice. *Arch. Toxicol.* **1993**, *67*, 55–60.

[47] Anglin, E. J.; Cheng, L.; Freeman, W. R.; Sailor, M. J. Porous Silicon in Drug Delivery Devices and Materials. *Adv. Drug Deliver. Rev.* **2008**, *60*, 1266–1277.

[48] Corriu, R. J. P.; Henner, B. J. L. Mechanism of Nucleophilic Substitution at Silicon: Kinetic Evidence on the Slow Formation of a Penta-Coordinate Silicon Intermediate. *J. Organomet. Chem.* **1975**, *102*, 407–416.

[49] Friedel, C.; Ladenburg, A. *Liebigs Annalen der Chemie,* **1868**, *145,* 174–178.

[50] Schuyten, H. A.; Weaver, J. W.; Reid, J. D. Preparation of Substituted Acetoxy Silanes. *J. Am. Chem. Soc.* **1947**, *69*, 2110–2112.

[51] Kopylov, V. M.; Kireev, V. V.; Ivanov, V. V.; Astaf'ev, G. Y.; Kozlov, Y. V. Reaction of Acetoxysilanes with Hydroxy Compounds. *Rus. J. Gen. Chem.* **2001**, *71*, 1924–1928.

[52] Roth, M. J.; Brook, M. A.; Penny, H. B. Hydrosilane Cleavage Reactions Accelerated by Tartaric Acid and Dimethyl Sulphoxide. *J. Organomet. Chem.* **1996**, *521*, 65–74.

[53] Crude ^{1}H NMR data for **2.38** (500 MHz, $CDCl_3$): δ = 3.94 [q, *J* = 7.1 Hz, 6H, $Si(OC\mathit{H}_2CH_3)_3$], 2.13 [s, 3H, $SiOC(O)C\mathit{H}_3$], and 1.25 [t, *J* = 7.1 Hz, 6H, $Si(OCH_2C\mathit{H}_3)_3$]. GC/MS: (Method: 50°C, hold for two min; ramp at 20°C/min for 10 min, hold at 250°C for three min) t_R = 5.48 min; *m/z* 222 (5, M^+), 177 (100, M^+ - OEt), and 135 (20).

[54] Crude ^{1}H NMR data (500 MHz, $CDCl_3$) showed a complex mixture of > 4 different products. Crude GC/MS for **2.40**: (Method: 50°C, hold for two min; ramp at 20°C/min for 11 min, hold at 270°C for three min) t_R = 7.90 min; *m/z* 194 (60, M^+), 179 (50, M^+ - Me), 135 (100), and 91 (10).

[55] Cragg, R. H.; Lane, R. D. Contributios to Group IV Organometallic Chemistry IV. Preparation and Properties of Some Organosilicon Derivatives of Salicylic and Related Acids. *J. Organomet. Chem.* **1981**, *212*, 301–310.

[56] This work was done jointly with National Science Foundation (NSF)/Lando fellowship undergraduate student Paul Alperin.

[57] No evidence consistent with the synthesis of either **2.56** or **2.57** was observed via TLC, GC/MS, or crude ^{1}H NMR spectroscopy.

[58] Theis, B.; Weib, J.; Lippert, W. P.; Bertermann, R.; Burschka, C.; Tacke, R. Zwitterionic and Anionic Multinuclear Pentacoordinate Silicon(IV) Complexes with Bridging (R,R)-Tartrato(4) Ligands and SiO_5 Skeletons: Synthesis and Reactivity in Aqueous Solution. *Chem. Eur. J.* **2012**, *18*, 2202–2206.

[59] Gabizon, A.; Shmeeda, H.; Barenholz, Y. Pharmacokinetics of Pegylated Liposomal Doxorubicin. *Clin. Pharmacokinet.* **2003**, *42*, 419–436.

[60] Diedrich, F.; Ebker, C.; Klingbiel, U.; Reiche, C.; Labahn, T.; Magull, J.; Noltemeyer, M. N,N-Bis(silyl)ethylenediamine und 1,3-Diaza-2-silacyclopentane – Synthese, Reaktionen, Strukturen. *Z. Naturforsch., B: Chem. Sci.* **2002**, *57*, 99–106.

[61] Wutz, P. G. M.; Greene, T. W. Protection for the Amino Group. In *Greene's Protective Groups in Organic Synthesis, Fourth Edition*. John Wiley & Sons, Inc: Hoboken, NJ, 2007.

[62] Crude GC/MS data for **2.63** (Method: 30°C, hold for 1.5 min; ramp at 27°C/min for 13 min, hold at 300°C for 1.5 min) t_R = 11.75 min; *m/z* 249 (20 M^+ - O^{t}Bu), 192 {40, $Si(O)[O(CH_3)CHCH_2NH_2]_2$}, 175 (300), 136 {100, $Si(OH)_2[O(CH_3)CHCH_2NH_2]_2$}, 97 (20), and 57 (20).

[63] Crude GC/MS data for **2.66** (Method: 30°C, hold for two min; ramp at 20°C/min for 14 min, hold at 310°C for five min) t_R = 9.34 min; *m/z* 282 (<5, M^+), 267/269 (100, M^+ - Me), 211/213 (80), 169/171 (40), 155/157 (40), 97 (30), and 57 (20).

[64] Crude GC/MS data for **2.67** (Method: 50°C, hold for two min; ramp at 20°C/min for 10 min, hold at 250°C for three min) t_R = 9.34 min; *m/z* 246 (5), M^+), 231 (20, M^+ - Me), 173 (20, M^+ - O^{t}Bu), 133 (40), and 117 (100).

[65] Alternatively, attempts to synthesize 1,3,2-azaoxasilinanes by treating 3-amino-1-propanol with di-*t*-butoxydichlorosilane again led to a disappointing mixture of products in the GC/MS trace. None of the products could be reliably assigned as a cyclized, non-chlorinated substrate.

[66] Crude GC/MS data for **2.68** (Method: Method: 30°C, hold for 1.5 min; ramp at 27°C/min for 13 min, hold at 300°C for 1.5 min) t_R = 9.07 min; *m/z* 219 (40, M^+ - Me) and 163 (100, M^+ - O^{t}Bu).

[67] Crude GC/MS data for **2.70** (Method: 50°C, hold for two min; ramp at 20°C/min for 10 min, hold at 250°C for three min) t_R = 5.05 min; *m/z* 233 (40, M^+ - Me), 177 (100), and 119 (20).

[68] Ismail, V. R. M. Herstellung von Tertiarbutoxy-(halogenphenoxy)-silanen. XIV. *Z. anorg. allg. Chem.* **1969**, *371,* 23–31.

[69] Crude GC/MS data for **2.73** (Method: Method: 30°C, hold for 1.5 min; ramp at 27°C/min for 13 min, hold at 300°C for 1.5 min) t_R = 12.46 min; *m/z* 339 (40, M^+), 324 (50, M^+ - Me), 282 (100, M^+ - ^{t}Bu), 268 (20), 226 (60), 184 (30), 139 (30), and 91 (20, Bn^+).

[70] Crude GC/MS data for **2.73** (Method: 50°C, hold for two min; ramp at 20°C/min for 10 min, hold at 250°C for three min) t_R = 5.05 min; *m/z* 386 (20, M^+), 371 (10, M^+ - Me), 329 (20, M^+ - ^{t}Bu), 313 (5, M^+ - O^{t}Bu), 295 (80, M^+ - Bn), 273 (30), 257 (10), 239 (40), 183 (100), 168 (30), 139 (40), 106 (30), and 91 (30, Bn^+).

[71] Overman, L. E.; Okazako, M. E.; Mishra, P. *tert*-Butyldipenylsilylamines: A Useful Protecting Group for Primary Amines. *Tet. Lett.* **1986**, *27*, 4391–4394.

[72] Liang, H.; Hu, L.; Corey, E. J. Di-*tert*-butylisobutylsilyl, Another Useful Protecting Group. *Org. Lett.* **2011**, *13*, 4120–4123.

[73] Lipshutz, B. H.; Papa, P.; Keith, J. M. Triisopropylsiloxycarbonyl (“Tsoc”): A New Protecting Group for 1° and 2° Amines. *J. Org. Chem.* **1999**, *64*, 3792–3793.

[74] Tao, M.; Park, C. H.; Bihovsky, R.; Wells, G. J.; Husten, J.; Ator, M. A.; Hudkins, R. L. Synthesis and Structure-Activity Relationships of Novel Poly(ADP-ribose) Polymerase-1 Inhibitors. *Bioorg. Med. Chem. Lett.* **2006**, *16*, 938–942.

[75] Crude GC/MS data for **2.76** (Method: 50°C, hold for two min; ramp at 20°C/min for six min, hold at 170°C for six min) t_R = 9.44 min; *m/z* 319 (5, M^+), 304 (100, M^+ - Me), 248 (20), 192 (20), and 136 (20).

[76] Development of hindered amonotrialkoxysilanes is continuing in collaboration with the laboratory of Prof. Michael Wentzel, Augsburg College, Minneapolis, MN.

[77] Gerrard, W.; Jones, J. V. Stability of Isomeric Butoxysilanes with Respect to Silicon Tetrachloride and Hydrogen Chloride. *J. Chem. Soc.* **1952**, 1690–1693.

[78] Gerrard, W.; Howe, B. K. The Behaviour of 1:1:1:3:3:3-hexachloropropan-2-ol with Inorganic Non-Metal Halides. *J. Chem. Soc.* **1955**, 505–510.

[79] Chappelow, C. C.; Elliot, R. L.; Goodwin, J. T. The Phenylation and Methylation of Alkoxychlorosilanes. *J. Org. Chem.* **1960**, *25*, 435–439.

[80] Pedlow, G. W.; Miner, C. S. Tertiary-Alkoxy Chlorosilanes. U.S. Patent 2,566,957, September 4, 1951.

[81] ^{1}H NMR assignments were made with the assistance of: Ciuffreda, P.; Casati, S.; Manzocchi, A. Complete ^{1}H and ^{13}C NMR Spectral Assignment of 17-Hydroxy Epimeric Sterols with Planar A or A and B Rings. *Magn. Reson. Chem.* **2004**, *42*, 360–363.

[82] ^{1}H NMR assignments were made with the assistance of: Kirk, D. N.; Toms, H. C.; Douglas, C.; White, K. A.; Smith, K. E.; Latif, S.; Hubbard, R. W. P. A Survey of the High-Field ^{1}H NMR Spectra of the Steroid Hormones, their Hydroxylated Derivatives, and Related Compounds. *J. Chem. Soc. Perkin Trans. 2* **1990**, 1567–1594.

[83] Stella, V. J. A Case for Prodrugs. In *Prodrugs.* Stella, V. J.; Borchardt, R. T.; Hageman, M. J.; Oliyai, R.; Maag, H.; Tilley, J. W., eds. Springer Science: New York, 2007, 3–33.

[84] Stella, V. J. Prodrugs as Therapeutics. *Expert Opin. Ther. Patents*, **2004**, *14*, 277–280.

[85] Ettmayer, P.; Amidon, G. L.; Clement, B.; Testa, B. Lessons Learned from Marketed and Investigational Prodrugs. *J. Med. Chem.* **2004**, *47*, 2393–2404.

[86] Testa, B. Prodrug Research: Futile or Fertile? *Biochem. Pharmacol.* **2004**, *68*, 2097–2106.

[87] Skwarczynski, M.; Hayashi, Y.; Kiso, Y. Paclitaxel Prodrugs: Toward Smarter Delivery of Anticancer Agents. *J. Med. Chem.* **2006**, *49*, 7253–7269.

[88] Wohl, A. R.; Kalscheuer, S.; Lee, H. S.; Han, J.; McCormick, A.; Macosko, C. W.; Panyam, J.; Hoye, T. R. A Silicate Ester Prodrug Strategy and in vivo Efficacy of Paclitaxel Prodrug-loaded Nanoparticles. *J. Am. Chem. Soc., submitted.*

[89] Corriu R. J. P.; Granier M.; Lanneau G. F. Synthesis and Reactivity of Bis(triethoxysilyl)methane, Tris(triethoxysilyl)methane and Some Derivatives. **1998** *J. Organomet. Chem. 562*, 79–88.

[90] Gitelman, H. J.; Alderman, F.; Perry, S. J. Renal Hnadling of Silicon in Normals and Patients with Renal Insufficiency. *Kidney Int.* **1992**, *42*, 957–959.

[91] Marco-Franco, J. E.; Torres, V. E.; Nixon, D. E.; Wilson, D. M; James, E. M.; Bergstrahl, E J.; McCarthy, J. T. Oxalate, Silicon, and Vanadium in Acquired Cystic Kidney Disease. *Clin. Nephrol.* **1991**, *35*, 52–58.

[92] Lai, W.; Garino, J.; Flaitz, C.; Ducheyne, P. Excretion of Resorption Products from Bioactive Glass Impanted in Rabbit Muscle. *J. Biomed. Mater. Res. Part A* **2005**, *75A*, 398–407.

[93] Mayne, A. H.; Bayliss, S. C.; Barr, P. Tobin, M.; Buckberry, L. D. Biologically Interfaced Porous Silicon Devices. *Phys. Status Solidi A – Appl. Res*. **2000**, *182*, 505–513.

[94] Kalscheuer, S.; Panyam, J. University of Minnesota, Minneapolis, MN. Personal communication, **2012**.

[95] Cory, A. H.; Owen, T. C.; Barltrop, J. A.; Cory, J. G. Use of an Aqueous Soluble Tetrazolium/Formazan Assay for Cell Growth Assays in Culture. *Cancer Comm.* **1991**, *3*, 207–212.

[96] Originally, compound **1.01** was named “taxol,” leading to the still persistent confusion over the name of the drug molecule (i.e., taxol with a lower case “t”) vs. the drug formulation (i.e., Taxol® with an upper case “T”). Historically, it was found after the name taxol was in widespread use, Taxol® was a previously trademarked name of a minor drug. By the time this came to be common knowledge, “taxol” was already widely recognized by the general public as a “miracle drug.” To maintain the positive publicity that had already been garnered by this molecule, Bristol-Meyers Squibb (BMS), the eventual commercial producer and marketer of this chemotherapeutic, purchased the legal rights to the name Taxol® during commercialization. Thus, the chemical entity was renamed “paclitaxel” to attempt to alleviate further confusion and to reserve the name Taxol® for the clinical formulation of paclitaxel in Cremophor EL® (CrEL®). For a more detailed history and commentary on this subject, see Kingston, D. G. I. The Shape of Things to Come: Structural and Synthetic Studies of Taxol and Related Compounds. *Phytochemistry* **2007**, *68*, 1844–1854 and references therein.

[97] Wani, M.C.; Taylor, H.L.; Wall, M.E.; Coggon, P.; McPhail, A.T. Plant Antitumor Agents. VI. The Isolation and Structure of Taxol, a Novel Antileukemic and Antitumor Agent from *Taxus brevifolia*. *J. Am. Chem. Soc.* **1971**, 2325–2327.

[98] Schiff, P. B.; Fant, J.; Horwitz, S. B. Promotion of Microtubule Assembly in vitro By Taxol. *Nature* **1979,** *277*, 665–667.

[99] Wang, Y.-F.; Shi, Q.-W.; Dong, M.; Kiyota, H.; Gu, Y.-C.; Cong, B. Natural Taxanes: Developments Since 1828. *Chem. Rev.* **2011**, *111*, 7652–7709.

[100] U.S. Food and Drug Administration. *TAXOL® (paclitaxel) INJECTION*. **2007**.

[101] ten Tije, A. J.; Verweij, J.; Loos, W. L.; Sparreboom, A. Pharmacological Effects of Formulation Vehicles: Implications for Cancer Therapy. *Clin. Pharmacokinet.* **2003**, *42*, 665–685.

[102] Wiernik, P. H.; Schwartz, E. L.; Einzig, A.; Strauman, J. J.; Lipton, R. B.; Dutcher, J. P. Phase I Trial of Taxol Given as a 24-Hour Infusion Every 21 Days: Responses Observed in Metastatic Melanoma. *J. Clin. Oncol.* **1987**, *5*, 1232–1239.

[103] Hennenfent, K. L.; Govindan, R. New Formulations of Taxol: A Review. Old Wine in a New Bottle? *Ann. Oncol.* **2006**, *17*, 735–749 and references therein.

[104] Gelderblom, H.; Verweij, J.; Nooter, K.; Sparreboom, A. Cremophor EL: The Drawbacks and Advantages of Vehicle Selection for Drug Formulation. *Eur. J. Cancer* **2001**, *37*, 1590–1598.

[105] Scripture, C. D.; Figg, W. D.; Sparreboom, A. Paclitaxel Chemotherapy: From Empiricism to a Mechanism-Based Formulation Strategy. *Ther. Clin. Risk Manag.* **2005**, *1*, 107–114.

[106] Sparreboom, A.; Baker, S. D.; Verweij, J. Paclitaxel Repackaged in an Albumin-Stabilized Nanoparticle: Handy or Just Dandy? *J. Clin. Oncol.* **2005**, *23*, 7765–7767.

[107] U.S. Food and Drug Administration. ABRAXANE™ for Injectable Suspension (paclitaxel protein-bound particles for injectable suspension) (albumin-bound). **2005**.

[108] Ibrahim, N. K.; Desai, N.; Legha, S.; Soon-Shiong, P.; Theriault, R. L.; Rivera, E.; Esmaeli, B.; Ring, S. E.; Bedikian, A.; Hortobagyi, G. N.; Ellerhorst, J. A. Phase I and Pharmacokinetics Study of ABI-007, a Cremophor-Free, Protein-Stabilized, Nanoparticle Formulation of Paclitaxel. *Clin. Cancer Res.* **2002**, *8*, 1038–1044.

[109] Gradishar, W. J.; Tjulandin, S.; Davidson, N.; Shaw, H.; Desai, N.; Bhar, P.; Hawkins, M.; O'Shaughnessy, J. Phase III Trial of Nanoparticle-Albumin Bound Paclitaxel Compared with Polyethylated Castor Oil-Based Paclitaxel in Women with Breast Cancer. *J. Clin. Oncol.* **2005**, *23*, 7794–7803.

[110] Harries, M.; Ellis, P.; Harper, P. Nanoparticle Albumin-bound Paclitaxel for Metastatic Breast Cancer. *J. Clin. Oncol.* **2005**, *23*, 7768–7771.

[111] Kim, S. C.; Kim, D. W.; Shim, Y. H.; Bang, J. S.; Oh, H. S.; Kim, S. W.; Seo, M. H. In vivo Evaluation of Polymeric Micellar Paclitaxel Formulation: Toxicity and Efficacy. *J. Control. Release* **2001**, *72*, 191–202.

[112] Hangal-Joshi, R.; Gore, A. Y.; Rubinfeld, J.; Shrotriya, R. Paclitaxel Formulation. U.S. Patent 6,538,020, August 1, 2002.

[113] Lee, K. S.; Chung, H. C.; Im, S. A.; Park, Y. H.; Kim, C. S.; Kim, S.-B.; Rha, S. Y.; Lee, M. Y.; Ro, J. Multicenter Phase II Trial of Genexol-PM, a Cremophor-Free Polymeric Micelle Formulation of Paclitasel, in Patients

with Metastatic Breast Cancer. *Breast Cancer Res. Treat.* **2008**, *108*, 241–250.

[114] Niu, F.; Roby, K. F.; Rajewski, R. A.; Decedue, C.; Subramaniam, B. Paclitaxel Nanoparticles: Production Using Compressed CO_2 as Antisolvent: Characterization and Animal Studies. In *Polymeric Drug Delivery II;* Svenson, S., ed. American Chemical Society: Washington, D. C., 2006, 262–277.

[115] Roby, K. F.; Niu, F.; Rajewski, R. A.; Decedue, C.; Subramaniam, B.; Terranova, P. F. Syngenic Mouse Model of Epithelial Ovarian Cancer: Effects of Nanoparticle Paclitaxel, Nanotax®. *Adv. Exp. Med. Biol.* **2008**, *622*, 169–181.

[116] Axiak, S. M.; Selting, K. A.; Decedue, C. J.; Henry, C. J.; Tate, D.; Howell, J.; Bilof, K. J.; Kim, D. Y. Phase I Does Escalation Study of Nanoparticulate Paclitaxel (CTI 52010) in Normal Dogs. *Int. J. Nanomedicine* **2011**, *6*, 2205–2212.

[117] Crown, J. Docetaxel and Paclitaxel in the Treatment of Breast Cancer: A Review of Clinical Experience. *Oncologist* **2004**, *9*, 24–32.

[118] Bernstein, B. Docetaxel as an Alternative to Paclitaxel after Acute Hypersensitivity Reactions. *Ann. Pharmacother.* **2000**, *34*, 1332–1335.

[119] Norris, L. B.; Qureshi, Z. P.; Bookstaver, P. B.; Raisch, D. W.; Sartor, O.; Chen, H.; Bennet, C. L. Polysorbate 80 Hypersensitivity Reactions: A Renewed Call to Action. *Commun. Oncol.* **2010**, *7*, 425–428.

[120] Echhoff, L.; Nielsen, M.; Moeller, S.; Knoop, A. TAXTOX – A Retrospective Study Regarding the Side Effects of Docetaxel Given as Part of the Adjuvant Treatment to Patients with Primary Breast Cancer in Denmark from 2007 to 2009. *Acta. Oncologica.* **2011**, *50*, 1075–1082.

[121] Vyas, D. M.; Wong, H.; Crosswell, A. R.; Casazza, A. M.; Knipe, J.O.; Mamber, S. W.; Doyle, T. W. Tumor targeting by covalent conjugation of a natural fatty acid to paclita. *Bioorg. Med. Chem. Lett*. **1993**, *3*, 1357–1360.

[122] Moosavi-Movahedi, A. A.; Hakimelahi, S.; Chamani, J.; Khodarahmi, G. A.; Hassanzadeh, F.; Luo, F. T.; Ly, T. W.; Shia, K.-S.; Yen, C. F.; Jain, M. L.; Kulatheeswaran, R.; Xue, C.; Pasdar, M.; Hakimelahi, G. H. Design, Synthesis, and Anticancer Activity of Phosphonic Acid Diphosphate Derivative of Adenine-Containing Butenolide and its Water Soluble Derivatives of Paclitaxel with High Antitumor Activity. *Bioorg. Med. Chem.* **2003**, *11*, 4303–4313.

[123] Paradis, R.; Page, M. New Active Paclitaxel Amino Acid Derivatives with Improved Water Solubility. *Anticancer Res.* **1998**, *18*, 2711–2716.

[124] Deutsch, H. M.; Glinski, J. A.; Hernandez, M.; Haugwitz, R. D.; Narayanan, V. L.; Suffness, M.; Zalkow, L. H. Synthesis of Congeners and Prodrugs. 3. Water-Soluble Prodrugs of Taxol with Potent Antitumor Activity. *J. Med. Chem.* **1989**, *32*, 788–792.

[125] Khmelnitsky, Y. L.; Budde, C.; Arnold, M. J.; Usyatinsky, A.; Clark, D. S.; Dordick, J. S. Synthesis of Water-Soluble Paclitaxel Derivatives by Enzymatic Acylation*. J. Am. Chem. Soc.* **1997**, *119*, 11554–11555.

[126] Greenwald, R. B.; Pendri, A.; Bolikal, D.; Gilbert, C. W. Highly Water Soluble Taxol Derivatives: 2-Polyethylene Glycol Esters as Potential Prodrugs. *Bioorg. Med. Chem. Lett*. **1994**, *4*, 2465–2470.

[127] Greenwald, R. B.; Gilbert, C. W.; Pendri, A.; Conover, C. D.; Xia, J.; Martinez, A. Drug Delivery Systems: Water Soluble Taxol 2'-Poly-(Ethylene Glycol) Ester Prodrugs. Design and in vivo Effectiveness. *J. Med. Chem*. **1996**, *39*, 424–431.

[128] Rodrigues, P. C. A.; Scheuermann, K.; Stockmar, C.; Maier, G.; Fiebig, H. H.; Unger, C.; Muelhaupt, R.; Kratz, F. Synthesis and in vitro Efficacy of Acid-Sensitive Poly(ethylene glycol) Paclitaxel Conjugates. *Bioorg. Med. Chem. Lett*. **2003**, *13*, 355–360.

[129] Luo, Y.; Prestwich, G. D. Synthesis and Selective Cytotoxicity of a Hyaluronic Acid-Antitumor Bioconjugate. *Bioconjugate Chem.* **1999**, *10*, 755–763.

[130] Li, C.; Yu, D. F.; Newman, R. A.; Cabral, F.; Stephens, L. C.; Hunter, N.; Milas, L.; Wallace, S. Complete Regression of Well-Established Tumors using a Novel Water-Soluble Poly(L-glutamic acid)-Paclitaxel Conjugate. *Cancer Res.* **1998**, *58*, 2404–2409.

[131] Stevens, P. J.; Sekido, M.; Lee, R. J. A Folate Receptor-Targeted Lipid Nanoparticle Formulation for a Lipophilic Paclitaxel Prodrug. *Pharm. Res.* **2004**, *21*, 2153–2157.

[132] Ansell, S. Lipophilic Drug Derivatives for Use in Liposomes. U.S. Patent 5,534,499, July 9, 1996.

[133] Zakharian, T. Y.; Seryshev, A.; Sitharaman, B.; Gilbert, B. E.; Knight, V.; Wilson, L. J. A Fullerene-Paclitaxel Chemotherapeutic: Synthesis, Characterization and Study of Biological Activity in Tissue Culture. *J. Am. Chem. Soc.* **2005**, *127*, 12508–12509.

[134] Ali, S.; Ahmad, I.; Peters, A.; Masters, G.; Minchey, S.; Janoff, A. S.; Mayhew, E. Hydrolyzable Hydrophobic Taxanes: Synthesis and Anticancer Activities. *Anti-Cancer Drugs* **2001**, *12*, 117–128.

[135] Lundberg, B. B.; Risovic, V.; Ramaswamy, M.; Wasan, K. M. A Lipophilic Pacltaxel Derivative Incorporated in a Lipid Emulsion for Parenteral Administration. *J. Control. Release* **2003**, *86*, 93–100.

[136] Rodrigues, D. C.; Maria, D. A.; Fernandes, D. C.; Valduga, C. J.; Couto, R. D.; Ibanez, O. C. M.; Maranhao, R. C. Improvement of Paclitaxel Therapeutic Index by Derivatization and Association to a Cholesterol-Rich Microemulsion: in vitro and in vivo Studies. *Cancer Chemother. Pharmacol.* **2005**, *55*, 565–576.

[137] Bradley, M. O.; Webb, N. L.; Anthony, F. H.; Devanesan, P.; Witman, P. A.; Hemamalini, S.; Chander, M. C.; Baker, S. D.; He, L.; Horwitz, S. B.; Swindell, C. S. Tumor Targeting by Covalent Conjugation of a Natural Fatty Acid to Paclitaxel. *Clin. Cancer Res*. **2001**, *7*, 3229–3238.

[138] Bedikian, A. Y.; DeConti, R. C.; Conry, R.; Agarwala, S.; Papadopoulos, N.; Kim, K. B.; Ernstoff, M. Phase 3 Study of Docosahexaenoic Acid-Paclitaxel Versus Dacarbazine in Patients with Metastatic Malignant Melanoma. *Ann. Oncol.* **2011**, *22*, 787–793.

[139] Harries, M.; O'Donnell, A.; Scurr, M.; Reade, S.; Cole, C.; Judson, I.; Greystoke, A.; Twelves, C.; Kaye, S. Phase I/II study of DHA-Paclitaxel in Combination with Carboplatin in Patients with Advanced Malignant Solid Tumours. *Br. J. Cancer* **2004**, *91*, 1651–1655.

[140] Hoye, T. R.; Wohl, A. W.; Macosko, C. W.; Panyam, J. Silicate Prodrugs and Nanoparticles. U.S. Patent Application PCT/US2012/040247, May 31, 2012. This application claims priority to a provisional application filed on May 31, 2011.

[141] Kim, I.-S.; Kim, S.-H. Development of a Polymeric Nanoparticulate Drug Delivery System: In vitro Characterization of Nanoparticles based on Sugar-Containing Particles. *Int. J. Pharm.* **2002**, *245*, 67–73.

[142] Görner, T.; Gref, R.; Michenot, D.; Sommer, F.; Tran, M. N.; Dellacherie, E. Lidocaine-loaded Biodegradable Nanospheres. I. Optimization of the Drug

Incorporation into the Polymer Matrix. *J. Control. Release* **1999**, *57*, 259–268.

[143] Zhu, Q.; Guo, Z.; Huang, N.; Wang, M.; Chu, F. Comparative Molecular Field Analysis of a Series of Paclitaxel Analogs. *J. Med. Chem*. **1997**, *40*, 4319–4328.

[144] Michel, A. University of Minnesota, Minneapolis, MN. Personal communication, **2012**.

[145] Hayashi, Y.; Skwarczynski, M.; Hamada, Y.; Sohma, Y.; Kumura, T.; Kiso, Y. A Novel Approach of Water-Soluble Paclitaxel Prodrug with No Auxiliary and no Byproduct: Design and Synthesis of Isotaxel. *J. Med. Chem.* **2003**, *46*, 3782–3784.

[146] Sohma, Y.; Hayashi, Y.; Skwarczynski, M.; Hamada, Y.; Sasaki, M.; Kimura, T.; Kiso, Y. O-N Intramolecular Acyl Migration Reaction in the Development of Prodrugs and the Synthesis of Difficult Sequence-Containing Bioactive Peptides. *Biopolymers* **2004**, *76*, 344–356.

[147] Analysis of crude ^{1}H NMR data demonstrated a characteristic shift of the C2' methine from a doublet (δ = 4.78) to a pair of diastereotopic doublets (δ = 5.03 and 5.01 in an ca. 3:2 ratio) assigned to **3.14**.

[148] This byproduct was later found to be the PTX-containing di-*t*-butoxysilanol **3.18**, confirmed by the HR-MS and the independent synthesis of **3.18**.

[149] Subjecting **3.17** to the "standard hydrolysis conditions" led to a $t_{1/2}$ > 400 h, at which point the experiment was discontinued.

[150] Damja, R. I.; Eaborn, C.; Saxena, A. K. Acyl-Oxygen Fission in Reactions of Oragnosilicon Carboxylates with Sodium Methoxide in Methanol. *J. Chem. Soc. Perkin Trans. II* **1985**, *2*, 597–598.

[151] These IC_{50} cytotoxicity studies were performed by Stephen Kalscheuer. Kalscheuer, S. University of Minnesota, Minneapolis, MN. Personal communication, **2012**.

[152] Mosmann, T. Rapid Colorimetric Assay for Cellular Growth and Survival: Application to Proliferation and Cytotoxicity Assays. *J. Immunol. Methods* **1983**, *65*, 55–63.

[153] Anand, P.; Kunnumakkara, A. B.; Newman, R. A.; Aggarwal, B. B. Bioavailability of Curcumin: Problems and Promises. *Mol. Pharm.* **2007**, *4*, 807–818.

[154] Hoehle, S. I.; Pfeiffer, E.; Metzler, M. Glucuronidation of Curcuminoids by Human Microsomal and Recombinant UDP-Glucuronosyltransferases. *Mol. Nutr. Food Res.* **2007**, *51*, 932–938.

[155] Pan, M.-H.; Huang, T.-M.; Lin, J.-K. Biotransformation of Curcumin through Reduction and Glucoronidation in Mice. *Drug Metab. Dispos.* **1998**, *27,* 486–494.

[156] O'Toole, M. G.; Henderson, R. M.; Soucy, P. A.; Fasciotto, B. H.; Hoblitzell, P. J.; Keynton, R. S.; Ehringer, W. D.; Gobin, A. S. Curcumin Encapsulation in Sub-Micron Chitosan/Tween 20 Particles. *Biomacromolecules*, **2012**, *13*, 2309–2314.

[157] These biological experiments were performed by Alex Grill. Grill, A. University of Minnesota, Minneapolis, MN. Personal communication, **2011**.

[158] Ireson, C. R.; Jones, D. J. L.; Orr, S.; Coughtrie, M. W. H.; Boocock, D. J.; Williams, M. L.; Farmer, P. B.; Steward, W. P.; Gescher, A. J. Metabolism of the Cancer Chemopreventive Agent Curcumin in Human and Rat Intestine. *Cancer Epidemiol. Biomarkers Prevent.* **2002**, *11*, 105–111.

[159] ^{1}H NMR assignments were made with the consideration of Oyama, M.; Itokawa, H. Physical Methods for Identification of the Structures of Taxoids. In *Taxus: The Genus Taxus*. Itokawa, H.; Lee, K.-H., Eds. Taylor & Francis, Inc: New York, **2003**, *32*; 79-133.

[160] Minor impurities were noted in the alkyl region of this product.

[161] Lohmeijer, B. G. G.; Pratt, R. C.; Leibfarth, F.; Logan, J. W.; Long, D. A.; Dove, A. P.; Nederberg, F.; Choi, J.; Wade, C.; Waymouth, R. M.; Hedrick, J. L. Guanidine and Amidine Organo-Catalysts for Ring-Opening Polymerization of Cyclic Esters. *Macromolecules* **2006**, *39*, 8574–8583.

[162] Qian, H.; Wohl, A. R.; Crow, J. T.; Macosko, C. W.; Hoye, T. R. A Strategy for Control of “Random” Copolymerization of Lactide and Glycolide: Application to Synthesis of PEG-*b*-PLGA Block Polymers Having Narrow Dispersity. *Macromolecules*, **2011**, *44*, 7132–7140.

[163] Jerome, C.; Lecomte, P. Recent Advances in the Synthesis of Aliphatic Polyesters by Ring-Opening Polymerization. *Adv. Drug Deliver. Rev*. **2008**, *60*, 1056–1076.

[164] Astente, C. E.; Sabliov, C. M. Synthesis and Characterization of PLGA Nanoparticles, *J. Biomater. Sci. Polymer Edn.* **2006**, *17*, 247–289.

[165] Albertsson, A. C.; Varma, I. K. Recent Developments in Ring Opening Polymerization of Lactones for Biomedical Applications. *Biomacromolecules* **2003**, *4*, 1466–1486.

[166] Mohamed, F.; Van der Walle, C. F. Engineering Biodegradable Polyester Particles with Specific Drug Targeting and Drug Release Properties. *J. Pharm. Sci.* **2008**, *97*, 71–87.

[167] Middleton, J. C.; Tipton, A. J. Synthetic Biodegradable Polymers as Orthopedic Devices. *Biomaterials* **2000**, *21*, 2335–2346.

[168] Drumright, R. E.; Gruber, P. R.; Henton, D. E. Polylactic Acid Technology. *Adv. Mater.* **2000**, *12*, 1841–1846.

[169] Chu, C. C. Biodegradable Polymeric Biomaterials: an Updated Overview. In *Biomaterials*; Wong, J. Y., Bronzino, J. D. CRC Press: Boca Raton, FL, 2007; 6/1–6/22.

[170] Vert, M. Polyglycolide and Copolyesters with Lactide. *Biopolymers* **2002**, *4*, 179–202.

[171] Stjerndahl, A.; Wistrand, A. F.; Albertsson, A. C. Industrial Utilization of Tin-Initiated Resorbable Polymers: Synthesis on a Large Scale with a Low Amount of Initiator. *Biomacromolecules* **2007**, *8*, 937–940.

[172] Li, J.; Stayshich, R. M.; Meyer, T. Y. Exploiting Sequence to Control the Hydrolysis Behavior of Biodegradable PLGA Copolymers. *J. Am. Chem. Soc.* **2011**, *133*, 6910–6913.

[173] Dong, C.-M.; Qiu, K.-Y.; Gu, Z.-W.; Feng, X.-D. Synthesis of Poly(D,L-lactic acid-*alt*-glycolic acid) from D,L-3-methylglycolide. *J. Polym. Sci., Part A: Polym. Chem.* **2000**, *38*, 4179–4184.

[174] Kreiser-Saunders, I.; Kricheldorf, H. R. Polylactones. Part 39. Zn Lactate-Catalyzed Copolymerization of L-lactide with Glycolide or ε-caprolactone. *Macromol. Chem. Phys.* **1998**, *199*, 1081–1087.

[175] O'Keefe, B. J.; Hillmyer, M. A.; Tolman, W. B Polymerization of Lactide and Related Cyclic Esters by Discrete Metal Complexes. *J. Chem. Soc., Dalton Trans.* **2001**, 2215–2224.

[176] Barakat, I.; Dubois, P.; Jérôme, R.; Teyssié, P. Living Polymerization and Selective End Functionalization of ε-caprolactone using Zinc Alkoxides as Initiators. *Macromolecules* **1991,** *24***,** 6542–6545.

[177] Baran, J.; Duda, A.; Kowalski, A.; Szymanski, R.; Penczek, S. Quantitative Comparison of Selectivities in the Polymerization of Cyclic Esters. *Macromol. Symp.* **1997**, *123*, 93–101.

[178] Ovitt, T. M.; Coates, G. W. Stereochemistry of Lactide Polymerization with Chiral Catalysts: New Opportunities for Stereocontrol using Polymer Exchange Mechanisms. *J. Am. Chem. Soc.* **2002**, *124*, 1316–1326.

[179] Shen, Y.; Shen, Z.; Shen, J.; Zhang, Y.; Yao, K. Characteristics and Mechanism of ε-caprolactone Polymerization with Rare Earth Halide Systems. *Macromolecules* **1996***, 29*, 3441–3446.

[180] Ravi, P.; Gröb, T.; Dehnicke, K.; Greiner, A. Novel $[Sm_2I(NPPh_3)_5(DME)]$ Initiator for the Living Ring-Opening Polymerization of ε-caprolactone and δ-valerolactone, *Macromolecules* **2001**, *34*, 8649–8653.

[181] Chamberlin, B. M.; Jazdzewski, B. A.; Pink, M.; Hillmyer, M. A.; Tolman, W. B. Controlled Polymerization of DL-lactide and ε-caprolactone by Structurally Well-Defined Alkoxo-Bridged Di- and Triyttrium(III) Complexes. *Macromolecules* **2000**, *33*, 3970–3977.

[182] Albertsson, A. C.; Srivastava, R. K. Recent Developments in Enzyme-Catalyzed Ring-Opening Polymerization. *Adv. Drug Deliver. Rev.* **2008**, *60*, 1077–1093.

[183] Nederberg, F.; Connor, E. F.; Möller, M.; Glauser, T.; Hedrick, J. L. New Paradigms for Organic Catalysts: the First Organocatalytic Living Polymerization. *Angew. Chem. Int. Ed.* **2001**, *40*, 2712–2715.

[184] Dove, A. P.; Pratt, R. C.; Lohmeijer, B. G. G.; Culkin, D. A.; Hagberg, E. C.; Nyce, G. W.; Waymouth, R. M.; Hedrick, J. L. *N*-Heterocyclic Carbenes: Effective Organic Catalysts for Living Polymerization. *Polymer* **2006**, *47*, 4018–4025.

[185] Myers, M.; Connor, E. F.; Glauser, T.; Mock, A.; Nyce, G.; Hedrick, J. L. Phosphines: Nucleophilic Organic Catalysts for the Controlled Ring-Opening Polymerization of Lactides. *J. Polym. Sci., Part A: Polym. Chem.* **2002**, *40*, 844–851.

[186] Zhang, L.; Nederberg, F.; Messman, J. M.; Pratt, R. C.; Hedrick, J. L.; Wade, C. G. Organocatalytic Stereoselective Ring-Opening Polymerization of Lactide with Dimeric Phosphazene Bases. *J. Am. Chem. Soc.* **2007,** *129*, 12610–12611.

[187] Dong, J.; Jiang, S.; Ping, Q. Development of Injectable Biodegradable in-situ forming Gel Implants. *Yaoxue Jinzhan* **2007**, *31*, 110–113.

[188] Avgoustakis, K. Pegylated Poly(lactide) and Poly(lactide-*co*-glycolide) Nanoparticles: Preparation, Properties and Possible Applications in Drug Delivery. *Curr. Drug Deliver*. **2004**, *1*, 321–333.

[189] Huh, K. M.; Cho, Y. W.; Park, K. PLGA-PEG Block Copolymers for Drug Formulations. *Drug Deliver. Tech*. **2003**, *42*, 44–49.

[190] Thakur, K. A. M.; Kean, R. T.; Hall, E. S.; Kolstad, J. J.; Munson, E. J. Stereochemical Aspects of Lactide Stereo-Polymerization Investigated by ^{1}H NMR: A Case of Changing Stereospecificity. *Macromolecules* **1998**, *21*, 1487–1497.

[191] Thillaye du Boullay, O.; Marchal, E.; Martin-Vaca, B.; Cossio, F. P.; Bourissou, D. An Activated Equivalent of Lactide toward Organocatalytic Ring-Opening Polymerization. *J. Am. Chem. Soc*. **2006**, *128*, 16442–16443.

[192] Each run of *i,i* moieties is terminated at each of its ends by a *i,s* moiety; there are two *i,s* moieties per run; and the number of runs is one half the number of *i,s* moieties. The average sequence length in any sample is the total

number of lactic acid units (#*i,i* + #*i,s*) divided by the total number of runs (#*i,s*/2).

[193] Hiemenz, P. C.; Lodge, T. P. Copolymers, Microstructure, and Stereoregularity. In *Polymer Chemistry*, 2nd Ed.; Taylor & Francis Group, LLC: Boca Raton, **2007**, *1*; 165–216.

[194] The reactivity ratio for a growing chain whose reactive terminal carbinol center has the *R* configuration is $r_{PLA\text{-}R}$ = (SL-2)/(2*[**R,R-1**]/[**S,S-1**]). Likewise, $r_{PLA\text{-}S}$ = (SL-2)/(2*[**S,S-1**]/[**R,R-1**]). Since **(±)-1** was used here, [**S,S-1**]/[**R,R-1**] = 1 and $r_{PLA\text{-}R} = r_{PLA\text{-}S} = r$ = (SL-2)/2.

[195] Kricheldorf, H. R.; Kreiser, I. Polylactones, 11. Cationic Copolymerization of Glycolide with L,L-Dilactide. *Makromol. Chem*. **1987**, *188*, 1861–1873.

[196] Gilding, D. K.; Reed, A. M. Biodegradable Polymers for Use in Surgery – Polyglycolic/Poly(lactic acid) Homo- and Copolymers: 1. *Polymer* **1979**, *20,* 1459–1464.

[197] Dotson, N. A.; Galván, R.; Laurence, R. L.; Tirrell, M. Reactor Configuration. In *Polymerization Process Modeling*; VCH Publishers, Inc.: New York, NY, **1996**; 259–303.

[198] To assess the accuracy of determining M_n via ^{1}H NMR spectroscopy, we analyzed three polymer samples by SEC/MALS to measure the absolute molecular weight each. The M_n values by these two approaches showed reasonably good agreement.

[199] Bandrup, J.; Immergut, E. H.; Grulke, E. A.; Abe, A.; Bloch, D. R. Polymer Handbook, 4th Edition, John Wiley & Sons, Inc. New York, 1999.

[200] Medrano, R.; Laguna, M. T. R.; Saiz, E.; Tarazona, M. P. Analysis of Copolymers of Styrene and Methyl Methacrylate using Size Exclusion

Chromatography with Multiple Detection. *Phys. Chem. Chem. Phys.* **2003**, *5*, 151–157.

[201] Huffman, K. R.; Casey, D. J. Effect of Carboxyl End Groups on Polyglycolic Acid. *J. Polym. Sci: Polym. Chem. Ed.* **1985**, *23*, 1939–1954.

[202] Khandpur, A. K.; Förster, S.; Bates, F. S.; Hamley, I W.; Ryan, A. J.; Bras, W.; Almdal, K.; Mortensen, K. Polyisoprene-Polystyrene Diblock Copolymer Phase Diagram near the Order-Disorder Transition. *Macromolecules* **1995**, *28*, 8796–8806.

[203] Bandrup, J.; Immergut, E. H.; Grulke, E. A.; Abe, A.; Bloch, D. R. Polymer Handbook, 4th Edition, John Wiley & Sons, Inc. New York, 1999.

[204] Kricheldorf, H. R.; Mang, T.; Jonte, J. M. Polylactones. 1. Copolymerization of Glycolide and ε-caprolactone. *Macromolecules* **1984**, *17*, 2173–2181.

[205] Grujpma, D. W.; Nijenhuis, A. J.; Pennings, A. J. Synthesis and Hydrolytic Degradation Behaviour of High-Molecular-Weight L-Lactide and Glycolide Copolymers. *Polymer* **1990**, *31*, 2201–2206.

[206] Odian, G., Principles of Polymerization, 4th Edition, Wiley-Interscience, New York, 2004, p 470.

[207] D'Addio, S. M.; Saad, W.; Ansell, S. M.; Squiers, J. J.; Adamson, D.; Herrera-Alonso, M.; Wohl, A. R.; Hoye, T. R.; Macosko, C. W.; Mayer, L. D.; Vauthier, C.; Prud'homme, R. K. Effects of Block Copolymer Properties on Nanocarrier Protection from *in vivo* Clearance. *J. Control. Release* **2012**, *162*, 208–217.

[208] Jain, R. A. The Manufacturing Techniques of Various Drug-Loaded Biodegradable Poly(lactide-*co*-glycolide) (PLGA) Devices. *Biomaterials*, **2000**, *21*, 2475–2490.

[209] Fetterly, G. J.; Straubinger, R. M. Pharmacokinetics of Paclitaxel-Containing Liposomes in Rats. *AAPS PharmSci.* **2003**, *5*, 90-100.

[210] Koudelka, S.; Turaneck-Knotigova, P.; Masek, J.; Korvasova, Z.; Skrbalova, M.; Plockova, J.; Bartheldyova, E.; Turanek, J. Liposomes with High Encapsulation Capacity for Paclitaxel: Preparation, Characterization, and *in vivo* Anticancer Effect. *J. Pharm. Sci.* **2010**, *99*, 2309–2319.

[211] Steele, T. W. J.; Huang, C. L.; Widjaja, E.; Boey, F. Y. C.; Loo, J. S. C.; Venkatraman, S. S.; The Effect of Polyethylene Glycol Strutcture on Paclitaxel Drug Release and Mechanical Properties of PLGA Thin Films. *Acta Biomater.* **2011**, *7*, 1973–1983.

[212] Quintanar-Guerrero, D.; Allèmann, E.; Fessi, H.; Doelker, E. Preparation Techniques and Mechanisms of Fromation of Biodegradable Nanoparticles from Preformed Polymers. *Drug Dev. Ind. Pharm.* **1998**, *24*, 1113–1128.

[213] Torchilin, V. P. Micellar Nanocarriers: Pharmaceutical Perspectives. *Pharm. Res.* **2007**, *24*, 1–16.

[214] Chavanpatil, M. D.; Patil, Y.; Panyam, J. Susceptibility of Nanoparticle-Encapsulated Paclitaxel to P-glycoprotein-mediated Drug Efflux. *Int. J. Pharm.* **2006**, *320*, 150–156.

[215] Patil, Y. B.; Toti, U. S.; Khdair, A.; Ma, L.; Panyam, J. Single-Step Surface Functionalization of Polymeric Nanoparticles for Targeted Drug Delivery. *Biomaterials*, **2009**, *30*, 859–866.

[216] Danhier, F.; Lecouturier, N.; Vroman, B.; Jèröme, C.; Marchand-Brynaert, J.; Feron, O.; Prèat, V. Paclitaxel-loaded PEGylated PLGA-based Nanoparticles: In vitro and in vivo Evaluation. *J. Control. Release* **2009**, *133*, 11–17.

[217] He, G.; Lwin, L.; Pan, J.; Venkatraman, S. ABA and BAB Type Triblock Copolymer of PEG and PLA: A Comparative Study of Drug Release Properties and "Stealth" Particle Characteristics. *Int. J. Pharm.* **2007**, *334*, 48–55.

[218] Johnson, B. K. Flash NanoPrecipitation of Organic Actives via Confined Micromixing and Block Copolymer Stabilization. Ph.D. Dissertation, Princeton University, Princeton, NJ, **2003**, 1–291.

[219] Zhu, Z.; Anacker, J. L.; Ji, S.; Hoye, T. R.; Macosko, C. W.; Prud'homme, R. K. Formation of Block Copolymer-Protected Nanoparticles via Reactive Impingement Mixing. *Langmuir*, **2007**, *23*, 10499–10504.

[220] Riess, G. Micellization of Block Copolymers. *Prog. Polym. Sci.* **2003**, *28*, 1107–1170 and references therein.

[221] Riley, T.; Stolnik, S.; Heald, C. R.; Xiong, C. D.; Garnett, M. C.; Illum, L; Davis, S. S.; Purkiss, S. C.; Barlow, R. J.; Gellert, P. R. Physicochemical Evaluation of Nanoparticles Assembled from Poly(lactic acid)-Poly(ethylene glycol) (PLA-PEG) Block Copolymers as Drug Delivery Vehicles. *Langmuir* **2001**, *17*, 3168–3174.

[222] Heald, C. R.; Stolnik, S.; Kujawinski, K. S.; De Matteis, C.; Garnett, M. C.; Illum, L.; Davis, S. S.; Purkiss, S. C.; Barlow, R. J.; Gellert, P. R. Poly(lactic acid)-Poly(ethylene oxide) (PLA-PEG) Nanoparticles: NMR Studies of the Central Solidlike PLA Core and the Liquid PEG Corona. *Langmuir*, **2002**, *18*, 3669–3675.

[223] Papadimitriou, S.; Bikiaris, D. Novel Self-Assembled Core–Shell Nanoparticles Based on Crystalline Amorphous Moieties of Aliphatic Copolyesters for Efficient Controlled Drug Release. *J. Control. Release* **2009**, *138*, 177–184.

[224] Zhang, X.-M.; Patel, A. B.; de Graaf, R. A.; Behar, K. L. Determindation of Liposomal Encapsulation Efficiency Using Proton NMR Spectroscopy. *Chem. Phys. Lipids* **2004**, *127*, 113–120.

[225] Hoo, C. M.; Starostin, N.; West, P.; Mecartney, M. L. A Comparison of Atomic Force Microscopy (AFM) and Dynamic Light Scattering (DLS) Methods to Characterize Nanoparticle Size Distributions. *J. Nanopart. Res.* **2008**, *10*, 89–96.

[226] Valentini, M.; Vaccaro, A.; Rehor, A.; Napoli, A.; Hubbell, J. A.; Tirelli, N. Diffusion NMR Spectroscopy for the Characterization of the Size and Interactions of Colloidal Matter: The Case of Vesicles and Nanoparticles. *J. Am. Chem. Soc.* **2004**, *126*, 2142–2147.

[227] Garcia-Fuentes, M.; Torres, D.; Martin-Pastor, M.; Alonso, M. J. Application of NMR Spectroscopy to the Characterization of PEG-Stabilized Lipid Nanoparticles. *Langmuir*, **2004**, *20*, 8839–8845.

[228] Dr. Letitia Yao provided critical expertise and assistance during these DOSY NMR experiments. Yao, L. University of Minnesota, Minneapolis, MN. Personal communication, **2011**.

[229] These studies are ongoing in collaboration with Ms. Jing Han and Prof. Christopher Macosko.

[230] Kang, E.; Robinson, J.; Park, K.; Cheng, J.-X. Paclitaxel Distribution in Poly(ethylene glycol) / Poly(lactide-*co*-glycolide) Blends and its Release by Coherent Anti-Stokes Raman Scattering Microscopy. *J. Control. Release* **2007**, *122*, 261–268.

[231] Mu, L.; Teo, M. M.; Ning, H. Z.; Tan, C. S.; Feng, S. S. Novel Powder Formulations for Controlled Delivery of Poorly Soluble Anticancer Drug:

Application and Investigation of TPGS and PEG in Spray-Dried Particulate System. *J. Control. Release* **2005**, *103*, 565–575.

[232] Ali, H.; El-Sayed, K.; Sylvester, P. W.; Nazzal, S. Molecular Interaction and Localization of Tocotrienol-Rich Fraction (TRF) within the Matrices of Lipid Nanoparticles: Evidence Studied by Differential Scanning Calorimetry (DSC and Proton Nuclear Magnetic Resonance Spectroscopy (^{1}H NMR). *Colloids Surf., B.* **2010**, *77*, 286–297.

[233] Essa, S.; Rabanel, J. M.; Hildgen, P. Effects of Polyethylene Glycol (PEG) Chain Organization on the Physicochemical Properties of Poly(D, L -lactide) (PLA) Based Nanoparticles. *Eur. J. Pharm. Biopharm.* **2010**, *75*, 96–106.

[234] Kulinski, Z.; Piorkowska, E.; Gadzinowska, K.; Stasiak, M. Plasticization of Poly(L-lactide with Poly(propylene glycol). *Biomacromolecules*, **2006**, *7*, 2128–2135.

[235] Lee, J. H.; Jho, J. Y. A Morphological Study of Semicrystalline Poly(L-lactic acid-*b*-ethylene oxide-*b*-L-lacitic acid) Triblock Copolymer. *Macromolecules* **2005**, *38*, 104–109.

[236] The cryo-TEM images were obtained by Mr. Han Seung Lee, a member of Prof. Alon McCormick's research group in Chemical Engineering and Materials Science.

[237] Oh, K. S.; Song, J. Y.; Cho, S. H.; Lee, B. S.; Kim, S. Y.; Kim, K.; Jeon, H.; Kwon, I. C.; Yuk, S. H. Paclitaxel-loaded Pluronic Nanoparticles Formed by a Temperature-Induced Phase Transition for Cancer Therapy. *J. Control. Release* **2010**, *148*, 344–350.

[238] Han, J. University of Minnesota,Minneapolis, M. Personal communication, **2012**.

[239] Guru, B. University of Minnesota, Minneapolis, MN. Personal communication, **2010**.

[240] Jenkins, D. E.; Oei, Y.; Hornig, Y. S.; Yu, S.-F.; Dusich, J.; Purchio, T.; Contag, P. R. Bioluminescent Imaging (BLI) to Improve and Redefine Traditional Murine Models of Tumor Growth and Metastasis. *Clin. Exp. Metastasis* **2003**, *20*, 733–744.

[241] http://www.criver.com/sitecollectiondocuments/rm_rm_r_NUNU_mouse_hematology_2008.pdf and http://www.criver.com/sitecollectiondocuments/rm_rm_r_NUNU_mouse_biochemistry_2008.pdf at http://www.criver.com/en-US/ProdServ/ByType/ResModOver/ResMod/Pages/NuNuNudeMouse.aspx (accessed May 31, 2012).

[242] Zhu, Z.; Margulis-Goshen, K.; Magdassi, S.; Talmon, Y.; Macosko, C. W. Polyelectrolyte Stabilized Drug Nanoparticles via Flash Nanoprecipitation: A Model Study With β-Carotene. *J. Pharm. Sci.* **2010**, *99*, 4295–4306.

[243] Paroo, Z.; Bollinger, R. A.; Braasch, D. A.; Richer, E.; Corey, D. R.; Antich, P. P.; Mason, R. P. Validating Bioluminescence Imaging as a High-Throughput, Quantitative Modality for Assessing Tumor Burden. *Mol. Imaging* **2004**, *3*, 117–124.

[244] Iha, R. K.; Wooley, K. L.; Nyström, A. M.; Burke, D. J.; Kade, M. J.; Hawker, C. J. Applications of Orthogonal “Click” Chemistries in the Synthesis of Functional Soft Materials. *Chem. Rev.* **2009**, *109*, 5620–5686.

[245] Acharya, S.; Sahoo, S. K. PLGA Nanoparticles Containing Various Agents and Tumour Delivery by EPR Effect. *Adv. Drug Deliver. Rev.* **2011**, *63*, 170–183.

[246] Brannon-Peppas, L.; Blanchette, J. O. Nanoparticle and Target Systems for Cancer Therapy. *Adv.Drug Delivery Rev*. **2004**, *56*, 1649–1659.

[247] Maeda, H.; Sawa, T.; Konno, T. Mechanism of Tumor-Targeted Delivery of Macromolecular Drugs,Including the EPR Effect in Solid Tumor and Clinical Overview of the Prototype Polymeric DrumSMANCS. *J. Control. Release* **2001**, *74*, 47–61.

[248] Peer, D.; Karp, J. M.; Hong, S.; Farokhzad, O. C.; Margalit, R.; Langer, R. Nanocarriers as an Emerging Platform for Cancer Therapy. *Nature Nanotech.* **2007**, *2*, 751–760.

[249] Adiseshaiah, P. P,. Hall, J. B., McNeil, S. E. Nanomaterial Standards for Efficacy and Toxicity Assessment. *Wiley Interdiscip. Rev. Nanomed. Nanobiotechnol.* **2010**, *2*, 99–112.

[250] Petros, R. A. & DeSimone, J. M. Strategies in the Design of Nanoparticles for Therapeutic Applications. *Nat. Rev. Drug Discov.* **2010**, *9*, 615–627.

[251] Betancourt, T.; Doiron, A.; Brannon-Peppas, L. Polymeric Nanoparticles for Tumor-Targeted Drug Delivery. In *Nanotechnology for Cancer Therapy.* Amiji, M. M., ed. CRC Press: Boca Raton, FL, 2007, pp 2115–229.

[252] Jäschke, A.; Fürste, J. P.; Cech, D.; Erdmann, V. A. Automated Incorporation of Polyethylene Glycol into Synthetic Oligonucleotides. *Tet. Lett.* **1993**, *34*, 301–304.

[253] Thompson, M. S.; Vadala, T. P.; Vadala, M. L.; Lin, Y.; Riffle, J. S. Synthesis and Applications of Heterobifunctional Poly(ethylene oxide) Oligomers. *Polymer* **2008**, *49*, 345–373 and references therein.

[254] Yagci, Y.; Ito, K. Macromolecular Architecture Based on Anionically Prepared Poly(ethylene oxide) Macromonomers. *Macromol. Symp.* **2005**, *226*, 87–96.

[255] Hiki, S.; Kataoka, K. A Facile Synthesis of Azido-Terminated Heterobifunctional Poly(ethylene glycol)s for “Click” Conjugation. *Bioconjugate. Chem.* **2007**, *18*, 2191–2196.

[256] Nagasaki, Y.; Iijima, M.; Kato, M.; Kataoka, K. Primary Amino-Terminal Heterobifunctional Poly(ethylene oxide). Facile Synthesis of Poly(ethylene oxide) with a Primary Amino Group on One End and a Hydroxyl Group at the Other End. *Bioconjugate Chem.* **1995**, *6*, 702–704.

[257] Ito, K.; Hashimura, K.; Itsuno, S. Poly(ethylene oxide) Macromolecules. 8. Preparation and Polymerization of ω-Hydroxypoly(ethylene oxide) Macromonomers. *Macromolecules* **1991**, *24*, 3977–3981.

[258] Reed, N. N,; Janda, K. D. A One-Step Synthesis of Monoprotected Polyethylene Glycol Ethers. *J. Org. Chem.* **2000**, *65*, 5843–5845.

[259] Hiki, S.; Kataoka, K. Versatile and Selective Synthesis of “Click Chemistry” Compatible Heterobifunctional Poly(ethylene glycol)s Possessing Azide and Alkyne Functionalities. *Bioconjugate Chem.* **2010**, *21*, 248–254.

[260] Additional samples (ca. 2K and 6K) were purchased at a later date from Adavanced Polymer Materials, Inc.

[261] Zhao, C.-L.; Winnik, M. A.; Riess, G.; Croucher, M. D. Fluorescence Probe Techniques Used to Study Micelle Formation in Water-Soluble Block Copolymers. *Langmuir*, **1990**, *6*, 514–516.

[262] Savic, R.; Luo, L.; Eisenberg, A.; Maysinger, D. Micellar Nanocontainers Distribute to Defined Cytoplasmic Organelles. *Science* **2009**, *300*, 615–618.

[263] Laitinen, O. H.; Hytönen, V. P.; Nordlund, H. R.; Kulomaa, M. S. Genetically Engineered Avidins and Streptavidins. *Cell Mol. Life Sci.* **2006**, *63*, 2992–3017.

[264] Tashiro, E.; Imoto, M. Target Identification of Bioactive Compounds. *Bioorg. Med. Chem.* **2012**, *20*, 1910–1921.

[265] Patil, Y.; Sadhukha, T.; Ma, L.; Panyam, J. Nanoparticle-Mediated Simultaneous and Targeted Delivery of Paclitaxel and Tariquidar Overcomes Tumor Drug Resistance. *J. Control. Rel.* **2009**, *136*, 21–29.

[266] Lee, E. S.; Na, K.; Bee, Y. H. Super pH-Sensitive Multifunctional Polymeric Micelle. *Nano Lett.* **2005**, *5*, 325–329.

[267] Salem, A. K.; Cannizzaro, S. M.; Davies, M. C.; Tendler, S. J. B.; Roberts, C. J.; Williams, P. M.; Shakesheff, K. M. Synthesis and Characterization of a Degradable Poly(lactic acid)-Poly(ethylene glycol) Copolymer with Biotinylated End Groups. *Biomacromolecules* **2001**, *2*, 575–580.

[268] Despras, G.; Robert, R.; Sendid, B.; Machez, E.; Poulain, D.; Mallet, J.-M. Biotin Sulfone Tagged Oligomannosides as Immunogens for Eliciting Antibodies against Specific Mannan Epitopes. *Bioorg. Med. Chem.* **2012**, *20*, 1817–1831.

[269] Newkome, G. R.; Kotta, K. K.; Mishra, A.; Moorefield, C. N. Synthesis of Water-Soluble Ester-Terminated Dendrons and Dendrimers Containing Internal PEG Linkages. *Macromolecules* **2004**, *37*, 8262–8268.

[270] Menger, F. M.; Zhang, H. Self-Adhesion among Phospholipid Vesicles. *J. Am. Chem. Soc.* **2006**, *128*, 1414–1415.

[271] Ryu, J.-H.; Jang, C.-J.; Yoo, Y.-S.; Lim, S.-G.; Lee, M. Supramolecular Reactor in an Aqueous Environment: Aromatic Cross Suzuki Coupling Reaction at Room Temperature. *J. Org. Chem.* **2005**, *70*, 8956–8962.

[272] Binder, W. H.; Sachsenhofer, R. “Click” Chemistry in Polymer and Materials Science. *Macromol. Rapid Commun.* **2007**, *28*, 15–54 and references therein.

[273] Opsteen, J. A.; van Hest, J. C. M. Modular Synthesis of Block Copolymers via Cycloaddition of Terminal Azide and Alkyne Functionalized Polymers. *Chem. Commun.* **2005**, 57–59.

[274] Ji, S.; Hoye, T. R.; Macosko, C. W. Primary Amine (-NH_2) Quantification in Polymers: Functionality by ^{19}F NMR Spectroscopy. *Macromolecules* **2005**, *38*, 4679–4686.

[275] Lin, P.-C.; Ueng, S.-H.; Yu, S.-C.; Jan, M.-D.; Adak, A. K.; Yu, C.-C.; Lin, L.-C. Surface Modification of Magnetic Nanoparticle via Cu(I)-Catalyzed Alkyne-azide [2 + 3] Cycloaddition. *Org. Lett.* **2007**, *9*, 2131–2134.

[276] Xu, W. Z.; Zhang, X.; Kadla, J. F. Design of Functionalized Cellulosic Honeycomb Films: Site-Specific Biomolecule Modification via "Click Chemistry." *Biomacromolecules* **2012**, *13*, 350–357.

[277] Weis, W. I.; Drickamer, K.; Hendrickson, W. A. Structure of a C-type Mannose-Binding Protein Complexed with an Oligosaccharide. *Nature* **1992**, *360*, 127–134.

[278] Irache, J. M.; Salman, H. H.; Gamazo, C.; Espuelas, S. Mannose-Targeted Systems for the Delivery of Therapeutics. *Expert Opin. Drug Dis.* **2008**, *5*, 703–724.

[279] Foged, C. Arigita, C.; Sundblad, A.; Jiskoot, W.; Storm, G.; Frokjaer, S. Interaction of Dendritic Cells with Antigen-Containing Liposomes: Effect of Bilayer Composition. *Vaccine* **2004**, *22*, 1903–1913.

[280] Taylor, M. E.; Drickamer, K. Structural Requirements for High-Affinity Binding of Complex Ligands by the Macrophage Mannose Receptor. *J. Bio. Chem.* **1993**, *268*, 399–404.

[281] Engel, A.; Chatterjee, S. K.; Al-arifi, A.; Riemann, D.; Langner, J.; Nuhn, P. Influence of Spacer Length on Interaction of Mannosylated Liposomes with Human Phagocytic Cells. *Pharm. Res.* **2003**, *20*, 51–57.

[282] Yeeprae, W.; Kawakami, S.; Yamashita, F.; Hashida, M. Effect of Mannose Density on Mannose Receptor-Mediated Cellular Uptake of Mannosylated O/W Emulstions by Macrophages. *J. Control. Release* **2006**, *114*, 193–201.

[283] Mahajan, S.; Prashant, C. K.; Koul, V.; Choudhary, V.; Dinda, A. K. Receptor Specific Macrophage Targeting by Mannose-Conjugated Gelatin Nanoparticles: An *in vitro* and *in vivo* Study. *Curr. Nanosci.* **2010**, *6*, 413–421.

[284] Nagahori, N.; Nishimura, S.-I. Tailoring Glycopolymers: Controlling the Carbohydrate-Protein Interaction Based on Template Effects. *Biomacromolecules* **2001**, *2*, 22–24.

[285] Hotha, S.; Kashyap, S.; "Click Chemistry" Inspired Synthesis of *pseudo*-Oligosaccharides and Amino Acid Glycoconjugates. *J. Org. Chem.* **2006**, *71*, 364–367.

[286] Fernandez-Megia, E.; Novoa-Carballal, R.; Quio, E.; Riguera, R. Conjugation of Bioactive Ligands to PEG-Grated Chitosan at the Distal End of PEG. *Biomacromolecules*, **2007**, *8*, 833–842.

[287] Berry, L. M.; Wollenberg, L.; Zhao, Z. Esterase Activities in the Blood, Liver and Intestine of Several Preclinical Species and Humans. *Drug Metab. Lett.* **2009**, *3*, 70–77.

[288] Synthesis of the mPEG-C(O)O$(CH_2)_3$CCH proceeded as expected and to high conversion. The key ^{1}H NMR resonances (500 MHz, $CDCl_3$): δ 4.24 [non-uniform t, *J* = 4.8 Hz, 2H, $CH_3O(CH_2CH_2O)_mCH_2CH_2OC(O)CH_2CH_2CH_2CCH$], 3.65 [s, 455 H,

$CH_3O(CH_2CH_2O)_mCH_2CH_2OC(O)CH_2CH_2CH_2CCH$], 3.38 [s, 3H, $CH_3O(CH_2CH_2O)_mCH_2CH_2OC(O)CH_2CH_2CH_2CCH$], 2.49 [t, J = 7.5 Hz, 3H $CH_3O(CH_2CH_2O)_mCH_2CH_2OC(O)CH_2CH_2CH_2CCH$], 2.27 [dt, J = 7.0, 2.7 Hz, 2H, $CH_3O(CH_2CH_2O)_mCH_2CH_2OC(O)CH_2CH_2CH_2CCH$], 1.98 [t, J = 2.6 Hz, 1H, $CH_3O(CH_2CH_2O)_mCH_2CH_2OC(O)CH_2CH_2CH_2CCH$], and 1.85 [app pent, J = 7.1 Hz, 2H $CH_3O(CH_2CH_2O)_mCH_2CH_2OC(O)CH_2CH_2CH_2CCH$].

[289] Iyer, S. S.; Anderson, A. S.; Reed, S.; Swanson, B.; Schmidt, J. G. Synthesis of Orthogonal End Functinoaled Oligotheylene Glycols of Defined Lengths. *Tetrahedron Lett.* **2004**, *45*, 4285–4288.

[290] Mereyala, H. B.; Gurrala, S. R. A Highly Diastereoselctive, Practical Synthesis of Allyl, Propargyl, 2,3,4,6-tetra-*O*-acetyl-β-D-gluco, β-D-galactopyranosides and Allyl, Propargyl, Heptaacetyl-β-D-lactosides. *Carbohydr. Res.* **1998**, *307*, 351–354.

[291] Wang, R.; Chen, G.-T.; Du, F.-S.; Li, Z.-C. Preparation and Aggregation Behavior of Mannose-Terminated Poly(ethylene glycol)-*b*-poly(L-leucine) in Water. *Colloids Surf., B* **2011**, *85*, 56–62.

[292] Kumar, K. K.; Kumar, R. M.; Subramanian, V.; Das, T. M. Expedient Synthesis of Coumarin-Coupled Triazoles via 'Click Chemistry' Leading to the Formation of Coumarin-Triazole-Sugar Hybrids. *Carbohydr. Res.* **2010**, *345*, 2297–2304.

[293] Singh, R. A Sensitive Assay for Maleimide Groups. *Bioconjugate Chem.* **1994**, *5*, 348–351.

[294] Durmaz, H.; Colakoglu, B.; Tunca, U.; Hizal, G. J. Preparation of Block Copolymers Via Diels Alder Reaction of Maleimide- and Anthracene-End Functionalized Polymers. *J. Polym. Sci., Part A: Polym. Chem.* **2006**, *44*, 1667–1675.

[295] Dag, A.; Durmaz, H.; Demir, E.; Hizai, G.; Tunca, U. Heterograft Copolymers via Double Click Reactions Using One-Pot Technique. *J. Polym. Sci., Part A: Polym. Chem.***2008**, *46*, 6969–6977.

[296] Kosif, I.; Park, E.-J.; Sanyal, R.; Sanyal, A. Fabrication of Maleimide Containing Thiol Reactive Hydrogels via Diels-Alder/Retro Diels-Alder Strategy. *Macromolecules* **2010**, *43*, 4140–4148.

[297] Durmaz, H.; Dag, A.; Altintas, O.; Erdogan, T.; Hizal, G.; Tunca, U. One Pot Synthesis of ABC Type Triblock Copolymers via in situ Click [3 + 2] and [4 + 2] Reactions. *Macromolecules* **2007**, *40*, 191–198.

[298] Gacal, B.; Durmaz, H.; Tasdelen, M. A.; Hizal, G.; Tunca, U.; Yagel, Y.; Demirel, A. L. Anthracene-Maleimide-Based Diels-Alder "Click Chemistry" as a Novel Route to Graft Copolymers. *Macromolecules* **2006**, *39*, 5330–5336.

[299] Olivier, J.-C.; Huertas, R.; Lee, H. J.; Calon, F.; Pardridge, W. M. Synthesis of Pegylated Immunonanoparticles. *Pharm. Res.* **2002**, *19*, 1137–1143.

[300] Nasongkla, N.; Shuai, X.; Ai, H.; Weinberg, B. D.; Pink, J.; Boothman, D. A.; Gao, J. cRGD-Functionalized Polymer Micelles for Targeted Doxorubicin Delivery. *Angew. Chem., Int. Ed*. **2004**, *116*, 6483–6487.

[301] Ji, S.; Hoye, T. R.; Zhu, Z.; Macosko, C. W. Maleimide Functionalized Poly(ε-caprolactone)-*b*-poly(ethylene glycol) (PCL-PEG-MAL) Nanoparticles: Formation and Thiol Conjugation. *Macromol. Chem. Phys.* **2009**, *210*, 823–831.

[302] Mehta, N. B.; Phillips, A. P.; Lui, F. F.; Brooks, R. E. Maleamic and Citraconamic Acids, Methyl Esters, and Imides. *J. Org. Chem.* **1960**, *25*, 1012–1015.

[303] Mitsunobu, O. The Use of Diethyl Azodicarboxylate and Triphenylphosphine in Synthesis and Transformation of Natural Products. *Synthesis* **1981** 1–28.

[304] Walker, M. A. The Mitsunobu Reaction: A Novel Method for the Synthesis of Bifunctional Maleimide Linkers. *Tetrahedron Lett.* **1994**, *35*, 665–668.

[305] Gill, H. S.; Tinianow, J. N.; Ogasawara, A.; Flores, J. E.; Vanderbilt, A. N.; Raab, H.; Scheer, J. M.; Vandlen, R.; Williams, S.-P.; Marik, J. A Modular Platform for the Rapid Site-Specific Radiolabelling of Proteins with ^{18}F Exemplified by Quantitative Positron Emission Tomography of Human Epidermal Growth Factor Receptor 2. *J. Med. Chem.* **2009**, *52*, 5826–5825.

[306] Walker, M. A. A High Yielding Synthesis of *N*-alkyl Maleimides Using a Novel Modification of the Mitsunobu Reaction. *J. Org. Chem.* **1995**, *60*, 5352–5355.

[307] Warnecke, A.; Kratz, F. Maleimide-oligo(ethylene glycol) Derivative of Camptothecin as Albumin-Binding Prodrugs: Synthesis and Antitumor Efficacy. *Bioconjugate Chem.* **2003**, *14*, 377–387.

[308] Given the limited discussion and spectroscopic data, it is difficult to judge the conversion (rather than the mass-based percent yield) of this reaction. See Schumacher, F. F.; Nobles, M.; Ryan, C. P.; Smith, M. E. B.; Tinker, A.; Caddick, S.; Baker, J. R. In Situ Maleimide Bridging of Disulfides and a New Approach to Protein PEGylation. *Bioconjugate Chem.* **2011**, *22*, 132–136.

[309] Veronese, F. M. Peptide and Protein PEGylation: A Review of Problems and Solutions. *Biomaterials* **2001**, *22*, 405–417 and references therein.

[310] Model **6.60** (17.5 mg, 0.088 mmol, 1 equiv) was co-dissolved with cysteine ethyl ester hydrochloride salt **6.68** (17.4 mg, 0.094 mmol, 1.1 equiv) in a buffered D_2O solution (pD = 7.4) in a 3 mL vial with stir bar. The vessel was capped with a Teflon-lined cap and allowed to stir for overnight at rt. The

product was analyzed crude and the major product was found to be **6.69**.LC/MS (Method: C18 column, gradient 50-100% methanol content MM-ES+APCI Positive and MM-ES+APCI Negative) t_R = 1.8 min ($M\text{-}H^+$ 349.0 and 350.0 for the di- and tri-deuterated species).

[311] http://www.creativepegworks.com/heterobifunctional%20PEG.html accessed July 18th, 2012.

[312] This procedure was completed with the help of Mr. Ligeng Yin in the lab of Prof. Marc Hillmyer. Their expertise, assistance, and provision of materials are greatly appreciated.

[313] Two primary singlets (and associated minor peaks due to differing repeat unit and/or stereoisomer patterns at the end of the polyester) are observed in the ^{1}H NMR spectrum. The total integration of these resonances in the fully acetylated BCP is 3H, although the ratio of the integrations varies by BCP batch.

[314] The ^{1}H NMR spectrum also exhibited resonances consistent with pyridine contamination.

[315] Some contaimination was noted from a PEG-*b*-PLGA polymer bearing the alkyne at both the polyether and polyester termini.

[316] The aromatic traizole resonance could not be observed, likely due to the minimal amount of material, low signal-to-noise ratio, and/or previously observed broadness of this resonance in $CDCl_3$.

[317] Relavent ^{1}H NMR data are reported from an impure sample. Impurities are omitted.

Bibliography

[1] Horn, D.; Rieger, J. Organic Nanoparticles in the Aqueous Phase – Theory, Experiment, and Use. *Angew. Chem. Int. Ed.* **2001**, *40*, 4330–4361.

[2] Johnson, B. K.; Prud'homme, R. K. Chemical Processing and Micromixing in Confined Impinging Jets. *AIChE* **2003**, *49*, 2264–2282.

[3] Johnson, B. K.; Prud'homme, R. K. Flash NanoPrecipitation of Organic Actives and Block Copolymers using a Confined Impinging Jets Mixer. *Aust. J. Chem.* **2003**, *56*, 1021–1024.

[4] Liu, Y.; Cheng, C.; Liu, Y.; Prud'homme, R. K.; Fox, R. O. Mixing in a Multi-Inlet Vortex Mixer (MIVM) for Flash Nano-Precipitation. *Chem. Eng. Sci.* **2008**, *63*, 2829–2842.

[5] Zhu, Z. Polymer Stabilized Nanosuspensions Formed via Flash Nanoprecipitation: Nanoparticle Formation, Formulation, and Stability. Ph.D. Dissertation, University of Minnesota, Minneapolis, MN, **2010**, 1–213.

[6] Han, J.; Zhu, Z.; Qian, H.; Wohl, A. R.; Beaman, C. J.; Hoye, T. R.; Macosko, C. W. A Simple Confined Impingement Jets Mixer for Flash NanoPrecipitation. *J. Pharm. Sci.* **2012**, *101*, 4018–4023.

[7] Saad, W. S. Drug Nanoparticle Formation via Flash Nanoprecipitation: Conjugation to Encapsulate and Control the Release of Paclitaxel. Ph.D. Dissertation, Princeton University, Princeton, NJ, **2007**. 1–198.

[8] Ansell, S. M.; Johnstone, S. A.; Tardi, P. G.; Lo, L.; Xie, S.; Shu, Y.; Harasym, T. O.; Harasym, N. L.; Williams, L.; Bermudes, D.; Liboiron, B. D.; Saad, W.; Prud'homme, R. K.; Mayer, L. D. Modulating the Therapeutic Activity of Nanoparticle Delivered Paclitaxel by Manipulating the Hydrophobicity of Prodrug Conjugates. *J. Med. Chem.* **2008**, *51*, 3288–3296.

[9] Dechy-Cabaret, O.; Martin-Vaca, B.; Bourissou, D. Controlled Ring-Opening Polymerization of Lactide and Glycolide. *Chem. Rev.* **2004**, *104*, 6147–6176.

[10] Ebelmen, M. *Ann. Chim. Phys.* **1845.** *15,* 319.

[11] Arkles, B. Silicon Esters. In *Kirk-Othmer Encyclopedia of Chemical Technology, Fourth Edition, Volume 22*; Kroschwitz, J. I.; Howe-Grant, M., ed. John Wiley & Sons, Inc: New York, 1997, 69–81.

[12] Wright, J. R. Bolt, R. O.; Goldschmidt, A.; Abbott, A. D. Silicate Esters and Related Compounds. I. Synthesis of Certain Tetraalkoxysilanes, Polyalkoxysilanes, Bis-(trialkoxysilyl)-alkanes, and Related Intermediates. *J. Am. Chem. Soc.* **1957**, *80*, 1733–1737.

[13] Hoye, T. R.; Ji, S.; Miura, Y.; Zhu, Z.; Macosko, C. W. PCL-b-PEG Nanoparticles for Drug Delivery: Package and Contents. Presented at IPRIME annual meeting. Minneapolis, MN, May 31, 2007.

[14] Wohl, A. R.; Hoye, T. R.; Zhu, Z.; Macosko, C. W. Orthosilicate Prodrug Models: Synthesis, Hydrolysis, and Encapsulation in Block Copolymer Nanoparticles. National Meeting of the AIChE, Nov. 2010.

[15] Tang, L.; Fan, T. M.; Borst, L. B.; Cheng, J. Synthesis and Biological Response of Size-Specific, Monodisperse Drug-Silica Nanoconjugates. *ACS Nano*, **2012**, *6*, 3954–3966.

[16] Kingston, D. G. I. The Shape of Things to Come: Structural and Synthetic Studies of Taxol and Related Compounds. *Phytochemistry* **2007**, *68*, 1844–1854.

[17] Parrott, M. C.; Luft, J. C.; Byrne, J. D.; Fain, J. H.; Napier, M. E.; DeSimone, J. M. Tunable Bifunctional SIlyl Ether Cross-Linkers for the Design of Acid-Sensitive Biomaterials. *J. Am. Chem. Soc.* **2010**, *132*, 17928–17932.

[18] Parrott, M. C.; Finniss, M.; Luft, J. C.; Pandya, A.; Gullapalli, A.; Napier, M. E.; DeSimone, J. M. Incorporation and Controlled Release of Silyl Ether Prodrugs from PRINT Nanoparticles. *J. Am. Chem. Soc.* **2012**, *134*, 7978–7982.

[19] Bassindale, A. R.; Taylor, P. G. Reaction Mechanisms of Nucleophilic Attack at Silicon. In *The Chemistry of Organic Silicon Comounds*. Patai, S.; Rappoport, Z., eds. John Wiley & Sons, Inc: New York, 1989, 839–892 and references therein.

[20] Holmes, R. R. The Stereochemistry of Nucleophilic Substitution at Tetracoordinated Silicon. *Chem. Rev.* **1990**, *90*, 17–31 and references therein.

[21] Aelion, R.; Loebel, A.; Eirich, F. Hydrolysis of Ethyl Silicate. *J. Am. Chem. Soc.* **1950**. *69*, 61–75.

[22] Brinker, C. J. Hydrolysis and Condensation of Silicates: Effects on Structure. *J.Non-Cryst. Solids* **1988**, *100*, 31–50.

[23] Ro, J. C.; Chung, I. J. Sol-Gel Kinetics of Tetraethylorthosilicate (TEOS) in Acid Catalyst. *J. Non-Cryst. Solids* **1989**, *110*, 26–32.

[24] Zerda, T. W.; Hoang, G. Effects of Solvents on the Hydrolysis Reaction of Tetramethyl Orthosilicate. *Chem. Mater.* **1990**, *2*, 372–376.

[25] Turner, C. W.; Franklin, K. J. Studies of the Hydrolysis and Condensation of Tetraethylorthosilicate by Multinuclear (^{1}H ^{17}O ^{29}Si) NMR Spectroscopy. *J. Non-Cryst. Solids* **1986**, *91*, 402–415.

[26] Assink, R. A.; Kay, B. D.; Study of Sol-Gel Chemical Reaction Kinetics by NMR. *Annu. Rev. Mater. Sci.* **1991**, *21*, 491–513.

[27] Zerda, T. W.; Hoang, G. Effects of Solvents on the Hydrolysis Reaction of Tetramethyl Orthosilicate. *Chem. Mater.* **1990**, *2*, 372–376.

[28] Brinker, C. J.; Scherer, G. W. Hydrolysis and Condensation II: Silicates. In *Sol-Gel Science: The Physics and Chemistry of Sol-Gel Processing*. Academic Press, Inc: San Diego, CA, **1990**, 97–233.

[29] Miura, Y. University of Minnesota, Minneapolis, MN. Personal communication, **2008**.

[30] Kalia, J.; Raines, R. T. Hydrolytic Stability of Hydrazones and Oximes. *Angew. Chem. Int. Ed.* **2008**, *47*, 7523–7526.

[31] Ridge, D.; Todd, M. Studies in the Formation Mechanisms of Alkyl Orthosilicates. *J. Chem. Soc.* **1949**, 2637–2640.

[32] Gerrard, W.; Woodhead, A. H. Interaction of Alcohols with Silicon Tetrachloride. *J. Chem. Soc.* **1951**, 519–522.

[34] Leo, A.; Hansch, C.; Elkins, D. Partition Coefficients and Their Uses. *Chem. Rev.* **1971**, *71*, 525–616 and references cited therein.

[35] Tetko, I. V.; Poda, G. I. Application of ALOGPS 2.1 to Predict log D Distribution Coefficient for Pfizer Proprietary Compounds. *J. Med. Chem*. **2004**, *47*, 5601–5604

[36] Tetko, I. V.; Bruneau, P. Application of ALOGPS to Predict 1-Octanol/Water Distribution Coefficients, logP, and logD, of AstraZeneca In-House Database. *J. Pharm. Sci*. **2004**, *93*, 3103–10.

[37] Tetko, I. V., Tanchuk, V. Y. Application of Associative Neural Networks for Prediction of Lipophilicity in ALOGPS 2.1 Program. *J. Chem. Inf. Comput. Sci.* **2002**, *42*, 1136–1145.

[38] http://www.vcclab.org/lab/alogps/ accessed June 19, 2012.

[39] Clausen, R. P.; Bols, M. The First Tri- and Tetraalkoxysilanes with Four Different Substituents. *J. Org. Chem.* **1997**, *62*, 4457–4464.

[40] Pedlow, G. W., Jr.; Miner, C. S., Jr. Organic Orthosilicates Stable Against Hydrolysis. U.S. Patent 2,566,365, June 15, 1946.

[41] Beckmann, J.; Dakternieks, D.; Tiekink, E. R. T. Chiral Trialkoxysilanols Derived from Terpene Alchols. Molecular Structures of Tris([(1*S*)-*endo*-]-(–)-bornoxy)silanols and tetrakis((–)-menthoxy)silane. *J. Organomet. Chem.* **2002**, *648*, 188–192.

[42] Miner, C. S., Jr.; Bryan, L. A.; Holysz, R. P.; Pedlow, G. W., Jr. *Ind. Eng. Chem.* Tert-Alkoxyaminosilanes. **1947**, *39*, 1368.

[43] Hyde, J. F.; Curry, J. W. The Preparation of Tetra-*i*-butoxysilane and Tri-*t*-butoxyfluorosilane. *J. Am. Chem. Soc.* **1955**, *77*, 3140–3141.

[46] Takebayashi, T. Acute Inhilation Toxicity of High Concentrations of Silane in Male ICR Mice. *Arch. Toxicol.* **1993**, *67*, 55–60.

[47] Anglin, E. J.; Cheng, L.; Freeman, W. R.; Sailor, M. J. Porous Silicon in Drug Delivery Devices and Materials. *Adv. Drug Deliver. Rev.* **2008**, *60*, 1266–1277.

[48] Corriu, R. J. P.; Henner, B. J. L. Mechanism of Nucleophilic Substitution at Silicon: Kinetic Evidence on the Slow Formation of a Penta-Coordinate Silicon Intermediate. *J. Organomet. Chem.* **1975**, *102*, 407–416.

[49] Friedel, C.; Ladenburg, A. *Liebigs Annalen der Chemie,* **1868**, *145,* 174–178.

[50] Schuyten, H. A.; Weaver, J. W.; Reid, J. D. Preparation of Substituted Acetoxy Silanes. *J. Am. Chem. Soc.* **1947**, *69*, 2110–2112.

[51] Kopylov, V. M.; Kireev, V. V.; Ivanov, V. V.; Astaf'ev, G. Y.; Kozlov, Y. V. Reaction of Acetoxysilanes with Hydroxy Compounds. *Rus. J. Gen. Chem.* **2001**, *71*, 1924–1928.

[52] Roth, M. J.; Brook, M. A.; Penny, H. B. Hydrosilane Cleavage Reactions Accelerated by Tartaric Acid and Dimethyl Sulphoxide. *J. Organomet. Chem.* **1996**, *521*, 65–74.

[55] Cragg, R. H.; Lane, R. D. Contributios to Group IV Organometallic Chemistry IV. Preparation and Properties of Some Organosilicon Derivatives of Salicylic and Related Acids. *J. Organomet. Chem.* **1981**, *212*, 301–310.

[58] Theis, B.; Weib, J.; Lippert, W. P.; Bertermann, R.; Burschka, C.; Tacke, R. Zwitterionic and Anionic Multinuclear Pentacoordinate Silicon(IV) Complexes with Bridging (R,R)-Tartrato(4) Ligands and SiO_5 Skeletons: Synthesis and Reactivity in Aqueous Solution. *Chem. Eur. J.* **2012**, *18*, 2202–2206.

[59] Gabizon, A.; Shmeeda, H.; Barenholz, Y. Pharmacokinetics of Pegylated Liposomal Doxorubicin. *Clin. Pharmacokinet.* **2003**, *42*, 419–436.

[60] Diedrich, F.; Ebker, C.; Klingbiel, U.; Reiche, C.; Labahn, T.; Magull, J.; Noltemeyer, M. N,N-Bis(silyl)ethylenediamine und 1,3-Diaza-2-silacyclopentane – Synthese, Reaktionen, Strukturen. *Z. Naturforsch., B: Chem. Sci.* **2002**, *57*, 99–106.

[61] Wutz, P. G. M.; Greene, T. W. Protection for the Amino Group. In *Greene's Protective Groups in Organic Synthesis, Fourth Edition*. John Wiley & Sons, Inc: Hoboken, NJ, 2007.

[68] Ismail, V. R. M. Herstellung von Tertiarbutoxy-(halogenphenoxy)-silanen. XIV. *Z. anorg. allg. Chem.* **1969**, *371,* 23–31.

[71] Overman, L. E.; Okazako, M. E.; Mishra, P. *tert*-Butyldipenylsilylamines: A Useful Protecting Group for Primary Amines. *Tet. Lett.* **1986**, *27*, 4391–4394.

[72] Liang, H.; Hu, L.; Corey, E. J. Di-*tert*-butylisobutylsilyl, Another Useful Protecting Group. *Org. Lett.* **2011**, *13*, 4120–4123.

[73] Lipshutz, B. H.; Papa, P.; Keith, J. M. Triisopropylsiloxycarbonyl ("Tsoc"): A New Protecting Group for 1° and 2° Amines. *J. Org. Chem.* **1999**, *64*, 3792–3793.

[74] Tao, M.; Park, C. H.; Bihovsky, R.; Wells, G. J.; Husten, J.; Ator, M. A.; Hudkins, R. L. Synthesis and Structure-Activity Relationships of Novel Poly(ADP-ribose) Polymerase-1 Inhibitors. *Bioorg. Med. Chem. Lett.* **2006**, *16*, 938–942.

[77] Gerrard, W.; Jones, J. V. Stability of Isomeric Butoxysilanes with Respect to Silicon Tetrachloride and Hydrogen Chloride. *J. Chem. Soc.* **1952**, 1690–1693.

[78] Gerrard, W.; Howe, B. K. The Behaviour of 1:1:1:3:3:3-hexachloropropan-2-ol with Inorganic Non-Metal Halides. *J. Chem. Soc.* **1955**, 505–510.

[79] Chappelow, C. C.; Elliot, R. L.; Goodwin, J. T. The Phenylation and Methylation of Alkoxychlorosilanes. *J. Org. Chem.* **1960**, *25*, 435–439.

[80] Pedlow, G. W.; Miner, C. S. Tertiary-Alkoxy Chlorosilanes. U.S. Patent 2,566,957, September 4, 1951.

[81] Ciuffreda, P.; Casati, S.; Manzocchi, A. Complete ^{1}H and ^{13}C NMR Spectral Assignment of 17-Hydroxy Epimeric Sterols with Planar A or A and B Rings. *Magn. Reson. Chem.* **2004**, *42*, 360–363.

[82] Kirk, D. N.; Toms, H. C.; Douglas, C.; White, K. A.; Smith, K. E.; Latif, S.; Hubbard, R. W. P. A Survey of the High-Field ^{1}H NMR Spectra of the Steroid Hormones, their Hydroxylated Derivatives, and Related Compounds. *J. Chem. Soc. Perkin Trans. 2* **1990**, 1567–1594.

[83] Stella, V. J. A Case for Prodrugs. In *Prodrugs.* Stella, V. J.; Borchardt, R. T.; Hageman, M. J.; Oliyai, R.; Maag, H.; Tilley, J. W., eds. Springer Science: New York, 2007, 3–33.

[84] Stella, V. J. Prodrugs as Therapeutics. *Expert Opin. Ther. Patents*, **2004**, *14*, 277–280.

[85] Ettmayer, P.; Amidon, G. L.; Clement, B.; Testa, B. Lessons Learned from Marketed and Investigational Prodrugs. *J. Med. Chem.* **2004**, *47*, 2393–2404.

[86] Testa, B. Prodrug Research: Futile or Fertile? *Biochem. Pharmacol.* **2004**, *68*, 2097–2106.

[87] Skwarczynski, M.; Hayashi, Y.; Kiso, Y. Paclitaxel Prodrugs: Toward Smarter Delivery of Anticancer Agents. *J. Med. Chem.* **2006**, *49*, 7253–7269.

[88] Wohl, A. R.; Kalscheuer, S.; Lee, H. S.; Han, J.; McCormick, A.; Macosko, C. W.; Panyam, J.; Hoye, T. R. A Silicate Ester Prodrug Strategy and in vivo Efficacy of Paclitaxel Prodrug-loaded Nanoparticles. *J. Am. Chem. Soc., submitted.*

[89] Corriu R. J. P.; Granier M.; Lanneau G. F. Synthesis and Reactivity of Bis(triethoxysilyl)methane, Tris(triethoxysilyl)methane and Some Derivatives. **1998** *J. Organomet. Chem. 562*, 79–88.

[90] Gitelman, H. J.; Alderman, F.; Perry, S. J. Renal Hnadling of Silicon in Normals and Patients with Renal Insufficiency. *Kidney Int.* **1992**, *42*, 957–959.

[91] Marco-Franco, J. E.; Torres, V. E.; Nixon, D. E.; Wilson, D. M; James, E. M.; Bergstrahl, E J.; McCarthy, J. T. Oxalate, Silicon, and Vanadium in Acquired Cystic Kidney Disease. *Clin. Nephrol.* **1991**, *35*, 52–58.

[92] Lai, W.; Garino, J.; Flaitz, C.; Ducheyne, P. Excretion of Resorption Products from Bioactive Glass Impanted in Rabbit Muscle. *J. Biomed. Mater. Res. Part A* **2005**, *75A*, 398–407.

[93] Mayne, A. H.; Bayliss, S. C.; Barr, P. Tobin, M.; Buckberry, L. D. Biologically Interfaced Porous Silicon Devices. *Phys. Status Solidi A – Appl. Res*. **2000**, *182*, 505–513.

[94] Kalscheuer, S.; Panyam, J. University of Minnesota, Minneapolis, MN. Personal communication, **2012**.

[95] Cory, A. H.; Owen, T. C.; Barltrop, J. A.; Cory, J. G. Use of an Aqueous Soluble Tetrazolium/Formazan Assay for Cell Growth Assays in Culture. *Cancer Comm.* **1991**, *3*, 207–212.

[96] Kingston, D. G. I. The Shape of Things to Come: Structural and Synthetic Studies of Taxol and Related Compounds. *Phytochemistry* **2007**, *68*, 1844–1854 and references therein.

[97] Wani, M.C.; Taylor, H.L.; Wall, M.E.; Coggon, P.; McPhail, A.T. Plant Antitumor Agents. VI. The Isolation and Structure of Taxol, a Novel Antileukemic and Antitumor Agent from *Taxus brevifolia*. *J. Am. Chem. Soc.* **1971**, 2325–2327.

[98] Schiff, P. B.; Fant, J.; Horwitz, S. B. Promotion of Microtubule Assembly in vitro By Taxol. *Nature* **1979,** *277*, 665–667.

[99] Wang, Y.-F.; Shi, Q.-W.; Dong, M.; Kiyota, H.; Gu, Y.-C.; Cong, B. Natural Taxanes: Developments Since 1828. *Chem. Rev.* **2011**, *111*, 7652–7709.

[100] U.S. Food and Drug Administration. *TAXOL® (paclitaxel) INJECTION*. **2007**.

[101] ten Tije, A. J.; Verweij, J.; Loos, W. L.; Sparreboom, A. Pharmacological Effects of Formulation Vehicles: Implications for Cancer Therapy. *Clin. Pharmacokinet.* **2003**, *42*, 665–685.

[102] Wiernik, P. H.; Schwartz, E. L.; Einzig, A.; Strauman, J. J.; Lipton, R. B.; Dutcher, J. P. Phase I Trial of Taxol Given as a 24-Hour Infusion Every 21 Days: Responses Observed in Metastatic Melanoma. *J. Clin. Oncol.* **1987**, *5*, 1232–1239.

[103] Hennenfent, K. L.; Govindan, R. New Formulations of Taxol: A Review. Old Wine in a New Bottle? *Ann. Oncol.* **2006**, *17*, 735–749 and references therein.

[104] Gelderblom, H.; Verweij, J.; Nooter, K.; Sparreboom, A. Cremophor EL: The Drawbacks and Advantages of Vehicle Selection for Drug Formulation. *Eur. J. Cancer* **2001**, *37*, 1590–1598.

[105] Scripture, C. D.; Figg, W. D.; Sparreboom, A. Paclitaxel Chemotherapy: From Empiricism to a Mechanism-Based Formulation Strategy. *Ther. Clin. Risk Manag.* **2005**, *1*, 107–114.

[106] Sparreboom, A.; Baker, S. D.; Verweij, J. Paclitaxel Repackaged in an Albumin-Stabilized Nanoparticle: Handy or Just Dandy? *J. Clin. Oncol.* **2005**, *23*, 7765–7767.

[107] U.S. Food and Drug Administration. ABRAXANE™ for Injectable Suspension (paclitaxel protein-bound particles for injectable suspension) (albumin-bound). **2005**.

[108] Ibrahim, N. K.; Desai, N.; Legha, S.; Soon-Shiong, P.; Theriault, R. L.; Rivera, E.; Esmaeli, B.; Ring, S. E.; Bedikian, A.; Hortobagyi, G. N.; Ellerhorst, J. A. Phase I and Pharmacokinetics Study of ABI-007, a Cremophor-Free, Protein-Stabilized, Nanoparticle Formulation of Paclitaxel. *Clin. Cancer Res.* **2002**, *8*, 1038–1044.

[109] Gradishar, W. J.; Tjulandin, S.; Davidson, N.; Shaw, H.; Desai, N.; Bhar, P.; Hawkins, M.; O'Shaughnessy, J. Phase III Trial of Nanoparticle-Albumin Bound Paclitaxel Compared with Polyethylated Castor Oil-Based Paclitaxel in Women with Breast Cancer. *J. Clin. Oncol.* **2005**, *23*, 7794–7803.

[110] Harries, M.; Ellis, P.; Harper, P. Nanoparticle Albumin-bound Paclitaxel for Metastatic Breast Cancer. *J. Clin. Oncol.* **2005**, *23*, 7768–7771.

[111] Kim, S. C.; Kim, D. W.; Shim, Y. H.; Bang, J. S.; Oh, H. S.; Kim, S. W.; Seo, M. H. In vivo Evaluation of Polymeric Micellar Paclitaxel Formulation: Toxicity and Efficacy. *J. Control. Release* **2001**, *72*, 191–202.

[112] Hangal-Joshi, R.; Gore, A. Y.; Rubinfeld, J.; Shrotriya, R. Paclitaxel Formulation. U.S. Patent 6,538,020, August 1, 2002.

[113] Lee, K. S.; Chung, H. C.; Im, S. A.; Park, Y. H.; Kim, C. S.; Kim, S.-B.; Rha, S. Y.; Lee, M. Y.; Ro, J. Multicenter Phase II Trial of Genexol-PM, a Cremophor-Free Polymeric Micelle Formulation of Paclitasel, in Patients with Metastatic Breast Cancer. *Breast Cancer Res. Treat.* **2008**, *108*, 241–250.

[114] Niu, F.; Roby, K. F.; Rajewski, R. A.; Decedue, C.; Subramaniam, B. Paclitaxel Nanoparticles: Production Using Compressed CO_2 as Antisolvent: Characterization and Animal Studies. In *Polymeric Drug Delivery II;* Svenson, S., ed. American Chemical Society: Washington, D. C., 2006, 262–277.

[115] Roby, K. F.; Niu, F.; Rajewski, R. A.; Decedue, C.; Subramaniam, B.; Terranova, P. F. Syngenic Mouse Model of Epithelial Ovarian Cancer: Effects of Nanoparticle Paclitaxel, Nanotax®. *Adv. Exp. Med. Biol.* **2008**, *622*, 169–181.

[116] Axiak, S. M.; Selting, K. A.; Decedue, C. J.; Henry, C. J.; Tate, D.; Howell, J.; Bilof, K. J.; Kim, D. Y. Phase I Does Escalation Study of Nanoparticulate Paclitaxel (CTI 52010) in Normal Dogs. *Int. J. Nanomedicine* **2011**, *6*, 2205–2212.

[117] Crown, J. Docetaxel and Paclitaxel in the Treatment of Breast Cancer: A Review of Clinical Experience. *Oncologist* **2004**, *9*, 24–32.

[118] Bernstein, B. Docetaxel as an Alternative to Paclitaxel after Acute Hypersensitivity Reactions. *Ann. Pharmacother.* **2000**, *34*, 1332–1335.

[119] Norris, L. B.; Qureshi, Z. P.; Bookstaver, P. B.; Raisch, D. W.; Sartor, O.; Chen, H.; Bennet, C. L. Polysorbate 80 Hypersensitivity Reactions: A Renewed Call to Action. *Commun. Oncol.* **2010**, *7*, 425–428.

[120] Echhoff, L.; Nielsen, M.; Moeller, S.; Knoop, A. TAXTOX – A Retrospective Study Regarding the Side Effects of Docetaxel Given as Part of the Adjuvant Treatment to Patients with Primary Breast Cancer in Denmark from 2007 to 2009. *Acta. Oncologica.* **2011**, *50*, 1075–1082.

[121] Vyas, D. M.; Wong, H.; Crosswell, A. R.; Casazza, A. M.; Knipe, J.O.; Mamber, S. W.; Doyle, T. W. Tumor targeting by covalent conjugation of a natural fatty acid to paclita. *Bioorg. Med. Chem. Lett*. **1993**, *3*, 1357–1360.

[122] Moosavi-Movahedi, A. A.; Hakimelahi, S.; Chamani, J.; Khodarahmi, G. A.; Hassanzadeh, F.; Luo, F. T.; Ly, T. W.; Shia, K.-S.; Yen, C. F.; Jain, M. L.; Kulatheeswaran, R.; Xue, C.; Pasdar, M.; Hakimelahi, G. H. Design,

Synthesis, and Anticancer Activity of Phosphonic Acid Diphosphate Derivative of Adenine-Containing Butenolide and its Water Soluble Derivatives of Paclitaxel with High Antitumor Activity. *Bioorg. Med. Chem.* **2003**, *11*, 4303–4313.

[123] Paradis, R.; Page, M. New Active Paclitaxel Amino Acid Derivatives with Improved Water Solubility. *Anticancer Res.* **1998**, *18*, 2711–2716.

[124] Deutsch, H. M.; Glinski, J. A.; Hernandez, M.; Haugwitz, R. D.; Narayanan, V. L.; Suffness, M.; Zalkow, L. H. Synthesis of Congeners and Prodrugs. 3. Water-Soluble Prodrugs of Taxol with Potent Antitumor Activity. *J. Med. Chem.* **1989**, *32*, 788–792.

[125] Khmelnitsky, Y. L.; Budde, C.; Arnold, M. J.; Usyatinsky, A.; Clark, D. S.; Dordick, J. S. Synthesis of Water-Soluble Paclitaxel Derivatives by Enzymatic Acylation*. J. Am. Chem. Soc.* **1997**, *119*, 11554–11555.

[126] Greenwald, R. B.; Pendri, A.; Bolikal, D.; Gilbert, C. W. Highly Water Soluble Taxol Derivatives: 2-Polyethylene Glycol Esters as Potential Prodrugs. *Bioorg. Med. Chem. Lett*. **1994**, *4*, 2465–2470.

[127] Greenwald, R. B.; Gilbert, C. W.; Pendri, A.; Conover, C. D.; Xia, J.; Martinez, A. Drug Delivery Systems: Water Soluble Taxol 2'-Poly-(Ethylene Glycol) Ester Prodrugs. Design and in vivo Effectiveness. *J. Med. Chem*. **1996**, *39*, 424–431.

[128] Rodrigues, P. C. A.; Scheuermann, K.; Stockmar, C.; Maier, G.; Fiebig, H. H.; Unger, C.; Muelhaupt, R.; Kratz, F. Synthesis and in vitro Efficacy of Acid-Sensitive Poly(ethylene glycol) Paclitaxel Conjugates. *Bioorg. Med. Chem. Lett*. **2003**, *13*, 355–360.

[129] Luo, Y.; Prestwich, G. D. Synthesis and Selective Cytotoxicity of a Hyaluronic Acid-Antitumor Bioconjugate. *Bioconjugate Chem.* **1999**, *10*, 755–763.

[130] Li, C.; Yu, D. F.; Newman, R. A.; Cabral, F.; Stephens, L. C.; Hunter, N.; Milas, L.; Wallace, S. Complete Regression of Well-Established Tumors using a Novel Water-Soluble Poly(L-glutamic acid)-Paclitaxel Conjugate. *Cancer Res.* **1998**, *58*, 2404–2409.

[131] Stevens, P. J.; Sekido, M.; Lee, R. J. A Folate Receptor-Targeted Lipid Nanoparticle Formulation for a Lipophilic Paclitaxel Prodrug. *Pharm. Res.* **2004**, *21*, 2153–2157.

[132] Ansell, S. Lipophilic Drug Derivatives for Use in Liposomes. U.S. Patent 5,534,499, July 9, 1996.

[133] Zakharian, T. Y.; Seryshev, A.; Sitharaman, B.; Gilbert, B. E.; Knight, V.; Wilson, L. J. A Fullerene-Paclitaxel Chemotherapeutic: Synthesis,

Characterization and Study of Biological Activity in Tissue Culture. *J. Am. Chem. Soc.* **2005**, *127*, 12508–12509.

[134] Ali, S.; Ahmad, I.; Peters, A.; Masters, G.; Minchey, S.; Janoff, A. S.; Mayhew, E. Hydrolyzable Hydrophobic Taxanes: Synthesis and Anticancer Activities. *Anti-Cancer Drugs* **2001**, *12*, 117–128.

[135] Lundberg, B. B.; Risovic, V.; Ramaswamy, M.; Wasan, K. M. A Lipophilic Pacltaxel Derivative Incorporated in a Lipid Emulsion for Parenteral Administration. *J. Control. Release* **2003**, *86*, 93–100.

[136] Rodrigues, D. C.; Maria, D. A.; Fernandes, D. C.; Valduga, C. J.; Couto, R. D.; Ibanez, O. C. M.; Maranhao, R. C. Improvement of Paclitaxel Therapeutic Index by Derivatization and Association to a Cholesterol-Rich Microemulsion: in vitro and in vivo Studies. *Cancer Chemother. Pharmacol.* **2005**, *55*, 565–576.

[137] Bradley, M. O.; Webb, N. L.; Anthony, F. H.; Devanesan, P.; Witman, P. A.; Hemamalini, S.; Chander, M. C.; Baker, S. D.; He, L.; Horwitz, S. B.; Swindell, C. S. Tumor Targeting by Covalent Conjugation of a Natural Fatty Acid to Paclitaxel. *Clin. Cancer Res*. **2001**, *7*, 3229–3238.

[138] Bedikian, A. Y.; DeConti, R. C.; Conry, R.; Agarwala, S.; Papadopoulos, N.; Kim, K. B.; Ernstoff, M. Phase 3 Study of Docosahexaenoic Acid-Paclitaxel Versus Dacarbazine in Patients with Metastatic Malignant Melanoma. *Ann. Oncol.* **2011**, *22*, 787–793.

[139] Harries, M.; O'Donnell, A.; Scurr, M.; Reade, S.; Cole, C.; Judson, I.; Greystoke, A.; Twelves, C.; Kaye, S. Phase I/II study of DHA-Paclitaxel in Combination with Carboplatin in Patients with Advanced Malignant Solid Tumours. *Br. J. Cancer* **2004**, *91*, 1651–1655.

[140] Hoye, T. R.; Wohl, A. W.; Macosko, C. W.; Panyam, J. Silicate Prodrugs and Nanoparticles. U.S. Patent Application PCT/US2012/040247, May 31, 2012. This application claims priority to a provisional application filed on May 31, 2011.

[141] Kim, I.-S.; Kim, S.-H. Development of a Polymeric Nanoparticulate Drug Delivery System: In vitro Characterization of Nanoparticles based on Sugar-Containing Particles. *Int. J. Pharm.* **2002**, *245*, 67–73.

[142] Görner, T.; Gref, R.; Michenot, D.; Sommer, F.; Tran, M. N.; Dellacherie, E. Lidocaine-loaded Biodegradable Nanospheres. I. Optimization of the Drug Incorporation into the Polymer Matrix. *J. Control. Release* **1999**, *57*, 259–268.

[143] Zhu, Q.; Guo, Z.; Huang, N.; Wang, M.; Chu, F. Comparative Molecular Field Analysis of a Series of Paclitaxel Analogs. *J. Med. Chem*. **1997**, *40*, 4319–4328.

[144] Michel, A. University of Minnesota, Minneapolis, MN. Personal communication, **2012**.

[145] Hayashi, Y.; Skwarczynski, M.; Hamada, Y.; Sohma, Y.; Kumura, T.; Kiso, Y. A Novel Approach of Water-Soluble Paclitaxel Prodrug with No Auxiliary and no Byproduct: Design and Synthesis of Isotaxel. *J. Med. Chem.* **2003**, *46*, 3782–3784.

[146] Sohma, Y.; Hayashi, Y.; Skwarczynski, M.; Hamada, Y.; Sasaki, M.; Kimura, T.; Kiso, Y. O-N Intramolecular Acyl Migration Reaction in the Development of Prodrugs and the Synthesis of Difficult Sequence-Containing Bioactive Peptides. *Biopolymers* **2004**, *76*, 344–356.

[150] Damja, R. I.; Eaborn, C.; Saxena, A. K. Acyl-Oxygen Fission in Reactions of Oragnosilicon Carboxylates with Sodium Methoxide in Methanol. *J. Chem. Soc. Perkin Trans. II* **1985**, *2*, 597–598.

[151] Kalscheuer, S. University of Minnesota, Minneapolis, MN. Personal communication, **2012**.

[152] Mosmann, T. Rapid Colorimetric Assay for Cellular Growth and Survival: Application to Proliferation and Cytotoxicity Assays. *J. Immunol. Methods* **1983**, *65*, 55–63.

[153] Anand, P.; Kunnumakkara, A. B.; Newman, R. A.; Aggarwal, B. B. Bioavailability of Curcumin: Problems and Promises. *Mol. Pharm.* **2007**, *4*, 807–818.

[154] Hoehle, S. I.; Pfeiffer, E.; Metzler, M. Glucuronidation of Curcuminoids by Human Microsomal and Recombinant UDP-Glucuronosyltransferases. *Mol. Nutr. Food Res.* **2007**, *51*, 932–938.

[155] Pan, M.-H.; Huang, T.-M.; Lin, J.-K. Biotransformation of Curcumin through Reduction and Glucoronidation in Mice *Drug Metab. Dispos.* .**1998**, *27,* 486–494.

[156] O'Toole, M. G.; Henderson, R. M.; Soucy, P. A.; Fasciotto, B. H.; Hoblitzell, P. J.; Keynton, R. S.; Ehringer, W. D.; Gobin, A. S. Curcumin Encapsulation in

Sub-Micron Chitosan/Tween 20 Particles. *Biomacromolecules*, **2012**, *13*, 2309–2314.

[157] Grill, A. University of Minnesota, Minneapolis, MN. Personal communication, **2011**.

[158] Ireson, C. R.; Jones, D. J. L.; Orr, S.; Coughtrie, M. W. H.; Boocock, D. J.; Williams, M. L.; Farmer, P. B.; Steward, W. P.; Gescher, A. J. Metabolism of the Cancer Chemopreventive Agent Curcumin in Human and Rat Intestine. *Cancer Epidemiol. Biomarkers Prevent.* **2002**, *11*, 105–111.

[159] ^{1}H NMR assignments were made with the consideration of Oyama, M.; Itokawa, H. Physical Methods for Identification of the Structures of Taxoids. In *Taxus: The Genus Taxus*. Itokawa, H.; Lee, K.-H., Eds. Taylor & Francis, Inc: New York, **2003**, *32*; 79-133.

[161] Lohmeijer, B. G. G.; Pratt, R. C.; Leibfarth, F.; Logan, J. W.; Long, D. A.; Dove, A. P.; Nederberg, F.; Choi, J.; Wade, C.; Waymouth, R. M.; Hedrick, J. L. Guanidine and Amidine Organo-Catalysts for Ring-Opening Polymerization of Cyclic Esters. *Macromolecules* **2006**, *39*, 8574–8583.

[162] Qian, H.; Wohl, A. R.; Crow, J. T.; Macosko, C. W.; Hoye, T. R. A Strategy for Control of “Random” Copolymerization of Lactide and Glycolide: Application to Synthesis of PEG-*b*-PLGA Block Polymers Having Narrow Dispersity. *Macromolecules*, **2011**, *44*, 7132–7140.

[163] Jerome, C.; Lecomte, P. Recent Advances in the Synthesis of Aliphatic Polyesters by Ring-Opening Polymerization. *Adv. Drug Deliver. Rev*. **2008**, *60*, 1056–1076.

[164] Astente, C. E.; Sabliov, C. M. Synthesis and Characterization of PLGA Nanoparticles, *J. Biomater. Sci. Polymer Edn.* **2006**, *17*, 247–289.

[165] Albertsson, A. C.; Varma, I. K. Recent Developments in Ring Opening Polymerization of Lactones for Biomedical Applications. *Biomacromolecules* **2003**, *4*, 1466–1486.

[166] Mohamed, F.; Van der Walle, C. F. Engineering Biodegradable Polyester Particles with Specific Drug Targeting and Drug Release Properties. *J. Pharm. Sci.* **2008**, *97*, 71–87.

[167] Middleton, J. C.; Tipton, A. J. Synthetic Biodegradable Polymers as Orthopedic Devices. *Biomaterials* **2000**, *21*, 2335–2346.

[168] Drumright, R. E.; Gruber, P. R.; Henton, D. E. Polylactic Acid Technology. *Adv. Mater.* **2000**, *12*, 1841–1846.

[169] Chu, C. C. Biodegradable Polymeric Biomaterials: an Updated Overview. In *Biomaterials*; Wong, J. Y., Bronzino, J. D. CRC Press: Boca Raton, FL, 2007; 6/1–6/22.

[170] Vert, M. Polyglycolide and Copolyesters with Lactide. *Biopolymers* **2002**, *4*, 179–202.

[171] Stjerndahl, A.; Wistrand, A. F.; Albertsson, A. C. Industrial Utilization of Tin-Initiated Resorbable Polymers: Synthesis on a Large Scale with a Low Amount of Initiator. *Biomacromolecules* **2007**, *8*, 937–940.

[172] Li, J.; Stayshich, R. M.; Meyer, T. Y. Exploiting Sequence to Control the Hydrolysis Behavior of Biodegradable PLGA Copolymers. *J. Am. Chem. Soc.* **2011**, *133*, 6910–6913.

[173] Dong, C.-M.; Qiu, K.-Y.; Gu, Z.-W.; Feng, X.-D. Synthesis of Poly(D,L-lactic acid-*alt*-glycolic acid) from D,L-3-methylglycolide. *J. Polym. Sci., Part A: Polym. Chem.* **2000**, *38*, 4179–4184.

[174] Kreiser-Saunders, I.; Kricheldorf, H. R. Polylactones. Part 39. Zn Lactate-Catalyzed Copolymerization of L-lactide with Glycolide or ε-caprolactone. *Macromol. Chem. Phys.* **1998**, *199*, 1081–1087.

[175] O'Keefe, B. J.; Hillmyer, M. A.; Tolman, W. B Polymerization of Lactide and Related Cyclic Esters by Discrete Metal Complexes. *J. Chem. Soc., Dalton Trans.* **2001**, 2215–2224.

[176] Barakat, I.; Dubois, P.; Jérôme, R.; Teyssié, P. Living Polymerization and Selective End Functionalization of ε-caprolactone using Zinc Alkoxides as Initiators. *Macromolecules* **1991,** *24***,** 6542–6545.

[177] Baran, J.; Duda, A.; Kowalski, A.; Szymanski, R.; Penczek, S. Quantitative Comparison of Selectivities in the Polymerization of Cyclic Esters. *Macromol. Symp.* **1997**, *123*, 93–101.

[178] Ovitt, T. M.; Coates, G. W. Stereochemistry of Lactide Polymerization with Chiral Catalysts: New Opportunities for Stereocontrol using Polymer Exchange Mechanisms. *J. Am. Chem. Soc.* **2002**, *124*, 1316–1326.

[179] Shen, Y.; Shen, Z.; Shen, J.; Zhang, Y.; Yao, K. Characteristics and Mechanism of ε-caprolactone Polymerization with Rare Earth Halide Systems. *Macromolecules* **1996***, 29*, 3441–3446.

[180] Ravi, P.; Gröb, T.; Dehnicke, K.; Greiner, A. Novel $[Sm_2I(NPPh_3)_5(DME)]$ Initiator for the Living Ring-Opening Polymerization of ε-caprolactone and δ-valerolactone, *Macromolecules* **2001**, *34*, 8649–8653.

[181] Chamberlin, B. M.; Jazdzewski, B. A.; Pink, M.; Hillmyer, M. A.; Tolman, W. B. Controlled Polymerization of DL-lactide and ε-caprolactone by Structurally Well-Defined Alkoxo-Bridged Di- and Triyttrium(III) Complexes. *Macromolecules* **2000**, *33*, 3970–3977.

[182] Albertsson, A. C.; Srivastava, R. K. Recent Developments in Enzyme-Catalyzed Ring-Opening Polymerization. *Adv. Drug Deliver. Rev.* **2008**, *60*, 1077–1093.

[183] Nederberg, F.; Connor, E. F.; Möller, M.; Glauser, T.; Hedrick, J. L. New Paradigms for Organic Catalysts: the First Organocatalytic Living Polymerization. *Angew. Chem. Int. Ed.* **2001**, *40*, 2712–2715.

[184] Dove, A. P.; Pratt, R. C.; Lohmeijer, B. G. G.; Culkin, D. A.; Hagberg, E. C.; Nyce, G. W.; Waymouth, R. M.; Hedrick, J. L. *N*-Heterocyclic Carbenes: Effective Organic Catalysts for Living Polymerization. *Polymer* **2006**, *47*, 4018–4025.

[185] Myers, M.; Connor, E. F.; Glauser, T.; Mock, A.; Nyce, G.; Hedrick, J. L. Phosphines: Nucleophilic Organic Catalysts for the Controlled Ring-Opening Polymerization of Lactides. *J. Polym. Sci., Part A: Polym. Chem.* **2002**, *40*, 844–851.

[186] Zhang, L.; Nederberg, F.; Messman, J. M.; Pratt, R. C.; Hedrick, J. L.; Wade, C. G. Organocatalytic Stereoselective Ring-Opening Polymerization of Lactide with Dimeric Phosphazene Bases. *J. Am. Chem. Soc.* **2007,** *129*, 12610–12611.

[187] Dong, J.; Jiang, S.; Ping, Q. Development of Injectable Biodegradable in-situ forming Gel Implants. *Yaoxue Jinzhan* **2007**, *31*, 110–113.

[188] Avgoustakis, K. Pegylated Poly(lactide) and Poly(lactide-*co*-glycolide) Nanoparticles: Preparation, Properties and Possible Applications in Drug Delivery. *Curr. Drug Deliver*. **2004**, *1*, 321–333.

[189] Huh, K. M.; Cho, Y. W.; Park, K. PLGA-PEG Block Copolymers for Drug Formulations. *Drug Deliver. Tech*. **2003**, *42*, 44–49.

[190] Thakur, K. A. M.; Kean, R. T.; Hall, E. S.; Kolstad, J. J.; Munson, E. J. Stereochemical Aspects of Lactide Stereo-Polymerization Investigated by ^{1}H NMR: A Case of Changing Stereospecificity. *Macromolecules* **1998**, *21*, 1487–1497.

[191] Thillaye du Boullay, O.; Marchal, E.; Martin-Vaca, B.; Cossio, F. P.; Bourissou, D. An Activated Equivalent of Lactide toward Organocatalytic Ring-Opening Polymerization. *J. Am. Chem. Soc*. **2006**, *128*, 16442–16443.

[193] Hiemenz, P. C.; Lodge, T. P. Copolymers, Microstructure, and Stereoregularity. In *Polymer Chemistry*, 2nd Ed.; Taylor & Francis Group, LLC: Boca Raton, **2007**, *1*; 165–216.

[195] Kricheldorf, H. R.; Kreiser, I. Polylactones, 11. Cationic Copolymerization of Glycolide with L,L-Dilactide. *Makromol. Chem*. **1987**, *188*, 1861–1873.

[196] Gilding, D. K.; Reed, A. M. Biodegradable Polymers for Use in Surgery – Polyglycolic/Poly(lactic acid) Homo- and Copolymers: 1. *Polymer* **1979**, *20,* 1459–1464.

[197] Dotson, N. A.; Galván, R.; Laurence, R. L.; Tirrell, M. Reactor Configuration. In *Polymerization Process Modeling*; VCH Publishers, Inc.: New York, NY, **1996**; 259–303.

[199] Bandrup, J.; Immergut, E. H.; Grulke, E. A.; Abe, A.; Bloch, D. R. Polymer Handbook, 4th Edition, John Wiley & Sons, Inc. New York, 1999.

[200] Medrano, R.; Laguna, M. T. R.; Saiz, E.; Tarazona, M. P. Analysis of Copolymers of Styrene and Methyl Methacrylate using Size Exclusion Chromatography with Multiple Detection. *Phys. Chem. Chem. Phys.* **2003**, *5*, 151–157.

[201] Huffman, K. R.; Casey, D. J. Effect of Carboxyl End Groups on Polyglycolic Acid. *J. Polym. Sci: Polym. Chem. Ed.* **1985**, *23*, 1939–1954.

[202] Khandpur, A. K.; Förster, S.; Bates, F. S.; Hamley, I W.; Ryan, A. J.; Bras, W.; Almdal, K.; Mortensen, K. Polyisoprene-Polystyrene Diblock Copolymer Phase Diagram near the Order-Disorder Transition. *Macromolecules* **1995**, *28*, 8796–8806.

[203] Bandrup, J.; Immergut, E. H.; Grulke, E. A.; Abe, A.; Bloch, D. R. Polymer Handbook, 4th Edition, John Wiley & Sons, Inc. New York, 1999.

[204] Kricheldorf, H. R.; Mang, T.; Jonte, J. M. Polylactones. 1. Copolymerization of Glycolide and ε-caprolactone. *Macromolecules* **1984**, *17*, 2173–2181.

[205] Grujpma, D. W.; Nijenhuis, A. J.; Pennings, A. J. Synthesis and Hydrolytic Degradation Behaviour of High-Molecular-Weight L-Lactide and Glycolide Copolymers. *Polymer* **1990**, *31*, 2201–2206.

[206] Odian, G., Principles of Polymerization, 4th Edition, Wiley-Interscience, New York, 2004, p 470.

[207] D'Addio, S. M.; Saad, W.; Ansell, S. M.; Squiers, J. J.; Adamson, D.; Herrera-Alonso, M.; Wohl, A. R.; Hoye, T. R.; Macosko, C. W.; Mayer, L. D.;

Vauthier, C.; Prud'homme, R. K. Effects of Block Copolymer Properties on Nanocarrier Protection from *in vivo* Clearance. *J. Control. Release* **2012**, *162*, 208–217.

[208] Jain, R. A. The Manufacturing Techniques of Various Drug-Loaded Biodegradable Poly(lactide-*co*-glycolide) (PLGA) Devices. *Biomaterials*, **2000**, *21*, 2475–2490.

[209] Fetterly, G. J.; Straubinger, R. M. Pharmacokinetics of Paclitaxel-Containing Liposomes in Rats. *AAPS PharmSci.* **2003**, *5*, 90-100.

[210] Koudelka, S.; Turaneck-Knotigova, P.; Masek, J.; Korvasova, Z.; Skrbalova, M.; Plockova, J.; Bartheldyova, E.; Turanek, J. Liposomes with High Encapsulation Capacity for Paclitaxel: Preparation, Characterization, and *in vivo* Anticancer Effect. *J. Pharm. Sci.* **2010**, *99*, 2309–2319.

[211] Steele, T. W. J.; Huang, C. L.; Widjaja, E.; Boey, F. Y. C.; Loo, J. S. C.; Venkatraman, S. S.; The Effect of Polyethylene Glycol Strutcture on Paclitaxel Drug Release and Mechanical Properties of PLGA Thin Films. *Acta Biomater.* **2011**, *7*, 1973–1983.

[212] Quintanar-Guerrero, D.; Allèmann, E.; Fessi, H.; Doelker, E. Preparation Techniques and Mechanisms of Fromation of Biodegradable Nanoparticles from Preformed Polymers. *Drug Dev. Ind. Pharm.* **1998**, *24*, 1113–1128.

[213] Torchilin, V. P. Micellar Nanocarriers: Pharmaceutical Perspectives. *Pharm. Res.* **2007**, *24*, 1–16.

[214] Chavanpatil, M. D.; Patil, Y.; Panyam, J. Susceptibility of Nanoparticle-Encapsulated Paclitaxel to P-glycoprotein-mediated Drug Efflux. *Int. J. Pharm.* **2006**, *320*, 150–156.

[215] Patil, Y. B.; Toti, U. S.; Khdair, A.; Ma, L.; Panyam, J. Single-Step Surface Functionalization of Polymeric Nanoparticles for Targeted Drug Delivery. *Biomaterials*, **2009**, *30*, 859–866.

[216] Danhier, F.; Lecouturier, N.; Vroman, B.; Jèröme, C.; Marchand-Brynaert, J.; Feron, O.; Prèat, V. Paclitaxel-loaded PEGylated PLGA-based Nanoparticles: In vitro and in vivo Evaluation. *J. Control. Release* **2009**, *133*, 11–17.

[217] He, G.; Lwin, L.; Pan, J.; Venkatraman, S. ABA and BAB Type Triblock Copolymer of PEG and PLA: A Comparative Study of Drug Release Properties and "Stealth" Particle Characteristics. *Int. J. Pharm.* **2007**, *334*, 48–55.

[218] Johnson, B. K. Flash NanoPrecipitation of Organic Actives via Confined Micromixing and Block Copolymer Stabilization. Ph.D. Dissertation, Princeton University, Princeton, NJ, **2003**, 1–291.

[219] Zhu, Z.; Anacker, J. L.; Ji, S.; Hoye, T. R.; Macosko, C. W.; Prud'homme, R. K. Formation of Block Copolymer-Protected Nanoparticles via Reactive Impingement Mixing. *Langmuir*, **2007**, *23*, 10499–10504.

[220] Riess, G. Micellization of Block Copolymers. *Prog. Polym. Sci.* **2003**, *28*, 1107–1170 and references therein.

[221] Riley, T.; Stolnik, S.; Heald, C. R.; Xiong, C. D.; Garnett, M. C.; Illum, L; Davis, S. S.; Purkiss, S. C.; Barlow, R. J.; Gellert, P. R. Physicochemical Evaluation of Nanoparticles Assembled from Poly(lactic acid)-Poly(ethylene glycol) (PLA-PEG) Block Copolymers as Drug Delivery Vehicles. *Langmuir* **2001**, *17*, 3168–3174.

[222] Heald, C. R.; Stolnik, S.; Kujawinski, K. S.; De Matteis, C.; Garnett, M. C.; Illum, L.; Davis, S. S.; Purkiss, S. C.; Barlow, R. J.; Gellert, P. R. Poly(lactic acid)-Poly(ethylene oxide) (PLA-PEG) Nanoparticles: NMR Studies of the Central Solidlike PLA Core and the Liquid PEG Corona. *Langmuir*, **2002**, *18*, 3669–3675.

[223] Papadimitriou, S.; Bikiaris, D. Novel Self-Assembled Core–Shell Nanoparticles Based on Crystalline Amorphous Moieties of Aliphatic Copolyesters for Efficient Controlled Drug Release. *J. Control. Release* **2009**, *138*, 177–184.

[224] Zhang, X.-M.; Patel, A. B.; de Graaf, R. A.; Behar, K. L. Determindation of Liposomal Encapsulation Efficiency Using Proton NMR Spectroscopy. *Chem. Phys. Lipids* **2004**, *127*, 113–120.

[225] Hoo, C. M.; Starostin, N.; West, P.; Mecartney, M. L. A Comparison of Atomic Force Microscopy (AFM) and Dynamic Light Scattering (DLS) Methods to Characterize Nanoparticle Size Distributions. *J. Nanopart. Res.* **2008**, *10*, 89–96.

[226] Valentini, M.; Vaccaro, A.; Rehor, A.; Napoli, A.; Hubbell, J. A.; Tirelli, N. Diffusion NMR Spectroscopy for the Characterization of the Size and Interactions of Colloidal Matter: The Case of Vesicles and Nanoparticles. *J. Am. Chem. Soc.* **2004**, *126*, 2142–2147.

[227] Garcia-Fuentes, M.; Torres, D.; Martin-Pastor, M.; Alonso, M. J. Application of NMR Spectroscopy to the Characterization of PEG-Stabilized Lipid Nanoparticles. *Langmuir*, **2004**, *20*, 8839–8845.

[228] Yao, L. University of Minnesota, Minneapolis, MN. Personal communication, **2011**.

[230] Kang, E.; Robinson, J.; Park, K.; Cheng, J.-X. Paclitaxel Distribution in Poly(ethylene glycol) / Poly(lactide-*co*-glycolide) Blends and its Release by Coherent Anti-Stokes Raman Scattering Microscopy. *J. Control. Release* **2007**, *122*, 261–268.

[231] Mu, L.; Teo, M. M.; Ning, H. Z.; Tan, C. S.; Feng, S. S. Novel Powder Formulations for Controlled Delivery of Poorly Soluble Anticancer Drug: Application and Investigation of TPGS and PEG in Spray-Dried Particulate System. *J. Control. Release* **2005**, *103*, 565–575.

[232] Ali, H.; El-Sayed, K.; Sylvester, P. W.; Nazzal, S. Molecular Interaction and Localization of Tocotrienol-Rich Fraction (TRF) within the Matrices of Lipid Nanoparticles: Evidence Studied by Differential Scanning Calorimetry (DSC and Proton Nuclear Magnetic Resonance Spectroscopy (^{1}H NMR). *Colloids Surf., B.* **2010**, *77*, 286–297.

[233] Essa, S.; Rabanel, J. M.; Hildgen, P. Effects of Polyethylene Glycol (PEG) Chain Organization on the Physicochemical Properties of Poly(D, L -lactide) (PLA) Based Nanoparticles. *Eur. J. Pharm. Biopharm.* **2010**, *75*, 96–106.

[234] Kulinski, Z.; Piorkowska, E.; Gadzinowska, K.; Stasiak, M. Plasticization of Poly(L-lactide with Poly(propylene glycol). *Biomacromolecules*, **2006**, *7*, 2128–2135.

[235] Lee, J. H.; Jho, J. Y. A Morphological Study of Semicrystalline Poly(L-lactic acid-*b*-ethylene oxide-*b*-L-lacitic acid) Triblock Copolymer. *Macromolecules* **2005**, *38*, 104–109.

[237] Oh, K. S.; Song, J. Y.; Cho, S. H.; Lee, B. S.; Kim, S. Y.; Kim, K.; Jeon, H.; Kwon, I. C.; Yuk, S. H. Paclitaxel-loaded Pluronic Nanoparticles Formed by a Temperature-Induced Phase Transition for Cancer Therapy. *J. Control. Release* **2010**, *148*, 344–350.

[238] Han, J. University of Minnesota,Minneapolis, M. Personal communication, **2012**.

[239] Guru, B. University of Minnesota, Minneapolis, MN. Personal communication, **2010**.

[240] Jenkins, D. E.; Oei, Y.; Hornig, Y. S.; Yu, S.-F.; Dusich, J.; Purchio, T.; Contag, P. R. Bioluminescent Imaging (BLI) to Improve and Redefine

Traditional Murine Models of Tumor Growth and Metastasis. *Clin. Exp. Metastasis* **2003**, *20*, 733–744.

[241] http://www.criver.com/sitecollectiondocuments/rm_rm_r_NUNU_mouse_hematology_2008.pdf and http://www.criver.com/sitecollectiondocuments/rm_rm_r_NUNU_mouse_biochemistry_2008.pdf at http://www.criver.com/en-US/ProdServ/ByType/ResModOver/ResMod/Pages/NuNuNudeMouse.aspx (accessed May 31, 2012).

[242] Zhu, Z.; Margulis-Goshen, K.; Magdassi, S.; Talmon, Y.; Macosko, C. W. Polyelectrolyte Stabilized Drug Nanoparticles via Flash Nanoprecipitation: A Model Study With β-Carotene. *J. Pharm. Sci.* **2010**, *99*, 4295–4306.

[243] Paroo, Z.; Bollinger, R. A.; Braasch, D. A.; Richer, E.; Corey, D. R.; Antich, P. P.; Mason, R. P. Validating Bioluminescence Imaging as a High-Throughput, Quantitative Modality for Assessing Tumor Burden. *Mol. Imaging* **2004**, *3*, 117–124.

[244] Iha, R. K.; Wooley, K. L.; Nyström, A. M.; Burke, D. J.; Kade, M. J.; Hawker, C. J. Applications of Orthogonal “Click” Chemistries in the Synthesis of Functional Soft Materials. *Chem. Rev.* **2009**, *109*, 5620–5686.

[245] Acharya, S.; Sahoo, S. K. PLGA Nanoparticles Containing Various Agents and Tumour Delivery by EPR Effect. *Adv. Drug Deliver. Rev.* **2011**, *63*, 170–183.

[246] Brannon-Peppas, L.; Blanchette, J. O. Nanoparticle and Target Systems for Cancer Therapy. *Adv.Drug Delivery Rev*. **2004**, *56*, 1649–1659.

[247] Maeda, H.; Sawa, T.; Konno, T. Mechanism of Tumor-Targeted Delivery of Macromolecular Drugs,Including the EPR Effect in Solid Tumor and Clinical Overview of the Prototype Polymeric DrumSMANCS. *J. Control. Release* **2001**, *74*, 47–61.

[248] Peer, D.; Karp, J. M.; Hong, S.; Farokhzad, O. C.; Margalit, R.; Langer, R. Nanocarriers as an Emerging Platform for Cancer Therapy. *Nature Nanotech.* **2007**, *2*, 751–760.

[249] Adiseshaiah, P. P,. Hall, J. B., McNeil, S. E. Nanomaterial Standards for Efficacy and Toxicity Assessment. *Wiley Interdiscip. Rev. Nanomed. Nanobiotechnol.* **2010**, *2*, 99–112.

[250] Petros, R. A. & DeSimone, J. M. Strategies in the Design of Nanoparticles for Therapeutic Applications. *Nat. Rev. Drug Discov.* **2010**, *9*, 615–627.

[251] Betancourt, T.; Doiron, A.; Brannon-Peppas, L. Polymeric Nanoparticles for Tumor-Targeted Drug Delivery. In *Nanotechnology for Cancer Therapy.* Amiji, M. M., ed. CRC Press: Boca Raton, FL, 2007, pp 2115–229.

[252] Jäschke, A.; Fürste, J. P.; Cech, D.; Erdmann, V. A. Automated Incorporation of Polyethylene Glycol into Synthetic Oligonucleotides. *Tet. Lett.* **1993**, *34*, 301–304.

[253] Thompson, M. S.; Vadala, T. P.; Vadala, M. L.; Lin, Y.; Riffle, J. S. Synthesis and Applications of Heterobifunctional Poly(ethylene oxide) Oligomers. *Polymer* **2008**, *49*, 345–373.

[254] Yagci, Y.; Ito, K. Macromolecular Architecture Based on Anionically Prepared Poly(ethylene oxide) Macromonomers. *Macromol. Symp.* **2005**, *226*, 87–96.

[255] Hiki, S.; Kataoka, K. A Facile Synthesis of Azido-Terminated Heterobifunctional Poly(ethylene glycol)s for “Click” Conjugation. *Bioconjugate. Chem.* **2007**, *18*, 2191–2196.

[256] Nagasaki, Y.; Iijima, M.; Kato, M.; Kataoka, K. Primary Amino-Terminal Heterobifunctional Poly(ethylene oxide). Facile Synthesis of Poly(ethylene oxide) with a Primary Amino Group on One End and a Hydroxyl Group at the Other End. *Bioconjugate Chem.* **1995**, *6*, 702–704.

[257] Ito, K.; Hashimura, K.; Itsuno, S. Poly(ethylene oxide) Macromolecules. 8. Preparation and Polymerization of ω-Hydroxypoly(ethylene oxide) Macromonomers. *Macromolecules* **1991**, *24*, 3977–3981.

[258] Reed, N. N,; Janda, K. D. A One-Step Synthesis of Monoprotected Polyethylene Glycol Ethers. *J. Org. Chem.* **2000**, *65*, 5843–5845.

[259] Hiki, S.; Kataoka, K. Versatile and Selective Synthesis of “Click Chemistry” Compatible Heterobifunctional Poly(ethylene glycol)s Possessing Azide and Alkyne Functionalities. *Bioconjugate Chem.* **2010**, *21*, 248–254.

[261] Zhao, C.-L.; Winnik, M. A.; Riess, G.; Croucher, M. D. Fluorescence Probe Techniques Used to Study Micelle Formation in Water-Soluble Block Copolymers. *Langmuir*, **1990**, *6*, 514–516.

[262] Savic, R.; Luo, L.; Eisenberg, A.; Maysinger, D. Micellar Nanocontainers Distribute to Defined Cytoplasmic Organelles. *Science* **2009**, *300*, 615–618.

[263] Laitinen, O. H.; Hytönen, V. P.; Nordlund, H. R.; Kulomaa, M. S. Genetically Engineered Avidins and Streptavidins. *Cell Mol. Life Sci.* **2006**, *63*, 2992–3017.

[264] Tashiro, E.; Imoto, M. Target Identification of Bioactive Compounds. *Bioorg. Med. Chem.* **2012**, *20*, 1910–1921.

[265] Patil, Y.; Sadhukha, T.; Ma, L.; Panyam, J. Nanoparticle-Mediated Simultaneous and Targeted Delivery of Paclitaxel and Tariquidar Overcomes Tumor Drug Resistance. *J. Control. Rel.* **2009**, *136*, 21–29.

[266] Lee, E. S.; Na, K.; Bee, Y. H. Super pH-Sensitive Multifunctional Polymeric Micelle. *Nano Lett.* **2005**, *5*, 325–329.

[267] Salem, A. K.; Cannizzaro, S. M.; Davies, M. C.; Tendler, S. J. B.; Roberts, C. J.; Williams, P. M.; Shakesheff, K. M. Synthesis and Characterization of a Degradable Poly(lactic acid)-Poly(ethylene glycol) Copolymer with Biotinylated End Groups. *Biomacromolecules* **2001**, *2*, 575–580.

[268] Despras, G.; Robert, R.; Sendid, B.; Machez, E.; Poulain, D.; Mallet, J.-M. Biotin Sulfone Tagged Oligomannosides as Immunogens for Eliciting Antibodies against Specific Mannan Epitopes. *Bioorg. Med. Chem.* **2012**, *20*, 1817–1831.

[269] Newkome, G. R.; Kotta, K. K.; Mishra, A.; Moorefield, C. N. Synthesis of Water-Soluble Ester-Terminated Dendrons and Dendrimers Containing Internal PEG Linkages. *Macromolecules* **2004**, *37*, 8262–8268.

[270] Menger, F. M.; Zhang, H. Self-Adhesion among Phospholipid Vesicles. *J. Am. Chem. Soc.* **2006**, *128*, 1414–1415.

[271] Ryu, J.-H.; Jang, C.-J.; Yoo, Y.-S.; Lim, S.-G.; Lee, M. Supramolecular Reactor in an Aqueous Environment: Aromatic Cross Suzuki Coupling Reaction at Room Temperature. *J. Org. Chem.* **2005**, *70*, 8956–8962.

[272] Binder, W. H.; Sachsenhofer, R. “Click” Chemistry in Polymer and Materials Science. *Macromol. Rapid Commun.* **2007**, *28*, 15–54

[273] Opsteen, J. A.; van Hest, J. C. M. Modular Synthesis of Block Copolymers via Cycloaddition of Terminal Azide and Alkyne Functionalized Polymers. *Chem. Commun.* **2005**, 57–59.

[274] Ji, S.; Hoye, T. R.; Macosko, C. W. Primary Amine (-NH_2) Quantification in Polymers: Functionality by ^{19}F NMR Spectroscopy. *Macromolecules* **2005**, *38*, 4679–4686.

[275] Lin, P.-C.; Ueng, S.-H.; Yu, S.-C.; Jan, M.-D.; Adak, A. K.; Yu, C.-C.; Lin, L.-C. Surface Modification of Magnetic Nanoparticle via Cu(I)-Catalyzed Alkyne-azide [2 + 3] Cycloaddition. *Org. Lett.* **2007**, *9*, 2131–2134.

[276] Xu, W. Z.; Zhang, X.; Kadla, J. F. Design of Functionalized Cellulosic Honeycomb Films: Site-Specific Biomolecule Modification via “Click Chemistry.” *Biomacromolecules* **2012**, *13*, 350–357.

[277] Weis, W. I.; Drickamer, K.; Hendrickson, W. A. Structure of a C-type Mannose-Binding Protein Complexed with an Oligosaccharide. *Nature* **1992**, *360*, 127–134.

[278] Irache, J. M.; Salman, H. H.; Gamazo, C.; Espuelas, S. Mannose-Targeted Systems for the Delivery of Therapeutics. *Expert Opin. Drug Dis.* **2008**, *5*, 703–724.

[279] Foged, C. Arigita, C.; Sundblad, A.; Jiskoot, W.; Storm, G.; Frokjaer, S. Interaction of Dendritic Cells with Antigen-Containing Liposomes: Effect of Bilayer Composition. *Vaccine* **2004**, *22*, 1903–1913.

[280] Taylor, M. E.; Drickamer, K. Structural Requirements for High-Affinity Binding of Complex Ligands by the Macrophage Mannose Receptor. *J. Bio. Chem.* **1993**, *268*, 399–404.

[281] Engel, A.; Chatterjee, S. K.; Al-arifi, A.; Riemann, D.; Langner, J.; Nuhn, P. Influence of Spacer Length on Interaction of Mannosylated Liposomes with Human Phagocytic Cells. *Pharm. Res.* **2003**, *20*, 51–57.

[282] Yeeprae, W.; Kawakami, S.; Yamashita, F.; Hashida, M. Effect of Mannose Density on Mannose Receptor-Mediated Cellular Uptake of Mannosylated O/W Emulstions by Macrophages. *J. Control. Release* **2006**, *114*, 193–201.

[283] Mahajan, S.; Prashant, C. K.; Koul, V.; Choudhary, V.; Dinda, A. K. Receptor Specific Macrophage Targeting by Mannose-Conjugated Gelatin Nanoparticles: An *in vitro* and *in vivo* Study. *Curr. Nanosci.* **2010**, *6*, 413–421.

[284] Nagahori, N.; Nishimura, S.-I. Tailoring Glycopolymers: Controlling the Carbohydrate-Protein Interaction Based on Template Effects. *Biomacromolecules* **2001**, *2*, 22–24.

[285] Hotha, S.; Kashyap, S.; “Click Chemistry” Inspired Synthesis of *pseudo*-Oligosaccharides and Amino Acid Glycoconjugates. *J. Org. Chem.* **2006**, *71*, 364–367.

[286] Fernandez-Megia, E.; Novoa-Carballal, R.; Quio, E.; Riguera, R. Conjugation of Bioactive Ligands to PEG-Grated Chitosan at the Distal End of PEG. *Biomacromolecules*, **2007**, *8*, 833–842.

[287] Berry, L. M.; Wollenberg, L.; Zhao, Z. Esterase Activities in the Blood, Liver and Intestine of Several Preclinical Species and Humans. *Drug Metab. Lett.* **2009**, *3*, 70–77.

[289] Iyer, S. S.; Anderson, A. S.; Reed, S.; Swanson, B.; Schmidt, J. G. Synthesis of Orthogonal End Functinoaled Oligotheylene Glycols of Defined Lengths. *Tetrahedron Lett.* **2004**, *45*, 4285–4288.

[290] Mereyala, H. B.; Gurrala, S. R. A Highly Diastereoselctive, Practical Synthesis of Allyl, Propargyl, 2,3,4,6-tetra-*O*-acetyl-β-D-gluco, β-D-galactopyranosides and Allyl, Propargyl, Heptaacetyl-β-D-lactosides. *Carbohydr. Res.* **1998**, *307*, 351–354.

[291] Wang, R.; Chen, G.-T.; Du, F.-S.; Li, Z.-C. Preparation and Aggregation Behavior of Mannose-Terminated Poly(ethylene glycol)-*b*-poly(L-leucine) in Water. *Colloids Surf., B* **2011**, *85*, 56–62.

[292] Kumar, K. K.; Kumar, R. M.; Subramanian, V.; Das, T. M. Expedient Synthesis of Coumarin-Coupled Triazoles via 'Click Chemistry' Leading to the Formation of Coumarin-Triazole-Sugar Hybrids. *Carbohydr. Res.* **2010**, *345*, 2297–2304.

[293] Singh, R. A Sensitive Assay for Maleimide Groups. *Bioconjugate Chem.* **1994**, *5*, 348–351.

[294] Durmaz, H.; Colakoglu, B.; Tunca, U.; Hizal, G. J. Preparation of Block Copolymers Via Diels Alder Reaction of Maleimide- and Anthracene-End Functionalized Polymers. *J. Polym. Sci., Part A: Polym. Chem.* **2006**, *44*, 1667–1675.

[295] Dag, A.; Durmaz, H.; Demir, E.; Hizai, G.; Tunca, U. Heterograft Copolymers via Double Click Reactions Using One-Pot Technique. *J. Polym. Sci., Part A: Polym. Chem.***2008**, *46*, 6969–6977.

[296] Kosif, I.; Park, E.-J.; Sanyal, R.; Sanyal, A. Fabrication of Maleimide Containing Thiol Reactive Hydrogels via Diels-Alder/Retro Diels-Alder Strategy. *Macromolecules* **2010**, *43*, 4140–4148.

[297] Durmaz, H.; Dag, A.; Altintas, O.; Erdogan, T.; Hizal, G.; Tunca, U. One Pot Synthesis of ABC Type Triblock Copolymers via in situ Click [3 + 2] and [4 + 2] Reactions. *Macromolecules* **2007**, *40*, 191–198.

[298] Gacal, B.; Durmaz, H.; Tasdelen, M. A.; Hizal, G.; Tunca, U.; Yagel, Y.; Demirel, A. L. Anthracene-Maleimide-Based Diels-Alder "Click Chemistry" as a Novel Route to Graft Copolymers. *Macromolecules* **2006**, *39*, 5330–5336.

[299] Olivier, J.-C.; Huertas, R.; Lee, H. J.; Calon, F.; Pardridge, W. M. Synthesis of Pegylated Immunonanoparticles. *Pharm. Res.* **2002**, *19*, 1137–1143.

[300] Nasongkla, N.; Shuai, X.; Ai, H.; Weinberg, B. D.; Pink, J.; Boothman, D. A.; Gao, J. cRGD-Functionalized Polymer Micelles for Targeted Doxorubicin Delivery. *Angew. Chem., Int. Ed*. **2004**, *116*, 6483–6487.

[301] Ji, S.; Hoye, T. R.; Zhu, Z.; Macosko, C. W. Maleimide Functionalized Poly(ε-caprolactone)-*b*-poly(ethylene glycol) (PCL-PEG-MAL) Nanoparticles: Formation and Thiol Conjugation. *Macromol. Chem. Phys.* **2009**, *210*, 823–831.

[302] Mehta, N. B.; Phillips, A. P.; Lui, F. F.; Brooks, R. E. Maleamic and Citraconamic Acids, Methyl Esters, and Imides. *J. Org. Chem.* **1960**, *25*, 1012–1015.

[303] Mitsunobu, O. The Use of Diethyl Azodicarboxylate and Triphenylphosphine in Synthesis and Transformation of Natural Products. *Synthesis* **1981** 1–28.

[304] Walker, M. A. The Mitsunobu Reaction: A Novel Method for the Synthesis of Bifunctional Maleimide Linkers. *Tetrahedron Lett.* **1994**, *35*, 665–668.

[305] Gill, H. S.; Tinianow, J. N.; Ogasawara, A.; Flores, J. E.; Vanderbilt, A. N.; Raab, H.; Scheer, J. M.; Vandlen, R.; Williams, S.-P.; Marik, J. A Modular Platform for the Rapid Site-Specific Radiolabelling of Proteins with ^{18}F Exemplified by Quantitative Positron Emission Tomography of Human Epidermal Growth Factor Receptor 2. *J. Med. Chem.* **2009**, *52*, 5826–5825.

[306] Walker, M. A. A High Yielding Synthesis of *N*-alkyl Maleimides Using a Novel Modification of the Mitsunobu Reaction. *J. Org. Chem.* **1995**, *60*, 5352–5355.

[307] Warnecke, A.; Kratz, F. Maleimide-oligo(ethylene glycol) Derivative of Camptothecin as Albumin-Binding Prodrugs: Synthesis and Antitumor Efficacy. *Bioconjugate Chem.* **2003**, *14*, 377–387.

[308] Schumacher, F. F.; Nobles, M.; Ryan, C. P.; Smith, M. E. B.; Tinker, A.; Caddick, S.; Baker, J. R. In Situ Maleimide Bridging of Disulfides and a New Approach to Protein PEGylation. *Bioconjugate Chem.* **2011**, *22*, 132–136.

[309] Veronese, F. M. Peptide and Protein PEGylation: A Review of Problems and Solutions. *Biomaterials* **2001**, *22*, 405–417 and references therein.